

Manuel Pérez Pueyo

Aportaciones de la Fm Tremp  
(Maastrichtiense superior) en la  
Ribagorza (Pirineo aragonés,  
(Huesca) al conocimiento de las  
comunidades de vertebrados  
finicretácicas de la isla Ibero-  
Armoricana.

VERSIÓN CORREGIDA

Director/es

Canudo Sanagustín, José Ignacio  
Bádenas Lago, Beatriz María  
Puértolas Pascual, Eduardo

<http://zaguan.unizar.es/collection/Tesis>



Universidad de Zaragoza  
Servicio de Publicaciones

ISSN 2254-7606

Tesis Doctoral

APORTACIONES DE LA FM TREMP  
(MAASTRICHTIENSE SUPERIOR) EN LA  
RIBAGORZA (PIRINEO ARAGONÉS, (HUESCA) AL  
CONOCIMIENTO DE LAS COMUNIDADES DE  
VERTEBRADOS FINICRETÁICAS DE LA ISLA  
IBERO-ARMORICANA.  
VERSIÓN CORREGIDA

Autor

Manuel Pérez Pueyo

Director/es

Canudo Sanagustín, José Ignacio  
Bádenas Lago, Beatriz María  
Puértolas Pascual, Eduardo

**UNIVERSIDAD DE ZARAGOZA**  
**Escuela de Doctorado**

Programa de Doctorado en Geología

2023





“Los últimos de Ribagorza”, paisaje cerca del actual Serraduy, hace 66.2 millones de años

(Autor: Eduardo Puértolas, ilustración realizada con apoyo de Inteligencia Artificial).

Tesis  
Doctoral

Aportaciones de la Fm Tresp (Maastrichtiense superior) en la Ribagorza (Pirineo aragonés, Huesca)  
al conocimiento de las comunidades de vertebrados finicretácicas de la isla Ibero-Armoricana.



Manuel Pérez Pueyo

2023

TESIS DOCTORAL

## Aportaciones de la Fm Tresp (Maastrichtiense superior) en la Ribagorza (Pirineo aragonés, Huesca) al conocimiento de las comunidades de vertebrados finicretácicas de la isla Ibero-Armoricana.

Contributions of the Tresp Fm (upper Maastrichtian) in Ribagorza (Aragonese Pyrenees, Huesca) to the knowledge of the latemost Cretaceous vertebrate communities of the Ibero-Armorican island.



Manuel Pérez Pueyo  
2023

Directores: Eduardo Puértolas Pascual, Beatriz Bádenas y José Ignacio Canudo  
Departamento de Ciencias de la Tierra  
Universidad de Zaragoza

**Tesis Doctoral**

**Aportaciones de la Fm Tresp (Maastrichtiense superior)  
en la Ribagorza (Pirineo aragonés, Huesca) al  
conocimiento de las comunidades de vertebrados  
finicretácicas de la isla Ibero-Armoricana.**

Contributions of the Tresp Fm (upper Maastrichtian) in Ribagorza (Aragonese Pyrenees, Huesca) to the knowledge of the finicretaceous vertebrate communities of the Ibero-Armorican island.

Manuel Pérez Pueyo

2023



Tesis doctoral dirigida por:

Eduardo Puértolas Pascual, Beatriz Bádenas Lago y

José Ignacio Canudo Sanagustín

Áreas de Paleontología y Estratigrafía, Departamento de Ciencias de la Tierra

Facultad de Ciencias, Universidad de Zaragoza



Departamento de  
Ciencias de la Tierra  
**Universidad Zaragoza**





La presente Tesis doctoral se realiza en la modalidad de **Compendio de publicaciones**. Este compendio cumple con la normativa de la Universidad de Zaragoza y se compone de tres artículos científicos publicados en revistas incluidas en el *Journal Citation Reports (Cretaceous Research, Journal of Vertebrate Paleontology y Historical Biology)*, indexados en el Science Citation Index Expanded (SCIE); y un artículo de calidad equiparable (*Geosciences*) incluido en el JCR, indexado en el Emerging Sources Citation Index (ESCI). La Tesis incluye además dos artículos publicados en sendas revistas con depósito legal y revisión por pares, pero no indexadas en el JCR (*Zubia y Ciências da Terra-Procedia*).

- 1) Puértolas-Pascual, E., Arenillas, I., Arz, J.A., Calvín, P., Ezquerro, L., García-Vicente, C., **Pérez-Pueyo, M.**, Sánchez-Moreno, E.M., Villalaín, J.J., Canudo, J.I. (2018). Chronostratigraphy and new vertebrate sites from the upper Maastrichtian of Huesca (Spain), and their relation with the K/Pg boundary. *Cretaceous Research*, 89, 36-59. <https://doi.org/10.1016/j.cretres.2018.02.016>
- 2) **Pérez-Pueyo, M.**, Cruzado-Caballero, P., Moreno-Azanza, M., Vila, B., Castanera, D., Gasca, J.M., Puértolas-Pascual, E., Bádenas, B., Canudo, J.I. (2021). The Tetrapod Fossil Record from the Uppermost Maastrichtian of the Ibero-Armorican Island: An Integrative Review Based on the Outcrops of the Western Tremp Syncline (Aragón, Huesca Province, NE Spain). *Geosciences*, 11 (4), 162. <https://doi.org/10.3390/geosciences11040162>
- 3) **Pérez-Pueyo, M.**, Puértolas-Pascual, E., Moreno-Azanza, M., Cruzado-Caballero, P., Gasca, J.M., Núñez-Lahuerta, C., Canudo, J.I. (2021). First record of a giant bird (Ornithuromorpha) from the uppermost Maastrichtian of the Southern Pyrenees, NE Spain. *Journal of Vertebrate Paleontology*, 41, e1900210. <https://doi.org/10.1080/02724634.2021.1900210>
- 4) Moreno-Azanza, M., **Pérez-Pueyo, M.**, Puértolas-Pascual, E., Núñez-Lahuerta, C., Mateus, O., Bauluz, B., Bádenas, B., Canudo, J.I. (2022). A new crocodylomorph related ootaxon from the late Maastrichtian of the Southern Pyrenees (Huesca, Spain). *Historical Biology*. Publicado online el 21 de julio de 2022 (pendiente de asignación de volumen).

- 5) **Pérez-Pueyo, M.**, Puértolas-Pascual, E., Canudo, J.I., Bádenas, B. (2019). Larra 4: Desenterrando a los últimos vertebrados del Maastrichtiense terminal del Pirineo aragonés. *Zubia*, 31, 175-180.
- 6) **Pérez-Pueyo, M.**, Moreno-Azanza, M., Núñez-Lahuerta, C., Puértolas-Pascual, E., Bádenas, B., Canudo, J.I. (2021). Eggshell association of the Late Maastrichtian (Late Cretaceous) at Blasi 2B fossil site: A scrambled of vertebrate diversity. *Ciências da Terra-Procedia*, 1, 58-61.  
<https://doi.org/10.21695/cterraproc.v1i0.410>

De acuerdo al Reglamento sobre Tesis Doctorales de la Universidad de Zaragoza (BOUZ 7-20), se incluye en esta memoria un apéndice (Apéndice I) en el que se recogen el factor de impacto de las revistas y las áreas temáticas de las publicaciones, así como la contribución del doctorando en aquellos trabajos en los que aparece como coautor. Las publicaciones que han sido incluidas en esta tesis aparecen en el Anexo I en su versión final publicada en inglés o castellano. El cuerpo principal de esta memoria de tesis está escrito también en inglés, excepto el resumen y las conclusiones, que también están escritos en castellano.

La presente Tesis doctoral se postula para la obtención de **Mención internacional**. Durante el periodo de realización de la Tesis, se realizaron dos estancias de investigación en un centro de investigación en el extranjero, en concreto en el **Departamento de Ciências da Terra de la Universidad de Nova de Lisboa** (Portugal). La primera estancia se llevó a cabo en 2019, con una duración de 61 días, mientras que la segunda se realizó en el año 2021, con una duración de 63 días. En total, la duración de ambas estancias fue de **4 meses y 4 días**. Las estancias se realizaron bajo la supervisión del Dr. Miguel Moreno Azanza, y tuvieron como objetivo fundamental el aprendizaje de técnicas de estudio de cáscaras de huevos fósiles, entre ellas el uso de microscopía electrónica, para el estudio de ejemplares de cáscaras recuperados en las sucesiones del Maastrichtiense del Pirineo aragonés estudiadas en la presente Tesis.

Además de estancias en el extranjero, se han realizado dos estancias breves en centros de investigación españoles, también con el objetivo de analizar aspectos específicos de las sucesiones maastrichtienses. La primera estancia, de 13 días, se realizó en 2020 en el **Departamento de Física de la Universidad de Burgos**, para realizar medidas de paleomagnetismo, supervisada por el Dr. Juan José Villalaín. La segunda estancia, de 5 días, se realizó en 2021 en el **Departament de Dinàmica de la Terra i l'Oceà de la Universitat de Barcelona**, para estudiar fósiles de carofitas, y fue supervisada por el Dr. Carles Martín Closas.

Durante el desarrollo de la tesis, el doctorando ha publicado y ha participado en otros artículos de investigación, algunos de ellos en revistas indexadas en el JCR. Estos artículos, debido a su temática **no forman parte del compendio de la tesis y no están incluidos en este volumen**. No obstante, han formado parte de la actividad investigadora del doctorando y de su formación, por lo que se enumeran a continuación:

- 1) **Pérez-Pueyo, M.**, Bádenas, B., Villas, E. (2018). Sedimentology and paleontology of the lower member of the Noguerras Fm. (Lower Devonian) at Santa Cruz de Noguerras (Teruel, NE Spain). *Revista de la Sociedad Geológica de España*, 31 (1), 89-104.
- 2) **Pérez-Pueyo, M.**, Moreno-Azanza, M., Barco, J.L., Canudo, J.I. (2019). New contributions to the phylogenetic position of the sauropod *Galvesaurus herreroi* from the late Kimmeridgian-early Tithonian (Jurassic) of Teruel (Spain). *Boletín Geológico y Minero*, 130 (3): 375-392.  
DOI: 10.21701/bolgeomin.130.3.001
- 3) Núñez-Lahuerta, C., Moreno-Azanza, M., **Pérez-Pueyo, M.** (2021). First approach for a taphonomic key for fossil eggs and eggshells accumulations using optic microscopy: The case of Blasi-2B (Upper Cretaceous, Spain). *Ciências da Terra Procedia*, 1, 42–45.

- 4) Canudo, J. I., Badiola, A., Belmonte, A., Cardiel, J., Cuenca-Bescós, G., Diaz Berenguer, E., Ferratges, F., Moreno Azanza, M., Pérez García, A., **Pérez Pueyo, M.**, Silva Casal, R. Zamora Iranzo, S. (2021). A Window onto the Eocene (Cenozoic): The Palaeontological record of the Sobrarbe-Pirineos UNESCO Global Geopark (Huesca, Aragon, Spain). *Geoconservation Research* 4 (2), 561-572.  
<https://doi.org/10.30486/gcr.2021.1912263.1043>
- 5) Puértolas-Pascual, E., Serrano-Martínez, A., **Pérez-Pueyo, M.**, Bádenas, B., & Canudo, J. I. (2022). New data on the neuroanatomy of basal eusuchian crocodylomorphs (Allodaposuchidae) from the Upper Cretaceous of Spain. *Cretaceous Research*, 135, 105170.  
<https://doi.org/10.1016/j.cretres.2022.105170>

*“There is a pleasure in the pathless woods,  
There is a rapture on the lonely shore,  
There is society, where none intrudes,  
By the deep Sea, and music in its roar:  
I love not Man the less, but Nature more,  
From these our interviews, in which I steal  
From all I may be, or have been before,  
To mingle with the Universe, and feel  
What I can ne’er express, yet cannot all conceal.”*

*Lord Byron*

*“Debo lo mejor de mí a la geología,  
pero todo lo que me ha enseñado  
tiende a alejarme de las cosas muertas.”*

*Pierre Teilhard de Chardin*



## **Agradecimientos**

*Creo que un GRACIAS (o varios) es la mejor palabra que se puede expresar al culminar una tesis doctoral. Tras un camino de varios años dedicado a ella en cuerpo y alma, me parece que agradecer es la mejor manera de recapitular y repasar todo lo vivido. Así puedo valorar todo lo bueno que esta etapa ha aportado a mi vida, que pienso que tiene mucho más peso que las cosas malas que han surgido (tampoco hay por qué negarlas). Pues venga, allá voy, aunque primero de todo, hay que cumplir con unas formalidades:*

*Esta tesis doctoral se ha realizado gracias a una ayuda predoctoral FPU del Ministerio de Educación, Cultura y Deporte, con nº de referencia FPU16/03064. Una vez finalizada la ayuda, se ha seguido contando con financiación durante 2022 y 2023 a través de un contrato N3 de Investigador iniciado de la Universidad de Zaragoza, obtenido a través del Procedimiento de urgencia PUI/2022-090.*

*Por otro lado, una gran parte de las labores de investigación realizadas han tenido el apoyo económico del grupo Aragosaurus-IUCA, a través de los proyectos de I+D+I CGL2017-85038-P y PID2021-122612OB-I00 financiados por el Ministerio de Ciencia e Innovación y, el Fondo Europeo de Desarrollo Regional; y también a través del Gobierno de Aragón mediante el grupo de referencia E18\_20R Aragosaurus: Recursos geológicos y Paleoambientes. También, se ha contado con una ayuda de investigación para estudiar el yacimiento de Veracruz 1, concedida por el Instituto de Estudios Altoaragoneses (Diputación de Huesca), obtenida en la XXXIV Convocatoria de ayudas a la investigación 2018' (Resolución N.º 169/2018). Finalmente se ha contado con una ayuda a la movilidad del Ministerio de Ciencia, Innovación y Universidades con referencia EST18/00257 para la realización de una estancia de investigación en la Universidad Nova de Lisboa en 2018. El mapa de la figura 1.1. ha sido cedido por Miguel Moreno-Azanza, y forma parte del proyecto PTDC/CTA-PAL/2217/2021 financiado por FCT –Fundação para a Ciência e a Tecnologia.*

*Dicho esto, me gustaría dar las gracias en primer lugar a mis tres directores de tesis: Eduardo Puértolas, Beatriz Bádenas y José Ignacio Canudo. Los tres se lanzaron conmigo a la piscina de la Formación Tremp, y durante estos 5 años y medio me han acompañado, aconsejado y apoyado en todo momento. También han tenido una enorme paciencia conmigo, especialmente a la hora de esperar envíos de borradores que*

*siempre me han costado más de lo que mi yo optimista creía. De ellos 3 he aprendido un montón durante estos años, y me han demostrado continuamente que no podría haber tenido mejores directores a nivel científico, pero sobre todo a nivel humano. Ha sido un viaje muy intenso, y me alegro de haberlo compartido con vosotros.*

*A Edu le tengo que dar las gracias por ser prácticamente mi hermano mayor en la ciencia, ayudándome con su experiencia previa y reciente de este mundillo de la investigación y de cómo hacer una tesis. También cobijándome en su casa durante las estancias en Lourinhã, compartiendo momentos fuera del trabajo, que también son necesarios para desconectar. Ah, y gracias también por enseñarme The Wire.*

*A Bea le tengo que agradecer sus numerosos y buenos consejos, su paciencia infinita y las charradas después del campo, con un par de cervezas (porque la primera no cuenta). Ella me ha enseñado la importancia de esforzarse y de poner cariño en lo que haces, que para hacer una buena investigación es necesario, pero también para muchas cosas en la vida. También por ser siempre optimista y encontrarle siempre el lado bueno a todo.*

*A Iñaki le tengo que agradecer por transmitirme su entusiasmo y también por su sentido común y buena mano izquierda en muchos temas. También por enseñarme con su ejemplo que la ciencia, si no se abre a los demás y se hace de todos, pierde un poco su sentido. Y que a veces para hablar de dinosaurios, valen más historietas y anécdotas cotidianas que 100.000 datos científicos. Habrá que seguir haciendo nuevas muescas en el revólver.*

*Agradecer a Luis Buatois (University of Saskatchewan), a Àngel Galobart (Instituto Catalán de Paleontología), a Xabier Pereda-Suberbiola (Universidad del País Vasco), Gabriela Mangano (University of Saskatchewan) y Luis Miguel Sender (Fundación Conjunto Paleontológico de Teruel-Dinópolis) por aceptar ser miembros de mi tribunal de tesis. Por otro lado, también tengo que dar las gracias a los dos revisores internacionales de esta tesis: Cristina Sequero y Maximiliano Paz. Les doy las gracias especialmente por su flexibilidad.*

*El lugar donde se ha gestado una tesis también es importante, y creo que en pocos lugares habría podido estar más a gusto que en la Facultad de Geológicas de Zaragoza. Gracias a las personas que han estado estos años llevando el Programa de Doctorado en Geología, y a todas las que componen el Departamento de Ciencias de la Tierra. Se va a trabajar siempre más a gusto sabiendo la cantidad de gente maja que está en La*

*Casa. Por supuesto, dentro del departamento tengo que mencionar a las áreas de Paleontología y Estratigrafía, mis áreas, que me han acogido tan bien estos años. Y por supuesto, no me olvido de la gente del Servicio de Apoyo a la Investigación (SAI). Esta tesis no se hubiera podido hacer sin el trabajo del servicio de preparación de rocas ni sin el de microscopía electrónica de materiales (SEM), tanto por su ayuda con las muestras como por las buenas charradas que nos hemos pegado.*

*Por circunstancias de la vida, la tesis la he tenido que terminar lejos de Zaragoza, nada más y nada menos que en Loarre. He tenido la suerte de formar parte del equipo del Laboratorio Paleontológico de Loarre, un proyecto muy bonito que pretende dar otro enfoque a lo que es el proceso de estudio y preparación de los fósiles. Les tengo que agradecer a todos su comprensión y paciencia por estos meses que he estado trabajando a dos (incluso a tres) bandas, y siento que no me haya podido implicar más. Gracias Moreno, Ester, Carmen (STM!!!) y especialmente gracias al equipo TOC, Laura y Lope, quienes han tenido que aguantarme (y ayudarme) más directamente durante esta etapa de locura finitésica.*

*Durante estos años he tenido la suerte de poder viajar mucho tanto dentro como fuera de España, habiendo pasado por Burgos, Barcelona, Cuenca, Huelva, Italia, Francia, Bélgica o Polonia. Pero sin duda alguna, la mejor experiencia que he tenido han sido mis dos estancias en Lourinhã. Las dos veces acabé en Portugal de rebote, tras fallar el plan A y fue gracias a Moreno y Edu, que acudieron al rescate para que no me quedara colgado. Estos meses en Lourinhã fueron muy productivos, y salir de mi burbuja de Zaragoza y conocer cómo se trabaja en otros equipos de paleontología me abrió bastante la mente. Me permitió valorar lo que tenía en casa, con sus virtudes y sus defectos. Allí conocí a gente muy maja que hizo que mi estancia allí se hiciera muy cómoda, a Pippo, Laura, André, Darío, María, Alex, Simone y muchos más. Por ellos, creo que siempre Lourinhã va a tener un huequito en mi corazón.*

*Y obviamente tengo que agradecer especialmente a Miguel Moreno, que aceptara dirigirme ambas estancias. Su vocación por la paleontología es contagiosa, y ha sido un gusto poder trabajar con él. Con Moreno he aprendido un poquito sobre los huevos fósiles de dinosaurios y otros amniotas y, de que, vaya, parece ser que la mineralogía mola bastante y que tiene papel muy importante en el estudio de los huevos. Con Miguel he podido compartir muchas horas en el SEM y en el coche camino a Lisboa, que han dado mucho de sí para hablar de muchos temas, y la calidez humana que me ha mostrado siempre hacen que le admire muchísimo. La espinita que se me queda clavada*

*es que mucho del trabajo que hemos hecho en esas estancias no ha podido verse reflejado en esta tesis, y es por culpa mía. Espero que podamos sacarlos pronto a la luz.*

*Por otro lado, tengo que dar las gracias a Gaby, a Luis y a Maxi por invitarme a participar en una aventura en el Paleozoico de Asturias, durante el penúltimo año de mi tesis sobre Mesozoico. He de reconocer que fue un rodeo inesperado, pero muy enriquecedor. Allá aprendí mucho sobre trazas fósiles, y aún más importante, conocí en persona a gente muy buena onda y muy apasionada. Se ha quedado en el tintero la visita a Saskatchewan, espero poder ir algún día.*

*Durante estos años he tenido a mucha gente buena acompañándome en este camino, y creo que sería injusto no mencionarlos aquí. Tanto en el área de Paleontología, otras áreas del departamento, y como en el grupo Aragosaurus (mi familia paleontológica), he tenido la suerte de formar parte de un grupo de compañeros y camaradas de fatigas increíbles con los que he compartido muchos buenos momentos, ratos de café y cerves en el Sportivo o la Badina. Esta tesis no hubiera sido la que es si no fuera por vosotros, así que gracias, Vicente, Álvaro, Irene, Edu, Ari Ferratges, Jara, Ester, Julia (Jules), Carmen, Toni, Alberto, Flavia, Andrea, Dani, Pere, Cristina, Luismi, Diego Castanera, Peny, Gasca, Diego Torromé, Raquel, Pilar, Julia foratas, Lucía, Francho, Alba, Pablo, Chema, Elisa, Sevil, Ángel, Úrbez, y alguno/a que seguro que me olvido (lo siento, sois demasiados).*

*Una mención especial para las nuevas generaciones de geólogos/as y paleontólogos/as que vienen pisando fuerte. Haber compartido raticos con vosotros, ya sea preparando fósiles o trabajando en el campo ha hecho que me contagié de vuestras ganas e ilusión, recuperando sensaciones que hacía tiempo que creía perdidas, de cuando yo estaba también empezando. Así que gracias, Jerome, Chantal, Cris, Asia, Pilar, Juan, Inma y Víctor; a seguir dando guerra.*

*Por otro lado, como no mencionar a todos mis colegas de promoción, a mi familia geológica original, con los que compartí unos años geniales durante la carrera, con mucha geología, muchas cerves y geofiestas, en los que sentamos las bases de una amistad que dura hasta hoy, y que espero que dure muchos años más. Esta tesis también tiene un poco de vosotros Francho, Álvaro, Alba, Lucía, Edu, Pablo, Diegu, Pilar, Nelson, Gonzalo y Chorche.*

*He tenido la suerte de poder realizar la tesis en una zona privilegiada de Aragón, en un área del Pirineo que aún parece que se mantiene a salvo de la masificación y del ruido.*

*La Ribagorza/Ribargorça es una región privilegiada por sus paisajes y naturaleza, por la historia que guarda y por seguir siendo refugio de las tres lenguas de nuestro Aragón. Pero sobre todo es rica por sus gentes, que también me han acogido siendo un forano que venía a estudiar sus tesoros paleontológicos. Un agradecimiento a todos esos vecinas y vecinos de Campo, Valle de Lierp, Rin, La Puebla de Roda, Roda de Isábena, Serraduy, Beranuy, Bascas de Obarra, Cagijar, Isclés y Arén/Areny, con los que alguna vez se ha cruzado mi camino y me han ayudado de una u otra forma.*

*Realizar campo en la Ribagorza es complicado, por el desnivel al que te enfrentas y que los lugares donde aparecen dinosaurios están muy aislados. Por suerte, siempre he podido contar con gente que me acompañara al campo. En especial me gustaría agradecer a Juan Carlos García Pimienta “Pimi”, paleontólogo de la Dirección General de Patrimonio de la DGA, por haberme acompañado al campo muchas veces, sobre todo a los sitios más inaccesibles y haber descubierto varios de los yacimientos nuevos de la Fm Tremp. Esos buenos ratos en el campo buscando fósiles también han venido acompañados por buenas recomendaciones de sitios donde comprar torta de manzana y charradas en el coche. Tendremos que volver al campo, que aún quedan afloramientos por prospectar.*

*Al igual que estar a gusto en tu trabajo es importante, también es importante encontrar momentos y personas para disfrutar fuera de él. Durante estos años he tenido la suerte de estar acompañado por mucha gente en muchos sitios que me han ayudado mucho a desconectar de la tesis, y salir de la burbuja que puede ser en ocasiones la investigación. Algunos amigos de toda la vida y otros que han llegado más tarde, todos ellos buena gente. Aquí están incluidos la gente de Alcubierre (Ángel, Eloy, Miguel, Miguel Ángel y toda la Otopaña), los amigos del cole (Marta, Miguel, Isa, Guille, Cris, Alexis), los del Movi (esos nifus!), los montañeros de Snow Mountain Ranch (Laura, Pablo, Irene, Miguel...) o los asiduos del Teatro (Sergio, Galán, Juan...) o a Chabi, que nos conocimos e hicimos amigos por la paleo, y nos estrechó los lazos por Aragón. No me quiero dejar tampoco a mis compañeros del equipo de biathlon del Stadium Casablanca (Héctor, Pablo, Miguel, Nora, Elena, Nacho, José Antonio, y nuestro jefe, Ángel), que han sido otra familia para mí durante estos años. Hemos competido y nos lo hemos pasado bastante bien durante estos años haciendo un deporte que nos mola. En 2019 pude viajar a Palestina una experiencia que me marcó mucho, y que no hubiera sido igual si no hubiera compartido ese viaje con un grupo de zagales muy majos (Los Cuquitos), que siendo cada uno de nuestra madre y de nuestro padre, hicimos una piña muy fuerte. Ojalá*

*podamos volver juntos en un futuro a una Palestina libre y en paz. Entre toda esta gente, hay tres personas que ocupan un lugar especial en mi corazón, tres personas con las que siempre voy a poder contar. Sé que puede pasar mucho tiempo sin vernos, y sin embargo cuando nos reunimos parece que no haya pasado el tiempo. Fran, Guille y Carlos, gracias a los 3 por poder llamaros mis amigos.*

*También le quiero dar gracias a mi familia, tanto los Pérez como los Pueyo, y sobre todo los Pérez Pueyo por su continuo apoyo y ánimos, porque sé que siempre van a estar ahí, pase lo que pase. Yo no hubiera llegado hasta aquí si no hubiera sido por ellos y por todo lo que me han dado, y me siento muy afortunado por ello. De mis padres Chus y Manu y de mis hermanas Elena y Cris no he hecho más que recibir, tanto cariño, buenos consejos y también empujones cuando necesitaba volver a arrancar en los momentos de incertidumbre. Sé que allá donde estéis es un sitio al que voy a poder llamar hogar y que voy a encontrar la puerta abierta.*

*Mención especial a mí tío Chivis, que ha sido uno de los culpables de que haya terminado siendo geólogo y haciendo una tesis. Creo que el martillo de geólogo es uno de los regalos de mi comunión que más me ha cundido, así que mira la que liaste, que hemos terminado haciendo una magneto y todo en Isclés.*

*Y por supuesto, tengo que dar las gracias a mis abuelos por su cariño y su ejemplo. Pertenecen a una generación que sufrió y que se esforzó mucho y sé que cualquier logro que consiga uno de vuestros nietos es una alegría inmensa. Lamentablemente tres de ellos no van a poder estar el día de la defensa de esta tesis, y sé que les hubiera gustado mucho estar, pero los voy a seguir sintiendo cerca siempre. Yaya Conchita, yaya Maritere, yayo Emilio y yayo José María, un beso muy fuerte de vuestro nieto.*

*Y, por último, tengo que dar las gracias a una persona muy especial. Una persona que apareció en mi vida sin esperarlo (afortunadas conexiones oscenses), y con la que he tenido la suerte de compartir estos dos últimos años. Muchas gracias, Julia, porque esta tesis también es un poco tuya. Realmente te ha tocado bailar con la más fea, tragándote todo el final de la tesis, con un Manu ultraestresado y con poco tiempo. Sin embargo, has sido la mejor compañera y consejera que podría haber tenido. Mi anclaje a la realidad, mi oasis donde recuperar la cordura, con quien sabía que todo iba a estar bien. Tú has conseguido sacarme siempre el lado positivo y hacer que mirará adelante con perspectiva, haciendo que los nubarrones se despejarán. Aún no sé qué vendrá después*

*de la tesis, pero eres una de mis certezas, y eso es una cosa que me tranquiliza bastante. Aún tenemos mucho de lo que hablar y mucho que vivir juntos. Te quiero.*

*Y ya está, creo que no me he dejado a nadie, y si lo he hecho, lo siento muchísimo y espero que me perdonéis. Tampoco iba a hacer unos agradecimientos más largos que la propia tesis, y aun así vaya tocho, jeje.*

*Ahora ya al final del camino, puedo decir que he cumplido el sueño de un niño que jugaba con sus muñecos de dinosaurios hace mucho tiempo, y que se soñaba con ser paleontólogo. Obviamente, el desenlace ha sido muy distinto a lo que ese niño pensaba que sería, pero sin duda ha sido mejor de lo que hubiera podido imaginar.*

*Solo me quedan unas palabras para esa investigadora o investigador del futuro al que pueda haber llegado esta tesis a sus manos. Espero que te pueda resultar útil, entretenida o que te pueda dar ideas. El camino de la investigación es a veces muy áspero e ingrato, pero también trae cosas muy bonitas. Disfruta del proceso, esfuérzate en lo que te gusta, y quédate con las buenas experiencias.*

*Mucho ánimo, merece la pena.*



*A mis abuelos*

# Table of Contents

Table of Contents.....	16
Abstract/Resumen.....	19
<b>CHAPTER 1. INTRODUCTION .....</b>	<b>23</b>
1.1. The K/Pg boundary extinction event.....	25
1.2. Upper Maastrichtian continental vertebrate record .....	29
1.2.1. <i>Hell Creek Fm (North America)</i> .....	31
1.2.2. <i>Marilía Fm (Brazil and Paraguay)</i> .....	34
1.2.3. <i>Densuş-Ciula, Sînpetru and Sebeş Fm (Romania)</i> .....	35
1.2.4. <i>Lameta Fm and inter-trappean beds (India)</i> .....	36
1.2.5. <i>Shanyang Fm (China)</i> .....	36
1.3. The upper Maastrichtian Ibero-Armorican record .....	37
<b>CHAPTER 2. OBJECTIVES.....</b>	<b>51</b>
<b>CHAPTER 3. MATERIAL AND METHODS .....</b>	<b>55</b>
3.1. Field work.....	57
3.1.1. <i>Stratigraphic-sedimentological fieldwork</i> .....	57
3.1.2. <i>Magnetostratigraphic fieldwork</i> .....	60
3.1.3. <i>Paleontological exploration</i> .....	61
3.1.4. <i>Paleontological excavation</i> .....	64
3.2. Laboratory work .....	68
3.2.1. <i>Macrofossil preparation</i> .....	68
3.2.2. <i>Microfossil preparation</i> .....	70
3.2.3. <i>Optical microscopy</i> .....	71
3.2.4. <i>Scanning electron microscope analysis</i> .....	73
3.2.5. <i>Laboratory treatment of magnetostratigraphic samples</i> .....	75
3.2.6. <i>Micro-CT scan</i> .....	76
3.3. Data treatment and interpretation .....	77
3.3.1. <i>Stratigraphic-sedimentological data</i> .....	77
3.3.2. <i>Magnetostratigraphic data</i> .....	77
3.3.3. <i>Paleontological data</i> .....	78
3.3.4. <i>Official reports</i> .....	80
3.4. Paleontological material .....	80

<b>CHAPTER 4. GEOGRAPHIC AND GEOLOGICAL SETTING .....</b>	<b>85</b>
<b>CHAPTER 5. STRATIGRAPHY AND SEDIMENTOLOGY .....</b>	<b>95</b>
5.1. Stratigraphy .....	97
5.1.1. Lithostratigraphy .....	97
5.1.2. Biostratigraphy .....	104
5.1.3. Magnetostratigraphy .....	109
5.1.4. Chronostratigraphic framework and K/Pg interval .....	122
5.2. Facies analysis and sedimentation model_.....	126
5.2.1. Topmost Arén Sandstone Fm .....	126
5.2.2. Tremp Fm .....	127
5.2.1. Sedimentary model .....	150
<b>CHAPTER 6. PALEONTOLOGY .....</b>	<b>155</b>
6.1. The vertebrate record of the Western Tremp Syncline.....	157
6.1.1. Dinosauria .....	160
6.1.2. Pterosauria .....	164
6.1.3. Crocodylomorpha .....	164
6.1.4. Testudines.....	168
6.1.5. Amphibia and Squamata.....	168
6.2. Systematic paleontology .....	169
6.2.1. The Veracruz 1 assemblage.....	169
6.2.2. Dolor ornithuromorph giant bird .....	196
6.2.3. Other vertebrates .....	210
6.3. Taphonomic modes of the Tremp Fm.....	214
6.4. Final remarks regarding the K/Pg boundary .....	223
<b>CHAPTER 7. OOLOGICAL RECORD OF THE TREMP FM IN THE WESTERN TREMP SYNCLINE .....</b>	<b>227</b>
<b>CONCLUSIONS/CONCLUSIONES.....</b>	<b>249</b>
Bibliography .....	259
Annexes.....	301
Annex I .....	303
Annex II .....	391
Annex III .....	409
Annex IV.....	423
Appendix I .....	439



## **ABSTRACT**

The K/Pg boundary (Maastrichtian-Danian) is one of the most relevant events in the history of planet Earth, since it supposed the extinction of several groups of animals which have been dominating the Mesozoic ecosystems, due to a meteoritic impact. Groups as the non-avian dinosaurs, the pterosaurs or the ammonoids are among those who disappeared. How this extinction affected to Late Cretaceous ecosystems of North America is well-known, but in other areas of the world still represents an unknown.

The Pyrenees is a mountainous range situated between Spain and France. In its southern site, the so-called Southern Pyrenees there are rocks of the Late Cretaceous in which are registered some of the last dinosaurs together with other vertebrates which lived in Iberia before the K/Pg extinction.

In this PhD Thesis, a combined stratigraphic and paleontological analysis has been carried out in the Western Tremp Syncline of the Ribagorza county (Aragón, Spain), situated in the Southern Pyrenees. The outcrops of the Tremp Fm, an upper Maastrichtian (66-67Ma) geological unit with vertebrate fossils, including dinosaurs have been studied. The main objective has been to study the paleodiversity of the end-Cretaceous vertebrate assemblages that inhabited this area and the environment where they lived

For that, a thorough stratigraphic work has been performed, to characterize the transitional and continental deposits of the Tremp Fm, improving their chronostratigraphic framework by the use of biostratigraphy and magnetostratigraphy. These studies point that these outcrops are dated within chron C30n and C29r, thus representing the last 300 ky before the K/Pg boundary. Besides, a sedimentological analysis of the Tremp Fm has been carried out, in order to reconstruct the depositional setting in which the vertebrates lived, and the fossils were preserved.

Concerning to the paleontological side, an intense field work has allowed to the discovery of 39 new vertebrates sites, which total 97 with the previous ones known. This vast record has permitted to reconstruct the vertebrate assemblage, conformed mainly by dinosaurs, crocodylomorphs, pterosaurs, turtles, lizards and amphibians, and even discovering new animals that were unknown to the date, like a giant ornithuromorph bird. The eggshells assemblages have been also studied, with the aim to find an alternative way to evaluate the vertebrate diversity.



## **RESUMEN**

El límite K/Pg (Maastrichtiense-Daniense) es uno de los acontecimientos más relevantes de la historia del planeta Tierra, ya que supuso la extinción de varios grupos de animales que habían estado dominando los ecosistemas mesozoicos, como consecuencia de un impacto meteorítico. Grupos como los dinosaurios no avianos, los pterosaurios o los ammonoideos se encuentran entre los que desaparecieron. Es bien conocido cómo afectó esta extinción a los ecosistemas del Cretácico Superior de Norteamérica, pero en otras zonas del mundo aún representa una incógnita.

Los Pirineos son una cadena montañosa situada entre España y Francia. En su parte sur, los llamados Pirineos Meridionales existen rocas del Cretácico Superior en las que se registran algunos de los últimos dinosaurios y otros vertebrados que habitaron Iberia antes de la extinción del K/Pg.

En esta Tesis Doctoral se ha realizado un análisis combinado estratigráfico y paleontológico en el Sinclinal de Tremp Occidental, en la comarca de la Ribagorza (Aragón, España), situada en los Pirineos Meridionales. Para ello, se han estudiado los afloramientos de la Fm. Tremp, una unidad geológica del Maastrichtiense superior (66-67Ma) con fósiles de vertebrados, incluidos dinosaurios. El objetivo principal ha sido estudiar la paleodiversidad de las asociaciones de vertebrados de finales del Cretácico que habitaron esta zona y el ambiente donde vivían.

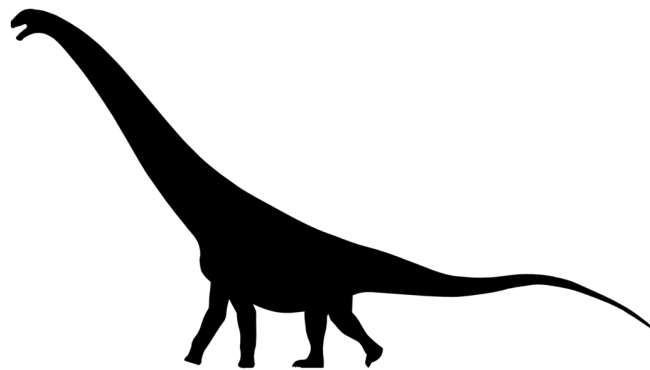
Para ello, se ha realizado un exhaustivo trabajo estratigráfico, para caracterizar los depósitos transicionales y continentales de la Fm Tremp, mejorando su marco cronoestratigráfico mediante el uso de bioestratigrafía y magnetoestratigrafía. Estos estudios apuntan a que estos afloramientos están datados dentro de los crones C30n y C29r, representando así los últimos 300.000 años antes del límite K/Pg. Además, se ha realizado un análisis sedimentológico de la Fm Tremp, con el fin de reconstruir el ambiente deposicional en el que vivieron los vertebrados y se conservaron los fósiles.

En cuanto al aspecto paleontológico, un intenso trabajo de campo ha permitido el descubrimiento de 39 nuevos yacimientos de vertebrados, que suman 97 con los anteriores conocidos. Este vasto registro ha permitido reconstruir el ensamblaje de vertebrados, conformado principalmente por dinosaurios, crocodilomorfos, pterosaurios, tortugas, lagartos y anfibios, e incluso descubrir nuevos animales desconocidos hasta la fecha, como un ave ornituomorfa gigante. También se han estudiado los conjuntos de cáscaras de huevo, con el fin de encontrar una forma alternativa de evaluar la diversidad de vertebrados.



# **Chapter 1.**

# **Introduction**





## **Chapter 1: Introduction**

### **1.1. *The K-Pg extinction event***

The Cretaceous-Paleogene boundary (K/Pg) ~66 Ma marks one of the most severe extinction events in the history of the life on Earth. This event caused the demise of non-avian dinosaurs and other groups of vertebrates, favoring the beginning of mammalian dominance. Without any doubt, the K/Pg extinction is one of the events of the history of our planet that most attention has brought to the scientific community in the last forty years. The discovery of an anomaly of iridium associated to the K/Pg boundary in Gubbio (Italy) by Alvarez et al. (1980), led to the proposal of a meteoritic impact as the cause of the extinction. Since then, a scientific debate between defenders and opponents to this theory has taken place (Keller et al., 1996; Arenillas et al., 2000; Archibald et al., 2010; Courtillot and Fluteau, 2010; Keller et al., 2010; Schulte et al., 2010a, b; Hull et al., 2020).

At the end of the Cretaceous, a set of destabilizing events occurring on Earth have been proposed, including a global marine regression (Miller et al., 2005), climate changes (Li and Keller, 1998; Barnet et al., 2018; Gilabert et al., 2022) and an intense volcanic activity in the Deccan Volcanic Province (India) (Fig. 1.1) with the emission of a huge amount of gases and volcanic material into the atmosphere (Courtillot et al., 1988; Courtillot and Renne, 2003; Tobin et al., 2012; Schoene et al., 2019; Sprain et al., 2019). All these events were culminated by the aforementioned meteoritic impact, which happened in Chicxulub (Mexico) (Fig. 1.1) (Hildebrand et al., 1991; Morgan et al., 1997), calibrated in  $66.052 \pm 0.008/0.043$  Ma (Sprain et al., 2018). Although all these causes seem to have contributed to the extinction to a certain degree, the meteorite impact hypothesis has the most solid arguments to be considered as the major disturbing mechanism and the main cause of the extinction (Schulte et al., 2010a; Witts et al., 2016; Chiarenza et al., 2020; Dzombak et al., 2020). The impact caused immediate catastrophic effects; including a blast wave; seismicity which triggered seiches and tsunamis (Scasso et al., 2005; Renne et al., 2018; DePalma et al., 2019; Range et al., 2022); an increase of thermal radiation by the re-entry of the ejecta back to the atmosphere (Goldin and Melosh, 2009); and abundant wildfires (Morgan et al., 2013; Santa Catharina et al., 2022) which affected primarily those areas close to the impact (mainly in North America and South America). Later, the impact caused more lingering effects which affected most of

the world; such as persistent clouds of dust coming from the Earth crust vaporized by the impact; ocean acidification and extinction of calcareous primary producers; and a general global cooling (Kring, 2007; Schulte et al., 2010a; Kaiho et al., 2016; Toon et al., 2016; Henehan et al., 2019; Lyons et al., 2020). The concatenation of these catastrophic effects generated the so-called 'impact winter' (Robertson et al., 2013), that was what finally led to the mass extinction. Although it has been argued that some groups of organisms were already in decline at a regional level before the impact (e.g. ammonites: Stinnesbeck et al., 2012; inoceramids: Dameron et al., 2017; or dinosaurs: Sakamoto et al., 2016), it is clear that the turning point was the Chicxulub impact.

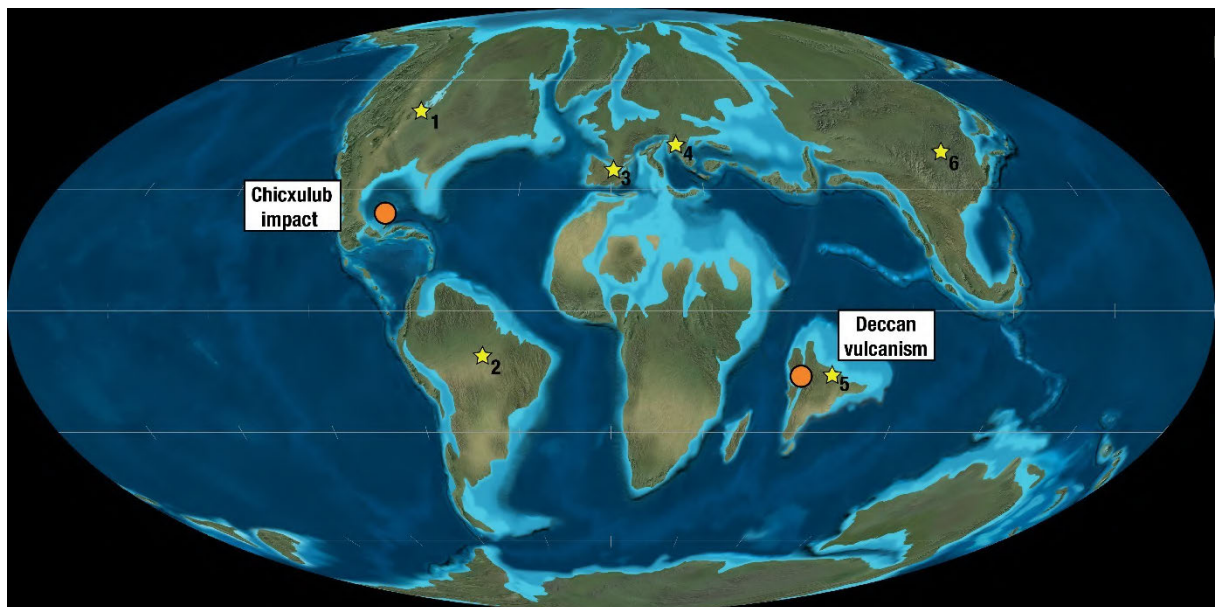


Figure 1.1. Global paleogeographic reconstruction of planet Earth at the end of the Maastrichtian (66 Ma), modified after Deep Time Maps™ (<https://deeptimemaps.com/>) to include the location of extinction-causing events (orange) and the main late Maastrichtian continental records with vertebrates (yellow stars): 1) Hell Creek Fm (USA), 2) Marília Fm (Brasil), 3) Garum facies (Spain/France)) 4) Densuș-Ciula, Sînpetru and Sebeș Fm (Romania) 5) Lameta Fm (India) and 6) Shanyang Fm (China).

Whatever the cause, the K-Pg extinction eradicated nearly 65-75% of the living species on Earth (Raup and Sepkoski, 1982; Jablonski, 1994) (Fig. 1.2) disappearing a great amount of groups that thrived during the Mesozoic. In the oceans, several groups disappeared (D'Hondt, 2005), including some groups of planktic foraminifera, rudist and inoceramid bivalves (Raup and Jablonski, 1993), ammonites (Landman et al., 2015) and

marine reptiles, including plesiosaurs and mosasaurs (Bardet, 1994; Jouve et al., 2008). Other marine groups were affected partially by the event, showing significant changes between their Maastrichtian and Danian assemblages; for example, benthic foraminifera (Alegret and Thomas, 2007), scleractinian corals (Kiessling and Baron-Szabo, 2004), elasmobranch fishes (Kriwet and Benton, 2004) and marine crocodylomorphs (Mannion et al., 2015; Puértolas-Pascual et al., 2016).

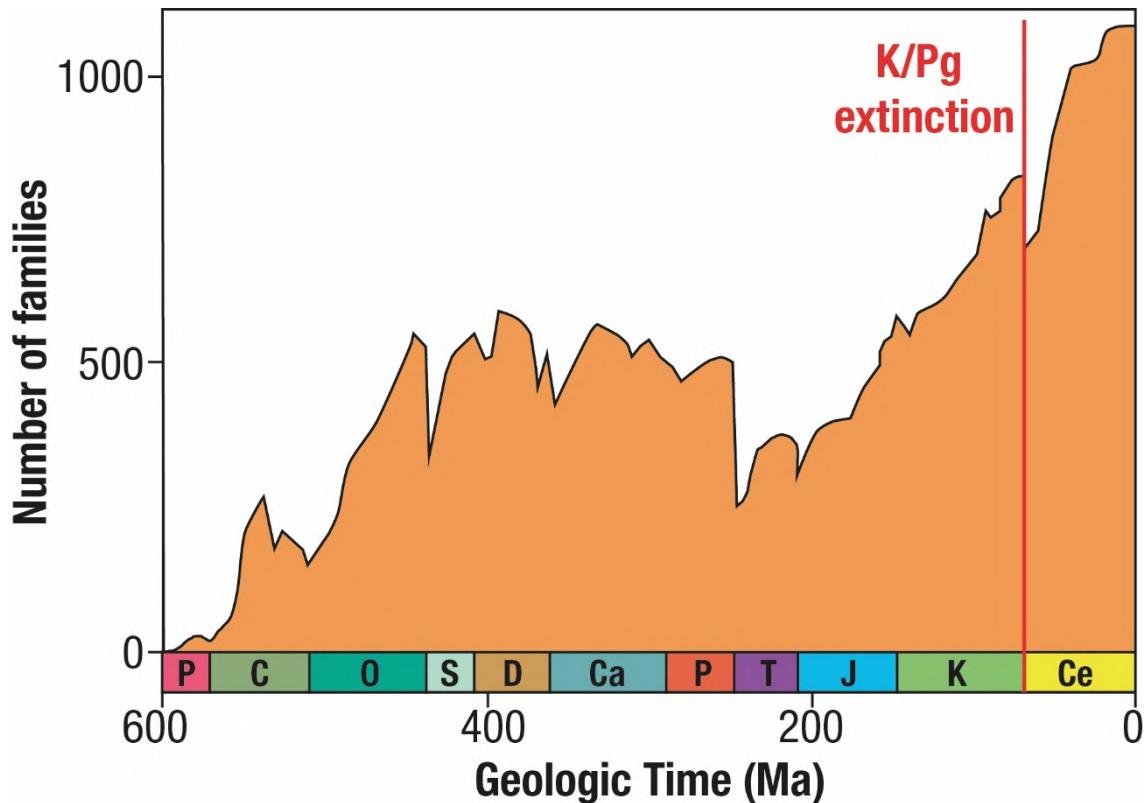


Figure 1.2. Evolution trend of diversity of living being species throughout the Phanerozoic, based on the variation of the number of families (After Sepkoski, 1993). Nearly 65-75% of the living species disappeared during the K-Pg extinction event.

The most notable effect of the K/Pg extinction on the continents was the disappearance of non-avian dinosaurs (Fastovsky and Sheehan, 2005; Lyson et al., 2011a; Brusatte et al., 2015); though other groups like the pterosaurs (Longrich et al., 2018) and enantiornithe or basal ornithuromorph birds (Longrich et al., 2011) became also extinct. Several groups of vertebrates remained during the Paleocene, although with diminished diversity. In this manner, the diversity of continental crocodylomorphs diversity was reduced (Bronzati et al., 2015; Mannion et al., 2015; Puértolas-Pascual et

al., 2016; De Celis et al., 2020), disappearing most of non-eusuchian clades and leading to the diversification of groups like Crocodylia during the Paleocene. Other reptiles also suffered the asteroid impact effects; for example, at least 83% of squamates reptiles became extinct in North America (Longrich et al., 2012). Nevertheless, other groups were less affected by the impact. This was the case of the turtles, though several lineages declined later in the Paleocene (Hutchison and Archibald, 1986; Lyson et al., 2011b; Vlachos et al., 2018); and the mammals, which slightly declined just after the impact, and then they experienced a rapid diversification (Springer et al., 2003; Pires et al., 2018; Lyson et al., 2019). However, it has been also postulated that the diversification of mammals occurred later, during the Eocene (Bininda-Emonds et al., 2007).

Continental plant communities were also heavily affected by the K/Pg extinction event, with the disappearance of nearly the 57% of the species in North America (Wilf and Johnson, 2004), although none of the major groups of plants disappeared (Nichols and Johnson, 2008). During the beginning of the Paleocene, the recovery of the plant communities was slow and done mainly by survivors of the extinction, involving first fern-dominated assemblages, which generated a 'fern-spore spike' that can be recognized globally (Vajda et al., 2001; Jolley et al., 2013; Vajda and Bercovici, 2014), and second, the recovery of gymnosperms and angiosperms, leading to new plant assemblages. The K/Pg event was also followed by the diversification of some angiosperm clades, such as the legumes (Koenen et al., 2021). A consequence related to this floral assemblages variation was the change of the plant-insect interactions between the Maastrichtian and the Paleocene, which indicates that insects were also affected to some extent, with the most specialized insects being the most affected (Labandeira et al., 2002; 2016; Wiest et al., 2018).

As it has been ascertained, in general terms the K/Pg extinction event is well understood, especially in the marine environments. However, concerning the continental environments, there is a geographic and geologic bias, especially with regard to the extinction of vertebrates. There are certain areas of the planet where the K/Pg event has been pretty well characterized, due to the presence of wide outcrops of latest Maastrichtian-earliest Paleocene continental deposits with vertebrate fossils, such as the case of North America. Nearly 80% of the continental sections studied until 2014, that included the K/Pg transition, were located in North America (Vajda and Bercovici, 2014) (Fig. 1.3). Although during the last decades there has been a huge effort to increase the available data in other areas of the world (e.g. Canudo et al., 2016; Csiki-Sava et al., 2016;

Verma et al., 2016; Vallati et al., 2020; Roberts et al., 2022), there is still a significant gap of knowledge to understand how the extinction happened and how their main driven mechanisms affected the ecosystems in areas that were further front the Chixchulub impact. For this reason, every new study of K/Pg continental sections is important to fill that gap.

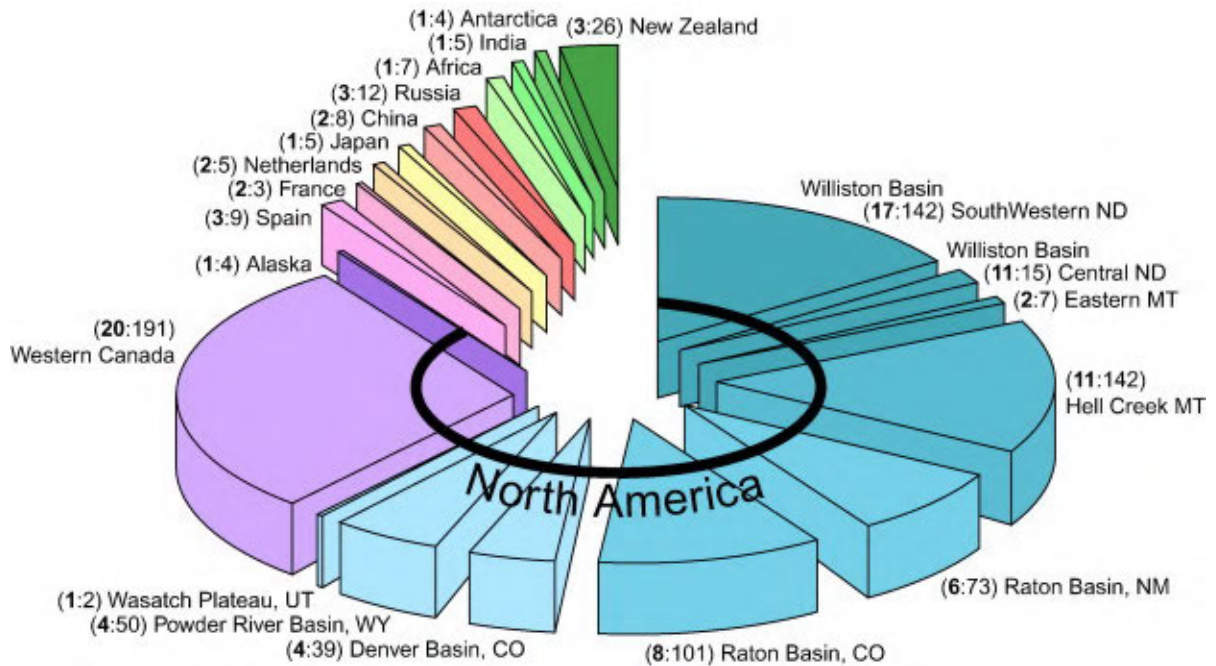


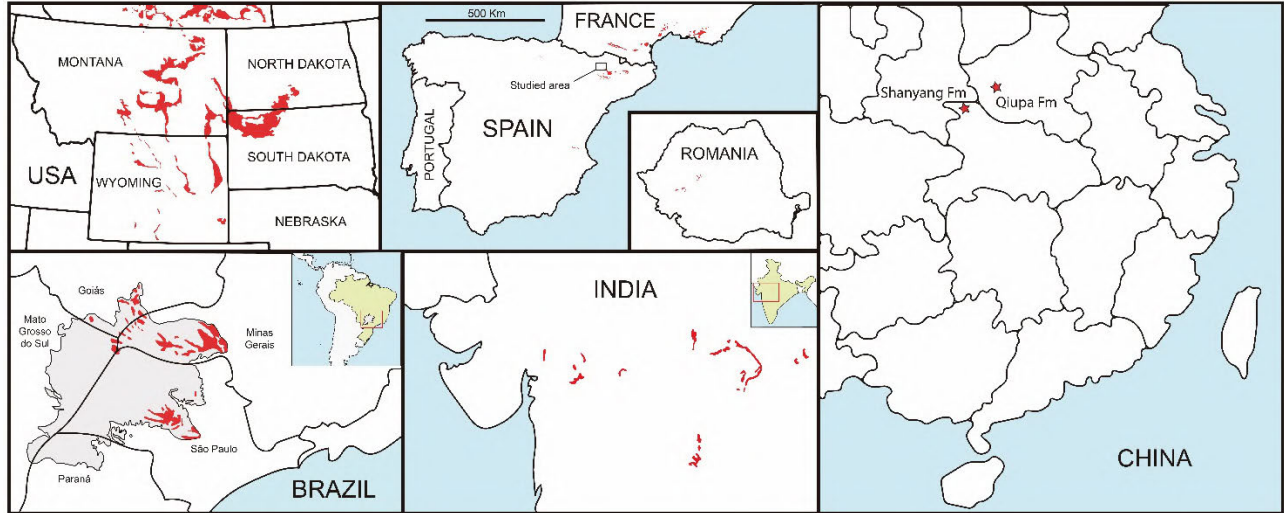
Figure 1.3. Continental K/Pg sections across the world. The numbers in the parenthesis indicate the number of sections from each different region (in bold), meanwhile the normal numbers indicate a score of the sections based on the robustness of the methodologies used to identify the K/Pg boundary (After Vajda and Bercovici, 2014). Note that since 2014, the number of K/Pg terrestrial sections studied has notably increased.

### 1.2. Upper Maastrichtian continental vertebrate record

The following is a brief description of the best examples of late Maastrichtian continental vertebrate records of the world. These records are found in geological units displaying a fairly continuous sedimentological record of the end of the Cretaceous and beginning of Paleocene, and thus including the K/Pg boundary (Table 1.1, Fig. 1.1 and 1.4). The study of these geological units has helped to better understand how the K/Pg extinction affected to continental vertebrates, although there are some of them that still have a lot of information to reveal.

Geological unit	Location	Sedimentary environment	Main vertebrate faunas
Hell Creek Fm	USA	Fluvial and coastal	<b>Theropods:</b> alvarezsaurids, tyrannosaurids, ornithomimids, dromaeosaurids, troodontids, caenagnathids, enantiornithine birds <b>Ornithischians:</b> ceratopsians, ankylosaurians, pachycephalosaurians, hadrosaurid and thescelosaurid ornithopods <b>Azhdarchid pterosaurs</b> <b>Eusuchian crocodylomorphs</b> <b>Turtles:</b> pan-trionychids, pleurosternids, baenids, macrobaenids, nanhsiungchelyids, adocids, chelydrids, kinosternoids <b>Squamates:</b> teiids, anguids, monstersaurids skinks, anguimorphs, necrosaurids, helodermatids, alethinophidian, boid snakes <b>Choristoderans</b> <b>Amphibians:</b> bombinatorid, pelobatid and other indeterminate anurans, salamanders <b>Mammals:</b> multituberculates, eutherians, metatherians <b>Elasmobranch and actinopterygian fishes</b>
Marília Fm	Brazil and Paraguay	Distal alluvial and anastomosing fluvial	<b>Titanosaurian sauropods</b> <b>Theropods:</b> carcharodontosaurids, abelisaurids, maniraptorans, megaraptorans, enantiornithine birds <b>Notosuchian crocodylomorphs</b> <b>Pelomedusoid turtles</b> <b>Iguanid lizards</b> <b>Amphibians:</b> neobatrachid anurans <b>Elasmobranch and actinopterygian fishes</b>
Garum facies	Spain and France	Lagoonal, coastal and fluvial	See Table 1.2
Densuş-Ciula, Sînpetru and Sebeş Fm	Romania	Alluvial and lacustrine with volcanoclastic deposits	<b>Titanosaurian sauropods</b> <b>Theropods:</b> maniraptorans, <i>Balaur</i> , <i>Elopteryx</i> , enantiornithine and gargantuavid birds <b>Ornithischians:</b> rhabdodontid and hadrosauroid ornithopods, nodosaurid ankylosaurs <b>Azhdarchid pterosaurs</b> <b>Crocodylomorphs:</b> eusuchians, notosuchians, “atoposaurids” <b>Turtles:</b> dortokids and <i>Kallokibotion</i> <b>Squamates:</b> anguimorph, ‘scincomorph,’ teioid, borioteioid and paramacellodid lizards, madtsoiid snakes <b>Amphibians:</b> albanerpetontids, alytid and bombinatorid anurans <b>Mammals:</b> kogaionid multituberculates <b>Elasmobranch and actinopterygian fishes</b>
Lameta Fm and inter-trappean beds	India	Alluvial and lacustrine with large lava flows	<b>Titanosaurian sauropods</b> <b>Abelisaurid theropods</b> <b>Crocodylomorphs:</b> dyrosaurids and crocodylians <b>Kurmadyemid bothremydid turtles</b> <b>Squamates:</b> anguid, anguimorph, skink and iguanid lizards, madtsoiid snakes <b>Amphibians:</b> discoglossid, ranid, leptodactylid, paleobatid anurans <b>Eutherian mammals</b> <b>Elasmobranch and actinopterygian fishes</b>
Shanyang Fm	China	Alluvial, lacustrine and meandering fluvial	<b>Indeterminate sauropods</b> <b>Theropods:</b> tyrannosaurids and oviraptorosaurs <b>Hadrosaurid ornithopods</b> <b>Indeterminate turtles</b>

*Table 1.1 (previous page). Main upper Maastrichtian continental geological units with fossil vertebrates.*



*Figure 1.4. Maps of the outcrops of the main upper Maastrichtian geological units with vertebrates around the world.*

### **1.2.1. Hell Creek Fm (North America)**

Without any doubt, the best studied K/Pg continental succession in the world is the Hell Creek Fm, in North America, with a vast extension of outcrops, along the Great Plains in Montana, South and North Dakota, to southern Canada (Fastovsky and Bercovici, 2016).

Since the early 20<sup>th</sup> century, research in the Hell Creek Fm has provided countless discoveries of fossil vertebrates, including some well-known dinosaurs such as *Tyrannosaurus rex* Osborn, 1905 or *Triceratops* (Scannella and Fowler, 2014). This geological unit represents fluvial environments fringing the coast of the Western Interior Seaway (Fastovsky, 1987; Johnson et al., 2002; Fowler, 2020). It has been dated as late Maastrichtian, encompassing the upper part of the magnetochron C30 and the C29r (Swisher III et al., 1993; Sprain et al., 2015; Fastovsky and Bercovici, 2016). The iridium anomaly that marks the K/Pg boundary is identified at the top of the formation (Bohor et al., 1984; Renne et al., 2013; Sprain et al., 2018).

The Hell Creek Fm has yielded a great diversity of fossil bones and eggs of vertebrates, and plants, as well as palynofossils, throughout the entire formation (Johnson et al., 2002; Jackson and Varricchio, 2010; Fastovsky and Bercovici, 2016), including vertebrate sites located at the K/Pg boundary itself (Lyson et al., 2011a; DePalma et al., 2019). Dinosaurs were abundant and diverse (Table 1.1, Fig. 1.5), with specimens of various clades of ornithischians (e.g., ceratopsians, pachycephalosaurians, ankylosaurians, and hadrosaurid and thescelosaurid ornithomimids). Diversity was also high regarding theropod dinosaurs, with a wide range of groups identified (e.g. tyrannosaurids, ornithomimids, alvarezsaurids, several maniraptorans, mainly dromaeosaurids, troodontids and caenagnathids-, and enantiornithine birds) (Pearson et al., 2002; Russell and Manabe, 2002; Lyson and Longrich, 2011; Brusatte et al., 2015). Though ornithischians seem to have suffered some type of decline prior to the impact, the communities were still pretty diverse prior to the meteorite impact (Fig. 1.5) (Vavrek and Larsson, 2010; Brusatte et al., 2015; Chiarenza et al., 2019).

Accompanying these rich faunas of dinosaurs, there were giant azhdarchid pterosaurs (Henderson and Peterson, 2006), eusuchian crocodylomorphs (Brochu, 1997; Pearson et al., 2002; Crawford and Evans, 2016), choristoderan reptiles (Brown, 1905; Pearson et al., 2002), and a great diversity of turtles with more than 19 species belonging to eight different families (Holroyd and Hutchison, 2002; Holroyd et al., 2014; Vitek and Joyce, 2015). Small vertebrates were also quite abundant in the Hell Creek Fm, with a rich and diverse record of elasmobranch and actinopterygian fishes (Brinkman et al., 2014; Cook et al., 2014), amphibians (Pearson et al., 2002; Wilson et al., 2014), lizards and snakes (Longrich et al., 2012), and mammals (Hunter and Archibald, 2002; Kielan-Jaworowska et al., 2005; Wilson, 2013).

The great diversity of vertebrates described from the Hell Creek Fm is complemented with the rich vertebrate record of geological units that are lateral equivalents to the Hell Creek Fm, such as the Lance Fm, the Frenchman Fm and the Ojo Alamo Fm. The total record of vertebrates of these formations (with some differences due to provincialism), reflects that North America ecosystems were far from decline before the impact of the meteorite.

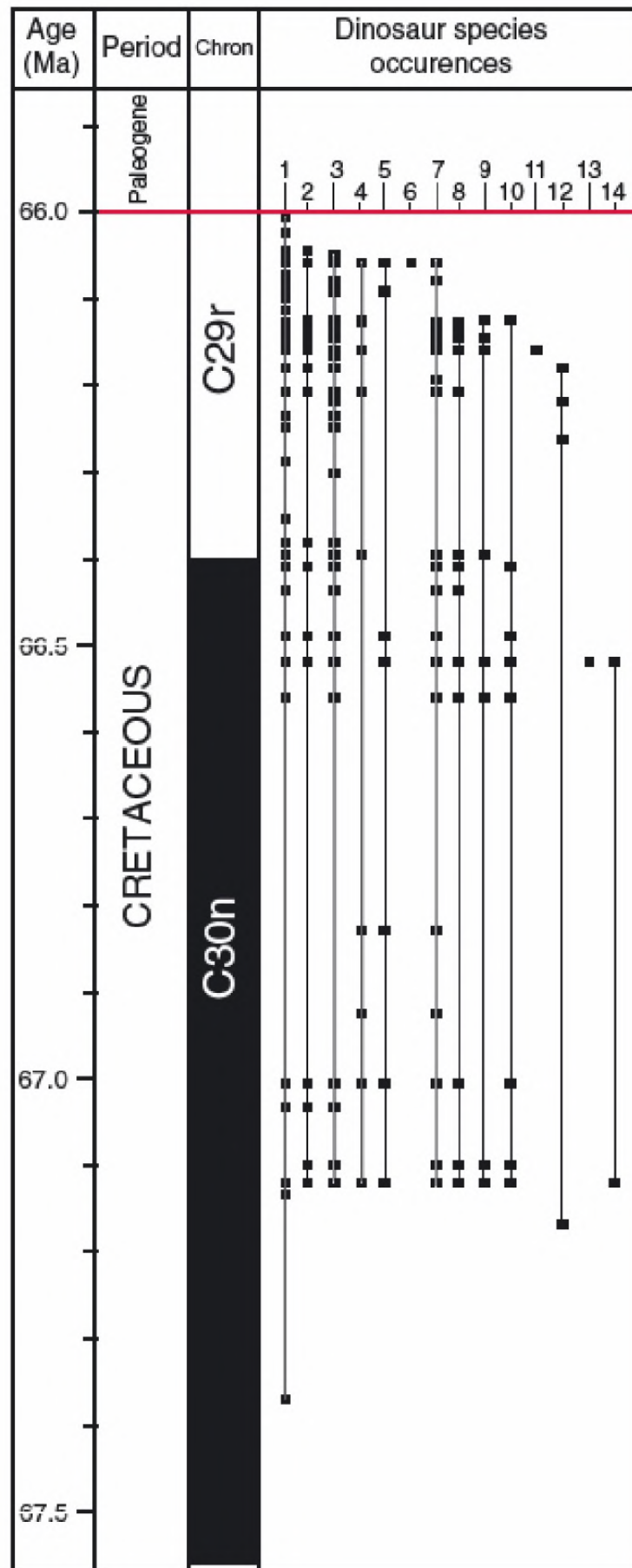


Figure 1.5 (previous page). Late Maastrichtian dinosaur record of the Hell Creek Fm in North Dakota (USA). Numbers correspond to the following dinosaur taxon: 1) *Ceratopsidae indet.*; 2) *Richardoestesia isosceles*; 3) *Hadrosaurinae indet.*; 4) *Caenagnathidae indet.*; 5) *Coelurosauria indet.*; 6) *Ornithomimidae indet.*; 7) *Tyrannosaurus rex*; 8) *Paronychodon lacustris*; 9) *Saurornitholestes*; 10) *Thescelosaurus neglectus*; 11) *Torosaurus latus*; 12) *Triceratops horridus*; 13) *cf. Avisaurus archibaldi* (probably of avian nature); 14) *Troodon sp.* (figure slightly modified from Brusatte et al. (2015), based on data from Pearson et al., (2002)).

### 1.2.2. Marília Fm (Brazil and Paraguay)

The Marília Fm corresponds to the uppermost unit of the Upper Cretaceous Bauru Group, which crops out in the south of Brasil and the northeast of Paraguay (Fernandes and Magalhães Ribeiro, 2015). This formation is composed by distal alluvial and fluvial deposits and local eolian deposits (Fernandes and Magalhães Ribeiro, 2015). It has been dated as late Maastrichtian, but its closeness to the K/Pg boundary is not clear (Dias-Brito et al., 2001; Brusatte et al., 2017). The unit has a rich fauna of vertebrates, including dinosaurs (Table 1.1): The main herbivores were large titanosaurian sauropods (Campos et al., 2005; Martinelli et al., 2015; Brusatte et al., 2017); meanwhile there was a high diversity of theropods, such as carcharodontosaurids and abelisaurids as large theropods (Candeiro and Martinelli, 2005; Novas et al., 2008; Méndez et al., 2014; Iori et al., 2021); accompanied by other smaller theropods such as maniraptorans and megaraptorans (Novas et al., 2005; Méndez et al., 2012); and enantiornithine birds (Candeiro et al., 2012).

Other vertebrates have been identified in the Marília Fm; including notosuchian crocodylomorphs, pelomedusoid turtles (de França and Langer, 2005), as well as iguanid lizards, amphibians and fishes (de França and Langer, 2005; Candeiro et al., 2006; Candeiro, 2009; Báez et al., 2012; Iori and Arrua-Campos, 2016).

The vertebrate record of the Marília Fm suggests rich and diverse ecological communities were thriving during the last millions of years of the Maastrichtian before the K/Pg. Nevertheless, the absence of small herbivorous and omnivorous dinosaurs compared to other areas of America is significant. This fact has been attributed to a sampling-bias and the occupation of these niches by abundant and diverse small crocodylomorphs (Brusatte et al., 2017).

### 1.2.3. *Densuș-Ciula, Sînpetru and Sebeș Fm (Romania)*

During the Late Cretaceous, the European landmass was partially covered by shallow seas, leaving an archipelago of emerged islands. The Hațeg island was one of those emerged landmasses, which encompassed part of present-day Transylvania (western Romania) (Nopcsa, 1915) (Fig. 1.6). During the Late Cretaceous, it was inhabited by an unusual community of vertebrates, with several groups showing dwarfism and other peculiar adaptations to insularity (Benton et al., 2010; Csiki-Sava et al., 2015) (Table 1.1). The upper Maastrichtian vertebrate fossils of Hațeg island have been recovered mainly from the Sînpetru, Densuș-Ciula and Sebeș formations, which represent alluvial and lacustrine deposits, with intercalated volcanoclastics, that range from the Santonian-Campanian to the upper Maastrichtian (see Csiki-Sava et al. (2016) for a detailed chronostratigraphic framework). However, these formations do not record the uppermost part of the Maastrichtian: most recent dating situates their upper parts around the boundary between the magnetochrons C30n and C29r; and their youngest vertebrate record are located in the upper part of the C30n. In this way, the vertebrates that might have inhabited the island at the moment of the K/Pg impact have not been preserved.

During the late Maastrichtian, the dinosaur assemblage of the Hațeg island consisted of dwarf and medium titanosaurian sauropods (Codrea et al., 2010; Csiki et al., 2010a; Mocho et al., 2022); rhabdodontid and hadrosauroid ornithopods (Weishampel et al., 1993, 2003; Godefroit et al., 2009; Csiki-Sava et al., 2016; Augustin et al., 2022); nodosaurid ankylosaurs (Ősi et al., 2014; Csiki-Sava et al., 2016) and small maniraptoran theropods (Csiki-Sava et al., 2016; Văcărescu et al., 2018), besides the enigmatic theropods *Balaur* and *Elopteryx* (Csiki et al., 2010c; Brusatte et al., 2013). Avian dinosaurs are represented by enantiornithine birds (Wang et al., 2011) and by the enigmatic giant gargantuavids (Mayr et al., 2020).

Other vertebrates present at the island were giant azhdarchid pterosaurs (Buffetaut et al., 2002; Solomon et al., 2020); eusuchian, notosuchian and “atoposaurid” crocodylomorphs (Delfino et al., 2008; Martin et al., 2010; Csiki-Sava et al., 2016); dortokid turtles and the basal turtle *Kallokibotion* (Rabi et al., 2013; Pérez-García and Codrea, 2018); kogaionid multituberculate mammals (Smith and Codrea, 2015; Csiki-Sava et al., 2018, 2022); as well as several amphibians and squamates, including

madtsoiid snakes and borioteioid lizards (Folie and Codrea, 2005; Vasile et al., 2013; Venczel et al., 2015, 2016; Csiki-Sava et al., 2016; Codrea et al., 2017).

#### **1.2.4. *Lameta Fm and inter-trappean beds (India)***

Several patchy outcrops of continental deposits appear associated to the basalts from the Deccan Traps in western and central of India. These continental successions were deposited in alluvial and lacustrine environments under semi-arid to humid conditions. Those deposits overlaid by the basalts belong to the Lameta Fm (Srivastava and Mankar, 2015; Kumari et al., 2021), meanwhile those intercalated within the basalt flows are known as inter-trappean beds. These continental deposits have been dated by means of biostratigraphy and magnetostratigraphy as late Maastrichtian (C30n-C29r magnetochrons). They yield a rich record of fossil vertebrates, including dinosaur bones and eggs (Mohabey and Samant, 2013; Kapur and Khosla, 2019) (Table 1.1).

The dinosaur faunal assemblage of the Lameta Fm is constituted by titanosaurian sauropods (Jain and Bandyopadhyay, 1997; Wilson et al., 2011a, 2019) and by several large and small abelisaurid theropods (Wilson et al., 2003; Novas et al., 2010). Non-dinosaurian vertebrates were represented by indeterminate crocodylomorphs and dyrosaurids (Rana and Sati, 2000; Prasad and de Lapparent de Broin, 2002; Khosla et al., 2009), kurmademydine bothremydid turtles (Gaffney et al., 2001; Joyce and Bandyopadhyay, 2020), anuran amphibians, matsoiid snakes and other squamates (Prasad and Rage, 1995, 2004; Rana and Mohabey, 2005; Mohabey et al., 2011). Mammals were represented by adapisoriculids eutherian mammals (Prasad et al., 2010). It has been suggested that the Lameta dinosaur fauna got extinct 350 ky before the K/Pg impact, due to the Deccan vulcanism (Mohabey and Samant, 2013), but a better stratigraphic and chronostratigraphic control of the paleontological sites is needed to corroborate this hypothesis.

#### **1.2.5. *Shanyang Fm (China)***

In central China, in the East Qinling region, there is a set of small pull-apart basins with an Upper Cretaceous continental sedimentary filling with fossils of dinosaurs and other vertebrates. Some of these basins include Maastrichtian deposits, thus allowing to study the ecosystems with vertebrates during the period prior to the K/Pg impact. In

particular, the Shanyang, Lushi, Lingbao and Luonan basins record upper Maastrichtian successions (Tong and Wang, 1980; Xue et al., 1996; Han et al., 2022), though only the Shanyang basin hold the closest vertebrate communities before the K/Pg boundary. In this latter basin, the Maastrichtian unit, known as Shanyang Fm, encompasses alluvial, meandering fluvial and lacustrine deposits with a diverse fauna of dinosaur eggs and bones, including sauropod, hadrosaurid ornithopods, and tyrannosaurid and oviraptorosaur theropods (Table 1.1). However, this assemblage is apparently less diverse than the dinosaur fauna of the Campanian-early Maastrichtian units. According to Han et al. (2022), this might be caused by a long-term decline of dinosaur communities during the last 2 My of the Maastrichtian before the K/Pg impact due to climatic and ecologic factors. Besides dinosaurs, in the Shanyang Fm, there are eggs of indeterminate turtles (Zhao et al., 2015). No information of other vertebrate groups is available.

### **1.3. *The upper Maastrichtian Ibero-Armorican record***

As it has mentioned before, during the Late Cretaceous, a great part of Europe was an archipelago. The Ibero-Armorican landmass, which encompassed the current south of France and a great part of the Iberian Peninsula, was the largest of these islands (Fig. 1.6.) (Csiki-Sava et al., 2015). The Ibero-Armorican island is one of the areas of Europe with the best continental records of the end of the Cretaceous.

Vertebrate fossils from the end of the Cretaceous (Campanian- Maastrichtian) are found in what are known as the Garum facies (Leymerie, 1868). This facies encompasses heterogenous and heterochronous deposits accumulated in fully continental (alluvial, fluvial, lacustrine), to transitional and lagoonal environments. To date, the upper Maastrichtian record of the Ibero-Armorican island is limited to the South-Pyrenean Basin in northeast Spain (Fondevilla et al., 2019; Pérez-Pueyo et al., 2021a); the Sobrepeña Fm, Torme Fm, and equivalent outcrops in northwest Spain (Berreteaga et al., 2008; Corral et al., 2016); eastern Spain near Tous (Valencia) (Company, 2004; Company et al., 2009); and the Haute-Garonne and Aude departments of Occitania in France (Laurent et al., 2002a; Fondevilla et al., 2019) (Fig. 1.7).

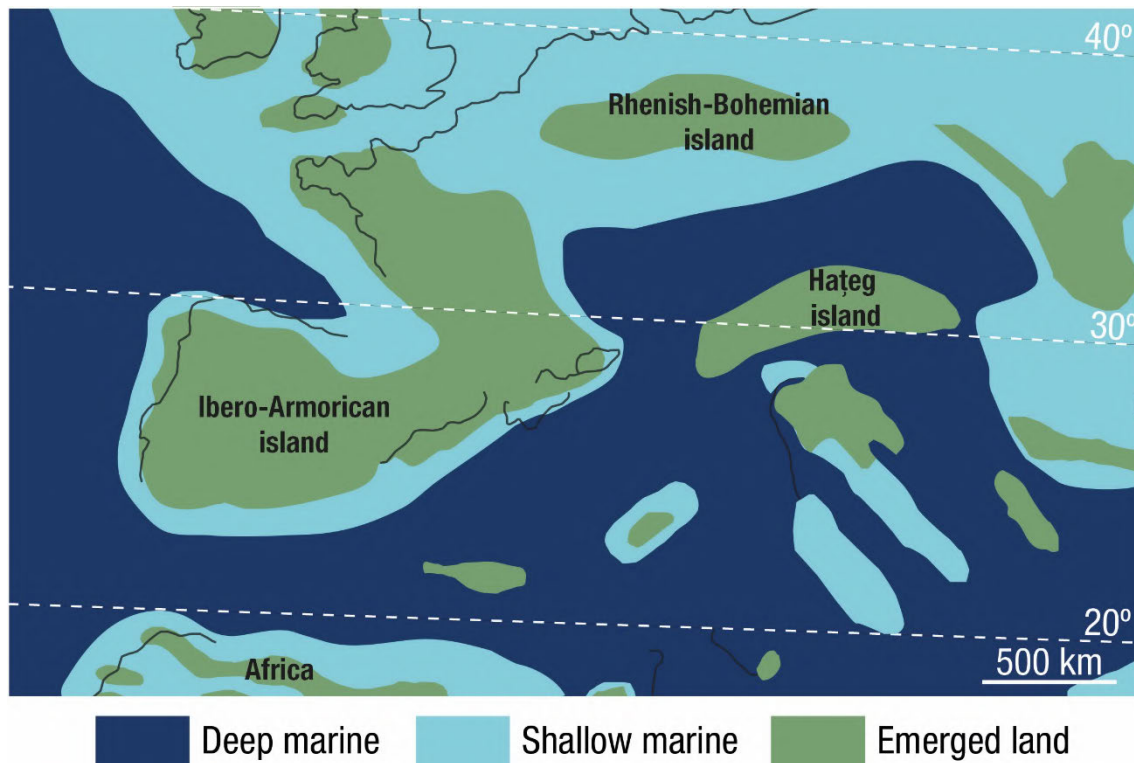


Figure 1.6. Late Maastrichtian paleogeography of the southwestern area of the European Archipelago. Dark lines represent current geography (Adapted from Dercourt et al., 2000).

The Ibero-Armorican island presents a rich and diverse record of vertebrates during the Maastrichtian, although it is important to note that the dinosaur faunas underwent a change in dominant herbivores during the so-called “Maastrichtian Dinosaur Turnover” (Le Loeuff et al., 1994b; Vila et al., 2016; Fondevilla et al., 2019). During the early Maastrichtian, ecosystems were inhabited by rhabdodontid ornithopods, titanosaurian sauropods and ankylosaurs, whereas in the late Maastrichtian, these communities were replaced by hadrosaurid ornithopods and new titanosaurian forms. However, nodosaurid ankylosaurians still persisted up to chron C30r, coexisting with these new assemblages for nearly 2 My (Fondevilla et al., 2019). On the other hand, it is not clear if this turnover affected to theropod dinosaurs, since their record is scarcer and more incomplete. Therefore, this faunal turnover supposed a decline in the diversity of herbivorous dinosaurs prior to the K/Pg boundary.

Lambeosaurine hadrosaurids were present in the Ibero-Armorican island from the late early Maastrichtian, mostly recorded from the Pyrenees. The lambeosaurine from Els Nerets in Vilamitjana (Lleida, Catalonia, NE Spain), within the chron C31r, is the oldest evidence of hadrosaurids in Europe (Conti et al., 2020). Lambeosaurines are also present

within the chron C29r, with some fossils recorded very close to the K-Pg boundary. At present, there are five species of lambeosaurine hadrosaurids described from the region: *Adynomosaurus* from the Costa de Les Solanes site in Basturs (Lleida, Catalonia, NE Spain) (Prieto-Márquez et al., 2019); *Arenysaurus* (Pereda-Suberbiola et al., 2009b) and *Blasisaurus* (Cruzado-Caballero et al., 2010a) from Blasi 3 and Blasi 1 sites in Arén (Ribagorza county, Huesca, Aragon, NE Spain), *Pararhabdodon* from the Sant Romà d'Abella site (Lleida, Catalonia, NE Spain) (Casanovas et al., 1993; Prieto-Marquez and Wagner, 2009; Prieto-Márquez et al., 2013; Serrano et al., 2021), and *Canardia* from the Lacarn and Tricouté sites (Haute-Garonne, Occitania, southern France) (Prieto-Márquez et al., 2013). Additional lambeosaurine remains include the aforementioned dinosaur from Els Nerets (Conti et al., 2020) and other indeterminate lambeosaurines from Basturs Poble and Les Llaus (Lleida, Catalonia, NE Spain) (Prieto-Márquez et al., 2006; Prieto-Márquez et al., 2013; Blanco et al., 2015c; Fondevilla et al., 2018;), and Blasi sites (Huesca, Aragon, NE Spain) (Cruzado-Caballero et al., 2005, 2008, 2010b, 2010c). Besides, there is also record of a non-hadrosaurid from Fontllonga-R (Lleida, Catalonia, NE Spain) (Casanovas et al., 1999; Pereda-Suberbiola et al., 2009a), which recently has been erected as the new species *Fylax thyrakolasus* Prieto-Marquez and Carrera Farias, 2021; an indeterminate euhadrosaurid from Blasi 3,4 in Arén (Huesca, Aragon, NE Spain) (Cruzado-Caballero et al., 2014); and a small hadrosaurid from Serraduy, also in the Ribagorza county (Huesca, Aragon, NE Spain) (Company et al., 2015). All through Ribagorza, there are also abundant sites with remains of indeterminate hadrosauroids (e.g. Cruzado-Caballero et al., 2012; Puértolas-Pascual et al., 2012; Pérez-Pueyo et al., 2019). This rich pyrenean osteological record of hadrosauroids is complemented by several track sites, with large ornithopod footprints, many of which have been referred to the ichnogenus *Hadrosauropodus* (Barco et al., 2001; Vila et al., 2013). On the other hand, there are also eggshells attributable to hadrosaurid dinosaurs described as *Spheroolithus europaeus* Sellés, Vila, Galobart, 2014a.

Outside the Pyrenees, there is a dentary from La Solana site near Tous (Valencia, Valencian Community, E Spain) that has been identified as belonging to an indeterminate hadrosaurid (Company et al., 1998; Pereda-Suberbiola et al., 2009a). Finally, there is a hadrosauroid femur from the Albaina site in Laño (Treviño county, Burgos, Castile and León, NW Spain) (Pereda-Suberbiola et al., 2015b). With between seven to thirteen taxa, Hadrosauroidea is the most speciose dinosaur clade in the Ibero-Armorican island, five of them being lambeosaurine hadrosaurids (Table 1.2., Fig. 1.8).

Ankylosaurs are represented by isolated and fragmentary material referred to nodosaurids during the early-late Maastrichtian transition of several sites in the Southern Pyrenees within the Lleida province (Catalonia, NE Spain), including Els Nerets (Santafé et al., 1997) and Biscarri (López-Martínez et al., 2000). However, they extend to the late Maastrichtian, since nodosaurid ankylosaurs fossils have been found in Fontllonga-6 site, also in Lleida (López-Martínez et al., 1998), and at the Lestailats site, in the Petite Pyrénées (Haute-Garonne, Occitania, southern France) (Laurent et al., 2002a). These two last sites represent the last occurrence of nodosaurid ankylosaurs in the island, being both within the chrons C30r and C30n (Figure 1.8).



Figure 1.7. Location of the main upper Maastrichtian records of continental vertebrates in the Ibero-Armorican island.

Taxon	Ibero Armorican island
<b>Amphibians</b>	
Anura	4 (1)
Albanerpetontidae	1
Salamandridae	1
<b>Turtles</b>	
Pleurodira	1 (2)
Cryptodira	1
<b>Squamates</b>	
Iguanidae	1
Scincomoprha	1?
Anguimorpha	1
Teiioidea	1
Alethinophidia	1
Gekkota	1
<b>Crocodyliforms</b>	
Ziphsuchia (Doratodon)	1
Mesoeucrocodylia Atoposauridae	1
Basal Eusuchia (Allodaposuchus)	4
Basal Eusuchia (Acynodon)	1
Eusuchia Gavialoidea	1
<b>Pterosaurs</b>	
Azhdarchidae	1
<b>Dinosaurs</b>	
<b>Sauropoda</b> , Titanosauria	3
<b>Theropoda</b>	
Abelisauroidae	1 (1)
Coelurosauria indet.	1
Dromaeosauridae	1
Troodontidae	1
Uncertain theropods	2
Paraves, Enantiornithes	1?
<b>Ornithopoda</b>	
Hadrosauroidae	7 (6)
Non-hadrosaurid Hadrosauroidae	1 (1)
Hadrosauridae	6 (5)
<b>Ankylosauria</b> , Nodosauridae	1
<b>Mammals</b>	
Therian	1

Table 1.2. Minimum number of tetrapod taxa present in the Ibero-Armorican island during the late Maastrichtian. Red numbers mark possible but not certain additional taxa.

The record of titanosaur sauropods from the late Maastrichtian of the Ibero-Armorican island consists of isolated bones, tracks, skin impressions and eggshells (Canudo, 2001; Laurent et al., 2002a; Vila et al., 2012; Vila and Sellés, 2015; Fondevilla et al., 2016, 2017b; Sellés et al., 2016). Vila et al. (2012) recognized three different femur morphotypes, which would correspond to three undetermined but distinct taxa of titanosaurs (Table 1.2, Fig. 1.8). One of the morphotypes corresponds to a large titanosaur, whereas the other two femora represent small-medium titanosaurs. Although not formally described, these titanosaurs represent different taxa from those of the early Maastrichtian assemblage (Vila et al., 2012). This is additionally supported by the distinct ootaxa association reported from the pre- and post-turnover assemblage (Vila and Sellés, 2015; Fondevilla et al., 2019; Vila et al., 2022). The upper Maastrichtian large femur morphotype could belong to members of a new group of large titanosaurs recently discovered within the upper part of the early Maastrichtian in the Southern-Pyrenees, and represented by the new taxon *Abditosaurus kuehnei* Vila, Sellés, Moreno-Azanza, Razzolini, Gil-Delgado, Canudo and Galobart, 2022. This new taxon might represent a new lineage of large saltasaurine titanosaurs which arrived to the Ibero-Armorican island from Gondwana (Vila et al., 2022).

Theropod record from the late Maastrichtian of the Ibero-Armorican island is quite scarce and fragmentary, mainly constituted by teeth, some isolated bones and eggshells. These fossils belong mainly to abelisaurid and maniraptoran theropods (dromaeosaurids and troodontids) (Laurent et al., 2002a; Baiano et al., 2014; Torices et al., 2015; Marmi et al., 2016; Puértolas-Pascual et al., 2018), found mainly in the South-Pyrenean Basin in Spain, and in Haute-Garonne in France. The number of taxa is difficult to determine due to the fragmentary and incomplete nature of the fossils. Tooth morphotypes from the Southern Pyrenees indicate that at least one abelisaurid taxon inhabited the island during the late Maastrichtian (Theropoda indet. 1 and 2 or cf. *Arcovenator*; Torices et al., 2015; Pérez-García et al., 2016) (Fig. 1.8). Maniraptoran record from the Southern Pyrenees is represented mainly by teeth, with at least three identified taxa (*Richardoestesia*, *Paronychodon*, and Dromaeosauridae indet. distinguished by Torices et al. (2015), and by a metatarsal of the troodontid *Tamarro insperatus* Sellés, Vila, Brusatte, Currie and Galobart 2021 (Fig. 1.8). However, the real abundance of theropods is hard to establish (Table 1.2) since there are several fragmentary skeletal remains attributable to undetermined dromaeosaurids. Moreover, there is an oological record comprising several ootaxa of maniraptoran-like eggshells, including *Prismatoolithus trempii* Sellés, Vila, Galobart, 2014b, and *Pseudogeckoolithus* (Vianey-Liaud and Lopez-Martinez, 1997;

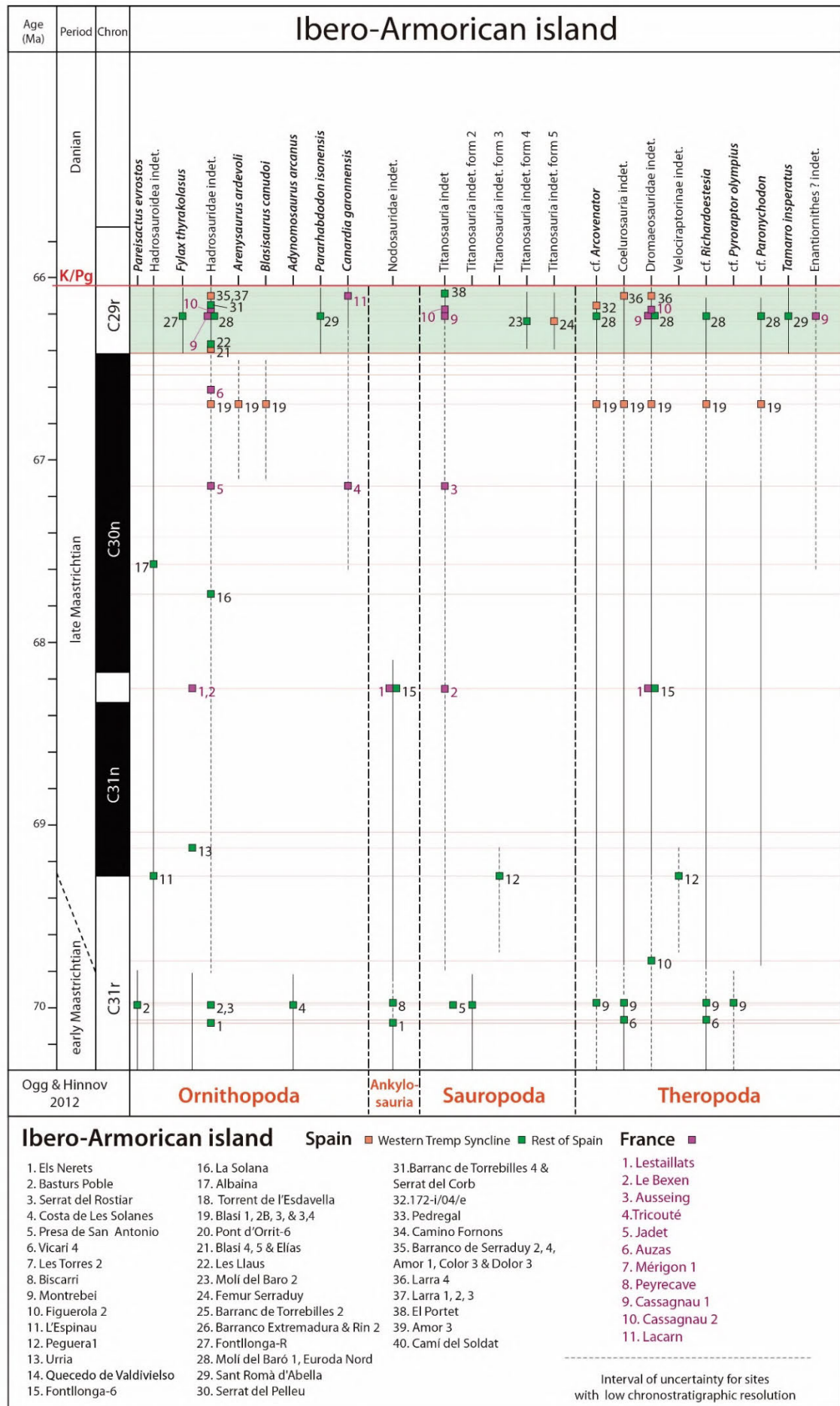
Sellés et al., 2014b; Choi et al., 2020). Avialan dinosaurs are represented only by a putative enantiornithines from southern France (Laurent, 2003) (Fig. 1.8).

The pterosaur record in the late Maastrichtian is scarce, with some isolated and fragmentary bones from the Pyrenees of France (Buffetaut et al., 1996, 1997; Buffetaut, 2008) and Spain (Dalla Vecchia et al., 2013; Pérez-Pueyo et al., 2021a), and outcrops near Valencia (Spain) (Company et al., 1999; Pereda-Suberbiola et al., 2007) (Figure 1.9). All of them have been identified as belonging to undetermined giant azhdarchids.

During the late Maastrichtian, the crocodylomorphs of the Ibero-Armorican island show great abundance, with a similar number of taxa than in the early Maastrichtian (Puértolas-Pascual et al., 2016). The best-represented clade is the eusuchian Allodaposuchidae, with two taxa described from the Southern Pyrenees: *Agaresuchus subjuniperus* Puértolas-Pascual, Canudo and Moreno-Azanza, 2014 and *Arenysuchus gascabadiolorum* Puértolas, Canudo and Cruzado-Caballero, 2011; and probably *Allodaposuchus palustris* Blanco, Puértolas-Pascual, Marmi, Vila and Sellés, 2014, whose characteristic teeth have been found up to the chron C29r (Marmi et al., 2016; Blanco et al., 2020). In addition, Blanco et al. (2020) described *Allodaposuchus* sp. 2 on the basis of a dentary from the Fontllonga-6 site in Lleida (Catalonia, NE Spain), within the chron C30r, which seems to be different from the allodaposuchids previously described, and could represent a new taxon. Finally, there are plenty of isolated teeth of allodaposuchids (Puértolas-Pascual et al., 2014, 2018; Blanco et al., 2015b; Marmi et al., 2016; Pérez-Pueyo et al., 2019) that due to their conical generalist shape are difficult to ascribe to more specific taxa. Gavialoidea is represented by a skull and other associated remains from the site of Cassagnau (Haute-Garonne, Occitania, southern France). These have been assigned to *Thoracosaurus neocesariensis* (Laurent et al., 2000), although they could belong to a new taxon (Brochu, 2004). In addition, more teeth referred to cf. *Thoracosaurus* have been found in the Spanish Pyrenees (Puértolas-Pascual et al., 2018; Blanco et al., 2020). The diversity of hylaeochampsid, “atoposaurid”, and notosuchian crocodylomorphs during the late Maastrichtian is difficult to determine, since most of their fossils are isolated teeth. There are several teeth referred to the hylaeochampsid cf. *Acynodon* from France (Le Loeuff et al., 1994a; Buffetaut and Le Loeuff, 1997) and the Spanish Pyrenees, (López-Martínez et al., 2001; Puértolas-Pascual et al., 2016; Blanco et al., 2020). “Atoposaurids” are represented by teeth from the Spanish Pyrenees identified as cf. *Theriosuchus* (López-Martínez et al., 2001; Marmi et al., 2016; Blanco et al., 2020). “Atoposauridae” is here written in quotes, since Tennant et al. (2016) have

argued that this clade is paraphyletic and some taxa previously assigned to this clade, such as “*Theriosuchus*” *ibericus* Brinkmann, 1992 and “*Theriosuchus*” *sympiestodon* Martin, Rabi and Csiki, 2010 belong to Paralligatoridae and, in consequence, both taxa were accordingly grouped under the new genus *Sabresuchus*. There are also some teeth from the Spanish Pyrenees identified as the notosuchian cf. *Doratodon* (Marmi et al., 2016; Blanco et al., 2020). It should further be noted that plenty of undetermined eusuchian and crocodylomorph remains have been discovered in the French and Spanish Pyrenees (see Puértolas-Pascual et al. 2016, and references therein), as well as tracks of crocodylomorphs (Vila et al., 2015; Pérez-Pueyo et al., 2018), but due to their limited diagnostic value, it is difficult to ascertain more precisely their taxonomic status. There are also indeterminate eusuchian remains from La Solana (Valencia, Valencian Community, E Spain) (Company, 2004) and Quecedo de Valdivielso (Burgos, Castile and León, NW Spain) (Berreteaga, 2008; Murelaga et al., 2005). Additionally, there are also crocodylomorph eggshells from the Blasi 2B site (Arén, Huesca, Spain). These were first reported as megaloolithid eggshells (López-Martínez et al., 1999), but they were later described as having a crocodyloid morphotype and were identified as *Krokolithes* sp. (Moreno-Azanza et al., 2014), implying that these eggs were laid by crocodylomorphs. Thus, Ibero-Armorican crocodylomorphs are represented during the late Maastrichtian by a minimum of eight taxa (Table 1.2, Figure 1.9).

Figure 1.8. (next page). Dinosaur groups and species in the Ibero-Armorican island during the late Maastrichtian. The green band marks the last ~350 ka of the Maastrichtian. Chronostratigraphic scale based on Ogg et al. (2012) (Modified after Pérez-Pueyo et al., 2021a).



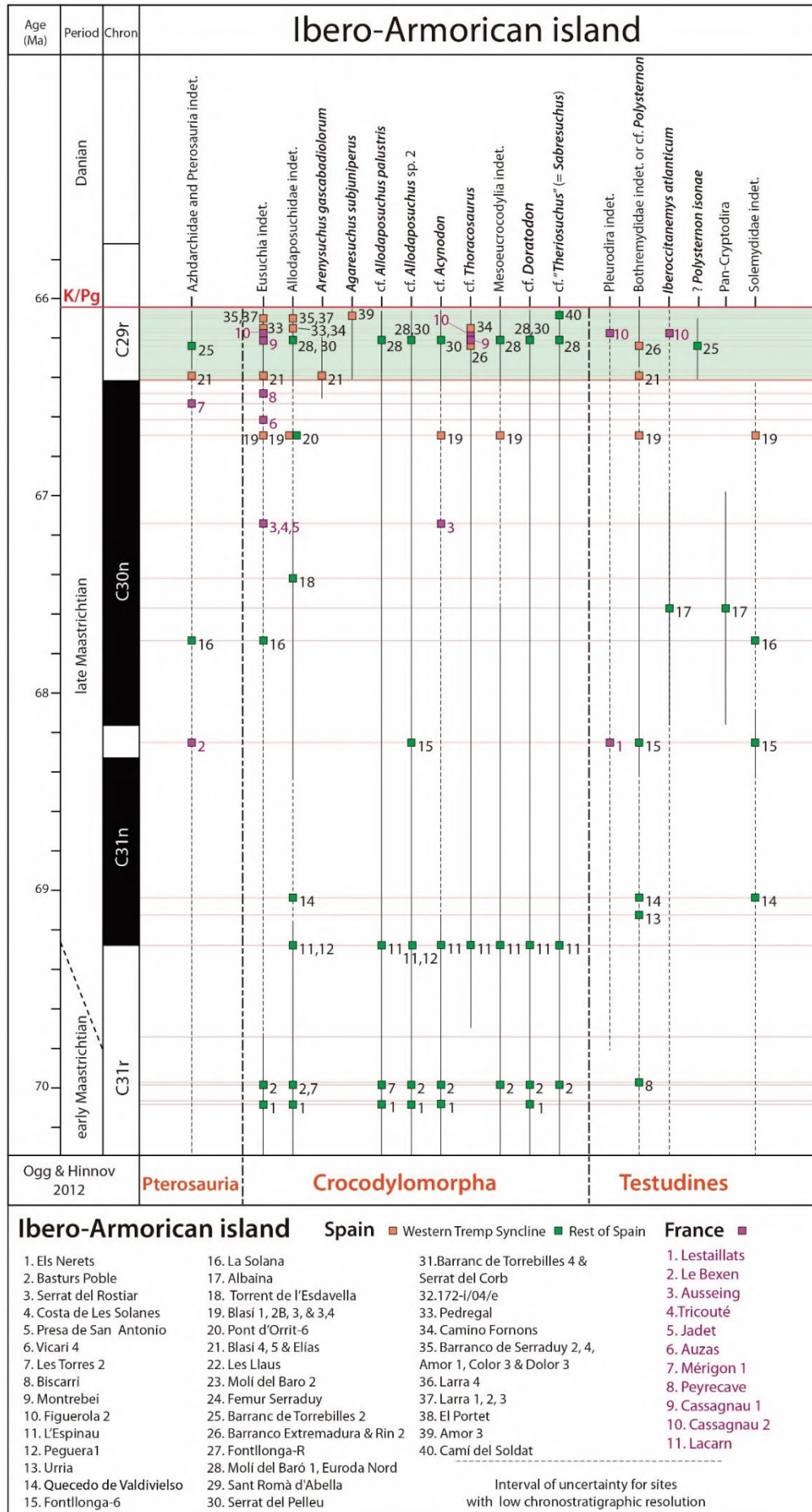


Figure 1.9. (previous page). Pterosaur, crocodylomorph, and testudine groups and species in the Ibero-Armorican island during the late Maastrichtian. The green band marks the last  $\approx 350$  ka of the Maastrichtian. Chronostratigraphic scale based on Ogg et al. (2012) (Modified after Pérez-Pueyo et al., 2021a).

The record of testudines during the late Maastrichtian of the Ibero-Armorican island is poorer than during the early Maastrichtian. In the Pyrenees, pleurodire turtles are represented by the bothremydid '*Elochelys convenarum*' Laurent, Tong, Claude, 2002b from Cassagnau-2 (Haute-Garonne, Occitania, southern France), and another bothremydid turtle, *Polysternon isonae* Marmi, Luján, Riera, Gaete, Oms, Galobart, 2012 from Isona (Lleida, Catalonia, NE Spain). However, Pérez-García (2017) considers *P. isonae* as *nomen dubium*, lacking enough diagnostic characters for a new species, and classifies the remains as *Foxemydina* indet. Isolated remains of indeterminate bothremydids are also present in other sites in the Pyrenees (Murelaga et al., 1998; Murelaga and Canudo, 2005; Pérez-Pueyo et al., 2019), and in the northwestern Spanish sites of Urria and Quecedo de Valdivielso (Burgos, Castile and León, NW Spain) (Murelaga et al., 2005; Berreteaga, 2008). In the fossil site of Albaina, also in Burgos, there is a plate identified as cf. *Polysternon atlanticum* de Lapparent de Broin, Murelaga 1996 (Pereda-Suberbiola et al., 2015b). Recently, Pérez-García et al. (2021) restudied the holotype material of *P. atlanticum*, reaching the conclusion that *P. atlanticum* and *E. convenarum* (newly combined as *Iberoccitanemys convenarum* by Pérez-García et al., 2012) are the same taxon, and he reformulated them as *Iberoccitanemys atlanticum*. For this reason, the diversity of pleurodire turtles during the late Maastrichtian of the Ibero-Armorican island is lower than previously thought. Pan-cryptodires are represented by the remains of solemydid turtles from the Spanish Pyrenees, from the sites of Blasi (Huesca) and Fontllonga-6 (Lleida) (Murelaga et al., 1998; Murelaga and Canudo, 2005); and from La Solana (Valencia) (Company, 2004; Company et al., 2009). Pereda-Suberbiola et al. (2015b) described a plate from a putative pan-cryptodire that differs from solemydids. This makes a minimum of one pan-pleurodire and two pan-cryptodires in the Ibero-Armorican island during the late Maastrichtian (Table 1.2, Figure 1.9).

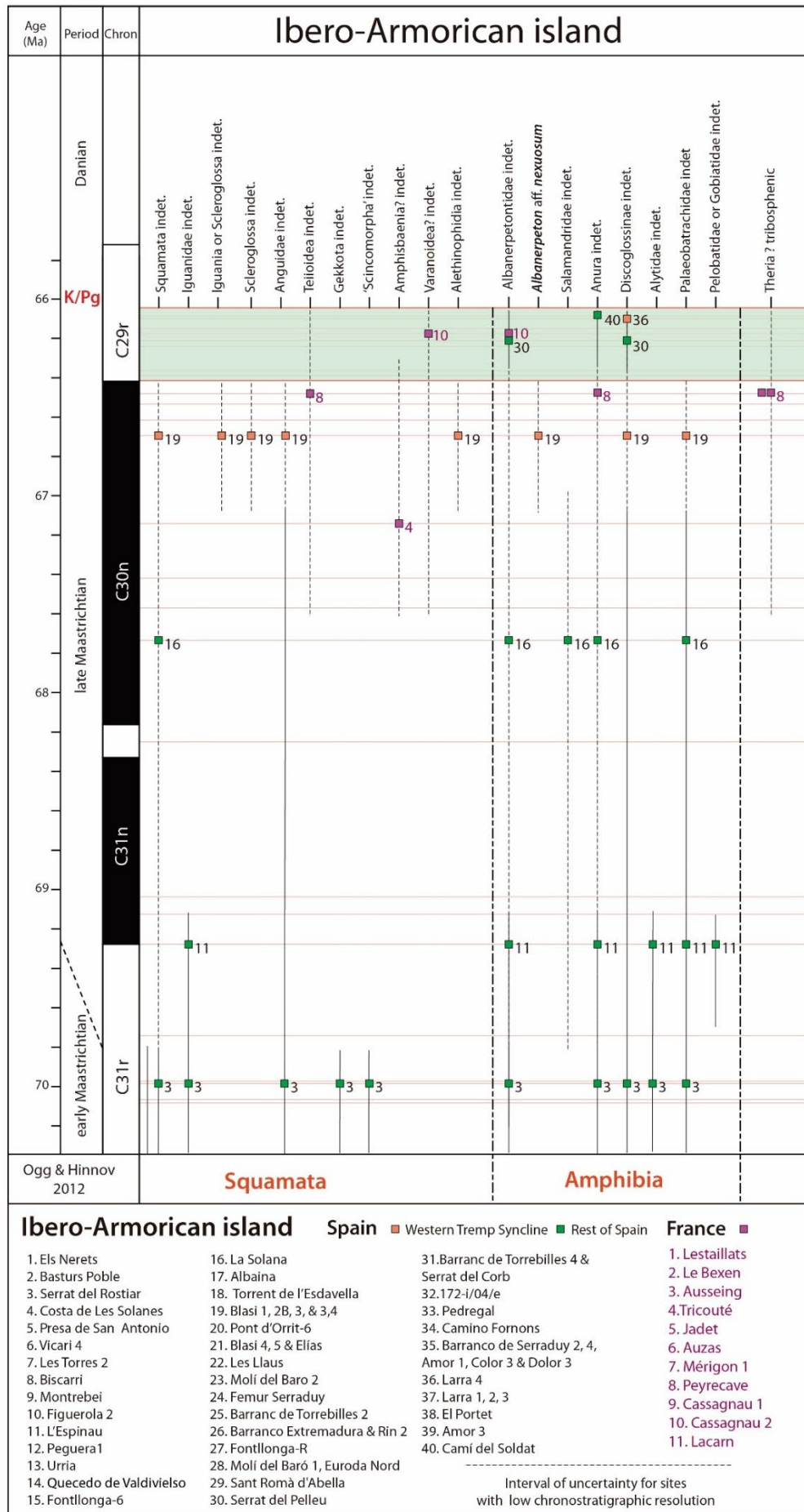


Figure 1.10 (previous page). Squamate, amphibian and mammal groups and species in the Ibero-Armorican island during the late Maastrichtian. The green band marks the last  $\approx 350$  ka of the Maastrichtian. Chronostratigraphic scale based on Ogg et al. (2012) (Modified after Pérez-Pueyo et al., 2021a).

Small-sized upper Maastrichtian tetrapods from the Ibero-Armorican island are represented only by amphibians and squamates from the Spanish and French Pyrenees (Laurent et al., 2002a; Laurent, 2003; Blain et al., 2010; Blanco et al., 2016; Puértolas-Pascual et al., 2018) and from Valencia (Szentesi and Company, 2017) (Table 1.2, Fig. 1.10).

The first group consists of albanerpetontids, with at least one taxon identified from Blasi 2B in Arén (Huesca, Aragon, NE Spain) as *Albanerpeton* aff. *nexuosum* Estes, 1981 (Blain et al., 2010), plus several albanerpetontid remains from the L'Espinau and Serrat del Rostiar 1 sites (Lleida, Catalonia, NE Spain) (Blanco et al., 2016), Cassagnau 1 (Haute-Garonne, Occitania, southern France) (Laurent et al., 2002a; Laurent, 2003), and La Solana (Valencia, Valencian Community, E Spain) (Szentesi and Company, 2017). In La Solana, the presence of a salamandrid is also documented (Szentesi and Company, 2017). Anurans are represented by at least four different groups, with one discoglossid and one palaeobatrachid recognized at Blasi 2B, L'Espinau, and Serrat del Rostiar (Blain et al., 2010; Blanco et al., 2016); and an alytid and a putative pelobatid or gobiatid at L'Espinau (Blanco et al., 2016). It is noteworthy that there are remains of a palaeobatrachid from Valencia (Szentesi and Company, 2017) that shows differences from the Blasi 2B taxon and could represent another taxon.

In the Upper Maastrichtian of the Aragonese Pyrenees, squamates are represented by two undetermined lizards, one anguid lizard, and one alethinophid snake from Blasi 2B site (Arén, Aragon, Spain) (Blain et al., 2010). Additionally, in the Catalan Pyrenees, the site of Serrat del Rostiar 1 has yielded several squamate remains (Blanco et al., 2016) including geckos, anguid, and “scincomorph” lizards, and an indeterminate iguanid. An indeterminate iguanid has also been found at L'Espinau. The Serrat del Rostiar 1 site is dated within chron C31r (early Maastrichtian), but due to its stratigraphic position, it lies very close to the boundary with the late Maastrichtian, so we have extended its faunal assemblage to the lower part of the late Maastrichtian (Fig. 10). In the French Pyrenees, there is also evidence of large varanoid, “scincomorph” lizards, and other indeterminate squamates (Laurent et al., 2002a; Laurent, 2003). Outside the Pyrenees, there are also undetermined squamate remains at the La Solana site in Valencia (Company, 2004).

It is interesting to note that during the late Maastrichtian, there is almost no evidence of mammals in the Spanish record of the Ibero-Armorican island (Fig. 1.10), despite their presence is documented during the early Maastrichtian (Pol et al., 1992; Gheerbrant and Astibia, 2012; Tabuce et al., 2013) and the earliest Paleocene (Lopez-Martinez and Pelaez-Campomanes, 1999; Peláez-Campomanes et al., 2000). The only evidence of mammals during the late Maastrichtian is some tribosphenic teeth from the Peyrecave site, in the Petites Pyrénées (Haute-Garonne, Occitania, southern France). These would have belonged to a therian mammal (Gheerbrant et al., 1997; Laurent, 2003).

# **Chapter 2.**

## **Objectives**





## **Chapter 2: Objectives**

The main objective of this PhD thesis is the study of the paleobiodiversity of the fossil vertebrate assemblages, just before the K/Pg extinction event, in the Maastrichtian transitional and continental sedimentary successions of the Western Tresp Syncline (Southern Pyrenees, NE Spain) belonging to the Tresp Fm. This goal has been addressed through an integrated paleontological and sedimentological study with the following specific objectives:

- I. Improving the knowledge of the sedimentary environments of the Maastrichtian successions of the Tresp Fm in this sector of the basin, by means of a stratigraphic-sedimentological analysis of the key outcrops.
- II. Refining the chronostratigraphic framework of the successions, through new biostratigraphic and magnetostratigraphic data.
- III. Analyzing the paleontological sites with fossil vertebrates in the studied key outcrops:
  - a. Increasing the knowledge about the diversity of vertebrates in the Pyrenean area during the late Maastrichtian: by the systematic study of fossils of groups not known to date and evaluating the chronological record of the different clades.
  - b. Paleoenvironmental interpretation of Veracruz 1 site: integrating sedimentological and micropaleontological data to provide an environmental context to this rich vertebrate site. Veracruz 1 represents a good approximation to the paleobiodiversity in a very specific place and time range close to the K/Pg boundary and was chosen as case study.

- IV. Evaluation of the vertebrate diversity based on the oological record: studying the fossil eggshell assemblage of Blasi 2B and Veracruz 1 site. Obtaining in this way complementary data to the osteological record.
- V. Integrating the sedimentological data with the vertebrate fossil record in order to evaluate the fossil preservation bias related to depositional and taphonomic factors.
- VI. Review of the late Maastrichtian vertebrate fossil record of the Ibero-Armorican island.

# **Chapter 3.**

# **Material and**

# **methods**





## **Chapter 3: Material and methods**

The analysis of the ‘Grey Garumnian’ and ‘Lower Red Garumnian’ successions and their fossil content in the Western Tremp Syncline studied in this PhD thesis required performing different tasks of field and laboratory work to obtain the main stratigraphic-sedimentological and paleontological data, as well as their posterior treatment and interpretation.

### **3.1. Field work**

To obtain the stratigraphic-sedimentological and paleontological data, **63** days of field work were carried out between 2017 and 2022. Several members of the Aragosaurus-IUCA research group, IGME, and other colleagues has participated and helped in these labors, that otherwise would have been impossible to perform alone. Below, there is a detailed information on the specific studied material and methodology used.

#### **3.1.1. Stratigraphic-sedimentological fieldwork**

For the stratigraphic-sedimentological characterization of the ‘Grey Garumnian’ and ‘Lower Red Garumnian’ successions of the Tremp Fm in the Western Tremp Syncline, 9 stratigraphic sections were studied: Campo, El Castellaz, Valle de Lierp, Rin, Serraduy, Beranuy, Isclés, San Pere de Cornudella and Arén. Their thickness range between 65 m to near 230 m (see figure 5.1 in Chapter 5 for their exact location). Lithology, color, geometry, thickness, texture, components (including fossil content) and sedimentary structures (including trace fossils and tracks) of the beds were studied in detail in each stratigraphic section. Paleocurrents were measured when possible and general and detailed photographs of the main sedimentary features were taken. Measuring tape, Jacob’s bar, compass, scale and a digital camera were used for these tasks (Fig. 3.1).

A total of 72 samples of coarse to medium-grained lithologies (e.g., limestones, sandstones, microconglomerates) were taken with a hammer for their later analysis in thin-sections to complete the observations concerning mainly texture and components. In addition, a total of 139 samples (in two batches of different years 94+45), (1-2 kg) of

soft fine-grained lithologies (mudstones, marls, marly mudstones) were collected at the Serraduy log for the analysis in the laboratory of their components and carbonate content. Finally, a detailed analysis was also performed at the Veracruz 1 paleontological site located in the Beranuy outcrop (sampling was performed every 0.5 m of the 7 m-thick marly mudstone bed of the site).

Good outcrop conditions allowed the analysis of the geometry of some deposits (e.g., sandstone packages) using field sketches and composite photographic overviews, as well as physical tracing of their lateral continuity/discontinuity. However, the physical correlation between outcrops was not possible due to bad outcrop conditions of the series in the intermediate areas. The exploration and tracking of the different layers led to the discovery of local and laterally constrained facies, which were not previously recognized in the studied logs. Their characterization was carried out and integrated in the general stratigraphic data set (e.g., bioclastic packstone with charophytes facies, see Chapter 5).



*Figure 3.1. A) Measuring the Arén log with a Jacob's staff. B) Measuring a mudstone interval at the Isclés outcrop.*

### **3.1.2. Magnetostratigraphic fieldwork**

Magnetostratigraphic sampling was carried out in two logs from different areas of the studied outcrops, Serraduy and Isclés. The aim was to improve and calibrate more precisely the age of the Tremp Fm in the area of study. The sampling was performed using both portable gas-powered and battery-powered drills cooled with water, orienting the samples *in situ* with a magnetic compass and an inclinometer (Fig. 3.2). In the case of soft lithologies, an unaltered surfaced of the bed was exposed with a hoe for the sampling with the drill. Oriented blocks were picked to those brittle soft fine-grained lithologies in which the sampling with the drill was unfeasible. Once the sample was extracted, a solution of sodium silicate dissolved in distilled water was applied to consolidate the sample, and then were wrapped in aluminum foil.

Sampling spacing was not regular, varying between 1 m to 6 m, depending on the outcrop conditions and the vertical variation of the different lithologies. In this way, 115 samples were taken at Serraduy log, including 6 samples in the marine Vallcarga Fm, 15 samples in the Aren Sandstone Fm, and 94 samples in the Tremp Fm (17 in the 'Grey Garumnian', 73 in the 'Lower Red Garumnian', and 4 in the 'Vallcebre limestone'). On the other hand, 106 levels were sampled at the Isclés section, of which 14 levels were from the Aren Sandstone Fm, 70 from the Tremp Fm, and 22 of the Cadí Alveoline-Limestone Fm. In the Tremp Fm, just a sample of each was extracted from the 'Grey Garumnian' and 'Vallcebre limestone' units respectively, since they are very thin at Isclés. By contrast, the sampling in the 'Lower Red Garumnian' (35 samples) and the 'Upper Red Garumnian' (33 samples) was more extensive, collecting a total of 68 samples between the two units. Besides, at the Isclés section, the magnetic susceptibility of the different lithologies was also measured, using a GF Instruments SM-20 magnetic susceptibility meter. In total, the susceptibility of 114 levels was measured.



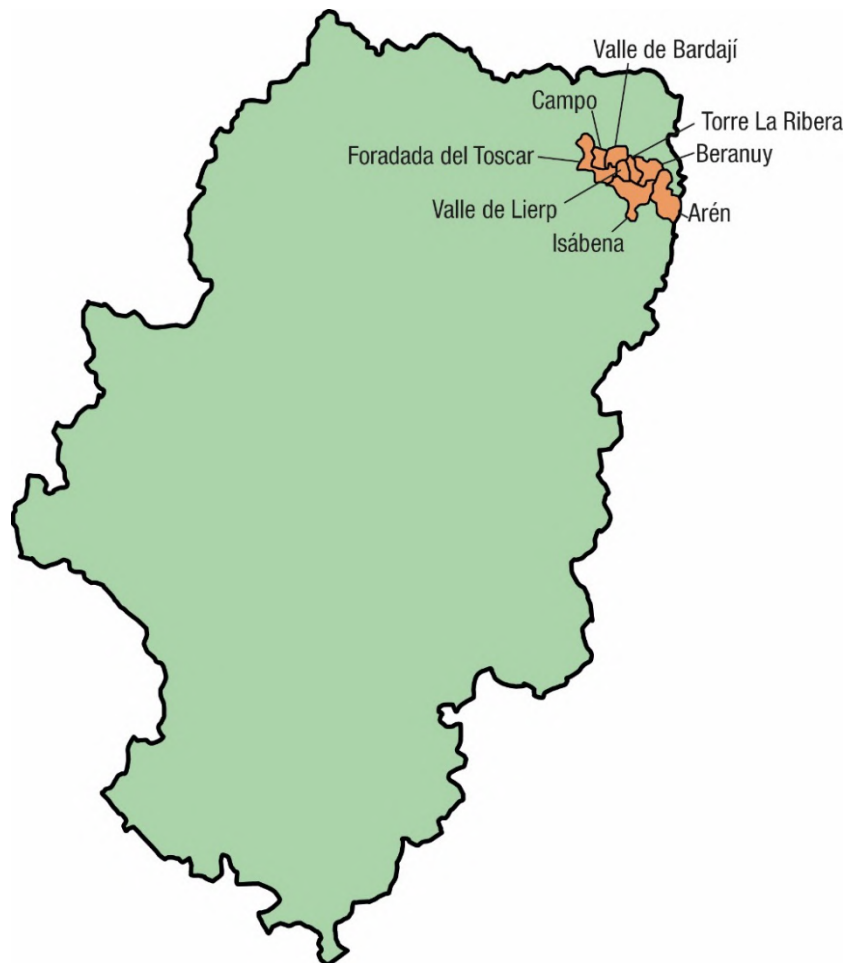
*Figure 3.2. A) Drilling red mudstones of the ‘Upper Red Garumnian’ at Isclés. B) Orienting in situ a drilled sample.*

### *3.1.3. Paleontological exploration*

According to the Law 3/1999 of Aragonese Cultural Heritage all fossils recovered in the Aragón region are considered as ‘paleontological heritage’, and thus have to be collected under exploration or excavation, to be later deposited in a public museum. The law also requires a yearly detailed report of the paleontological campaigns to be submitted to the Aragon Government. In this PhD thesis five exploration campaigns in the Tremp Fm were carried out between the years 2018 and 2022, with the institutional permits from the Aragón Government (Table 3.1). These paleontological campaigns allowed the discovery of 39 new paleontological sites (Table 3.1), with a total of 581 number of fossils and 20 microfossil samples. Several levels and outcrops with vertebrate tracks have been also found After each year of exploration, a detailed report has been submitted to the Aragon Government as it is required by law. Thereby, the territory of eight municipalities of the Ribagorza county have been prospected, including: Foradada del Toscar, Campo, Valle de Lierp, Valle de Bardají, Torre La Ribera, Beranuy, Isábena and Arén (Fig. 3.3).

Aragon Government file number	Exploration campaign director	New paleontological sites discovered	Number of fossils recovered	Sediment samples for microfossils
044/2018	Manuel Pérez Pueyo	20	324	6
044/18-2019	Manuel Pérez Pueyo	6	101	6
044/18-2020	Manuel Pérez Pueyo	4	66	8
044/18-20-21	Manuel Pérez Pueyo	9	70	0
044/18-2022	Manuel Pérez Pueyo	0	20	0
TOTAL	-	39	581	20

*Table 3.1. Summary of the exploration campaigns carried out in the Tremp Fm outcrops of the northern flank of the Western Tremp Syncline.*



*Figure 3.3. Location of the municipalities explored during this PhD within the territory of Aragón (Spain).*

Beside the discovering of new paleontological sites, the paleontological exploration also consisted in monitoring the already known paleontological sites discovered in previous works, to pick up any new fossil material exposed by washing and weathering of the rocks (Fig. 3.4 A-C).

For the proper location of the new paleontological sites discovered, a photographic documentation of the site and outcropping fossils and GPS location using ETRS-89 coordinate system as datum were performed. Then, as part of the prospection labor, all the fossils dispersed on the surface, or slightly showing up, are picked up, consolidating them with Paraloid B72 acrylic resin dissolved in acetone at 5-10% concentration. If the fossil shows a brittle state or need certain reinforcement to avoid its fracture, a protective film is made with rectangular pieces of gauze, consolidated with Paraloid B72 at 15% concentration (Fig. 3.2 D). Exploration also includes the sampling of levels of fine lithology, such as mudstones and marls, in order to check the richness in microfossils of those levels. The sample varied between 2 kg to 12 kg, depending on if it was the first sample taken or if the level was an already contrasted microfossil site.

All the information on the paleontological exploration was summarized in a data base created with File Maker Pro software, encompassing the geography, the geology (including the stratigraphic location), the faunal content and specific types of fossils of each paleontological site. This information was complemented by field and aerial photographs.



Figure 3.4. A) Picking up fossils exposed on the surface of the site El Castellaz 4. B) A coracoid of an hadrosauroid dinosaur found at Veracruz 3 site. C) A sauropod caudal vertebra found at Rin 1 site. D) Applying a film of gauze to a fragile bone at Amor 3 site.

#### 3.1.4. Paleontological excavation

The paleontological excavations were performed on the fossil sites discovered during exploration and prospection labors, with a particular emphasis on those showing good preservation, abundance or exceptionality of their fossils. Different kinds of excavations were carried out:

- Excavation of fossils on new and/or already know paleontological sites requiring emergency actions for collection and preservation of isolated but exceptional fossils which were at risk of suffering environmental weathering (Fig. 3.5). These fossils were swiftly excavated and protected appropriately previously to their stratigraphic and sedimentological setting characterization, to avoid their potential loss.



*Figure 3.5. Emergency excavation of a turtle shell from Larra 10 site.*

- Systematic paleontological excavation, following a thorough methodology. Just one fossil site has been excavated in that way: Larra 4, situated in Valle de Lierp municipality (Fig. 3.5 A, see Figs. 5.1 and 5.2 in Chapter 5 for stratigraphic location). In this site, the vertebrate remains appeared disarticulated, but well preserved; scattered in a discrete layer of intraclastic limestone. This site was previously prospected before the start of this PhD by members of Aragosaurus research team under Aragon Government exploration permit 115/2016. The excavation took place during a week in 2018, under the excavation permit 244/2018.

Firstly, a preliminary preparation of the dig site was carried out, setting up some reference points to create a system of coordinates for the cartography of the site. Because part of the fossiliferous level was partially covered by azoic carbonated sandstones, a jackhammer was used to remove those levels (Fig. 3.6 B), unearthing a larger surface of the fossiliferous level. The digging of the fossils was performed with screwdrivers, punches, chisels, and hammers, used to remove the sediment around the fossils and outline the fossils (Fig. 3.6 C). Paraloid B72 diluted in acetone and cellulose nitrate glue were used to consolidate and to paste broken fragments of the bones. All the fossils recovered were listed with a site number and referenced within the set cartesian

coordinate system before their extraction (Fig. 3.4 D), taking a triad of coordinates (X, Y, Z), including the relative depth of each fossil. The orientation of those fossils with an elongated shape was also registered, measuring the trend and plunge of their major axis.

For the extraction, those fossils that showed certain fragility, were reinforced by a film of gauze consolidated with concentrated paraloid B72, and once extracted, placed on cushioned packages. The excavation of Larra 4 site led to the recovery of 55 fossil remains of different vertebrates, decapod crustaceans and amber droplets. With all the data collected during the excavation, a map of the site was sketched, appearing on it the position of the fossils and the main structures (sedimentary and tectonic) recognized at the site (Fig. 3.7).

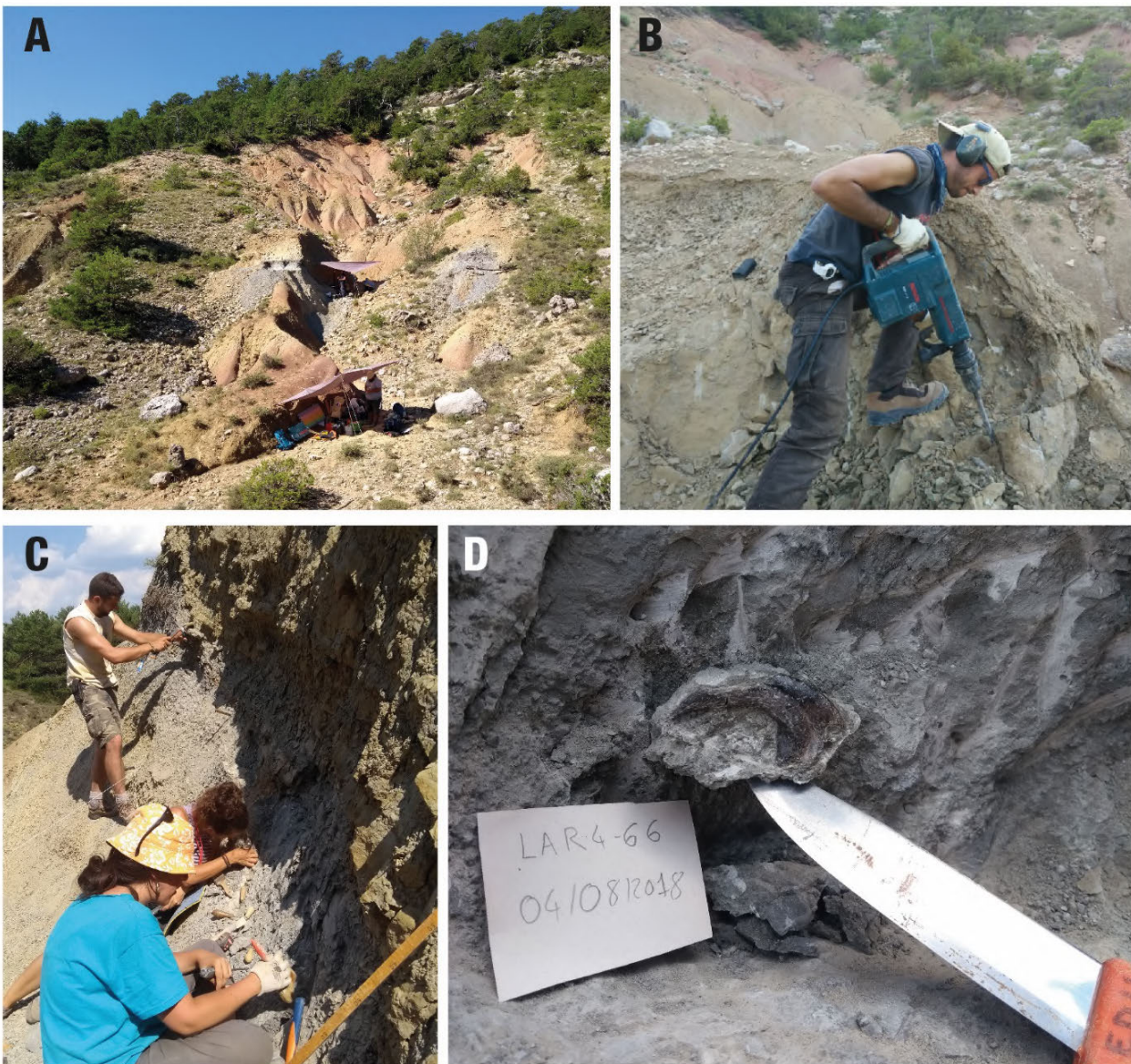


Figure 3.6. (previous page). Paleontological excavation of Larra 4 site. A) General view of the site during 2018 campaign. B) Removal of the azoic coverage with a jackhammer. C) Some of the excavation team members working on Larra 4 site. D) A theropod ungual phalanx with its site number before being extracted.

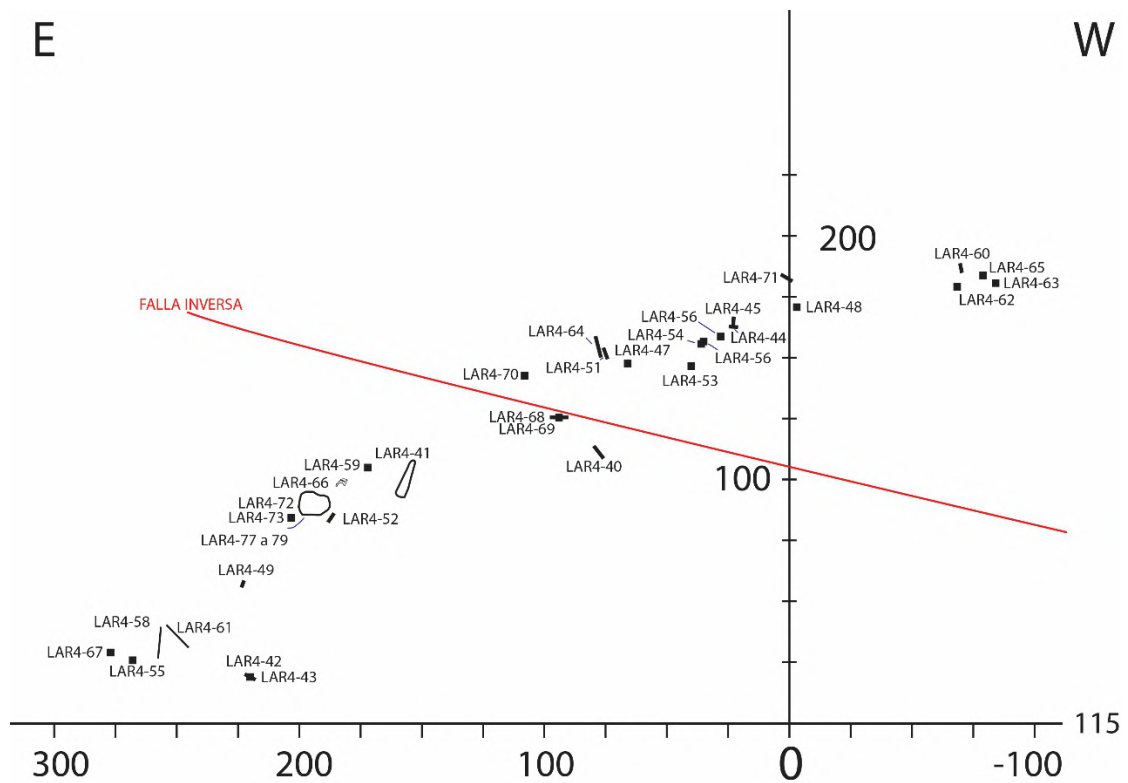


Figure 3.7. Map of Larra 4 site sketched during the excavation campaign of 2018. Scale bar is set in cm.

### **3.2. Laboratory work**

#### **3.2.1. Macrofossil preparation**

All fossils recovered during the exploration and excavation campaigns were prepared in the laboratory using conventional techniques of fossil preparation. Firstly, the protective packaging and the gauze film of each fossil was removed, as well as the glues applied at the field and the superficial dirt. For this, acetone was carefully applied with a small pencil or a hyssop. Once the fossil was cleaned, it was again consolidated with a new layer of Paraloid B72. Fossil preparation included mechanic preparation and/or chemical preparation, depending on the lithology in which the fossil was hosted and the status of the fossil, being the most common situation the use of both techniques.

- Mechanical preparation consists of the removal of the rock surrounding the fossil using different tools such as an air scribe (Fig. 3.8), a punch or a scalpel. Little by little, the matrix is removed, making the sediment let loose and individualization the fossil. If the fossil broke during preparation or some parts needed to be joined, concentrated Paraloid B72 (around 20-25%) was used to glue them.
- Chemical preparation was mainly used for fossils held in carbonate samples. Firstly, those parts of the fossil visible on the surface of the sample were protected with several layers of concentrated Paraloid B72 (20-25%). After that, the sample was submerged around 6 to 8 hours in a solution of acetic acid diluted in water at 10%-15% (cleaning vinegar has been also used) and placed under a fume hood. After this bath, the sample was extracted and cleaned with water to neutralize the acid. In some cases, this bathing process was repeated several times until the fossil could be extracted from the sample. Alternatively, some samples were later prepared using the mechanical removal of already weakened rock matrix. At the end of the process, it is very important to check that the acid has been neutralized correctly and to consolidate the fossil again.



*Figure 3.8. A) Using an air incisor for the removal of rock of a sandstone sample. B) Detail of the sample, with a partially cleaned dinosaur bone.*

Once the preparation is done, the fossil is marked with an acronym and packed for storage and transport. For delicate fossils, custom foam boxes are used, cutting the foam to adjust to the shape of the fossil, avoiding thus any type of movement of the fossil within the box. All the fossils were or will be deposited in the Museo de Ciencias Naturales de la Universidad de Zaragoza (Canudo, 2018).

### *3.2.2. Microfossil preparation*

Sediment samples picked at the field to recover microfossils were processed at the laboratory using the following procedure. All samples were disaggregated in a solution of water and hydrogen peroxide ( $H_2O_2$ ) for a period between 4 and 12 hours, depending on the sample. Then they were washed and wet-sieved with mesh sieves of 2000, 1000, 500  $\mu m$ . Additionally, a 100  $\mu m$  sieve was exclusively used for the samples collected from the Veracruz 1 site, in order to recover foraminifera and small charophyte gyrogonites. Once the sediment was cleaned, the residue was finally oven-dried at 50°C for 24 hours. The picking of the microfossils was performed using a Motic SMZ-140 binocular microscope (Fig. 3.9). The residue of the sediment of each sample was poured little by little in a plate, and sorted with a fine-bristled brush, picking the microfossils found between the sediment grains. Foraminifera, charophytes, vertebrate bones and eggshell fragments were the four main types of microfossils picked up.

Small samples (1-2 kg) were used to check the richness of microfossils of the different facies, meanwhile bigger samples (10-12 kg) were used to develop a detailed study of the microfossil association of Veracruz 1 site.



*Figure 3.9. Picking microfossils from sieved sediment using a binocular microscope.*

### *3.2.3. Optical microscopy of rock samples and eggshells*

Optical microscope was used both for a more detailed characterization of the texture and components of rock samples and the analysis of cristalographic features of fossil eggshells. The rock samples and the eggshell fragments were cut into 20  $\mu\text{m}$ -thick thin sections. In the case fragile rock samples and the eggshells, an embedding in epoxy resin was done previously to cut them. This process was carried out by the 'Servicio de Preparación de Rocas y Materiales Duros' (Rock and Hard Materials Preparation Service) which belongs to the SAI 'Servicio de Apoyo a la Investigación' (Research Support Service) of the Universidad de Zaragoza of Zaragoza.

Thin section observations were performed with an Olympus BX53M petrographic microscope equipped with an Olympus DP27 digital camera (Fig. 3.10.), housed in the

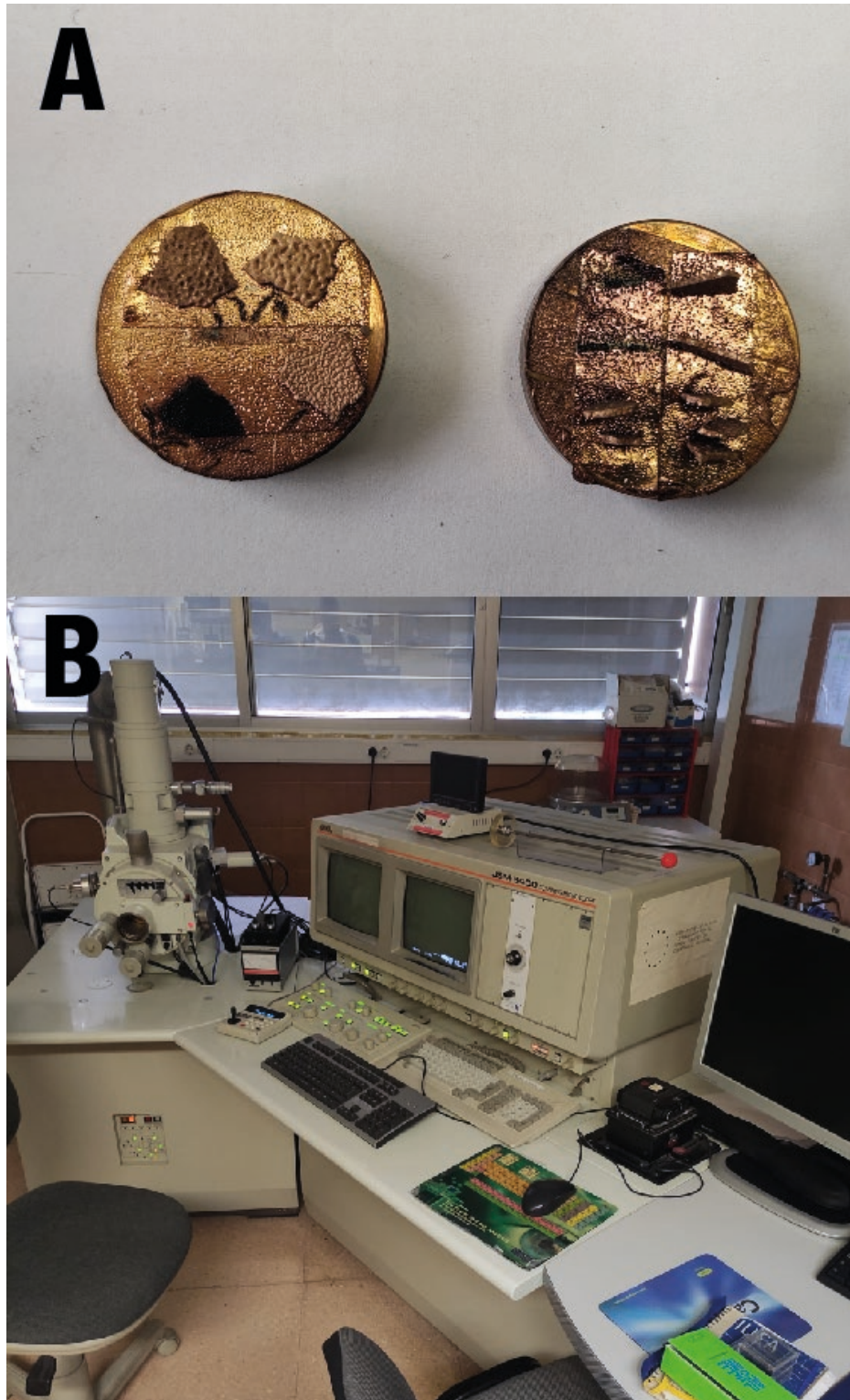
IUCA 'Instituto Universitario de Ciencias Ambientales' (University Institute of Environmental Sciences) (IUCA) of the Universidad de Zaragoza. Pictures of the thin sections were taken with the camera of the microscope. Besides, thin sections of rock samples were also scanned using a photographic negative scanner, with the aim of obtain high resolution images.



*Figure 3.10. Olympus BX53M petrographic microscope housed at the IUCA of Universidad de Zaragoza.*

#### *3.2.4. Scanning electron microscope analysis*

Some of the microfossils recovered were prepared for their observation and characterization using a Scanning Electron Microscope (SEM). Most of the microfossils were previously cleaned with an ultrasound bath for a period between 1 min to 15 min, depending on the type of fossil and were dried later. Then, the fossils were mounted on a circular holder, which was previously covered with several stripes of carbon tape. Before entering the samples in the microscope, they were coated with a powdered metal in vacuum, to make their surface conductive (Fig. 3.11 A). All the samples were coated with gold, except those ones that were observed at the Universidade Nova de Lisboa, which were covered with iridium. The main SEM used was a JEOL JSM 6400 housed at 'Servicio de Microscopía Electrónica de Materiales' (Electron Microscopy of Materials Service) of the Universidad de Zaragoza of Zaragoza (Fig. 3.11 B). Punctually, a XXX SEM was also used at the Departamento de Engenharia Mecânica e Industrial (Department of Mechanical and Industrial Engineering) of the Universidade Nova de Lisboa, in Portugal.



*Figure 3.11. A) Fossil eggshells mounted and coated with gold for SEM observation. B) JEOL JSM 6400 SEM microscope housed at 'Servicio de Microscopía Electrónica de Materiales' of Universidad de Zaragoza.*

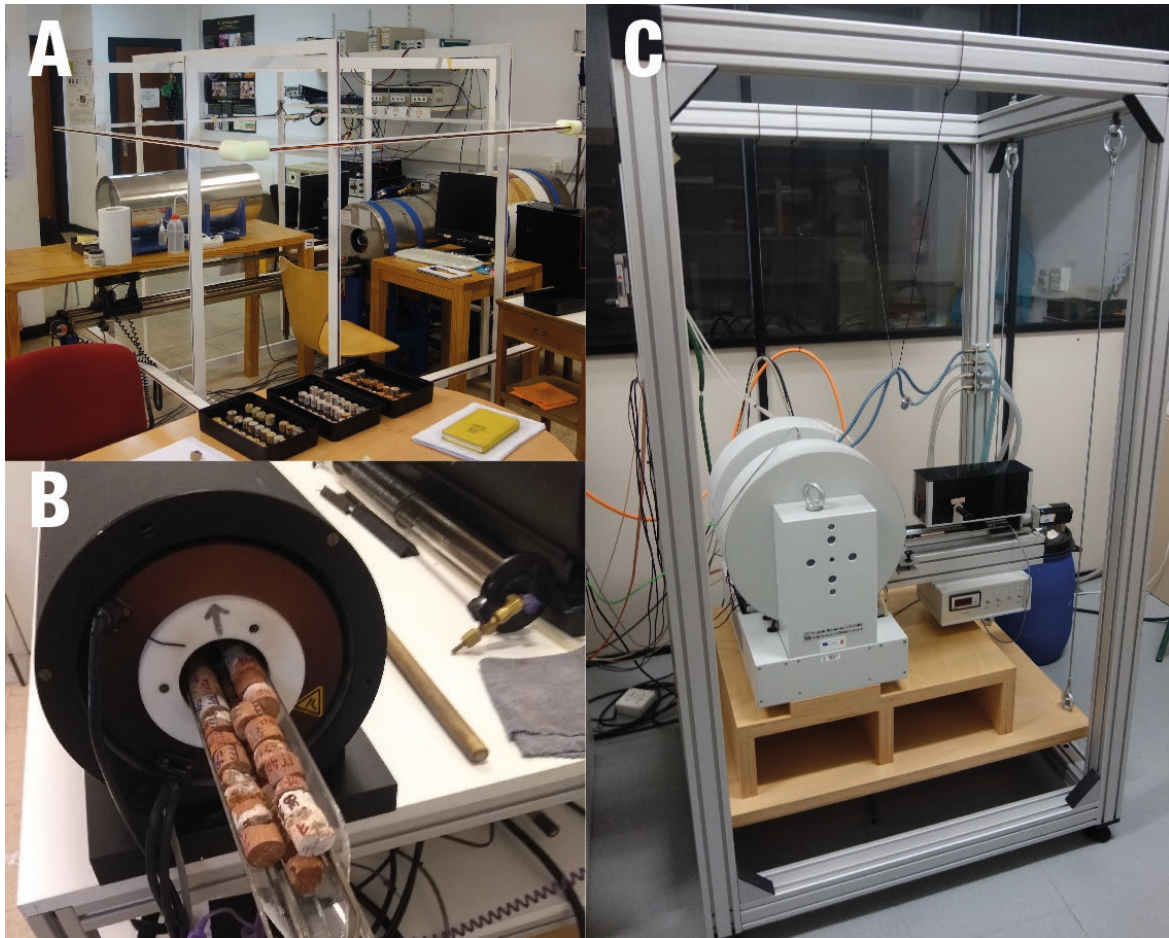
### **3.2.5. Laboratory treatment of magnetostratigraphic samples**

Samples were prepared following the methodology of Pueyo et al. (2006), first consolidating them with a solution of sodium silicate, and using aluminum cement for fracture repair. After that, they were cut with a non-magnetic saw in two or three subsamples, as a function of the size of the original sample cylinder.

The paleomagnetic analysis of the samples collected at Serraduy and Isclés were carried out in the paleomagnetic laboratory of the University of Burgos. Both, stepwise thermal (TH) and alternating field (AF) demagnetization were applied aiming to separate all magnetic components present in the sampled rocks, using a TD48-DC (ASC) oven and a LDA3 (Agico) alternating field demagnetizer (Fig. 3.12 A, B).

Different procedures were used for the two sections analyzed. The 198 samples taken in the Serraduy log were demagnetized with different stepwise temperatures and applied alternating fields according to the sample lithology. 145 of these were Th-demagnetized, heating up to 400-575 °C for marls, sandstones, calcarenites and limestones and up to 475-675 °C for mudstones (several samples of all lithologies were heated up to 675 °C in order to check their magnetic behaviors). In addition, 39 samples were demagnetized by automatic Alternating Field (Af), 14 with manual Af trying to improve the accuracy of the method, and an Af protocol with an initial thermal step of 130 °C to delete the part of the signal carried by goethite (all Af up to 100 mT). From the 121 samples of the Isclés log, 100 samples were Th-demagnetized (6 of them were lost during preparation), being heated successively up to 650-680 °C not considering the different lithologies. The remaining 21 samples were subjected to automatic Af demagnetization.

In addition, rock-magnetic experiments including hysteresis loops ( $H_c$ ,  $J_s$  and  $J_{rs}$ ), backfield curves ( $H_{cr}$ ), and thermomagnetic loops were carried out at the University of Burgos with a variable field translation balance (VFTB) (Fig. 3.12 C). Powdered whole-rock specimens from all lithologies were underwent to experiments on IRM acquisition and backfield curves, hysteresis loops and strong field magnetization versus temperature ( $M_s$ - $T$ ) curves. A total of 20 samples (14 from the Serraduy section, 6 from Isclés section) were analyzed. Analyses of these measurements were performed with RockMagAnalyzer 1.0 software (Leonhardt, 2006).



*Figure 3.12. A) Superconducting magnetometer used for the demagnetization of the samples, housed at the Universidad de Burgos. B) Sample introduction into the oven for their demagnetization. C) Variable field translation balance used for additional magnetic measures housed at the Universidad de Burgos.*

### 3.2.6. Micro-CT scan

One of the fossils studied in this PhD thesis (a bird cervical vertebra, MPZ 2019/264) was scanned with a micro-CT scan, with the aim of characterizing its inner pneumatic cavities. The micro computed tomography was carried out using a GE V|Tome|X scanner at the CENIEH (Centro Nacional de Investigación sobre la Evolución Humana, Burgos, Spain). To examine the internal features of the vertebra, the images obtained from the scanner were processed using Dragonfly software (Version 4.1, Object Research Systems (ORS) Inc., Montreal, Canada, 2018; software available at <http://www.theobjects.com/dragonfly>).

### **3.3. Data treatment and interpretation**

Field and laboratory data were compiled and interpreted. This includes search and compilation of bibliographic sources; the inventory, digitalization and processing of data, the study of the fossils and the sedimentary facies or the generation of graphic support to illustrate the research.

Most of the data processing consisted in the creation and organization of different databases. The management of most of the field and laboratory data has been carried using software such as Microsoft Excel, File Maker Pro and Google Earth. The organized data are very diverse in nature, such as the geographic location of fossil sites, the typology of recovered fossils, the stratigraphic location of the sedimentological and magnetostratigraphic samples, or field photographs. The representation of data and other graphic support has been created using software from Adobe (Illustrator and Photoshop). It has consisted of drawings, sketches and photo montages of fossils, outcrops or sedimentary features.

#### **3.3.1. Stratigraphic-sedimentological data**

Field and laboratory data allowed the differentiation of facies based on their particular sedimentary features (mainly lithology, color, texture, components and sedimentary structures). Duhham (1962) classification was used for textural characterization of facies. Terrigenous-clastic facies were classified following Folk (1980) size-classes. Flügel (2010) were used for the identification of components in thin sections. Lateral and vertical relations of the different lithological units and facies have been studied, as well as their architecture.

#### **3.3.2. Magnetostratigraphic data**

Evaluation of the demagnetization diagrams and the estimation of the characteristic remanent magnetization (ChRM) directions was done using the Virtual Paleomagnetic Directions (VPD) (Ramón et al., 2017) and the Remasoft (Chadima and Hrouda, 2006) software packages. ChRM directions were fitted using standard principal component analysis (Kirschvink, 1980), although, demagnetization circles (Bailey and Halls, 1989),

stacking routine (Scheepers and Zijdeveld, 1992), linearity spectrum analysis (Schmidt, 1982) and the virtual directions methods (Pueyo, 2000; Ramón & Pueyo, 2012; Ramón, 2013) were also applied with the VPD software. Fisher (1953) and Bingham (1974) statistics were applied to obtain the section mean using the stereonet software (Allmendinger et al., 2012).

Due to the scattered paleomagnetic signal and focusing on avoiding unnecessary noise, characteristic remanent magnetization (ChRM) direction was classified in three quality groups: class I samples addressing to the origin, class II poorer directions with an unambiguous polarity, class III includes the remaining set (the worst dataset not used in further calculation; neither profile means nor for the VGP profile construction).

### 3.3.3. *Paleontological data*

Several fossils, including vertebrate bones, eggshell fragments, invertebrates and microfossils were studied using different approaches. The study of vertebrate macrofossils consisted in the description and measurement of anatomical dimensions, and taxonomic determination based on the comparison with those described from the bibliography. The anatomical description of the fossils was carried out using the nomenclature usually used in works of vertebrate paleontology: Baumel and Witmer (1993) to describe the main anatomical features; Britt (1997, 1993) to describe the internal pneumatic cavities, taking into account also the recommendations from other authors for vertebral laminae and pneumatic fossae (Wedel et al., 2000; Wilson, 1999; Wilson et al., 2011b). Those macrofossils which were especially relevant were photographed with a Nikon D7100 digital camera with a macro-60-mm-lens, sometimes using a sublimated ammonium chloride cover to accentuate relevant morphological features. Besides, a cladistic analysis was performed for the cervical vertebra MPZ 2019/264, to analyze its phylogenetic affinities. It was included in two different datasets (Cau, 2018; Wang et al., 2020), which were edited using Mesquite V.3.31 (Maddison and Maddison, 2017) and analyzed using TNT v.1.5 (Goloboff and Catalano, 2016).

Microfossils and eggshell fragments were described by direct observations in transmitted light and SEM microscopes, meanwhile measurements were taken on the images obtained by microscopy, using the software Image J. Eggshell thickness were measured with a digital caliper. For the study of charophyte fructifications, at least 100 gyrogonites (when it was possible) per taxa were measured, with the aim of characterize

properly the shape variation of each morphotype, based on stable mean measures (Soulié-Märsche and Joseph, 1991). The description of fossil eggshell fragments was done using the terminology proposed by Mikhailov (1991, 1997) (Fig. 3.13), describing the macrostructure, the histostructure and the ultrastructure of the eggshell by combined use of SEM and transmitted polarized light microscope images. For crocodylomorph eggshells some specific terms were used after Hirsch (1985) and Moreno-Azanza et al. (2014). The main macrostructural features described were shell thickness, outer ornamentation, and pore patterns. Meanwhile, histostructural features included shell unit type, shell unit size, pore canal system, mammilla shape and size, and the type of basal plate group. The ultrastructure of the eggshell (arrangement mode of crystalline and organic elements of the shell) was also analyzed. With the main histo- and ultrastructural features, a structural morphotype for the eggshell can be assigned.

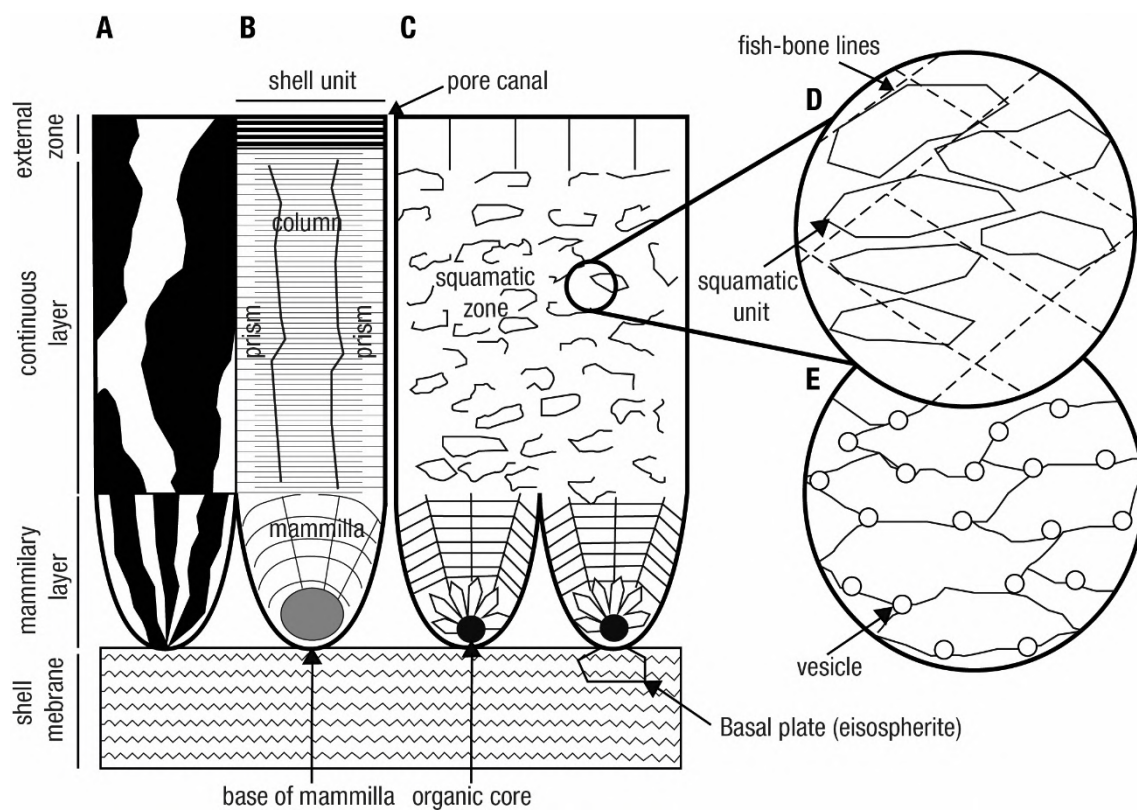


Figure 3.13. General terminology of eggshell structure based on the avian eggshell. Sketch drawings of real view seen in radial section: A) under transmitted polarized light microscope; B) under light microscope; C) under SEM; D) 'fish-bone pattern' superimposed on a pattern of the squamatic shell units; E) organic matrix consisting of large membranes, fine fibrils and vesicles (modified after Mikhailov, 1997).

Besides the paleontological analysis based on bibliography, the visits to two paleontological centers for comparison purposes were conducted. The aim of these collection visits was to examine their fossil material and compare with the specific fossils obtained during this PhD thesis: the institutions Musée de l'Association Culturelle, Archéologique et Paléontologique de l'Ouest Biterrois in Cruzy (Hérault, Occitania, France) and the Musée des Dinosaurés in Espéraza (Aude, Occitania, France) were visited. In particular, these short research stays were focused on the fossil remains of the enigmatic Maastrichtian giant bird *Gargantuavis* and the dromaeosaur dinosaur *Variraptor*.

### **3.3.4. Official reports**

Finally, another task performed during this PhD has been the fulfillment of abundant bureaucratic documents, to meet administrative obligations with several official organisms related to the completion of this doctoral thesis. In this way near **180** documents have been fulfilled, including progress reports, paleontological permit applications and field campaign reports, research stay documents, CVs, teaching planning documents, per diem forms, grant applications, and other documents of similar nature. Though this work is not directly related to the scientific topic of this PhD, it is time consuming, and it is important to show that it was part of the PhD candidate work.

## **3.4. Paleontological material**

All the fossil material studied and published during this PhD has been collected in the Tremp Fm outcrops of the Ribagorça county (Huesca, Aragón, NE Spain) under exploration or excavation permits of the Aragón Government, and thus it is deposited in the Museo de Ciencias Naturales de la Universidad de Zaragoza (Table 3.2). It is important to note that the material recovered during field campaigns is very abundant, with around 580 vertebrate fossils, and not considering microfossils. For this reason, not all the fossils recovered have been studied, since there are some of them that are still under preparation, and thus they have not been studied nor published. In Table 3.3. are listed those fossils that has been studied for this PhD, but not published yet, all coming from the Veracruz 1 site. A great amount of material has been studied superficially for the classification of taphonomic modes and record.

## Material and methods

Museum acronym	Material	Taxonomy	Paleontological site	Publication
MPZ 2018/17	Swimming tracks	Crocodylomorpha	Beranuy	Pérez-Pueyo et al., 2018
MPZ 2019/182	Caudal vertebra	Hadrosauridae indet.	Larra 4	Pérez-Pueyo et al., 2019
MPZ 2019/183	Maxilla fragment	Hadrosauridae indet.	Larra 4	Pérez-Pueyo et al., 2019
MPZ 2019/184	Tooth	cf. Allodaposuchidae	Larra 4	Pérez-Pueyo et al., 2019
MPZ 2019/185	Tooth	cf. Allodaposuchidae	Larra 4	Pérez-Pueyo et al., 2019
MPZ 2019/186	Tooth	cf. Allodaposuchidae	Larra 4	Pérez-Pueyo et al., 2019
MPZ 2019/187	Tooth	cf. Allodaposuchidae	Larra 4	Pérez-Pueyo et al., 2019
MPZ 2019/188	Tooth	cf. Allodaposuchidae	Larra 4	Pérez-Pueyo et al., 2019
MPZ 2019/189	Tooth	Theropoda	Larra 4	Pérez-Pueyo et al., 2019
MPZ 2019/190	Tooth	cf. Allodaposuchidae	Larra 4	Pérez-Pueyo et al., 2019
MPZ 2019/191	Fragment of neural spine	Hadrosauridae indet.	Larra 4	Pérez-Pueyo et al., 2019
MPZ 2019/192	Osteoderm	Eusuchia	Larra 4	Pérez-Pueyo et al., 2019
MPZ 2019/193	Shell plates fragments	Bothremydidae indet.	Larra 4	Pérez-Pueyo et al., 2019
MPZ 2019/194	Distal end of right ulna	Theropoda Dromaeosauridae?	Larra 4	Pérez-Pueyo et al., 2019
MPZ 2019/195	Chevron	Hadrosauridae indet.	Larra 4	Pérez-Pueyo et al., 2019
MPZ 2019/196	II ungual phalanx	Dromaeosauridae	Larra 4	Pérez-Pueyo et al., 2019
MPZ 2019/197	Shell plate	Bothremydidae indet.	Larra 4	Pérez-Pueyo et al., 2019
MPZ 2019/198	Large bone shard	Indeterminate	Larra 4	Pérez-Pueyo et al., 2019
MPZ 2019/199	Long bone fragment	Dinosauria	Larra 4	Pérez-Pueyo et al., 2019
MPZ 2019/200	Tooth	cf. Allodaposuchidae	Larra 4	Pérez-Pueyo et al., 2019
MPZ 2019/201	Caudal neural spine	Hadrosauridae indet.	Larra 4	Pérez-Pueyo et al., 2019
MPZ 2019/202	Long bone fragment	Indeterminate	Larra 4	Pérez-Pueyo et al., 2019
MPZ 2019/203	Proximal end of rib	Dinosauria	Larra 4	Pérez-Pueyo et al., 2019
MPZ 2019/204	Distal end of femur	Hadrosauridae?	Larra 4	Pérez-Pueyo et al., 2019
MPZ 2019/205	Atlas	Hadrosauridae indet.	Larra 4	Pérez-Pueyo et al., 2019
MPZ 2019/206	Anterior caudal vertebra	Hadrosauridae indet.	Larra 4	Pérez-Pueyo et al., 2019
MPZ 2019/207	Anterior caudal vertebra	Hadrosauridae indet.	Larra 4	Pérez-Pueyo et al., 2019

## Material and methods

MPZ 2019/208	Posterior caudal vertebra	Hadrosauridae indet.	Larra 4	Pérez-Pueyo et al., 2019
MPZ 2019/209	Posterior caudal vertebra	Hadrosauridae indet.	Larra 4	Pérez-Pueyo et al., 2019
MPZ 2019/264	Cervical vertebra	Ornithuromorpha indet.	Dolor 2/3	Pérez-Pueyo et al., 2021b
MPZ2021/1	Posterior caudal vertebra	Titanosauria indet	Barranco Serraduy 4	Pérez-Pueyo et al., 2021a
MPZ 2021/54	Phalanx fragment?	Pterosauria indet.	Blasi 5	Pérez-Pueyo et al., 2021a
MPZ 2022/268	Eggshell fragment (holotype)	<i>Pachykrokolithus excavatum</i> (crocodylomorph eggshell)	Veracruz 1	Moreno-Azanza et al., 2022
MPZ 2022/252 to 277	26 eggshell fragments (gold coated)	<i>Pachykrokolithus excavatum</i> (crocodylomorph eggshell)	Veracruz 1	Moreno-Azanza et al., 2022
MPZ 2022/278 to 283	6 thin sections with eggshells	<i>Pachykrokolithus excavatum</i> (crocodylomorph eggshell)	Veracruz 1	Moreno-Azanza et al., 2022
MPZ 2022/286 to 569	284 eggshell fragments	<i>Pachykrokolithus excavatum</i> (crocodylomorph eggshell)	Veracruz 1	Moreno-Azanza et al., 2022
MPZ 2013/20 to 31	13 eggshell fragments	<i>Pachykrokolithus excavatum</i> (crocodylomorph eggshell)	Blasi 2B	Moreno-Azanza et al., 2022
MPZ 2022/284	1 eggshell fragment	<i>Pachykrokolithus excavatum</i>	127-i/04/e	Moreno-Azanza et al., 2022
MPZ 2022/284	1 eggshell fragment	(crocodylomorph eggshell)	Areny 1 site	Moreno-Azanza et al., 2022

Table 3.2. Studied vertebrate fossil material which have been already published during this PhD.

## Material and methods

Material	Clade	Taxonomy	Number of specimens	Paleontological site
Test	Foraminifera	<i>Heterohelix globulosa</i>	3	Veracruz 1
Test	Foraminifera	<i>Heterohelix planata</i>	3	Veracruz 1
Test	Foraminifera	<i>Heterohelix labellosa?</i>	1	Veracruz 1
Test	Foraminifera	<i>Guembelitra cretacea</i>	1	Veracruz 1
Test	Foraminifera	<i>Guembelitra blowi</i>	1	Veracruz 1
Test	Foraminifera	<i>Globotruncana mariei?</i>	1	Veracruz 1
Test	Foraminifera	<i>Globotruncana linneiana</i>	1	Veracruz 1
Charcoal wood fragments	Pinopsida	Pinopsida indet.	85	Veracruz 1
Gyrogonites	Charophyta	<i>Feistiella malladae</i>	2	Veracruz 1
Gyrogonites	Charophyta	<i>Lychnothamnus begudianus</i>	19	Veracruz 1
Gyrogonites	Charophyta	<i>Peckichara sertulata</i>	110	Veracruz 1
Gyrogonites	Charophyta	<i>Peckichara llobregatensis</i>	65	Veracruz 1
Gyrogonites	Charophyta	<i>Platychara</i> sp.	300 (105 measured)	Veracruz 1
Gyrogonites	Charophyta	<i>Microchara cristata</i>	116	Veracruz 1
Gyrogonites	Charophyta	<i>Microchara punctata</i>	12	Veracruz 1
Gyrogonites	Charophyta	<i>Microchara nana</i>	22	Veracruz 1
Gyrogonites	Charophyta	<i>Lamprothamnium</i> sp.	4	Veracruz 1
Incrustant bryozoan	Bryozoa	Bryozoa indet.	4	Veracruz 1
Incrustant serpulids	Annelida	Serpulidae indet.	Not counted	Veracruz 1
Inner casts	Mollusca, Bivalvia	<i>Corbicula laletana</i>	6	Veracruz 1
Shells	Mollusca, Bivalvia	<i>Anomia</i> sp.	6	Veracruz 1
Shells	Mollusca, Bivalvia	<i>Saccostrea elhuyari</i>	10	Veracruz 1
Calcified syphons	Mollusca, Bivalvia	<i>Teredo?</i>	16	Veracruz 1
Shells	Mollusca, Gastropoda	<i>Melanopsis</i> sp.	26	Veracruz 1
Shells	Mollusca, Gastropoda	<i>Cerithium</i> sp.	9	Veracruz 1
Shells	Mollusca, Gastropoda	<i>Pyrgulifera saginata</i>	1	Veracruz 1
Shells	Mollusca, Gastropoda	<i>Pyrgulifera stillans</i>	59	Veracruz 1
Shells	Mollusca, Gastropoda	Physidae indet.	1	Veracruz 1
Shells	Arthropoda, Ostracoda	Ostracoda indet.	3	Veracruz 1
Coprolites	Arthropoda, Insecta	<i>Microcarpolithes hexagonalis</i>	Not counted	Veracruz 1
Mobile and fixed fingers	Arthropoda, Decapoda	Decapoda indet. morphotype 1	32	Veracruz 1
Mobile and fixed fingers	Arthropoda, Decapoda	Decapoda indet. morphotype 2	9	Veracruz 1
Scales, hemitrichia and teeth	Osteichthyes	Lepisoteidae indet.	15	Veracruz 1
Scales	Osteichthyes	<i>Lepisosteus</i> sp.	3	Veracruz 1

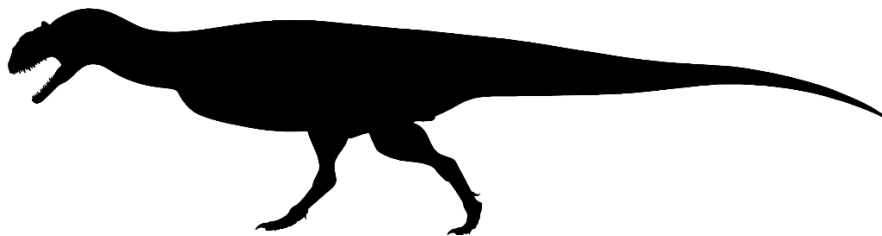
## Material and methods

Tooth	Osteichthyes	Amiidae?	1	Veracruz 1
Tooth	Osteichthyes	<i>Paralbula</i> sp.	1	Veracruz 1
Tooth	Osteichthyes	<i>Pseudoeogertonia</i> ?	1	Veracruz 1
Teeth	Osteichthyes	<i>Phyllodus</i> sp.	2	Veracruz 1
Tooth	Osteichthyes	Actinopterygii indet.	1	Veracruz 1
Premaxilla?	Amphibia	Albanerpentotidae indet.	1	Veracruz 1
Shell plates	Testudines	Bothremydidae indet.	27	Veracruz 1
Eggshell fragments	Testudines	Testudoolithidae indet.	Not counted	Veracruz 1
Teeth	Crocodylomorpha	Allodaposuchidae indet. morphotype 1	33	Veracruz 1
Teeth	Crocodylomorpha	Allodaposuchidae indet. morphotype 2	9	Veracruz 1
Tooth	Crocodylomorpha	cf. <i>Allodaposuchus palustris</i>	1	Veracruz 1
Osteoderms	Crocodylomorpha	Eusuchia indet.	2	Veracruz 1
Eggshell fragments	Crocodylomorpha	Krokolithidae indet.	Not counted	Veracruz 1
Tooth and bones	Dinosauria, Ornithopoda	Hadrosauroidea indet.	11	Veracruz 1
Tooth	Dinosauria, Theropoda	cf. <i>Richardoestesia</i> sp.	1	Veracruz 1
Eggshell fragments	Dinosauria, Theropoda	Prismatoolithidae indet.	Not counted	Veracruz 1
Eggshell fragments	Dinosauria, Theropoda	<i>Pseudogeckoolithus</i> sp.	Not counted	Veracruz 1
Bones	Dinosauria	Dinosauria indet.	3	Veracruz 1
Bones	Vertebrata	Vertebrata indet.	29	Veracruz 1

Table 3.3. Studied vertebrate fossil material from Veracruz 1 site, not published during the PhD.

# **Chapter 4.**

## **Geographic and geological setting**





## Chapter 4: Geographic and geological setting

The upper Maastrichtian (Upper Cretaceous) successions studied in this PhD thesis crop out in Ribagorza, a small county of the Huesca province in the autonomous region of Aragón (NE of Spain). Geologically, these outcrops are part of the north flank of the Tremp Syncline, located in the South-Central Pyrenees (South-Pyrenean Central Unit *sensu* Séguret, 1972).

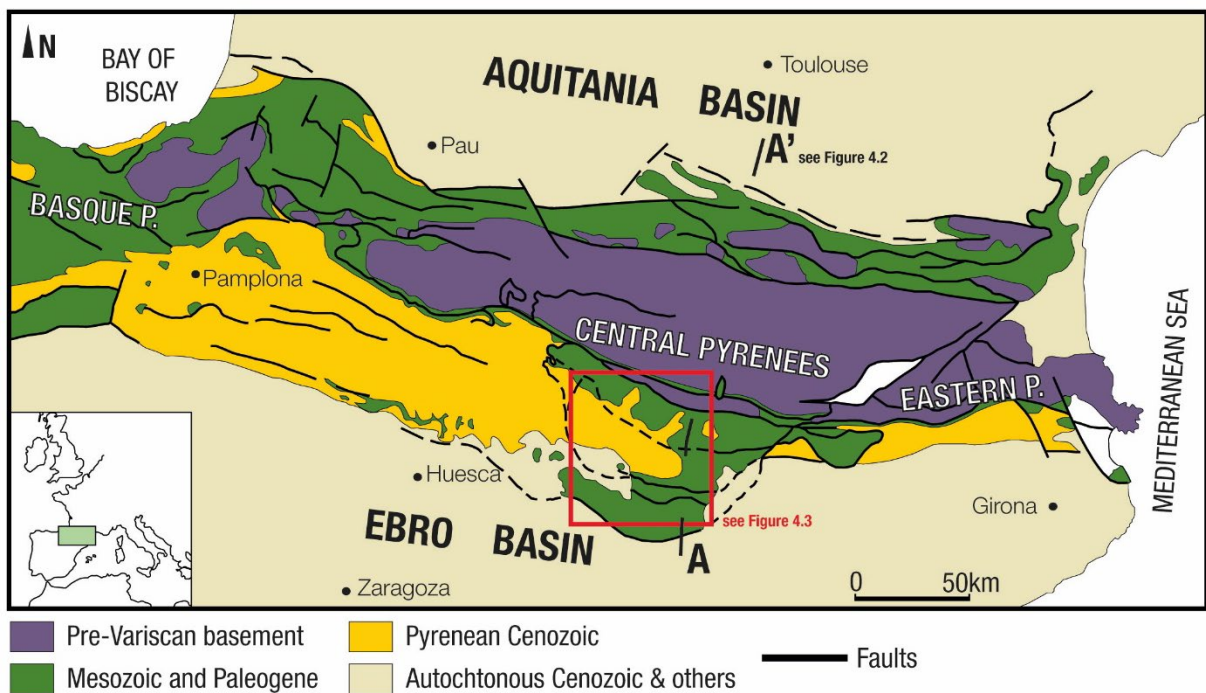
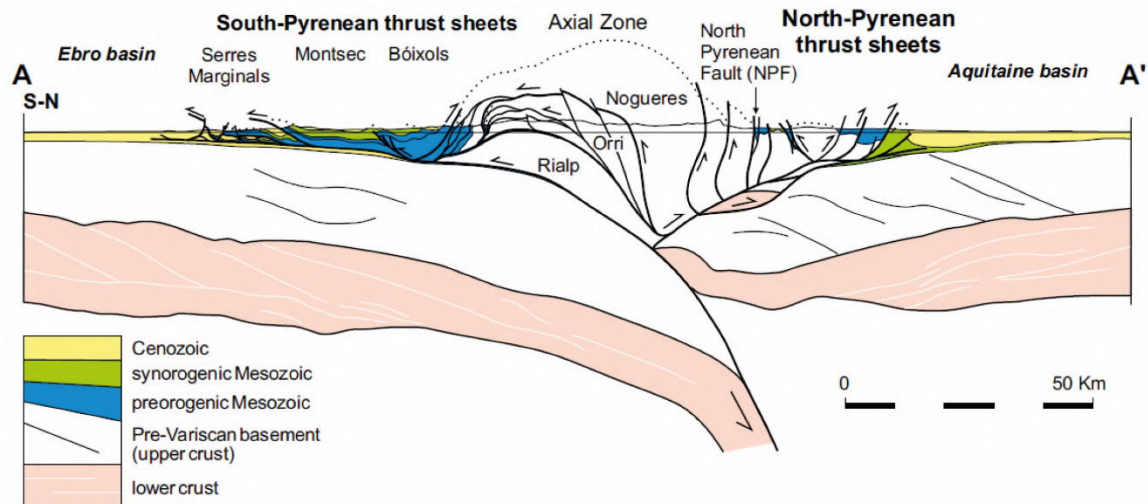


Figure 4.1. General geologic map of the Pyrenees (adapted from Muñoz et al., 2018).

The Pyrenees is a NNW-SSE-oriented collision range located in the northeast of the Iberian Peninsula, between Spain and France (Fig. 4.1). It is structured as an asymmetric fold and thrust belt with double vergence (NE-SW) (Fig. 4.2), being the result of the collision between the European and the Iberian plates during the Alpine orogeny, between the end of the Cretaceous and the Miocene (Puigdefregas et al., 1986; Muñoz, 1992; Teixell, 1998, 2004; Sibuet et al., 2004). The thrust sheets of the orogen controlled the development of a series of foreland basins, parallel to the axis of the mountain range,

which were active in different tectonic stages and were later stacked in a piggy-back sequence (Choukroune, 1989; Muñoz, 1992; Chanvry et al., 2018; Muñoz et al., 2018) (Fig. 4.2). The South-Pyrenean Basin was one of these foreland basins, limited in the north by the Axial Zone and in the south by the Ebro Basin (Fig. 4.1). This South-Pyrenean Basin was active between the Late Cretaceous and the Oligocene, with marine, transitional and continental sedimentation, until the late Eocene when it became permanently a continental basin (Costa et al., 2010). In the South-Central Pyrenees, several synsedimentary synclines (Àger, Coll de Nargó, Tremp and Vallcebre) with Pyrenean orientation can be found, result of the activity of the different thrust sheets of the orogen (Cadí, Pedraforca, Boixolls, Montsec and Serres Marginals). The activity of these thrust sheets generated growth structures which acted as structural heights that compartmentalized the sedimentation in several subbasins (Teixell and Muñoz, 2000; Fondevilla et al., 2016; Gómez-Gras et al., 2016; Oms et al., 2016).

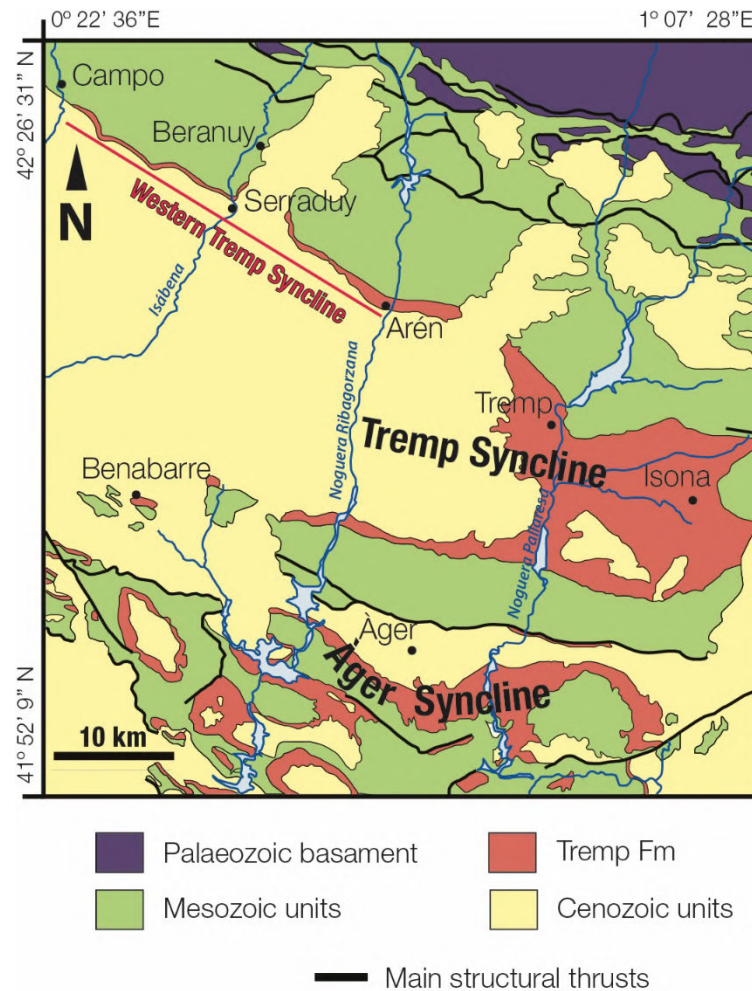


*Figure 4.2. Geological cross-section of the Central Pyrenees based on the deep seismic reflection data from ECORS (taken from Muñoz et al., 2018).*

The Tremp Syncline (also known as the Tremp-Graus Basin) is the largest of these subbasins. It is bounded in the north by the Boixolls thrust and in the south by the Montsec thrust (Fig. 4.3). Its sedimentary filling is constituted mainly by Upper Cretaceous marine sediments, although coeval to the latest Cretaceous global sea level fall (Miller et al., 2005), the basin was progressively filled with westward-prograding

turbiditic and deltaic sediments (Santonian-Maastrichtian) (Ardévol et al., 2000) and transitional and continental deposits (lower to upper Maastrichtian) (Gómez-Gras et al., 2016; Oms et al., 2016), lasting the continental sedimentation up to the Paleocene.

In the Tresp Syncline, the uppermost Cretaceous-lowermost Paleocene transitional and continental deposits consist of two closely related stratigraphic units, the Arén and Tresp formations (Figs. 4.3 and 4.4).



*Figure 4.3. Geological map of the western part of the South-Pyrenean Basin, focusing on the Tresp and Àger synclines (modified after López-Martínez and Vicens, 2012).*

The Arén Sandstone Fm, defined by Mey et al. (1968), is a middle Campanian–Maastrichtian transitional unit constituted by a thick succession of calcarenites with large-scale cross-bedding, composed mainly of quartz grains and

bioclasts (Nagtegaal et al., 1983). It represents deposition in different transitional sedimentary environments including delta (Mutti and Sgavetti, 1987), barrier-island (Nagtegaal, 1972; Nagtegaal et al., 1983) and beach deposits (Mutti et al., 1975; Díaz-Molina et al., 2007). These deposits overlay the marine sediments of the Vallcarga Fm and pass laterally and vertically to the Tresp Fm, interdigitating both units continuously throughout the basin (Díaz-Molina, 1987; Eichenseer, 1988; Ardévol et al., 2000) .

The Tresp Fm was also defined by Mey et al. (1968), although it is traditionally known in the Pyrenees as the 'Garumnian Facies' or 'Garum Facies' (Leymerie, 1868). It is a coastal to continental heterogeneous and diachronous lithostratigraphic unit that ranges between the Maastrichtian and the Paleocene. It shows a great variability of facies and thickness (between 400 to 30 m), as a consequence of its syntectonic sedimentation (Liebau, 1973; Eichenseer, 1988; Deramond et al., 1993; Ardévol et al., 2000). It can be subdivided into four minor lithostratigraphic units, which have received different names in the proposed stratigraphic subdivisions (Mey et al., 1968; Cuevas, 1992; Rosell et al., 2001; Pujalte and Schmitz, 2005; Oms et al., 2016) (Fig. 4.4). The scheme used here is that of Rosell et al. (2001), who divided the Tresp Fm into four informal units recognizable throughout the South-Pyrenean Basin. This division has been selected because it is the most useful for the area of study to differentiate lithostratigraphic units, since it avoids certain chronostratigraphic problems. Other divisions proposed are complicated to extrapolate to the area of study, since they were proposed in other areas of the basin (see justification at the end of the chapter).

The lowermost unit is the so-called 'Grey Garumnian', characterized by a succession of grey marls and mudstones, with intercalations of sandstones, limestones and coal beds and a rich fossil content of brackish and continental invertebrate faunas. It is interpreted as transitional deposits, including lagoon, tidal mud flats, swamp and marsh subenvironments (Nagtegaal, 1972; Díaz-Molina, 1987; Eichenseer, 1988; Cuevas, 1992; Rosell et al., 2001; Riera et al., 2009; Díez-Canseco et al., 2014; Oms et al., 2016). The overlying unit is the 'Lower Red Garumnian', composed of reddish, brown ochre and multi-colored mudstones, with local paleosoils and intercalated lenticular sandstone packages, locally with channelized bases and point-bar deposits. There are also intercalations of lacustrine carbonates. The 'Lower Red Garumnian' has been interpreted either as fluvial and alluvial deposits (Cuevas, 1992; Rosell et al., 2001; Riera et al., 2009) or as deltaic-plain and perilagoonal deposits in the Western Tresp Syncline (Eichenseer,

1988). The fluvial deposits show features indicative of a marked tidal influence (Eichenseer, 1988; Díez-Canseco et al., 2014, 2016; Blanco et al., 2017; Ghinassi et al., 2020).

Mey et al. (1968)	Rosell et al. (2001)	Cuevas (1992)	Pujalte & Schmitz (2005)
Trempe Fm	'Upper Red Garumnian'	La Guixera Mb Claret Fm	La Guixera Mb Claret Fm Cg. Claret Mb
		Esplugafreda Fm	Esplugafreda Fm
	'Vallcebre limestones & equivalents'	St. Salvador de Toló Fm	St. Salvador de Toló Fm
	'Lower Red Garumnian'	Talarn Fm	Talarn Fm
		Tossal d'Oba Mb Conques Fm	Tossal d'Oba Mb Conques Fm
		Basturs Mb	Basturs Mb
Arén Fm & lateral equivalents	'Grey Garumnian'	La Posa Fm	La Posa Fm Fumanya Mb*
		Arén Fm & lateral equivalents	Arén Fm & lateral equivalents

\* defined by Oms et al., 2016

Figure 4.4. Stratigraphic proposals for the upper Campanian to Paleocene successions of the Trempe Syncline (modified after Riera, 2010).

The facies of the 'Grey Garumnian' and the 'Lower Red Garumnian' units are laterally related and have been dated as latest Campanian-Maastrichtian, based on planktonic foraminifera, charophytes, palynomorphs and rudists (Feist and Colombo, 1983; De Porta et al., 1985; Vicens et al., 2004; Villalba-Breva and Martín-Closas, 2013; Díez-Canseco et al., 2014; Vicente et al., 2015, 2016) and by magnetostratigraphy (Pereda-Suberbiola et al., 2009; Canudo et al., 2016; Fondevilla et al., 2016; Puértolas-Pascual et al., 2018). Nevertheless, due to sedimentary evolution and syntectonic activity during the Maastrichtian, the age of these units varies throughout the basin, being younger westwards (Ardévol et al., 2000; Fondevilla et al., 2016). Thus, the lower

Maastrichtian is only represented in the eastern part of the basin, whereas the upper Maastrichtian is much better recorded in its western part. This distribution implies the presence of a sedimentary gap within the 'Lower Red Garumnian' in the eastern part, between the chron C31r and the chron C29r (Fondevilla et al., 2016).

The third unit of the Tremp Fm is the 'Vallcebre limestones and equivalents', a laterally discontinuous sedimentary unit of limestones with charophytes and *Microcodium*, which represent coastal lacustrine deposits (Rosell et al., 2001; López-Martínez et al., 2006). In the Eastern Tremp Syncline, this unit has been dated as late Danian (Díez-Canseco et al., 2014), which would indicate the existence of an unconformity between the 'Lower Red Garumnian' and the 'Vallcebre limestones' unit. The K-Pg boundary would accordingly be situated somewhere between the topmost part of the 'Lower Red Garumnian' and the boundary with the 'Vallcebre limestones', with dinosaur-bearing sites lying just few meters below the Vallcebre limestones (Riera, 2010; Canudo et al., 2016; Puértolas-Pascual et al., 2018). However, up to now the iridium anomaly has never been recognized in the Tremp Syncline within this stratigraphic interval (Rosell et al., 2001).

The last unit of the Tremp Fm is the 'Upper Red Garumnian', a succession of red mudstones, sandstones and conglomerates, with occasional paleosoils, gypsum and limestones, representing fluvial and alluvial deposits (Cuevas, 1992; Rosell et al., 2001). Its age is constrained in the Tremp Syncline between the Selandian and the late Thanetian (Masriera and Ullastre, 1990; Robador et al., 1990; Serra-Kiel et al., 1994; Ullastre and Masriera, 1998), and at the top of the unit, the Paleocene-Eocene Thermal Maximum has been recognized (Pujalte et al., 2014). It is also worth mentioning the Colmenar-Tremp Horizon (Eichenseer, 1988), a stratigraphic catena of caliche paleosoils and gypsum that can be traced across the basin. This horizon overlies the more modern sedimentary units westwards, marking a progressive unconformity within the Garumnian deposits. This is explained by the absence of some units by consequence of non-deposition due to tectonic uplift (Eichenseer, 1988; López-Martínez et al., 2006). Finally, it is noteworthy to point that the Tremp Fm is overlain by the marine deposits of the Eocene Serraduy Fm (Alveoline Limestone) (Mey et al., 1968; Serra-Kiel et al., 1994). Westwards, the continental deposits of the Tremp Fm pass laterally to the marine Laspún and Navarri formations (Garrido Megías and Ríos Aragües, 1972; Serra-Kiel et al., 1994;

López-Martínez et al., 2006), being recognized the 'Garumnian' facies up to Foradada del Toscar, west of the Ésera river (Fig. 4.3).

The lithostratigraphic schemes used by other authors are indicated in Fig. 4.4. The 'Grey Garumnian' of Rosell et al. (2001) is equivalent to the Posa Fm, whereas the 'Lower Red Garumnian' is equivalent to the Conques and Talarn formations of Cuevas (1992). Paleogene units also change their names, thus, the 'Vallcebre limestones and equivalents' are equal to the St. Salvador de Toló and Suterranya formations, and the 'Upper Red Garumnian' is equivalent to the Esplugafreda and Claret formations. Furthermore, Cuevas (1992) named as members the limestones intercalated with the mudstones of the Lower and Upper Red Garumnian, including (from older to younger) the Basturs, Tossal d'Oba and la Guixera members. Later, Pujalte and Schmitz (2005) and Oms et al. (2016) followed the proposal by Cuevas (1992), with some modifications. Pujalte and Schmitz (2005) define the Claret Conglomerates member within the Claret Fm, and Oms et al. (2016) differentiate the Fumanya Member (lower Maastrichtian tidal flat deposits within La Posa Fm), preserved only in the eastern part of the South-Pyrenean Basin.

The successions studied in this PhD thesis correspond to the 'Grey Garumnian' and the 'Lower Red Garumnian', as well as the uppermost part of the Arén Sandstone Fm. They are outcropping in the north flank of the Tremp Syncline, extending in a NW-SE aligned stripe of near 32 km cut by the rivers Ésera, Isábena and Noguera Ribagorzana, being this area known as the Western Tremp Syncline (Fondevilla et al., 2019) (Fig. 4.3). These NW-SE aligned outcrops are near 32 km in lateral extent and are cut by the Ésera, Isábena and Noguera Ribagorzana rivers.

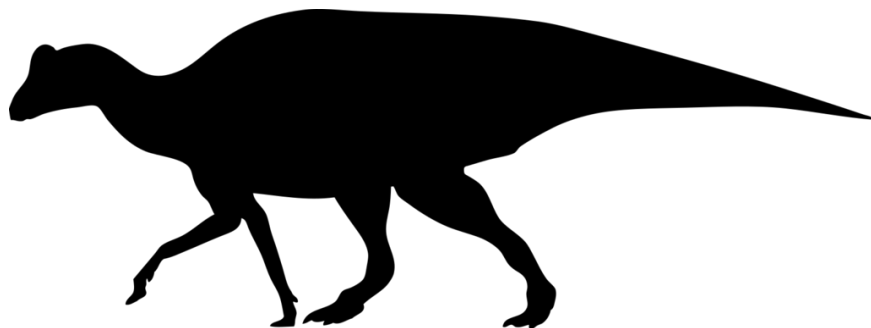
In the Western Tremp Syncline, there are some sedimentological particularities that sometimes make it difficult to locate the formations and boundaries proposed in the Eastern Tremp Syncline. The boundary between the Conques and Talarn formations (equivalent units to the 'Lower Red Garumnian') is defined by the sharp contact between mudstones and conglomerates, or a swift change of light-colored mudstones to red mudstones and sandstones (Cuevas, 1992); however, neither of these contacts can be observed in the Western Tremp Syncline. Moreover, chronostratigraphic data in the eastern part of the Tremp Syncline (Vila et al., 2012; Fondevilla et al., 2016) restrict the Conques Fm to the early Maastrichtian (within chron C31r) and the Talarn Fm to the late

Maastrichtian (chron C29r), a great part of the late Maastrichtian not being recorded (hiatus between C31r and C29r). By contrast, in the Western Tremp Syncline, the lateral equivalents to these units ('Lower Red Garumnian') are dated to within the late Maastrichtian chron C30n-C29r (López-Martínez et al., 2001; Pereda-Suberbiola et al., 2009; Canudo et al., 2016; Puértolas-Pascual et al., 2018), thus being the only part of the basin where chron C30n is recorded. According to the lithostratigraphic and depositional model proposed by Ardèvol et al. (2000) and updated by Fondevilla et al. (2016), the Tarn Fm is limited to the eastern part of the basin (see Figure 8c of Fondevilla et al., 2016). As a direct correlation is not possible, since part of the succession is overlaid by discordant Neogene conglomerates (Fig. 4.1.), it is quite difficult to determine whether the 'Lower Red Garumnian' in the Western Tremp Syncline corresponds to an upper Maastrichtian Conques Fm or the Tarn Fm. A similar pattern is observed with the 'Vallcebre limestone' of the Western Tremp Syncline, which cannot be directly correlated with the St. Salvador de Toló and Suterranya formations to the east due to their lateral discontinuity. This is the main reason for the choosing of the lithostratigraphic division from Rosell et al. (2001) for this work.

# **Chapter 5.**

# **Stratigraphy and**

# **sedimentology**





## **Chapter 5: Stratigraphy and sedimentology of the Tremp Fm in the Western Tremp Syncline**

In this chapter the stratigraphy and sedimentology of the Tremp Fm in the outcrops of the Western Tremp Syncline are analyzed. It includes an update of the lithostratigraphy and the chronostratigraphic framework. Besides, a sedimentological analysis has been carried out, describing a series of facies and a sedimentary model for the studied successions.

### **5.1. *Stratigraphy***

The Tremp Fm, in the Western Tremp Syncline, was characterized in nine outcrops (Campo, El Castellaz, Valle de Lierp, Rin, Serraduy, Beranuy, Isclés, San Pere de Cornudella and Arén) situated along a 32 km-long (without restoring tectonic shortening) NW-SE oriented stripe (Figs. 5.1 and 5.2). Here, this geological unit crops out continuously, except in the area between Beranuy and Isclés, where it is covered by the Oligocene conglomerates of the Sierra del Sis (Figs 5.1 and 5.2). Detailed logging was performed in each one of the outcrops (e.g., Beranuy: Fig. 5.3), from the boundary between the Arén and Tremp Fm to the base of the 'Vallcebre limestones and lateral equivalents' unit or the Colmenar-Tremp Horizon. A detailed representation of the logs is offered in the Annex II.

#### **5.1.1. *Lithostratigraphy***

The analysis of the Mesozoic part of the Tremp Fm in the Western Tremp Syncline has required reviewing the information of the different lithostratigraphic units described by several authors in the eastern part of the basin (Fig. 5.2). In this work, the division by Rosell et al. (2001) is used, differentiating two units in the Mesozoic part of the Tremp Fm: 'Grey Garumnian' and 'Lower Red Garumnian'. This division has been chosen since it is the most helpful for field work in this part of the basin (see reasoning in Chapter 4). Throughout the studied outcrops, the units show a great lateral variability, in thickness and facies association, which make sometimes hard to find laterally continuous key levels. The Mesozoic Tremp Fm shows a decrease in thickness towards the NW, from

235 m in Arén to 30 m in Campo (Fig. 5.2 and 5.4). This is caused by its progressive lateral change to the Arén Sandstone Fm and Laspún Fm towards the west.

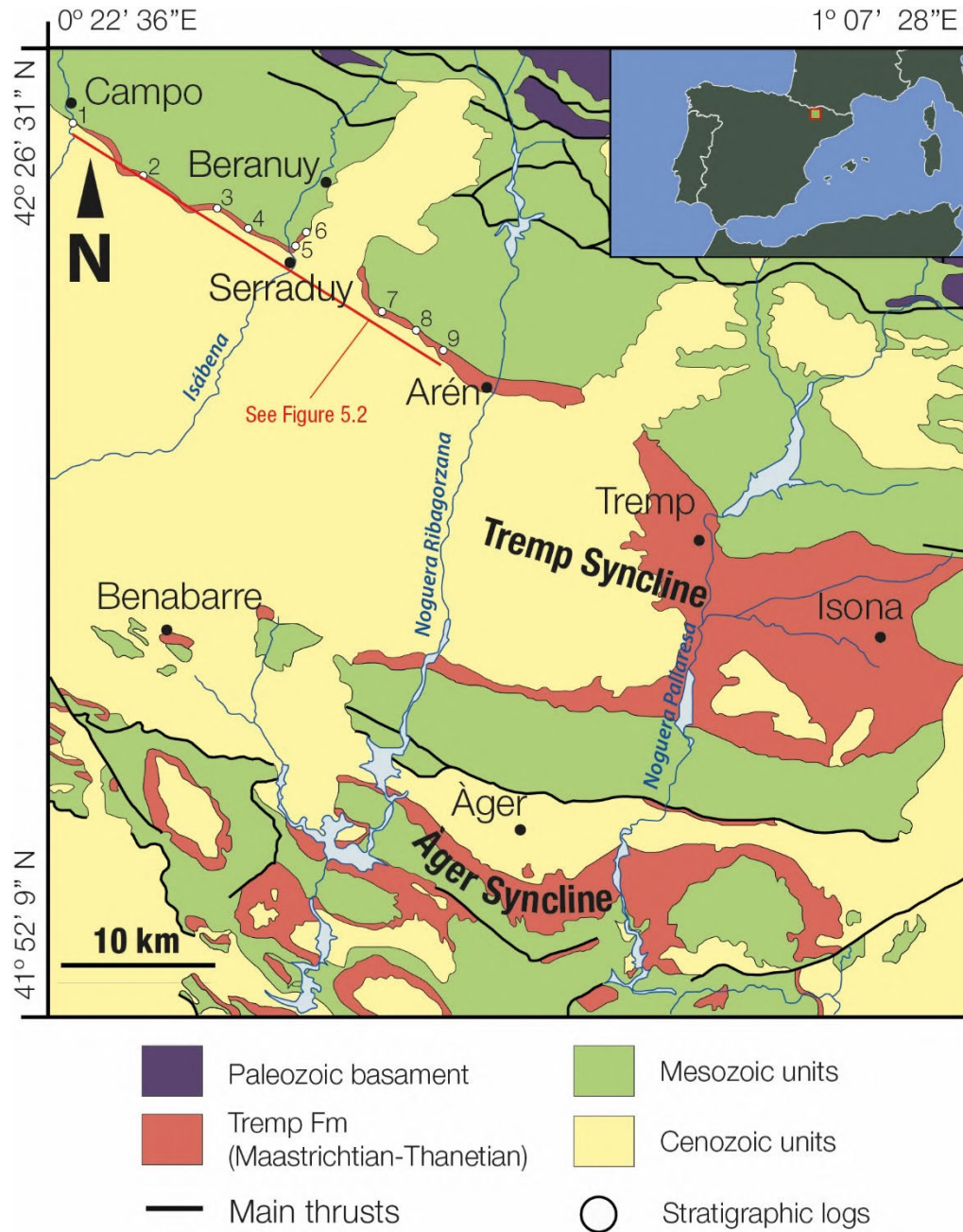


Figure 5.1. Geological map of the Tremp Syncline, with the location of the nine stratigraphic logs studied in the Western Tremp Syncline: 1) Campo, 2) El Castellaz, 3) Valle de Lierp, 4) Rin, 5) Serraduy, 6) Beranuy, 7) Isclés, 8) San Pere de Cornudella and 9) Arén. Figure modified after López-Martínez and Vicens (2012).

1. Campo    2. El Castellaz    3. Valle de Lierp    4. Rin    5. Serraduy    6. Beranuy    7. Isclés    8. Sant Pere    9. Arén

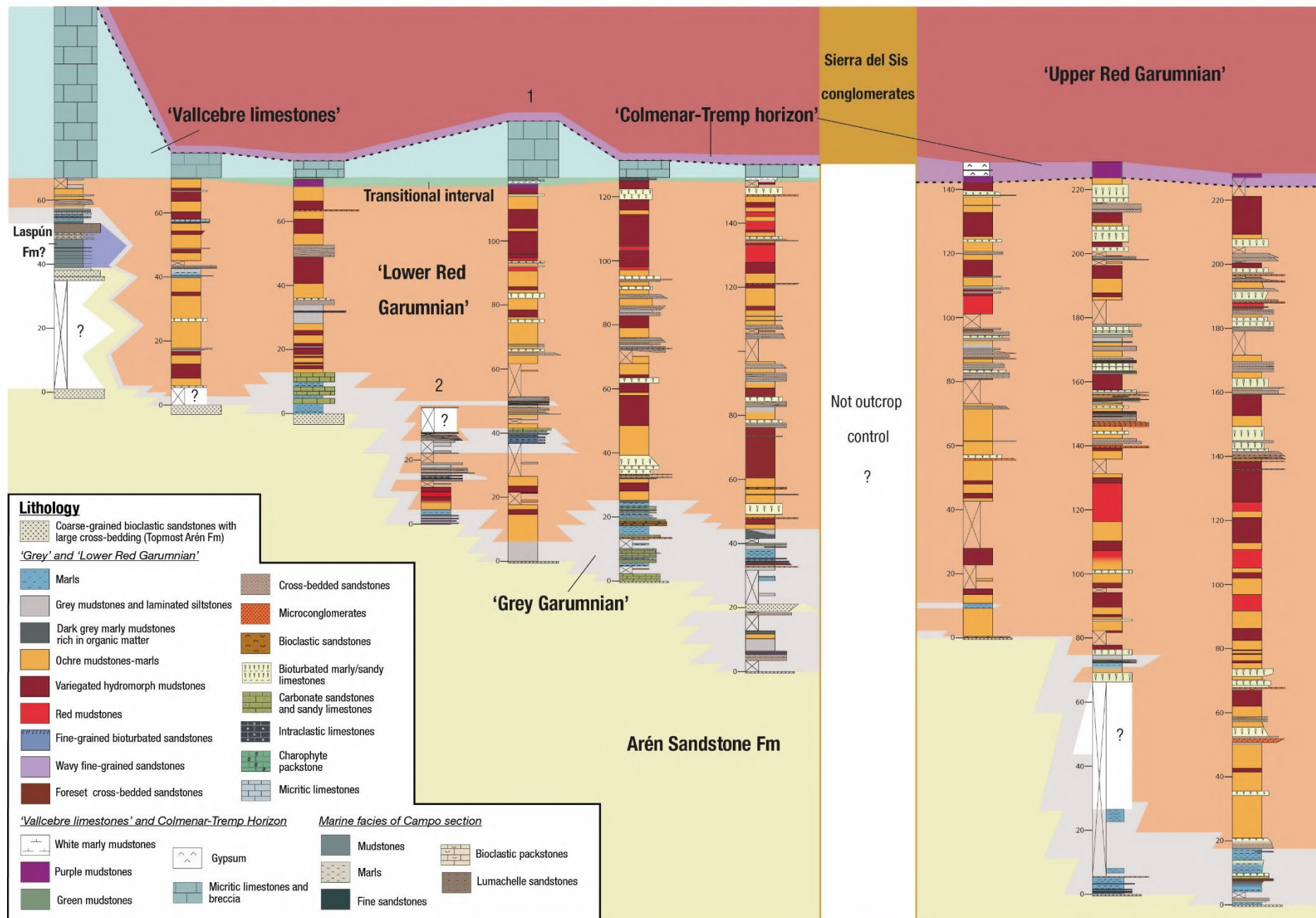


Figure 5.2 (previous page). Correlation panel of the nine stratigraphic logs studied in the Mesozoic part of the Tremp Fm in the Western Tremp Syncline with the main lithostratigraphic units, lithology and facies identified. The correlation panel is W-E oriented (see Fig. 5.1 for location).

The 'Grey Garumnian' unit is formed by an alternation of marls, marly mudstones, sandstones and sandy limestones. It shows a variable thickness, ranging from near 70 m in San Pere de Cornudella outcrop to be almost absent in some of the outcrops, such is the case of Isclés (Fig. 5.2). It interdigitates with the upper part of the Arén Fm (Beranuy outcrop) (Fig. 5.3), but also with the 'Lower Red Garumnian' (Rin outcrop). In addition, in the area of Campo, there is transitional marine interval between the Arén Sandstone Fm and the 'Grey Garumnian' (Fig. 5.2) composed by grey and beige mudstones and marls, with intercalations of fine sandstones and bioclastic packstones bearing non- to little reworked specimens of macroforaminifera (cf. *Laffitenia*), rudists, and ammonoids (López-Martínez et al., 2006a; Canudo et al., 2016). This marine interval may be assigned tentatively to the marine Laspún Fm, defined by Garrido Megías and Ríos Aragües (1972).

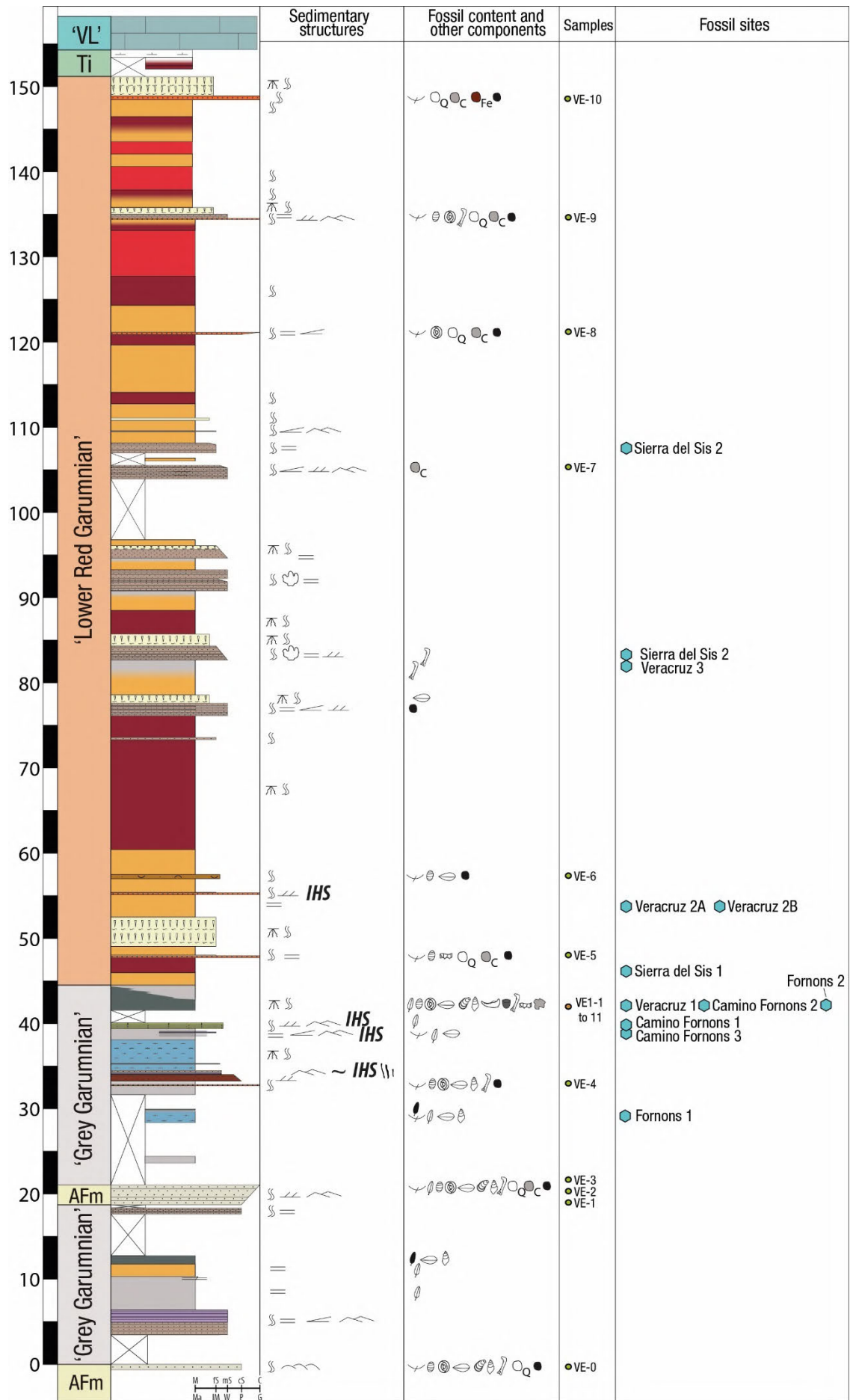
The 'Lower Red Garumnian' is conformed by a succession of mudstones of varied colours with intercalations of sandstones and microconglomerates. It decreases its thickness gradually towards the west, from 210 m in Arén to the scarce 20 m in Campo (Fig. 5.2 and 5.4). This reduction in thickness is gradual, though it displays an abrupt step between Rin (116 m) and Valle de Lierp (60 m) outcrops, separated just by 1.8 km. This thinning is due to the lateral pass of the 'Lower Red Garumnian' to the Areny Sandstone Fm westwards. Eichenseer (1988) already recognized this lateral change in this area and linked it to a major progradational cycle consequence of the uplifting of the Turbón anticline, which acted as a structural high and made the depositional system migrate to the west.

The upper boundary of the 'Lower Red Garumnian' is variable along the study area depending on the presence of the 'Vallcebre limestones and lateral equivalents' or the Colmenar-Tremp Horizon (Fig. 5.4 A, B and C). In the outcrops located to the west of the Sierra del Sis, on top of the 'Lower Red Garumnian', there is a 3-5 m-thick transitional interval formed by purple, white, maroon and green marls and marly mudstones, with occasional lime mudstone levels (Fig. 5.2 and 5.4 C and D). They are overlain by a package of limestones, dolostones and brecciated levels that thickens towards the west (3 m in Beranuy to around 55 m in Campo), which corresponds to the 'Vallcebre limestones and lateral equivalents'. The muddy 3-5 m-thick transitional interval between

the detritic deposits of the 'Lower Red Garumnian' and the carbonates of the 'Vallcebre limestones and lateral equivalents' was also recognized by other authors (López-Martínez et al., 2006a). According to López-Martínez et al. (2006a) and Eichenseer, (1988), the base of the 'Vallcebre limestones and lateral equivalents' in this area is an isochronous boundary, since its loss of thickness towards the east is related to the wedging of the unit and not to a lateral change of facies. To the east of the Sierra del Sis, the upper boundary of the 'Lower Red Garumnian' is the contact with the Colmenar-Tremp Horizon, a discrete level of calcimorph paleosoils. This horizon displays a great lateral variability: it is formed by pink to purple mudstones with carbonate nodules in the area of Arén (Fig. 5.4 A), whereas in Isclés it is composed by pinkish white mudstones with veins and nodules of gypsum, and local carbonate nodules (Fig. 5.4 B). Eichenseer (1988) suggested that the contact between the 'Vallcebre Limestones' and the Colmenar-Tremp Horizon is an unconformity (Eichenseer, 1988). However, at the studied area, the relationship between the Colmenar-Tremp Horizon to the east and the 'Vallcebre Limestones' to the west of the Sierra del Sis is uncertain due to the absence of intermediate outcrops (Fig 5.2). Apparently, during the deposition of the 'Vallcebre Limestones', the eastern area was an uplifted paleorelief with no deposition of the lacustrine facies, due to the activity of the Boixolls-San Corneli thrust (López-Martínez et al., 2006a), so that gap in the sedimentation also between the 'Lower Red Garumnian' and the Colmenar-Tremp cannot be ruled out. In addition, as noted by López-Martínez et al. (2006a), the age of the 'Vallcebre limestones' and the temporal entity of the aforementioned gap is uncertain due to the no finding of the K/Pg boundary level and a significant lack of index fossils in the limestones.

*Figure 5.3 (next page). Stratigraphic log of Beranuy outcrop. AFm: Arén Sandstone Formation, Ti: Transitional interval, 'VL': 'Vallcebre Limestones' unit. See Fig. 5.2 for legend of lithology and facies and Annex II for the legend of symbols.*

## Stratigraphy and sedimentology



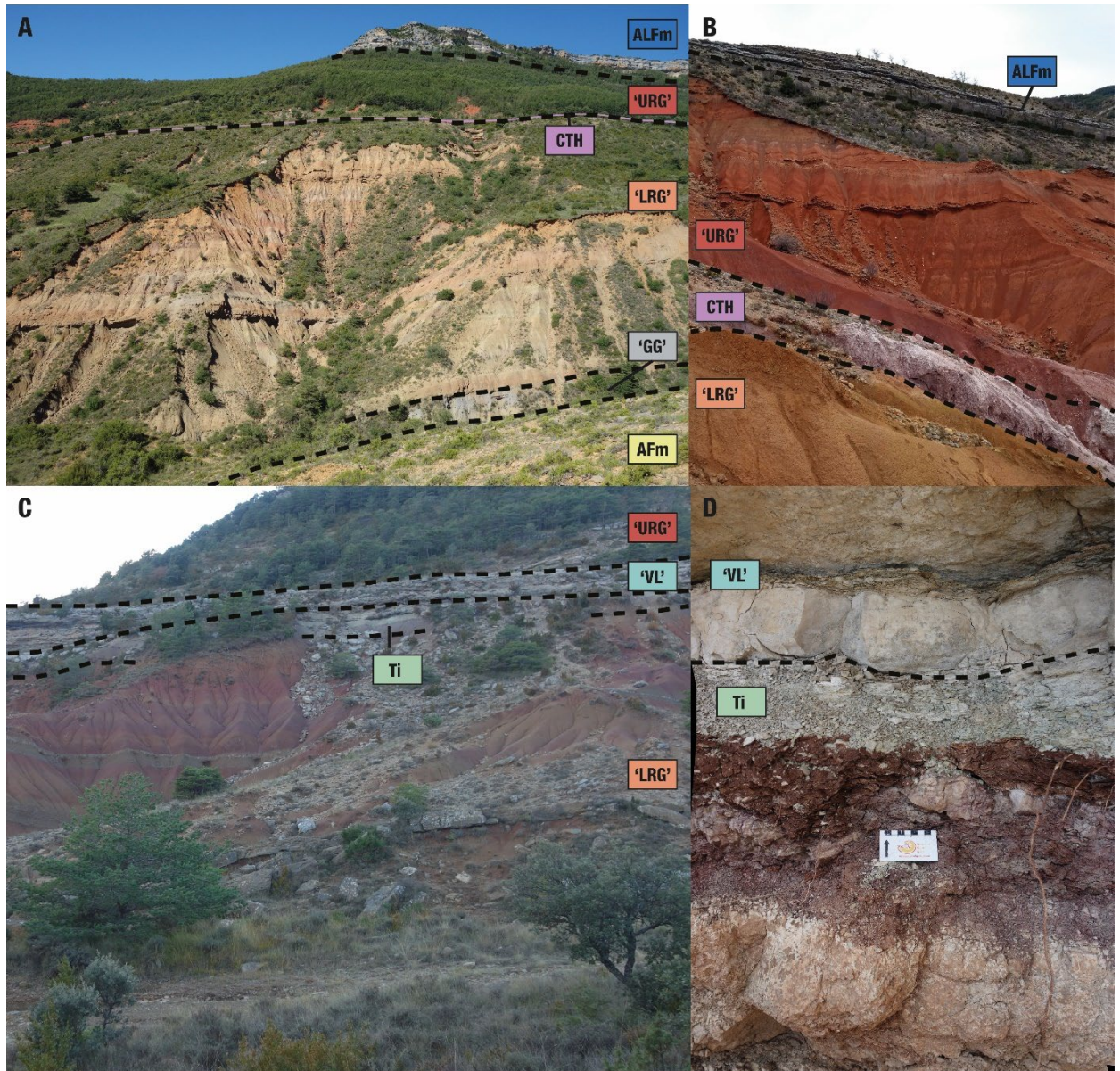


Figure 5.4. Main lithostratigraphic units of the Tremp Fm in the Western Tremp Syncline. A) General view of the Arén outcrop. B) Colmenar-Tremp Horizon in the Isclés outcrop. C) General view of the Rin outcrop. D) Detailed view of the transitional interval between the 'Lower Red Garumnian' and the 'Vallcebre Limestones' near Serraduy. AFm: Arén Sandstone Fm, ALFm: Alveoline Limestone Fm, CTH: Colmenar-Tremp Horizon, 'GG': 'Grey Garumnian' unit, 'LRG': 'Lower Red Garumnian' unit, Ti: Transitional interval, 'URG': 'Upper Red Garumnian' unit, 'VL': 'Vallcebre Limestones' unit.

**5.1.2. Biostratigraphy**

The biostratigraphic data of the Tremp Fm in the Western Tremp Syncline has been based mainly on planktonic foraminifera found in this unit and underlying units. The foraminifera found in the transitional and continental deposits of the Tremp Fm correspond to both allochthonous foraminifera transported landwards by tidal currents and to reworked foraminifera eroded from older Santonian rocks (Díez-Canseco et al., 2014). Thanks to this, the marine biozones proposed for the Maastrichtian can be extrapolated to the continental deposits of the Tremp Syncline. López-Martínez et al. (2001) identified the foraminifera *Abathomphalus mayaroensis* Bolli, 1951 (early late Maastrichtian age: Gale et al., 2020) in the marine deposits of the Vallcarga Fm, below the Arén Sandstone Fm in the Campo section (Fig. 5.1). Therefore, in this area, the 'Grey Garumnian' and the 'Lower Red Garumnian' would probably be late Maastrichtian in age. Correlation with the dated outcrops of the eastern part of the Tremp Syncline support this age assignment. For example, Díez-Canseco et al. (2014) determined an age of early Maastrichtian for the 'Grey Garumnian' and early and late Maastrichtian for the 'Lower Red Garumnian' in the area between Isona and Tremp (Lleida, Catalonia, Spain), about 28 km east from the Arén outcrops. They dated the Suterranya limestone, equivalent of the 'Vallcebre limestones', as late Danian in age based on planktonic foraminifera, corroborated also with the charophytes association described by Masrera and Ullastre (1990). However, the Suterranya Limestone disappears towards the west and cannot be directly correlated to the 'Vallcebre Limestones' of the Western Tremp Syncline, so its late Danian age cannot be extrapolated to the 'Vallcebre Limestones'. Another additional biostratigraphic marker is the macroforaminifer *Laffiteina bibensis* Marie, 1946, which appears in the marine levels between the Arén Fm and the Tremp Fm in Campo section. This foraminifer was considered Danian in age, but it has been determined recently as exclusively Cretaceous (Serra-Kiel et al., 2020).

López-Martínez et al. (2001) studied the charophyte association of Blasi 2B site located near Arén in the 'Grey Garumnian' (Fig. 5.1 and 5.2), identifying four taxa: *Feistiella* sp., *Peckichara sertulata* Grambast, 1971, '*Amblyochara*' *concava* Grambast-Fessard, 1980 and '*Amblyochara*' sp. A Feist. The genus '*Amblyochara*' was synonymized by Soulié-Märsche (1989) to the genus *Lychnothamnus*. The assemblage was interpreted as late Maastrichtian in age and is concordant with new biostratigraphic proposals. For example Vicente et al. (2019) marks *Lychnothamnus concavus* Grambast-

Fessard, 1980 as a late Maastrichtian to Danian fructification, meanwhile *P. sertulata* does not reach the Danian.

The last stratigraphic evidences of dinosaur fossils has been used to calibrate the position of the K/Pg boundary between the 'Lower Red Garumnian' and the 'Vallcebre Limestones' (López-Martínez et al., 2006a; Canudo et al., 2016; Puértolas-Pascual et al., 2018). However, without the evidence of the iridium anomaly in the Tremp Syncline, this criterion could led to circular reasoning, and must be evaluated cautiously. In the Campo section, ammonoids and rudists found in the marine interval situated between the Arén and the Tremp formations have been used also to corroborate the Maastrichtian age of the 'Grey Garumnian' and the 'Lower Red Garumnian' (Eichenseer, 1988; López-Martínez et al., 2001; Canudo et al., 2016).

In the Serraduy section (Fig. 5.1 and 5.2), the whole Mesozoic succession, including the 'Grey Garumnian', the 'Lower Red Garumnian', and the lower part of the 'Vallcebre Limestones', was analyzed for micropaleontological content (see detailed description in Puértolas-Pascual et al., 2018). Foraminifera are absent in the 'Grey Garumnian' unit, meanwhile planktonic and benthic foraminifera appear in almost all samples of the 'Lower Red Garumnian' (Fig. 5.5.). The assemblage is a mix of species of different ages, including probably reworked older foraminifera and contemporaneous allochthonous foraminifera, as it has been proposed by Díez-Canseco et al. (2014). There are some pre-Maastrichtian species such as *Favusella washitensis* Carsey, 1926; species such as *Heterohelix globulosa* Ehrenberg, 1840 or *Contusotruncana fornicata* Plummer, 1931, which are present in the Maastrichtian, but their first appearance is previous to this age; and exclusively Maastrichtian taxa such as *Globotruncanita fareedi* El Naggar, 1966 and *Pseudoguembelina hariaensis* Nederbragt, 1991.

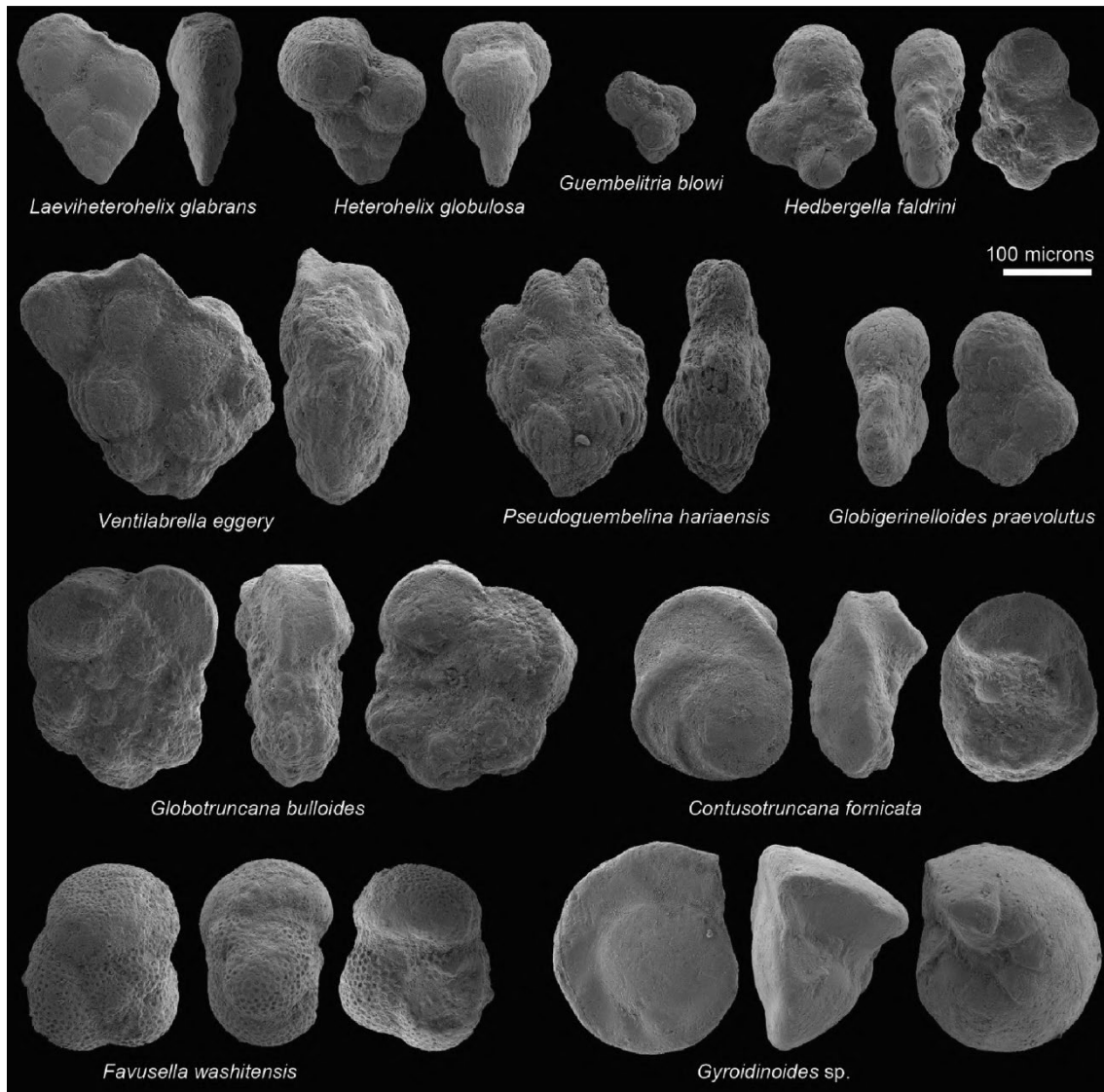


Figure 5.5. Some representative planktonic and benthic foraminifera species identified in the Serraduy section. *Laeviheterohelix glabrans* (MPZ 2018/25), *Heterohelix globulosa* (MPZ 2018/23), *Guembelitra blowi* (MPZ 2018/28), *Hedbergella faldrini* (MPZ 2018/24), *Ventilabrella eggery* (MPZ 2018/22), *Pseudoguembelina hariaensis* (MPZ 2018/21), *Globigerinelloides praevolutus* (MPZ 2018/27), *Globotruncana bulloides* (MPZ 2018/26), *Contusotruncana fornicata* (MPZ 2018/20), *Favusella washitensis* (MPZ 2018/18), *Gyroidinoides* sp. (MPZ 2018/19) (after Puértolas-Pascual et al., 2018).

Although the mixing of reworked and allochthonous foraminifera makes difficult the assignation of a concrete biozone for the studied successions, the presence of *P. hariaensis* in the lower part of the 'Lower Red Garumnian' allows the assignation of maximum and minimum age for these deposits. This species appears for the first time at 67.3 Ma, in the upper part of chron C30n (Gradstein et al., 2012), and disappears in the

K/Pg boundary, which confirms that at least the 'Lower Red Garumnian' is late Maastrichtian in age. In the "Vallcebre Limestones", some specimens of *Guembelitra cretacea* Cushman, 1933 and *Guembelitra blowi* Arz, Arenillas and Náñez, 2010 have been identified. *Guembelitra* is the only genus whose survival beyond the Cretaceous/Paleogene mass extinction event has been clearly proven (Smit, 1982). As the temporal calibration of the 'Vallcebre Limestones' in the Western Tresp Syncline is not well-constrained, is difficult to ascertain if these foraminifera are reworked, since the supposed lateral equivalent in the Eastern Tresp Syncline, the Suterranya Limestone, has been dated as late Danian (Díez-Canseco et al., 2014), and *Guembelitra* only reach the early Danian.

The Veracruz 1 site, located in the upper part of the 'Grey Garumnian' unit in the Beranuy area (Figs. 5.1, 5.2, 5.3) has also yielded microfossils with biostratigraphical value. Some few foraminifera have been recovered, but they are not good biostratigraphic markers (Fig. 5.6); for example, *Guembelitra cretacea*, *G. blowi*, *Heterohelix planata* Cushman, 1938, *Globotruncana mariei* Banner and Blow, 1960, and *Globotruncana linneiana* d'Orbigny, 1839, which are present during the Maastrichtian but have their first record well before this stage, (Nederbragt, 1991; Pérez-Rodríguez et al., 2012). The foraminifera tests recovered (Fig. 5.6) show very different preservation state; moreover, different color of the test (white, grey and red) suggests their provenance from different stratigraphic horizons. This points again to a mix of reworked and transported foraminifera. Therefore, no unequivocal age attribution or biozone determination can be made on the basis of planktonic foraminifera distribution for this interval. Nonetheless, a minimum age can be assigned based on the most modern planktonic foraminifera species identified, *Heterohelix labellosa*? Nederbragt, 1991, which ranges up to the late Campanian. This minimum age is far below the estimations of other microfossils analyzed, which may indicate the test of *H. labellosa*? studied is reworked, which is also supported by the poor preservation of the test (Fig. 5.6 A). Thus, the foraminifera assemblage of Veracruz 1 site is not very useful in a biostratigraphic way. Nevertheless, these taxa correspond to the first foraminifera assemblage described in the 'Grey Garumnian' of the Western Tresp Syncline, since this type of fossils are very scarce in this geological unit, as it has been mentioned before.

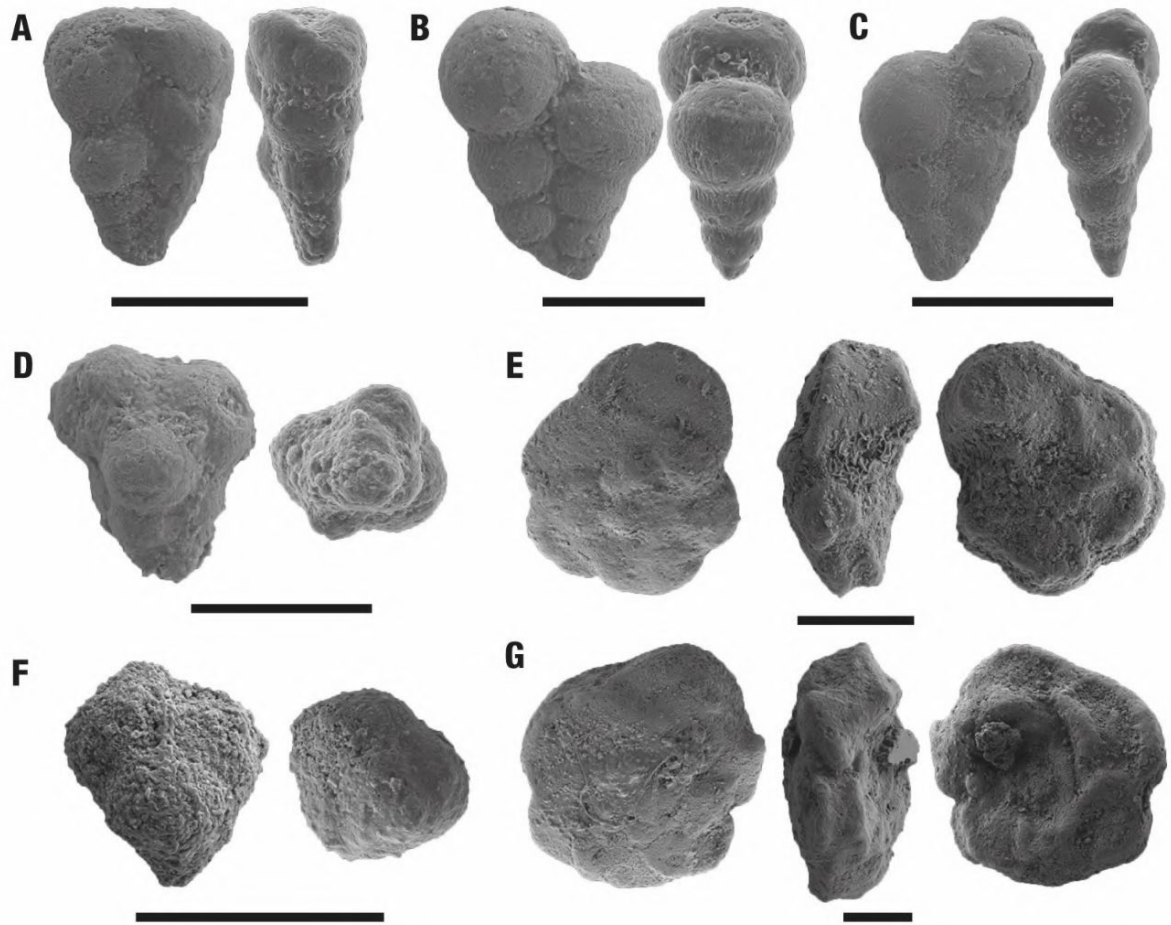


Figure 5.6. Planktonic foraminifera specimens found at VE1 site. A) *Heterohelix labellosa*? (VE1T-01). B) *Heterohelix globulosa* (VE1T-02). C) *Heterohelix planata* (VE1T-03). D) *Guembelitra cretacea* (VE1T-04). E) *Globotruncana mairei*? (VE1T-05). F) *Guembelitra blowi* (VE1T-06). G) *Globotruncana linneiana* (VE1T-07). Scale bar equals to 100  $\mu\text{m}$ .

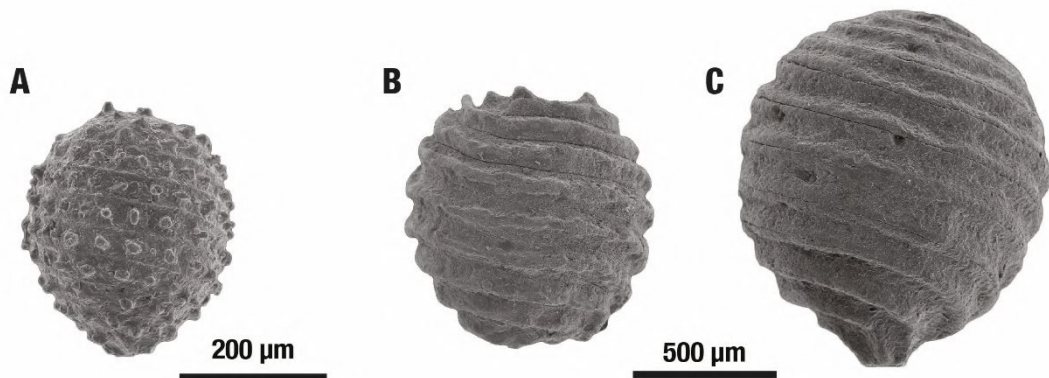


Figure 5.7. Relevant biostratigraphic charophyte gyrogonites from Veracruz 1 site in lateral view. A) *Microchara puntacta* (specimen VE1T-16). B) *Peckichara sertulata* (specimen VE1T-10). C) *Lychnothamnus begudianus* specimen VE1T-09.

The charophyte association of Veracruz 1 site was also studied (see section 6.2 of Chapter 6 for the taxonomic description). The occurrence of very well-preserved *Microchara punctata* Feist in Feist and Colombo, 1983 (Fig. 5.7 A) indicates that VE1 belongs to the homonymous *Microchara punctata* biozone described by Vicente et al. (2016b), which spans from the magnetochron C32n.1n (lower Maastrichtian) to the magnetochron C29r (lower Danian). The absence of clavatoraceans in the site, specially *Clavator ultimus* Grambast, 1971, may indicate that the site is situated above the *Clavator ultimus* subzone, which encompasses the lower Maastrichtian part of the *Microchara punctata* biozone (chron C32n to C31n). Besides, the association of *M. punctata* with *Peckichara sertulata* Grambast, 1971 (Fig. 5.7 B), and *Lychnothamnus begudianus* Grambast, 1962 (Fig. 5.7 C), which do not reach the Danian (Vicente et al., 2019), suggests that the age of the assemblage may be constrained to the upper Maastrichtian, between chron C31n and the middle part of C29r.

### 5.1.3. Magnetostratigraphy

The Cretaceous and Paleogene successions of Western Tresp Syncline has been the subject of various magnetostratigraphic studies, especially those of Tresp Fm since this geological unit potentially contains the K/Pg boundary. The first published magnetostratigraphy in this sector corresponds to Pereda-Suberbiola et al. (2009), which analyzed in the Arén outcrops (Figs. 5.1 and 5.2), the Vallcarga and Arén Fm, and the 'Grey Garumnian' and 'Lower Red Garumnian' of the Tresp Fm, though the uppermost part of this later unit was not sampled. They identified a normal magnetozone encompassing the Vallcarga and Arén formations, the 'Grey Garumnian' and the lower part of the 'Lower Red Garumnian', meanwhile the upper part of the 'Lower Red Garumnian' displayed reverse directions. Both magnetozones were separated by an interval of 25 m of uncertain polarity. By correlation with the biostratigraphic data of López-Martínez et al. (2001) in the section of Campo, they correlated the normal magnetozone with chron C30n and the reverse one with C29r.

The second magnetostratigraphic analysis was performed by Canudo et al. (2016) in a composite log of the Campo outcrops (Figs. 5.1 and 5.2). They sampled from the Vallcarga Fm to the top of the 'Lower Red Garumnian' of the Tresp Fm. Their results show an extensive normal magnetozone in the Vallcarga and Arén Fm, identified as the C30n, meanwhile a short reverse magnetochron is constrained from the upper part of

the Arén Fm the top of the 'Lower Red Garumnian'. This reverse zone has been identified as the chron C29r.

Finally, is important to mention another magnetostratigraphic section studied by López-Martínez et al. (2006b) in the area of Rin (Figs. 5.1 and 5.2). Though it was never properly published, it was presented in a meeting (Climate & Biota of the Early Paleogene congress in Bilbao 2006), and the authors have uploaded the poster in an accessible data repository. This relevant work introduces two new magnetostratigraphic profiles (Rin and Esplugafreda) being the first sections in which the Paleocene part of the Tremp Fm was sampled in the Western Tremp Syncline. Although this magnetostratigraphic profile is nearby but not at the same place of the Rin section studied in this Thesis (Dinarès-Turell, pers. comm.), the data can be extrapolated, since both logs show a similar thickness for the 'Grey Garumnian' and 'Lower Red Garumnian' (around 110 m). In this unpublished magnetostratigraphic section, there is a short normal magnetozone between the top of the Arén Fm and the middle part of the 'Grey Garumnian' identified as the chron C30n, followed by a 107 m-thick reverse magnetozone which reach the upper part of the 'Lower Red Garumnian', identified as the chron C29r. This is followed by a short interval without data followed by a short reverse and a short normal magnetozones, which would be situated in the topmost part of the 'Lower Red Garumnian' and the transitional interval described in section 5.1.1. The correlation proposed by López-Martínez et al. (2006b) for this last short normal magnetozone is C29n or C28n. The 'Vallcebre Limestones' unit has not paleomagnetic data, meanwhile the 'Upper Red Garumnian' shows a long and continuous reverse magnetozone whose correlation with the GPTS is unclear, having an uncertainty interval between chrons C26r, C25r or C24r. The lack of relevant biostratigraphic markers in the Paleocene units hinders a more precise calibration.

Aiming to shed more light on this issue, two new magnetostratigraphic studies have been included in this Doctoral Thesis, which correspond to Serraduy and Isclés sections respectively (Figs. 5.1 and 5.2).

**Serraduy section**

In the Serraduy section (Puértolas-Pascual et al., 2018), magnetostratigraphic sampling encompassed the uppermost part of the Vallcarga Fm, the Arén Fm, the 'Grey Garumnian', 'Lower Red Garumnian' and 'Vallcebre Limestones' of the Tremp Fm (Fig. 5.8.).

The different lithologies sampled show different paleomagnetic behaviors (see Puértolas-Pascual et al., 2018 for an extended description of the magnetic properties of the different lithologies). Sandstones and green/violet mudstones have moderate NRM intensities (0.1-0.5 mA/m) and a heterogeneous paleomagnetic behavior, being paleomagnetically unstable. Grey marls and mudstones sampled from the Vallcarga Fm show higher NRM values between 1.1 and 1.78 mA/m, meanwhile grey marls and mudstones from the 'Grey Garumnian' and punctual levels of the 'Lower Red Garumnian' usually have lower NRM intensity, between 0.4 and 0.5 mA/m. Nevertheless, in most of them two different components in thermal (TH) demagnetization can be recognized: a low-temperature component (250/300-450 °C in Vallcarga Fm marls and 250-400 °C in Tremp Fm marls) and a high-temperature component (up to 500 °C). Red and ocher mudstones of the Tremp Fm display low-medium NRM intensities ranging from 0.1 to 1.8 mA/m, but some of them have higher intensities around 3 mA/m. Low intensity samples (~0.2-0.8 mA/m) usually show a single component (350/550 °C), meanwhile in those of higher intensity two overlapped components (low and intermediate) are deduced between 350 °C and 550 °C. Finally, a high temperature up to 500°C and above is also present. Rock magnetic properties points to magnetite as primary carrier of both components in marls, meanwhile hematite would be the main carrier in red mudstones (Puértolas-Pascual et al., 2018).

Though part of the local magnetic stratigraphy of the Serraduy section shows an undetermined polarity in the Arén and Vallcarga formations (in the latter most probably related to the formation of secondary magnetite) (Fig. 5.8), the 'Grey Garumnian' and 'Lower Red Garumnian' can be assigned to a reverse polarity chron (Fig. 5.8). The 'Vallcebre Limestones' does not display clear directions.

The presence of the planktonic foraminifer *P. hariaensis* (see section 5.1.2) in sample SR35 indicates that this level has a maximum age of 67.3 Ma (oldest age range of the species), or younger if it is reworked. The age range for this species is between 67.3 and 66.0 Ma, its lowermost and uppermost occurrences being coincident

respectively with the upper part of C30n and the K/Pg boundary in the middle part of C29r. Thus, all the reverse polarity section between levels SR35 and SR90 can only correspond with chron C29r (Fig. 5.8).

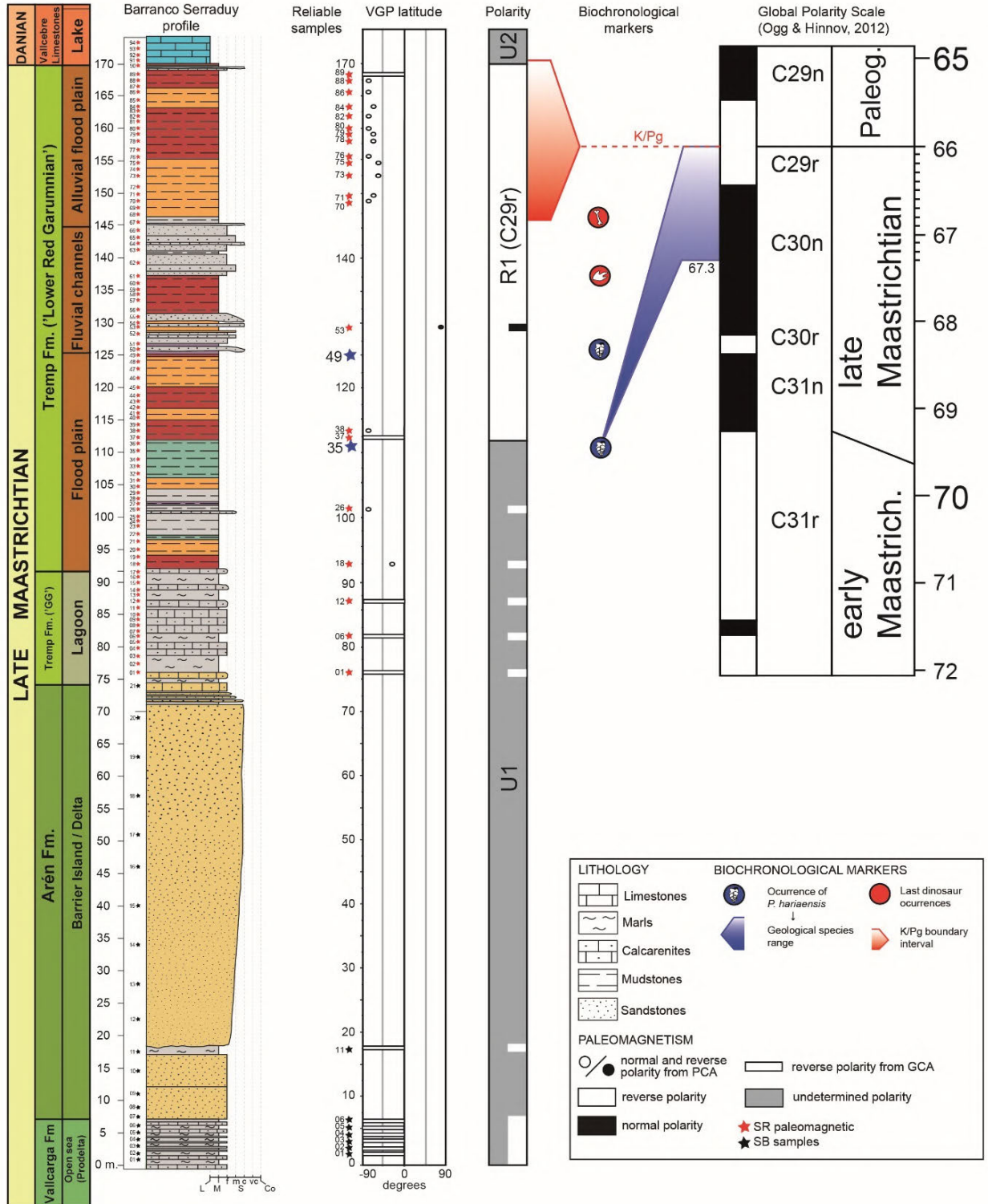


Figure 5.8 (previous page). Lithology, last dinosaur occurrences, and the proposed magnetostratigraphy from the Serraduy section. VGP latitude logs along the Arén Formation (SB) and Tremp Formation (SR) profiles are shown by circles (black or white) when the polarity has been calculated from paleomagnetic directions obtained by principal component analysis (PCA) or by bars (white) when it has been obtained by great circle analysis (GCA) (modified after Puértolas-Pascual et al., 2018).

### Isclés section

In Isclés section, several units were sampled in 5 partial profiles, including the Arén Fm, all the Tremp Fm ('Grey Garumnian', 'Lower Red Garumnian', Colmenar-Tremp Horizon and 'Upper Red Garumnian') and the Alveoline Limestone Fm, totaling an overall magnetostratigraphic profile of near 380 m (Fig. 5.9).

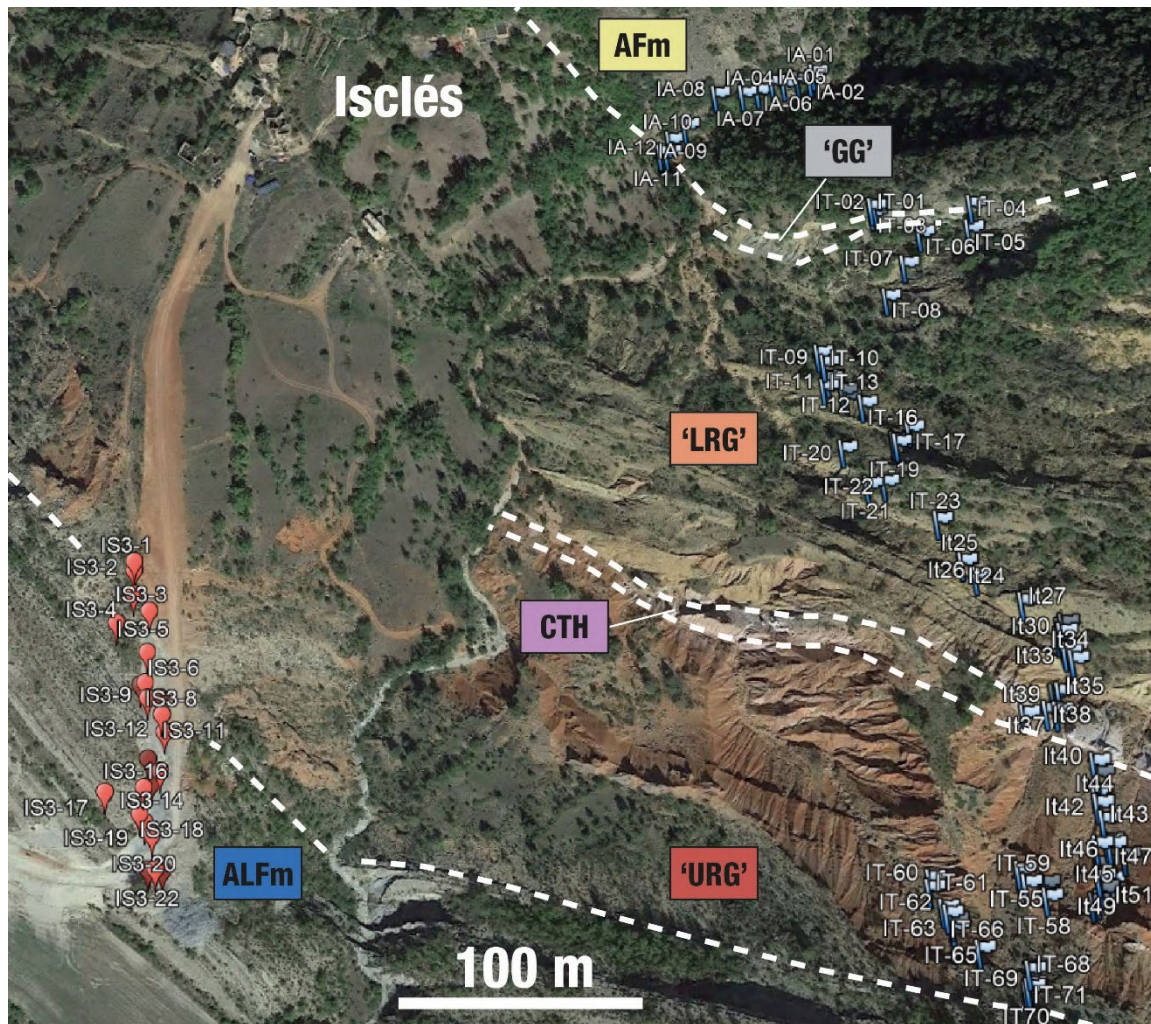


Figure 5.9. Aerial photograph of the outcrop of Isclés, with the location of all the samples of the magnetostratigraphic profile.

Magnetic carriers and paleomagnetic directions

The Isclés section displays a great variety of magnetic behavior as expected from the lithological diversity, similar to previous studies (Pereda-Suberbiola et al., 2009; Canudo et al., 2016; Fondevila et al., 2016; Puértolas-Pascual et al., 2018). Due to the scattered paleomagnetic signal and focusing on avoiding unnecessary noise, samples were classified in three quality groups according to their characteristic remanent magnetization (ChRM) direction: class I samples addressing to the origin, class II poorer directions with an unambiguous polarity, class III includes the remaining set (the worst dataset not used in further calculation; neither profile means nor for the VGP profile construction).

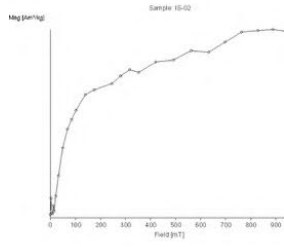
The Arén Fm, the 'Grey Garumnian' and the Alveoline Limestone Fm are dominated by low coercivity ( $H_c$ ) carriers (magnetite and iron sulphides) as it follows from the quick saturation of the magnetization (IRM curves in Fig. 5.10) and the low values of the coercivity force ( $H_{cr}$ ). This is also supported by some AF demagnetizations (unblocking between 25-70mT) and several TH ones with dominant decays in the 300-575°C temperature interval. On the other hand, the red sandstone, siltstones and mudstones of the 'Lower' and 'Upper Red Garumnian' also have evidences of hematite, non saturated IRM curves (high  $H_c$ ) and much higher values of the coercivity of the remanence ( $H_{cr}$ ). Thermal demagnetizations unblocking until 675°C partially support this evidence. However, these high-temperature components only show up in less than 25% of the analyzed rocks and intermediate temperature decays ( $\approx$  400-500°C) are dominant in our collection (> 50%) independently of the facies.

Apart from a viscous component without geological meaning (Fig. 5.11), most samples display mono-directional components. The ChRM, in average out, includes 5 (+/- 2) steps and is characterized by MAD angles (Kirschvink, 1980) of 15° (+/- 7°). The class grading reflects the moderate-low quality of the paleomagnetic directions:  $\approx$ 20% Q1,  $\approx$  60% Q2 and  $\approx$  20% Q3 totally useless directions.

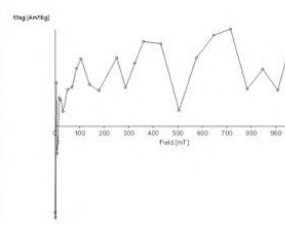
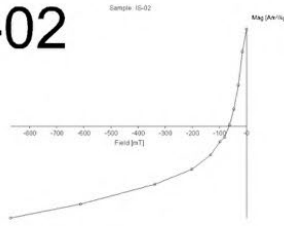
The data from the Isclés section alone preclude to run a fold test and to check the paleomagnetic stability, although several paleomagnetic studies have effectively demonstrated the primary character of the paleomagnetic signal in the South Pyrenean Central Unit (Beamud et al., 2004) nearby the Isclés section. In any case, the normal and reverse polarities (Fig. 5.12); 357, 24 ( $\alpha_{95}$ : 18°, k: 3.8 and R: 0.7514) and 181, -37 ( $\alpha_{95}$ : 14.2°, k: 3.3 and R: 0.7073) share a common true mean. Except for some assumable

inclination shallowing, the mean vector in the lower hemisphere (358, 33 [ $\alpha_{95}$ : 11°, k: 3.5 and R: 0.7175]) resembles the expected Late Cretaceous reference direction (Dec: 359, Inc: 46;  $\alpha_{95}$  5°, k: 294, after Corral et al., 2016) as well as the Cenozoic mean obtained in the Ebro Foreland Basin (Dec: 003, Inc: 49;  $\alpha_{95}$  5.4°, k: 5.4, and R: 0.8152, after Oliva-Urcia and Pueyo, 2019). Comparatively, the Isclés section has yielded better results than closer magnetostratigraphic sections. It is worth mentioning that only classes I and II directions were used to estimate the paleolatitude of the virtual geomagnetic pole (VGP).

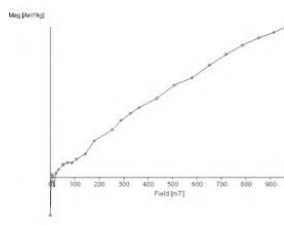
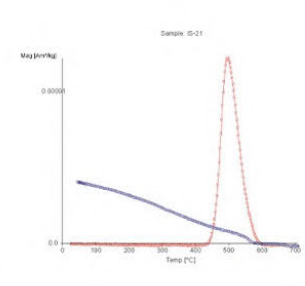
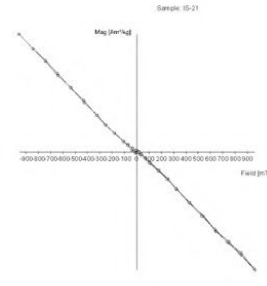
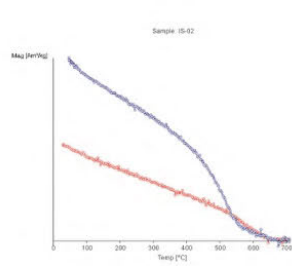
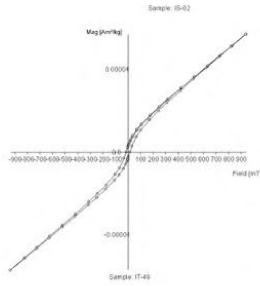
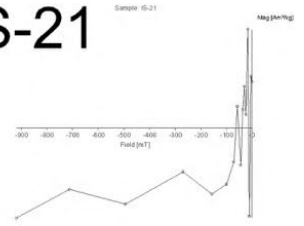
*Figure 5.10 (next page). Rock-magnetism analyses in some representative samples of the Isclés section. Upper part: Isothermal Remanent Magnetization (IRM) acquisition curve and its back field experiment to deduce the coercitivity of the remanence ( $H_{cr}$ ). Lower part: Hysteresis loop (without paramagnetic correction) and thermomagnetic run, red heating and blue cooling down curves.*



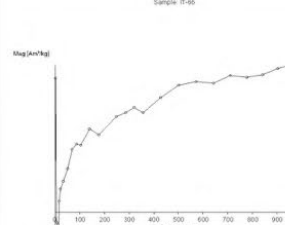
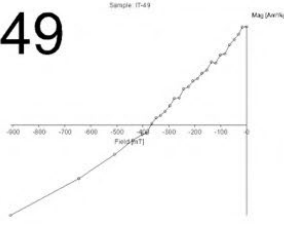
**IS-02**



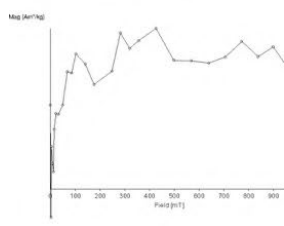
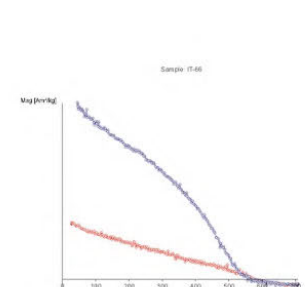
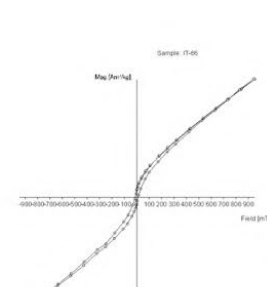
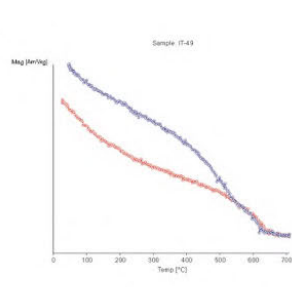
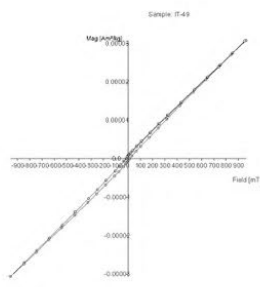
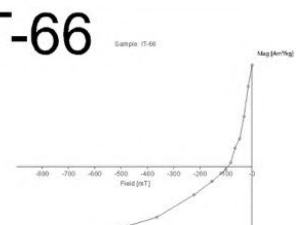
**IS-21**



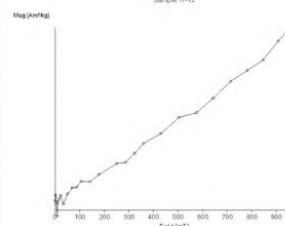
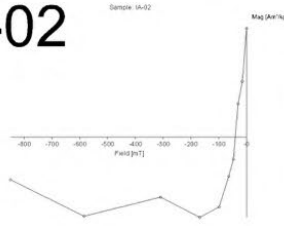
**IT-49**



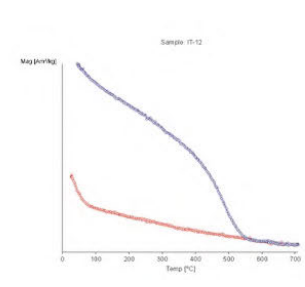
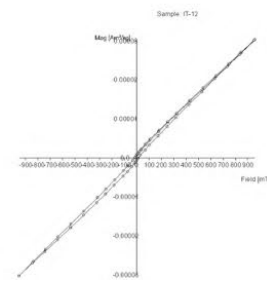
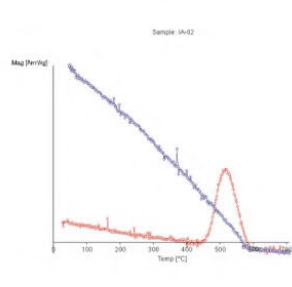
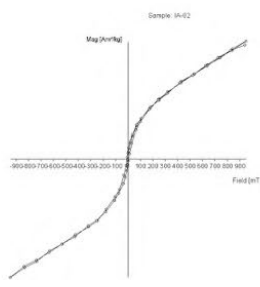
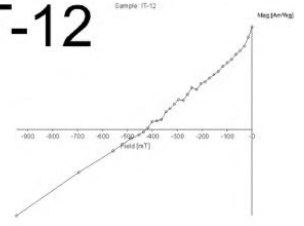
**IT-66**



**IA-02**



**IT-12**



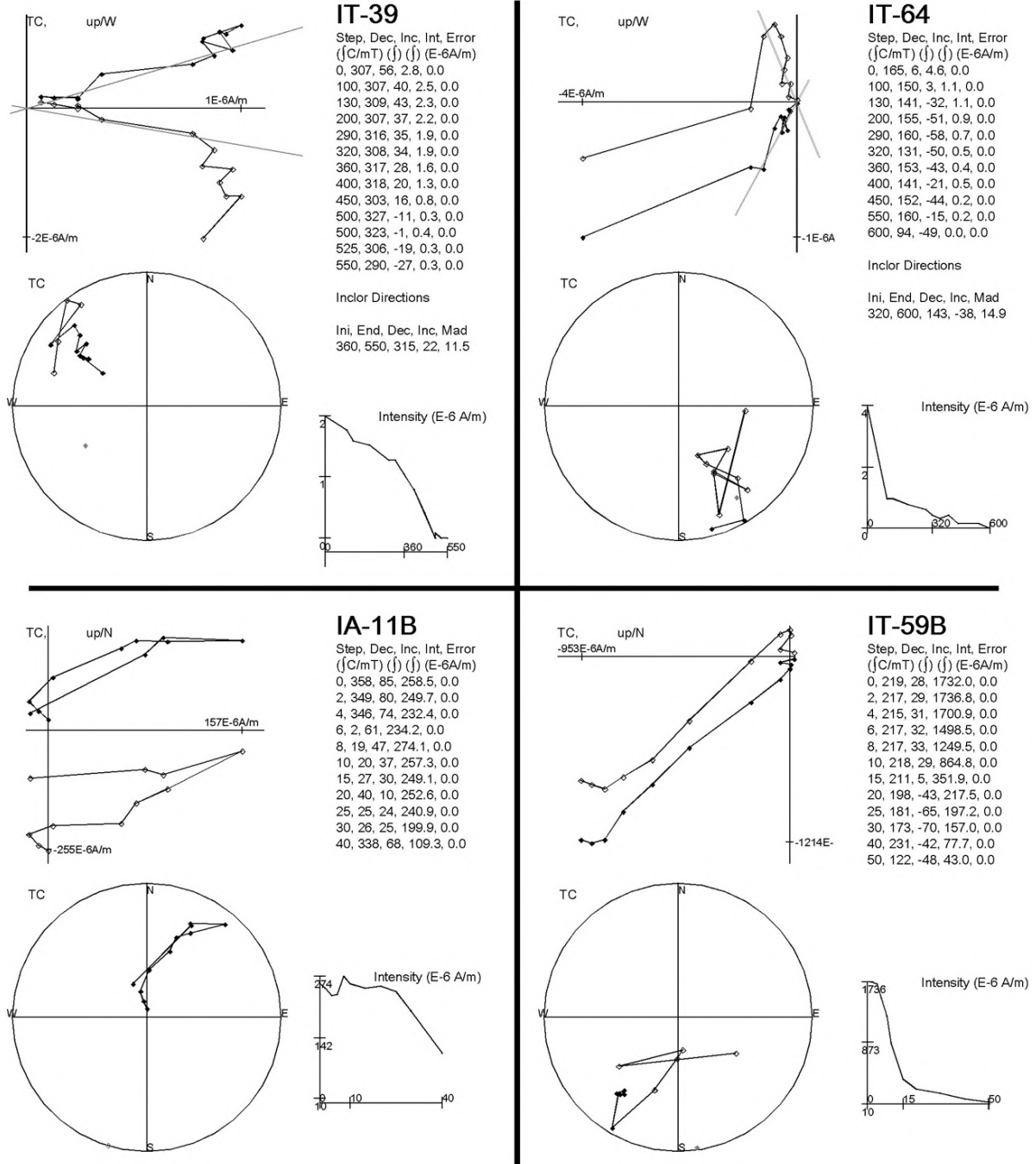


Figure 5.11. Demagnetization of the natural remanent magnetization in some representative samples of the Isclés section. Orthogonal diagram, stereoplot and intensity decay curve for all examples are shown. The upper samples (IT-38 and IT-64) are TH samples while the lowermost ones (IA-11B and IT59B) are AF examples.

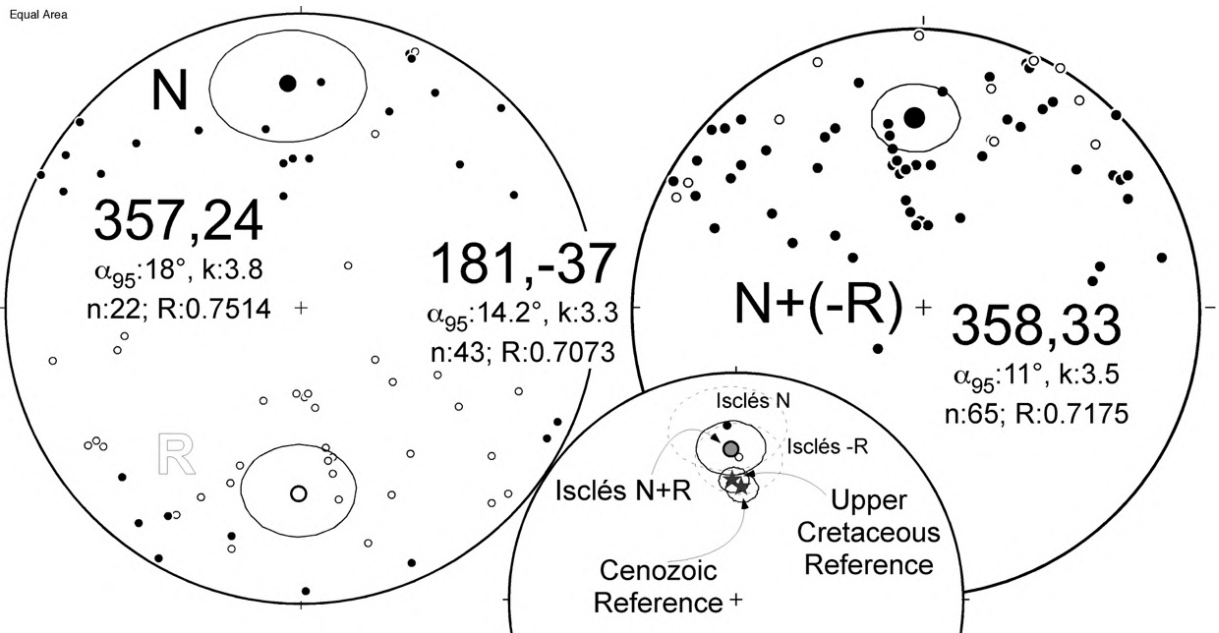


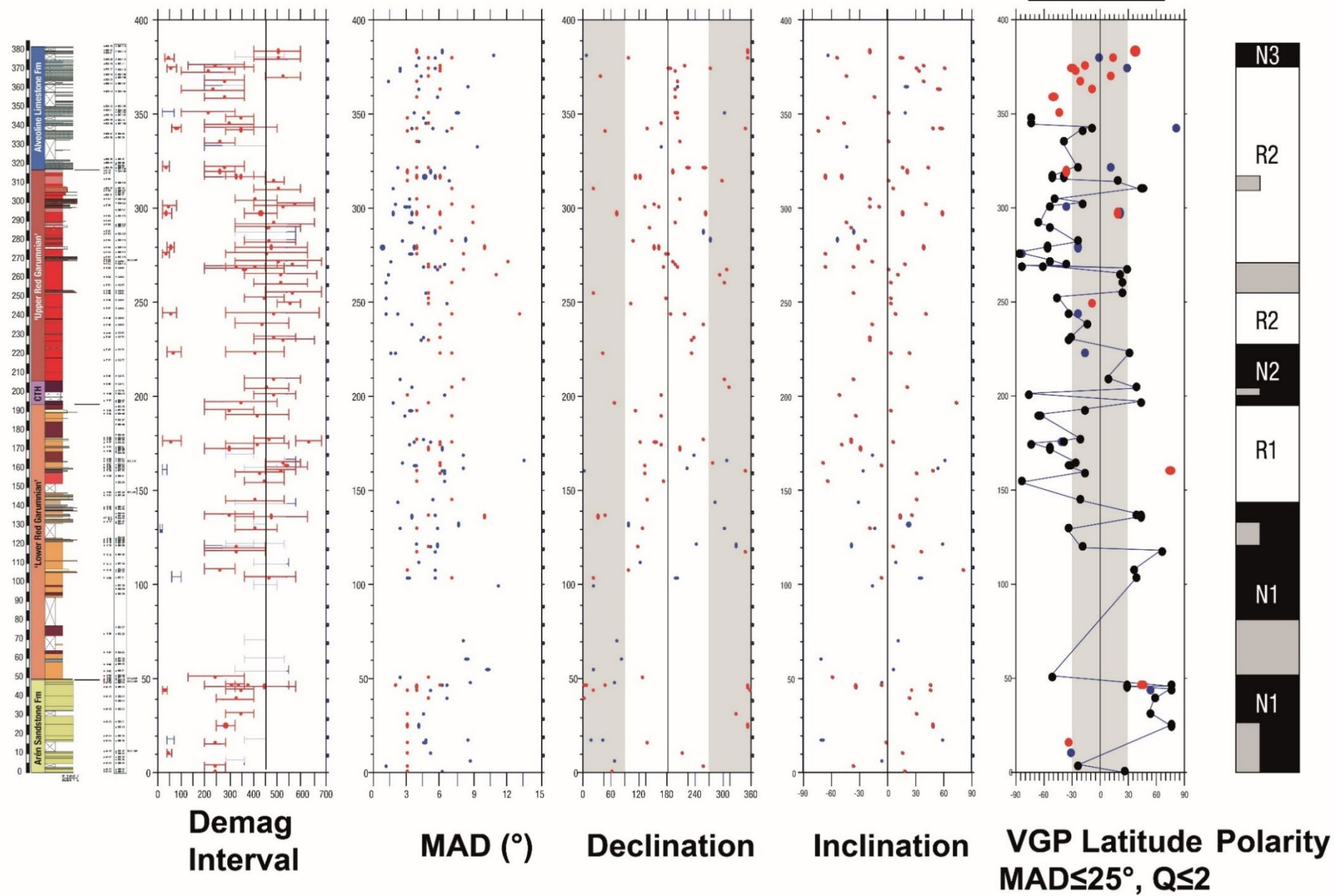
Figure 5.12: Stereographic projections of Q1 and Q2 CHRM of the Isclés section. ChRMs after bedding correction (paleogeographical reference system. Left: Normal and reverse components are plotted in both projections hemispheres. Right: All reverse directions converted to normal ones. Fisherian means and standard statistical parameters are also shown. Lower stereonet displays Isclés mean vectors and confidence regions together with the Upper Cretaceous and Cenozoic paleomagnetic references (stars).

The Local Polarity Sequence (LPS) calculated for Isclés section show some magnetozones, most of them showing a high degree of confidence (several consecutive levels with the same polarity) although in few intervals the determined polarity is not conclusive (Fig. 5.13). The first 50 meters of the section, which correspond with coarse-grained sandstone levels of the Arén Fm, displays a normal direction, not so clear in the lower part, but consistent in the last 25 meters of the formation. The first meters of the Tremp Fm, constituted by a very thin 'Grey Garumnian' and a partially covered muddy 'Lower Red Garumnian', represent an interval of undetermined polarity, due to the outcropping conditions and the subsequent sparsely sampling (some of the samples were lost during preparation since they were brittle). Between meters 90 to 140, with better outcrop condition for sampling, normal directions are again recognized (Figs. 5.13 and 5.14). These two normal intervals separated by an uncertain segment as a whole have been considered as normal magnetozones (N1). It is followed by a reverse magnetozones (R1) located between meters 140 to 190 within the upper part of the 'Lower

Red Garumnian', practically reaching the top. The uppermost levels of the 'Lower Red Garumnian' are followed by a short interval (~12 m) of purple mudstones and gypsum levels with carbonate nodules, which represents the Colmenar-Tremp Horizon (Eichenseer, 1988), followed upwards by the red mudstones of the 'Upper Red Garumnian'.

Apparently, the base of the Colmenar-Tremp Horizon marks the start of a normal magnetozone (N2), which extends approximately up to meter 225, including the first 20 meters of the 'Upper Red Garumnian'. The rest of this unit shows reverse directions, except a short interval between meters 250 and 270, in which a clear polarity could not be determined (Figs. 5.13 and 5.14). The detritic interval of the 'Upper Red Garumnian' is overlaid by the Alveoline Limestone Fm, which was only sampled in its first 60 meters. The samples from the 50 first meters (meters 320 to 360 of the composite profil) gave inverse directions (Figs. 5.13 and 5.14). This reverse interval in conjunction with the underlying reverse interval of the 'Upper Red Garumnian' has allowed to define a second reverse magnetozone (R2). Finally, the last 10 meters of the Alveoline Limestone Fm show again normal polarities, constituting a third normal magnetozone (Figs. 5.13 and 5.14)

The main problem that the Isclés magnetostratigraphic section has for correlation its LPS with the Global Polarity Time Scale is the absence of good biostratigraphic markers to anchor them. Thus, the main tool has been the correlation with nearby magnetostratigraphic sections from previous works, specially the Arén and Serraduy sections (Fig. 5.15). In this way, magnetozones N1 and R1 have been correlated with chron C30n and C29r respectively (Fig. 5.14). The presence of dinosaur fossils (bones and tracks) in the levels of these two magnetozones is the only 'biostratigraphic' marker identified. However, as it has been mentioned before, the presence of dinosaurs could lead to circular reasoning, specially concerning to chron C29r, where the K/Pg boundary is located. The last record of dinosaurs, which is a sandstone level with hadrosaur tracks, is located around the meter 160 of the section, in the chron C29r, albeit Vila et al. (2013) located a higher level with tracks (Isclés 5), very close to the Colmenar-Tremp Horizon (Fig 5.14). This track level could not be identified during the works of this thesis, so the exact stratigraphic position remains unknown.



*Figure 5.13 (previous page). Magnetostratigraphic analysis of Isclés section, including the stratigraphy, demagnetization interval, MAD, declination, inclination, VPG latitude and Local Polarity Sequence.*

The normal magnetozone N2 is the most problematic, since it is partially contained in the Colmenar-Tremp Horizon. This level of paleosoils is marking a progressive unconformity according to Eichenseer (1988), and appears above the 'Vallcebre Limestones' in the outcrops west of Serraduy, so that its age must be younger than that of the 'Vallcebre Limestones'. In consequence, the Colmenar-Tremp Horizon might have a minimum age of late Danian, assuming the direct correlation with the Suterranya Limestones from the eastern part of the Tremp Syncline (Díez-Canseco et al., 2014), though the problematic of this correlation has been already mentioned earlier. Then, the N2 magnetozone could be representing the chron C28n, the chron C27n, or the chron C26n, or could even represent two concatenated normal chrons, since it is unknown if there was an interruption of the sedimentation between the 'Upper Red Garumnian' and the Colmenar-Tremp Horizon. The lack of any relevant microfossil in the later hinders any accurate answer to that question.

Magnetozones R2 and N3 are less difficult to correlate with the GPTS. Previous works performed in the area of Isclés and other parts of the Western Tremp Syncline (Robador et al., 1990; Molina et al., 1992; Serra-Kiel et al., 1994, 2020; Pujalte et al., 2009), have calibrated temporally by means of magneto- and biostratigraphy the Alveoline Limestone Fm and the marine equivalent of the 'Upper Red Garumnian' (Fm Navarri). In this way, the 'Upper Red Garumnian' is Thanetian in age, meanwhile the Alveoline Limestone Fm lays in the Ilerdian (regional stage of the early Eocene, equivalent to the early Ypresian). Serra-Kiel et al., (1994) identified the presence of a regional unconformity between the Alveoline Limestone Fm and the 'Upper Red Garumnian', pointing to the existence of an stratigraphic hiatus, not being represented the chron C25n. For this reason the reverse magnetozone R2 is representing two different reverse chrons: the part of the 'Upper Red Garumnian' would correspond to the chron C25r and the part of the Alveoline Limestone Fm to the chron C24r (Fig. 5.14). This would imply that the N2 magnetozone, or at least the part that lays in the 'Upper Red Garumnian' could correlate with the chron C26n. Finally, the short normal magnetozone N3 would correspond with the C24n chron.

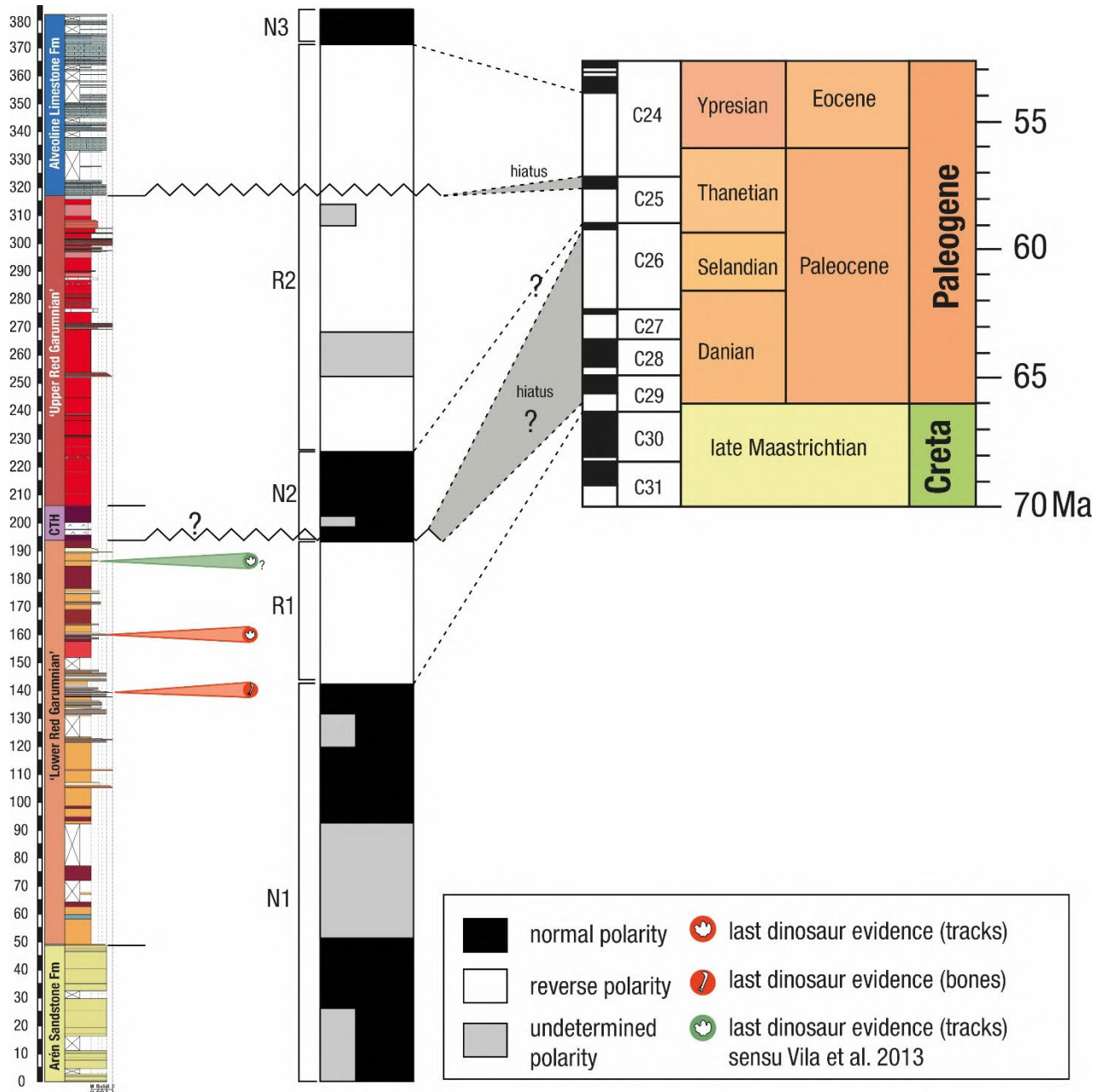


Figure 5.14. Correlation proposal of the Isclés Local Polarity Sequence (LPS) with the Global Polarity Time Scale (Ogg et al., 2012).

#### 5.1.4. Chronostratigraphic framework and K/Pg interval

The integration of previous data with the new contributions presented in this Thesis allows to improve the chronostratigraphic framework of the studied successions in the Western Tresp Syncline. A calibrated chronostratigraphic model is proposed (Fig. 5.15). The datings performed indicate an age between the upper part of chron C30n to the chron C29r for the top of the Arén Fm and the Mesozoic part of the Tresp Fm. However,

the stratigraphic position of the boundary between both chrons varies throughout the outcrops, tending to be situated in lower stratigraphical units towards the west, as a consequence of the thinning and progressive lateral passing of the 'Grey Garumnian' and Lower Red Garumnian' to their marine equivalents. So, all the Mesozoic Tremp Fm outcrops to the west of the Sierra del Sis are exclusively dated within chron C29r, meanwhile in the east their lower part lays within C30n. Rin section (López-Martínez et al., 2006b), represents an exception, since the top of the C30n reach the 'Grey Garumnian' (Fig. 5.15).

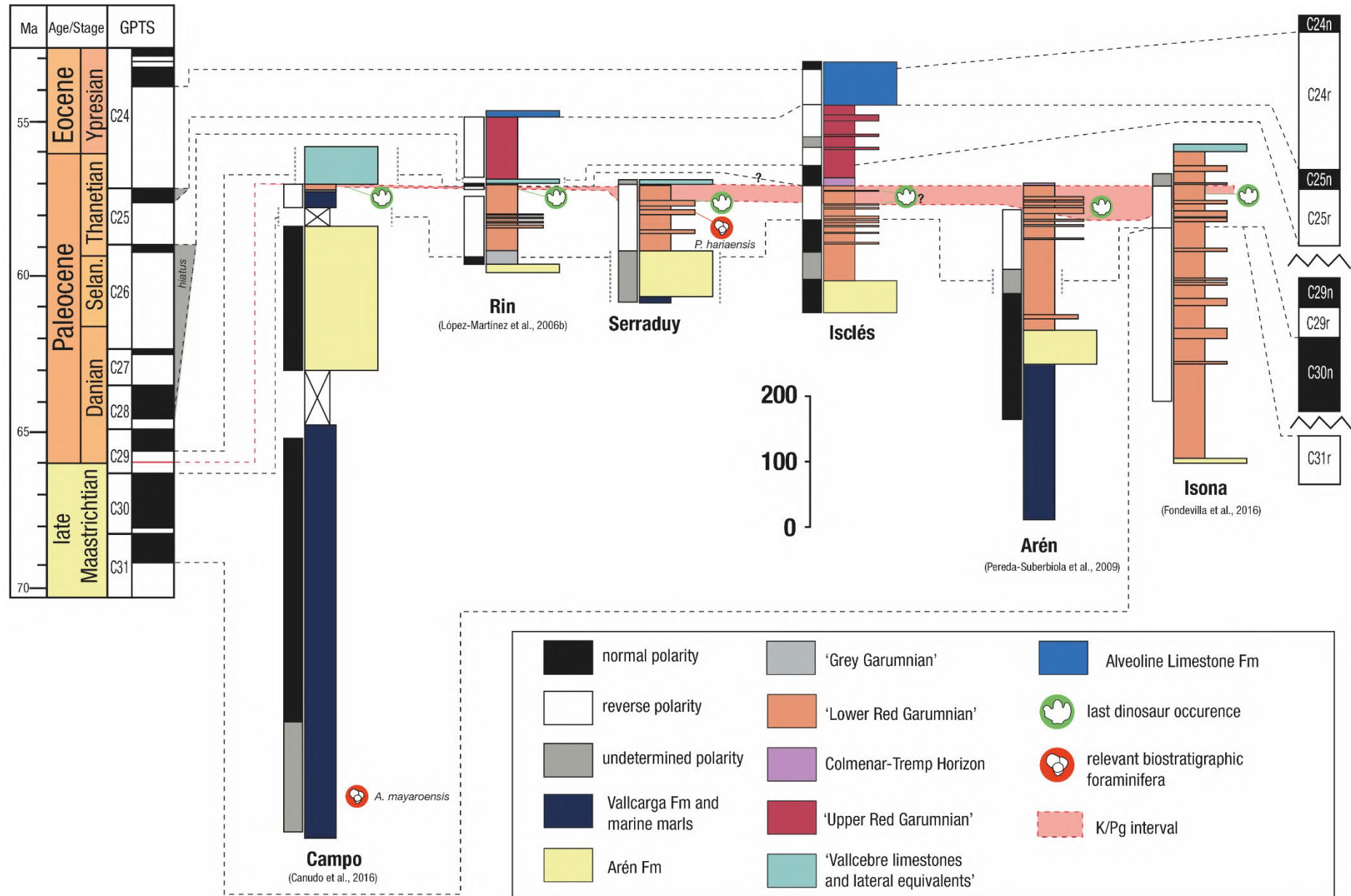
The stratigraphic position of the K/Pg is difficult to ascertain, since no layer with evidence of the impact (e.g., ejecta, iridium anomaly) has been found to the date. Thus, indirect methods have been used to constrain the K/Pg boundary, but there are some difficulties. In the Western Tremp Syncline, the reverse magnetozone identified as the C29r show different thickness (Arén: 90.5 m, Isclés: 50 m, Serraduy: 93.95 m, Rin: 104.6 m and Campo: 63.8 m). This variation in thickness may be related to variation in the spacing of sampling, by variations in the accumulation rates and the presence of intervals of undetermined polarity, which blur the exact position of the boundary between C30n and C29r (e.g., Arén, Fig. 5.15). This problem might be also related with the fact that the C29r is not preserved completely, especially the upper part. The only area where the top of the chron seems to be preserved is in the Rin section in which pass to a short normal magnetozone in the upper part of the 'Lower Red Garumnian', interpreted as the C29n by López-Martínez et al. (2006b) (Fig. 5.15), though it is preceded by an interval without data, which introduces some uncertainty. Fondevilla et al. (2016) estimated a sedimentation rate of  $\approx 18$  cm/kyr for the Tremp Fm during the chron C31r in the area of Isona, in the Eastern Tremp Syncline (Fig. 5.15). The K/Pg boundary is dated in 66.052 Ma (Sprain et al., 2018), meanwhile the chron C29r base is located in 66.311 Ma and the top in 65.724 Ma. This means that only the first 259 kyr of the chron are Maastrichtian, whereas 328 kyr would be Danian. Assuming that the rate from Fondevilla et al. (2016) remained constant during the deposition of the Tremp Fm in the chron C29r, the estimated thickness for the whole chron would be 105.6 m, meanwhile the Maastrichtian part would be around 46.6 m. The first number is quite close to the thickness preserved in the only area where the chron seems to be complete (Rin, 104.6 m), and all the preserved thicknesses of C29r in the 'Lower Red Garumnian' are higher than the estimated. This assumption would imply three consequences: 1) part of the preserved C29r in the 'Lower Red Garumnian' is Danian in age, 2) in some outcrops, a percentage

of the upper part of C29r is not preserved, and 3) some of the dinosaur sites could be then early Danian in age.

However, there are some flaws in these hypotheses. The constancy of the sedimentation rate may be challenged by the tectonic activity consequence of the initial uplift of the Pyrenees. The activity of the Bóixols s.s., Riu, Turbón and Campanué thrusts (from east to west) would conditionate the sedimentation in the area by uplift and growth of local anticlines (Ardévol et al., 2000; López-Martínez et al., 2006a; Fondevilla et al., 2016). This tectonic activity is related too with the lack of the upper part of chron C29r in some outcrops. For example, in all the outcrops east of Sierra del Sis, the 'Vallcebre Limestones' is not present because of the uplift of the Boixoll anticline, (López-Martínez et al., 2006a), and could have avoided the deposition of the upper part of the C29r too, avoiding even the preservation of the K/Pg boundary. Regarding to non-avian dinosaur fossils, they have previously used to determine the situation of the K/Pg interval by their last stratigraphic occurrence, assuming that they do not pass the Maastrichtian with the related problem with circular reasoning mentioned before. There are some few examples of non-avian dinosaur bones occurrences in rocks of the early Danian (Lofgren et al., 1990; Fassett et al., 2002), thought they are considered reworked or incorrectly dated (Lucas et al., 2009; Renne and Goodwin, 2012). However, in the Western Tremp Syncline there are several levels with tracks that could lay in the early Danian (e.g., Isclés 5 site from Vila et al., 2013), and if confirmed, would clearly represent survivors of the K/Pg event, since tracks cannot be reworked. Nevertheless, this is more likely a correlation/dating problem than the true presence of Paleogene non-avian dinosaurs.

In conclusion, there is chronostratigraphic evidence that points that the 'Lower Red Garumnian' was deposited in some areas of the Western Tremp Syncline up to the early Danian, whereas in others sedimentation was interrupted prior to the end of chron C29r. More chronostratigraphic data is needed to confirm or dismiss this theory, such as a proper temporal calibration of the 'Vallcebre Limestones' unit or the finding of the K/Pg boundary layer. Until then, the chronostratigraphic framework for this area present certain gaps, but it is quite solid to determine that record some of the vertebrates that inhabited the Ibero-Armorican island the last 300 kyr prior to the K/Pg boundary.

*Figure 5.15 (next page). Chronostratigraphic framework of the Western Tremp Syncline, based on biostratigraphic and magnetostratigraphic data. K/Pg interval has been proposed based on the last occurrence of dinosaur in each section.*



## **5.2. *Facies analysis and sedimentation model***

The facies identified have been differentiated according to the main lithostratigraphic units (topmost Arén Fm, 'Grey Garumnian', 'Lower Red Garumnian'). However, there are facies that are present in both in the 'Grey Garumnian' and in the 'Lower Red Garumnian' due to the lateral relationship of units, and locally Arén Fm facies are intercalated within the 'Grey Garumnian'. Thus, a clear distinction between lagoonal and fluvial facies is sometimes difficult. To solve this problem, some of them have been grouped in a perilagoonal facies association, since they show transitional characteristics between a lagoonal and strictly fluvial environment. This perilagoonal condition of the Tremp Fm in this area has been proposed previously by Eichenseer, (1988). Facies of the 'Transitional interval' described in section 5.1.1 are also included in this section.

### **5.2.1. *Topmost Arén Sandstone Fm: coarse-grained bioclastic sandstones with large scale cross-bedding***

The uppermost part of the Arén Fm was studied, since some vertebrate sites appear in those beds (e.g., Blasi 1 or Rin 1). This is characterized by metric-thick beds of coarse-grained sandstones with carbonate cement, rich in well-sorted quartz grains, though lateral variations in the grain size have been observed (Fig 5.16). Carbonate grains are also present with variable proportion, being mainly bioclasts of different type of invertebrates (gastropods, rudists, oysters, other bivalves) (Fig. 5.16 F, G) and rounded intraclasts of micrite. Vertebrate bones (Fig. 5.16 G), charophytes and plant remains appear occasionally, as well as calcareous and quartzite pebbles (Fig. 5.16 D). These sandstone beds display large cross-bedding (m-thick sets). Decimetric- to centimetric-thick sets of minor scale crossbedding and ripple marks are also present in some levels (Fig 5.16 E). This facies is also present intercalated within the 'Grey Garumnian' facies (e.g., Beranuy) (Fig. 5.2 and 5.3).

At the study area, the coarse-grained bioclastic sandstones of the uppermost part of the Arén Fm show a series of features that might indicate that the contact between the Arén and Tremp formations would not be an isochronous surface. In some areas, the top of the Arén Fm appears covered by a ferruginous crust; in other areas, it is heavily bioturbated by vertical traces (Fig. 5.16 B, C). Besides, locally the lowermost beds of the Tremp Fm have sandstone pebbles of the Arén Fm. This indicates that there were local

areas of the basin in which the Arén Fm could be exposed and eroded during the initial stages of deposition of the studied Tremp Fm.

### *5.2.2. Tremp Fm*

#### ***Lagoonal facies association***

##### *- Grey marls/mudstones and laminated siltstones (Gmls and Gm)*

This facies formed by grey fine-grained rocks of mixed composition arranged in decimetric to metric packages (Fig. 5.17 A). Carbonate content ranges between 28-40%. Quartz grains, carbonate nodules, plant debris and bioclasts of bivalves (veneroids and oysters) and gastropods are also present occasionally (Fig. 5.3), together with fossils of charophytes, foraminifera and fragments of bones of microvertebrates, though they have not been found in all the levels that have been sampled. The facies usually shows a massive aspect (Fig. 5.17 A), with usual presence of bioturbation, though is reduced to mottling, since traces determination is difficult.

Occasional intervals of laminated siltstones with parallel and low-angle lamination also appear, generally related to those muddy interval with less carbonate content (Fig. 5.17 B). These coarser intervals locally preserve two-dimensional impressions of plants (e.g. Camino Fornons 3) (Fig. 5.17 C).

##### *- Wavy fine-grained sandstones (Wfs)*

This facies is formed by fine-grained sandstones in cm- to dm-thick beds, which pinch out laterally. The sandstones have fine (< 0.3 mm) quartz grains and local carbonate grains, including undetermined bioclasts, algae fragments and foraminifera (Fig. 5.17 F).

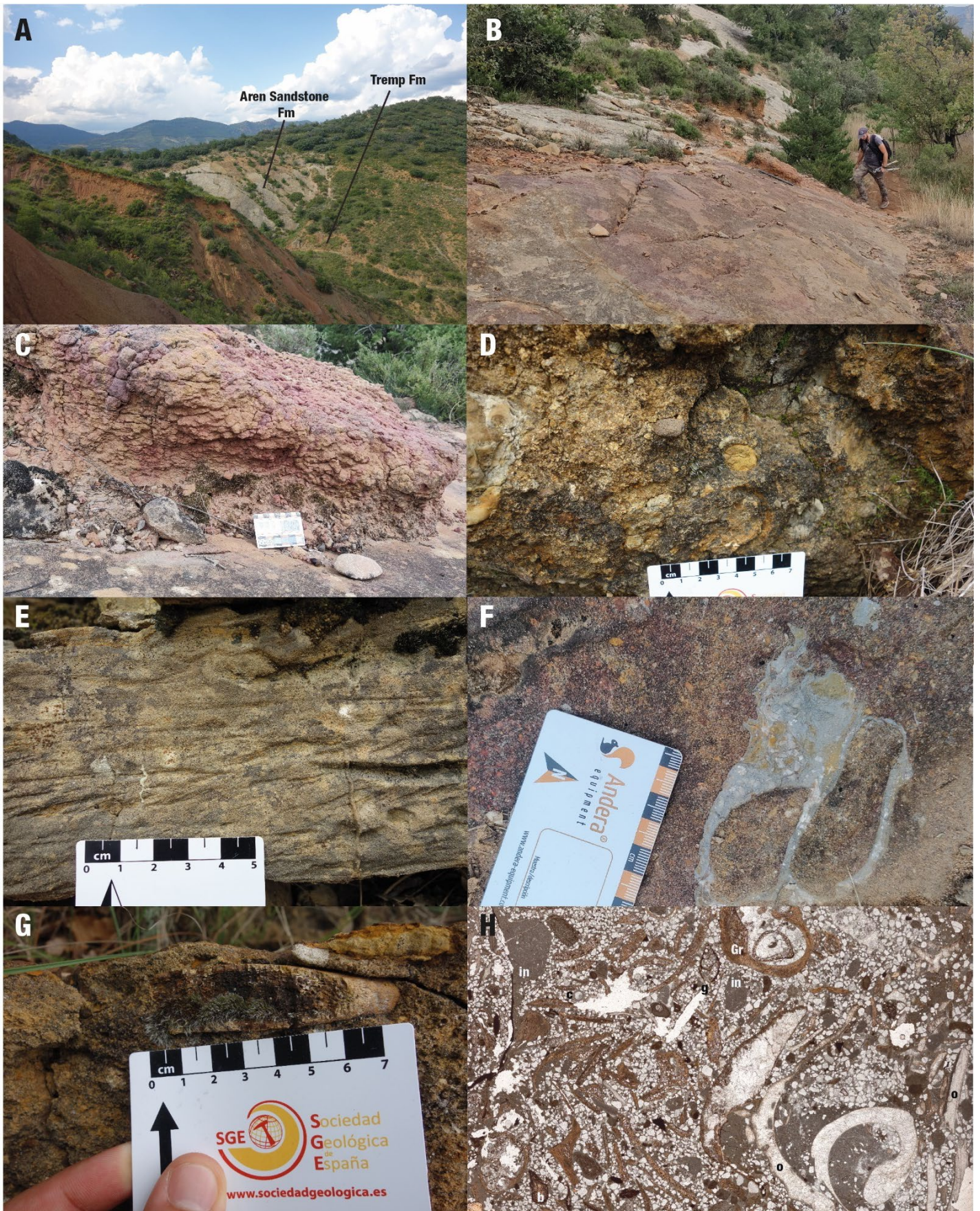
They always appear interbedded within the grey marls and mudstones and laminated siltstones (*Gmls* and *Gm* facies) (Fig. 5.17 D). The facies presents flow structures such as ripple marks, parallel and inclined lamination, flaser bedding and mud drapes (Fig. 5.17 E). Locally it has inclined heterolithic stratification (IHS) of small scale, passing some of the inclined laminae of sandstone to siltstone or even mudstones. Crocodylomorph swimming tracks have been recognized, including scratch marks and

partial or complete casts of hands and feet which appear as convex hyporeliefs at the bases of the strata (Pérez-Pueyo et al., 2018) (Fig. 5.18).

- *Micritic limestones (Mil)*

The micritic limestones facies only appears in the 'Grey Garumnian' of the Campo section (Fig. 5.2). It is formed by pure micritic limestones arranged in cm- to dm thick beds which are interbedded with grey marls (Fig. 5.17 G). Locally there are carbonate nodules and some levels present dinosaur tracks at their bases (Fig. 5.17 H), preserved as convex hyporeliefs, corresponding to casts of hands and feet of hadrosauroid ornithopods. The tracks are referable to the ichnogenus *Hadrosauropodus*.

*Figure 5.16 (next page). Coarse-grained bioclastic sandstones with large cross-bedding. A) Contact between the Arén Sandstone Fm and the Tremp Fm at the Arén outcrop. B) Bioturbated and Fe-rich top layer of the Arén Sandstone Fm at the Arén outcrop. C) Detail of the heavily bioturbated layer of photo B). D) Calcareous and quartzite pebbles found in a sandstone package at the Beranuy outcrop. E) Cross-bedding and ripples marks in a sandstone layer at the Beranuy outcrop. F) Oyster shell found at the top layer of the Arén Sandstone Fm at the Arén outcrop. G) Vertebrate bone at the top of a sandstone bed at the Beranuy outcrop. H) Thin-section image of sample VE-0, displaying the main components of a coarse-grained bioclastic sandstone: b: bone fragment, c: carophyte, g: gastropod, in: intraclast, o: oyster.*



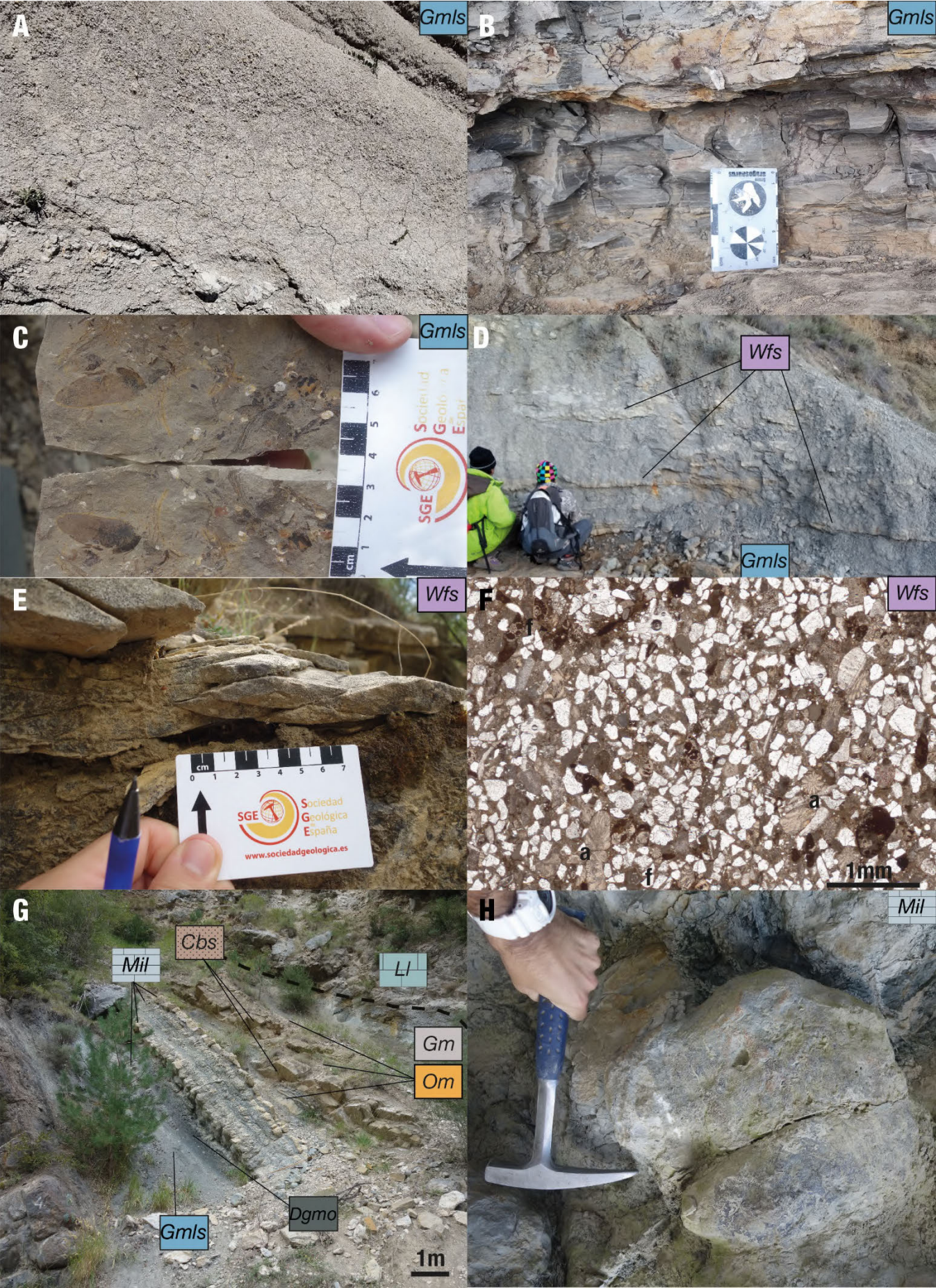


Figure 5.17 (previous page). Lagoonal facies association I. A) Grey marls at San Pere de Cornudella outcrop (Gmls). B) Detail of grey mudstones and siltstones with parallel and low-angle lamination (Gmls) (Beranuy outcrop). C) Plant fossils from Camino Fornons 3 site, preserved in the laminated siltstones (Gmls). D) Intercalation of wavy fine-grained sandstones and grey marls at the Serraduy outcrop. E) Detail of some wavy ripples in a level of fine-grained sandstones (Wfs) (Beranuy outcrop). F) Thin-section image of sample STH-1 of wavy fine-grained sandstone (Wfs) with fragments of algae (a) and foraminifera (f). G) Tremp Fm in the Campo section, with the main sedimentary facies pointed. H). Hadrosaur track preserved at the base of a micritic limestone bed at the Campo section.

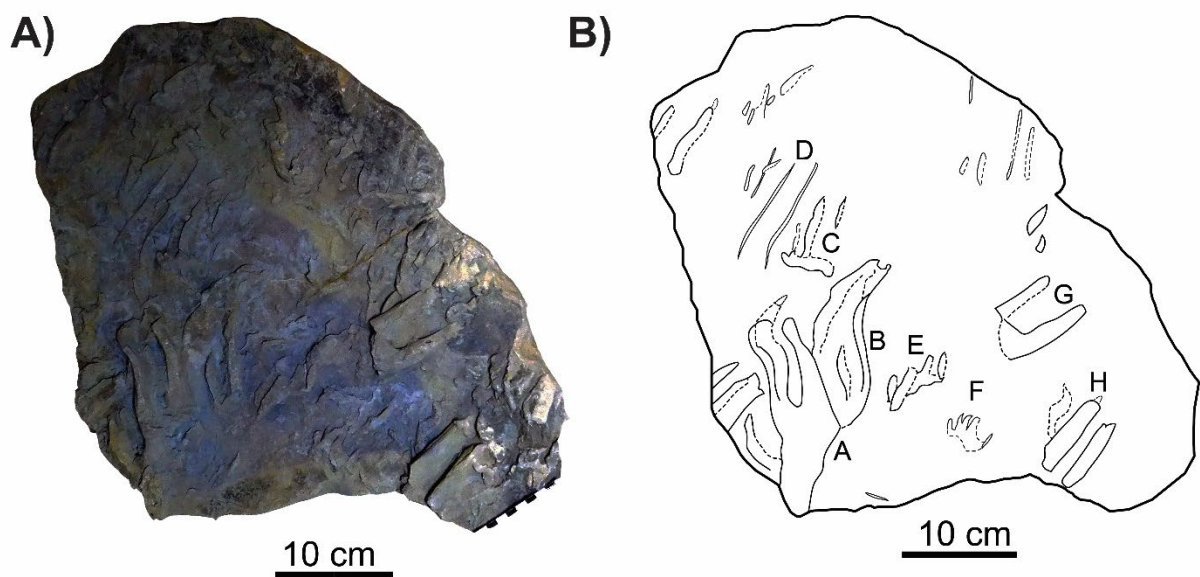


Fig. 5.18. Rock slab with crocodylomorph swimming tracks from Beranuy site (MPZ 2018/17), preserved as convex casts in the base of a wavy fine-grained sandstone (Wfs) bed. A) General view. B) Schematic drawing pointing the different tracks recognized (A–H) (after Pérez-Pueyo et al., 2018).

### **Perilagoonal facies association**

#### **- Carbonate sandstones and sandy limestones (CsSl)**

Sandy limestones and carbonate sandstones are arranged in dm-thick tabular, nodular and lenticular beds, which usually appear grouped in bed packages (Fig. 5.19 A and C). They present tabular cross-bedding, flaser bedding with mud drapes (Fig. 5.19

D and E), and in some cases, inclined heterolithic stratification (IHS), passing laterally to grey siltstones and mudstones, noting the tidal influence in their deposit (Fig. 5.19 C).

They exhibit a mixed composition, variable proportion of fine sand size quartz grains and a carbonated micritic matrix. Other minor components are bioclasts and intraclasts. They are usually highly bioturbated (Fig. 5.19 B), displaying both vertical and horizontal traces of invertebrates, and occasionally dinosaur tracks, though those last, when appearing, are very distorted, limiting ichnotaxonomic inferences. Vertebrate bones and plant remains also appear occasionally. Though this facies is mainly related to lagoonal facies, sometimes it has been observed associated also with facies of the 'Lower Red Garumnian', like ochre mudstones, which would indicate that would fit within the perilagoonal fringe too (see below).

- *Bioclastic sandstones (Bcs)*

This facies is conformed by discrete irregular dm-thick coquina beds of medium-grained sandstones with abundant skeletal remains of invertebrates, mainly bivalves and gastropods, generally with a carbonate matrix (Fig. 5.20). The most common bivalve represented is the genus *Corbicula*, being even some beds exclusively composed by shells of this veneroid bivalve (Fig. 5.20 B, C). This genus has been recognized in the Tremp Fm in transitional environments, usually associated with brackish molluscs (Vila et al., 2011; Oms et al., 2016). The bivalve shells sometimes appear preserved (Fig. 5.20 D), and other times dissolved, leaving only inner casts of the bivalves (Fig. 5.20 F). Other minor skeletal components are plant remains, charophyte gyrogonites and talli, foraminifera and calcispheres. Less common there are non-skeletal grains including carbonate and sandy pebbles and intraclasts (Fig. 5.20 D and F). Two types of bioclastic sandstones can be recognized: shell-supported bioclastic coquina sandstones being quartz grains minority (Fig. 5.20 A-D); and a second one in which shells are less abundant, and quartz grains or intraclasts are more abundant (Fig. 5.20 E, F). In the first one, bivalve shells appear mostly articulated, meanwhile in the second one, they appear disarticulated and imbricated, and in hydrodynamic position (Fig. 5.20 D).

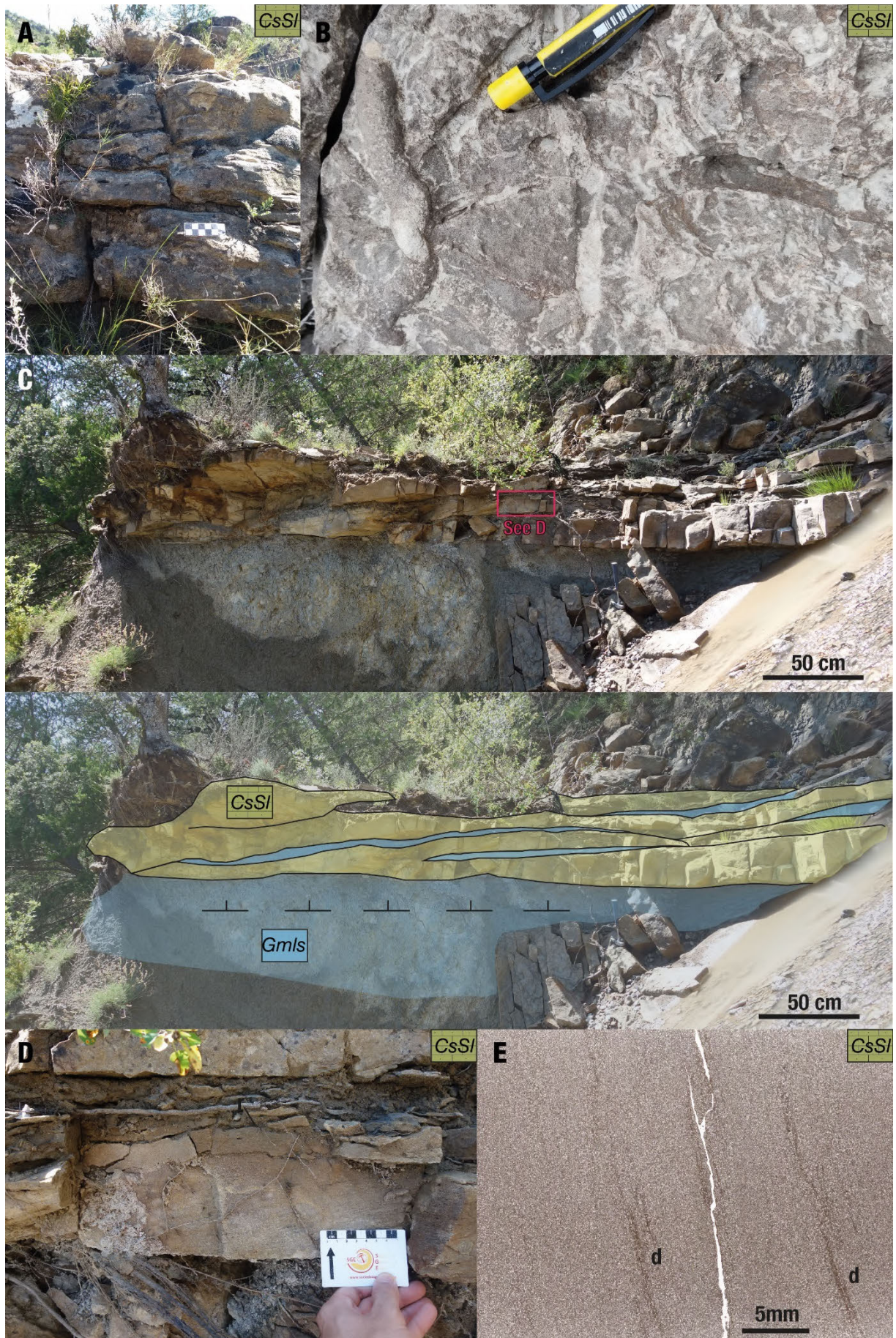


Fig. 5.19 (previous page). *Perilagoonal facies association*. Carbonate sandstones and sandy limestones facies (CsSl). A) Package of nodular carbonate sandstones at Serraduy outcrop. B) Detail of infauna horizontal traces at Serraduy outcrop. C) A package of sandy limestones and carbonate sandstones from San Pere de Cornudella outcrop with inclined heterolithic stratification (IHS), in which sandstones layers (CsSl) pass laterally to grey marly mudstones (Gmls). The geometric relationships of both facies have been sketched. Note that the bedding of the package was restore to the horizontal. D) Detail of one of the layers of C), which shows planar cross-bedding with mud drapes and subtle ripples at the top. E) Thin-section image of sample SE1-2. Some mud drapes (d) can be observed.



Fig. 5.20 (previous page). *Perilagoonal facies association. Bioclastic sandstones facies (Bcs)*. A) *Coquina bed of bivalves and gastropods found at Isclés section, with a fossilized tree trunk*. B) *Detail of A9, displaying several shells of Corbicula*. C) *Monospecific Corbicula coquina sandstone bed near the Serraduy outcrop; all bivalves are preserved as inner casts*. D) *Thin-section image of sample IS-2, picked from A) bed*. E) *Bioclastic sandstone found at Serraduy outcrop, with disarticulated and imbricated bivalve shells*. F) *Thin-section image of sample SE1-6*. *b: bivalve, c: charophyte, f: foraminifera, g: gastropod, i: intraclast, p: plant debris*.

- *Fine-grained bioturbated sandstones (Fbs)*

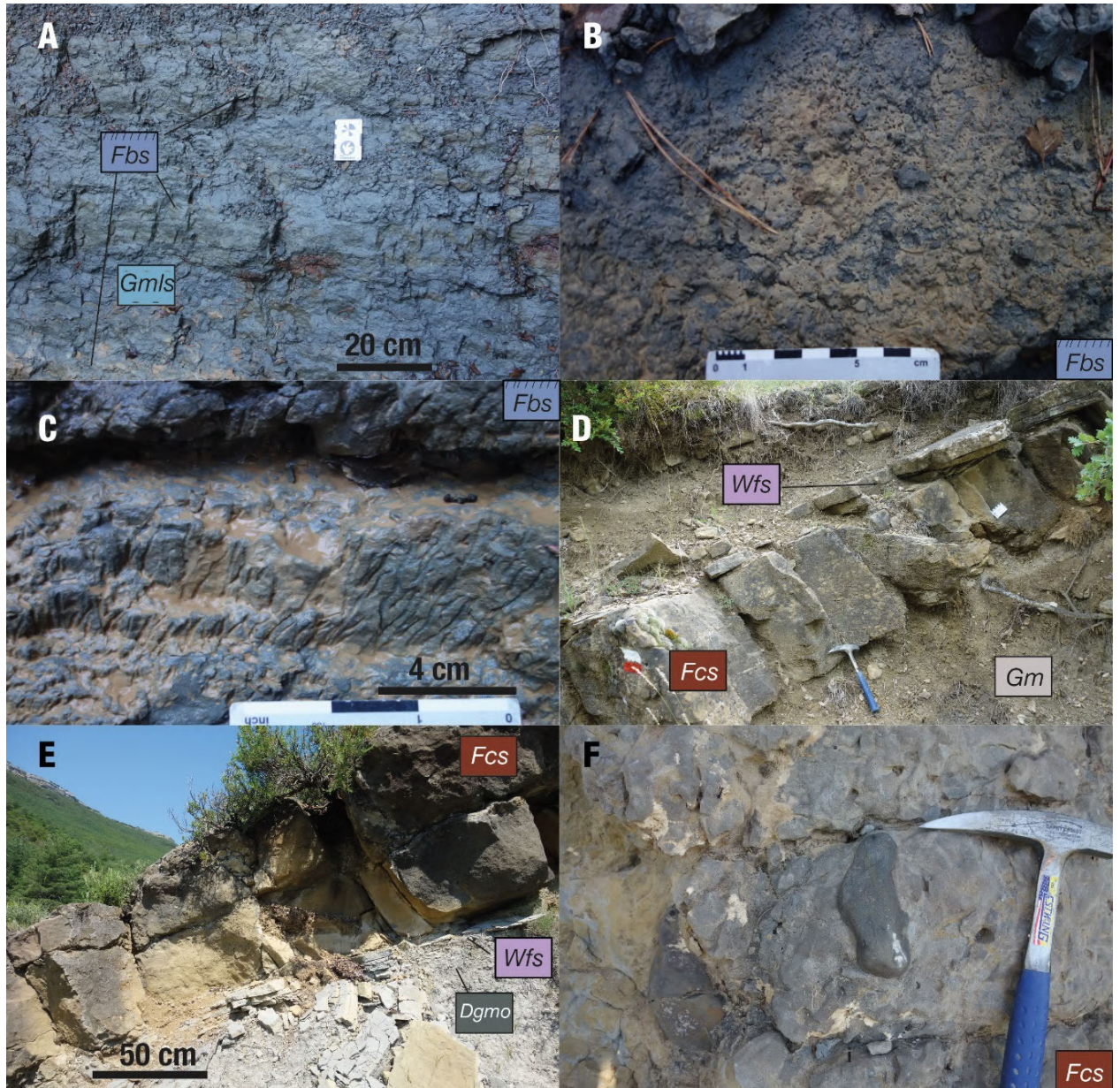
Only found in the outcrop of Rin (Fig. 5.2), this facies is constituted by an alternation of very thin (2-5 cm thick) fine-grained sandstones to siltstones, with also grey marls and mudstones (Fig. 5.21 A). Sandstone beds display a quite penetrative bioturbation, consisting of millimetric tubes, which traverse the sediment vertically or slightly oblique, but always with a main vertical component (Fig. 5.21 B, C). The traces are not straight but irregular, gently sinuous, and branching in some cases. Thus, they are probably rhizoliths of small plants. These fine levels are found in an area where the 'Grey Garumnian' interdigitates with the 'Lower Red Garumnian' (Fig. 5.2).

- *Foreset cross-bedded sandstones (Fcs)*

This is a locally limited facies, which has been recognized only in two beds in Beranuy and Arén outcrops, which probably represent event (storm) beds. It is formed by isolated decimetric 0.6 and 1m-thick beds of medium to coarse-grained sandstones. In the case of Beranuy, the bed is an isolated set of planar cross-bedding (Fig. 5.21 D). The paleocurrent measured is 350-360° (N-NNW). Few scape traces can also be observed in the sandstone. It is overlaid by fine-grained wavy sandstones facies (*Wfs*). The bed from Arén is highly bioturbated sandstone level (Fig. 5.21 E), that obliterates the cross-bedding, thus no paleocurrent was measured. However, in the bed there were abundant numerous dinosaur bones, including partially articulated skeleton of the holotype of the hadrosaur *Arenysaurus*, being the bed the horizon of Blasi 3 site.

Both beds present some isolated limestone boulders of decimetric diameter (Fig. 5.21 F), which point that the energy was high in the moment of the deposition. Cruzado-Caballero et al. (2021) also indicates that Blasi 3 level is conformed by texturally

immature greywacke, with poor grain sorting; implying that the sedimentation was consequence of a rapid event. Thin-section from Blasi 3 level confirm this, with a grain-supported texture, with angular grains of quartz and carbonate.



*Fig. 5.21 Perilagoonal facies association. A) Alternation of fine-grained bioturbated sandstones (Fbs) with grey marls (Gmls) at Rin section. B) Detail of the top of a heavily bioturbated sandstone level at Rin section. C) Detail of B), showing the high degree of bioturbation. D) Foreset cross-bedded sandstone (Fcs) level at Beranuy, showing planar cross-bedding. E) Foreset cross-bedded sandstone (Fcs) level at Arén. F) Limestone boulders found a top of a foreset cros-bedded sandstone at Arén section (level of Blasi 3 site)*

- *Dark grey marly mudstones rich in organic matter (Dgmo)*

This is a local facies of levels of the 'Grey Garumnian', which usually appears in the upper part of the unit, close to the boundary with the 'Lower Red Garumnian'. This reinforces their inclusion within the perilagoonal facies association. These facies are usually limited laterally, since they pass sometimes to non-fossiliferous grey mudstones (Fig. 5.2). It is characterized by discrete massive m-thick levels of dark-grey mudstones rich in organic matter (Fig. 5.22 A). The carbonate ( $\text{CaCO}_3$ ) content is around 20-39%, ranging between marly mudstones and marls. Plant remains are abundant, including charcoalified fossil wood fragments and small amber droplets. Carbonate nodules can also be found. Some levels show intense plant bioturbation, in the form of centimetric ocherish vertical mottling and grey-ocher cemented silt-filled rhizocretions (Fig. 5.22 B and C). The rhizocretions range in sizes from few centimeters to up to 15 cm. They sometimes branch out and include fragments of carbonaceous wood.

The facies is notably fossiliferous, including microfossils of charophyte gyrogonites (Fig. 5.7), foraminifera (Fig. 5.6) and ostracods, and invertebrates represented by a mix of marine, and brackish tolerant forms, such as veneroid bivalves, oysters, gastropods, crustacean decapods, insect coprolites, serpulids and bryozoans (Fig. 5.22 E). (See section 6.2.1 for the description of the invertebrate assemblage of Veracruz 1). Vertebrates are represented by isolated bones (Fig. 5.22 D), teeth, scales, eggshell fragments, and coprolites, including remains of fishes, amphibians, turtles, crocodylomorphs and dinosaurs, as well as eggshell fragments. Bones appear isolated, with abraded surfaces and sometimes carbonate encrusted. The paleontological site Veracruz 1, studied in detail in this PhD was found in this facies (see section 6.2.1 or the description of the vertebrate assemblage of Veracruz 1 site).



Fig.5.22). Perilagoonal facies association. Dark grey marly mudstones rich in organic matter facies (Dgmo). A) Panoramic view of Veracruz 1 site (VE1), located in a thick package of dark grey marly mudstones rich in organic matter. B) Detail view of A), with several in situ rhizoconcretions and ochre mottling. C) General view and cross section of one of the rhizoconcretions recovered from VE1. D) Fragmented dinosaur bone from the interval B of VE1. E) Detail of an outcrop of dark grey marly mudstones rich in organic matter with shells of veneroid bivalves and gastropods (in white), at the Beranuy area.

- *Ochre mudstones-marls (Om)*

This facies is characterized by m-thick packages of ochre to light brown mudstones to marls, with a carbonate content between 13 to 40%, (average 23.5%). Locally silty mudstones are also present. Bioclasts of gastropods and bivalves are common, but they do not represent more than the 3-5% of the samples. Other occasional skeletal elements are foraminifera, charophytes, ostracods, vertebrate bones (Fig. 5.23 C) and small eggshell fragments of theropod dinosaurs. Besides, quartz grains, ferrous nodules and specially carbonate pebbles are also present. The facies is in general bioturbated, though sometimes this is difficult to identify, since the infilling sediment of traces have the same ochre color than the matrix. Invertebrate knobby traces like *Loloichnus* can be observed usually in the boundary between ochre mudstones and overlying sandstone levels, showing the traces a sandy infilling. The facies is closely related with the variegated hydromorphic mudstones (*Vhm*) (see below), as they pass gradually to each other (Figs. 5.2. and 5.23 A, B). In fact, sometimes the ochre mudstones-marls display hydromorphic mottled texture.

***Fluvial facies association***

- *Variegated hydromorphic mudstones (Vhm)*

The variegated hydromorphic mudstones facies corresponds to m-thick packages of reddish to pinkish brown mudstones, though when unaltered rock is exposed, they display a high range of colors (red, yellow, green, brown), which appear with a mottled texture, being all present and intermingled. This is due to penetrative bioturbation of plants and invertebrates, being more common root vertical traces (Fig. 5.23 D). The facies has a carbonate content that ranges between 2 to 23 % (average 14%). In some levels, charophytes and dinosaur eggshells appear, but less frequently than in the ochre mudstones-marls facies. Bioclasts are also scarcer but other grains are more abundant, especially ferruginous nodules, quartz and carbonate pedogenic grains. It is highly related with ochre mudstones-marls (*Om*) and the bioturbated marly/sandy limestones (*Bmsl*) (see below) facies (Fig. 5.23 A, B), and it is usual to see lateral changes between them over short distances.

- *Red mudstones (Rm)*

This facies is formed by several dm-thick levels of red and reddish brown mudstones (Fig. 5. 23 A, E, F). Their average carbonate content is 14%, ranging between 13-15% (only two levels of this facies were sampled: see Annex II). Ferruginous nodules are more abundant than in the other fine-grained facies. Quartz grains and grey and white carbonate nodules and concretions are also present in some beds.

All the sampled mudstones are azoic, without micro- and macrofossils, except some trace fossils of invertebrates (Fig. 5.23 E). The distribution of this facies is mainly restricted to the middle and upper part of the 'Lower Red Garumnian' (Fig. 5.2) being usually in alternation with ochre mudstones-marls (*Om*) and variegated hydromorphic mudstones (*Vhm*) facies (Fig. 5.2, 5.3 and 5.23 A) and showing no relationship with the facies of the 'Grey Garumnian', discarding thus its location in the perilagoonal fringe. It has been also noted that red mudstones are only present in the eastern part of the studied outcrops, not being observed west of the Rin section (Fig. 5.2)

- *Grey mudstones (Gm)*

In contrast with the grey fine-grained lagoonal facies described for the 'Grey Garumnian', grey mudstones also locally appear in the 'Lower Red Garumnian' but with different characteristics. They usually form laterally limited dm-thick levels, which are usually found underlying sandstone packages of cross-bedded sandstones (*Cbs*) facies (see below) (Fig. 5.2 and 5.24 A) or included alternating with ochre and variegated mudstones, to which they pinch out. In some cases, they can be also found as small interbeds in sandstones packages, as small lenses between the inclined sandstone strata. They show a massive texture (Fig. 5.24 B), only disrupted by invertebrate traces, which are simple (Fig. 5.24 C) or by occasional laminations or pebble lineations. Vegetal remains and vertebrate bones also appear in some levels.

- *Intraclastic limestones (Ilm)*

Only one level of this lithology has been recognized in the 'Lower Red Garumnian', in the Valle de Lierp section (Fig. 5.2). It is a lenticular bed of a maximum thickness of 40 cm, which is limited a base, a top and laterally by grey mudstones (Fig. 5.24 D). Both the

grey mudstones and the intraclastic limestone pinch out laterally, being this set of facies enclosed in a thick interval of ocher and variegated hydromorphic mudstones.

At first sight this facies seems like a microconglomerate. However, it has been classified as intraclastic limestone because it is dominated by carbonate intraclasts (85%) supported by a carbonate muddy matrix. The intraclasts are rounded ( $\varphi \sim 0,2$  cm), and occasionally present irregular oncolitic coatings (Fig. 5.24 F). Subrounded to angular. poorly sorted ( $\varphi < 1$  mm) quartz grains are also present (10 %), they are poorly sorted ( $\varphi < 1$  mm) and range between subrounded to angular. Other components are bones of vertebrates, decapod fingers, foraminifera, charophytes, plant remains and ambar droplets. Vertebrate bones are disarticulated, having sizes between 15 to 2 cm, showing fragmentation and abraded edges (Fig. 5.24 E). The bed has normal grading, and its top is bioturbated by horizontal and vertical simple traces of invertebrates, which show a diameter of around 1 cm. Larra 4 vertebrate site is located in this level.

- *Charophyte packstone (Cp)*

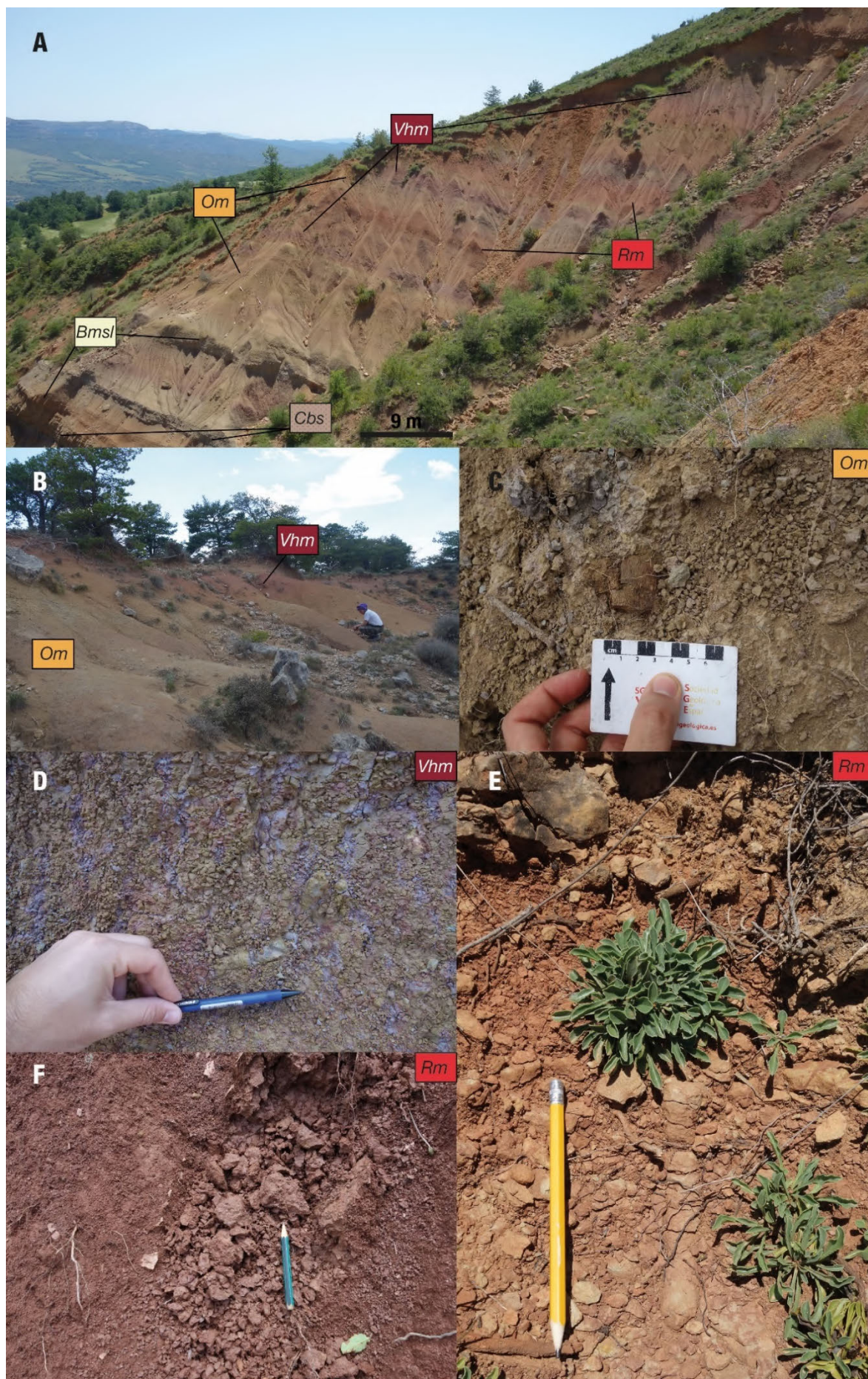
Only one bed of this facies has been recognized in the studied outcrops, in San Pere de Cornudella (Fig. 5.2, Annex II). This ~30 cm thick whitish grey nodular limestone layer is located in a muddy interval, in the lower part of the 'Lower Red Garumnian', and it is limited spatially, passing to ochre mudstones, having a lateral extension of around 70 m (Fig. 5.24 G). The limestone has abundant charophyte gyrogonites (Fig. 5.24 H), shells of gastropods and veneroid bivalves, crocodylomorph teeth and other indeterminate bioclasts. Its texture is grain-supported with a micritic matrix. Some invertebrate traces have been observed also. The charophytes were only analyzed through thin section, avoiding thus a proper taxonomic assignation.

- *Bioturbated marly/sandy limestones (Bmsl)*

This facies is characterized by m-thick beds of highly bioturbated sandy limestones and carbonate fine-grained sandstones. The beds have irregular geometry, sometimes showing bulging dome shapes, sometimes located at the top of sandstone or microconglomerate beds (Figs 5.23 and A 5.25 A, B, C). They present an obscured texture (mixing of carbonate matrix and small quartz grains) obliterated by the bioturbation produced by plants and infauna. Those less bioturbated beds are sandier.

Plant bioturbation is represented by pink to purple or grey rhizohalos oriented vertically (Fig. 5.25 D), meanwhile the invertebrates traces appear as circular burrows on the top, with paired openings (cf. *Arenicolites*) (Fig.5.25 B) or as knobby galleries (cf. *Loloichnus*), besides multitude of simple traces. They are composed by a carbonated matrix accompanied by small quartz grains, most of them mobilized by the action of the infauna and the plants. The amount of quartz grains seems to be related to the action of the bioturbation (Fig. 5.25 E), thus those beds less bioturbated are sandier. Tough is not something common, isolated vertebrate bones appear in this facies. They tend to pass upwards gradually to ochre mudstones (*Om*) or variegated hydromorphic (*Vhm*) facies without a clear boundary.

*Fig.5.23 (next page). Fluvial facies association. A) Panoramic view of the Arén section, showing an alternation of some muddy facies of the 'Lower Red Garumnian'. B) Ochre (Om) and variegated hydromorphic mudstones (Vhm) at El Castellaz section. C) Detail of ochre mudstones (Om) in Enebro site (Serraduy), with a fragment of a vertebrate bone. D) Variegated hydromorph mudstones (Vhm), with penetrative vertical root traces and an invertebrate trace, in the area of Rin. E) Red mudstones (Rm) at Arén outcrop, with a vertical invertebrate trace cf. Loloichnus? F) Red mudstones (Rm) in the area of San Pere de Cornudella.*



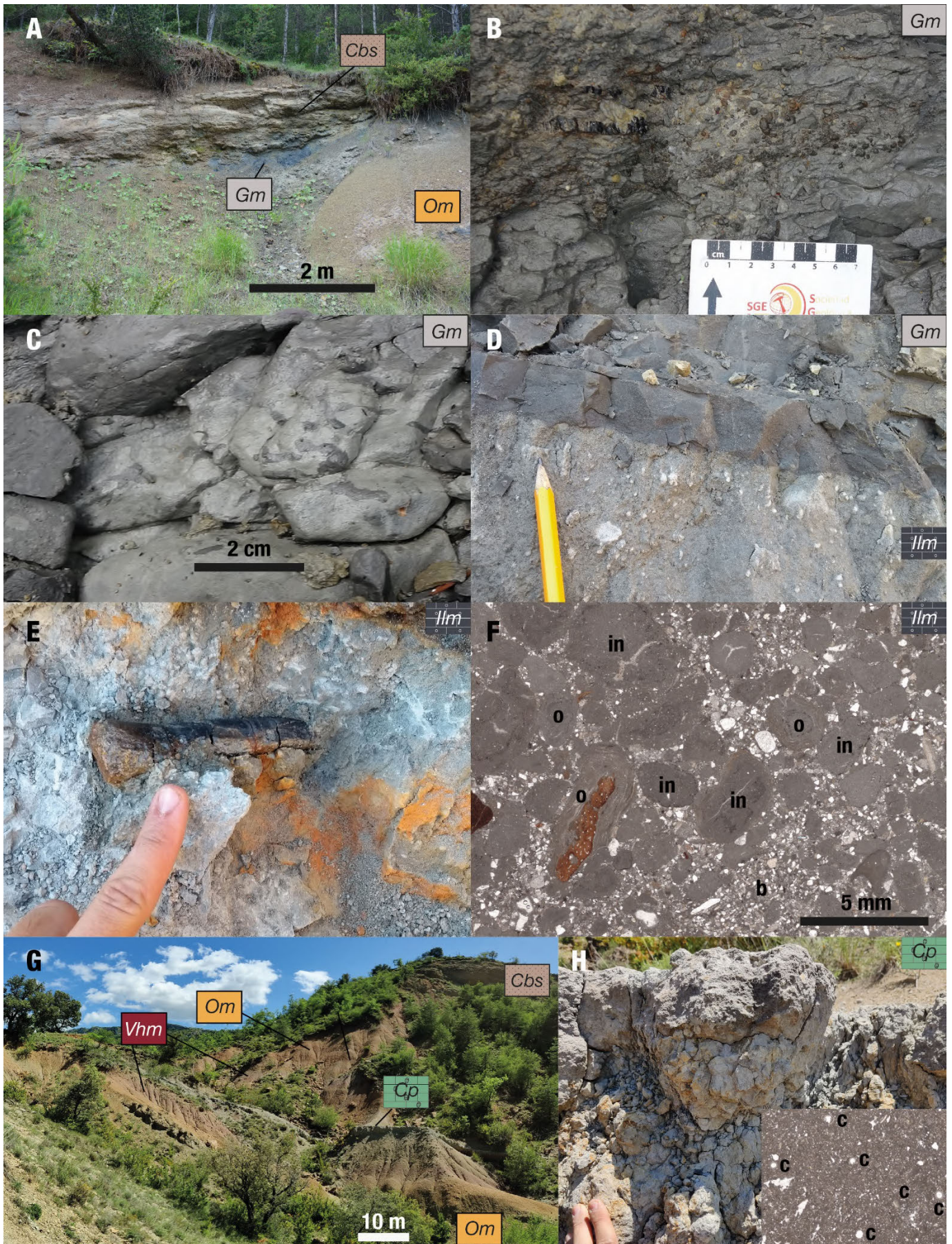


Fig.5.24 (previous page). Fluvial facies association. A) View of a small outcrop in the area of Beranuy, where a cross-bedded sandstone (Cbs) package is overlaying a level of grey mudstones (Gm). B) Detail of the grey mudstone (Gm) level of A). A fragment of charcoal and some pebbles can be observed within the matrix. C) Simple invertebrate traces in the grey mudstones. Same level than A) and B). D) Boundary between grey mudstones (Gm) and intraclastic limestones (Ilm) facies in Valle de Lierp section. E) A theropod bone preserved in the intraclastic limestone (Ilm) level of Valle de Lierp (Larra 4 site). F) Thin-section image of sample LAR4. b: bioturbation, in: intraclast, o: oncoid. G) Panoramic view of the charophyte packstone (Cp) level of San Pere de Cornudella. H) Detail of the limestone bed of G) and detail of thin-section STH-CL, with several charophyte gyrogonites (C).

- *Microconglomerates (Mc)*

This facies corresponds to dm-thick beds of both grain-supported and matrix-supported microconglomerates. The beds are lenticular, having short lateral continuity and pinching out to muddy intervals (Fig. 5.25 F), or they appear underlying sandstone packages of the Cbs facies (Fig. 5.25 C), or as thin levels that are part of the sandstones (Fig. 5.25 G). The pebble grains are millimetric to centimetric in size and polygenic in origin, including carbonate grains (intraclasts, oncoids and bioclasts), but also quartzitic, sandy, silty and ferrous pebbles (Fig. 5.25 H). The average size of the pebbles tends to be higher in the eastern outcrops; for example, in the Arén area some levels of conglomerate bear pebbles of around 3 cm, meanwhile in the west, they barely reach 5 mm. Locally, the facies has foraminifera (Fig. 5.23 H), charophytes and disarticulated vertebrate bones. The facies has erosive scours at the bases of beds, lamination (parallel or low angle), and bioturbation on top.

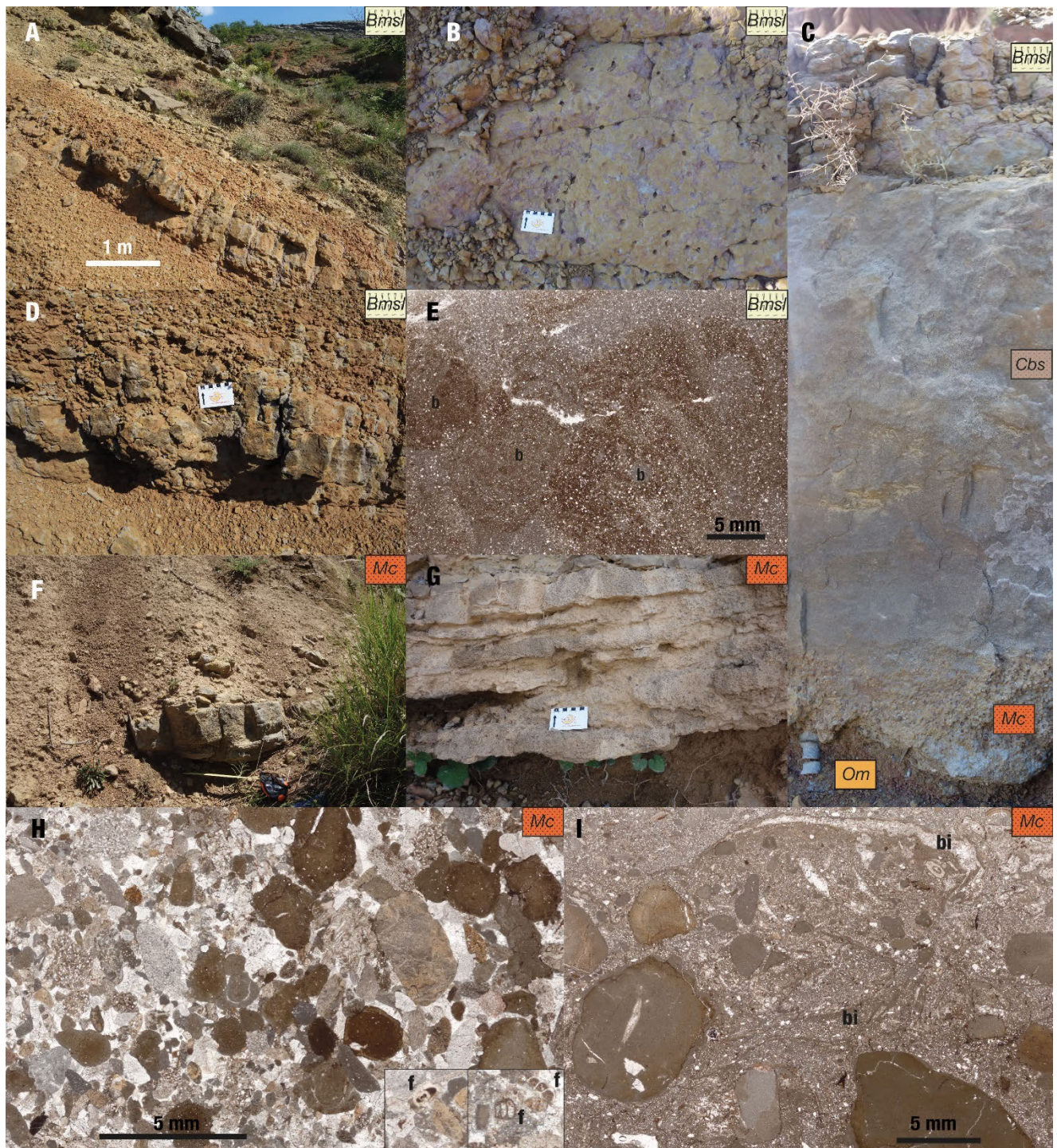
Mc facies also appears on some occasions in the 'Grey Garumnian' unit, or in relationship with perilagoonal facies. The most remarkable difference with their counterpart in the 'Lower Red Garumnian' is that the proportion of bioclasts of bivalves and gastropods is higher, being sometimes the shells complete (Fig. 5.25 I).

- *Cross-bedded (IHS) sandstones (Cbs)*

This facies is conformed by packages of cross-bedded sandstones intercalated within the muddy facies of the 'Lower Red Garumnian'. These packages tend to be thicker in the eastern outcrops (Arén, San Pere de Cornudella). Towards the west (El Castellaz, Rin) their thickness and number decrease (Fig.5.2). The grain size also varies,

tending to be coarser in the east, where even conglomerate levels can be found within the sandstone levels (see *Mc facies*) meanwhile in the west are finer and more laminated (Fig. 5.2). The sandstones often present erosive scours (Fig. 5.26 C), and locally channelized bases. They present planar and trough cross-bedding, ripple marks, and flaser and wavy bedding. Notwithstanding, their most relevant feature is their inclined heterolithic stratification (IHS sensu Thomas et al., 1987) (Fig. 5.26 A, B). The sandstone strata are intercalated with grey or ochre mudstone (*Gm* and *Om*) and siltstone lenses, to which pass laterally and vertically. Besides, in some sandstone levels, geometries similar to point bars have been observed, recognized lateral accretion surfaces (Fig. 5.26 B). The sandstones display a certain degree of bioturbation, with several traces of invertebrates such as *Taenidium* (Fig. 5.26 E), *Loloichnus* and *Palaeophycus*. Besides, big almond-shaped traces have been found at some bed bases in the western part of the studied area (El Castellaz and Rin) (Fig. 5.26 D), which might be related to bivalves resting traces assignable to the ichnogenus *Lockeia* (Buatois and Mángano, 2011). At the base of the sandstone beds dinosaur tracks are also common, being usual to find positive hyporreliefs of hands and feet of hadrosaurid ornithopods (Fig. 5.26 E), referable to the ichnogenus *Hadrosauropodus* (Vila et al., 2013). Other fossils common in these beds are vertebrate bones, usually present at the base or at the top of the levels. Transported foraminifera are locally present in some of the sandstone levels.

Fig.5.25. (next page). Fluvial facies association. A) Bed of bioturbated marly/sandy limestones (*Mmsl*) in Isclés. B) Top of a bed of bioturbated marly/sandy limestones with burrows (cf. *Arenicolites*) close to area of Isclés. C) Bed from Rin section, which encompasses three different facies from base to top: Microconglomerate (*Mc*), cross-bedded sandstone *Cbs* and *Bmsl*. Note the invertebrate trace and the scour at the base of the bed. D) Detail of A), Root vertical rhizohalos in the bioturbated limestone. E) Thin-section image of sample SE1-13, b: bioturbation. F) Microconglomerate (*Mc*) lense in the upper part of Beranuy section. G) Several layers of microconglomerates at the base of a sandstones package. Arén outcrop. H) Thin-section image of sample AR-6, with detailed view of some allochthonous foraminifera (f). I) Thin-section image of sample SE1-5, bi: bivalve.



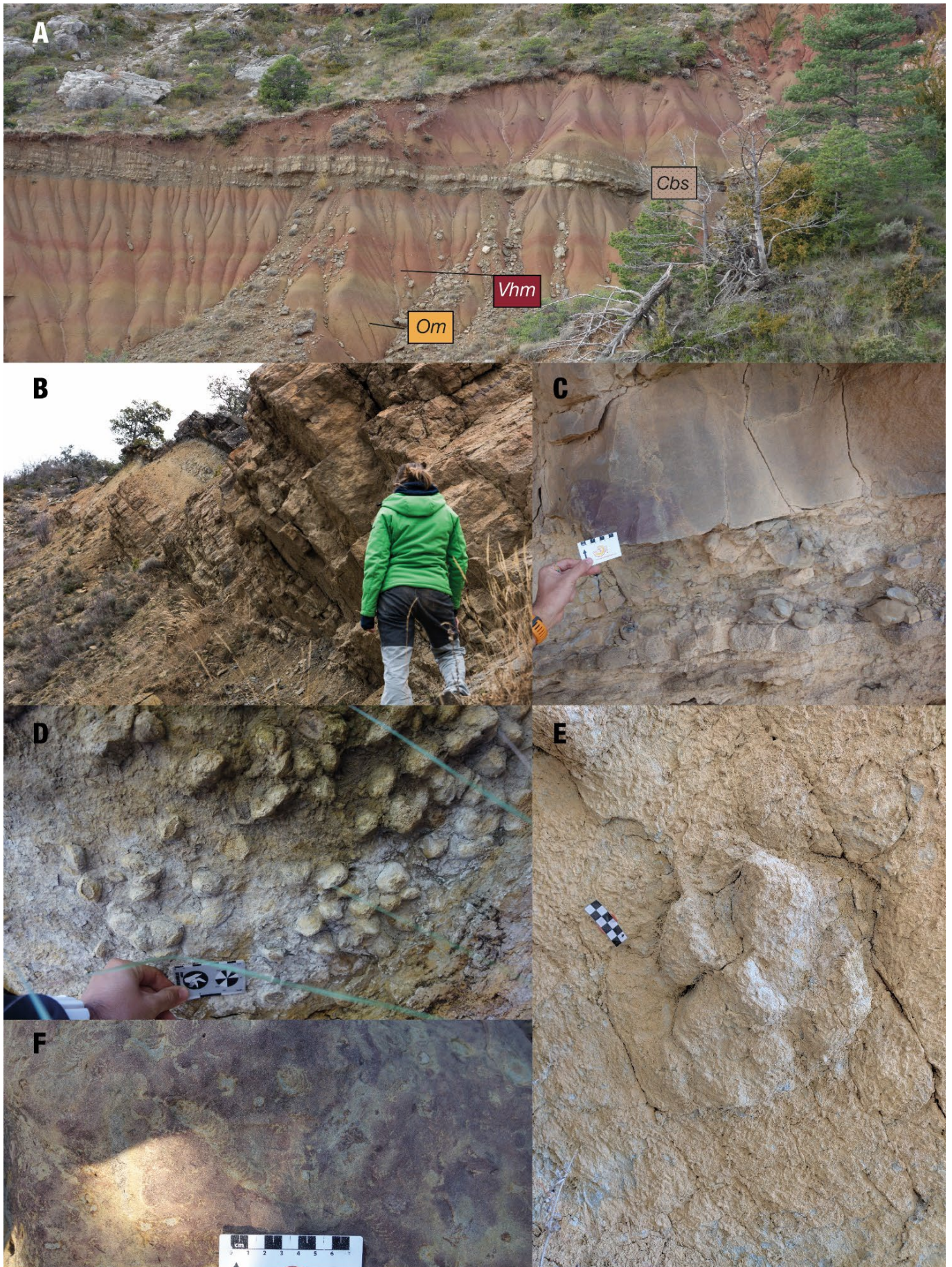


Fig.5.26. (previous page). Fluvial facies association. A) IHS in a sandstone body in the area of Rin. B) Sandstone body with HIS and lateral accretion at the Isclés section. C) Erosive base with trough cross-bedding at the Arén section. D) Almond-shaped invertebrate traces referred to *cf. Lockeia* sp. (Rin section). E) Hadrosaur track at the Isclés section. F) Taenidium traces atop of a sandstone level near Isclés.

### **Transitional lacustrine facies association**

This facies association is characterized by those lithologies that conform the 'Transitional interval' described in section 5.1.1, which represents a change in the sedimentary conditions that have ruled during the sedimentation of the 'Grey Garumnian' and the 'Lower red Garumnian'. This change represents a break with previous conditions, setting the beginning of the lacustrine environment of the 'Vallcebre Limestones'. Since there are not vertebrate fossils in this thin interval, a shallow description of them is offered (Fig. 5.4 D):

- *Green mudstones (Grm)*

This facies is formed by thin dm-beds of green mudstones, without bioturbation nor fossils. The only significant component identified are carbonate nodules and some sparse quartz grains.

- *Purple mudstones (Pm)*

This facies is formed by purple to garnet mudstones, sometimes showing a kind of metallic shining. It appears as a cm-thick levels within the green mudstones or sometimes within white marly mudstones. One individual bed has been traced laterally at least along the outcrops from Beranuy to Rin. In other areas up to two horizons of the purple mudstones can be recognized. The mudstones contain abundant spherical iron nodules smaller than 1 mm.

- *White marly mudstones (Wmm)*

This facies of whitish marly mudstones and marls is present in the 'Transitional interval', but with limited lateral continuity. Its most relevant feature is the presence of invertebrate traces with knobby structures. The presence of microfossils is unknown since this facies was not sampled.

- *Micritic limestones and breccia (Mlb)*

It is formed by discrete decimetric beds (20-25 cm) of micritic limestones and breccia. It contains scarce carbonate nodules, and eventually charophytes. Bioturbation may occur, but traces are difficult to identify. This facies is very similar to that of the limestones observed in the 'Vallcebre Limestones' unit.

**5.2.3. Sedimentary model**

Based on the observations at the studied area and previous works on sedimentology of the Tresp Fm (Eichenseer, 1988; Riera, 2010; Díez-Canseco et al., 2014; Oms et al., 2016), a sedimentary model establishing the lateral relationships of the great variety of facies of the Tresp Fm in this area is offered (Fig. 5.27). This model tries to shed a light about how sedimentation worked during the late Maastrichtian in the Western Tresp Syncline. For the model, has been taken into account that the Turbón anticline was already growing during the Maastrichtian (Eichenseer, 1988; Ramos et al., 2020), and thus it was representing a structural high which would conditionate the sedimentation. Unfortunately, the proximal sintectonic facies of the Arén and Tresp formations that would have been deposited close to the Turbón High are not preserved, and then cannot be characterized.

The coarse-grained sandstones of the Arén Fm (including those of the topmost part) would correspond to the coastal deposits of the barrier island, protecting the lagoon. The *Gmls* marly facies would represent the subtidal deposits of the lagoon, meanwhile fine-grained sandstones of (*Wfs*) would correspond to sands carried out from open area and affected by tides and waves. The micritic limestones (*Mc*) of Campo could correspond to a muddy carbonate area in the margin of the lagoon, through which dinosaurs were able to walk. The huge variability of thickness and facies within the 'Grey Garumnian' might point to a not linear but complex margin of the lagoon. None of the lagoonal deposits studied in the Grey Garumnian fits with deposits associated to tidal inlets, such as flood tidal deltas or ebb tidal delta.

Fringing the lagoon would be all the perilagoonal facies situated in the intertidal and supratidal areas of the lagoon depending on the facies. The carbonate sandstones and sandy limestones (*CsSl* facies) might represent the reworking of the fluvial and marine sediment, forming sandy banks in the marginal areas, or even the deposits of

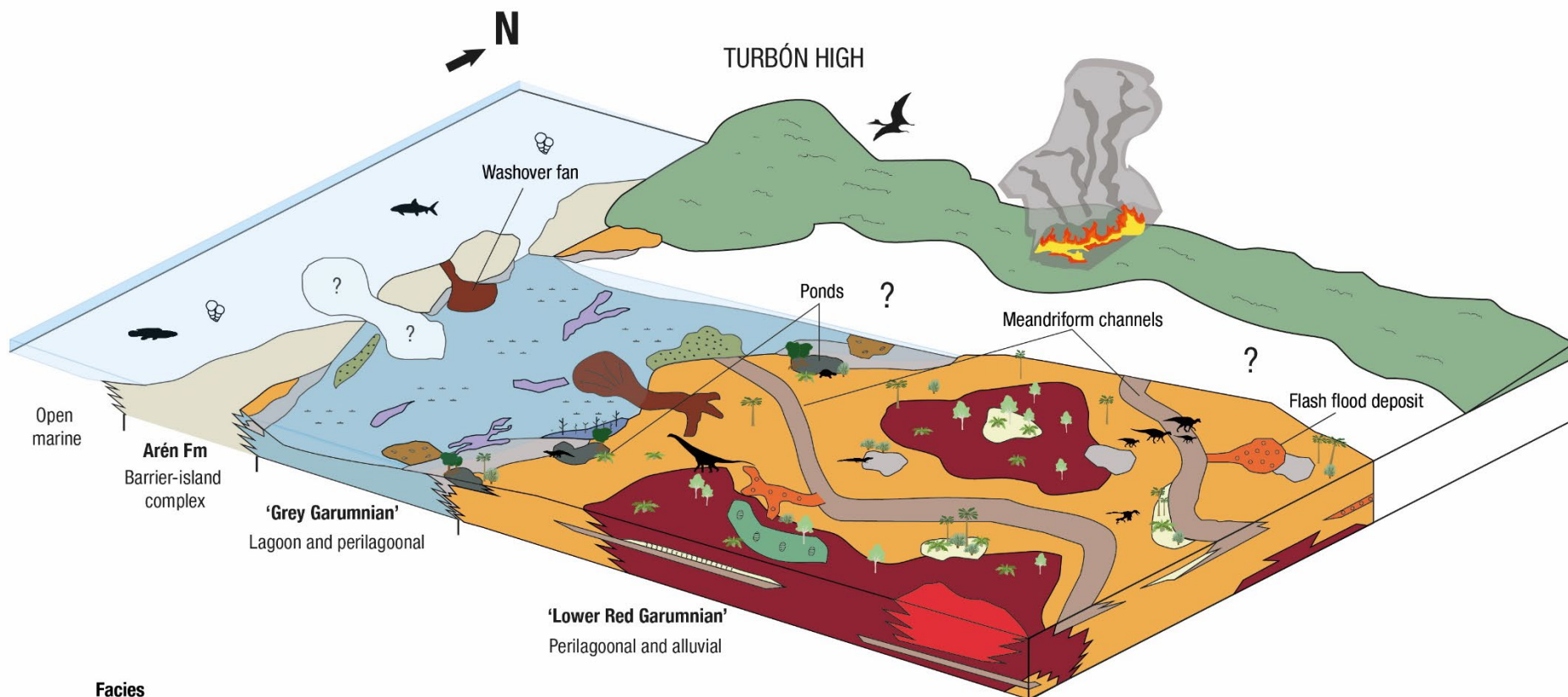
fluvial channels entering the lagoon. The bioclastic sandstones (*Bcs*) of veneroid bivalves could represent subtidal to perilagoonal areas colonized by these bivalves (Zuschin and Ebner, 2015). Foreset cross-bedded sandstones (*Fcs*) represent marine storm deposits (washover fan) breaking the barrier island or flood events from the continent (Cruzado-Caballero et al., 2021). The fine-grained bioturbated sandstones (*Fbs*), correspond to perilagoonal areas colonized by riparian small plants (reed like) and small invertebrates, stabilizing and fixing the fine sediment and helping to its cementation.

The interpretation of the marly mudstones rich in organic matter (*Dgmo*) is complex. Taking into account the paleontological data of the Veracruz 1 site found in this facies, whose fossil association has been studied (see Chapter 6), some inferences has been done. Since this type of mudstones are laterally limited, this might point to a spatially limited depositional setting, such as a small body of water, pond-like, separated from the lagoon. The ochre vertical mottling and the grey-ochre silt-filled rhizocretions recognized within the sediment indicate the presence of vegetation and the formation of a paleosoil in very poorly drained conditions (McCarthy and Guy Plint, 1998; Kraus and Hasiotis, 2006). The fossil association at VE1 (including microfossils, plant remains, invertebrates and vertebrates) is diverse, with mixed fossils from marine, transitional and continental environments. This mixed condition points towards a complex taphonomic story to explain the genesis of the site. The charophyte assemblage from VE1 (see Chapter 6) is dominated by *P. sertulata* and *P. llobregatensis* associated with many other species known to thrive exclusively in alkaline freshwater lakes (Vicente et al., 2016a, 2019). However, the large population of *Platychara* sp., which belongs to a brackish tolerant genus, associated with less abundant gyrogonites from brackish species, such as *Feistella malladae* and *Lamprothamnium* sp. (Soulié-Märsche, 1989; Villalba-Breva and Martín-Closas, 2013; Vicente et al., 2016a, 2019), suggests that the assemblage may be time-averaged, from a depositional setting recording minor marine influences in a dominantly freshwater environment. Other invertebrates such *Corbicula*, *Cerithium*, *Pyrgulifera* and *Melanopsis* are tolerant to brackish waters, meanwhile they usually inhabit fresh waters (Bandel, 2006; Vila et al., 2011), and something similar occurs with the vertebrates, having Lepisosteiformes fishes are typical of freshwater environments, but also capable of tolerate euryhaline conditions in transitional settings (Grande, 2010), but there are also marine fishes such phyllodontids, and terrestrial vertebrates as dinosaurs. For all these reasons, VE1 deposit and *Dgmo* facies are interpreted as the filling of partially vegetated ponds, situated in the margin of the lagoon or in the proximal area of the perilagoonal fringe (Fig. 5.27), which may hold fresh water, but could certainly

show fluctuations of salinity, which would allow the proliferation of euryhaline tolerant charophytes and animals in the pond.

The mudstones of the 'Lower Red Garumnian' (*Om*, *Vhm* and *Rm*), usually intercalated represent a transition of muddy deposits with paleosoils between the perilagoonal plain and the fully alluvial plain, being *Om* and *Rm* facies the distal facies, and *Vhm* an intermediate condition. In this perilagoonal/fluvial plain (Fig. 5.27) there would be some few meandriform fluvial channels represented by the *Cbs* facies. The presence of IHS in this facies points to a tidal influence in these channels (Díez-Canseco et al., 2014; Ghinassi et al., 2020), corroborated also by the presence of planktonic foraminifera in these sandstones. Grey mudstones (*Gm*) would represent small ponds in the plain, meanwhile microconglomerates (*Mc*) correspond to flash flood deposits (*Mc* in isolated beds) or the most energetic areas of the channels (*Mc* associated to sandstones of *Cbs* facies). The local intraclastic limestone (*IIM*) deposit of Larra 4 could correspond to one of these flash floods events that dropped part of its charge into a small pond. The bioturbated marly sandy limestones (*Bmsl*) represent heavily vegetated areas, or when they appear a top of a fluvial channel, the final stages of channel fill, in which it is colonized by plants. Finally, the charophyte bioclastic limestone (*Cbl*) might be not a pond, but more extensive freshwater lake within the alluvial plain, perhaps an oxbow lake.

*Fig.5.27 (next page). Sedimentary model proposed for the Arén and Tremp Fm in the Western Tremp Syncline during the late Maastrichtian.*

**Facies**

- Coarse-grained bioclastic sandstones with large cross-bedding (Topmost Arén Fm)
- Marls
- Grey mudstones and laminated siltstones
- Dark grey marly mudstones rich in organic matter

- Ochre mudstones-marls
- Variegated hydromorph mudstones
- Red mudstones
- Fine-grained bioturbated sandstones

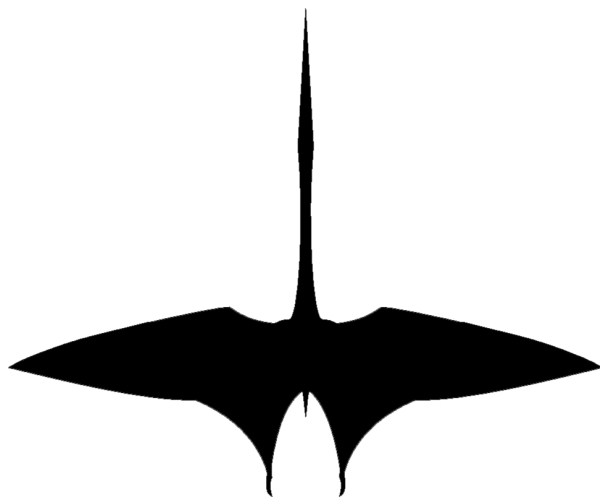
- Wavy fine-grained sandstones
- Foreset cross-bedded sandstones
- Bioclastic sandstones
- Carbonate sandstones and sandy limestones

- Cross-bedded sandstones
- Microconglomerates
- Charophyte packstone
- Bioturbated marly/sandy limestones



# **Chapter 6.**

# **Paleontology**





## Chapter 6: Paleontology of the Tremp Fm in the Western Tremp Syncline

In this chapter, the upper Maastrichtian vertebrate record of the Western Tremp Syncline is analyzed, considering all the discoveries and research performed since the late 90's. In this way, the diversity and stratigraphic range of the main clades of vertebrates has been reviewed. In addition to this, the relationship between the different paleontological sites and the sedimentary facies described in Chapter 5 has been studied, to evaluate the different taphonomic modes of preservation of vertebrate fossils and how the paleoenvironment facilitated, or not, the record of the vertebrate remains. Besides, new fossil material to this record is added, with the description and taxonomic assignments of the fossils, some of them belonging to vertebrate clades never identified before in the South-Pyrenean Basin.

### 6.1. *The vertebrate record of the Western Tremp Syncline*

Since the discovery in the 90s of the first sites with dinosaurs in Arén (Ribagorza county, Huesca), an intense research activity has taken place to characterize the diversity of tetrapods of the late Maastrichtian of the Western Tremp Syncline (see Canudo et al., 2016; Pérez-Pueyo et al., 2021a for a review of all the research). The outcrops of the Tremp Fm in this area have yielded a great amount of fossil sites with vertebrate, accounting a total of 97 paleontological sites (39 of them firstly described in this Doctoral thesis), and more than 1200 fossil remains, including bones, eggshell fragments, tracks and coprolites (Fig. 6.1). Because of its chronostratigraphy (see Chapter 5), this area is key for high-resolution study of the diversity patterns of vertebrates during the last 400.000 years of the Mesozoic in Europe. All the relevant information about the sites and their stratigraphic position can be found at Annex II and III.

*Figure 6.1 (next page). Correlation panel of the Western Tremp Syncline (W-E oriented) with the stratigraphic position of the vertebrate fossil sites. The equivalence of the numbers that designate each site is located in Table 6.1.*



<b>Fossil site</b>	<b>Number</b>	<b>Fossil site</b>	<b>Number</b>	<b>Fossil site</b>	<b>Number</b>
172-i/04/a	52	Camino Rin 2	33	Isclés Gris	77
172-i/04/b	56	Camino Rin 3	25	La Solana	49
172-i/04/c	37	Campo 1	1	Larra 1	21
172-i/04/d	39	Campo 2	2	Larra 10	20
172-i/04/e	40	Casa Bonet	82	Larra 2A	22
172-i/04/f	42	Color	44	Larra 2B	23
Altero Negro 1	63	Dolor 1	54	Larra 2C	24
Altero Negro 2	64	Dolor 2	55	Larra 3A	11
Amor 1	58	Dolor 3	57	Larra 3B	14
Amor 2	59	El Blocas 1	46	Larra 3C	12
Amor 3	62	El Blocas 2	53	Larra 4	17
Areny 1	90	El Castellaz 1	3	Larra 5	15
Barranc del Solá	88	El Castellaz 2	9	Larra 6	19
Barranco Extremadura	28	El Castellaz 3	6	Larra 7	18
Barranco Generador	10	El Castellaz 4	7	Larra 8	16
Barranco Serraduy 1	36	El Castellaz 5	8	Larra 9	13
Barranco Serraduy 2	41	El Castellaz 6	5	Las Llempías 1	48
Barranco Serraduy 3	50	El Castellaz 7	4	Las Llempías 2	43
Barranco Serraduy 4	60	Elías	95	L'Aspra	78
Barranco Serraduy 5	61	Enebro	47	Pedregal	31
Barranco Vayart	32	Femur	35	Rin 1	26
Beranuy	38	Fornons 1	65	Rin 2	27
Blasi 1	89	Fornons 2	69	Rin 3	29
Blasi 2a & 2b	91 and 92	Fornons 3	76	Sabor	45
Blasi 3	93	Isclés 1	80	San Cristobal	34
Blasi 3,4	94	Isclés 2	84	Serraduy Norte	51
Blasi 4	96	Isclés 3	85	Sierra del Sis 1	71
Blasi 5	97	Isclés 4	86	Sierra del Sis 2	75
Camino Fornons 1	67	Isclés 5	87	Veracruz 1	70
Camino Fornons 2	68	Isclés 6	83	Veracruz 2A	72
Camino Fornons 3	66	Isclés 7	81	Veracruz 2B	73
Camino Rin 1	30	Isclés 8	79	Veracruz 3	74

*Table 6.1. List of vertebrate fossil sites from the Western Tremp Syncline, which their correspondent number in Figure 6.1.*

### 6.1.1. *Dinosauria*

#### 6.1.1.1. *Hadrosauroidea*

Hadrosauroid dinosaurs are the clade of Cretaceous ornithopods with the most abundant fossil record, especially in the Northern Hemisphere. In the Western Tresp Syncline, hadrosauroids are recorded in the upper Maastrichtian deposits of the Arén Sandstone Fm and the 'Grey' and 'Lower Red Garumnian' of the Tresp Fm; these are among the youngest non-avian dinosaurs in the world (Puértolas-Pascual et al., 2018). The first hadrosauroid bones were found in the 1990s near the locality of Arén (Areny in Catalan) (Huesca, Aragon, NE Spain). Early work on several sites (Blasi 1 to 5 and Blasi 3,4) (Fig. 6.1) by a multidisciplinary team yielded fossil remains of indeterminate euhadrosaurids, together with bones and eggshells of several dinosaurs and other terrestrial and aquatic vertebrates (López-Martínez et al., 2001). Later studies on specimens from the Blasi 1 and Blasi 3 sites resulted in the erection of two lambeosaurine hadrosaur species: *Blasisaurus canudo* Cruzado-Caballero, Pereda-Suberbiola and Ruiz-Omeñaca 2010a (Fig. 6.1 and 6.2 A) and *Arenysaurus ardevoli* Pereda-Suberbiola, Canudo, Cruzado-Caballero, Barco, López-Martínez, Oms and Ruiz-Omeñaca 2009 (Pereda-Suberbiola et al., 2009b, Cruzado-Caballero et al., 2013) (Fig. 6.1 and 6.2 B, C). Both sites fall within the upper part of chron C30n (Fig. 6.1). These two species are recovered within Arenysaurini, which is a recently erected clade of lambeosaurines from Europe (Longrich et al., 2020).

In addition to this, other remains of indeterminate hadrosaurids and euhadrosaurids have been described from the Blasi sites (Cruzado-Caballero et al., 2009, 2010a, 2010b, 2014). The findings from these sites have also led to the first description of a pathological bone from a hadrosaurid in Spain (Canudo et al., 2005), and the first paleoneuroanatomical description of a European lambeosaurine, *Arenysaurus ardevoli* (Cruzado-Caballero et al., 2015). Recent studies on the paleohistology of the hadrosauroids from the Blasi sites reveal the presence of hadrosaurid individuals at different ontogenetic stages, including early and late juveniles, subadults, and mature adults (Mayayo-Lainez et al., 2021). New areas with hadrosaurid remains have been found in the vicinities of Serraduy (Isábena, Huesca, Aragon, NE Spain) and Beranuy (Huesca, Aragon, NE Spain) (Fig. 6.1) (Cruzado-Caballero et al., 2012; Puértolas-Pascual et al., 2012, 2018; Pérez-Pueyo et al., 2019). The new sites are characterized by the

presence of fossil remains of the smallest adult hadrosaurids (maybe affected by insular dwarfism) from Europe, which coexisted alongside larger hadrosaurids (Company et al., 2015) (Fig. 6.2 D).

This rich osteological record of hadrosauroids in the Western Tremp Syncline is complemented by several track sites. These tracks appear in several levels from Arén to Campo (Huesca, Aragon, NE Spain), with large ornithopod footprints, many of which have been referred to the ichnogenus *Hadrosauropodus* (Barco et al., 2001; Canudo et al., 2016; Vila et al., 2013) (Figs. 6.1 and 6.3), spanning from the top of chron C30n into chron C29r.

#### **6.1.1.2. Sauropoda**

The sauropod remains in the Western Tremp Syncline are very scarce compared to those in the eastern part, where titanosaur bones, eggshells, and tracks are moderately abundant (Vila et al., 2012; Vila and Sellés, 2015; Fondevilla et al., 2019). A remarkable specimen is the proximal half of a femur (MPZ 99/143) that probably corresponds to a large and indeterminate titanosaur (Canudo, 2001; Vila et al., 2012) (Fig. 6.2 E). MPZ 99/143 was recovered northwest of the town of Serraduy, in the 'Grey Garumnian' unit (Femur site in Fig. 6.1.). Interestingly, the femur was originally correlated to the top of chron C30n, but the new chronostratigraphical data provided by this thesis indicate that this fossil lies within chron C29r. Thus, this femur is one of the youngest records of titanosaurian sauropods in the Ibero-Armorican island, along with those recorded in fossil sites in the Catalonia region, including the Molí del Baró-2 femur (Vila et al., 2012), the vertebra from El Portet site (Sellés et al., 2016), and the skin impressions and footprints from the Mirador de Vallcebre (Fondevilla et al., 2017b). The rest of fossils assignable to Sauropoda from the Western Tremp Syncline are too fragmentary or inconclusive, except a caudal vertebra from Barranco Serraduy 4, that is described properly in this thesis (see section 6.2.3).

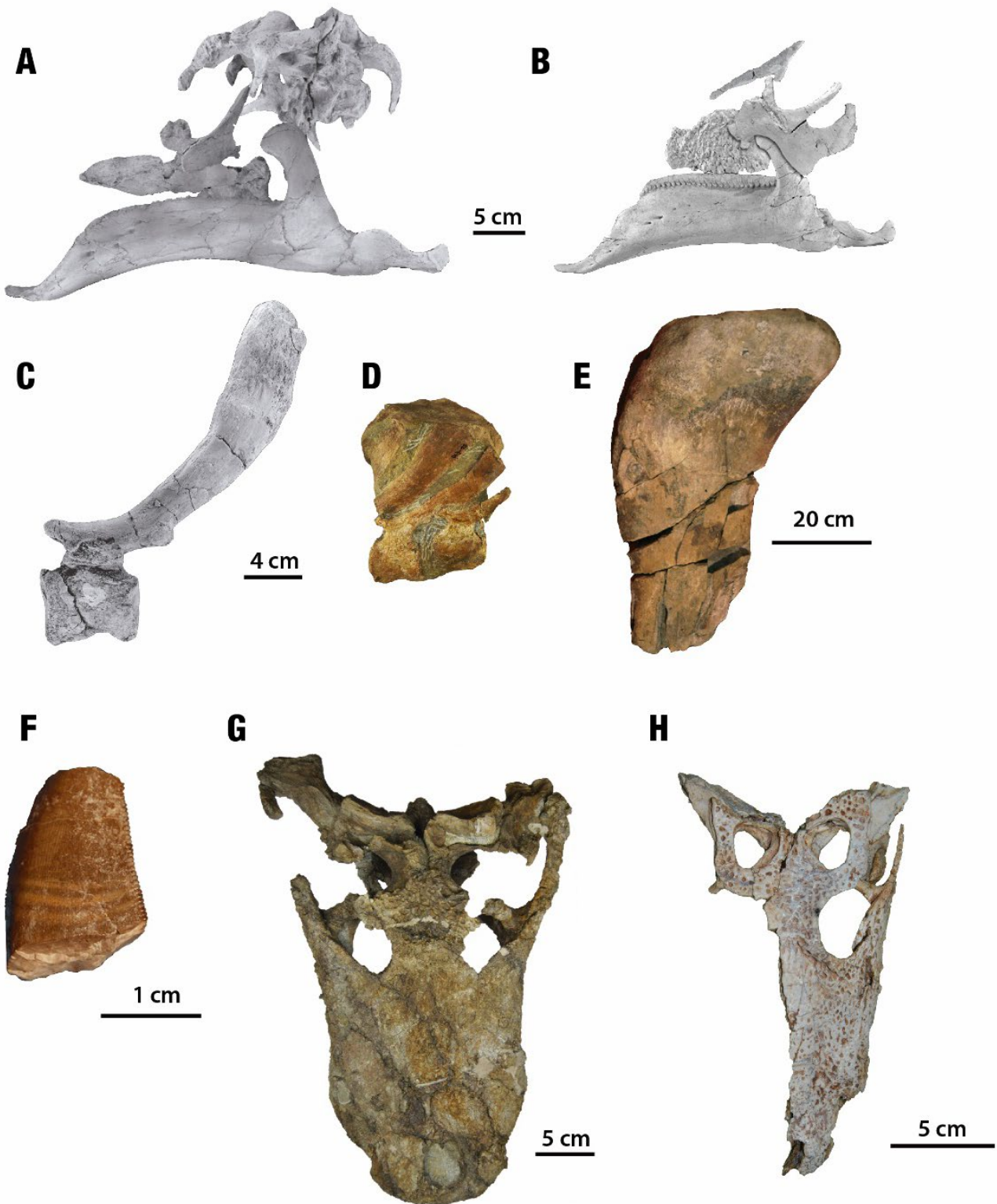


Figure 6.2 (previous page). Main tetrapod remains from the Western Tremp Syncline. A) Cranial elements of *Arenysaurus ardevoli* (MPZ2008/17, MPZ2008/256, MPZ2008/258, MPZ2008/259, MPZ2011/01), in left lateral view (modified from Cruzado-Caballero et al., 2013). B) cranial elements of *Blasisaurus canudo* (MPZ 99/664, MPZ 99/665, MPZ99/666a, MPZ99/666b, MPZ99/667, MPZ 2009/348), in left lateral view. C) mid-caudal vertebra of *Arenysaurus* (MPZ204/480), in left lateral view (modified from Cruzado-Caballero et al., 2013). D) articulated mid-caudal vertebrae of the small hadrosaurid from Serraduy (MPZ 2013-371), in left lateral view. E) femur (proximal end) of *Titanosauria* indet. from Serraduy (MPZ 99/143), in posterior view (modified from Puértolas-Pascual et al., 2018). F) cf. *Arcovenator* tooth (MPZ 2017/804), in lingual view. G) skull of *Agaresuchus subjuniperus* (MPZ 2012/288), in dorsal view. H) skull of *Arenysuchus gascabadiolorum* (MP Z2011/184), in dorsal view.

### **6.1.1.3. Theropoda**

Theropod fossils are scarce in the Western Tremp Syncline, and these are mainly represented by teeth, eggshells, and some isolated bones. Torices et al. (2015) described several teeth from the Blasi sites of Arén/Areny (Fig. 6.1.). They identify one morphotype as *Coelurosauria* indet. (MPZ 98/79 to 82) and three morphotypes belonging to maniraptoran theropods, including *Richardoestesia* sp. (MPZ 98/72 to 74; MPZ 2004/7), cf. *Paronychodon* (MPZ 98/76 to 78), and *Dromaeosauridae* indet. (MPZ 2004/6). Finally, they describe two different morphotypes of large teeth whose assignation is problematic and that are referred to *Theropoda* indet. 1 (MPZ 98/67; MPZ 2004/3 to 5, and 8) and *Theropoda* indet. 2 (MPZ 98/68), although a possible relation with neoceratosaurs is suggested. In fact, these two morphotypes were identified by Pérez-García et al. (2016) as cf. *Arcovenator*, which is an abelisaurid genus from the Campanian of southern France. The Blasi sites 1, 2, and 3 are dated within chron C30n (Fig. 6.1).

Two more theropod teeth have been described from the fossil sites of 172-i/04/e (Serraduy) and Larra 4 (Valle de Lierp, Huesca, Aragon, NE Spain) (Puértolas-Pascual et al., 2018). The first tooth (MPZ 2017/804) (Fig. 6.2 F) is large and resembles the *Theropoda* indet. morphotype 1 (cf. *Arcovenator*) from Torices et al. (2015), and the second one has been identified as *Coelurosauria* indet. Both sites are situated in outcrops of the ‘Lower Red Garumnian’ dated within chron C29r (Fig. 6.1). Postcranial fossils of theropods are not very common and are usually fragmentary. In this thesis a ungual phalanx of a paravian theropod from Larra 4 site, and a cervical vertebra of a

large ornithuromorph bird from Dolor site have been described. Both sites lay into the C29r chron (see section 6.2.2 and 6.2.3).

### 6.1.2. *Pterosauria*

The presence of pterosaurs in the upper Maastrichtian of the Tremp Syncline has only been reported from the site of Torrebilles-2 in the Eastern Tremp Syncline (Lleida, Catalonia, NE Spain, within chron C29r (Dalla Vecchia et al., 2013). In the Western Tremp Syncline, Puértolas-Pascual et al. (2018) reported a possible mandible of a pterosaur from the upper part of the 'Lower Red Garumnian' near Serraduy (Isábena). This specimen has been reexamined, and although its identification as a dentary has been refuted, its affinity to a pterosaurian bone cannot be ruled out. However, until a future study identifies this bone more precisely, it cannot be assigned to Pterosauria. Nevertheless, we have identified a fragment of a long bone from the Blasi 5 site (Fig. 6.1.) that might belong to a pterosaur (see section 6.2.3).

### 6.1.3. *Crocodylomorpha*

The crocodylomorph record in the Western Tremp Syncline is dominated by eusuchians. Two skulls belonging to two different genera have been identified. The first one is *Arenysuchus gascabadiolorum* Puértolas, Canudo and Cruzado-Caballero 2011 (MPZ 2011/184) (Fig. 6.2 H), from the Elias site near Arén/Areny ('Lower Red Garumnian', C29r, Fig. 6.1). Phylogenetically, MPZ 2011/184 was initially placed within Crocodyloidea (crown-group Crocodylia), but later cladistic studies have situated it as a more basal eusuchian within Allodaposuchidae (Blanco et al., 2014, 2015a; Narváez et al., 2015, 2016; Mateus et al., 2019). The second species is the allodaposuchid *Agaresuchus subjuniperus* (Puértolas-Pascual, Canudo and Moreno-Azanza, 2014) (MPZ 2012/288) (Fig. 6.2 G). MPZ 2012/288 was initially identified as a member of the genus *Allodaposuchus* (Puértolas-Pascual et al., 2014), but it was later reassigned to the newly described genus *Agaresuchus* (Narváez et al., 2016). This crocodylomorph comes from the Amor 3 site near the town of Serraduy, from one of the uppermost levels of the 'Lower Red Garumnian' (C29r, Fig. 6.1). As such, it could be one of the youngest crocodylomorphs on the Ibero-Armorican island before the K-Pg extinction. In addition, allodaposuchids are also represented by isolated teeth in several sites throughout the C30n–C29r interval (Fig. 6.1) (Puértolas-Pascual et al., 2016, 2018; Blanco et al., 2020).

All these teeth are conical with pointed crowns, showing the typical morphology of crocodylomorphs with a generalist diet. These dental morphologies have been observed in several allodaposuchid species from the Late Cretaceous of Europe (e.g. Blanco et al., 2020). As the presence of other crocodylomorph clades with generalist dentition cannot be ruled out, these teeth were assigned to cf. Allodaposuchidae, since this is the most abundant clade in this region and time interval. Some new allodaposuchid material is described in this thesis from Veracruz 1 site (Beranuy, Huesca, Aragon NE Spain), including the first record of *Allodaposuchus palustris* Blanco, Puértolas-Pascual, Marmi, Vila and Sellés 2014 in the Western Tremp Syncline (see section 6. 2. 1.).

Gavialoidea is another clade of crocodylomorphs that may be present in the upper Maastrichtian of the Western Tremp Syncline. A few elongated conical teeth with basiapical ridges have been assigned to cf. *Thoracosaurus*. These are restricted to the transitional environments of the Arén Fm and the 'Grey Garumnian' unit of the Tremp Fm close to Arén/Areny, Beranuy and Serraduy (Fig. 6.1) (Puértolas-Pascual et al., 2016, 2018; Blanco et al., 2020).

Hylaeochampsidae is represented by tribodont teeth from the Blasi 2B site close to Arén, which were identified as cf. *Acynodon* (MPZ-2017/1137) (López-Martínez et al., 2001; Puértolas-Pascual et al., 2016, 2018; Blanco et al., 2020). The eusuchian record is complemented by teeth, osteoderms, and vertebrae from the Blasi and Serraduy sites (Fig. 6.1), whose taxonomical position within Eusuchia is difficult to assign with precision. They are accordingly identified as Eusuchia indet.

López-Martínez et al. (2001) pointed out the presence of “trematochampsid”-like and alligatoroid teeth from the sites of Blasi 1, 2, and 3 (Fig. 6.1). However, although the authors did not provide pictures or specimen numbers, the morphotypes in question probably correspond to more recently erected taxa that had not been described at the time of publication of that paper. The “trematochampsid”-like teeth may correspond to non-eusuchian crocodylomorphs more typical of the Late Cretaceous of Europe, such as *Sabresuchus*, *Doratodon* or *Ogresuchus* (Sellés et al., 2020), and the alligatoroid teeth probably correspond to allodaposuchids. In addition, Blanco et al. (2020) mentioned the presence of a conical tooth (MPZ 2010/948) with enamel striations and crenulated carinae assigned to Mesoeucrocodylia indet.

Finally, the crocodylomorph record also includes several swimming and plantigrade tracks from the Serraduy, Beranuy, and Campo outcrops, all within chron

C29r (Vila et al., 2015; Puértolas-Pascual et al., 2016; Pérez-Pueyo et al., 2018) (Fig. 6.1 and Fig. 6.3 C). These tracks are the youngest record of crocodylomorph tracks in Europe. These tracks represent digit scratch marks produced by the manus and pes of buoyant crocodylomorphs, and they have been assigned to the ichnogenus *Characichnos*. One pedal impression has been assigned to cf. *Crocodylopodus*, and although its assignation cannot be confirmed with certainty due to the scarce material, this is the youngest occurrence of this ichnotaxon (Vila et al., 2015).



Figure 6.3. Tetrapod tracks from the Western Tremp Syncline. A) *Hadrosauropodus* trackway from the Areny 1 site. B) foot cast of a hadrosaurid dinosaur from the 172-i/04/a site. C) crocodylomorph tracks from the Serraduy Norte site.

#### 6.1.4. Testudines

Testudines are represented mainly by disarticulated plates of the carapace or the plastron. They appear at most of the paleontological sites from the topmost part of the Arén Fm to the upper levels of the 'Lower Red Garumnian' (Fig. 6.1). Most of these remains show fine ornamentation comprising thin dichotomic grooves, which is a distinctive character of the bothremydids (de Lapparent de Broin and Murelaga, 1996). Among these remains, Murelaga and Canudo (2005) described several plates from the Blasi sites near Arén/Areny (Fig. 6.1), including nuchal, pleural, and peripheral plates, a hyoplastron, a hypoplastron, and a xiphiplastron from bothremydids. At the site of Rin 2, near the town of Serraduy, situated in the topmost part of the Arén Fm, Murelaga and Canudo (2005) describe a xiphiplastron and a mesoplastron from a bothremydids. Pérez-Pueyo et al., 2019) also describe indeterminate plates from this kind of turtle from the Larra 4 site (Fig. 6.1). Thus, the record of this group of pleurodiran turtles extends from the upper part of chron C30r to near the K-Pg boundary interval. It is also important to note that Murelaga and Canudo (2005) identified a peripheral plate from a Solemydidae (=Helochelydridae) turtle from the Blasi 2 site (Fig. 6.1), which would represent a second turtle taxon in this area, though no other evidence of solemydids have been found up to date. This plate shows its characteristic vermiculate ornamentation, although it is not well preserved.

#### 6.1.5. Amphibia and Squamata

The Blasi 2 site has yielded a rich microvertebrate fossil assemblage, which includes bones of small tetrapods, mainly amphibians and squamates (Blain et al., 2010) (Fig. 6.1). Amphibian remains dominate, with at least one albanerpetontid (resembling the North American taxon *Albanerpeton nexuosum*) Estes, 1981 and two anurans, a discoglossid and a palaeobatrachid. The squamate remains comprise at least two undetermined lizards, one anguillid lizard, and a snake. Blasi 2B is dated to the top of chron C30n in the 'Grey Garumnian', and is the only well-studied microvertebrate site in the Western Tresp Syncline. However, it is noteworthy that the Larra 4 site (C29r) has yielded remains from discoglossid amphibians (Puértolas-Pascual et al., 2018), making it the youngest microvertebrate site in the Western Tresp Syncline. In this thesis a new fossil of albanerpetontid has been studied from Veracruz 1 site (see section 6.2.1).

## **6.2. Systematic paleontology**

In this section several new fossils are described from some sites mentioned above. In order to avoid missing the context of each site, a brief sedimentological description is included. In the same manner, the systematic description of Veracruz 1 site also includes foraminifera, charophytes, flora and invertebrates; though described in a less thorough way, they give important information about the paleoenvironment in which the fossil accumulation was formed.

### **6.2.1. The Veracruz 1 assemblage**

Veracruz 1 site (VE1) is found in the Tremp Fm outcrops near the small town of Biascas de Obarra, in the Beranuy area (Huesca, Aragon, NE Spain). VE1 is situated within a 6.7-7 m thick marly mudstone deposit a top of the 'Grey Garumnian' (Fig. 6.1). This sedimentary interval displays a dark-grey color and is rich in organic material. The lower part of the interval is intensely bioturbated by plants in the form of centimetric ocherish vertical mottling and grey-ocher cemented silt-filled rhizocretions, which diminish in intensity to the upper part. It is very rich in fossils, including foraminifera, charophytes, vegetal charcoal, invertebrates, vertebrates, and eggshells, presenting a mixed association of marine, transitional and continental fossils. VE1 deposit corresponds to the facies of *dark grey marly mudstones rich in organic matter*, and the site has been interpreted as a small, partially vegetated pond. It would be situated in the margin of the lagoon or in the proximal area of the perilagoonal fringe (see interpretation of the facies in Chapter 5). The study of the charophyte association points that this pond may hold freshwater. Nevertheless, it also shows fluctuations of salinity related to the input of waters coming to the lagoon, since it is composed by a mix of fresh water and euryhaline forms with no signs of reworking (see Annex IV for measurements).

Class FORAMINIFERA Lankester, 1885

Order GLOBOTRUNCANIDA Arenillas, Arz and Gilabert 2022

**Material:** 11 foraminifera tests.

**Commentaries:** Foraminifera are scarce at the VE1 site (N=11), being typically rare in the 'Grey Garumnian' unit (Díez-Canseco et al., 2014; Puértolas-Pascual et al., 2018), and just planktonic foraminifera have been recognized. The preservation state of the foraminifera ranges from very poor to moderately good (Fig. 5.6), furthermore, different color of the planktonic foraminiferal tests is identified. The species recognized are imprecise biostratigraphic markers and correspond to: *Heterohelix globulosa*, *H. planata*, *H. labellosa*, *Guembelitra cretacea*, *G. blowi*, *Globotruncana mariei*, and *Gl. linneiana*,

STREPTOPHYTA Jeffrey, 1967

Class CHAROPHYCEAE Smith 1938

Order CHARALES Lindley 1836

Family POROCHARACEAE Grambast 1962

*Feistiella malladae* Bataller, 1945 nov. comb. Villalba-Breva and Martín-Closas,  
2012

**Material:** 2 gyrogonites.

**Commentaries:** (Fig. 6.4 A–C) Gyrogonites are very large, ca. 665 µm high and 578 µm wide, sub-spherical to sub-prolate in shape, and with a mean ISI (Isopolarity Index = height x100/ maximum width) of 117. Usually, 8 convolutions are visible in lateral view. Spiral cells are convex, but sometimes slightly flat and devoid of ornamentation. The apex and base are flat or rounded. The apex shows a large apical pore, about 179 µm across. The basal pore is pentagonal and smaller than the apical one. The plate has not been observed but is known to be simple in this genus. The VE1 population is more spherical than the type population, however, the intraspecific polymorphism is well-known to be high in this species (Fondevilla et al., 2017a).

Family CHARACEAE Agardh 1824

*Lychnothamnus begudianus* Grambast, 1962

**Material:** 19 gyrogonites.

**Commentaries:** (Fig. 6.4 D–F) Gyrogonites are prolate spheroidal to subprolate, and large to very large in size, with an average 1032  $\mu\text{m}$  in height and 887  $\mu\text{m}$  in width. They are usually ovoidal in shape, and with a mean ISI of 117. Ten spiral cells are visible in lateral view, separated by a marked suture, usually bicarinate. Spiral cells are concave and devoid of ornamentation. The apex is flat or slightly rounded, with a faint narrowing of the cells. The base is elongated, with a marked pentagonal pore, sometimes at the end of a funnel. Some specimens show a basal column similar to those *Lychnothamnus* previously described as *Pseudoharrisichara* by Musacchio (1973).

*Peckichara sertulata* Grambast, 1971

**Material:** 110 gyrogonytes.

**Commentaries:** (Fig. 6.4 G–I) Gyrogonites are subprolate, medium in size, showing an average of 781  $\mu\text{m}$  in height and 687  $\mu\text{m}$  in width. They are ovoid in shape, and with an ISI of 113. Usually, eight spiral cells are visible in lateral view, separated by a fine intercellular suture. Spiral cells are concave and ornamented with a wide mid-cellular crest, sometimes undulated, which disappears near the apex. The apex is flat, showing a poorly marked periapical depression and wide apical nodules at the cell tips. The base is rounded, with a small pentagonal pore and with the ornamentation reaching the pore.

*Peckichara llobregatensis* Feist in Feist and Colombo, 1983

**Material:** 65 gyrogonites.

**Commentaries:** (Fig. 6.4 J–L) Gyrogonites are subprolate, medium in size, with an average of 486  $\mu\text{m}$  high and 471  $\mu\text{m}$  wide, spheroidal in shape, and with a mean ISI of 104. Usually, six spiral cells are visible in lateral view. They are slightly convex or flat, ornamented with large, and regularly spaced tubercles of the same width as the spiral cell width. The apex is rounded, showing periapical narrowing and with well-marked apical nodules. The base is rounded, with a small and pentagonal basal pore.

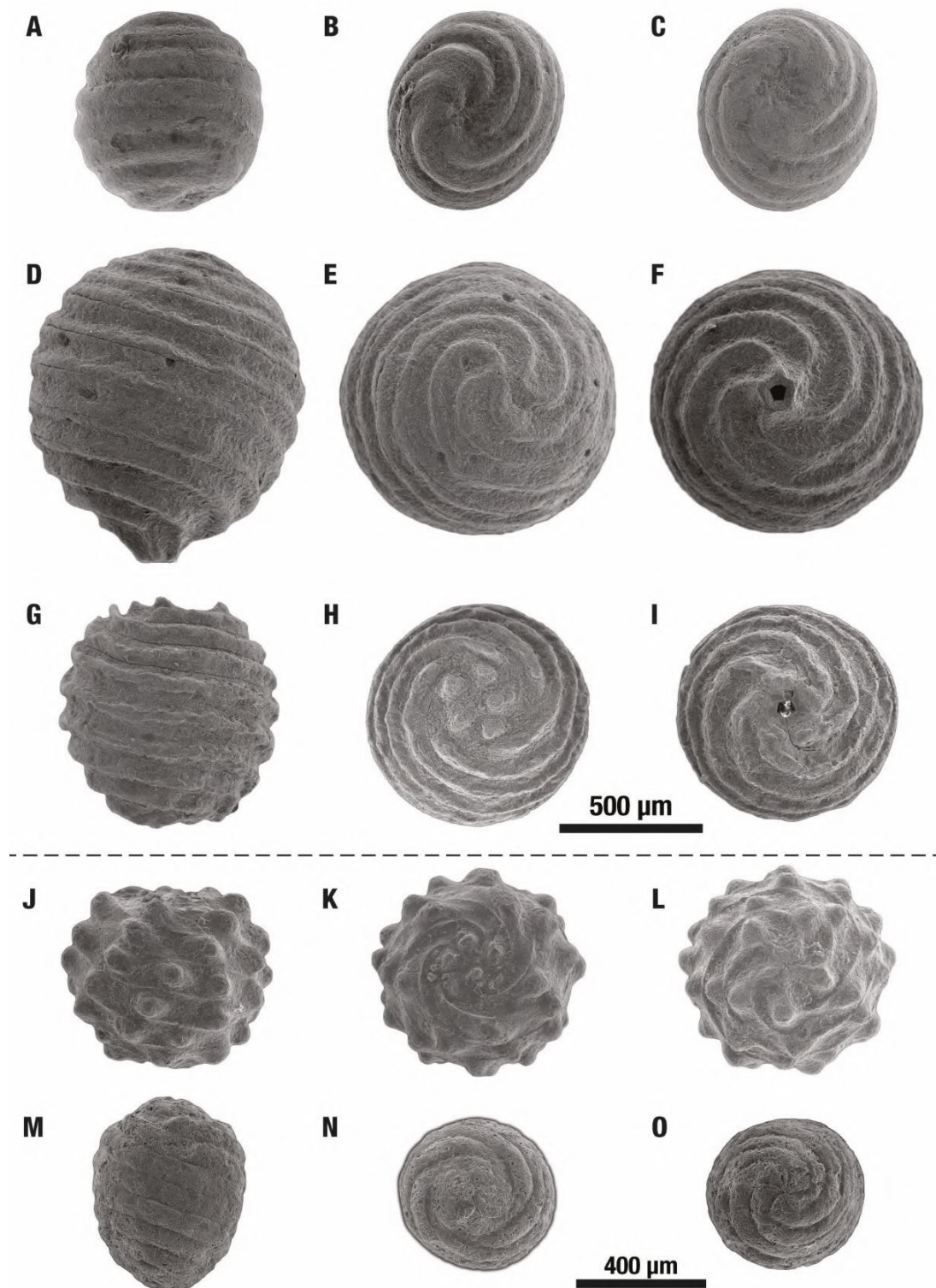


Figure 6.4. Charophyte gyrogonites of the most abundant taxa found in the upper Maastrichtian paleontological VE1 site. A-C) *Feistiella malladae*, A) lateral view (specimen VE1T-08), B) apical view, C) basal view. D-F) *Lychnothamnus begudianus*, D) lateral view (VE1T-09), E) apical view, F) basal view. G-I) *Peckichara sertulata*, G) lateral view (VE1T-10), H) apical view, I) basal view. J-L) *Peckichara llobregatensis*, J) lateral view (VE1T-11), K) apical view, L) basal view. M-O) *Lamprothamnium* sp., M) lateral view (VE1T-12), N) apical view, O) basal view.

*Lamprothamnium* sp. Groves 1916

**Material:** 4 gyrogonites.

**Commentaries:** (Fig. 6.4 M–O) Fructifications are very small in size, with a mean of 614  $\mu\text{m}$  in height and 449  $\mu\text{m}$  in width. Gyrogonites are subprolate in shape and with a mean ISI of 137. Eight convex spiral cells are visible in lateral view. The apex is flat with large nodules and with a marked periapical furrow typical in this genus. The base is slightly pointed with a small basal pore.

*Platychara* sp. Grambast, 1962

**Material:** 105 gyrogonites.

**Commentaries:** (Fig. 6.5 A–F) Small-sized gyrogonites, 245–442  $\mu\text{m}$  high (mean 337  $\mu\text{m}$ ) and 312–469  $\mu\text{m}$  wide (mean 402  $\mu\text{m}$ ) (Fig. 7). The ISI ranges 75–94 (mean 84), and they are suboblate in shape. Spiral cells are wide, slightly concave and with 5–6, most frequently 6, spiral cells visible in the lateral view. The ornamentation consists of a wide and undulated mid-cellular crest ranging from the proximities of the basal pore and disappearing near the periapical area. The apex is convex, sometimes showing a faint periapical narrowing. Apical nodules occur at the end of the spiral cells. The base is rounded, sometimes elongated, showing a small pentagonal pore rarely preluded by a funnel. The basal plate is not observed in the specimens studied. *Platychara* sp. from VE1 has gyrogonites similar to *Platychara cristata* Grambast, 1975 from the Maastrichtian deposits of Cuenca. However, *P. cristata* displays larger gyrogonites (475–500  $\mu\text{m}$  high and 675–800  $\mu\text{m}$  wide) and is devoid of apical nodules, which is one of the diagnostic features of VE1 *Platychara*. It is also similar to *Maedleriella* sp. A, described at the Maastrichtian south-Pyrenean basins (Feist and Colombo, 1983), but VE1 *Platychara* does not display its basal plate visible from the outside, as in genus *Maedleriella*. This indicates that the specimens from VE1 might represent a new species of the genus *Platychara*. Besides, few specimens (Form B, N=6) show less calcified gyrogonites resulting in a thinner midcellular crest along with an elongation of the base (Fig. 6.5 D–F) and might represent another species. However, more specimens of this second morphotype are needed to confirm this hypothesis.

*Microchara cristata* Grambast, 1971

**Material:** 116 gyrogonites.

**Commentaries:** (Fig. 6-5 G-I) Gyrogonites are small in size, with a mean height of 521  $\mu\text{m}$  and a mean width of 429  $\mu\text{m}$ . They are mainly subprolate and ovoidal in shape, with a mean ISI of 122. This species usually shows eight spiral cells visible in lateral view. The cells are concave, ornamented with a prominent and slightly undulated mid-cellular crest. This crest is continuous towards the apex, where it develops coma-shaped apical nodules. The apex is rounded and devoid of periapical modifications. The base is pointed, commonly forming a small, elongated column, ended with a small pentagonal basal pore.

*Microchara punctata* Feist in Feist and Colombo, 1983

**Material:** 12 gyrogonites.

**Commentaries:** (Fig. 6.5 J-L) Fructifications are very small in size, with a mean of 362  $\mu\text{m}$  in height and 293  $\mu\text{m}$  in width. They were subprolate and ovoid in shape and with a mean ISI of 124. Usually, eight spiral cells are visible in lateral view. They are usually flat and ornamented with well-developed and individualized tubercles. These tubercles are regularly spaced, disappearing near the periapical area. The apex is rounded, devoid of periapical modifications but with small apical tubercles. The base is pointed, sometimes forming a small column, and ended in a small pentagonal basal pore.

*Microchara nana* Vicente and Martín-Closas in Vicente et al., 2015

**Material:** 22 gyrogonites

**Commentaries:** (Fig. 6.5 M-O) Fructifications are very small in size, with a mean of 301  $\mu\text{m}$  in height and 259  $\mu\text{m}$  in width. They were subprolate and ovoid in shape, with a mean ISI of 117. Seven, usually flat to concave spiral cells are visible in lateral view. The gyrogonites are ornamented with a well-developed mid-cellular crest which are absent in some specimens. The apex is rounded, devoid of periapical modifications but with small apical tubercles. The base is generally rounded and ends in a small pentagonal basal pore.

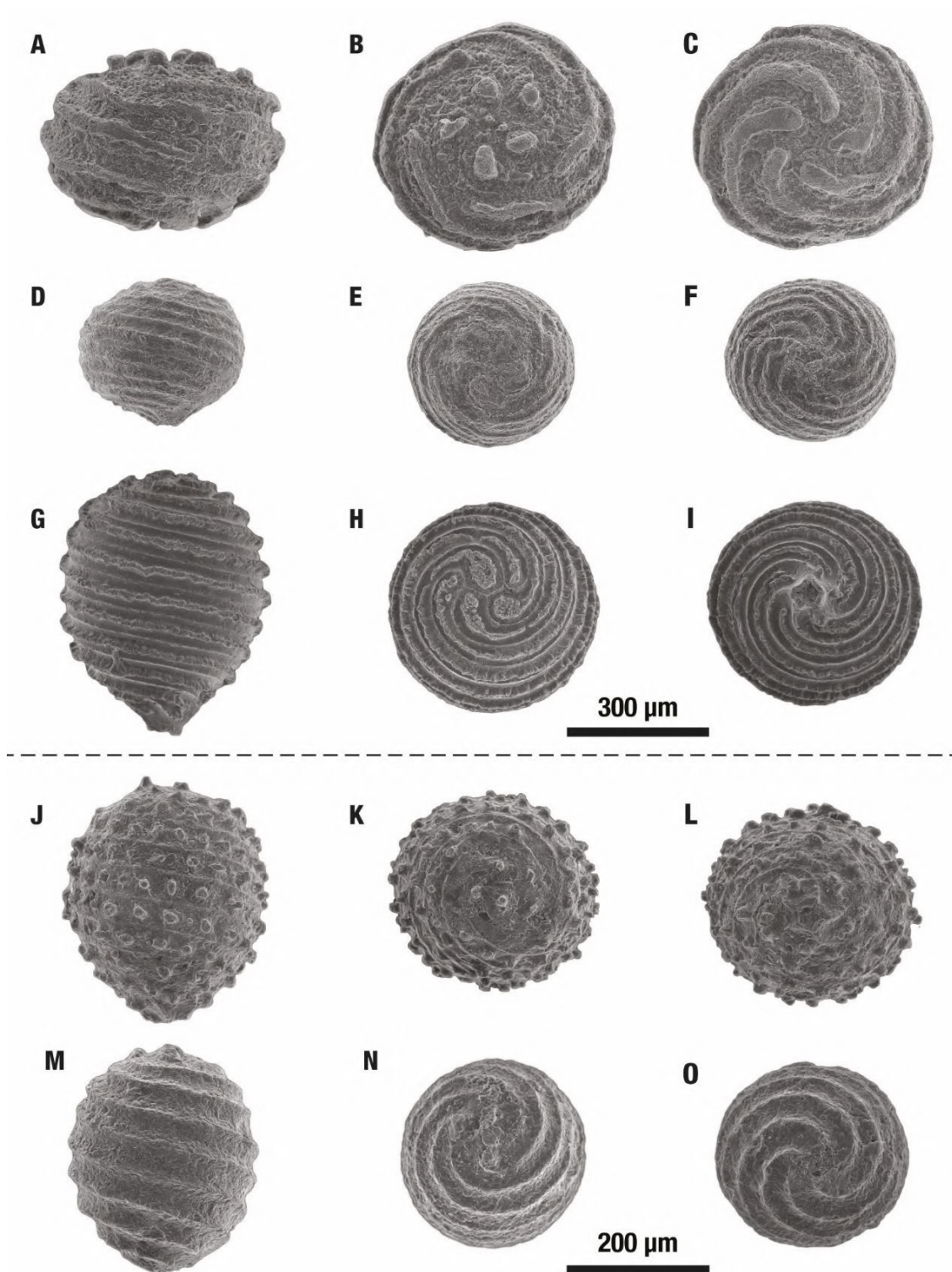


Figure 6.5. Charophyte gyrogonites of the most abundant taxa found in the upper Maastrichtian paleontological VE1 site. A-C) *Platychara* sp. form A, A) lateral view (VE1T-13), B) apical view, C) basal view. D-F) *Platychara* sp. form B, D) lateral view (VE1T-14), E) apical view, F) basal view. G-I) *Microchara cristata*, G) lateral view (VE1T-15), H) apical view, I) basal view. J-L) *Microchara punctata*, J) lateral view (VE1T-16), K) apical view, L) basal view. M-O) *Microchara nana*, M) lateral view (VE1T-17), N) apical view, O) basal view.

EMBRYOPHYTA Engler 1892

Superdivision TRACHEOPHYTA Sinnott 1935

EUPHYLLOPHYTA Kenrick and Crane 1997

Division SPERMATOPHYTA Willkomm 1854

Subdivision GYMNOSPERMAE Lindley, 1830

Class PINOPSIDA Burnett 1835

**Material:** 85 charcoal wood fragments

**Commentaries:** The dark gray colored mudstone levels in the fossil site contain abundant remains of charcoalified fossil wood. These remains are fundamentally prismatic-shaped but some of them have planar morphologies (Fig. 6.6 A to F) ranging in sizes from 63 mm long, 55 mm wide and 54 mm high to 12 mm long, 6 mm wide and 3 mm high, with the most abundant remains being fragments of elongated prismatic morphology 25 to 30 mm long, 10 to 15 mm wide and 7 to 10 mm high in average. Some of the remains have a stepped-shaped appearance (Fig. 6.6 A, D, E) that is typical of wood burned by natural fires that have suffered some kind of transport prior to deposition (Tanner and Lucas, 2016). However, mostly charcoalified wood fragments present variable sizes, straight margins and acute or slightly rounded corners (Fig. 6.6 B, C, F), which would indicate little transport from the fire site to its final depositional environment (Scott, 2000).

The internal structure of the charcoalified wood fragments was studied under the SEM showing homoxyllic type wood (Fig. 6.6 G) that corresponds to conifers. The wood fragments present both abundant rays and tracheid pitting of the abietinoid type with a single row of spacing radial punctuations (Fig. 8 H). Cross sections of the charcoalified wood show that the lamellae of the tracheids are completely fused (Fig. 6.6 I) indicating that the wood suffered the action of an intense and continuous wildfire, which would have reached temperatures of combustion ranging between 300° and 400° degrees centigrade (Scott, 2010). In some of the remains, the cell lumina is filled with diagenetic calcitic cement (Fig. 6.6 I), while others show iron mineralization that can be both superficial in the form of ferruginous crusts (Fig. 6.6 E) or as a mineral replacement (Fig. 6.6 D). These mineralizations provide these charcoalified wood remains both a greater weight and hardness than the others.

Some of the wood fragments showing flatter and wider surfaces present marine exobiont organisms on them –in this case colonies of calcitic serpulid worms– that are partially covering one of their surfaces (Fig. 6.6 F). The presence of these fossils on the surfaces of charred wood fragments would indicate that they had remained exposed outside the sediment for some time –up to several months– before being buried, thus providing a hard substrate to grow for these sessile marine invertebrates with filtering habits (Thiel and Gutow, 2005).

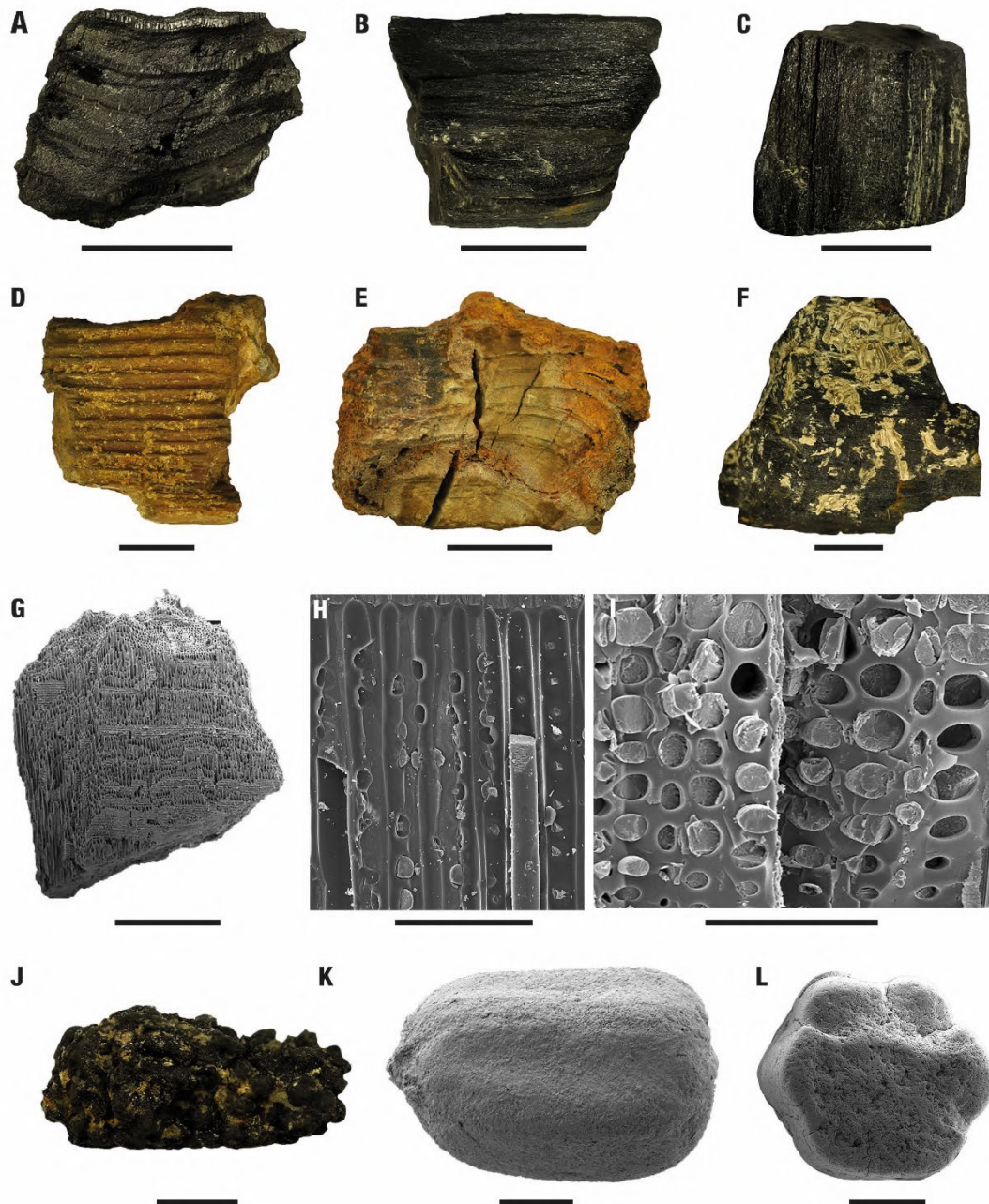


Figure 6.6. Paleobotanical remains and ichnological evidence of insect-plant interactions. A-C) Prismatic-shaped fragments of charcoalfied wood showing the typical both color and texture (VE1T-18, VE1T-19 and VE1T-20). D-E) Mineralized –ferruginous – charcoalfied wood (VE1T-21 and VE1T-22). F) Flat-shaped fragment of charcoalfied wood covered by tubes of calcitic serpulid worms (VE1T-23). G-I) Photographs of charcoalfied wood under SEM, G) fragment in tangential section showing both tracheids and rays (VE1T-24), H) uniseriate tracheid pitting in radial section (VE1T-25), I) tracheids in cross section showing completely fused lamellae and some lumina filled with calcite (VE1T-26). J) Cluster of termite coprolites (VE1T-27). K) A single coprolite in lateral view (VE1T-28). L) coprolite in transverse section with the characteristic hexagonal shape (VE1T-29). Scale bars: A, B, C, D, F = 1 cm; E = 2 cm; G, J = 1 mm; H, I = 100  $\mu$ m; K, L = 200  $\mu$ m.

Phylum MOLLUSCA Linnaeus, 1758

Class BIVALVIA Linnaeus, 1758

**Material:** 6 shell casts of *Corbicula laletana*, 6 shells of *Anomia* sp., 10 shells of '*Saccostrea*' *elhuyari* and 16 calcified syphons of shipworms

**Commentaries:** Several shells of veneroid bivalves (subclass Heterodonta) have been found, preserved as inner casts (Fig. 6.7 A) (N=6). They resemble closely to the genus *Corbicula laletana* Vidal, 1874, quite abundant in the transitional facies of the Tremp Fm (Oms et al., 2016; Vila et al., 2008, 2011). On the other hand, two different bivalves of the subclass Pteriomorpha have been recognized, including *Anomia* sp. (Anomiidae) (N=6), with its distinctive byssus foramen, which is always preserved disarticulated (Fig. 6.7 B), and the oyster '*Saccostrea*' *elhuyari* Vidal, 1921 (Ostreidae) (N=10), with a marked sickle shape (Fig. 6.7 C). However, the fragmentary condition of most of the oyster shells of VE1 (e.g., Fig. 6.7 E) may blur the identification of another possible different taxon of oyster. These two bivalves are also common in the shallow marine and transitional facies of the Eastern Tremp Syncline (Oms et al., 2016; Vila et al., 2011). Besides, some carbonated tubular structures have been found at VE1 (Fig. 6.7 D) and may represent calcified syphons of some type of shipworms (Teredo, family Teredinidae) (N=16). Nonetheless, none of them were found associated with the wood fragments, which did not show any kind of boring (Fig. 6.6 A to F), so that this assignation is tentative until new and better-preserved fossils were found.

Class GASTROPODA Cuvier 1795

**Material:** 26 shells of *Melanopsis* sp., 9 shells of *Cerithium* sp., 1 shell of *Pyrgulifera saginata*, 59 shells and casts of *Pyrgulifera stillans* and 1 shell of Physidae indet.

**Commentaries:** At least 5 different taxa of gastropods appear within the deposits of VE1 site. These include abundant shells of *Melanopsis* sp. (Fig. 6.7 F) (N=26) and *Cerithium* sp. (Fig. 6.7 G and H) (N=9). The turriculate and significantly ornamented genus *Pyrgulifera* has also been found, represented by the shell-elongated *Pyrgulifera stillans* Vidal, 1874 (Fig. 6.7 I and J) (N=59), which is very abundant at the site, and by the shell-compressed *Pyrgulifera saginata* Vidal, 1874, which is less abundant with only one shell found (N=1). These gastropods are common in the transitional deposits of the Tremp Fm (Marmi et al., 2014; Vila et al., 2011) and appear at VE1 as corporal fossils, though some

inner casts of *Pyrgulifera* have been found too. Finally, another fourth indeterminate small gastropod has been recognized (Fig. 6.7 K), which shows a sinistral coiling, while the rest of VE1 gastropods have a dextral coiling. It resembles to gastropods of the family Physidae (N=1), but this assignation is tentative.

Phylum ARTHROPODA Latreille, 1829  
Subphyllum CRUSTACEA Brünnich, 1772  
Class MALACOSTRACA Latreille, 1802  
Order DECAPODA Latreille, 1802

**Material:** 32 mobile and fixed fingers of Decapoda indet. (morphotype 1) and 9 mobile and fixed fingers of Decapoda indet. (morphotype 2).

**Commentaries:** Remains of decapod crustaceans from VE1, consist only of isolated fingers, including mobile (dactyli) and fixed fingers (pollices). Two different morphotypes of paired fingers are present at VE1, the first one (Fig. 6.7 L-M) (N=32) is characterized by robust, big, and strongly calcified mobile and fixed fingers. They bear between 4 and 5 molariform teeth in their occlusal margin, indicating a durophagous diet. The inner and outer margins show several lined setal pits, and fixed fingers display one extra lineation in the lower margin. When preserved, the mottled texture of the cuticle can be observed. The second morphotype (Fig. 6.7 N-O) (N=9) is represented by slender and elongated fingers with small sharp triangular teeth (not molariform) in the occlusal margin. These fingers are smaller than the first morphotype, having sometimes lengths under 4 mm (Fig. 6.7 O). Both fingers also show the lineation of setal pits in the inner and outer margins, and in the dorsal/ventral margin. As both morphotypes preserve repeated elements (right dactylus) (Fig. 6.7 L and M) with significant differences between them, it is reasonable to think that they belong to two different taxa.

The first morphotype shows certain resemblances to the crab fingers of *Dinocarcinus velauciensis* Van Bakel, Hyžný, Valentin and Robin, 2019 (in Robin et al., 2019), described in the upper Campanian of southern France as a freshwater crab. However, although VE1 fingers shares the molariform teeth with *Dinocarcinus*, they have sometimes more teeth, a lineation of setal pits, and they are slightly more recurved towards their inner margin. Thus, VE1 fingers clearly represent a different taxon. The mobile fingers of the second morphotype share some similarities with another dactylus described from the uppermost Maastrichtian Molí del Baró-1 site, also from Tremp Fm outcrops (Marmi et

al., 2016). They share the lineation of setal pits in the outer margin or the shape of the teeth, but they lack the tubercles of the inner margin observed in the Molí del Baró-1 fingers. For these reasons, we classify the fossils crabs from VE1 as belonging to indeterminate decapods. Further taxonomical assignation is tangled, since no more anatomical elements from the decapods have been found.

Class OSTRACODA Latreille, 1802

**Material:** 3 carapaces

**Commentaries:** it is interesting to mention the presence of ostracod carapaces (N=3) at VE1, some of them with their outer surface smooth, while others show ornamentation. However, their relative low abundance and their fragmentary condition has avoided proper taxonomical identifications.

Subphylum HEXAPODA Latreille, 1825

Class INSECTA Linnaeus, 1758

Order BLATTODEA Wattenwyl, 1882

Infraorder ISOPTERA Brullé, 1832

*Microcarpolithes hexagonalis* Vangerow, 1954.

**Material:** Hundreds of coprolites and clusters of coprolites, not counted

**Commentaries:** Hundreds of tiny structures preserved as carbonaceous compressions have been recovered from the sediment of VE1. They occur both isolated, or grouped in clusters composed of ten specimens to more than a hundred of them (Fig. 6.6 J). These structures are ellipsoid to cylindrical in shape, up to 1 mm long and 500 µm wide (Fig. 6.6 K, L), and they present a smooth surface that is externally organized in 6 longitudinal rounded lobes separated by slightly concave depressions (Fig. 6.6 K). These cylindrical bodies show a rounded to slightly pointed apex ending in a small terminal protrusion, a rounded base, and they are hexagonal in cross-section (Fig. 6.6 L). Similar structures were identified as small seeds of angiosperms and named as *Microcarpolithes hexagonalis* Vangerow, 1954. Nevertheless, the similarities in size, shape and their hexagonal transverse section with extant coprolites produced by insects, led to Colin et al. (2011) to reclassify them as fossil fecal pellets of termites (Insecta: Isoptera). These kind of coprolites have been identified in Mesozoic and Cenozoic deposits all around the

world, including the Maastrichtian deposits of the Southern Pyrenees (Liebau, 1971, 1973).

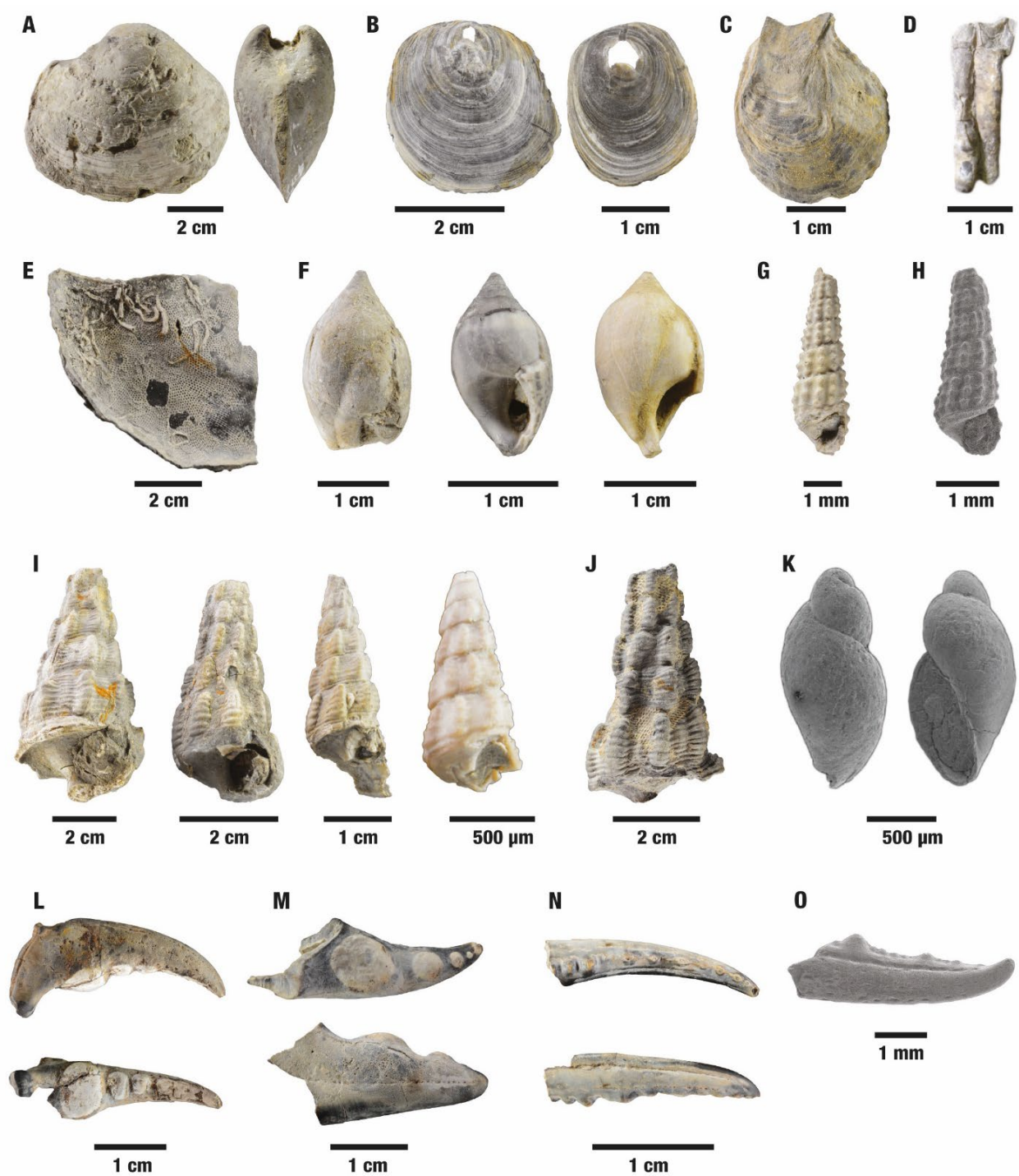


Figure 6.7 (previous page) Main invertebrate fossils from the late Maastrichtian VE1 site. A) *Corbicula laetana* (VE1T-30 and VE1T-31). B) *Anomia* (MPZ VE1T-32 and VE1T-33). C) ‘*Saccostrea*’ *elhuyari*’ (VE1T-34). D) Syphons of *Teredo*? (VE1T-35). E) Fragment of an indeterminate oyster colonized by bryozoans and serpulid worms (VE1T-36). F) *Melanopsis* sp. (VE1T-37, VE1T-38 and VE1T-39). G) and H) *Cerithium* sp. (VE1T-40 and VE1T-41). I) *Pyrgullifera stillans* (VE1T-42, VE1T-43, VE1T-44 and VE1T-45). J) *Pyrgullifera stillans* colonized by an incrustant bryozoan (VE1T-46). K) *Physidae* indet. (VE1T-47). L) Indeterminate decapod crustacean, right mobile finger in outer and occlusal view (MPZ2022/184). M) Indeterminate decapod crustacean, right fixed finger in outer and occlusal view (MPZ2022/187). N) Indeterminate decapod crustacean, right mobile finger in outer and occlusal view (MPZ2022/188). O) Indeterminate decapod crustacean, right mobile finger in inner view (VE1T-48).

Phylum CHORDATA Haeckel, 1874  
Subphylum VERTEBRATA Lamarck, 1801  
Superclass OSTEICHTHYES Huxley, 1880  
Class ACTINOPTERYGII Klein, 1885  
Order LEPISTOSTEIFORMES Hay, 1929  
Family LEPISTOSTEIDAE Cuvier 1825  
Lepistosteidae indet.

**Material:** 12 ganoid scales, 1 hemitrich and 2 teeth.

**Commentaries:** Lepistosteid fishes, also known as gar fishes, are represented at VE1 by several ganoid scales, one hemitrich and teeth. The ganoid scales (Fig. 6.8 A-F) have generally a rhomboidal or diamond shape and display a shiny layer of ganoine in its external surface. This ganoid ornamentation is composed by many tiny subcircular tubercles. Some of the scales have an anterodorsal process (Fig. 6.8 C), used for the attachment of the scale to the body of the gar. There is certain disparity on their size, ranging from 12.4 mm to 3 mm. The hemitrich (Fig. 6.8 H, I) recovered from VE1 is a small rod-like element with a subrectangular contour, which displays three transversal ridges ornamented with ganoine. These ridges also show tiny tubercles as the ganoid scales (Fig. 6.8 I). They are modified scales which compose the fin rays of lepidosteids. The lepidosteid teeth recovered at VE1 are conical and apicobasally elongated, with a circular cross-section (Fig. 6.8 G). They show a plicidentine structure displaying the teeth an opaque dark enamel with longitudinal striations, while the tip presents a translucent acrodine cap, without striations. The features of these elements allow to identify them as

remains of indeterminate lepisosteids ( Wiley, 1976; Szabó et al., 2016; Blanco et al., 2017), but without any further taxonomical inference.

*Lepisosteus* sp. Lacepède, 1803

**Material:** 3 ganoid scales.

**Commentaries:** Due to the lack of diagnostic features, most of the material of Lepisosteidae from VE1 cannot be assigned to any known genus of this group of fishes, nevertheless, three scales could be assigned to *Lepisosteus* sp. thanks to SEM microscopy. Gayet et al. (2002) point that the size and the distribution of the ganoine tubercles of the scales allow to distinguish the lepisosteid genera. In this way, the three scales imaged under SEM microscopy could be measured (Fig. 6.8 F), focusing on the diameter of their tubercles and the distance between them. Until now, two genera of lepisosteid fishes have been identified in the Maastrichtian of Ibero-Armorica: *Actractosteus* and *Lepisosteus* (Blanco et al., 2017; Cavin, 1999). The results (Fig. 6.9; Table 6.2) show that the three scales analyzed from VE1 fit well within the genus *Lepisosteus* (N=3).

Scale	Average tubercle diameter	Average inter-tubercular distance
VE1T-53	4.99 µm (n= 114)	4.48 µm (n= 142)
VE1T-54	4.37 µm (n= 137)	3.92 µm (n= 176)
VE1T-55	4.12 µm (n= 167)	4.68 µm (n= 203)

Table 6.2. Measurements on the lepisosteid scales from VE1 of size and distance between the ganoid tubercles.

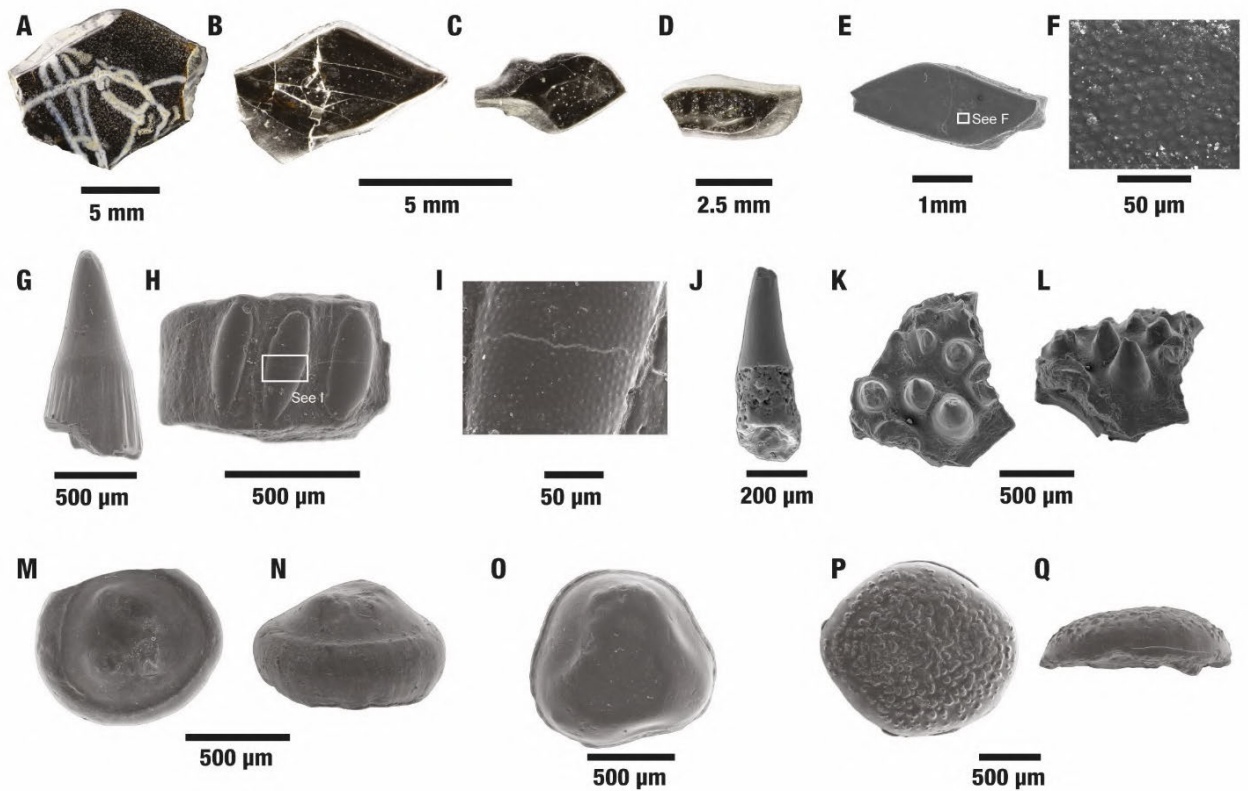


Figure 6.8. Bony fish remains from the late Maastrichtian VE1 site. A-D) Ganoid scales of *Lepisosteidae* indet. (VE1T-49, VE1T-50, VE1T-51, VE1T-52). E-F) Ganoid scale of *Lepisosteus* sp. (VE1T-53), E) general view, F) detail of the ganoid ornamentation. G) Tooth of *Lepisosteidae* indet. (VE1T-56). H-I) Hemitrich of *Lepisosteidae* indet. sp. (VE1T-57), H) general view, I) detail of the ganoid ornamentation. J) Tooth of an indeterminate actinopterygian (VE1T-58). K-L) Teeth-bearing element of an indeterminate *Amiidae*? (VE1T-59) K) apical view, L) lateroapical view. M-N) Tooth of *Paralbula* sp. (VE1T-60), M) occlusal view, N) lateral view. O) Tooth of *Pseudoegertonia*? (VE1T-61) in occlusal view. P-Q) Tooth of *Phyllodus* sp. (VE1T-62), P) occlusal view, Q) lateral view(P).

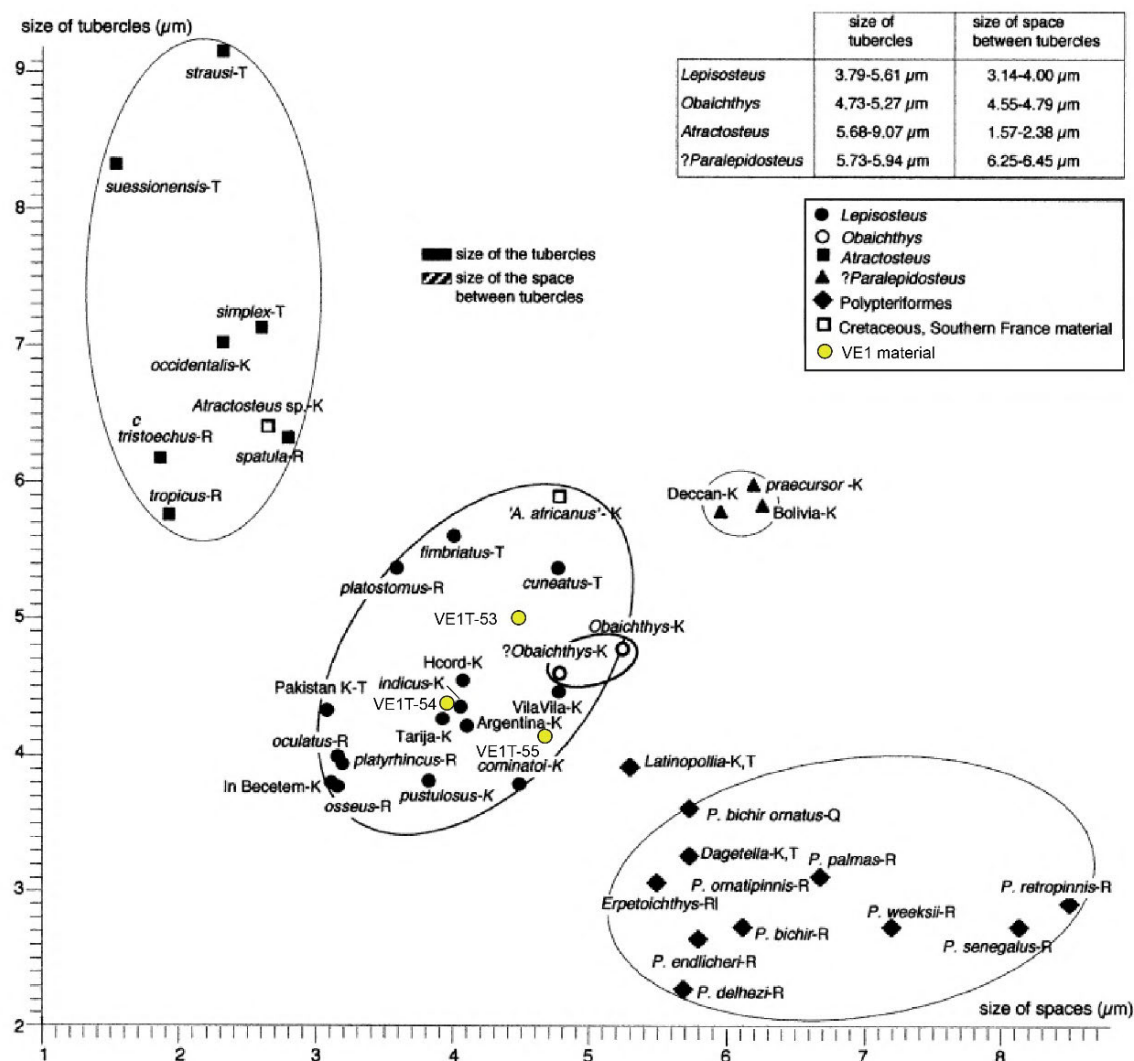


Figure 6.9. Measurements of the ganoid ornamentation of scales of extinct and extant lepisosteoid fishes, including *Lepisosteus* sp. from VE1 site. Abbreviations: F., fossil; K., Cretaceous; T., Tertiary; Q., Quaternary; R., Recent (Modified after Gayet et al., 2002).

Order ELOPIFORMES Greenwood, Rosen Weitzman and Myers 1966

Family PHYLLODONTIDAE Sauvage 1875

Subfamily PARALBULINAE Estes 1969

*Paralbula* sp. Blake 1940

**Material:** 1 tooth.

**Commentaries:** Phyllodontid fishes are represented at VE1 just by isolated round teeth, that can be sometimes globular or sometimes flattened, with foramina observable in basal view. None superposed sets of teeth (phyllodont dentition) have been found, a diagnostic character of this group (Estes, 1969). This would imply that some of the teeth could belong to pycnodontiform fishes, but none of the teeth found at VE1 are attached to jaw fragments, which avoid any kind of differentiation between stacked phyllodont dentition or non-stacked pycnodontiform fishes. Nevertheless, the teeth from VE1 identified as phyllodontids are quite similar to other phyllodontids described from the South-Central Pyrenees (Blanco et al., 2017), so this assignation seems the most plausible. At least three different types of teeth have been recognized. The first two types of teeth (Fig. 6.8 M-O) correspond to paralbuline phyllodontids, being bulbous to hemispherical, and bearing a well-developed basilar foramen. The first morphotype (N=1) is more globular in lateral view (Fig. 6.8 N) and shows a protruding margin around the base of the crown. In occlusal view (Fig. 6.8 M) the tooth is subcircular and has a central papilla or subcircular tubercles surrounding the central area, though in the preserved specimen these features are poorly marked due to weathering. These features fit properly with the genus *Paralbula* Blake, 1940, which have been reported previously in other areas of the Southern-Pyrenees (Blanco et al., 2017).

*Pseudoegertonia* sp.? Darteville and Casier 1949

**Material:** 1 tooth.

**Commentaries:** The other paralbuline morphotype is represented by one tooth (N=1). It also shows a globular crown, but it is rather partially flattened. It also bears a protruding margin around the crown, but it is thinner than in the first morphotype. In occlusal view (Fig. 6.8 O), the tooth shows a distorted morphology being more polygonal than circular, due to growth compression. The only specimen recovered shows an enamel that is kind of smooth (Fig. 6.8 O), but some reminiscences of granular ornamentation can be observed, being the actual state product of weathering or abrasion. In basal view, a large

basilar foramen can be observed. By its distorted shape and its apparent granular ornamentation, this tooth fits well within the genus *Pseudoegertonia* Darteville and Casier, 1949, which has been recognized in the Pyrenees, in the early Maastrichtian site of L'Espinou (Blanco et al., 2017). As just one worn tooth has been recovered, we classify it as *Pseudoegertonia*? with the premise of more material appearing to corroborate it.

Subfamily PHYLLODONTINAE Sauvage, 1875

*Phyllodus* sp. Agassiz, 1843

**Material:** 2 teeth.

**Commentaries:** The last phyllodontid morphotype (N=2) (Fig. 6.8 P, Q) has a quite flattened crown, without a protruding margin. It is subcircular in occlusal view and displays an ornamented enamel with tiny tubercles that cover almost all its occlusal surface. The flattened nature of the crown indicates that these teeth belong to a phyllodontine phyllodontid (Estes, 1969). These teeth are similar to the teeth referred to the genus *Phyllodus* from other sites of the Southern Pyrenees (Blanco et al., 2017), and the Phyllodontinae indet. from Quintanilla de Ojada, Albaina and Laño (Burgos, NW Spain) (Poyato-Ariza et al., 1999; Berreteaga et al., 2011; Pereda-Suberbiola et al., 2015a; Corral et al., 2021). For this reason, we refer VE1 specimens to the genus *Phyllodus*.

Order AMIIFORMES Hay 1929

Family AMIIDAE Bonaparte 1838

Amiidae indet.?

**Material:** 1 teeth-bearing element.

**Commentaries:** One teeth-bearing element (Fig. 6.8 K, L) has been recovered from VE1. It bears several styliform teeth, higher than wider, lined in at least two rows. The teeth are conical and straight, with a circular cross-section and the tip of their crowns display a translucent acrodine cap. They do not show any kind of ornamentation. Other similar teeth-bearing elements and isolated teeth have been described in other Cretaceous sites of Europe and the Pyrenees (Grande and Bemis, 1998; Berreteaga et al., 2011; Blanco et al., 2017; Szabó and Ősi, 2017), being referred sometimes to indeterminate Amiidae

or as indeterminate actinopterygians. We tentatively refer this element to Amiidae, since their teeth are quite similar to the ones of the coronoid element described by Blanco et al. (2017) from the Upper Cretaceous of the Southern Pyrenees; though the future discovery of new and more complete elements would help to confirm this assignment.

Actinopterygii indet.

**Material:** 1 tooth.

**Commentaries:** One isolated conic styliiform tooth was recovered from VE1 (Fig. 6.8 J). It is basiapically elongated and lacks any kind of ornamentation in its crown. Its fragmentary and isolated nature hinders more precise taxonomical assignment further than an indeterminate actinopterygian.

Class AMPHIBIA Linnaeus, 1758

Subclass LISSAMPHIBIA Haeckel, 1866

Order ALLOCAUDATA Fox and Naylor, 1982.

Family ALBANERPETONTIDAE Fox and Naylor, 1982.

**Material:** 1 premaxilla?

**Commentaries:** Just one fossil (N=1) that can be assigned to amphibians has been identified at VE1. It is a small cranial fragment (Fig. 6.10 G-H) that bears two teeth with pleurodont implantation. The bone bears a nutritious foramen in its external surface and lacks a subdental shelf, discarding it as a dentary. However, its fragmentary nature prevents us to discern if it is a maxilla or a premaxilla. The teeth have an elongated root and a labio-lingually flattened crown (Fig. 6.10 G). Though one of the teeth is partially eroded, the other one shows three distinct cusps (Fig. 6.10 G-H), which is a characteristic feature of the albanerpetontids (Gardner, 2001, 2002). By this reason, we classify this fossil within this group of amphibians. Other remains of albanerpetontids, including similar jaw elements, have been documented in the Maastrichtian outcrops of the Tremp Fm, in the nearby site of Blasi 2B in Huesca (Blain et al., 2010) and in other sites of Catalonia (Blanco et al., 2016). Alongside the other remains from the Serrat del Peleu site in Lleida (Blanco et al., 2016) and the Cassagnau 2 in France (Laurent et al., 2002a; Laurent, 2003), the albanerpetontid from VE1 constitutes the youngest record (C29r) of this group of amphibians of the Maastrichtian of the Ibero-Armorican island.

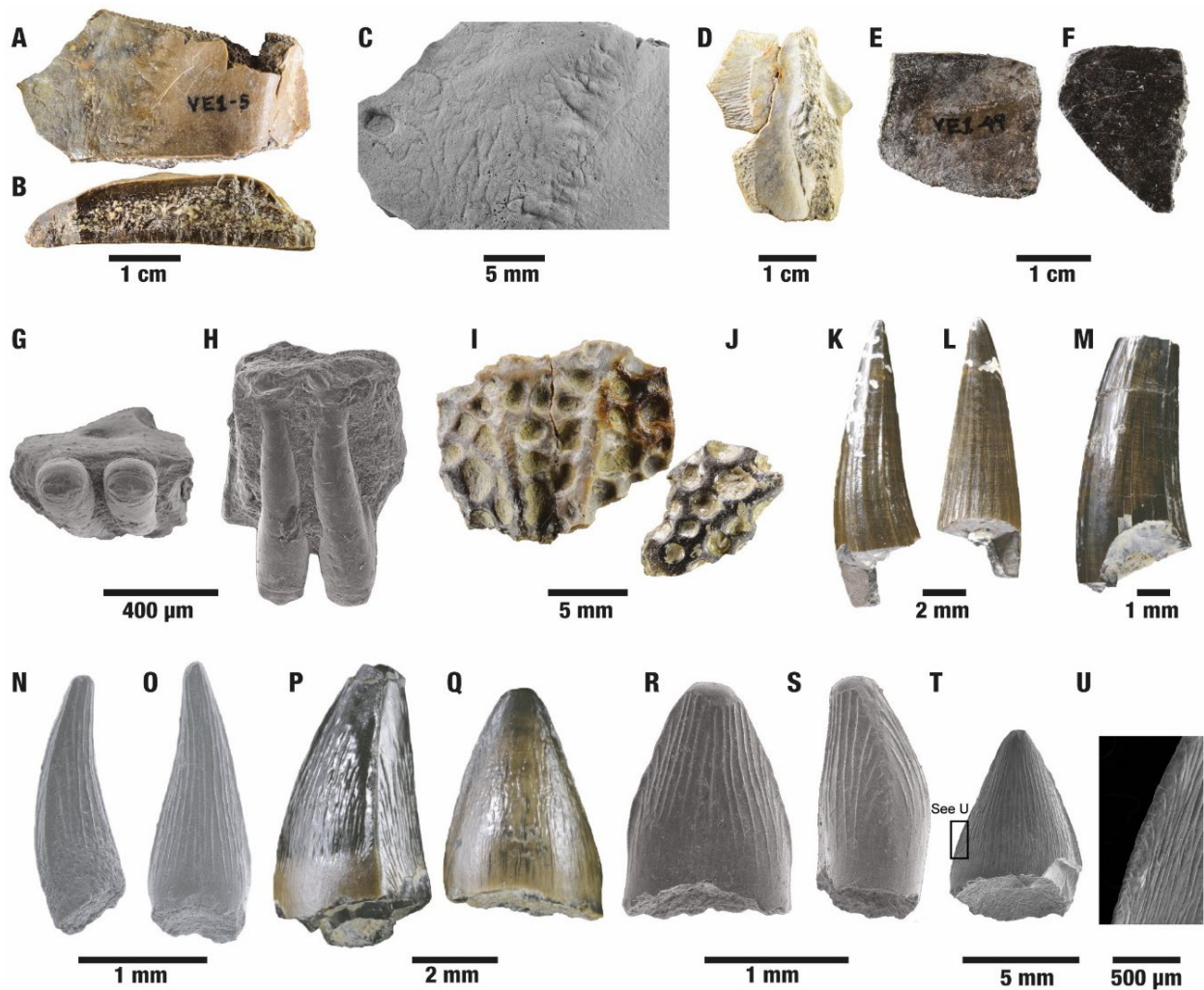


Figure 6.10. Tetrapod remains from the late Maastrichtian VE1 site. A-C) Peripheral plate of *Bothremydidae* indet. (VE1T-63), A) ventral view, B) transversal view, C) detail of the ornamentation. D) Neural plate of *Bothremydidae* indet. in ventral view (VE1T-64). E-F) Indeterminate plastron plates of *Bothremydidae* indet. (VE1T-65 and VE1T-66). G-H) Premaxilla? of *Albanerpetontidae* indet. (VE1T-67), G), occlusal view, H) lingual view. I-J) Osteoderms of *Crocodylomorpha* indet. (VE1T-68 and VE1T-69). K-L) Tooth of *Allodaposuchidae* indet. (morphotype 1) (VE1T-70), K) lateral view, L) lingual view. M) Tooth of *Allodaposuchidae* indet. (morphotype 1) (VE1T-71) in lateral view. N-O) Tooth of *Allodaposuchidae* indet. (morphotype 1) (VE1T-72), N) lateral view, O) lingual view. P) Tooth of *Allodaposuchidae* indet. (morphotype 2) (VE1T-73) in lateral view. Q) Tooth of *Allodaposuchidae* indet. (morphotype 2) (VE1T-74) in labial view. R-S) Tooth of *Allodaposuchidae* indet. (morphotype 2) (VE1T-75), R) lingual view, S) lateral view. T-U). Tooth of cf. *Allodaposuchus palustris* (VE1T-76), T) lingual view, U) detail of the carina.

Order TESTUDINES Batsch, 1788

Sub-order PLEURODIRA Cope, 1864

Hyperfamily PELOMEDUSOIDES Cope, 1868

Family BOTHREMYDIDAE Baur, 1891

**Material:** 27 fragments of plates.

**Commentaries:** Turtles are represented by isolated and fragmented plates of the carapace and the plastron (Fig. 6.10 A-F) (N=27), including a peripheral and a neural plate. Unfortunately, the condition of this material avoids any proper identification and further taxonomic inferences. Nevertheless, most of the plates display a characteristic ornamentation conformed by shallow dichotomic grooves or sulci (Fig. 6.10 C), which is a characteristic ornamentation of the clade Bothremydidae (e.g. de Lapparent de Broin and Murelaga, 1996; Murelaga and Canudo, 2005; Blanco et al., 2015b), due to the high vascularization of the shell. This clade of pan-pleurodiran turtles is well-represented in the Maastrichtian of the Ibero-Armorican island by several taxa (see section 1.3. of Chapter 1). However, the material from VE1 is too fragmentary to compare it with any defined taxa of the Ibero-Armorican island.

Superorder CROCODYLOMORPHA Walker, 1970

Order CROCODYLIFORMES Hay, 1930

MESOEUCROCODYLIA Whetstone and Whybrow, 1983

NEOSUCHIA Gervais, 1871 (sensu Benton and Clark, 1988)

Suborder EUSUCHIA Huxley, 1875

**Material:** 2 osteoderms of indeterminate eusuchians.

**Commentaries:** Some few fragments of crocodylomorph osteoderms have been found (Fig. 6.10 I, J) (N=2). They show an ornamented dorsal surface with elliptical to subcircular pits. We classify them tentatively as Eusuchia indet., since no further taxonomic assignments could be made.

Family ALLODAPOSUCHIDAE Nárvaez, Brochu, Escaso, Pérez-García and Ortega,  
2015

**Material:** 33 teeth of *Allodaposuchidae* indet. (morphotype 1), 9 teeth of *Allodaposuchidae* indet. (morphotype 2).

**Commentaries:** At VE1 site, crocodylomorphs are mainly represented by isolated teeth. At least two different teeth morphotypes of *Allodaposuchidae* indet. have been recognized. The first morphotype (Fig. 6.10 K-O) (N=33) is characterized by conical and elongated pointy teeth. The crowns have a subcircular to lemon-shaped section and do not show a basal constriction. Carinae are slightly marked, lacking denticles and situated in the mesial and distal margins. The enamel shows fine parallel ridges to the carinae, both in lingual and labial sides. They have a wide size range, showing basiapically heights from 13.9 mm (Fig. 6.10 K-M) to small teeth with heights around 2 mm (Fig. 6.10 N-O). It resembles to the morphotype 2 from the Molí del Baró-1 site (Marmi et al., 2016) and to morphotype X from Blanco et al. (2020), both from the Maastrichtian of the Southern Pyrenees.

The second morphotype (Fig. 6.10 P-S) (N=9) is represented also by conical teeth, but they are wider and blunter than morphotype 1. They display a lemon-shape or D-shape cross-section, being sometimes their lingual margin slightly flattened, whereas their labial one is always convex (Fig. 6.10. P and S). The crowns of the teeth display a faint basal constriction in most of the cases (Fig. 6.10 Q and R), and their carinae are well-marked and smooth, lacking denticles. The enamel displays longitudinal ridges going from the base to almost the tip of the tooth (Fig. 6.10 P-S). They have marked size and heights differences ranging from 4.2 mm (Fig. 6.10 P-Q) in the bigger tooth to 1.4mm (Fig. 6.10 R-S) in the smallest. This morphotype is similar to the morphotype 3 from the Molí del Baró-1 site (Marmi et al., 2016) and morphotype XIII from Blanco et al. (2020), also from the Maastrichtian of the Southern Pyrenees.

These two teeth morphologies are associated to the dentition of generalist crocodylomorphs, barely changing throughout the geological record (e.g. Turner, 2006; Buscalioni et al., 2008; Puértolas-Pascual et al., 2015; Blanco et al., 2020). By this reason, we associate them to *allodaposuchid* crocodylomorphs, since they are the most abundant group of crocodylomorphs with generalist dentition in the Maastrichtian of the Ibero-Armorican island and the European Archipelago (Puértolas-Pascual et al., 2016). Assigning them to any particular genus or species is a difficult task, since most of the

allodaposuchids from Ibero-Armorica display teeth similar to these morphotypes. It is plausible also that they even belong to the same taxon since they could represent different positions within the same tooth row. For all these reasons, we prefer to describe these two types of teeth as *Allodaposuchidae* indet.

cf. *Allodaposuchus palustris* Blanco, Puértolas-Pascual, Marmi, Vila and Sellés, 2014

**Material:** 1 tooth of cf. *Allodaposuchus palustris*.

**Commentaries:** The third morphotype (Fig. 6.10 T-U) (N=1) is defined by a blunt conical tooth, similar in shape to morphotype 2, but slightly more acute on its tip. Its cross-section has a D shape, with the labial side being more convex than the lingual one. It is 8.16 mm high from the base to the apex. The carinae are well-developed, and slightly displaced towards the lingual face. The enamel of the crown has several fine ridges which are subparallel to oblique to the carinae (Fig. 6.10 T). The convergence of the ridges with the carinae creates crenulations, which resemble to denticles (Fig. 6.10 U), displaying a false-ziphodonty. It corresponds to morphotype 4 from the Molí del Baró-1 site (Marmi et al., 2016) and to morphotype IX from Blanco et al. (2020), also found in the Pyrenees. This morphotype has also a generalist shape, which led us to refer it also to *Allodaposuchidae*. However, within this clade, the false-ziphodont condition has been only described in *Allodaposuchus palustris* (Marmi et al., 2016; Blanco and Brochu, 2017; Blanco et al., 2014, 2020). For this reason, we assign this tooth to cf. *Allodaposuchus palustris*.

Superorder DINOSAURIA Owen, 1842

Order ORNITHISCHIA Seeley, 1887

Infraorder ORNITHOPODA Marsh, 1881

IGUANODONTIA Dollo, 1888

Superfamily HADROSAUROIDEA Sereno, 1986

**Material:** 1 tooth, 1 dentary fragment, 1 caudal vertebral centrum, 1 proximal part of a rib and 7 ossified tendons.

**Commentaries:** At VE1, some isolated elements belonging to hadrosauroid ornithopods have been identified. They include a tooth, a fragment of a dentary, a large caudal centrum, a probable proximal part of a rib (Fig 6.11 A, B, E-H, J), and some fragments of ossified tendons (N=7). The tooth is partially broken, preserving only the upper part of

the crown, and albeit not complete, the characteristic lanceolate shape of hadrosauroid ornithopods can be recognized (Fig. 6.11 A-B). It has a slightly curved median ridge in its lingual enameled surface (Fig. 6.11 A), and apparently lacks secondary ridges. It has small rectangular denticles (papillae) in their lateral margins, similar to the teeth described from Els Nerets and Basturs Poble sites (early-late Maastrichtian, Southern Pyrenees) (Blanco et al., 2015b; Fondevilla et al., 2018; Conti et al., 2020), or the teeth of the indeterminate hadrosaurid from La Solana (late Maastrichtian, Valencia) (Company et al., 1998), but unlike *Arenysaurus* and *Blasisaurus* teeth (Cruzado-Caballero et al., 2010a, 2013). The tooth has a maximum width of 8.97 mm, and a preserved height of 13.1 mm. However, more than the half of the tooth is lost, and we prefer to be cautious and not calculate a height/width ratio.

A fragment of a dentary (Fig. 6.11 E-F) has been also found at VE1. It does not keep any of the teeth, but seven rows of alveoli are preserved. It is noteworthy to mention that this fragment has its edges rounded and it is colonized by an incrustant bryozoan in its lateral margin (Fig. 6.11 F).

Another element recovered is a big centrum of a caudal vertebra (Fig. 6.11 G-H). This centrum is amphiplatyan, with hexagonal articular surfaces, compressed craniocaudally, and showing some nutrient foramina in its lateral surfaces (Fig. 6.11 G). Only a small fragment of the left transverse process is preserved, joining the vertebra in the dorsal margin of the centrum (Fig. 6.11 G-H). The area of the neural arch and part of the caudal surface display a carbonate crust. By its dorso-caudal compression and size, it may belong to the anterior sector of the tail of a big hadrosauroid dinosaur. Finally, what it seems to be a proximal part of a dorsal rib was found also in VE1 (Fig. 6.11 K). The rib is broken, encrusted and the tuberculum is not preserved. The onset of the shaft of the rib conforms an angle of approximately 90° with the capitulum process.

These hadrosauroid dinosaurs remains are too fragmentary and incomplete to perform any kind of taxonomic determination within Hadrosauroidea. However, they reinforce the presence of big hadrosauroid dinosaurs in the latest Maastrichtian of the Ibero-Armorican island, as have been demonstrated by the findings of the medium to big sized lambeosaurines, *Arenysaurus* (Pereda-Suberbiola et al., 2009b; Cruzado-Caballero et al., 2013), *Blasisaurus* (Cruzado-Caballero et al., 2010a), *Canardia* (Prieto-Márquez et al., 2013) and *Pararhabdodon* (Casanovas-Cladellas et al., 1993; Prieto-Marquez and Wagner, 2009; Serrano et al., 2021).

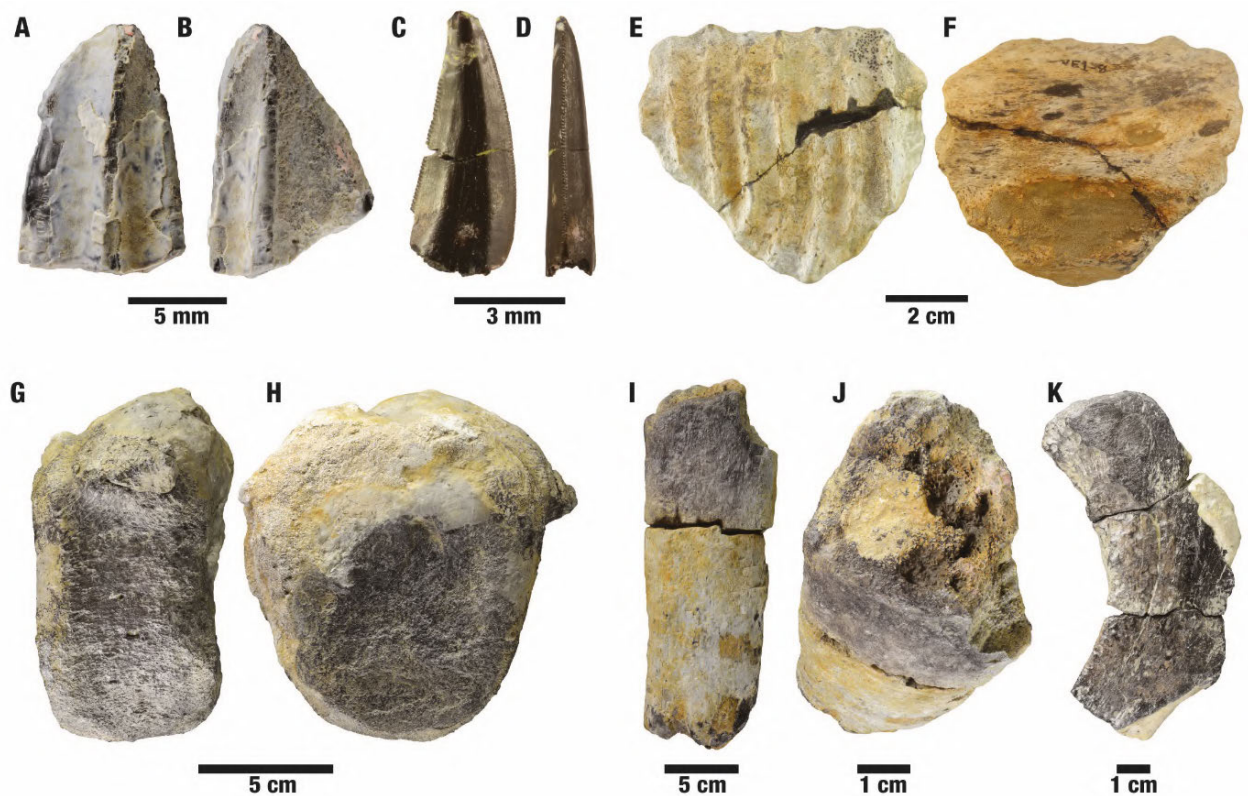


Figure 6.11. Dinosaur remains from the late Maastrichtian VE1 site. A-B) *Hadrosauroidea* indet. tooth (VE1T-77), A) lingual view, B) lateral view. C-D) cf. *Richardoestesia* (Theropoda, family indet.) tooth (MPZ2022/90), C) labial view, D) mesial view. E-F) *Hadrosauroidea* indet. fragment of dentary (VE1T-78), E) medial view, F) lateral view. G-H) *Hadrosauroidea* indet. anterior caudal vertebral centrum (VE1T-79), G) left lateral view, H) anterior view. I-J) *Dinosauria* indet. fragment of a long bone (VE1T-80). K) *Hadrosauroidea* indet.? proximal part of a rib (VE1T-81).

Order SAURISCHIA Seeley, 1887

THEROPODA Marsh, 1881

Family INDET.

cf. *Richardoestesia* Currie, Rigby and Sloan, 1990

**Material:** 1 tooth.

**Commentaries:** The only theropod fossil recovered in VE1 is a small, isolated ziphodont tooth MPZ2022/90 (Fig. 6.11 C, D) (N=1). This tooth is elongated and straight with a crown height of 6.1 mm. Its mesial surface shows a slightly convex curvature while the

distal one is straight (Fig. 6.11 C). Its basal cross-section shape is reniform (sensu Hendrickx et al., 2015). Carinae are serrated, bearing small rectangular denticles which grow in size towards the apex, though the mesial ones seems to be relatively smaller than the distal ones (Fig. 6.11 C). They are straight, centered labiolingually and reach practically the cervix of the tooth (Fig. 6.11 D). Its enamel texture is smooth and lack ornamentation.

It resembles to teeth ascribed to the genus *Richardoestesia* (Currie, et al 1990). This taxon has been identified mostly by isolated teeth from North America, Asia and Europe (e.g. Larson, 2008; Csiki-Sava et al., 2016; Văcărescu et al., 2018; Averianov and Sues, 2019), including the Upper Cretaceous outcrops of the Ibero-Armorican domain (Valentin et al., 2012; Torices et al., 2015; Marmi et al., 2016; Isasmendi et al., 2022). In Europe, *Richardoestesia* teeth display two distinct morphotypes, one shortened and curved distally (e.g., MCD5032 in Marmi et al., 2016; cf. *Richardoestesia* sp. A in Isasmendi et al., 2022) and one elongated and straighter (e.g. cf. *Richardoestesia* sp. B in Isasmendi et al., 2022). In this case, the straight and elongated shape of MPZ2022/90 resembles to the cf. *Richardoestesia* sp. B morphotype from Laño (upper Campanian, Treviño, northern Spain) (Isasmendi et al., 2022), and to some of the elongated *Richardoestesia* teeth from the Maastrichtian of Romania (Fig. 2D of Văcărescu et al., 2018).

Therefore, we classify MPZ2022/90 as cf. *Richardoestesia* sp., representing a tooth of a small theropod with uncertain taxonomic affinities. Further findings would help to determine the taxonomic affinities of this teeth and other *Richardoestesia* teeth from the Ibero-Armorican domain.

### 6.2.2. *Dolor ornithuromorph giant bird*

The fossil site of Dolor is located in the middle part of the ‘Lower Red Garumnian’ (Fig. 6.1) and was first reported by Cruzado-Caballero et al. (2012). The vertebra studied in this section was found in a sandstone block that had fallen from an outcrop of a detrital interval comprising several sandstone levels, two of them containing vertebrate fossils. Although the precise fossiliferous layer could not be determined, the aforementioned sandstone package is continuous regionally, allowing the site to be correlated with the nearby stratigraphic section of Serraduy. The correlation situates Dolor site in the lower half of chron C29r (see Chapter 5 for age calibration). This indicates that the site

corresponds to the last 259 ka of the Cretaceous. Besides the giant bird vertebra, the Dolor outcrop has yielded vertebrate fossil remains of hadrosaurid dinosaurs, eusuchian crocodylomorphs and testudines (Cruzado-Caballero et al., 2012; Puértolas-Pascual et al., 2016; Blanco et al., 2020).

AVIALAE Gauthier, 1986

ORNITHOTHORACES Chiappe, 1995

ORNITHUROMORPHA Chiappe, 2002

**Material:** an isolated cervical vertebra (MPZ 2019/264) (full research in Pérez-Pueyo et al., 2021c).

**Description:** MPZ 2019/264 is an isolated cervical vertebra, which is not deformed and moderately well preserved (Fig. 6.12). It shows some bone modifications due to taphonomic effects, such as a low stage of weathering (stage 1, Behrensmeyer, 1978) and a low-to-medium stage of abrasion (stage 1-2, Fiorillo, 1988). It lacks the caudal articular surface, the prezygapophysis, and part of the transverse processes. Some small specific areas show a heavily pneumatized inner bone tissue exposed by the effect of abrasion.

The centrum is craniocaudally elongated (Cau, 2018, character 222:1), with the cranial articular surface dorsoventrally shorter. The mediolaterally width of the cranial and caudal articular surfaces are similar (Table 6.3). In ventral view, the centrum shows a smooth ventral medial keel (Cau, 2018, character 207: 1; Wang et al., 2020, character 54: 1) in its caudal section, which gradually disappears cranially towards the *sulcus caroticus* (Fig. 6.12 A, F). The caudal part of the ventral surface of the centrum is connected with the cranial part through a craniodorsally inclined triangular facet (Fig. 4F). In ventral view, the cranial area of the centrum possesses a smooth wide medial depression or *sulcus caroticus*, which is laterally limited by two ridges or prominences (Cau, 2018, character 210: 1) (Fig. 6.12 A, F). These ridges indicate the presence of carotid processes (*processi carotici*) (Cau, 2018, character 520: 1; Wang et al., 2020, character 52: 1) that would be located at the lateroventral margins of the cranial region of the centrum; however, they are not preserved.

In lateral view, the centrum shows, on both lateral sides, an elongated groove that is craniocaudally oriented (Fig. 6.12 B, E), which, together with the ventral keel, gives the centrum an inverted-arrow-shaped section in caudal view (Fig. 6.12 D). On both lateral

sides of the cranial half of the centrum, there is a pneumatic foramen (pleurocoel) divided into two subforamina by a bone septum (Wang et al., 2020, character 50:0) (Fig. 6.12 B). The subforamina would be partially covered by the *ansae costotransversariae*, but they are also not preserved. Thus, it is impossible to determine the size and the position of the transverse foramina (*foramina transversarium*). However, we can infer that they would be situated far from the centrum, as the part of the transverse processes that is preserved exceeds the width of the centrum (Fig. 6.12 A). Each transverse foramen would also be connected with the inner part of the neural arch through a pneumatic foramen, which is situated in a slightly anterior position just above the foramina of the centrum (Fig. 6.12E).

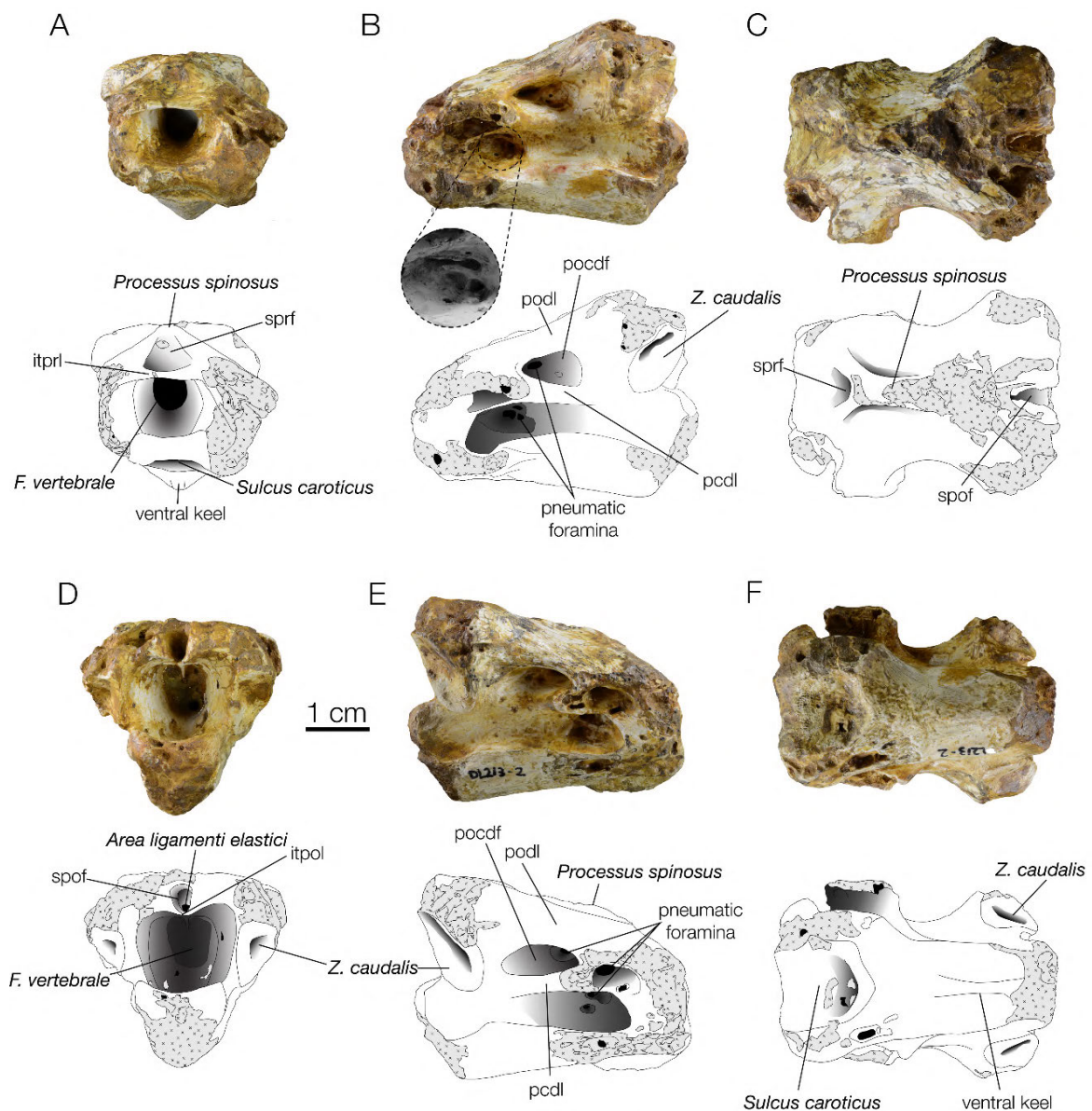


Figure 6.12 (previous page). MPZ 2019/264. Cervical vertebra from the Dolor site (Serraduy, NE Spain). A) cranial view; B) right lateral view, with a detailed view of the pneumatic foramen; C) dorsal view; D) caudal view; E) left lateral view; F) ventral view. Each photograph has a schematic drawing with the main osteological elements pointed out. Grey texture identifies eroded or broken areas. Abbreviations: *itpol*, interpostzygapophyseal lamina; *itprl*, interprezygapophyseal lamina; *pcdl*, posterior centrodiapophyseal lamina; *pocdf*, postzygapophyseal centrodiapophyseal fossa; *podl*, postzygodiapophyseal lamina; *sprf*, spinoprezygapophyseal fossa; *spof*, spinopostzygapophyseal fossa. Scale bar equals 1 cm.

The caudal articular surface (*facies articularis caudalis*) is almost completely eroded, except for its dorsal margin (Fig. 6.12 D). This dorsal margin extends more posteriorly than the caudal margin of the postzygapophyses (Cau, 2018, character 782:1; character 1083:0) (Fig. 6.12 B, E, F) (Table 6.3). This latter feature, along with the shape of the cranial articular surface (*facies articularis cranialis*), which is narrow, concave transversely, convex dorsoventrally, and with concave dorsal and ventral margins (Fig. 6.12 A; Fig. 6.13 F), points to a well-developed heterocoelous (i.e., saddle-shaped) articulation. Although most of the morphology of the caudal articular face is unknown, the lateromedially convex shape (Fig. 6.12 B, D, E) of the preserved dorsal margin would also suggest a heterocoelous articulation, with a transversely convex and dorsoventrally concave articular surface (Cau, 2018, character 684: 1; Wang et al., 2020, character 51:1&2).

The caudal aperture of the neural canal (*foramen vertebrale*) is bigger than the cranial one (Fig. 6.12 A, D) (Table 6.3). There is also a thin inner medial keel in the dorsal roof of the caudal region of the neural canal (Fig. 6.12 D). The neural arch is lateromedially wider than it is dorsoventrally high. In lateral view, its dorsal surface is tilted and faces dorsocranially, as well as the neural canal (*foramen vertebrale*) (Fig. 6.12 B, E; Fig. 6.13 F). It has a dorsoventrally compressed pneumatic oval foramen in the middle part of each lateral side (Fig. 6.12 B, E), which is enclosed within the postzygapophyseal centrodiapophyseal fossa (*pocdf*, sensu Wilson et al., 2011b). This fossa is bounded dorsally by a well-marked, craniolaterally oriented postzygodiapophyseal lamina (*podl*) (Cau, 2018; character 848:1), and ventrally by a posterior centrodiapophyseal lamina (*pcdl*) (Fig. 6.12 B, E). This latter lamina is craniolaterally directed and does not face ventrally (Cau, 2018, character 1424:1). The prezygapophyses (*zygapophysis cranialis*) are not preserved (Fig. 6.12 A); however, they would be situated laterally to the lateral

sides of the centrum, since they are not in the well-preserved craniomedial portion of the arch (Cau, 2018, character 216:1). The postzygapophyses (*zygapophysis caudalis*) are elliptical, craniocaudally elongated, and are situated near the base of the neural arch (Fig. 6.12 B, D, E). Their articular facets are slightly concave, lateroventrally oriented and subvertical, oriented at an angle of about 70° with respect to the horizontal plane. Although the dorsal margins of the postzygapophyses are not well preserved, they seem relatively flat, without any kind of bump-like protuberance, suggesting that they lack well-developed epipophyses (*torus dorsalis*) (Fig. 6.12 C, D, E) (Cau, 2018, character 208:0; Wang et al., 2020, character 53:1).

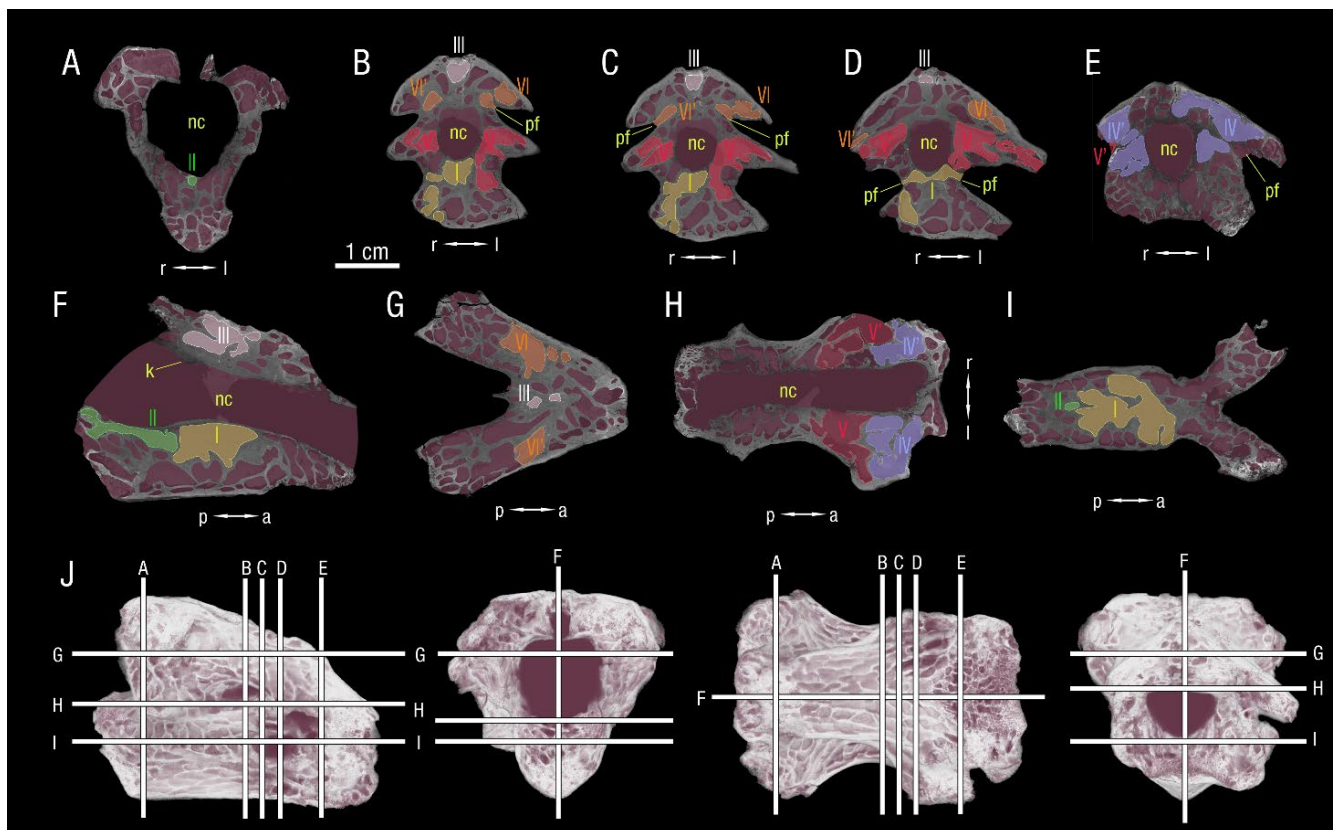


Figure 6.13. CT-Scan cross-sections (A-I) of MPZ 2019/264 and their corresponding position on the vertebra (J) in lateral, caudal, ventral and cranial views respectively. Abbreviations: a, anterior; k, keel; l, left; nc, neural canal; p, posterior; pf, pneumatic foramen; r, right.

Measurement	Description of the measure	Length
<b>M1</b>	Maximum length	4.64cm*
<b>M2</b>	Maximum height	3.23 cm*
<b>M3</b>	Cranial width	2.92 cm*
<b>M4</b>	Caudal width	3.17 cm*
<b>M5</b>	Distance between articular surfaces	4.35 cm
<b>M6</b>	Length of the centrum (ventral view)	4.57 cm*
<b>M7</b>	Length of the neural arch (Distance between the borders of the neural canal) (dorsal view)	4.34 cm
<b>M8</b>	Height of cranial articular surface	0.23 cm
<b>M9</b>	Width of cranial articular surface	1.33 cm
<b>M10</b>	Height of caudal articular surface	1.61 cm*
<b>M11</b>	Width of caudal articular surface (dorsal margin)	1.42 cm
<b>M12</b>	Width of caudal articular surface (narrowest part)	0.9 cm
<b>M13</b>	Length of the ventral keel	1.19* cm
<b>M14</b>	Cranial height of the neural canal	1.02 cm
<b>M15</b>	Cranial width of the neural canal	1.07 cm
<b>M16</b>	Caudal height of the neural canal	1.4 cm
<b>M17</b>	Caudal width of the neural canal	1.76 cm
<b>M18</b>	Width of the dorsal spine	0.52 cm
<b>M19</b>	Length of dorsal spine	1.66 cm*
<b>M20</b>	Distance between postzygapophyses (between their middle point)	2.64 cm
<b>M6/M8</b>	Relation between centrum length and dorsoventral height of the cranial surface (Cau 2018, character 222)	19.8

*Table 6.3. Main measurements of MPZ 2019/264. The measurements with an asterisk are estimated or represent just the preserved bone.*

A horizontal, interpostzygapophyseal lamina (itpol) (Fig. 6.12 D) (Cau, 2018, character 1162:1) joins both postzygapophyses medially. The neural spine (*processus spinosus*) is craniocaudally elongated, being slightly less than half the length of the neural arch (Cau, 2018, character 211: 1) (Table 6.3), and situated in its middle part (Cau, 2018, character 213:0) (Fig. 6.12 C). Although the distalmost part of its dorsal margin is not preserved, the neural spine shows a slight vertical development (Cau, 2018, character 212:0) (Fig. 6.12 A, B, E). Just ahead of the cranial margin of the spine, there is a shallow depression, which corresponds to the spinoprezygapophyseal fossa (sprf) (Fig. 6.12 A, C). In caudal view, just below the base of the spine and above the neural canal, there is a lateromedially narrow but dorsoventrally deep fossa, which would correspond to the spinopostzygapophyseal fossa (spof). Within this fossa, there is a tiny foramen (Fig. 6.12 D), corresponding to the insertion of the elastic interlaminar ligament (*area ligamenti elastici*).

The CT-scan images of MPZ 2019/264 reveal its inner pneumatic system (Fig. 6.13). They show that both centrum and neural arch are strongly pneumatized, with an asymmetric pattern of distribution of the camerae. Its pneumatic system could be described as ‘camellate’ (sensu Wedel et al., 2000), as it is constituted by numerous small and irregular chambers or camellae separated by thin bone walls. This system is only connected with the exterior through the six pneumatic foramina or pleurocoels (three per side) (Fig. 6.12 B, E; Fig. 6.13). An extended description of the inner pneumatic structure of the vertebra can be found in Supplementary Data 2.

Determining the position of MPZ 2019/264 in the neck is difficult, given the lack of any associated material. The absence of hypapophyses in its ventral surface rules it out as one of the cranial-most or one of the cervicothoracic vertebrae. The presence of two elongated ridges on the ventral surface of the centrum, which would support the carotid processes, may indicate an intermediate position in the neck. Rauhut (2003) notes the presence of a ventral keel in the cranial cervical vertebrae of several dinosaurs, including theropods. For all these reasons, MPZ 2019/264 would be situated in the cranial middle part of the neck. In addition, the spacing between the two ventral ridges and the shape of the cranial articulation of the centrum (thin dorsoventrally and elongated transversely) may indicate that the vertebra was capable of dorsal bending and limited ventral bending. This supports the notion that this vertebra was situated at a transitional point between section I and II of the neck (see Boas, 1929; Tambussi et al., 2012), again suggesting a middle-cranial position. Recently, Terray et al. (2020) have proposed a modular structure

for the neck of birds, differentiating nine different morphofunctional modules. MPZ/2019/264 shares features with module 2 and module 7, and fits better (despite some differences) within module 7. This module is characterized by vertebrae with an elongated centrum, small neural spine, well-marked *sulcus caroticus* and ventrolaterally oriented postzygapophyses, which do not project further than the caudal margin of the centrum. Vertebrae from module 7 are specific to long-necked birds, and usually occupy posterior positions, but they can also occupy anterior to medium positions, as is the case in *Struthio* (see Terray et al., 2020).

**Cladistic analysis:** To test the affinity of MPZ 2019/264 within Avialae, it was included in an extensive matrix comprising a sample of all major pan-avian clades (Cau, 2018). Our Analysis A1 resulted in 21624 MPTs of 6795 steps (ensemble consistency index, CI = 0.244; ensemble retention index, RI = 0.563; rescaled consistency index, RC = 0.137). The general topology of the consensus tree (Fig. 6.14 A) is the same as that originally recovered by Cau (2018, see Supplementary Figure 1 for the full consensus tree), although the addition of MPZ 2019/264 has resulted in the collapse of the clade Ornithothoraces. MPZ 2019/264 is recovered as a sister taxon of *Piscivoravis*, an Early Cretaceous ornithuromorph, closely related to the Carinatae (Zhou et al., 2014; Cau, 2018), based on the relatively long centrum (A1 character 222:1), a condition shared with some Neornithes such as *Meleagris* (turkey), but also with some dromaeosaurs such as *Fukuivenator* and *Halszkaraptor*. Nevertheless, its position within Ornithothoraces is supported by the presence of a saddle-shaped articular surface, a character exclusive to this clade and shared with most of its members (A1 character 648:1). The presence of a ventral keel on the centrum (A1 character 207:1) also supports its inclusion within Ornithothoraces.

To further specify the position of MPZ 2019/264 within Ornithothoraces, a second analysis (A2) was carried out, using the dataset of Wang et al. (2020), which focuses on Mesozoic birds. This resulted in 4872 trees of 1271 steps (consistency index, CI = 0.306; retention index, RI = 0.665; rescaled consistency index, RC = 0.203). The consensus tree (Fig. 6.14 B) is identical to that recovered by Wang et al. (2020). MPZ 2019/264 is recovered as an ornithuromorph ornithothoraces, forming a clade with *Patagopteryx*, *Apsaravis* and *Vorona*, based on certain derived conditions shared with *Apsaravis*, such as the presence of pneumatic foramina at the level of the parapophysis-diapophysis (A2, character 50:0), and heterocoelous articular surfaces (A2, character 51:1-2). The placement within Ornithuromorpha is nonetheless well supported on the basis of the

presence of a prominent carotid process, a synapomorphy of this clade (A2, character 52:1).

It is also important to note that in both cladistics analyses carried out, bootstrap values are low (Fig. 6). The inclusion of MPZ 2019/264 in both datasets does not have an impact on the general topology of the tree and does not significantly lower the already low bootstrap values and Bremer indexes recovered for both consensus topologies (Cau, 2018, Wang et al., 2020). This is due to the scarce number of characters of MPZ 2019/264 scored in both matrixes (1.8% of the overall in both analyses). In any case, we consider our consensus topologies informative, but more complete material from this putative ornithuromorph and related taxa would help to refine its phylogenetic position and the robustness of the phylogenetic hypothesis.

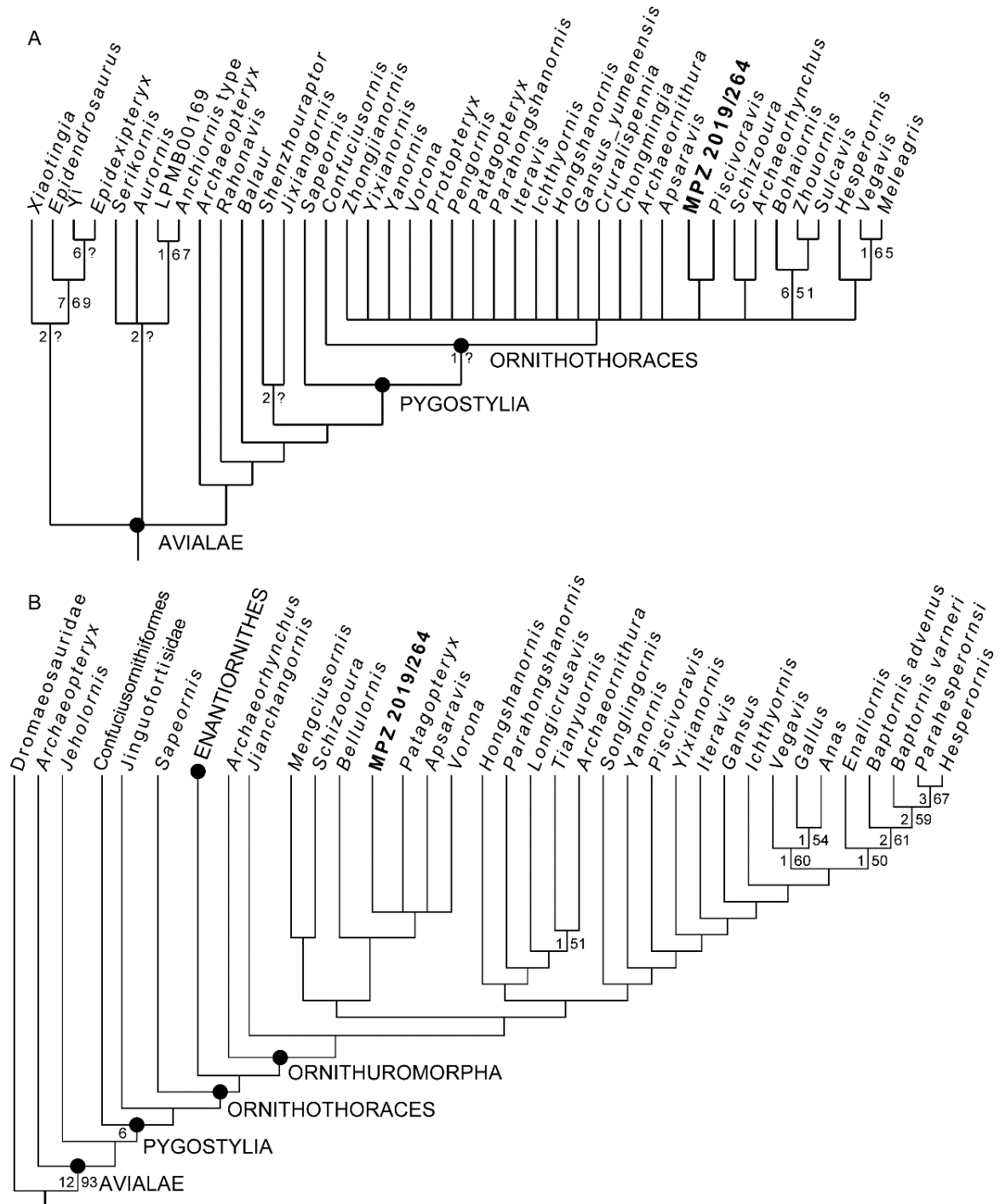


Figure 6.14. Phylogenetic position of MPZ 2019/264 as an ornithuromorph ornithothoraces. A) the clade Avialae, as recovered in the strict consensus tree of the 21624 most parsimonious trees recovered after the inclusion of MPZ 2019/264 in the dataset of Cau (2018). See Supplementary Figure 1 for the full topology of the strict consensus; B) strict consensus tree of the 4872 most parsimonious trees recovered after the inclusion of MPZ 2019/264 in the dataset of Wang et al. (2020). Numbers at the left of branches represent Bremer supports (values below 2 are not shown). Numbers to the right of the branches represent bootstrap index after 1000 replications (values below 50 are not shown).

**Discussion:** The key feature of MPZ 2019/264 with relevant phylogenetic implications is its heterocoelous vertebral articulation. This characteristic has been recognized as an avialan character (Marsh, 1879; Martin, 1991), mainly in the clade Ornithuromorpha (Clarke and Norell, 2002; Clarke et al., 2006; O'Connor et al., 2011), but also in a few enantiornitheans such as *Vescornis* (Zhang et al., 2005), *Pengornis* (Zhou et al., 2008) and the enantiornithean LP-4450-IEI from El Montsec (Sanz et al., 1997). A few paravian theropods, such as dromaeosaurids (e.g. *Buitreraptor*) and troodontids (e.g. *Mei*), also show a slight, incipient saddle-shaped articulation (Xu and Norell, 2004; Novas et al., 2018), but not as developed as in MPZ 2019/264. On the other hand, the cervical vertebra from Beranuy shares some characters with these paravian theropods, such as the presence of lateral pneumatic excavations (e.g. Makovicky and Sues, 1998; Makovicky and Norell, 2004; Sues and Averianov, 2014) (Fig. 6.15 B2), and the presence of a camellate inner pneumatic system. This system is present in most coelurosaurs (Benson et al., 2012), but in MPZ 2019/264 it is clearly more complex than those in most non-avian theropods, and more similar to that of modern birds (compare for example *Archaeornithomimus* and *Catharacta*) (Gutzwiller et al., 2013; Watanabe et al., 2015). Another feature shared with troodontids and dromaeosaurids is the presence of carotid processes on the ventral surface (Makovicky and Norell, 2004; Makovicky et al., 2005). Unlike these two clades, MPZ 2019/264 lacks well-developed epiphyses above the postzygapophysis, it is more elongated craniocaudally (Fig. 6.15 A1, B1), and its caudal articular face would project far beyond the postzygapophyses (Fig. 6.15 A2, B2).

The systematic attribution of MPZ 2019/264 within Avialae is well supported even though it is an isolated element, as some of its characters are decisive. First is the above-mentioned well-developed heterocoelous articulation, which would situate it within Ornithothoraces (Ornithuromorpha + Enantiornithes), and most probably within Ornithuromorpha (O'Connor et al., 2011). On the other hand, the presence of well-marked lateral pneumatic foramina (pleurocoels) in the centrum is a character that is present within Ornithuromorpha and Ornithurae, but not in Enantiornithes (Chiappe and Walker, 2002; O'Connor et al., 2011). In most neornitheans the pleurocoels become superficial and reduced or absent (Hope, 2002). Although there are exceptions with some developed pleurocoels, as in *Chloephaga*, *Catharacta*, or *Struthio* (e.g. O'Connor, 2004, 2009; Apostolaki et al., 2015), these are never as developed as in other, more basal avialans.

When MPZ 2019/264 is compared with other Late Cretaceous avialans, it is found to share its elongated shape with Enantiornithes, such as specimen LP-4450-IEI from El Montsec (Sanz et al., 1997), *Enantiornis* (Walker and Dyke, 2009) and *Pengornis* (Zhou et al., 2008), and with some of them, such as *Pengornis* and *Vescornis*, it shares the presence of a keel on the ventral surface. By contrast, it differs in its more developed heterocoelous articulation, in the presence of pneumatic excavations on the lateral sides of the centrum and in the extension of the caudal articular surface further than the postzygapophyses.

Comparisons with the sister clade of Enantiornithes, Ornithuromorpha, should begin with the cervical vertebra MC-MN 478 (Fig. 6.15 C), referred to *Gargantuavis* (Buffetaut and Angst, 2013), recovered in the Upper Cretaceous of the Ibero-Armorican island (Southern France and NE Spain). This vertebra was identified as belonging to a giant bird that would be included within Ornithuromorpha and closely related to Ornithurae, due to its marked heterocoelous articulation. MPZ 2019/264 and MC-MN 478 are similar in size (cassowary-size according to Buffetaut and Angst, 2013), and in both, the caudal articular surfaces of the centra project further than the postzygapophyses (Fig. 6.15 C2). MC-MN 478 differs from MPZ 2019/264 in the presence of epipophyses above the postzygapophyses (A1, character 782:1; character 1083:0) (Fig. 6.15 C2, C3), and in the scarce craniocaudal and ample dorsoventral development of the dorsal spine (Fig. 6.15 A, C). Furthermore, MC-MN 478 has little lateromedial development of the neural arch (Fig. 6.15 C1), and just a tiny pneumatic foramen at the base of the neural arch is present (Fig. 6.15 C2). By contrast, the neural arch of MPZ 2019/264 is wider, with less dorsoventral development, and it has three pleurocoels per side. All these differences are enough to establish that these specimens represent two different taxa. Given its well-marked pleurocoels (Hope, 2002), the taxon from Beranuy would probably occupy a more basal position within Avialae.

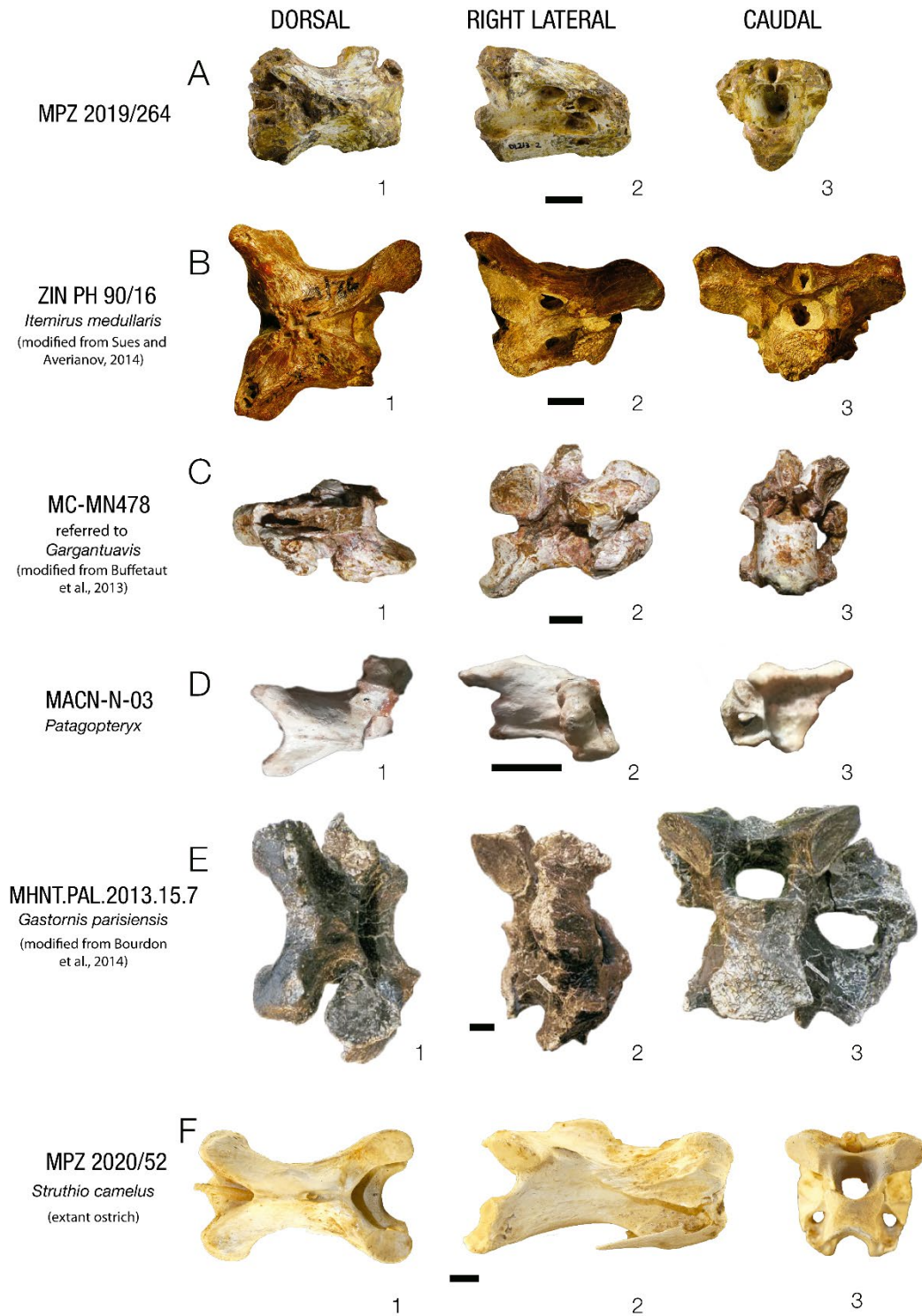


Figure 6.15. Comparative plate of A) MPZ 2019/264 with several cervical vertebrae of maniraptoran theropods in dorsal (1), right lateral (2) and caudal (3) views; B) ZIN PH 90/16, *Itemirus medullaris*. Dromaeosauridae (modified from Sues and Averianov, 2014) (mirrored); C) MC-MN478, referred to *Gargantuavis*. Ornithurae? (modified from Buffetaut and Angst, 2013); D) MACN-N-03, *Patagopteryx deferrariisi*. Ornithuromorpha (mirrored); E) MHNT.PAL.2013.15.7, *Gastornis parisiensis*. Gastornithidae (modified from Bourdon et al., 2014); F) MPZ 2020/52 *Struthio camellus*. Palaeognathae. Scale bar equals 1 cm.

MPZ 2019/264 has also been compared with other Late Cretaceous birds of relatively 'large' size, with preserved cervical vertebrae. For example, *Patagopteryx* (MACN-N-03) (Alvarenga and Bonaparte, 1992; Chiappe, 2002), a non-flying hen-sized ornithuromorph bird from Argentina, has the anterior cervical vertebrae (Fig. 6.15 D) smaller in size, lack pneumatic foramina in their centrum or neural arch, have tiny epipophyses above the postzygapophyses (Fig. 6.15 D2, D3), and the centrum does not project beyond the postzygapophyses (Fig. 6.15 D2). On the other hand, MACN-N-03 and MPZ 2019/264 share the elongated shape, the low and long neural spine, and their well-developed heterocoelous articulation. Other ornithuromorphs, such as *Longicrusavis* (O'Connor et al., 2010) and *Piscivoravis* (Zhou et al., 2014), have elongated anterior-middle centra (A1, character 222: 1), heterocoelous articulation, a keeled ventral surface, long and low neural spines, and they lack pneumatic foramina. The ornithurine *Apsaravis* (Clarke and Norell, 2002) shares some characteristics with MPZ 2019/264, such as the heterocoelous articulation and the presence of pleurocoels in the centra, in a caudal position relative to the diapophyses, as well as the ventral keel and the absence of epipophyses.

MPZ 2019/264 also differs from the cervical vertebrae of Hesperornithiformes, the large Late Cretaceous diving ornithurines. Hesperornithiforms, such as *Hesperornis* and *Chupkaornis* (e.g., Marsh, 1880; Tanaka et al., 2018), possess more craniocaudally elongated heterocoelous cervical vertebrae, without pneumaticity, but with the postzygapophyses projecting further than the centrum, and epipophyses above the postzygapophyses.

MPZ 2019/264 is not similar to the giant flightless birds present in Europe during the Palaeogene either. The cervical vertebrae of neornithean giant birds, gastornithids (Bourdon et al., 2014), and phorusrhacids (Alvarenga et al., 2011; Tambussi et al., 2012) are clearly more robust and bigger than MPZ 2019/264 (Fig. 6.15 E). The cervical vertebrae of gastornithids such as *Gastornis* are craniocaudally compressed (Fig. 6.15 E1, E2), they lack pneumatic foramina, the caudal articular surface does not project further than the postzygapophyses, and they have marked epipophyses. The cervical vertebrae of phorusrhacids, such as *Andalgalornis* or *Paraphysornis*, do not show pneumatic openings, their postzygapophyses extend further than the caudal articular surface, and they generally have a bony bridge between the transverse processes and the middle part of the neural arch. Finally, comparison with Palaeogene palaeognaths is difficult since their remains are scarce. Sometimes there are no cervical vertebrae preserved, as is the case with *Remiornis* (Martin, 1992; Smith et al., 2014), and

sometimes they are preserved in two-dimensional slabs, as is the case with *Palaeotis* (Houde and Haubold, 1987; Peters, 1988). Comparison of MPZ 2019/264 with modern palaeoagnaths (e.g., *Struthio*) (Fig. 6.15 F) shows that they share the absence of epipophyses above the postzygapophyses, and have a low, long neural spine (Fig. 6.15 F1, F2), and a caudal articular surface that projects further than the postzygapophyses. On the other hand, palaeoagnaths have more elongated vertebrae, generally without pneumatic foramina, but when present, they are very reduced (Apostolaki et al., 2015).

Even though the affinities of *Gargantuavis* within Ornithuromorpha have been questioned on the basis of the pelvic material (Mayr et al., 2020), MC-MN 478, the vertebra assigned to *Gargantuavis* from Montplo-Nord (Cruzy, France), clearly has avialan features (Buffetaut et al., 2013; 2020). Whether or not the Montplo-Nord vertebra belongs to *Gargantuavis*, there is no doubt of its avialan affinities, but more derived than the avialan vertebra MPZ 2019/264. This suggests that at least two different taxa of large-sized birds inhabited the Ibero-Armorican Island during the Late Cretaceous, although it seems they did not coexist at the same time. Due to the scarceness and fragmentary nature of most of these remains, establishing their phylogenetic position is complicated and, until new fossils are discovered, the degree of kinship between them will remain unknown. Further research should exercise caution in the assignation of new giant bird material from the Late Cretaceous of the Ibero-Armorican Island.

### 6.2.3. *Other vertebrates*

Here are briefly described some additional fossils that expands the stratigraphic range of certain tetrapod groups or suppose the first record of new groups in the record of the Western Tremp Syncline. These fossils come from Barranco Serraduy 4, Larra 4 and Blasi 5 sites (Fig. 6.1)

Superorder DINOSAURIA Owen, 1842

Order SAURISCHIA Seeley, 1887

Infraorder SAUROPODA Marsh, 1878

TITANOSAURIA Bonaparte and Coria, 1993

**Material:** one caudal vertebra (MPZ 2021/1).

**Commentaries:** The caudal vertebra MPZ 2021/1 was found in the Barranco de Serraduy 4 site (Serraduy), situated in the 'Lower Red Garumnian' (Fig. 6.1). It was firstly reported by Cruzado-Caballero et al. (2012). It is situated stratigraphically above the Femur site, making it the youngest evidence of sauropods in the Western Tremp Syncline. MPZ 2021/1 is a slightly deformed centrum from a posterior caudal vertebra, which is elongated craniocaudally and compressed dorsoventrally. It is amphiplatyan, with both articular surfaces flat to slightly concave and with a rounded contour (Fig. 6.16 A and C). In anteroposterior view, the centrum has a subcircular outline (Fig. 6.16 A). Its ventral surface is slightly concave and lacks chevron facets (Fig. 6.16 C). Together with its length and the absence of transverse processes, this indicates that it was situated distally in the caudal series (Díez Díaz et al., 2013). The neural arch is not preserved, but its attachment facets can be observed in the anterior area of the centrum (Fig. 6.16 B), which is a synapomorphy of Titanosauriformes (Salgado et al., 1997). The amphiplatyan condition in the middle and posterior caudal vertebrae is plesiomorphic within Titanosauria (Salgado et al., 1997; Upchurch et al., 2019). Some basal titanosaurs show this condition, as is the case of *Andesaurus* (Calvo and Bonaparte, 1991; Mannion and Calvo, 2011) or the distalmost vertebrae of *Lirainosaurus* (Díez Díaz et al., 2013). Titanosaurian sauropods are the only group of sauropods recorded in the Ibero-Armorican island during the Maastrichtian, reaching the uppermost levels of the upper Maastrichtian (see Chapter 1). Therefore, MPZ 2021/1 is referred as Titanosauria indet.

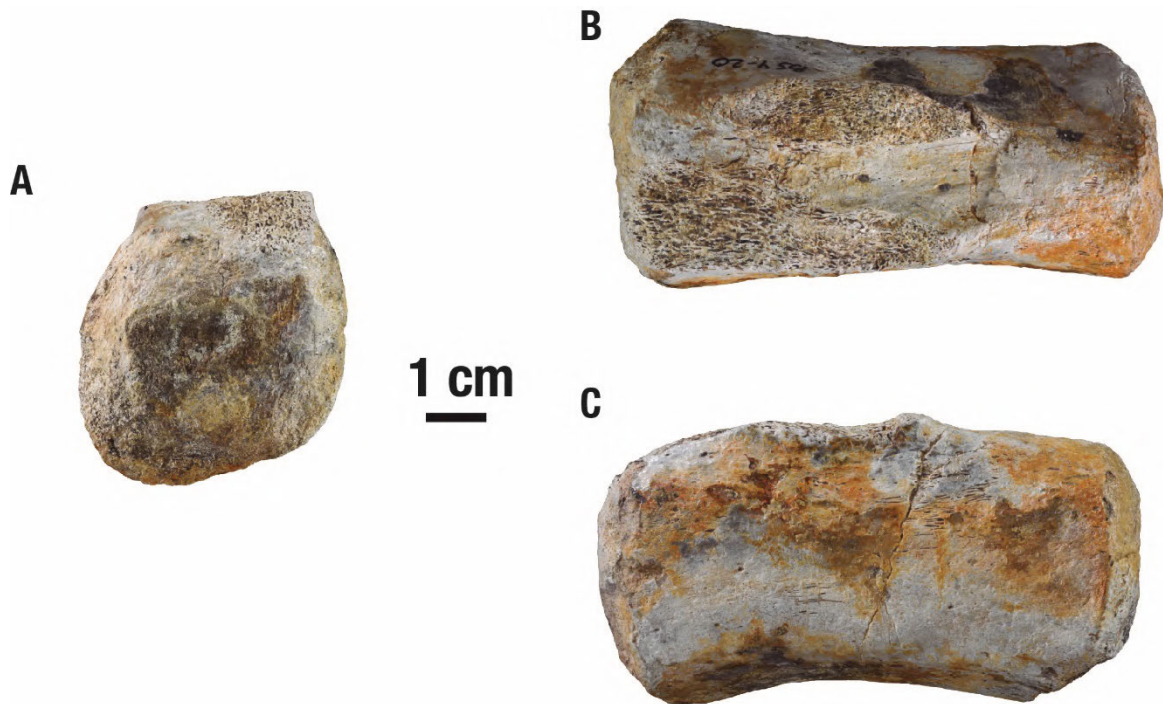


Figure 6.16. MPZ2021/1, posterior caudal vertebra of *Titanosauria indet.* from Barranco Serraduy 4. A) Anterior view. B) Dorsal view. C) Left lateral view.

Suborder THEROPODA Marsh, 1881

MANIRAPTORA Gauthier, 1986

PENNARAPTORA Foth, Tischlinger and Rauhut, 2014

PARAVES Sereno, 1997

**Material:** 1 manual? ungual phalanx (MPZ2019/196).

**Commentaries:** This fossil comes from Larra 4 site (Valle de Lierp) (Fig. 6.1) situated in the 'Lower Red Garumnian'. MPZ 2019/196 is an incomplete left ungual phalanx that lacks part of its dorsal margin and the distalmost tip (Fig. 6.17). It is strongly curved and sickle-shaped (Fig. 6.17 A and C), being also lateromedially compressed (Fig. 6.17 B), pointing to a paravian affinity. The cross-section of MPZ 2019/196 is dorsoventrally elongated, with flattened lateral and medial margins. Its blood grooves are simple and slightly asymmetrical, with the medial one slightly shifted ventrally relative to the lateral one (Fig. 6.17 A, B). The dorsal surface is strongly tapered (Fig. 6.17 D), whereas the ventral one is broad and flat (Fig. 6.17 E). The articular surface is not preserved, causing that the presence of a proximodorsal lip and the projection of the flexor tubercle cannot

be assessed. By its sickle-shape this ungual phalanx might correspond to a manual claw of a paravian theropod or to the modified pedal ungual phalanx II of a dromaeosaurid or a troodontid (Ostrom, 1969; Currie and Peng, 1993; Senter, 2007). Previously, MPZ 2019/196 was described as a pedal ungual phalanx II of an indeterminate dromaeosaurid (Pérez-Pueyo et al., 2019; 2021a), however, the missing state of the articular facet hinders the identification of the ungual as manual or pedal. Nevertheless, the flat shape of the ventral margin suggest that the phalanx might be from the forelimb, by lacking the typical blade-like shape of pedals II (Ostrom 1969; Novas et al., 2005; Longrich and Currie, 2009). The re-evaluation provided here supports the classification of MPZ 2019/196 within Paraves, but the lack of a well-marked asymmetry and the absence of accessory blood grooves excludes its inclusion within Eudromaeosauria (Longrich and Currie, 2009), pointing more to an early-branched dromaeosaurid (Forster et al., 1998; Longrich and Currie, 2009) or a troodontid (Novas and Pol, 2005); or even to a large avialan. MPZ2019/196 show some similarities with the pedal phalanxes of *Pyroraptor*, a dromaeosaur described in the Upper Cretaceous of France (Allain and Taquet, 2000; Santos Brilhante et al., 2022) though MPZ2019/196 seems to be more recurved than *Pyroraptor* and lacks a secondary blood groove.

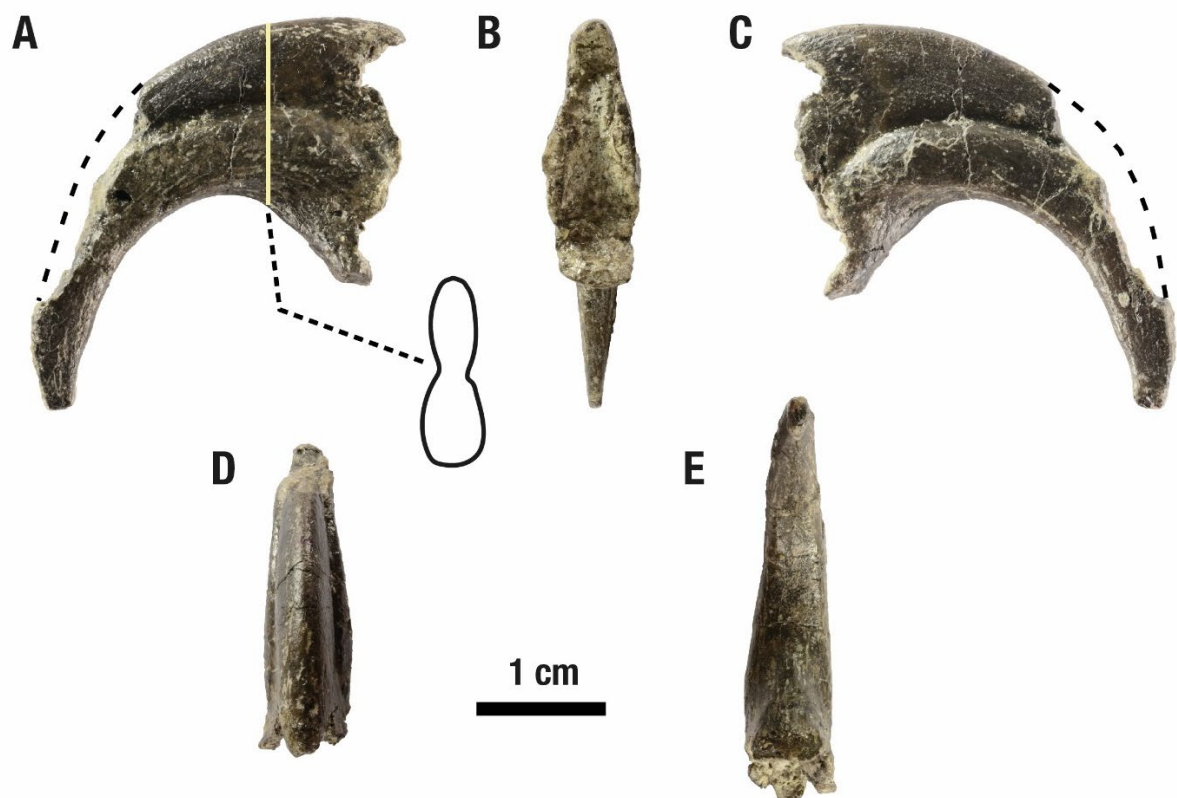


Figure 6.17. MPZ2019/196 ungual pedal phalanx II of an indeterminate paravian from Larra 4. A) Lateral view and section outline. B) Proximal view. C) Medial view. D) Dorsal view. E) Ventral view.

Order PTEROSAURIA Kaup, 1934

Suborder PTERODACTYLOIDEA Plieninger, 1901

Superfamily ORNITHOCHEIROIDEA sensu Kellner, 2003

**Material:** 1 indeterminate long bone (MPZ 2021/54).

**Commentaries:** MPZ 2021/54 is a tiny fragment from a long bone with a subcircular section (Fig. 6.18), which was found in Blasi 5 (Arén). It measures 4.89 cm long and displays a very thin cortex (0.5 mm), being hollow inside, with its medular cavity filled with sediment (Fig. 6. 18 B). These features allow to identify it as a pterosaur bone. The bone narrows towards one of its ends, having around half the diameter than its other end. The assignation is difficult due to the lack of epiphyses, but it might be part of the diaphysis of one of the phalanxes of the wing (digit IV). Only three families of pterosaurs are known during the late Maastrichtian: Pteranodontidae, Nyctosauridae and Azhdarchidae, all belonging to the superfamily Ornithocheiroidea (Longrich et al., 2018), meanwhile in the Ibero-Armorican island only the giant azhdarchids have been identified (Company et al., 1999; Pereda-Suberbiola et al., 2007; Buffetaut, 2008; Dalla Vecchia et al., 2013). Nevertheless, the fragmentary condition of MPZ 2021/54 hinders any further taxonomical inference beyond Ornithocheiroidea.



Figure 6.18. MPZ 2021/54, indeterminate bone of a putative pterosaur from Blasi 5. A) lateral view. B) transverse view

### 6.3. Taphonomic modes of the Tremp Fm

In order to assess the control of the sedimentary setting in the preservation of vertebrate fossils, an analysis on the typology of the fossil sites has been carried out, considering the taphonomic features and their relationship with the sedimentary facies

in which they fossils were preserved. In the study 96 sites were analyzed. Camino Fornons 3 was discarded, as it is a paleobotanical site, without vertebrate remains.

14 sedimentary facies with vertebrate fossils have been recognized, including detritic, carbonated and mixed lithologies:

- Grey mudstones (*Gm*)
- Variegated hydromorphic mudstones (*Vhm*)
- Ochre mudstones-marls (*Om*)
- Dark grey marly mudstones rich in organic matter (*Dgmo*)
- Bioturbated marly/sandy limestones (*Bmsl*)
- Micritic limestones (*Mil*)
- Intraclastic limestones (*Ilm*)
- Wavy fine-grained sandstones (*Wfs*)
- Carbonate sandstones and sandy limestones (*CsSl*)
- Bioclastic sandstones (*Bcs*)
- Foreset cross-bedded sandstones (*Fcs*)
- Cross-bedded sandstones (*Cbs*)
- Coarse-grained bioclastic sandstones with large scale cross-bedding
- Microconglomerates (*Mc*)

On the other hand, inspired in the categories described by Behrensmeyer and Hook (1992) and Erberth et al., (2007), and the approach taken by Csiki et al. (2010b) and Gasca et al. (2017), 5 different taphonomic modes has been recognized (Fig. 6. 19 and 6.20):

- **Isolated bones:** In some lithologies, solitary bones have been found punctually, specially in muddy facies of the 'Lower Red Garumnian'. Those bones are usually more or less complete and are classifiable, though the general rule is they being incomplete or with some type of abrasion or deterioration (Fig. 6.19 A and B). Occasionally in some of these beds, one or two more fossils have been found, because they do not represent the features and genesis of a bonebed. 26 of the studied sites fall within this category.
- **Articulated/associated elements:** This category includes those cases in which two or more elements of the same individual are preserved in the same layer, sometimes keeping their anatomical connection (Fig. 6.19 C and D). These associated or articulated elements can be alone, or accompanied by fossils of other vertebrates,

constituting also bonebed. 7 paleontological sites show this type of preservation, standing out specially Blasi 1 and Blasi 3 in Arén.

- **Macrofossils bonebeds:** They correspond to accumulations of disarticulated bones which belongs to several individuals and to different taxa (Fig. 6.19 E, G, H). Fossils can be broken and partially abraded, but most of them are recognizable. It occurs both in muddy and hard lithologies, having at least 30 sites included in this taphonomic mode.
- **Microfossil bonebeds:** This category encompasses fossil sites conformed by abundant vertebrate fossils, including disarticulated bones and eggshells of different taxa, but the main size of the fossils is under 5 cm. Nevertheless, bigger fossils may appear, but punctually. Only 3 sites of this type have been found and only in muddy lithologies (Fig. 6.19 H).
- **Undifferentiated bonebeds:** in some levels, accumulations of vertebrate bones have been found, but the general preservation they display is so fragmentary that taxonomic assignments are difficult to do. Bones appear broken, abraded and corroded, and with bioerosions, mostly in levels of paleosoils (Fig. 6.19 I). Nevertheless, in some cases, proper identification of some few fossils has been possible. 17 sites correspond to this category.

*Figure 6.19 (next page). Taphonomic modes of the Tremp Fm. A) Isolated bone of an hadrosauroid dinosaur from Barranc del Solá site. B) Isolated pterosaur bone from Barranco Vayart site. C) Almost complete turtle shell from Larra 10 site. D) An articulated section of the tail of an hadrosauroid dinosaur from Camino Rin 3 site. E-G) Several bones recovered from Larra 4 site, including a dromaeosaurid pedal phalanx, a theropod ulna and a plate of a turtle. H) General view of Veracruz 1 site. I) Fragmented bones from Enebro site.*



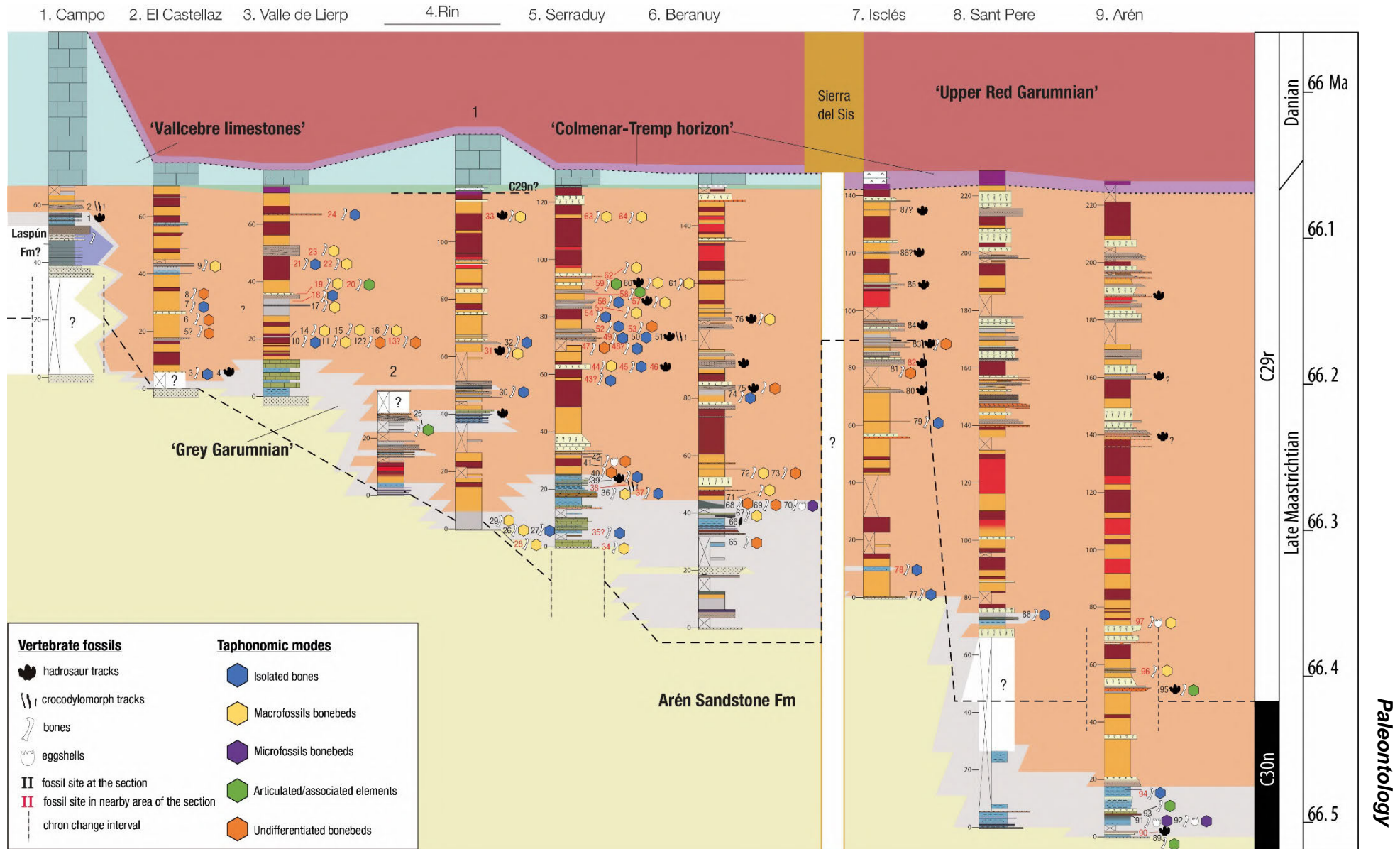


Figure 6.20 (previous page). Taphonomic modes of the paleontological vertebrate fossil sites of the Western Tremp Syncline. The equivalence of the numbers that designate each site is located in Table 6.1.

For the analysis, the population of sites has been divided between bone sites and tracks sites, though some of the bone fossils have been added to the counting of tracks sites, since there are cases in which a site has both bones and tracks (e.g., Pedregal, Fig. 6.20). Thus, 83 sites have been analyzed for bones and 18 for tracks (Table 6. 4)

	Isolated bones	Associated elements	Macrofossil bonebed	Microfossil bonebed	Undifferentiated bonebed	Tracks
Coarse bioclastic sandstones with large scale cross-stratification	1	1	3	-	-	-
Bioclastic sandstones	2	-	-	-	-	1
Bioturbated marly/sandy limestones	1	-	2	-	-	1
Carbonated sandstones and sandy limestones	1	-	2	-	1	-
Cross-bedded sandstones	7	3	10	-	2	13
Dark grey marly mudstones rich in organic matter	2	-	1	3	3	-
Foreset sandstones	-	1	-	-	-	-
Grey mudstones	3	-	2	-	1	-
Intraclastic limestone	-	-	1	-	-	-
Micritic limestones	-	-	-	-	-	1
Microconglomerates	1	1	6	-	-	1
Ochre mudstones	4	1	2	-	6	-
Variegated hydromorphic mudstones	-	-	-	-	1	-
Wavy sandstones	-	-	-	-	-	1
Level not located	4	-	1	-	3	-
	<b>26</b>	<b>7</b>	<b>30</b>	<b>3</b>	<b>17</b>	<b>18</b>

Table 6.4. Distribution of taphonomic modes in the Western Tremp Syncline.

Results show that cross-bedded sandstones (Cbs) have more fossil sites (26% of total) (Fig. 6.21). They are also the facies where vertebrate tracks are more like to be found (72% of the total tracks record) (Fig. 6.22). This indicates that fluvial channels with

tidal influence were the most suitable environment for the preservation of vertebrate fossils.

Regarding taphonomic modes, macrofossil bonebeds and isolated bones are the most common (36% and 31% respectively) (Fig. 6.20), being quite transversal. These preservation modes can be recognized in both lagoonal, perilagoonal and fluvial environments (Fig. 6.21). Macrofossil bonebeds are more usual in energetic facies of the fluvial setting as cross-bedded sandstones (fluvial channels) (*Cbs*), microconglomerates (*Mc*) (flash flood events) or deposits of the barrier-island system (Fig. 6.22). Nevertheless, they can be found sometimes in less energetic facies like ochre mudstones, but that is not usual (Fig. 6.22).

This dominance of energetic facies for the formation of macrofossil bonebeds may be related to the tidal dynamic of the fluvial channels. This would imply a high mobility and reworking of the fossils through the fluvial plain, tending to create accumulations of bones of different taxa. Isolated bones are a taphonomic mode more polyvalent, which appear both in energetic and low energy facies (Fig. 6.22). The double action of tides and fluvial dynamics would facilitate the dispersal of anatomical elements in the different environments, and variations of the energy of the transport processes or the sediment input would facilitate the accumulation of bonebeds or the dispersal of the different anatomical elements (Behrensmeyer, 2007).

Microfossil bonebeds have been only found in the dark grey mudstones rich in organic matter (*Dgmo*) (Fig. 6.22), which would correspond to deposits of small ponds of the perilagoonal fringe. The small ponds would act as collector of small fossils, receiving inputs both from the lagoon and the fluvial system. Their position within this tidal influenced system, between the lagoon and the fluvial facies, would help to the formation of this sites following an attritional model (Rogers and Kidwell, 2007). However, it is important to note that the small amount of microfossil sites identified could be related to a sampling bias. It is difficult to identify this type of sites in the field at first sight, and usually washing and sieving of sediment is needed to locate them. If a thorough sampling of all muddy facies of the Tremp Fm was carried out, probably more microfossil sites would appear.

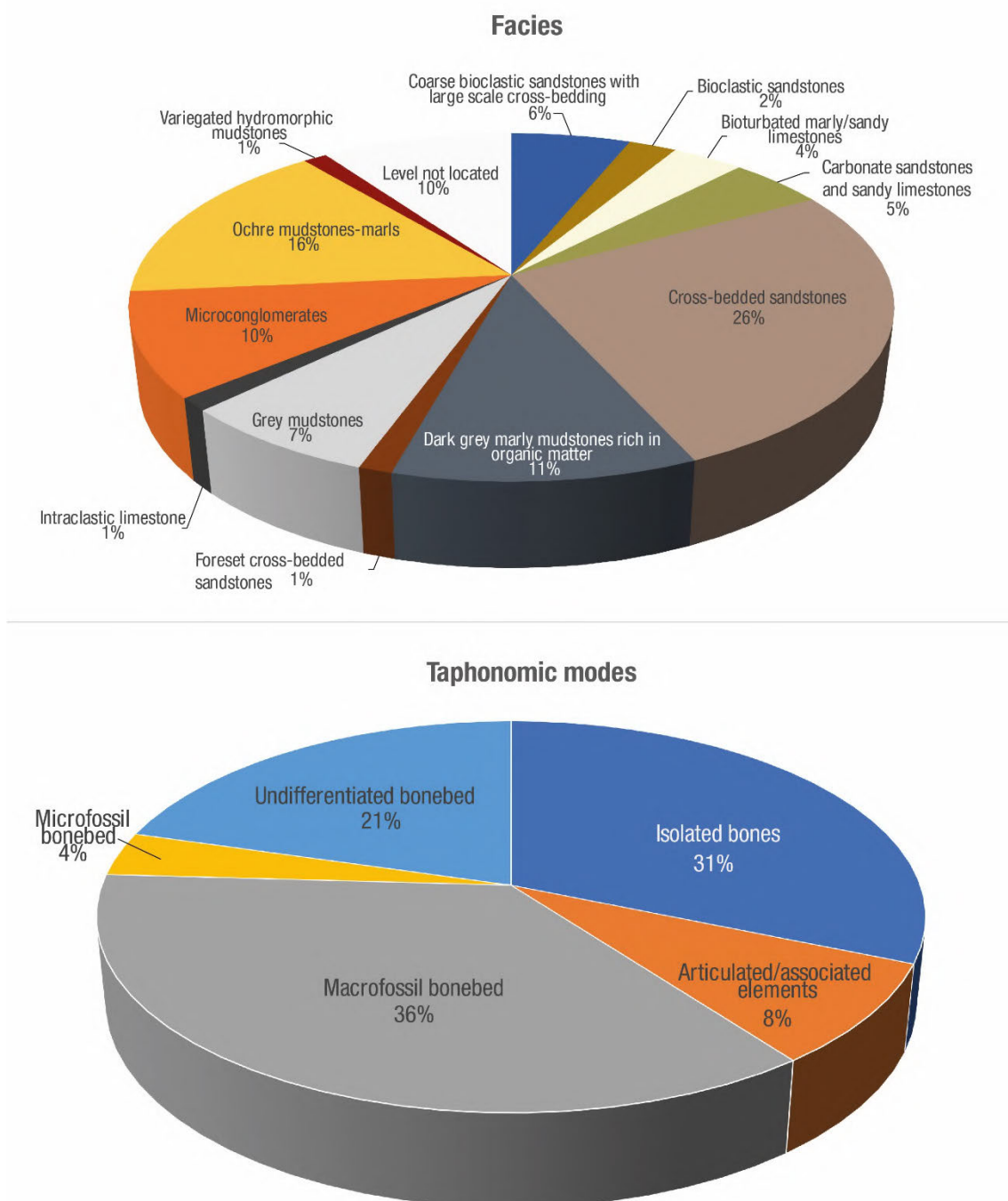


Figure 6.21. Pie charts showing the relative abundance of the fossil sites regarding to in which sedimentary facies appear, and the relative abundance of the different taphonomic modes.

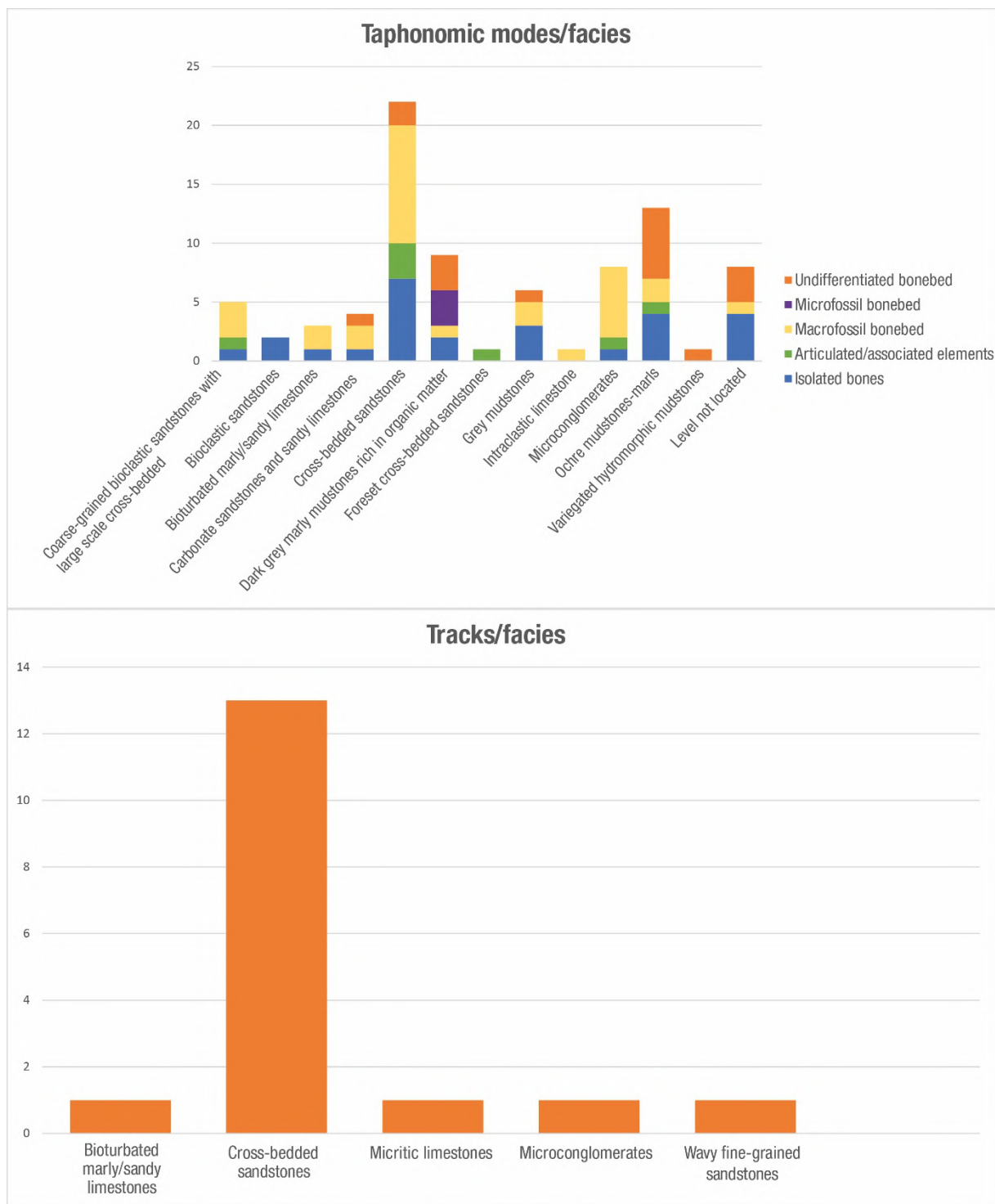


Figure 6.22. Bar charts showing the abundance of the difference taphonomic mode within each facies, and the occurrence of vertebrate tracks within each facies.

Articulated and associated elements constitute the 8% of the sites (Fig. 6.21), being usually found in energetic settings in the perilagoonal and fluvial environments (Fig. 6.22). In some few occasions, they appear in the ochre mudstones-marls facies (*Om*). The preserved elements range from partial skeletons, such as tails of hadrosauroid dinosaurs (Fig. 6.19 D), crocodylomorph skulls, and an almost complete shell of a turtle (Fig. 6.19 C). Some of these elements favor an associated preservation, such as hadrosauroid tails, which usually preserve their vertebrae held together by the action of ossified tendons, or crocodylomorph skulls, which are firmly fused by strong sutures. Nevertheless, a swift burial, such as the storm deposit of Blasi 3, might be necessary for this kind of preservation since long exposure would facilitate the dispersal of the bones by scavenging or by resedimentation. Finally point that a quick burial would not save the bones of the activity of infaunal invertebrates, such is the case of *Arenysaurus* holotype (Cruzado-Caballero et al., 2021).

Undifferentiated bonebeds tend to occur more in muddy facies, especially in ochre (*Om*) and dark grey mudstones rich in organic matter (*Dgmo*) (Fig. 6.22). The bad preservation in fossils found in these sites may be explained due to their high reworking, but also due to the high biological activity of these settings. The facies where this taphonomic mode is usual, display abundant plants and invertebrates bioturbation, being most of them paleosoils horizons. Thus, bones deposited here might be affected by this biological activity, which would increase the degradation of the fossils.

Finally, it is interesting that most dinosaur tracks are preserved as positive hyporeliefs in fluvial sandstones (*Cbs*) (Fig. 6.22). At it has been pointed by other authors (Vila et al., 2013; Gasca et al., 2017), the formation of these casts may be related by the alternation between low water and high water stages, being the tracks recorded in muddy lithologies during low water stages, and later being infilled during high water ones. The only site with negative epireliefs is recorded in perilagoonal facies.

#### **6.4. Final remarks regarding the K/Pg boundary**

At it has been stated, the Tresp Fm in the Western Tresp Syncline has a rich record of Maastrichtian vertebrates. All the main late Maastrichtian groups are preserved in the upper part of the 'Lower Red Garumnian' (Fig. 6.1), very close to the K/Pg boundary. However, this rich record is certainly limited by a series of factors including geological history, rock outcrop area, taphonomy, and study and sampling biases

(Benton et al., 2011; Benton and Pearson, 2001; Brocklehurst et al., 2013; Purnell and Donoghue, 2005), as well as uncertainties in the taxonomic identification of specimens. Such biases strongly influence the measurement of diversity (i.e., taxonomic richness over a given time period).

Geological and rock outcrop area biases of the uppermost Maastrichtian beds are controlled by the following factors: the geological history of the basin, the outcrop area, and the number of exposures. In the Pyrenean region, the Alpine orogeny has had an important impact on the availability of outcrops and localities. Thus, a significant reduction in outcrops occurred due to a series of thrusts that caused a shortening of circa 120 km (Teixell et al., 2016). Second, highly erosive fluvial and glacial valleys, generated during and after the last glaciation, have eroded the Mesozoic formations for thousands of years, further limiting the presence of potential outcrops. The number of exposures (i.e., sedimentary bedrock that is visibly exposed at the surface) is constrained by the Pyrenean climate, which favors a high level of vegetation cover. However, in general terms, the southern Pyrenean regions are less forested than the northern foothills, and this enhances the number of available exposures. Nevertheless, it is a small area if compared with the huge surface of outcrops of other late Maastrichtian fossiliferous formations, such as the Hell Creek Fm (see Fig. 1.4 of Chapter 1).

As regards taphonomic biases, the fragmentary nature of most of the fossil remains found in the Tresp Fm favors major uncertainties in their taxonomical assignation of most of the collected specimens. Consequently, their taxonomic assignment is usually to what is commonly held to be a family rank (e.g., Azhdarchidae, Bothremydidae, Titanosauridae,) or superfamily rank (Hadrosauroidea, Varanoidea). Besides, in the Western Tresp Syncline, the uppermost part of the 'Lower Red Garumnian' is dominated by facies that has poor preservation potential (Fig. 6.1), which limits the information for the closest time to the K/Pg boundary. However, when adequate facies occur in that interval, vertebrate fossils appear (e.g. Altero Negro 1 and sites, Fig. 6.1), which reinforces the idea of a taphonomic bias in the vertebrate fossil record.

With respect to study and sampling biases, the accessibility of sedimentary rock exposures and variations in the efforts of paleontologists in the region are the two main factors affecting the fossil recovery. First, the complex relief of the Western Tresp Basin reduces accessibility to some of the outcrops, hindering the collection of large macroremains or representative amounts of bulk rock for sieving. Sampling efforts made by paleontologists are unequal as well. Indeed, there are microvertebrate fossil

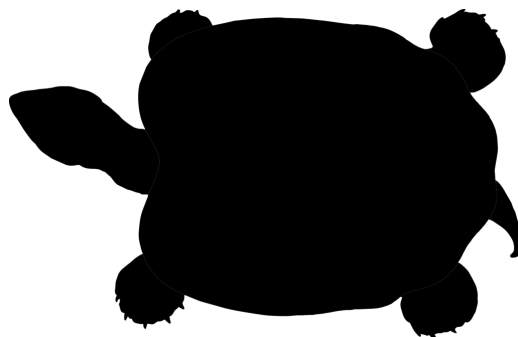
assemblages present in the Maastrichtian outcrops of the Tremp Basin that have not been sampled. One exception is the great effort made by some teams during the 1990s in their pursuit of mammal microfossils (Lopez-Martinez and Pelaez-Campomanes, 1999). This otherwise unsuccessful survey resulted in the discovery of important localities such as Blasi 2 and Fontllonga 6 (Vianey-Liaud and López-Martinez, 1997; Blain et al., 2010). Prospecting efforts are currently being carried out in selected localities, (e.g., Veracruz 1), but an extensive microfossil sampling campaign is lacking. Regarding macrovertebrates, the greater amount of hadrosaur and crocodylomorph fossils, probably because their osteological remains are both more resilient and easier to identify identifiable compared with other vertebrate clades, produced a clear study bias in the faunal diversity of the Tremp Formation. These two clades of vertebrates have been the subject of further studies, probably because their fossils are more informative or better preserved, and thus allow greater taxonomic resolution. By contrast, other groups such as pterosaurs, turtles, sauropods, and theropods have a more fragmentary and less diagnostic fossil record that makes assessment of their abundance more difficult.

By all these reasons, interpreting if there was or not a decline in the diversity of some groups of tetrapods before the K-Pg boundary in the Ibero-Armorican island is difficult. However, during the last years, the discovery of new taxa whose presence was not known in the island, such as the troodontid *Tamarro* (Sellés et al., 2021), the ornithomorph from Beranuy (Pérez-Pueyo et al., 2021c), or the titanosaur *Abditosaurus* (Vila et al., 2022), points that the late Maastrichtian tetrapod ecosystems were in fact more diverse than previously thought. By this reason, it seems plausible to think that diversity was far from declining prior to the extinction, but this would perhaps be a daredevil judgment, since a higher resolution of the Maastrichtian fossil record (in number of specimens and age constraints) is needed to observe differences and clear trends in the diversity evolution.



# **Chapter 7.**

## **Oological record of the Tremp Fm in the Western Tremp Syncline**





## **Chapter 7: Oological record of the Tremp Fm in the Western Tremp Syncline**

The Upper Cretaceous continental deposits of the South-Pyrenean Basin have yielded a rich Maastrichtian record of dinosaur fossil eggs. In this record, fossil eggs associated to titanosaur sauropods stand out, with a great number of clutches, eggs and eggshell fragments belonging to several different ootaxa (Díaz-Molina et al., 2007; Vila et al., 2010; Sellés et al., 2013; Bravo and Gaete, 2015, Marmi et al., 2016) recovered in some areas of the basin, including the Tremp Syncline. Besides eggs and eggshells attributed to theropod dinosaurs (Vianey-Liaud and López-Martínez, 1997; López-Martínez and Vicens, 2012; Sellés et al., 2014b), hadrosauroid ornithopods (Sellés et al., 2014a) and probably ankylosaurs (Sellés and Galobart, 2016)

On the contrary to the eastern areas of the Tremp Syncline, the record of fossil eggs in the Western Tremp Syncline is rather scarce. No clutches nor eggs of titanosaurian sauropod dinosaurs have been found, and the only paleontological site with fossil eggshells found is Blasi 2B (Arén, Huesca) (Fig. 6.1). The oological association recovered from this site was studied preliminary by López-Martínez et al. (1999), who identified up to six types of prismatoolithid eggshells attributable to theropod dinosaurs, and one megaloolithid eggshell type, which was later reidentified as a crocodyloid eggshell referred to the oogenus *Krokolithes* (Moreno-Azanza et al., 2014), attributable to crocodylomorphs.

Part of the work of this Doctoral Thesis consisted in the re-evaluation of the oological assemblage of Blasi 2B site (Pérez-Pueyo et al. 2019). This new analysis of the fossil eggshells of Blasi 2B has allow to identify spheroolithid eggshells (Fig. 7.1). These eggshells have been assigned to the oospecies *Spheroolithus* aff. *europaeus* (Sellés et al., 2014a), described from outcrops nearby Arén, and referable to hadrosauroid ornithopods. Besides, four different types of prismatoolithid eggshells have been recognized, two of them referable to the oogenus *Prismatoolithus*, and the other two to the oogenus *Pseudogeckoolithus* (Fig. 7.2), with a characteristic outer dispersituberculate ornamentation (Fig. 7.2 A) and two structural layers with a squamatic zone (Fig. 7.2 B, C, D). *Pseudogeckoolithus* has been postulated to belong to maniraptoran theropods (Choi et al., 2020). Additionally, two different crocodyloid type eggshells and one testudoid morphotype have been recognized, adding

crocodylomorphs and testudines to the assemblage, though the size of the samples is small, with just some few eggshells per morphotype. This ootaxonomical study of Blasi 2B has been complemented by a taphonomical study of the eggshells, showing different state of conservation depending on the morphotype, pointing to an attritional origin for the eggshell accumulation (Núñez-Lahuerta et al., 2021).

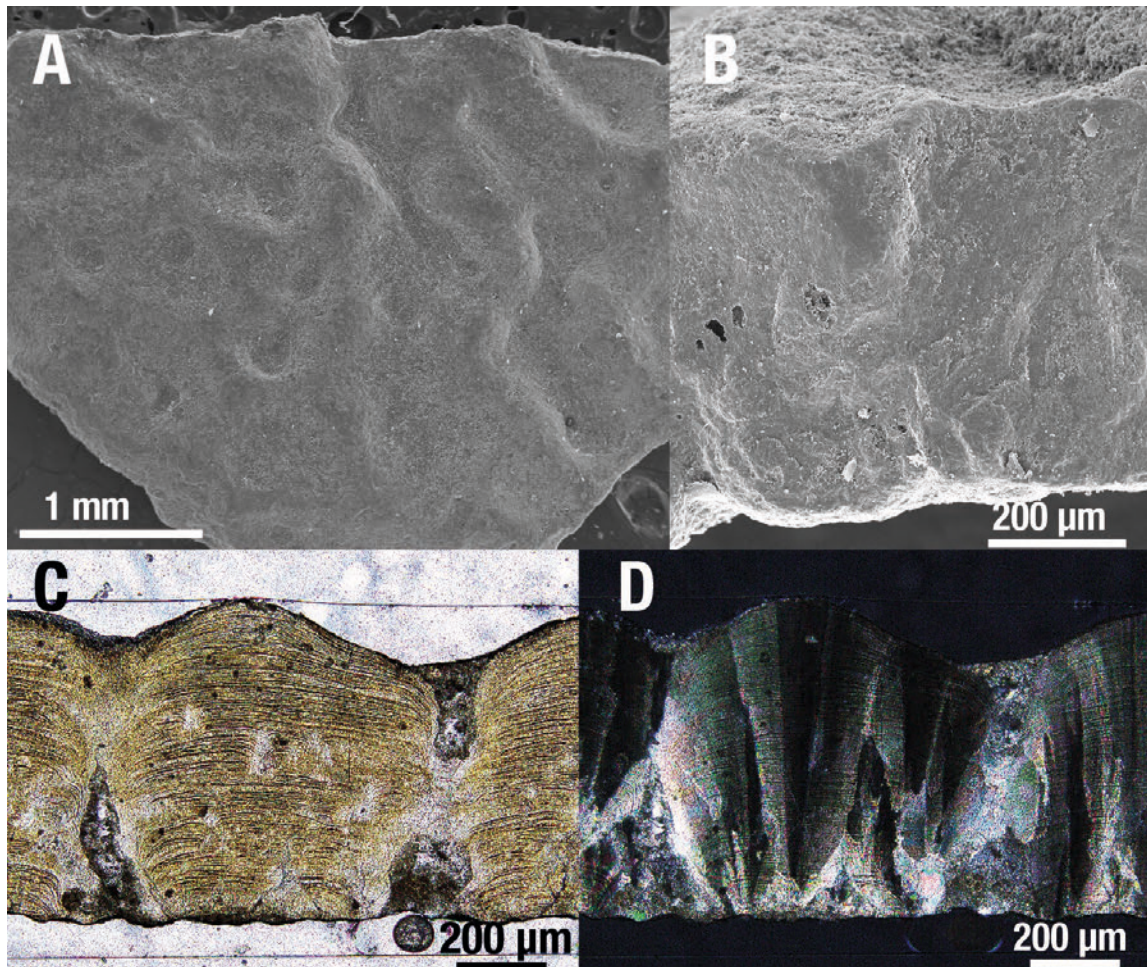


Figure 7.1. *Spheroolithus aff. europaeus* eggshells from Blasi 2B site. A) Outer surface (SEM image). B) Radial section (SEM image). C) Radial thin-section in parallel-polarized light (Petrographic microscope image). D) Radial thin-section in cross-polarized light (Petrographic microscope image).

During the works of this Doctoral Thesis, a new paleontological site with fossil eggshells has been discovered: Veracruz 1 (Fig. 6.1). From this site, the most remarkable finding is a great number (N= 327) of thick and ornamented crocodyloid eggshells, which have allowed to the erection of a new ootaxon: *Pachykrokolithus excavatum* Moreno-Azanza,

Pérez-Pueyo, Puértolas-Pascual, Núñez-Lahuerta, Mateus, Bauluz, Bádenas and Canudo, 2022. *Pachykrokolithus* is one thickest eggshell attributable to crocodylomorphs of the fossil record, and allodaposuchid eusuchians have been pointed as the most probable producers of these eggs. Besides eggshells of theropod dinosaurs, other crocodylomorphs and testudines have been identified, though the oological assemblage has not been described.

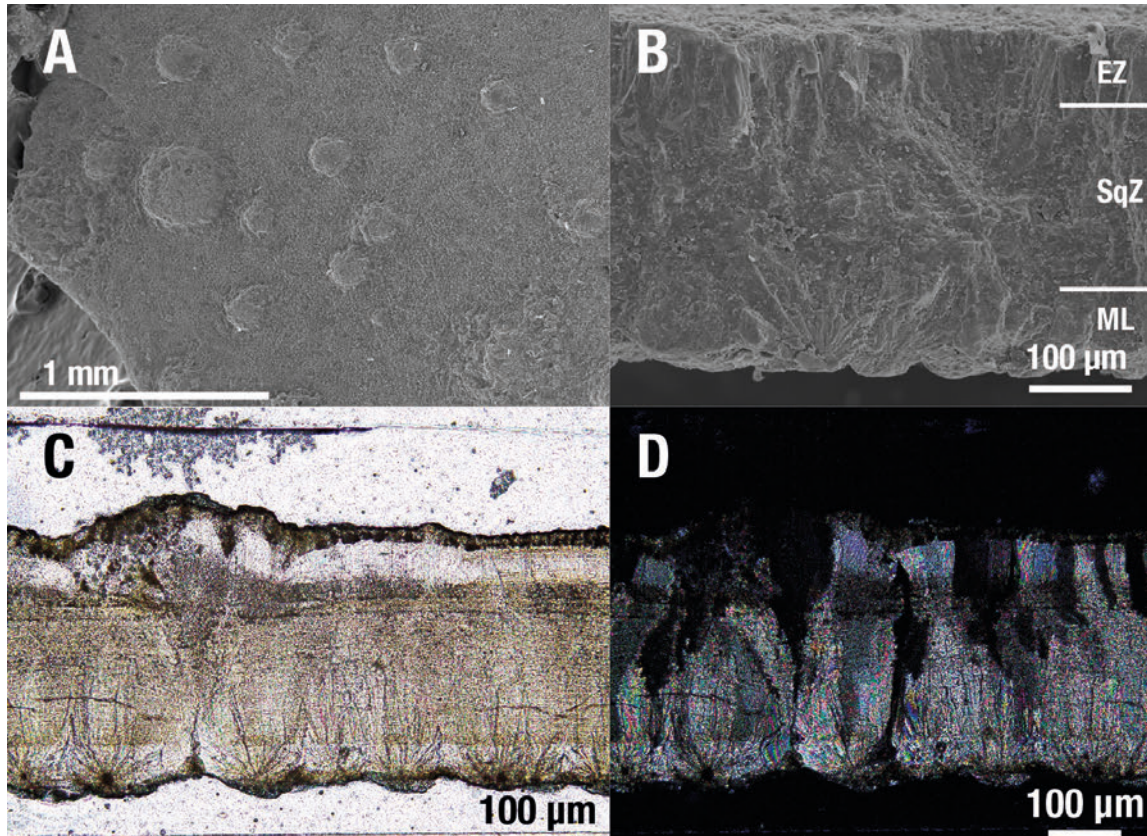


Figure 7.2. *Pseudogeckoolithus* sp. eggshells from Blasi 2B site. A) Outer surface (SEM image). B) Radial section (SEM image). C) Radial thin-section in parallel-polarized light (Petrographic microscope image). D) Radial thin-section in cross-polarized light (Petrographic microscope image). Abbreviations: EZ: external zone, ML: mammillary layer, SqZ: squamatic zone.

These new data is included in the following research articles:

- 1) **Pérez-Pueyo, M.**, Moreno-Azanza, M., Núñez-Lahuerta, C., Puértolas-Pascual, E., Bádenas, B., Canudo, J.I. (2021). Eggshell association of the Late Maastrichtian (Late Cretaceous) at Blasi 2B fossil site: A scrambled of vertebrate diversity. *Ciências da Terra-Procedia*, 1, 58-61.  
<https://doi.org/10.21695/cterraproc.v1i0.410>
- 2) Moreno-Azanza, M., **Pérez-Pueyo, M.**, Puértolas-Pascual, E., Núñez-Lahuerta, C., Mateus, O., Bauluz, B., Bádenas, B., Canudo, J.I. (2022). A new crocodylomorph related ootaxon from the late Maastrichtian of the Southern Pyrenees (Huesca, Spain). *Historical Biology*. Published online on the 21st June 2022 (volume assignation pending).  
<https://doi.org/10.1080/08912963.2022.2098024>



#### Corresponding author:

M. Pérez-Pueyo  
manuppueyo@unizar.es

#### Journal webpage:

<http://cienciasdaterra.novaidfct.pt/>

#### Copyright:

© 2021 M. Pérez-Pueyo *et al.* This is an open access article distributed under the terms and conditions of the [Creative Commons Attribution License \(CC BY\)](https://creativecommons.org/licenses/by/4.0/), which permits unrestricted use, distribution, and reproduction in any medium, provided the original author and source are credited.

ISSN: 0254 - 055X  
eISSN: 2183 - 4431

## Eggshell association of the Late Maastrichtian (Late Cretaceous) at Blasi 2B fossil site: a scrambled of vertebrate diversity

M. Pérez-Pueyo<sup>1</sup>, M. Moreno-Azanza<sup>1,2</sup>, C. Núñez-Lahuerta<sup>1,2</sup>, E. Puértolas-Pascual<sup>1,2</sup>, B. Bádenas<sup>1</sup> & J. I. Canudo<sup>1</sup>

<sup>1</sup> Grupo Aragosaurus-IUCA. Departamento de Ciencias de la Tierra, Facultad de Ciencias, Universidad de Zaragoza. c/Pedro Cerbuna 12, 50009 Zaragoza, Spain.

<sup>2</sup> Departamento de Ciências da Terra, Faculdade de Ciências e Tecnologia FCT, Universidade Nova de Lisboa, 2829-516 Caparica, Portugal.

### Abstract

Upper Cretaceous outcrops of the South-Central Pyrenees in north-eastern Spain show a rich palaeontological record of eggs and eggshells of vertebrates, in particular dinosaurs. The fossil site of Blasi 2B (Arén, Huesca) is added to the oological record of the Late Maastrichtian, with an association of at least five ootypes of dinosaur eggshells (one Spheroolithidae and four Prismatoolithidae), two Krokoolithidae and one Testudoolithidae. Blasi 2B represents one of the most diverse Maastrichtian eggshell sites of the Southern Pyrenees, and remarks the presence of a diverse theropod dinosaur fauna during the Late Maastrichtian in the Ibero-Armorican Island, with at least 4 ootaxa recognised.

**Keywords:** South-Central Pyrenees, Tremp Fm, Chron C30n, Prismatoolithidae, Spheroolithidae.

## 1. Introduction

The Upper Cretaceous outcrops of the South-Central Pyrenees (Tremp Basin, NE Spain) have yielded a rich record of fossil vertebrates, including amphibians, squamates, testudines, crocodylomorphs, pterosaurs and dinosaurs (Canudo *et al.*, 2016). Among dinosaurs, titanosaurid sauropods, rhabdodontids and hadrosaurid ornithopods, nodosaurid ankylosaurians and abelisaurid and maniraptoran theropods have been lately identified (Fondevilla *et al.*, 2019). From this record, eggshells and eggs remains stand out, being the most abundant those attributed to sauropod dinosaurs, represented by complete eggs and clutches (Vianey-Liaud & López-Martínez, 1997; Vila *et al.*, 2010). Besides, there are several sites with eggshells of theropods (Sellés *et al.*, 2014a), hadrosaurid ornithopods (Sellés *et al.*, 2014b) and putative ankylosaurs (Sellés & Galobart, 2016).

In this work, we present a new study about the oodiversity of the palaeontological site of Blasi 2B (referred as Blasi 2 in López-Martínez *et al.*, 2001), located north-western of the town of Arén (Huesca, NE Aragón). Blasi 2B occurs at the base of the informally called 'Grey Unit' of the Tremp Fm, which corresponds

to transitional and lagoonal deposits (Rosell *et al.*, 2001). Based on biostratigraphy (López-Martínez *et al.*, 2001) and magnetostratigraphy (Pereda-Suberbiola *et al.*, 2009), it has been dated as Late Maastrichtian, in particular within the upper part of magnetochron C30n. Blasi 2B corresponds to a 6.5 m-thick level of grey marls, directly overlaying the top of the Arén Fm, and is very rich and diverse in vertebrate microfossils, including bones and eggshells. The oodiversity of Blasi 2B was shallowly identified by López-Martínez *et al.* (1999; 2001), with the exception of Krokolithidae eggshells (Moreno-Azanza *et al.*, 2013). Here, we present preliminary results of the study of the oodiversity and the Blasi 2 site, considering all the new progresses made in the knowledge of palaeoology and palaeoological record of the Southern Pyrenees.

## 2. Material and methodology

Over 2000 eggshell fragments have been recovered in the Blasi 2B site, after sieving over 5 tons of rock previously disaggregated with water and hydrogen peroxide. These eggshell samples were carefully examined under a stereomicroscope, and a subsample of 61 specimens was selected on the

basis of observed differences in eggshell thickness, shell unit shape and outer surface ornamentation. These fragments were photographed with secondary electrons with a JEOL JSM 6400 SEM. Measurements were taken using the software ImageJ. The material from Blasi 2B is housed at the palaeontological collection of the Museo de Ciencias Naturales de la Universidad de Zaragoza.

### 3. Results

We have identified 8 different ootaxa in the Blasi 2B site, including one *Spheroolithidae*, 4 *Prismatoolithidae*, 2 *Krokolithidae* and 1 *Testudoolithidae* eggshells types.

*Spheroolithidae* eggshells have a mean thickness of 572  $\mu\text{m}$  ( $N=4$ ) and their outer surface shows a sagenotuberculate ornamentation (Fig.1A), with anastomosing ridges. In radial section, the shells show a prolatospherulitic morphotype (Fig. 1B), with radial calcitic ultrastructure. Shell units are partially fused towards the outer surface. No pores have been observed in the few thin sections available. We assign them tentatively to the taxon *Spheroolithus* aff. *europaeus* (Sellés *et al.*, 2014b) described in the nearby locality of Porrit-6, which share the morphotype and ornamentation pattern. We prefer to use open nomenclature since the fragments from Blasi 2B are significantly thinner than those of *Spheroolithus europaeus*. However, the few specimens available hinder further discussion.

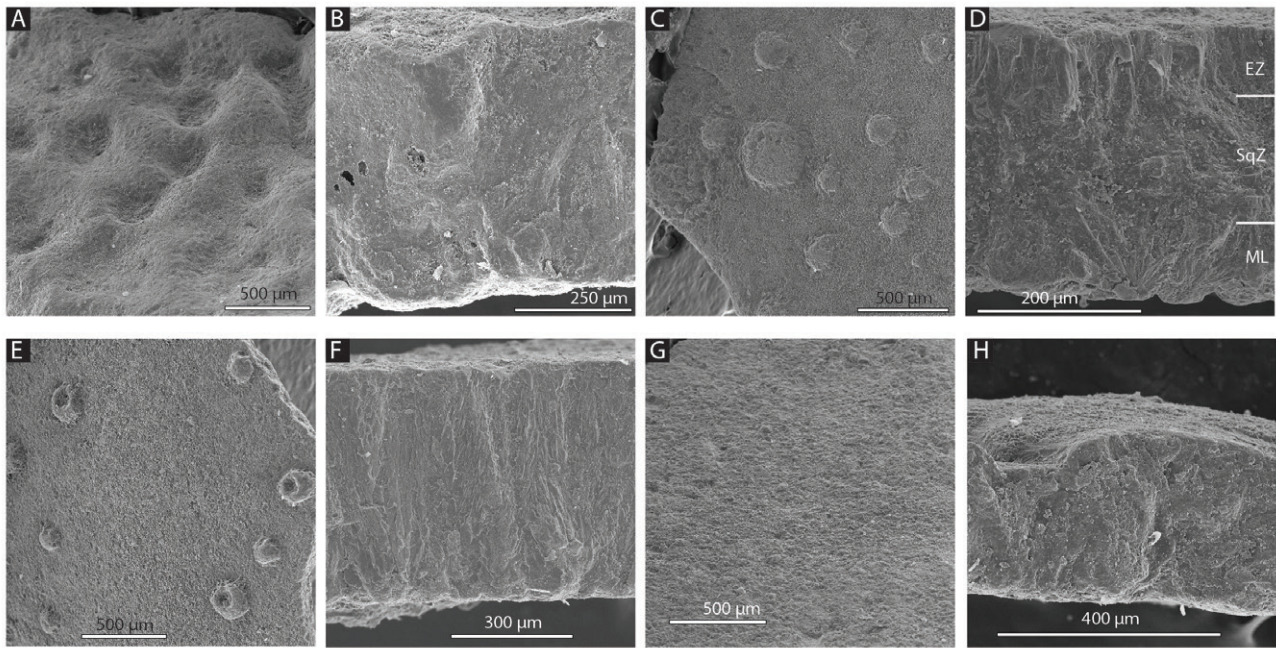
The four prismatoolithic ootypes identified have a prismatic structure, two of them show a distinctive dispersituberculate outer surface ornamentation with isolated domed tubercles (Fig. 1C). In radial section, two layers can be recognised (Fig. 1D): a mamillary layer, and a continuous layer, which can be subdivided in a squamatic zone and an external zone. Based on these features, we have interpreted them as belonging to the genus *Pseudogeckoolithus* (Vianey-Liaud & López-Martínez, 1997), in particular to *Pseudogeckoolithus* oosp. 1, which is thicker (mean 285  $\mu\text{m}$ ,  $N=30$ ), and *Pseudogeckoolithus* oosp. 2, which is thinner (141  $\mu\text{m}$  in average,  $N=2$ ) and sometimes presents cratered tubercles (Fig. 1E). Vianey-Liaud & López-Martínez (1997) did not observe an external zone in *Pseudogeckoolithus*. Nevertheless, this has been recently reported in other *Pseudogeckoolithus* eggshell fragments from several localities of the Upper Cretaceous of Europe (Choi *et al.*, in press).

The other two prismatoolithid eggshells present columnar-shaped shell units composed of mamillary and a continuous layer. No squamatic ultrastructure can be distinguished (Fig. 1F). Both show a smooth outer surface (Fig. 1G). These characters allow us to refer them to the oofamily *Prismatoolithidae*. The poor preservation of the eggshells prevents further comparison, but both can be easily differentiated by their eggshell thickness (*Prismatoolithidae* indet. 1 averages 572  $\mu\text{m}$  ( $N=11$ ) whereas *Prismatoolithidae* indet. 2 averages 276  $\mu\text{m}$  ( $N=9$ ). Several *Prismatoolithidae* ootaxa have been recognized in the Tremp Basin (Sellés *et al.*, 2014a). *Prismatoolithidae* indet 1. and 2 differ from *Ageroolithus* eggshells both in the lack of the ratite morphotype and the squamatic ultrastructure. They also differ from *Sankofa pyrenaica* in lacking the distinct interlocking pattern in the middle part of the continuous layer. Finally, they can be easily differentiated from *Prismatoolithus trempi* by the absence of dispersituberculate ornamentation with flattened nodes.

Besides eggshells referable to dinosaurs, *Krokolithidae* eggshells are also present in the Blasi 2B assemblage. They are characterized by a crocodyloid morphotype, with trapezoidal-shape shell units that broaden towards the outer surface (Fig. 1H). Externally, the eggshells have wavy outer surfaces, with circular depressions. The two ootypes differ in their thickness: *Krokolithes* sp. 1 (370  $\mu\text{m}$ ,  $N=3$ ) and *Krokolithes* sp. 2 (276  $\mu\text{m}$ ,  $N=1$ ). Finally, a single eggshell fragment with testudoid morphotype has been identified. It is badly preserved but can be ascribed to *Testudoolithidae* on the basis of its toughly packaged subcylindrical shell units with radial ultrastructure.

### 4. Discussion and conclusions

Blasi 2B shows a highly diverse assemblage of eggshells, with at least 7 ootaxa. *Spheroolithus* aff. *europaeus* was probably laid by hadrosaurid dinosaurs; whereas the four ootaxa here attributed to *Prismatoolithidae* would correspond to theropod dinosaurs. *Pseudogeckoolithus* eggshells had in the past an uncertain attribution (see Vianey-Liaud & López-Martínez, 1997; Sellés, 2012), but recent research (Choi *et al.*, in press) has postulated that they belong to maniraptoran theropods. The other two prismatoolithid ootaxa are not so well-preserved and their assignation to a particular taxon is difficult, as *Prismatoolithidae*-like eggshells have been identified



**Fig. 1.** -SEM images of the vertebrate eggshells from Blasi 2B site (Huesca, Aragón): A- Outer surface and B- radial section of *Spheroolithus* aff. *europaeus* eggshell; C- Outer surface and D- radial section of *Pseudogeckolithus* sp. 1 eggshell; E- Outer surface of *Pseudogeckolithus* sp. 2 eggshell; F- Radial section G- and outer surface of Prismatoolithidae indet. 1; H- Radial section of *Krokolithes* sp. 2. Abbreviations: EZ: external zone, ML: mammillary layer, SqZ: squamatic zone.

in many theropod groups, including allosauroids, maniraptoran and avian theropods. Furthermore, López-Martínez *et al.*, (1999, 2001), recognised six types of prismatoolithid eggshells in Blasi 2B, based on thin section analysis, three of which are not presented in our sample. Further research is needed to precise the number of putative theropod taxa. Nevertheless, the eggshell record in Blasi 2B points to a high diversity of theropods during the Late Maastrichtian, as reported by previous works (Sellés *et al.*, 2014a). This is concordant with the Theropoda record in the Ibero-Armorican island during the Late Maastrichtian (Torices *et al.*, 2015; Fondevilla *et al.*, 2019), with dromaeosaurids and abelisaurids (cf. *Arcovenator*) recognised specially by dental remains.

Crocodylomorphs are represented in the Southern Pyrenees by four species described and named therein, but according to fossil teeth and other fragmentary cranial remains there would be up to ten taxa (Blanco *et al.*, in press). Although the diversity of clades is wide, basal eusuchians belonging to Allodaposuchidae and Hylaeochampsidae predominate. Within Blasi 2B, teeth from allodaposuchids, aff. *Acynodon* and an indeterminate mesoeucrocodylian have been recovered. However, the assignment of the Blasi 2B eggshells to a concrete genus or family is, for the moment, impossible. It is interesting to note that none of the ootypes match in thickness with *Krokolithes* oosp. eggshells (~0,75 mm) described

by Moreno-Azanza *et al.* (2013), not present in our sample, probably pointing to the presence of three different *Krokolithes* oosps. Further Testudoolithidae eggshells are needed to confirm that their presence is not anecdotal in the Blasi 2B assemblage.

The preliminary analysis of the Blasi 2B eggshell assemblage shows a high eggshell diversity, with between eight and eleven ootaxa. Nevertheless, some of the ootaxa are represented by few specimens, possibly representing an intraoospecific variation that would be detected if the sample size is increased. Even when the oodiversity is underestimated, Blasi 2 is one of the most diverse oological sites of the Maastrichtian of the Tremp Basin.

### Acknowledgments

This research forms part of the project CGL2017-85038-P and is subsidized by the Spanish Ministry of Science and Innovation, the European Regional Development Fund, the Government of Aragón (Grupo Aragosaurus: Recursos geológicos y Paleoambientes) the Fundação para a Ciência e a Tecnologia project PTDC/CTA-PAL/31656/2017 and the GeoBioTec (UIDB/04035/2020). M.P-P is supported by the Spanish Ministry of Education, Culture and Sport (Grant Number FPU 16/03064). M.M-A, C.N-L and E.P-P are supported by the Fundação para a Ciência e a Tecnologia, Portugal (Grant numbers SFRH/BPD/113130/2015, SFRH/BPD/116759/2016, PTDC/CTA-PAL/31656/2017). We are grateful to Xavier Pereda-Suberbiola and Bernat Vila for their valuable comments on the original version of the manuscript. The authors would like to thank the use of the 'Servicio General de Apoyo a la Investigación'-SAI, Universidad de Zaragoza.

## References

- Blanco A., Puértolas-Pascual E., Marmi J., Moncunill-Solé B., Llácer S. & Rössner G. E. (In press) - Late Cretaceous (Maastrichtian) crocodyliforms from north-eastern Iberia: a first attempt to explain the crocodyliform diversity based on tooth qualitative traits. *Zool. J. Linn. Soc-Lond.* zlz106.
- Canudo J.I., Oms O., Vila B., Galobart À., Fondevilla V., Puértolas-Pascual E., Sellés A. G., Cruzado-Caballero P., Dinarès-Turell J., Vicens E., Castanera D., Company J., Burrell L., Estrada R., Marmi J. & Blanco A. (2016) - The upper Maastrichtian dinosaur fossil record from the southern Pyrenees and its contribution to the topic of the Cretaceous–Palaeogene mass extinction event. *Cretac. Res.* 57, 540–551.
- Choi S., Moreno-Azanza M., Csiki-Sava Z., Prondvai E. & Lee Y. (In press) - Comparative crystallography suggests maniraptoran theropod affinities for latest Cretaceous European ‘Geckoid’ eggshell. *Pap. in Palaeontol.* doi.org/10.1002/spp2.1294
- Fondevilla V., Riera V., Vila B., Dinarès-Turell J., Vicens E., Gaete R., Oms O. & Galobart À. (2019) - Chronostratigraphic synthesis of the latest Cretaceous dinosaur turnover in south-western Europe. *Earth-Sci. Rev.* 191, 168–189.
- López-Martínez N., Canudo J. I. & Cuenca G. (1999) - Latest Cretaceous eggshells from Arén (Southern Pyrenees, Spain). In: *First International Symposium on Dinosaur Eggs and Babies*, Isona i Conca Dellà, Spain, 35–36.
- López-Martínez N., Canudo J. I., Ardévol L., Pereda-Suberbiola X., Orue-Etxebarria X., Cuenca-Bescós G., Ruiz-Omeñaca J. I., Murelaga X. & Feist M. (2001) - New dinosaur localities near the Cretaceous/Tertiary boundary (Arén south central Pyrenees, Spain). *Cretac. Res.* 22, 41–61.
- Moreno-Azanza M., Bauluz B., Canudo J. I., Puértolas-Pascual E. & Sellés A. G. (2013) - A re-evaluation of aff. *Megaloolithidae* eggshell fragments from the uppermost Cretaceous of the Pyrenees and implications for crocodylomorph eggshell structure. *Hist. Biol.* 26, 195–205.
- Pereda-Suberbiola X., Canudo J. I., Cruzado-Caballero P., Barco J. L., López-Martínez N. & Ruiz-Omeñaca J. I. (2009) - The last hadrosaurid dinosaurs of Europe: a new lambeosaurine from the uppermost Cretaceous of Arén (Huesca, Spain). *C.R. Palevol* 8, 559–572.
- Rosell J., Linares R. & Llompart C. (2001) - El “Garumniense” prepirenaico. *Revista de la Sociedad Geológica de España* 14, 47–56.
- Sellés A. G. (2012) - *Oological record of dinosaurs in South-Central Pyrenees (SW Europe): Parataxonomy, diversity and biostratigraphical implications*. PhD Thesis, Universitat de Barcelona, 237 p.
- Sellés A. G., Vila B. & Galobart À. (2014a) - Diversity of theropod ootaxa and its implications for the latest Cretaceous dinosaur turnover in southwestern Europe. *Cretac. Res.* 49, 45–54.
- Sellés A. G., Vila B. & Galobart À. (2014b) - *Spheroolithus europaeus*, oosp. nov. (late Maastrichtian, Catalonia), the youngest oological record of hadrosauroids in Eurasia. *J. Vertebr. Paleontol.* 34, 725–729.
- Sellés A. G. & Galobart À. (2016) - Reassessing the endemic European Upper Cretaceous dinosaur egg *Cairanoolithus*. *Hist. Biol.* 28(5), 583–596.
- Torices A., Currie P. J., Canudo J. I. & Pereda-Suberbiola X. (2015) - Theropod dinosaurs from the Upper Cretaceous of the South Pyrenees Basin of Spain. *Acta Palaeontol. Pol.* 60(3), 611–626.
- Vianey-Liaud M. & López-Martínez N. (1997) - Late Cretaceous dinosaur eggshells from the Tremp Basin, southern Pyrenees, Lleida, Spain. *J. Paleontol.* 71, 1157–1171.
- Vila B., Jackson F. D., Fortuny J., Sellés A. G. & Galobart À. (2010) - 3-D modelling of megaloolithid clutches: insights about nest construction and dinosaur behaviour. *PLoS ONE* 5, e10362.

# Historical Biology

An International Journal of Paleobiology



ISSN: (Print) (Online) Journal homepage: <https://www.tandfonline.com/loi/ghbi20>

## A new crocodylomorph related ootaxon from the late Maastrichtian of the Southern Pyrenees (Huesca, Spain)

Miguel Moreno-Azanza, Manuel Pérez-Pueyo, Eduardo Puértolas-Pascual, Carmen Núñez-Lahuerta, Octávio Mateus, Blanca Bauluz, Beatriz Bádenas & José Ignacio Canudo

To cite this article: Miguel Moreno-Azanza, Manuel Pérez-Pueyo, Eduardo Puértolas-Pascual, Carmen Núñez-Lahuerta, Octávio Mateus, Blanca Bauluz, Beatriz Bádenas & José Ignacio Canudo (2022): A new crocodylomorph related ootaxon from the late Maastrichtian of the Southern Pyrenees (Huesca, Spain), Historical Biology, DOI: [10.1080/08912963.2022.2098024](https://doi.org/10.1080/08912963.2022.2098024)

To link to this article: <https://doi.org/10.1080/08912963.2022.2098024>



Published online: 21 Jul 2022.



Submit your article to this journal [↗](#)




View related articles [↗](#)



View Crossmark data [↗](#)



## A new crocodylomorph related ootaxon from the late Maastrichtian of the Southern Pyrenees (Huesca, Spain)

Miguel Moreno-Azanza <sup>a,b,c</sup>, Manuel Pérez-Pueyo <sup>a</sup>, Eduardo Puértolas-Pascual <sup>a,b,c</sup>, Carmen Núñez-Lahuerta <sup>d,e</sup>, Octávio Mateus <sup>b,c</sup>, Blanca Bauluz <sup>a</sup>, Beatriz Bádenas <sup>a</sup> and José Ignacio Canudo <sup>a</sup>

<sup>a</sup>Aragosaurus reconstrucciones paleoambientales-IUCA, Departamento de Ciencias de la Tierra, Universidad de Zaragoza, Zaragoza, Spain; <sup>b</sup>GeoBioTec, Department of Earth Sciences, NOVA School of Sciences and Technology, Universidade NOVA de Lisboa, Campus de Caparica, Caparica, Portugal; <sup>c</sup>Museu da Lourinhã, Lourinhã, Portugal; <sup>d</sup>Història de l'Art, Universitat Rovira i Virgili, AvDepartament d'Història i, Tarragona, Spain; <sup>e</sup>Institut Català de Paleocologia Humana i Evolució Social (IPHES-CERCA), Tarragona, Spain

### ABSTRACT

Crocodylomorph eggs and eggshells are known as old as the Late Jurassic and are frequent components of most multiootaxic eggshell assemblages. Classified within the oofamily Krokolithidae, their histo- and ultrastructures are conservative throughout geological time, characterised by inverted-trapezoid-shaped shell units that grow from highly spaced basal knobs and present a diagnostic tabular ultrastructure. Here, we report 327 eggshell fragments from a new fossil site from the Maastrichtian of the Southern Pyrenees, Veracruz 1, and erect a new oogenus and oospecies, *Pachykrokolithus excavatum* oogen. et oosp. nov. characterised by crocodyloid morphotype and a prominent rugosocavate ornamentation. Eggshells from the slightly older locality of Blasi 2b, previously reported as aff. Krokolithidae, are also assigned to this new ootaxon. Different crocodylomorph taxa coexisted during the Late Cretaceous of the Tremp Basin, hindering the attribution of *Pachykrokolithus excavatum* oogen. et oosp. nov. to a single clade. Nevertheless, allodaposuchid eusuchians were dominant in this ecosystem, and are the most probable producers of *Pachykrokolithus excavatum* oogen. et oosp. nov. eggs.

### ARTICLE HISTORY

Received 26 May 2022  
Accepted 29 June 2022

### KEYWORDS

Crocodylomorpha;  
Krokolithidae; eggshell  
fragments; Tremp Basin; Late  
Cretaceous

### Introduction

Fossil crocodylomorphs are important components of most Mesozoic continental faunal assemblages, being significantly more diverse and disparate than their current representatives (Felice et al. 2021 and references within). Nevertheless, crocodylomorph eggs and eggshells are relatively scarce in the fossil record, especially when compared with dinosaurs (Carpenter and Alf 1994). Despite the osteological record of the clade Crocodylomorpha dates back to the Carnian, Late Triassic (Irmis et al. 2013), the oldest crocodylomorph eggshells known are almost 80 My younger, dating from the Kimmeridgian-Tithonian, Late Jurassic (Russo et al. 2017). First crocodylomorph eggshells had ultrastructure and histostructure very similar to that of their modern relatives, which remarkably remained constant through fossil record with few exceptions – e.g. *Mycomorphoolithus kohringii* Moreno-Azanza, Gasca and Canudo 2015, an eggshell with uncertain ootaxonomic affinities that has been postulated to be crocodylomorph related based on the extinction pattern observed in its shell units. These conservative features are as follows: (1) calcite composition; (2) tabular ‘book-like’ ultrastructure, with remarkable horizontal cleavage of the calcite crystals; (3) subtriangular shell units; presence of basal knobs – subspherical microcrystalline agglomerates at the base of the shell units – that clearly differ from the eisospherites observed in other amniotes; and (4) shell units comprised by very few large crystals that comprise all the eggshell thickness, and laterally expand towards the external surface, showing blocky extinction pattern under cross-polarised light (Hirsch 1985; Mikhailov 1991, 1997; Kohring and Hirsch 1996; Moreno-Azanza et al. 2014).

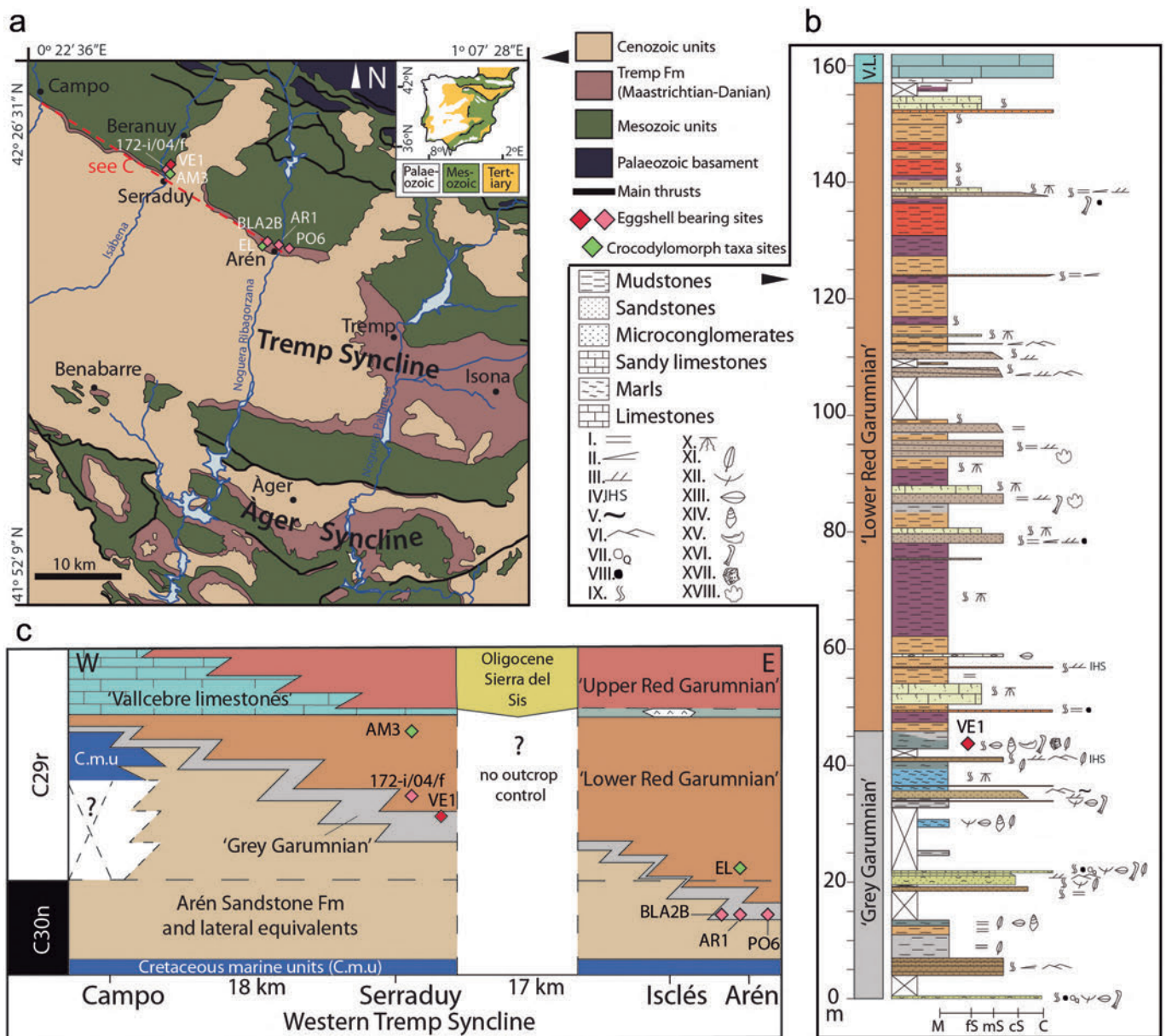
The fossil record of Crocodylomorpha from the Tremp Formation (Southern Pyrenees, Spain) is rich and diverse and comprises both osteological and oological fossils (Pérez-Pueyo et al. 2021). Concerning the osteological record, five major clades have been recognised: Allodaposuchidae, Hylaeochampsidae, Crocodylia, Atoposauridae and Sebecosuchia (Puértolas-Pascual et al. 2016; Blanco et al. 2020; Sellés et al. 2020). The fossil record of Eusuchia (clade that includes all extant crocodylians and several extinct clades) recovered within the Tremp Basin corresponds to: postcranial bones, isolated teeth, cranial fragments and several skulls of allodaposuchids; isolated teeth and a mandible of hylaeochampsids; and few isolated teeth tentatively assigned to Crocodylia (Puértolas et al. 2011; Blanco et al. 2014, 2015, 2020; Puértolas-Pascual et al. 2014; Puértolas-Pascual 2016). Besides Eusuchia, only isolated teeth of atoposaurids, and scarce isolated teeth and a partial skeleton assigned to sebecosuchians have been recovered within the basin (Puértolas-Pascual et al. 2016; Blanco et al. 2020; Sellés et al. 2020).

Concerning the oological record of Crocodylomorpha, Moreno-Azanza et al. (2014) described 13 eggshell fragments collected from the Blasi 2b microfossil site from the upper Maastrichtian part of the Tremp Formation. These eggshells were previously interpreted as presenting dinosaur spherulithic morphotype and attributed to aff. Megaloolithidae (López-Martínez et al. 1999; López Martínez 2003). However, Moreno-Azanza et al. (2014) reassigned them to Krokolithidae indet., based on a detailed analysis of their histo- and ultrastructure that revealed the presence of tabular ultrastructure, blocky extinction patterns and absence of true eisospherites. Due to the small sample size, these authors refrained to erect new ootaxa.

In this work, we describe hundreds of eggshells collected from the Maastrichtian part of the Tremp Formation, from the Veracruz 1 (VE1) fossil site. These eggshells are attributable to the oofamily Krokolithidae, and indistinguishable from the aff. Krokolithidae from Blasi 2b (BLA2B), although better preserved. This wider sample allows us to erect a new oogenus and oospecies of the oofamily Krokolithidae to include the eggshells from both localities, and compare them other Krokolithidae ootaxa and with *Stromatoolithus* (*Spheroolithus*) *europaeus*, a dinosaur ootaxon that is found in the same outcrops which, despite being ultrastructurally very different, can be easily misidentified in hand sample.

## Geographical and geological setting

The fossil eggshells studied mostly come from the Veracruz 1 site, and in minor number, from Blasi 2b. Two additional eggshell fragments were also collected from 172-i/04/f site, and from a level close to the Areny 1. All these palaeontological sites were found in the Upper Cretaceous continental outcrops of the Southern Pyrenees (Ribargorza county, Huesca, NE Spain; Figure 1a): Veracruz 1 site is close to the town of Biascas de Obarra (municipality of Beranuy), 172-i/04/f is located near the town of Serraduy (municipality of Isábena) and Blasi 2b and Areny 1 lay within the municipality of Arén.



**Figure 1.** Geographic and geological context of the palaeontological sites with crocodylomorph sites of the Southern Pyrenees. a. Geological map of the Southern Pyrenees, focused on the Tremp Syncline and its Upper Cretaceous-Palaeogene outcrops (modified from López-Martínez and Vicens, 2012). b. Stratigraphic log of the upper Maastrichtian Tremp Formation from the Beranuy outcrops. Colour of rocks are indicated. Key: I. Parallel lamination II. Low-angle cross-bedding III. Planar cross-bedding. IV. Inclined heterolithic cross-bedding V. Flaser, wavy and lenticular bedding VI. Ripples VII. Quartz pebbles VIII. Mud pebbles IX. Bioturbation X. Root marks-mottling XI. Plant remains XII. Undifferentiated bioclasts XIII. Bivalves XIV. Gastropods XV. Decapods XVI. Vertebrate bones XVII. Eggshells XVIII. Dinosaur tracks. c. Chronostratigraphic framework of the Western Tremp Syncline (magnetostratigraphic data after Pereda-Suberbiola et al. (2009); Canudo et al. (2016); Puértolas-Pascual et al. (2018), with the stratigraphic position of the sites studied in this paper. AM3: Amor 3: type locality of *Agaresuchus subjuniperus*, AR1: Areny-1, BLA2B: Blasi 2B, EL: Elias: type locality of *Arenysuchus gascabadiolorum* PO6: Porrit-6, VE1: Veracruz 1. (Lopez-Martínez 2012)

In the Southern Pyrenees, there are a series of sedimentary domains developed during the Late Cretaceous to the Palaeogene filled with marine to continental sediments (Muñoz 1992; Teixell 2004; Costa et al. 2010; Fondevilla et al. 2016), and all together conform the South-Pyrenean Basin. The materials described here come from the so-called Tremp Basin, whose sedimentary record widely crops out in the Tremp Syncline (Figure 1a). The sedimentary unit including the fossil sites studied correspond to the Tremp Formation (Mey et al. 1968). It is a Maastrichtian-Palaeocene transitional to continental unit, with an important record of Maastrichtian vertebrate fossils, including dinosaurs, pterosaurs, crocodylomorphs, testudines, squamates, amphibians and fishes, representing some of the last Mesozoic biological communities of vertebrates prior the K/Pg extinction event, being one of the few assemblages preserved in Europe for this age (Puértolas-Pascual 2016; Vila et al. 2016; Puértolas-Pascual et al. 2018; Fondevilla et al. 2019; Pérez-Pueyo et al. 2021). According to the stratigraphical proposal of Rosell et al. (2001), the Tremp Formation can be divided into four informal units, with the two lower units dated as Maastrichtian. These lower units are the 'Grey Garumnian', formed by mudstones, sandstones and limestones deposited in transitional and lagoonal environments (Eichenseer 1988; Riera et al. 2009; Oms et al. 2016), and the overlaying 'Lower Red Garumnian', dominated by multicoloured mudstones and intercalations of sandstones, representing fluvial and alluvial deposits with certain marine influence (Riera et al. 2009; Díez-Canseco et al. 2014).

Veracruz 1 fossil site is situated in the upper part of the 'Grey Garumnian' (Figure 1b, c). The eggshells appear in a 6.7–7 m-thick level of bioturbated grey marly mudstones with charcoal fragments, invertebrate shells – molluscs and crustaceans –, vertebrate bones, and eggshells which are more abundant at the top of the level. Several vertebrate clades have been identified, including osteichthyans, testudines, crocodylomorphs, hadrosaurid dinosaurs (Pérez-Pueyo et al. 2019) and, more recently, amphibians and theropod dinosaurs (Pérez-Pueyo 2022, obs. pers.). The 172-i/04/f fossil site is situated in the lower part of the 'Lower Red Garumnian' (Figure 1c), not so far from Veracruz 1. This site has produced isolated bones of Hadrosauridae indet. and abundant crustacean fingers. A single eggshell fragment was recovered. Both sites have been dated within the magnetochron C29r (Puértolas-Pascual et al. 2018) (Figure 1c), thus laying within the last 400 kyr of the Maastrichtian.

Blasi 2b is situated in the lower part of the 'Grey Garumnian' (Figure 1c) and has yielded abundant eggshell fragments (López-Martínez et al. 1999; López-Martínez 2003; Moreno-Azanza et al. 2014) and numerous microvertebrate remains assigned to dinosaurs (López-Martínez et al. 2001; Torices et al. 2004; Pereda-Suberbiola et al. 2009; Cruzado-Caballero et al. 2013), crocodylomorphs (López-Martínez et al. 2001; Blanco et al. 2020); testudines (López-Martínez et al. 2001; Murelaga and Canudo 2005); amphibians, squamates (López-Martínez et al. 2001; Blain et al. 2010) and fishes (López-Martínez et al. 2001). One eggshell with crocodylomorph affinity was found in the 'Grey Garumnian' above the fossil tracksite of Areny 1 (Barco et al. 2001), in a similar stratigraphic position to Blasi 2b (Figure 1c). Both sites (Blasi 2b and Areny 1) have been dated as late Maastrichtian (top of chron C30n; Figure 1c), by means of magnetostratigraphy (Pereda-Suberbiola et al. 2009).

## Material and methods

Veracruz-1 site has yielded several hundreds of eggshell fragments, among other macro- and microfossils remains. Among these, 317 eggshells are included in this study, most of them big enough to be

observed at naked eye and be picked up in situ during field surveys. No complete eggs have been recovered. Additionally, smaller fragments were recovered during microfossil sorting. Bulk rock samples were dried at room temperature and soaked in water with 5–10% hydrogen peroxide for ~24 h. The resulting sediment was screen washed using 2-, 1- and 0.5-mm sieves.

All 317 eggshell fragments were measured using a digital caliper, of which 25 were cleaned with an ultrasound bath for 15 min, dried and mounted and gold-coated for secondary electron imaging in a JEOL 3600 Scanning Electron Microscope housed at Servicios de Apoyo a la Investigación (SAI) of the University of Zaragoza. Six additional fragments were embedded in epoxy resin and cut into 20 µm thick thin sections, as standard 30 µm thin sections where too thick to observe certain crystallographic features of the eggshell. Thin section observations were performed with an Olympus BX53M petrographic microscope equipped with an Olympus DP27 digital camera, housed in the 'Instituto Universitario de Ciencias Ambientales' (IUCA) of the University of Zaragoza. All specimens were collected with permission under the regional and national Cultural Heritage law and are currently housed in the Museo de Ciencias Naturales de la Universidad de Zaragoza (Canudo 2018). The new names published here are nomenclaturally available according to the requirements of the amended International Code of Zoological Nomenclature, including registration of the work in ZooBank (<http://zoobank.org>) with the following Life Science Identifier: urn:lsid:zoobank.org:pub:BA86B702-A1BB-4D7F-AF60-94E92A9E7207

Nomenclature follows Hirsch (1985) and Moreno-Azanza et al. (2014).

### Systematic palaeontology

#### Oofamily Krokolithidae Kohring and Hirsch 1996

#### Oogenus *Pachykrokolithus* oogen. nov.

urn:lsid:zoobank.org:act:70871E72-2C84-4347-8F8E-5C50F5B3E460

## Diagnosis

as for the type and only oospecies

## Etymology

Combined from the ancient Greek terms: 'pachy' (meaning thick), 'krokos' (from the combining form for the krokódilos meaning lizard), 'oo' (from the combining form for ova, meaning egg) and 'lithos' (meaning stone).

Oospecies *Pachykrokolithus excavatum* oogen. et oosp. nov.

urn:lsid:zoobank.org:act:503DE743-CE5C-4102-9A63-DEEEC34A5C9A

## Etymology

From Latin 'excavatum' = excavated, in reference to the prominent rugosocavate outer surface.

## Type material

Holotype, a single eggshell fragment (MPZ 2022/268), gold coated for SEM. Paratype: 26 eggshell fragments gold coated, prepared for SEM (MPZ 2022/252 to MPZ 2022/277); 6 eggshell fragments prepared as thin sections (MPZ 2022/278 to MPZ 2022/283); and 284 unprepared eggshell fragments (MPZ 2022/286 to MPZ 2022/569).

## Type locality and horizon

Veracruz 1 site, Bascas de Obarra, Ribagorza county (Huesca province, Spain). Tremp Formation, uppermost Maastrichtian (chron C29r).

### Stratigraphy and geographical range

Lower Red Garumnian and Grey Garumnian units of Tremp Formation, Upper Maastrichtian, Ribagorza county (Huesca, NE Spain). Additional sites, other than the type locality, include Blasi 2b site and an unnamed fossiliferous bed near Areny 1 site (top C30n), and 127-i/04/f (C29r).

### Material

In addition to the type material, 13 eggshell fragments (MPZ 2013/20 to MPZ 2013/31) from the Blasi 2b locality, previously described by Moreno-Azanza et al. (2014); One eggshell fragment from 127-i/04/e (MPZ 2022/284); and one eggshell fragment found near Areny 1 site (MPZ 2022/285).

#### Synonymia

Dinosauroid-spherulitic type eggshell; López-Martínez et al. 1999, pp. 35–36.

Aff. Megaloolithidae; López-Martínez 2003, p. 136, pl. 1

Krokolithidae indet; Moreno-Azanza et al. 2014, p. 197, (Figures 2, 3).

*Spheroolithus* aff. *europaeus*; Pérez-Pueyo, Gilabert, Moreno-Azanza, Puértolas-Pascual, Bádenas, Canudo 2019, p. 111

### Diagnosis

Thick Krokolithidae eggshells (Mean thickness 814  $\mu\text{m}$ , range 500–1100  $\mu\text{m}$ ), combining prominent rugosocavated ornamentation in the external surface and shell units packed together in the two outer thirds of the eggshell, with small pyramidal interstices between shell units in the inner third.

Figures 2, 4c–d

### Description

Thick Krokolithidae eggshells with a mean thickness of 814  $\mu\text{m}$  –  $N = 317$ ,  $SD = 0.08$ , range 500–1100  $\mu\text{m}$ ; Figure 2a–d. Eggshell units are taller than wider with width to height ratios ranging from 0.5 to 0.8, although some shell units can be as wide as tall. They are trapezoidal in shape, and are tightly packed (Figure 2d), but for the inner third of the eggshell, where small pyramidal interstices are present between shell units – interstices being smaller than in other Krokolithidae eggshells. Occasionally there are some smaller shell units compressed between larger ones, partially filling these interstices.

The eggshell has three different layers: inner, middle and outer (Figure 2a): (1) The inner layer is comprised of microcrystalline basal knobs, which at high magnification has an irregular crystal arrangement (Figure 2a), forming an irregular rosette-like arrangement of the basal plate and showing some vesiculation. These basal knobs act as nucleation centres for the shell units and are loosely spaced throughout the inner surface of the eggshell; (2) The middle layer is more compact than the inner layer and has the characteristic book-like tabular ultrastructure of the crocodylomorph eggshell (Figure 2a). Vesicles are very scarce (Figure 2a), and the massiveness of this layer results in some fragments showing conchoidal fractures when broken and prepared for examination; (3) The outer layer is also thick, representing more than half of the eggshell, and it is formed by large wedges with a marked cleavage following three directions, one parallel to the eggshell surface and two of them oblique to the eggshell surface (Figure 2a). Vesicles are much more abundant in this layer. Some fragments have a fibrous ultrastructure, resulting from the abundant vesicles being aligned by the cleavage (Moreno-Azanza et al. 2014) (Figure 2a).

Pore channels are straight, very wide and funnel shaped (Figure 2b), increasing their diameter towards the external and internal surfaces of the eggshell (Figure 2e). They appear between

shell units, and open to the interstices of the inner part of the eggshell, which are interconnected in a secondary horizontal pore system, as in other crocodylomorph eggshells.

In thin section, shell unit boundaries are clearly distinguished throughout most of the eggshell thickness, although some degree of fusion hinders their limits at the outer layer (Figure 2c). Brownish-yellowish organic matter is present on the inner layer, the upper half of the middle layer and in the outer layer, whereas the lower half of the middle layer is white (Figure 2c). Sinuous growth lines are present in the outer layer, parallel to the undulating outer surface (arrow in Figure 2c). In cross-polarised light, the characteristic blocky extinction of the crocodylomorph eggshell can be observed (Figure 2d). Each shell unit is formed by at least three extinction domains, shaped as irregular wedges, which comprise both the middle and outer layers of the eggshell. The microcrystalline nature of the basal knobs agrees with the lack of extinction pattern.

The external surface shows prominent rugosocavate ornamentation (sensu Marzola et al. 2015) (Figure 2e, f). The surface is undulant, with bulges and depressions, which are subcircular to elliptical, and sometimes coalesce. The pore openings are subcircular and locate inside of some of these depressions. The general aspect of the surface ornamentation is thus similar to that observed in *Paleosuchus palpebrosus* eggshells (Marzola et al. 2015) but much more marked. Some circular dissolution pits can be observed (Figure 2e).

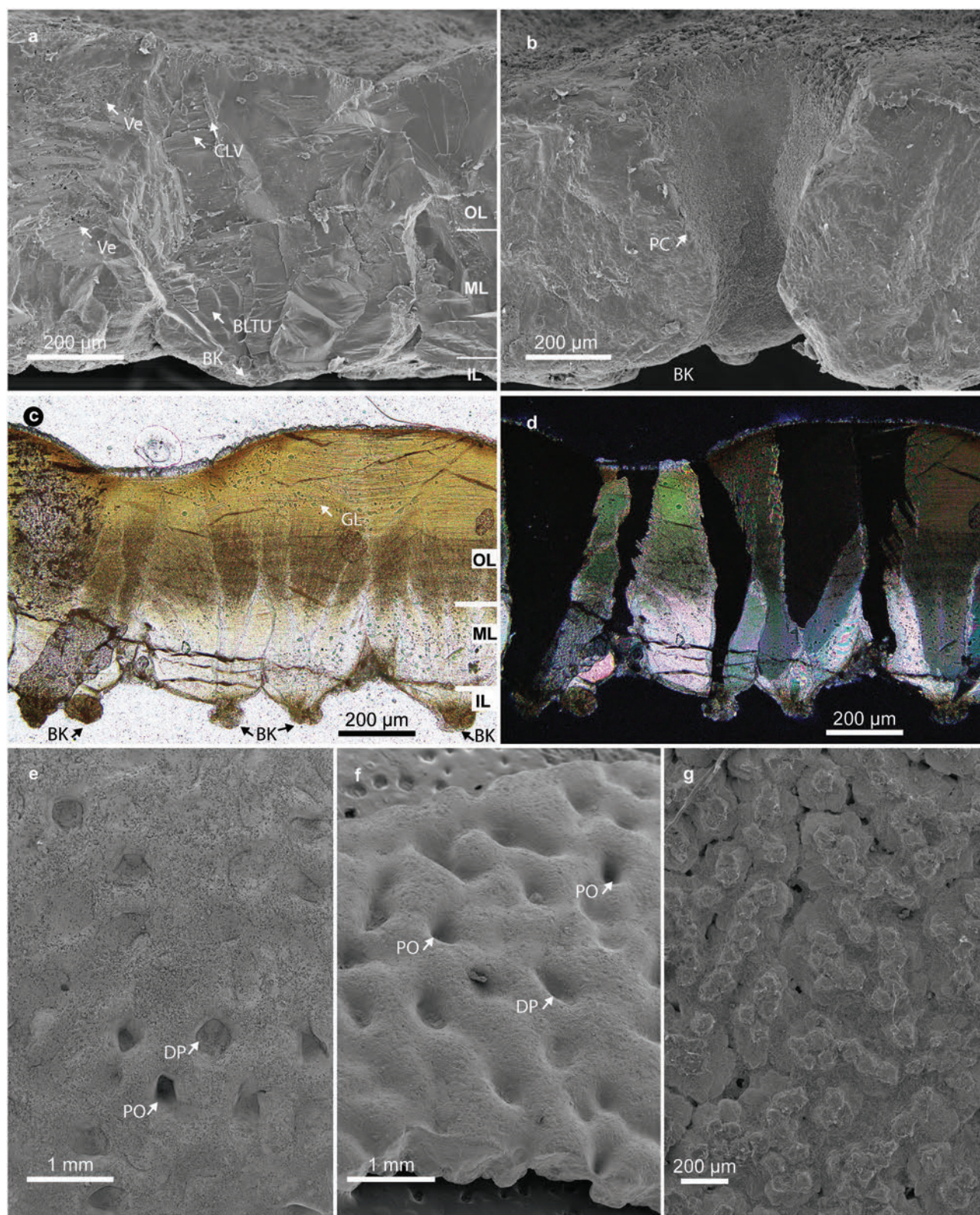
The inner surfaces have bulbous, irregular basal plate groups (Figure 2g). They are randomly spaced, originating shell units of different sizes, depending on the available space between adjacent units. The contact between shell units is distinct and straight, with somewhat zigzagging profiles, giving the shell units a polygonal contour in inner view. Irregular polygonal gaps, somewhat elongated, locate in the junction points between three and five shell units, causing the secondary horizontal pore system (Figure 2g).

### Discussion

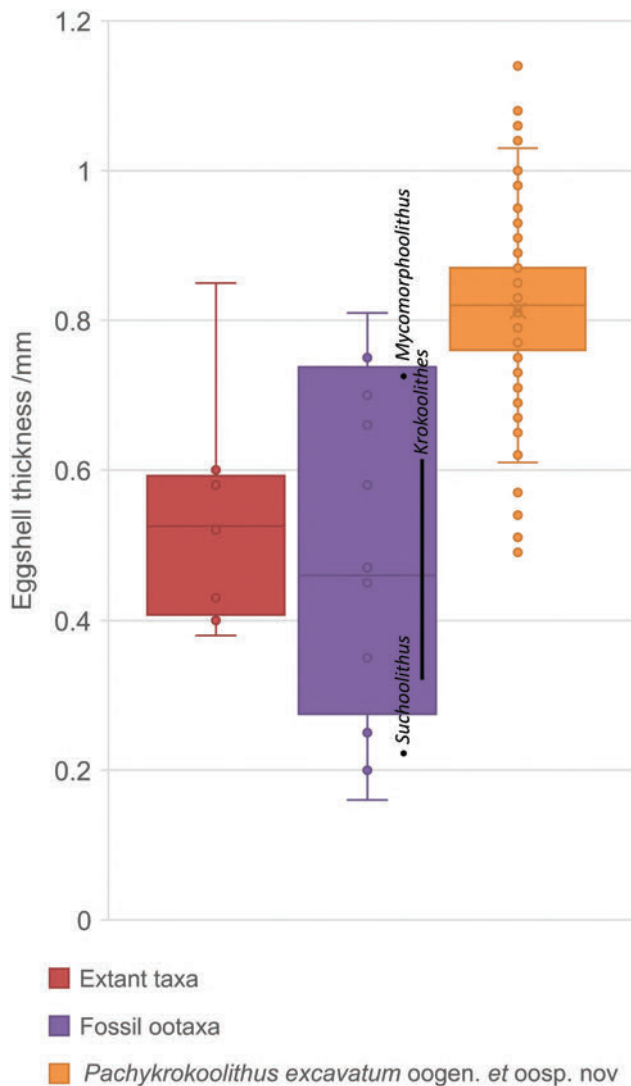
#### Comparison with other crocodylomorph-related ootaxa

Well-preserved fragments of *Pachykrokolithus excavatum* oogen. et oosp. nov. have diagnostic features of the Krokolithidae oofamily, according to the emended diagnosis proposed by Jackson and Varricchio (2016), namely multi-layered eggshells with basal knobs and shell units with book-like tabular ultrastructure. Among the Krokolithidae, *Pachykrokolithus* oogen. nov. presents the thickest eggshells (Figure 3, Supplementary Table 1). Among Crocodylomorpha, the thickness of *Pachykrokolithus excavatum* oogen. et oosp. nov. is comparable to that of some eggshells of *Caiman latirostris*, that have been reported to reach up to 850  $\mu\text{m}$  in thickness (Schleich and Kästle 1988) although recent studies have shown that the eggshell thickness in this taxon highly varies within a single egg, as well as during incubation (Piazza et al. 2021).

Three valid oogenera are recognised within the oofamily Krokolithidae: *Krokolithes* Hirsch 1985; *Suchoolithus*, Russo, Mateus, Marzola and Balbino 2017; and *Neokrokolithes* Bravo, Sevilla and Barroso-Barcenilla 2018. In addition, *Bauruoolithus* Oliveira, Santucci, Andrade, Fuljaro, Basílio and Benton 2011, was originally described as a Krokolithidae, but was moved out of the oofamily by Jackson and Varricchio (2016) based on some features incompatible with Krokolithidae (e.g. lack of tabular book-like ultrastructure, absence of basal plate groups, and presence of sweeping extinction pattern), and even regard it as a nomen nudum due to the lack of appropriate illustration of the type specimens. Finally, *Mycomorophoolithus* Moreno-Azanza, Gasca and Canudo 2015 is



**Figure 2.** *Pachyrokrolithus excavatum* oogen. et oosp. nov. from the Upper late Maastrichtian Veracruz 1 site (Trempe Formation) a). Scanning Electron Microscope secondary electron images (a, b, e–f) and thin section microphotographs (c, d). A, MPZ-2022/268 holotype eggshell fragment in radial section, showing a three-layered eggshell and trapezoidal shell units. The inner layer (IL) has a rosette-like structure, with basal knobs. The middle layer (ML) has book-like tabular ultrastructure (BLTU) and sparse vesiculation (Ve). The thicker outer layer (OL) represents more than half of the eggshell thickness, has more vesicles (Ve) and shows marked cleavage (CLV). b, MPZ-2022/277 eggshell fragment in radial section, showing a funnel shaped pore channel (PC) and a basal knob (BK). c, MPZ 2022/282 eggshell fragment thin section under parallel-polarised light, showing the brownish colour of the basal knobs (BK) of the inner layer (IN) and the outer layer (OL), compared with a much clearer medium layer (ML) due to the different distribution of organic matter. Note the sinuous growth lines (GL) parallel to the eggshell surface. d, MPZ 2022/282 eggshell fragment in radial section under cross-polarised light, showing the blocky extinction, with extinction domains expanding in lateral development in the outer layer. e, MPZ 2022/251 eggshell fragment outer surface, having a prominent rugosocavate ornamentation with bulges and depressions, with subcircular pore openings within the depressions (PO), and incipient dissolution pits (DP). f, MPZ 2022/252 eggshell fragment outer surface, with even more marked rugosocavate ornamentation, with some of the bulges coalescing into ridges. g, MPZ/2022/265 eggshell fragment inner surface with irregular, randomly spaced basal plate groups. Irregular polygonal gaps locate in the junction points between shell units, resulting in the interstices that connect with pore openings.



**Figure 3.** Box and whiskers plot comparing the maximum eggshell thickness of modern taxa, fossil ootaxa, and the measured thickness of *Pachyrokoolithus excavatum* oogen. et oosp. nov., with boxes representing the two medium percentiles with inclusive medians. Note that *Pachyrokoolithus excavatum* oogen. et oosp. nov. is thicker than most other crocodylomorph-related eggshells.

classified as oofamily incertae sedis, but its affinity to Krokoolithidae was established due to the presence of blocky extinction pattern and sub-trapezoidal shell units.

The comparison of *Pachyrokoolithus excavatum* oogen. et oosp. nov. with the oogenera of the oofamily Krokoolithidae supports its proposals as a new ootaxon. *Pachyrokoolithus excavatum* oogen. et oosp. nov. is up to four times thicker than the Jurassic oogenus *Suchoololithus* and can be further differentiated in having taller than wider shell units and lacking the faint dispersituberculated ornamentation of *Suchoololithus* (Russo et al. 2017). *Neokrokoolithes* is much thinner than *Pachyrokoolithus excavatum* oogen. et oosp. nov. and presents characteristic triangular nodes on the outer surface (Bravo et al. 2018) instead of the rugosocavate ornamentation of *Pachyrokoolithus excavatum* oogen. et oosp. nov. *Krokoolithes* eggshells are generally much thinner, usually 250–550  $\mu\text{m}$ , and with a maximum thickness of 760  $\mu\text{m}$  present in the unnamed Bridger Formation Eggshells described by Hirsch and Kohring (1992). In addition, the interstices between shell units are significantly larger in *Krokoolithes*

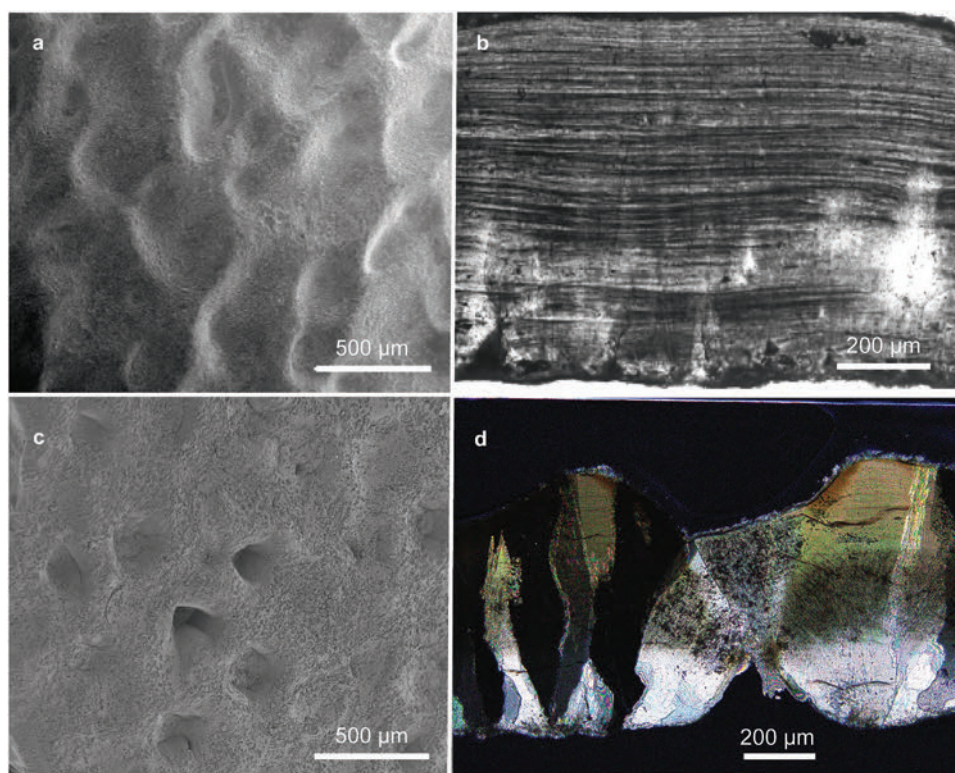
eggshells (Hirsch 1985; Kohring and Hirsch 1996), whereas in *Pachyrokoolithus excavatum* oogen. et oosp. nov. they are restricted to the inner third of the eggshell.

The oogenus *Mycomorphoolithus* from the Lower Cretaceous of Europe was originally described as having a smooth to wavy surface, ‘... although extrinsic erosion of the numerous pore openings confers a reticulate appearance upon the outer surface’ (Moreno-Azanza et al. 2015). This oogenus was described prior to the definition of the rugosocavate ornamentation by Marzola et al. (2015), but its ornamentation is somewhat similar to the exaggerated rugosocavate ornamentation present in *Pachyrokoolithus excavatum* oogen. et oosp. nov. The ornamentation of *Mycomorphoolithus* is highly related to the degree of development of the porosity – number and width of the pore channels –, which was postulated to increase during embryogenesis, reaching its maximum prior to hatch (Moreno-Azanza et al. 2015). A similar trend on the development of the porosity can be observed in *Pachyrokoolithus excavatum* oogen. et oosp. nov., with some fragments having small circular pores in the bottom of the valleys excavated in the eggshell surface (Figure 2e), to wider circular pores between large ridges, and finally a heavily ornamented eggshell surface with prominent ridges and multiple pores (Figure 2f). These similitudes reinforce the original interpretation of *Mycomorphoolithus* as a crocodylomorph eggshell. Nevertheless, *Pachyrokoolithus excavatum* oogen. et oosp. nov. can be easily differentiated by the absence of anastomosing pores and mushroom shape of the shell units with larger interstices between shell units compared to *Mycomorphoolithus*.

Finally, Hirsch and Quinn (1990) describe a single 1100  $\mu\text{m}$ -thick eggshell fragment from the Two Medicine Formation (Campanian, Late Cretaceous), as a putative crocodile eggshell, a determination supported by other authors (Jackson and Varricchio 2010). This eggshell fragment is poorly preserved, but presents large shell units arranged in wedges, which would support its crocodylomorph affinity. Nevertheless, in radial cross section, it has a rhombohedral fracture (Hirsch and Quinn 1990 figure 13C), which suggests the eggshell is recrystallised, and an overlaying granular layer with remains of sedimentary grains embedded that hinders any further comparison.

### Similitudes with the dinosaurian ootaxa *Stromatoolithus* (*Spheroolithus*) *europaeus*

The oospecies *Spheroolithus europaeus* Sellés, Vila and Galobart 2014 was described from Porrit-6 site in the upper Maastrichtian outcrops of the Tremp Formation in the village of El Pont d’Orrit (Lleida, Spain), which locates 17 km to the east of Veracruz 1 site and 5 km to the east of Blasi 2b site (Figure 1a, C). Porrit-6 is located in the lower part of the ‘Grey Garumnian’, having a roughly equivalent stratigraphic position to Blasi 2b, within the upper part of chron C30n (Figure 1c). Since the original description of this oospecies, Zhou et al. (2021) have proposed that it belongs to the oogenus *Stromatoolithus*, based on its straight pore canals and fine ornamentation. It is important to note that this attribution was based on the original description and without direct examination of the type material by Zhou et al. (2021). To acknowledge this taxonomic proposal but to avoid confusion if this assignment is disregarded after future revision, we chose to refer to this ootaxon as *Stromatoolithus* (*Spheroolithus*) *europaeus* Sellés et al. 2014). *Stromatoolithus* (*Spheroolithus*) *europaeus* has a slightly thicker eggshell than *Pachyrokoolithus excavatum* oogen. et oosp. nov. (Figure 4). It has a well-defined prolatospherulithic morphotype with highly fused shell units with radial calcite structure and is



**Figure 4.** Comparison between *Stromatoolithus (Spheroolithus) europaeus* (a, b) and *Pachykrokolithus excavatum* oogen. et oosp. nov. (c, d). A, IPS-64162, *Stromatoolithus (Spheroolithus) europaeus* Scanning Electron Microscope secondary electron image of the outer surface composed of fine ridges. B, IPS-58973 g, *Stromatoolithus (Spheroolithus) europaeus* thin section microphotograph, showing fused spherulitic shell units, with tightly packed growth lines and swapping extinction. c, MPZ 2022/251, *Pachykrokolithus excavatum* oogen. et oosp. nov. Scanning Electron Microscope secondary electron image of the outer surface showing prominent rugosocavate ornamentation, with pore openings. d, MPZ 2022/278, *Pachykrokolithus excavatum* oogen. et oosp. nov. thin section microphotograph showing a slightly thinner eggshell with wide trapezoidal shell units and growth lines limited to the outer layer. Extinction pattern is blocky.

characterised by sagenotuberculate ornamentation comprising fine irregular ridges, and two types of pore openings, one elliptical and large and another circular and small (Sellés et al. 2014).

The similar thickness and ornamented outer surface of *Pachykrokolithus excavatum* oogen. et oosp. nov. and *Stromatoolithus (Spheroolithus) europaeus*, causes that weathered specimens of can be easily misidentified during sample picking, and even with low magnification SEM images. Furthermore, the ultra-structure of both ootaxa may be obliterated by minimal recrystallisation, making it even more difficult to properly identify and differentiate them. Nevertheless, thin sections are unequivocal to differentiate both oospecies (Figure 4 b, d), as *Stromatoolithus (Spheroolithus) europaeus* has slender shell units, marked growth lines throughout the shell thickness and sweeping extinction, whereas *Pachykrokolithus excavatum* oogen. et oosp. nov. has wider shell units, with faint grown lines restricted to the upper part of the eggshell, and blocky extinction. This emphasises the importance of thin sections in the study of fossil eggs together with scanning electron microscope imaging, two complementary techniques required for a proper diagnosis of ootaxa.

#### Taxonomic affinities of *Pachykrokolithus excavatum* oogen. et oosp. nov.

The lack of embryonic remains or gravid females associated with eggs in Veracruz 1 site hinders the precise identification of the egg laying taxon that produced *Pachykrokolithus excavatum* oogen. et oosp. nov. eggshells. Nevertheless, the crocodylomorph affinities of

this ootaxon can be discussed by reviewing the diverse crocodylomorph osteological record of the Tremp Formation to search for putative egg layers.

Allodaposuchidae (basal eusuchians closely related to the crown group Crocodylia) is the most abundant crocodylomorph clade in the Tremp Basin. Indeed, their recovered fossils consist of the most reliably taxonomically identified and well-studied crocodylomorph remains of the whole Basin. During the last decade, four skulls assigned to four different species, *Arenysuchus gascabadiolorum* Puértolas, Canudo and Cruzado-Caballero, 2011, *Agaresuchus subjuniperus* (Puértolas-Pascual, Canudo and Moreno-Azanza, 2014), *Allodaposuchus palustris* Blanco, Puértolas Pascual, Marmi, Vila and Sellés, 2014 and *Allodaposuchus hulki* Blanco, Fortuny, Vicente, Luján, García-Marçà and Sellés, 2015, have been found within the Maastrichtian of the Tremp Basin. Besides, dozens of isolated generalist conical teeth and several fragmentary cranial remains assigned to Allodaposuchidae indet. have also been recovered, including teeth found in Veracruz 1 and Blasi 2b (Puértolas-Pascual et al. 2016; Blanco et al. 2020). Interestingly, the holotype of *A. subjuniperus* (C29r, latest Maastrichtian, Huesca, Spain) was geographically recovered only 800 m from Veracruz 1 and 300 m from 127-i/04/f (Figure 1a); and the holotype of *A. gascabadiolorum* (C30n–C29r, late Maastrichtian, Huesca, Spain) was located 100 m from Blasi 2b and 3 km from Areny 1 (Figure 1a). Therefore, both taxa were recovered in the same geographic area and very close stratigraphic levels to the sites where eggshells of *Pachykrokolithus excavatum* oogen. et oosp. nov. specimens have been recovered (Figure 1c).

Regarding Hylaeochampsidae (another clade of basal eusuchians closely related to Allodaposuchidae and crown group Crocodylia), only remains assigned to cf. *Acynodon* have been identified within the Tremp Formation (Puértolas-Pascual et al. 2016; Blanco et al. 2020). The most important fossil of this taxon is an almost complete small mandible from Els Nerets (C31r, early Maastrichtian, Lleida, Spain) assigned to *Acynodon* sp. (Blanco et al. 2020). The rest of the remains recovered in the Tremp Formation consist of isolated teeth assigned to cf. *Acynodon*. Although very scarce, they are distributed throughout the basin (including Blasi 2b) and throughout the Maastrichtian (from C31r to C29r) (Puértolas-Pascual et al. 2016; Blanco et al. 2020).

The presence of the crown group Crocodylia within the Tremp basin is less reliable as only three isolated teeth assigned to cf. *Thoracosaurus* have been found. However, more complete remains, such as a skull, have been found in the Maastrichtian of France (Laurent et al. 2000). Therefore, its presence in the Tremp Basin is possible and the assignment as a producer of *Pachykrokolithus excavatum* oogen. et oosp. nov. cannot be completely ruled out.

Besides eusuchians, other crocodylomorphs recovered within the basin are Atoposauridae. Although two species have been described in other Maastrichtian localities of Europe, *Aprosuchus ghirai* Venczel and Codrea, 2019 and *Sabresuchus* (= *Theriosuchus*) *sympiestodon* (Martin, Rabi and Csiki, 2010), both from the Hăţeg Basin (Romania), only a few isolated teeth assigned to Atoposauridae indet. have been found in the Maastrichtian of the Tremp basin (Puértolas-Pascual et al. 2016; Blanco et al. 2020).

The rarest clade corresponds to Sebecosuchia. Of this clade, isolated teeth assigned to cf. *Doratodon* have been recovered from several sites of the Tremp basin with ages ranging from C30r to C29r (Blanco et al. 2020). However, no teeth of this type have been recovered from nearby sites where eggshells of *Pachykrokolithus excavatum* oogen. et oosp. nov. have been found. On the other hand, the Sebecidae *Ogresuchus furatus* Sellés, Blanco, Vila, Marmi, López-Soriano, Llácer, Frigola, Canals and Galobart, 2020, from the early Maastrichtian (C32n–C31r) of the Tremp basin (Coll de Nargó, Lleida, Spain), have been recently described (Sellés et al. 2020). No other material assigned to *Ogresuchus* has been identified at other locations of the Tremp Basin.

Considering the high abundance of the osteological fossil remains of Eusuchia within the Tremp basin and their geographical/stratigraphical proximity to the sites where *Pachykrokolithus excavatum* oogen. et oosp. nov. has been found, the most likely producers are the basal eusuchians Allodaposuchidae or, although less probable, Hylaeochampsidae.

## Concluding remarks

*Pachykrokolithus excavatum* oogen. et oosp. nov. is a new oogenus and oospecies of the oofamily Krokolithidae, which has been identified in four localities of the Maastrichtian (Late Cretaceous) of the southern Pyrenees. Its ornamented external surface, unusual thickness for a crocodile eggshell and large shell units have led to several misidentifications as a dinosaurian (*Megaloolithus* and *Spheroolithus*) eggshell, but the combination of a rugosocavate ornamentation, presence of basal knobs tabular book-like ultrastructure, and blocky extinction pattern confirm its belonging to Krokolithidae. These emphasise the importance of combining thin-section analysis and high magnification scanning electron microscope images in the study of fossil eggshells. Among the putative egg layers, allodaposuchid crocodylomorphs are the most likely producers of *Pachykrokolithus excavatum* oogen. et oosp. nov. eggs.

## Acknowledgments

This research is supported by the PLEC2021-008203 project, funded by MCIN/AEI/10.13039/501100011033 and by the European Union “NextGenerationEU”/PRTR, the Spanish Ministry of Science and Innovation (project PID2021-122612OB-I00) and by the Government of Aragón-FEDER 2014–2020 *Construyendo Europa desde Aragón* (Group E18: *Aragosaurus: Recursos Geológicos y Paleoambientales*) and Fundação para a Ciência e a Tecnologia (grant number PTDC/CTA-PAL/31656/2017 and research unit UIDB/04035/2020; GeoBioTec). Authors would like to acknowledge the use of Servicio General de Apoyo a la Investigación-SAI, Universidad de Zaragoza. MMA and EPP funded by Ministerio de Universidades and Unión Europea-NextGenerationEU “Requalification of Spanish university system for 2021–2023”. MPP is supported by the Spanish Ministry of Education, Culture and Sport (Grant Number FPU 16/03064). CNL is the recipient of a Juan de la Cierva-Formación contract (FJC2020-044561-I), supported by the MCIN and co-financed by the NextGenerationEU/PRTR. We thank the contribution of the two anonymous reviewers and the editor, Dr Gareth Dyke.








## Disclosure statement

No potential conflict of interest was reported by the author(s).

## Funding

This work was supported by the Fundação para a Ciência e a Tecnologia [PTDC/CTA-PAL/31656/2017, UIDB/04035/2020]; Gobierno de Aragón [Group E18: *Aragosaurus: Recursos Geológicos y Pal*]; Ministerio de Educación, Cultura y Deporte [FPU 16/03064]; Ministerio de Universidades Unión Europea-NextGenerationEU [Maria Zambrano. Requalification of Spanish univerts]; Ministerio de Universidades (by Unión Europea-NextGenerationEU) [Maria Zambrano. Requalification of Spanish univerts]; MCIN/AEI/10.13039/501100011033 and by the European Union “NextGenerationEU”/PRTR, [FJC2020-044561-I, PLEC2021-008203]; Spanish Ministry of Science and Innovation [CGL2017-85038-P; MCIN/AEI/10.13039/501100011033 and by the European Union “NextGenerationEU”/PRTR, MCIN/AEI/10.13039/501100011033 and by the European Union “NextGenerationEU”/PRTR, [FJC2020-044561-I, PLEC2021-008203].

## ORCID

Miguel Moreno-Azanza  <http://orcid.org/0000-0002-7210-1033>  
Manuel Pérez-Pueyo  <http://orcid.org/0000-0002-6792-1563>  
Eduardo Puértolas-Pascual  <http://orcid.org/0000-0003-0759-7105>  
Carmen Núñez-Lahuerta  <http://orcid.org/0000-0002-2882-6061>  
Octávio Mateus  <http://orcid.org/0000-0003-1253-3616>  
Blanca Bauluz  <http://orcid.org/0000-0002-4970-6333>  
Beatriz Bádenas  <http://orcid.org/0000-0003-4970-6333>  
José Ignacio Canudo  <http://orcid.org/0000-0003-1732-9155>

## References

- Barco J, Ardèvol L, Canudo J. 2001. Descripción de los primeros rastros asignados a Hadosauridae (Ornithopoda, Dinosauria) del Maastrichtense de la Península Ibérica (Areny, Huesca). *Geogaceta*. 30:235–238.
- Blain H-A, Canudo J-I, Cuenca-Bescós G, López-Martínez N. 2010. Amphibians and squamate reptiles from the latest Maastrichtian (Upper Cretaceous) of Blasi 2 (Huesca, Spain). *Cretaceous Res*. 31(4):433–446. doi:10.1016/j.cretres.2010.06.001.
- Blanco A, Puértolas-Pascual E, Marmi J, Vila B, Sellés AG. 2014. *Allodaposuchus palustris* sp. nov. from the Upper Cretaceous of Fumanya (South-Eastern Pyrenees, Iberian Peninsula): systematics, Palaeoecology and Palaeobiogeography of the Enigmatic Allodaposuchian Crocodylians. *PLOS ONE*. 9(12):e115837. doi:10.1371/journal.pone.0115837.
- Blanco A, Fortuny J, Vicente A, Luján AH, García-Marçá JA, Sellés AG. 2015. A new species of *Allodaposuchus* (Eusuchia, Crocodylia) from the Maastrichtian (Late Cretaceous) of Spain: phylogenetic and paleobiological implications. *PeerJ*. 3:e1171. doi:10.7717/peerj.1171
- Blanco A, Puértolas-Pascual E, Marmi J, Moncunill-Solé B, Llácer S, Rössner GE. 2020. Late Cretaceous (Maastrichtian) crocodylians from north-eastern Iberia: a first attempt to explain the crocodylians diversity based on tooth qualitative traits. *Zool J Linn Soc*. 189(2):584–617. doi:10.1093/zoolinnean/zlzl06.
- Bravo AM, Sevilla P, Barroso-Barcenilla F. 2018. Avian and crocodilian eggshells from the upper Barremian site of Vadillos-1 (Lower Cretaceous, Cuenca province, Spain). *Cretaceous Res*. 85:28–41. doi:10.1016/j.cretres.2018.01.003

- Canudo JI, Oms O, Vila B, Galobart À, Fondevilla V, Puértolas-Pascual E, Sellés AG, Cruzado-Caballero P, Dinarès-Turell J, Vicens E, et al. 2016. The upper Maastrichtian dinosaur fossil record from the southern Pyrenees and its contribution to the topic of the Cretaceous–Palaeogene mass extinction event. *Cretaceous Res.* 57:540–551. doi:10.1016/j.cretres.2015.06.013
- Canudo JI. 2018. The Collection of Type Fossils of the Natural Science Museum of the University of Zaragoza (Spain). *Geoheritage*. 10(3):385–392. doi:10.1007/s12371-017-0228-1.
- Carpenter K, and Alf K. 1994. Global distribution of dinosaur eggs, nests and babies. In: Carpenter K, Hirsch KF, Horner JR, editors. *Dinosaur eggs and babies*. Cambridge: Cambridge University Press; p. 15–30.
- Costa E, Garcés M, López-Blanco M, Beamud E, Gómez-Paccard M, Larrasoana JC. 2010. Closing and continentalization of the South Pyrenean foreland basin (NE Spain): magnetochronological constraints. *Basin Res.* 22(6):904–917. doi:10.1111/j.1365-2117.2009.00452.x.
- Cruzado-Caballero P, Canudo JI, Moreno-Azanza M, Ruiz-Omeñaca JI. 2013. New material and phylogenetic position of *Arenysaurus ardevoli*, a lambeosaurine dinosaur from the late Maastrichtian of Arén (northern Spain). *J. Vertebr. Paleontol.* 33(6):1367–1384. doi:10.1080/02724634.2013.772061.
- Díez-Canseco D, Arz JA, Benito MI, Díaz-Molina M, Arenillas I. 2014. Tidal influence in redbeds: a palaeoenvironmental and biostratigraphic reconstruction of the Lower Tremp Formation (South-Central Pyrenees, Spain) around the Cretaceous/Paleogene boundary. *Sediment Geol.* 312:31–49. doi:10.1016/j.sedgeo.2014.06.008
- Eichenseer H. 1988. Facies geology of late Maastrichtian to early Eocene coastal and shallow marine sediments, Tremp-Graus basin, northeastern Spain [PhD Thesis]. [place unknown]: Institut und Museum für Geologie und Paläontologie der Universität Tübingen.
- Felice RN, Pol D, Goswami A. 2021. Complex macroevolutionary dynamics under the evolution of the crocodyliform skull. *Proc R Soc B: Biol Sci.* 288(1954):20210919. doi:10.1098/rspb.2021.0919.
- Fondevilla V, Dinarès-Turell J, Oms O. 2016. The chronostratigraphic framework of the South-Pyrenean Maastrichtian succession reappraised: implications for basin development and end-Cretaceous dinosaur faunal turnover. *Sediment Geol.* 337:55–68. doi:10.1016/j.sedgeo.2016.03.006
- Fondevilla V, Riera V, Vila B, Sellés AG, Dinarès-Turell J, Vicens E, Gaete R, Oms O, Galobart À. 2019. Chronostratigraphic synthesis of the latest Cretaceous dinosaur turnover in south-Western Europe. *Earth Sci Rev.* 191:168–189. doi:10.1016/j.earscirev.2019.01.007
- Hirsch KF. 1985. Fossil Crocodilian Eggs from the Eocene of Colorado. *J. Paleontol.* 59(3):531–542.
- Hirsch KF, Quinn B. 1990. Eggs and eggshell fragments from the Upper Cretaceous Two Medicine Formation of Montana. *J. Vertebr. Paleontol.* 10(4):491–511. doi:10.1080/02724634.1990.10011832.
- Hirsch KF, Kohring R. 1992. Crocodilian eggs from the middle Eocene Bridger Formation, Wyoming. *J. Vertebr. Paleontol.* 12(1):59–65. doi:10.1080/02724634.1992.10011431.
- Irmis RB, Nesbitt SJ, Sues H-D. 2013. Early Crocodylomorpha. *Geol Soc London Spec Publ.* 379(1):275–302. doi:10.1144/SP379.24.
- Jackson FD, Varricchio DJ. 2010. Fossil eggs and eggshell from the lowermost Two Medicine Formation of western Montana, Sevenmile Hill locality. *J. Vertebr. Paleontol.* 30(4):1142–1156. doi:10.1080/02724634.2010.483537.
- Jackson FD, Varricchio DJ. 2016. Fossil egg and eggshells from the Upper Cretaceous Hell Creek Formation, Montana. *J. Vertebr. Paleontol.* 36(5):e1185432. doi:10.1080/02724634.2016.1185432.
- Kohring R, Hirsch KF. 1996. Crocodilian and avian eggshells from the Middle Eocene of the Geiseltal, Eastern Germany. *J. Vertebr. Paleontol.* 16(1):67–80. doi:10.1080/02724634.1996.10011285.
- Laurent Y, Buffetaut E, Le Loeuff J. 2000. Un crâne de Thoracosaurine (Crocodylia, Crocodylidae) dans le Maastrichtien supérieur du Sud de la France. *Oryctos*. 3:19–27.
- López-Martínez N. 2003. Dating dinosaur oodiversity: chronostratigraphic control of Late Cretaceous oospecies succession. *Palaeovertebrata*. 32(2–4):121–148.
- López-Martínez N, Canudo JI, Ardévol L, Suberbiola XP, Orue-Etxebarria X, Cuenca-Bescós G, Ruiz-Omeñaca JI, Murelaga X, Feist M. 2001. New dinosaur sites correlated with Upper Maastrichtian pelagic deposits in the Spanish Pyrenees: implications for the dinosaur extinction pattern in Europe. *Cretaceous Res.* 22(1):41–61. doi:10.1006/cres.2000.0236.
- López-Martínez N, Canudo JI, and Cuenca-Bescós G. 1999. Latest Cretaceous eggshells from Arén (Southern Pyrenees, Spain). In: First International Symposium on Dinosaur Eggs and Babies. Isona i Conca Dellà (Spain); p. 35–36.
- López-Martínez NIEVES, and Vicens E. (2012). A new peculiar dinosaur egg, *Sankofa pyrenaica* oogen. nov. oosp. nov. From the Upper Cretaceous coastal deposits of the Aren Formation, south-central Pyrenees, Lleida, Catalonia, Spain. *Palaeontology*, 55(2):325–339.
- Martin JE, Rabi M, and Csiki Z. 2010. Survival of *Theriosuchus* (Mesoeucrocodylia: Atoposauridae) in a Late Cretaceous archipelago: a new species from the Maastrichtian of Romania. *Naturwissenschaften*. 97(9):845–854.
- Marzola M, Russo J, Mateus O. 2015. Identification and comparison of modern and fossil crocodilian eggs and eggshell structures. *Hist Biol.* 27(1):115–133. doi:10.1080/08912963.2013.871009.
- Mey PHW, Nagtegaal PJC, Roberti KJ, Harteveldt JJA. 1968. Lithostratigraphic subdivision of Post-Hercynian deposits in the South-Central Pyrenees, Spain. *Leidse Geol Mededelingen*. 41(1):221–228.
- Mikhailov KE. 1991. Classification of fossil eggshells of amniotic vertebrates. *Acta Palaeontol Polonica*. 36(2):193–238.
- Mikhailov KE. 1997. Fossil and recent eggshell in amniotic vertebrates: fine structure, comparative morphology and classification. London: Palaeontological association. [place unknown].
- Moreno-Azanza M, Bauluz B, Canudo JI, Puértolas-Pascual E, Sellés AG. 2014. A re-evaluation of aff. *Megaloolithidae* eggshell fragments from the uppermost Cretaceous of the Pyrenees and implications for crocodylomorph eggshell structure. *Hist Biol.* 26(2):195–205. doi:10.1080/08912963.2013.786067.
- Moreno-Azanza M, Canudo JI, Gasca JM. 2015. Enigmatic Early Cretaceous ootaxa from Western Europe with signals of extrinsic eggshell degradation. *Cretaceous Res.* 56:617–627. doi:10.1016/j.cretres.2015.06.019
- Muñoz JA. 1992. Thrust Tectonics McClay KR (editor), Evolution of a continental collision belt: ECORS-Pyrenees crustal balanced cross-section [Internet]. Dordrecht: Springer Netherlands; [accessed 2021 Dec 7]; 235–246. doi:10.1007/978-94-011-3066-0\_21.
- Murelaga X, and Canudo J. 2005. Descripción de los restos de quelonios del Maastrichtense superior de Arén y Serraduy (Huesca). *Geogaceta*. 38(5):51–54.
- Oliveira CE, Santucci RM, Andrade MB, Fulfaro VJ, Basilio JA and Benton MJ. (2011). Crocodylomorph eggs and eggshells from the Adamantina Formation (Bauru Group), Upper Cretaceous of Brazil. *Palaeontology*, 54(2):309–321. doi:10.1111/j.1475-4983.2010.01028.x.
- Oms O, Fondevilla V, Riera V, Marmi J, Vicens E, Estrada R, Anadón P, Vila B, Galobart À. 2016. Transitional environments of the lower Maastrichtian South-Pyrenean Basin (Catalonia, Spain): the Fumanya Member tidal flat. *Cretaceous Res.* 57:428–442. doi:10.1016/j.cretres.2015.09.004
- Pereda-Suberbiola X, Canudo JI, Cruzado-Caballero P, Barco JL, López-Martínez N, Oms O, Ruiz-Omeñaca JI. 2009. The last hadrosaurid dinosaurs of Europe: a new lambeosaurine from the Uppermost Cretaceous of Aren (Huesca, Spain). *C R Palevol.* 8(6):559–572. doi:10.1016/j.crpv.2009.05.002.
- Pérez-Pueyo M, Gilabert V, Moreno-Azanza M, Puértolas-Pascual E, Bádenas B, Canudo JI. 2019. Late Maastrichtian fossil assemblage of Veracruz 1 site (Beranuy, NE Spain): wildfires and bones in a transitional environment. *Proceedings of the VIII Jornadas Internacionales sobre Paleontología de Dinosaurios y su Entorno*, Burgos, Spain. 5–9.
- Pérez-Pueyo M, Cruzado-Caballero P, Moreno-Azanza M, Vila B, Castanera D, Gasca JM, Puértolas-Pascual E, Bádenas B, Canudo JI. 2021. The Tetrapod Fossil Record from the Uppermost Maastrichtian of the Ibero-Armorican Island: an Integrative Review Based on the Outcrops of the Western Tremp Syncline (Aragón, Huesca Province, NE Spain). *Geosciences*. 11(4):162. doi:10.3390/geosciences11040162.
- Piazza MV, Fernández MS, Leiva PML, Piña CI, Simoncini MS. 2021. “Intracascar space” an eggshell structure of Caiman latirostris eggs. *Sci Rep.* 11(1):5579. doi:10.1038/s41598-021-85113-9.
- Puértolas E, Canudo JI, Cruzado-Caballero P. 2011. A New Crocodylian from the Late Maastrichtian of Spain: implications for the Initial Radiation of Crocodyloids. *PLoS ONE*. 6(6):e20011. doi:10.1371/journal.pone.0020011.
- Puértolas-Pascual E, Canudo JI, Moreno-Azanza M. 2014. The eusuchian crocodylomorph *Allodaposuchus subjuniiperus* sp. nov., a new species from the latest Cretaceous (upper Maastrichtian) of Spain. *Hist Biol.* 26(1):91–109. doi:10.1080/08912963.2012.763034.
- Puértolas-Pascual E. 2016. Contribución a la paleobiodiversidad de crocodylomorpha en el cretácico de la Península Ibérica: implicaciones filogenéticas y paleobiogeográficas [Unpublished PhD Thesis]. Zaragoza: Universidad de Zaragoza.
- Puértolas-Pascual E, Blanco A, Brochu CA, Canudo JI. 2016. Review of the Late Cretaceous-early Paleogene crocodylomorphs of Europe: extinction patterns across the K-PG boundary. *Cretaceous Res.* 57:565–590. doi:10.1016/j.cretres.2015.08.002

- Puértolas-Pascual E, Arenillas I, Arz JA, Calvín P, Ezquerro L, García-Vicente C, Pérez-Pueyo M, Sánchez-Moreno EM, Villalain JJ, Canudo JI. 2018. Chronostratigraphy and new vertebrate sites from the upper Maastrichtian of Huesca (Spain), and their relation with the K/Pg boundary. *Cretaceous Res.* 89:36–59. doi:[10.1016/j.cretres.2018.02.016](https://doi.org/10.1016/j.cretres.2018.02.016)
- Riera V, Oms O, Gaete R, Galobart À. 2009. The end-Cretaceous dinosaur succession in Europe: the Tremp Basin record (Spain). *Palaeogeogr Palaeoclimatol Palaeoecol.* 283(3):160–171. doi:[10.1016/j.palaeo.2009.09.018](https://doi.org/10.1016/j.palaeo.2009.09.018).
- Rosell J, Linares R, Llompart C. 2001. El “Graundiense” prepirenaico. *Rev de Soc Geol de España.* 14(1–2):47–56.
- Russo J, Mateus O, Marzola M, Balbino A. 2017. Two new ootaxa from the late Jurassic: the oldest record of crocodylomorph eggs, from the Lourinhã Formation, Portugal. *PLOS ONE.* 12(3):e0171919. doi:[10.1371/journal.pone.0171919](https://doi.org/10.1371/journal.pone.0171919).
- Schleich HH, Kästle W. 1988. *Reptile Egg-Shells. SEM Atlas.* Stuttgart: Gustav Fischer Verlag.
- Sellés AG, Vila B, Galobart À. 2014. *Stromatoolithus (Spheroolithus) europaeus*, oosp. nov. (late Maastrichtian, Catalonia), the youngest oological record of hadrosauroids in Eurasia. *J Vertebr Paleontol.* 34(3):725–729. doi:[10.1080/02724634.2013.819360](https://doi.org/10.1080/02724634.2013.819360).
- Sellés AG, Blanco A, Vila B, Marmi J, López-Soriano FJ, Llácer S, Frigola J, Canals M, Galobart À. 2020. A small Cretaceous crocodyliform in a dinosaur nesting ground and the origin of sebecids. *Sci Rep.* 10(1):15293. doi:[10.1038/s41598-020-71975-y](https://doi.org/10.1038/s41598-020-71975-y).
- Teixell A. 2004. Estructura de los Pirineos: generalidades. In: Vera JA, editor. *Geología de España.* Madrid: SGE-IGME; p. 321–323.
- Torices A, Ruiz-Omeñaca JI, Canudo JI, López-Martínez N. 2004. Nuevos datos sobre los dinosaurios terópodos (Saurischia: Theropoda) del Cretácico superior de los Pirineos Sur-Centrales (Huesca y Lleida). *Geotemas.* 6(5):71–74.
- Venczel M, Codrea VA. 2019. A new Theriosuchus-like crocodyliform from the Maastrichtian of Romania. *Cretaceous Research.* 100:24–38.
- Vila B, Sellés AG, Brusatte SL. 2016. Diversity and faunal changes in the latest Cretaceous dinosaur communities of southWestern Europe. *Cretaceous Res.* 57:552–564. doi:[10.1016/j.cretres.2015.07.003](https://doi.org/10.1016/j.cretres.2015.07.003)
- Zhu X, Wang Q, Wang X. 2021. Restudy of the original and new materials of *Stromatoolithus pinglingensis* and discussion on some *Spheroolithidae* eggs. *Hist Biol.* 34(2):283–297. doi:[10.1080/08912963.2021.1910817](https://doi.org/10.1080/08912963.2021.1910817).



# **Conclusions/ Conclusiones**





## Conclusions

An integrated stratigraphical and paleontological analysis of the Cretaceous part of the Tremp Fm in the Western Tremp Syncline (Ribargorza, NE Huesca province, Aragón, Spain) has been carried out. The main objective has been the characterization of the upper Maastrichtian successions with fossil vertebrates of this area of the Southern Pyrenees and evaluate their diversity prior to the K/Pg extinction event. The result of this study has allowed to reach the following conclusions:

- I. The lithostratigraphic study of the Tremp Fm in this area has allowed to recognize several lithostratigraphical units with variable thickness and complex vertical and lateral relations. Thus, starting from the top of the Arén Fm, the units identified are the 'Grey Garumnian', the 'Lower Red Garumnian', the 'Vallcebre Limestones and lateral equivalents', and the 'Upper Red Garumnian'. The two first units are the most interesting for the purposes of this Doctoral Thesis, since they contain Maastrichtian vertebrates. It has been noted the presence of a 'Transition interval' between the 'Lower Red Garumnian' unit and the 'Vallcebre Limestones and lateral equivalents' unit, sharing mixed features between them.
- II. New biostratigraphic and magnetostratigraphic data has been apported. The study of the foraminifera from Serraduy and Veracruz 1 site, and the charophyte assemblage from Veracruz 1, together with two magnetostratigraphic sections (Serraduy and Isclés), have allowed to reinforce the chronostratigraphic framework of the Western Tremp Syncline. The deposits of the Arén Fm, the 'Grey Garumnian' and the 'Lower Red Garumnian' have been dated within the magnetochrons C30n and C29r (late Maastrichtian). These datings confirm that the fossil record from the Western Tremp Syncline is one of the youngest before the K/Pg boundary in the Iberian Peninsula, registering the last 300 ky of the Cretaceous. It has also been observed that the uppermost part of the 'Lower Red Garumnian' might be early Danian. However, more chronostratigraphic information about this interval and the 'Vallcebre Limestones' unit in order to constrain the K/Pg boundary is necessary, avoiding the use of data that could lead to circular reasoning.
- III. The sedimentary analysis has allowed to characterize 22 sedimentary facies for the top of the Arén Fm, the 'Grey Garumnian', the 'Lower Red Garumnian', and

the 'Transitional interval'. By their sedimentary features, they have been classified within 4 facies assemblages, including lagoonal, perilagoonal, fluvial, and transitional lacustrine facies. This allowed to establish a sedimentary model for the Tresp Fm during the late Maastrichtian.

- IV. A thorough field stratigraphic control for all the paleontological sites of the Western Tresp Syncline has allowed to integrate a total of 97 fossil sites in the chronostratigraphic framework, 39 of them newly found during the labors of this doctoral thesis. The evaluation of previously discovered material and the finding of new fossils points that all the main vertebrate groups, including hadrosauroid, theropod and sauropod dinosaurs, crocodylomorphs and testudines reached the upper part of the 'Lower Red Garumnian', being then situated very close to the K/Pg boundary. Other groups that have worse record due to their small size and facies restriction, such as fishes, squamates or amphibians, are not so well-constrained.
- V. The combination of the sedimentary facies and paleontological sites has been embodied in a taphonomic analysis. 14 facies and 5 taphonomic modes were established. It has been constated that fluvial sandstones are the facies with more vertebrate sites, counting both bones and tracks. On other hand, vertebrate microfossils sites are less abundant, and limited to perilagoonal grey mudstones rich in organic matter. This is probably due to a sampling bias of muddy lithologies, and because microvertebrates are difficult to see with the naked eye during prospection. Finally, it is interesting to mention that the facies more likely to preserve vertebrate fossils are scarcer or absent in the uppermost part of the 'Lower Red Garumnian' and in the 'Transitional interval', introducing a taphonomic bias to study the fossil record in this interval.
- VI. The study of several vertebrate fossils permitted to mark new records of several already known groups, such as sauropod dinosaurs or eusuchian crocodylomorphs. It also has led to the identification of new taxa without a previous record in the Western Tresp Syncline, such as a giant ornithuromorph bird, a putative dromaeosaurid theropod, an indeterminate pterosaur or the allodaposuchid crocodylomorph *Allodaposuchus palustris*. These new data increases the diversity known of the late Maastrichtian assemblages.

- VII. The study of the eggshell assemblages from Blasi 2B and Veracruz 1 has allowed to increase the knowledge about the oodiversity in the Western Tresp Syncline. A new ootaxon related to crocodylomorphs has been erected with eggshells from Veracruz 1 site: *Pachykrokolithus excavatum*. Besides, hadrosauroid dinosaur eggshells identified as *Spheroolithus* aff. *europaeus* have been recognized for the first time in the Western Tresp Syncline, in the site of Blasi 2B. Besides, the presence of at least 4 different types of theropod eggshell indicates that the diversity of this group may be higher than has been previously assessed.



## Conclusiones

Se ha realizado un análisis estratigráfico y paleontológico integrado de la parte cretácica de los afloramientos de la Fm Tresp del Sinclinal de Tresp Occidental (Ribargorza; NE de la provincia de Huesca, Aragón, España), con el objetivo principal de caracterizar las sucesiones del Maastrichtiense superior con vertebrados fósiles de esta zona del Pirineo meridional y evaluar su diversidad previa al evento de extinción K/Pg. El resultado de este estudio ha permitido alcanzar las siguientes conclusiones:

- I. El estudio litoestratigráfico de la Fm Tresp en esta zona ha permitido reconocer varias unidades litoestratigráficas de espesor variable y relaciones verticales y laterales complejas. Así, partiendo del techo de la Fm Arén, las unidades identificadas son el 'Garumniense Gris' el 'Garumniense Rojo Inferior' las 'Calizas de Vallcebre y equivalentes laterales', y el 'Garumniense Rojo Superior'. Las dos primeras unidades son las de mayor interés para los objetivos de esta tesis, ya que son las unidades en las que se encuentran vertebrados del Maastrichtiense. Se ha constatado la presencia de un 'Intervalo de transición' entre el 'Garumniense Rojo Inferior' y las 'Calizas de Vallcebre y equivalentes laterales', compartiendo rasgos mixtos entre ambas unidades.
- II. Se han aportado nuevos datos bioestratigráficos y magnetoestratigráficos. El estudio de los foraminíferos de los yacimientos de Serraduy y Veracruz 1, y de la asociación de carofitas de Veracruz 1, junto con dos secciones magnetoestratigráficas (Serraduy e Isclés) ha permitido reforzar el marco cronoestratigráfico del Sinclinal de Tresp Occidental. Los depósitos de la Fm Arén, el 'Garumniense Gris' y el 'Garumniense Rojo Inferior' han sido datados dentro de los magnetocrones C30n y C29r (Maastrichtiense tardío), lo que confirma que el registro fósil del Sinclinal de Tresp Occidental es uno de los más jóvenes antes del límite K/Pg en la Península Ibérica, registrando los últimos 300.000 años del Cretácico. También se ha observado que la parte superior del 'Garumniense Rojo Inferior' podría ser Daniense basal. No obstante, es necesaria más información cronoestratigráfica sobre este intervalo y la unidad de 'Calizas de Vallcebre' para restringir el límite K/Pg, evitando el uso de datos que podrían conducir a razonamientos circulares.

- III. El análisis sedimentológico ha permitido caracterizar 22 facies sedimentarias para el techo de la Fm Arén, el 'Garumniense Gris', el 'Garumniense Rojo Inferior' y el 'Intervalo transicional'. Por sus características sedimentarias, se han clasificado con 4 conjuntos de facies, incluyendo facies lagunares, facies perilagunares, facies fluviales y facies lacustres transicionales, estableciendo así un modelo sedimentario para la Fm Tresp durante el Maastrichtiense tardío.
- IV. Un exhaustivo control estratigráfico de campo de todos los yacimientos paleontológicos del Sinclinal de Tresp Occidental ha permitido integrar en el marco cronoestratigráfico un total de 97 yacimientos fósiles, 39 de ellos hallados recientemente durante las labores de esta tesis doctoral. La evaluación del material previamente descubierto y el hallazgo de nuevos fósiles apunta a que todos los principales grupos de vertebrados, incluyendo dinosaurios hadrosauroideos, terópodos y saurópodos, crocodilomorfos y testudines, alcanzan la parte superior del "Garumniense Rojo Inferior", situándose por tanto muy cerca del límite K/Pg. Otros grupos con peor registro debido a su pequeño tamaño y restricción de facies, como los escamosos o los anfibios, no están tan bien delimitados.
- V. La combinación de las facies sedimentarias y los yacimientos paleontológicos se ha plasmado en un análisis tafonómico. Para este análisis se han utilizado 14 facies y 5 modos tafonómicos. Se ha constatado que las areniscas fluviales son las facies con más yacimientos de vertebrados, contando tanto huesos como huellas. Por otro lado, los yacimientos de microfósiles de vertebrados son escasos y se limitan a lutitas grises perilagunares ricas en materia orgánica. Esto se debe probablemente a un sesgo de muestreo de litologías fangosas, y porque los microvertebrados son difíciles de observar directamente en el campo durante las prospecciones. Por último, es interesante mencionar que las facies más propensas a preservar fósiles de vertebrados son más escasas o están ausentes en la parte superior del "Garumniense Rojo Inferior" y en el "Intervalo Transicional", introduciendo de este modo un sesgo tafonómico a la hora de estudiar el registro fósil en este intervalo.
- VI. El estudio de varios fósiles de vertebrados ha permitido marcar nuevos registros de varios grupos ya conocidos, como los dinosaurios saurópodos o los crocodilomorfos eusuquios. También ha conducido a la identificación de nuevos taxones sin registro previo en el Sinclinal de Tresp Occidental, como un ave

gigante ornituomorfa, un terópodo paraviano indeterminado, un pterosaurio indeterminado o el crocodilomorfo *Allodaposuchus palustris*. Estos nuevos datos aumentan la diversidad conocida de los conjuntos del Maastrichtiense tardío.

- VII. El estudio de los conjuntos de cáscaras de huevo de Blasi 2B y Veracruz 1 ha permitido aumentar el conocimiento sobre la oodiversidad en el Sinclinal de Tresp Occidental. Un nuevo ootaxon relacionado con los crocodilomorfos ha sido erigido con las cáscaras de huevo del yacimiento de Veracruz 1. Se trata de *Pachykrokolithus excavatum*. Además, se han reconocido por primera vez cáscaras de huevo de dinosaurios hadrosauroideos, identificadas como *Spheroolithus* aff. *europaeus* en el Sinclinal de Tresp Occidental, en el yacimiento de Blasi 2B. Además, la presencia de al menos 4 tipos diferentes de cáscaras de huevo de terópodos indica que la diversidad de este grupo puede ser mayor de lo que se ha evaluado previamente.



# **Bibliography**



## Bibliography

- Alegret, L., Thomas, E., 2007. Deep-Sea environments across the Cretaceous/Paleogene boundary in the eastern South Atlantic Ocean (ODP Leg 208, Walvis Ridge). *Marine Micropaleontology* 64, 1–17. <https://doi.org/10.1016/j.marmicro.2006.12.003>
- Allain R, Taquet P., 2000. A new genus of Dromaeosauridae (Dinosauria, Theropoda) from the Upper Cretaceous of France. *Journal of Vertebrate Paleontology*. 20 (2):404–407. doi:10.1671/0272-4634(2000)020[0404:ANGODD]2.0.CO;2.
- Allmendinger, R. W., Cardozo, N. C., Fisher, D., 2013. Structural geology algorithms: Vectors & tensors: Cambridge: Cambridge University Press. 289 pp.
- Alvarenga, H. M. F., J.F. Bonaparte., 1992. A new flightless land bird from the Cretaceous of Patagonia; pp. 51–64 in K.E. Campbell (ed.), *Papers in Avian Paleontology, Honoring Pierce Brodkorb*. Science Series 36. Natural History Museum of Los Angeles County, Los Angeles.
- Alvarenga, H. M. F., L. Chiappe, S. Bertelli., 2011. Phorusrhacids: the terror birds; pp. 187–208 in G. Dyke, and G. Kaiser (eds.), *Living dinosaurs. The evolutionary history of modern birds*. John Wiley & Sons Ltd, Chichester, West Sussex.
- Alvarez, L.W., Alvarez, W., Asaro, F., Michel, H. V., 1980. Extraterrestrial Cause for the Cretaceous-Tertiary Extinction. *Science* 208, 1095–1108. <https://doi.org/10.1126/science.208.4448.1095>
- Apostolaki, N.E., E.J. Rayfield, P.M. Barrett., 2015. Osteological and soft-tissue evidence for pneumatization in the cervical column of the ostrich (*Struthio camelus*) and observations on the vertebral columns of non-volant, semi-volant and semi-aquatic birds. *PloS One*, 10(12): e0143834.
- Archibald, J.D., Clemens, W.A., Padian, K., Rowe, T., Macleod, N., Barrett, P.M., Gale, A., Holroyd, P., Sues, H.D., Arens, N.C., Horner, J.R., Wilson, G.P., Goodwin, M.B., Brochu, C.A., Lofgren, D.L., Hurlbert, S.H., Hartman, J.H., Eberth, D.A., Wignall, P.B., Currie, P.J., Weil, A., Prasad, G.V.R., Dingus, L., Courtillot, V., Milner, A., Milner, A., Bajpai, S., Ward, D.J., Sahni, A., 2010. Cretaceous Extinctions: Multiple Causes. *Science* 328, 973–973. <https://doi.org/10.1126/science.328.5981.973-a>
- Ardévol, L., Klimowitz, J., Malagón, J., Nagtegaal, P.J.C., 2000. Depositional sequence response to foreland deformation in the upper Cretaceous of the Southern Pyrenees, Spain. *AAPG Bulletin* 84, 566–588. <https://doi.org/10.1306/c9ebce55-1735-11d7-8645000102c1865d>
- Arenillas, I., Arz, J.A., Molina, E., Dupuis, C., 2000. An independent test of planktic foraminiferal turnover across the Cretaceous/Paleogene (K/P) boundary at El Kef, Tunisia; catastrophic mass extinction and possible survivorship. *Micropaleontology* 46, 31–49.
- Arenillas, I., Arz, J.A., Gilabert, V., 2022. An updated suprageneric classification of planktic foraminifera after growing evidence of multiple benthic-planktic transitions. *Spanish Journal of Palaeontology* 37(1), 1-34 <https://doi.org/10.7203/sjp.22189>
- Arz, J.A., Arenillas, I., Nájuez, C., 2010. Morphostatistical analysis of Maastrichtian populations of *Guembelitra* from El Kef, Tunisia. *The Journal of Foraminiferal Research* 40, 148–164. <https://doi.org/10.2113/gsjfr.40.2.148>
- Augustin, F.J., Bastiaans, D., Dumbravă, M.D., Csiki-Sava, Z., 2022. A new ornithomimid dinosaur, *Transylvanosaurus platycephalus* gen. et sp. nov. (Dinosauria: Ornithischia), from the Upper

- Cretaceous of the Hațeg Basin, Romania. *Journal of Vertebrate Paleontology*, 42:2. <https://doi.org/10.1080/02724634.2022.2133610>
- Averianov, A., Sues, H.-D., 2019. Morphometric analysis of the teeth and taxonomy of the enigmatic theropod *Richardoestia* from the Upper Cretaceous of Uzbekistan. *Journal of Vertebrate Paleontology* 39, e1614941. <https://doi.org/10.1080/02724634.2019.1614941>
- Báez, A.M., Gómez, R.O., Ribeiro, L.C.B., Martinelli, A.G., Teixeira, V.P.A., Ferraz, M.L.F., 2012. The diverse Cretaceous neobatrachian fauna of South America: *Uberabatrachus carvalhoi*, a new frog from the Maastrichtian Marília Formation, Minas Gerais, Brazil. *Gondwana Research* 22, 1141–1150. <https://doi.org/10.1016/j.gr.2012.02.021>
- Baiano, M., Galobart, À., Dalla, F.M., Vila, B., 2014. Aplicación de la microtomografía en el estudio de dientes aislados de dinosaurios terópodos, in: Arreguín-Rodríguez, G., Colmenar, J., Díaz-Berenguer, E., Galán, J., L.-L., A., Parrilla-Bel, J., Puértolas-Pascual, E., Silva-Casal, R. (Eds.), *New Insights on Ancient Life. XII Encuentro de Jóvenes Investigadores En Paleontología*. Boltaña (Huesca), pp. 57–59.
- Bailey, R.C., Halls, H.C., 1984. Estimate of confidence in paleomagnetic directions derived from mixed remagnetization circle and direct observational data. *Journal of Geophysics*, 54, 174–182
- Bandel, K., 2006. Families of the Cerithioidea and related superfamilies (Palaeo-Caenogastropoda; Mollusca) from the Triassic to the Recent characterized by protoconch morphology-including the description of new taxa. *Freiberger Forschungshefte C* 511, 59–138.
- Banner, F. T., Blow, W. H. 1960. Some primary types of species belonging to the superfamily Globigerinaceae. *Contributions from the Cushman Foundation for Foraminiferal Research*. 11: 1-41.
- Barco, J.L., Ardevol, L., Canudo, J.I., 2001. Descripción de los primeros rastros asignados a Hadrosauridae (Ornithopoda, Dinosauria) del Maastrichtiense de la Península Ibérica (Areny, Huesca). *Geogaceta* 30, 235–238.
- Bardet, N., 1994. Extinction events among Mesozoic marine reptiles. *Historical Biology* 7, 313–324. <https://doi.org/10.1080/10292389409380462>
- Barnet, J.S.K., Littler, K., Kroon, D., Leng, M.J., Westerhold, T., Röhl, U., Zachos, J.C., 2018. A new high-resolution chronology for the late Maastrichtian warming event: Establishing robust temporal links with the onset of Deccan volcanism. *Geology* 46, 147–150. <https://doi.org/10.1130/G39771.1>
- Bataller, J.R., 1945. Enumeración de las especies nuevas del Cretácico de España. *Memorias de la Real Academia de Ciencias y Artes de Barcelona, Tercera Época* 571, 373–441.
- Baumel, J.J., Witmer, L.M., 1993. Osteologia, in: Baumel, J.J., King, A.S., Breazile, J.E., Evans, H.E., Vanden Berge, J.C. (Eds.), *Handbook of Avian Anatomy: Nomina Anatomica Avium*. Publications of the Nuttall Ornithological Club, Cambridge, Massachusetts, pp. 45–132.
- Beamud, E., Garcés, M., Muñoz, J.A., Cabrera, L., Almar, Y., 2004. Distribución de las rotaciones paleomagnéticas en la cuenca de Graus-Tremp durante el Terciario. *Geotemas*, 6 (4), 283–286.
- Behrensmeyer, A.K., 1978. Taphonomic and ecologic information from bone weathering. *Paleobiology* 4, 150–162.
- Behrensmeyer, A.K., 1992. Paleoenvironmental contexts and taphonomic modes. In: Behrensmeyer, A.K., Damuth, J.D., Potts, R., Sues, H.-D., Wing, S.L. (Eds.), *Terrestrial*

- Ecosystems Through Time: Evolutionary Paleoecology of Terrestrial Plants and Animals. University of Chicago Press, Chicago, pp. 15–136.
- Behrensmeyer, A.K., 2007. Bonebeds through time. In: Rogers, R.R., Eberth, D.A., Fiorillo, A.R. (Eds.), Bonebeds: Genesis, Analysis, and Paleobiological Significance. University of Chicago Press, Chicago, pp. 65–101.
- Benson, R.B.J., Butler, R.J., Carrano, P.M., O'Connor, M.T., 2012. Air-filled postcranial bones in theropod dinosaurs: physiological implications and the 'reptile'-bird transition. *Biological Reviews* 87: 168–193.
- Benton, M. J., Clark, J. M., 1988. Archosaur phylogeny and the relationships of the Crocodylia. *The Phylogeny and Classification of the Tetrapods*, 1, 295–338.
- Benton, M.J., Pearson, P.N., 2001. Speciation in the fossil record. *Trends in Ecology & Evolution* 16, 405–411. [https://doi.org/10.1016/S0169-5347\(01\)02149-8](https://doi.org/10.1016/S0169-5347(01)02149-8)
- Benton, M.J., Csiki, Z., Grigorescu, D., Redelstorff, R., Sander, P.M., Stein, K., Weishampel, D.B., 2010. Dinosaurs and the island rule: The dwarfed dinosaurs from Hateg Island. *Palaeogeography, Palaeoclimatology, Palaeoecology* 293, 438–454. <https://doi.org/10.1016/j.palaeo.2010.01.026>
- Benton, M.J., Dunhill, A.M., Lloyd, G.T., Marx, F.G., 2011. Assessing the quality of the fossil record: insights from vertebrates. *Geological Society, London, Special Publications* 358, 63–94. <https://doi.org/10.1144/SP358.6>
- Berreteaga, A., 2008. Estudio estratigráfico, sedimentológico y paleontológico de los yacimientos con fósiles de vertebrados del Cretácico final de la región Vasco-Cantábrica. Universidad del País Vasco. Doctoral Thesis, 387 pp.
- Berreteaga, A., Pereda Suberbiola, X., Floquet, M., Olivares, M., Etxebarria, N., Iriarte, E., Badiola Kortabitarte, A., Elorza, J., Astibia Ayerra, H., 2008. Datos sedimentológicos y tafonómicos de enclaves finicretácicos con fósiles de vertebrados de la Formación Sobrepeña (Burgos, Región Vasco-Cantábrica). *Geo-Temas* 10, 1278–1280.
- Berreteaga, A., Poyato-Ariza, F.J., Pereda-Suberbiola, X., 2011. A new actinopterygian fauna from the latest Cretaceous of Quintanilla la Ojada (Burgos, Spain). *Geodiversitas* 33, 285–301. <https://doi.org/10.5252/g2011n2a6>
- Bingham, C., 1974. An antipodally symmetric distribution on the sphere. *The Annals of Statistics*, 1201–1225.
- Bininda-Emonds, O.R.P., Cardillo, M., Jones, K.E., MacPhee, R.D.E., Beck, R.M.D., Grenyer, R., Price, S.A., Vos, R.A., Gittleman, J.L., Purvis, A., 2007. The delayed rise of present-day mammals. *Nature* 446, 507–512. <https://doi.org/10.1038/nature05634>
- Blain, H.A., Canudo, J.I., Cuenca-Bescós, G., López-Martínez, N., 2010. Amphibians and squamate reptiles from the latest Maastrichtian (Upper Cretaceous) of Blasi 2 (Huesca, Spain). *Cretaceous Research* 31, 433–446. <https://doi.org/10.1016/j.cretres.2010.06.001>
- Blake, S.F., 1940. *Paralbula*, a new fossil fish based on dental plates from the Eocene and Miocene of Maryland. *Washington Academy of Sciences Journal* 30, 205–209.
- Blanco, A., Puértolas-Pascual, E., Marmi, J., Vila, B., Sellés, A. G., 2014. *Allodaposuchus palustris* sp. nov. from the Upper Cretaceous of Fumanya (South-Eastern Pyrenees, Iberian Peninsula): systematics, palaeoecology and palaeobiogeography of the enigmatic allodaposuchian crocodylians. *PLoS One*, 9(12), e115837.

- Blanco, A., Fortuny, J., Vicente, A., Luján, À.H., García-Marçà, J.A., Sellés, A.G., 2015a. A new species of *Allodaposuchus* (Eusuchia, Crocodylia) from the Maastrichtian (Late Cretaceous) of Spain: phylogenetic and paleobiological implications. *PeerJ* 3, e1171. <https://doi.org/10.7717/peerj.1171>
- Blanco, A., Méndez, J.M., Marmi, J., 2015b. The fossil record of the uppermost Maastrichtian Reptile Sandstone (Trempe Formation, northeastern Iberian Peninsula). *Spanish Journal of Paleontology* 30, 147–160. <https://doi.org/10.7203/sjp.30.1.17231>
- Blanco, A., Prieto-Márquez, A., De Esteban-Trivigno, S., 2015c. Diversity of hadrosauroid dinosaurs from the Late Cretaceous Ibero-Armorican Island (European Archipelago) assessed from dentary morphology. *Cretaceous Research* 56, 447–457. <https://doi.org/10.1016/j.cretres.2015.04.001>
- Blanco, A., Bolet, A., Blain, H.-A., Fondevilla, V., Marmi, J., 2016. Late Cretaceous (Maastrichtian) amphibians and squamates from northeastern Iberia. *Cretaceous Research* 57, 624–638. <https://doi.org/10.1016/j.cretres.2015.07.005>
- Blanco, A., Brochu, C.A., 2017. Intra- and interspecific variability in allodaposuchid crocodylomorphs and the status of western European taxa. *Historical Biology* 29, 495–508. <https://doi.org/10.1080/08912963.2016.1201081>
- Blanco, A., Szabó, M., Blanco-Lapaz, À., Marmi, J., 2017. Late Cretaceous (Maastrichtian) Chondrichthyes and Osteichthyes from northeastern Iberia. *Palaeogeography, Palaeoclimatology, Palaeoecology* 465, 278–294. <https://doi.org/10.1016/j.palaeo.2016.10.039>
- Blanco, A., Puértolas-Pascual, E., Marmi, J., Moncunill-Solé, B., Llácer, S., Rössner, G.E., 2020. Late Cretaceous (Maastrichtian) crocodyliforms from north-eastern Iberia: a first attempt to explain the crocodyliform diversity based on tooth qualitative traits. *Zoological Journal of the Linnean Society* 189, 584–617. <https://doi.org/10.1093/zoolinnean/zlzlz106>
- Boas, J. E. V., 1929. Biologisch-anatomische Studien über den Hals der Vögel. *Det Kongelige Danske Videnskabernes Selskabs Skrifter, Naturvidenskabelig og Matematisk Afdeling* 9: 105–222.
- Bohor, B.F., Foord, E.E., Modreski, P.J., Triplehorn, D.M., 1984. Mineralogic Evidence for an Impact Event at the Cretaceous-Tertiary Boundary. *Science* 224, 867–869. <https://doi.org/10.1126/science.224.4651.867>
- Bolli, H., 1951. The Genus *Globotruncana* in Trinidad, B. W. I.: Notes on Occurrence, Nomenclature and Relationships between species. *Journal of Paleontology* 25, 187–199.
- Bonaparte, J. F., Coria, R. A., 1993. A new and huge titanosaur sauropod from the Rio Limay Formation (Albian-Cenomanian) of Neuquen Province, Argentina. *Ameghiniana*, 30, 271–282.
- Bourdon, E., C. Mourer-Chauvire, Y. Laurent., 2014. The birds (Aves) from the Early Eocene of La Borie, southern France. *Acta Palaentologica Polonica* 61(1), 175–190.
- Bravo, A.M., Gaete, R., 2015. Titanosaur eggshells from the Trempe Formation (Upper Cretaceous, Southern Pyrenees, Spain). *Historical Biology* 27 (8), 1079–1089
- Brinkman, D.B., Newbrey, M.G., Neuman, A.G., 2014. Diversity and paleoecology of actinopterygian fish from vertebrate microfossil localities of the Maastrichtian Hell Creek Formation of Montana, in: Wilson, G.P., Clemens, W.A., Horner, J.R., Hartman, J. (Eds.), *Through the End of the Cretaceous in the Type Locality of the Hell Creek Formation in*

- Montana and Adjacent Areas: : Geological Society of America Special Paper 503. Geological Society of America, pp. 247–270. [https://doi.org/10.1130/2014.2503\(09\)](https://doi.org/10.1130/2014.2503(09))
- Brinkmann, W., 1992. Die krokodilier-fauna aus der Unter-Kreide (Ober-Barremium) von Uña (Provinz Cuenca, Spanien). *Berliner Geowissenschaftliche Abhandlungen* 5, 1–123.
- Britt, B.B., 1993. Pneumatic postcranial bones in dinosaurs and other archosaurs. University of Calgary. Doctoral Thesis, 383 pp.
- Britt, B.B., 1997. Postcranial pneumaticity, in: Currie, P.J., Padian, K. (Eds.), *Encyclopedia of Dinosaurs*. Academic Press, San Diego, pp. 590–593.
- Brochu, C.A., 1997. A review of “*Leidyosuchus*” (Crocodyliformes, Eusuchia) from the Cretaceous through Eocene of North America. *Journal of Vertebrate Paleontology* 17, 679–697.
- Brochu, C.A., 2004. A new Late Cretaceous gavialoid crocodylian from eastern North America and the phylogenetic relationships of thoracosaurids. *Journal of Vertebrate Paleontology* 24, 610–633.
- Brocklehurst, N., Kammerer, C.F., Fröbisch, J., 2013. The early evolution of synapsids, and the influence of sampling on their fossil record. *Paleobiology* 39, 470–490. <https://doi.org/10.1666/12049>
- Bronzati, M., Montefeltro, F.C., Langer, M.C., 2015. Diversification events and the effects of mass extinctions on Crocodyliformes evolutionary history. *Royal Society Open Science* 2, 140385. <https://doi.org/10.1098/rsos.140385>
- Brown, B., 1905. The osteology of *Champsosaurus* Cope. *Memoirs of the American Museum of Natural History* 9, 1–26.
- Brusatte, S.L., Vremir, M., Csiki-Sava, Z., Turner, A.H., Watanabe, A., Erickson, G.M., Norell, M.A., 2013. The Osteology of *Balaur bondoc*, an Island-Dwelling Dromaeosaurid (Dinosauria: Theropoda) from the Late Cretaceous of Romania. *Bulletin of the American Museum of Natural History* 374, 1–100. <https://doi.org/10.1206/798.1>
- Brusatte, S.L., Butler, R.J., Barrett, P.M., Carrano, M.T., Evans, D.C., Lloyd, G.T., Mannion, P.D., Norell, M.A., Peppe, D.J., Upchurch, P., Williamson, T.E., 2015. The extinction of the dinosaurs. *Biological Reviews* 90, 628–642. <https://doi.org/10.1111/brv.12128>
- Brusatte, S.L., Candeiro, C.R.A., Simbras, F.M., 2017. The last dinosaurs of Brazil: The Bauru Group and its implications for the end-Cretaceous mass extinction. *Anais da Academia Brasileira de Ciências* 89, 1465–1485. <https://doi.org/10.1590/0001-3765201720160918>
- Buatois, L.A., Mángano, M.G., 2011. *Ichnology: Organism-substrate interactions in space and time*. Cambridge University Press. 366 pp.
- Buffetaut, E., 2008. Late Cretaceous pterosaurs from France: a review. *Zitteliana* B28, 249–255.
- Buffetaut, E., Clarke, J.B., Le Loeuff, J., 1996. A terminal Cretaceous pterosaur from the Corbieres (southern France) and the problem of pterosaur extinction. *Bulletin of the Societe geologique de France* 167, 753–759.
- Buffetaut, E., Laurent, Y., Le Loeuff, J., Bilotte, M., 1997. A terminal Cretaceous giant pterosaur from the French Pyrenees. *Geological Magazine* 134, 553–556. <https://doi.org/10.1017/S0016756897007449>
- Buffetaut, E., Le Loeuff, J., 1997. Late Cretaceous dinosaurs from the foothills of the Pyrenees. *Geology Today* 13, 60–68.

- Buffetaut, E., Grigorescu, D., Csiki, Z., 2002. A new giant pterosaur with a robust skull from the latest Cretaceous of Romania. *Naturwissenschaften* 89, 180–184. <https://doi.org/10.1007/s00114-002-0307-1>
- Buffetaut, E., D. Angst., 2013. New evidence of a giant bird from the Late Cretaceous of France. *Geological Magazine* 150:173–176.
- Buffetaut, E., D. Angst., 2020. *Gargantuavis* is an insular basal ornithurine: a comment on Mayr et al., 2020, 'A well preserved pelvis from the Maastrichtian of Romania suggests that the enigmatic *Gargantuavis* is neither an ornithurine bird nor an insular endemic'. *Cretaceous Research* 112:104438.
- Buscalioni, A.D., Fregenal, M.A., Bravo, A., Poyato-Ariza, F.J., Sanchíz, B., Báez, A.M., Cambra Moo, O., Martín Closas, C., Evans, S.E., Marugán Lobón, J., 2008. The vertebrate assemblage of Buenache de la Sierra (Upper Barremian of Serranía de Cuenca, Spain) with insights into its taphonomy and palaeoecology. *Cretaceous Research* 29, 687–710. <https://doi.org/10.1016/j.cretres.2008.02.004>
- Calvo, J.O., Bonaparte, J.F., 1991. *Andesaurus delgadoi* gen. et. sp. nov. (Saurischia-Sauropoda), dinosaurio Titanosauridae de la Formación Río Limay (Albiano-Cenomaniano), Neuquén, Argentina. *Ameghiniana* 28, 303–310.
- Campos, D.D.A., Kellner, A.W., Bertini, R.J., Santucci, R.M., 2005. On a titanosaurid (Dinosauria, Sauropoda) vertebral column from the Bauru group, Late Cretaceous of Brazil. 565–593. *Arquivos do Museu Nacional* 63, 565–593.
- Candeiro, C.R.A., Martinelli, A.G., 2005. Abelisauroides and Carcharodontosauridae (Theropoda, Dinosauria) in the Cretaceous of South America. Paleogeographical and geochronological implications. *Sociedade & Natureza Uberlândia* 17, 5–19.
- Candeiro, C.R.A., Martinelli, A.G., Avilla, L.S., Rich, T.H., 2006. Tetrapods from the Upper Cretaceous (Turonian–Maastrichtian) Bauru Group of Brazil: a reappraisal. *Cretaceous Research* 27, 923–946. <https://doi.org/10.1016/j.cretres.2006.05.002>
- Candeiro, C.R.A., 2009. Vertebrates of the Marília Formation (Late Maastrichtian) from the Peirópolis Paleontological Site: toward a better understanding. *Earth Sciences Research Journal* 13, 6–15.
- Candeiro, C.R.A., Agnolin, F., Martinelli, A.G., Buckup, P.A., 2012. First bird remains from the Upper Cretaceous of the Peirópolis site, Minas Gerais state, Brazil. *Geodiversitas* 34, 617–624. <https://doi.org/10.5252/g2012n3a8>
- Canudo, J.I., 2001. Descripción de un fragmento proximal de fémur de Titanosauridae (Dinosauria, Sauropoda) del Maastrichtense superior de Serraduy (Huesca), in: *Actas de Las XVII Jornadas de La Sociedad Española de Paleontología. Los Fósiles y La Paleogeografía*. Albarracín, pp. 255–262.
- Canudo, J.I., 2018. The Collection of Type Fossils of the Natural Science Museum of the University of Zaragoza (Spain). *Geoheritage* 10, 385–392. <https://doi.org/10.1007/s12371-017-0228-1>
- Canudo, I., Cruzado-Caballero, P., Moreno-Azanza, M., 2005. Possible theropod predation evidence in hadrosaurid dinosaurs from the Upper Maastrichtian (Upper Cretaceous) of Arén (Huesca, Spain). *Kaupia. Darmstädter Beiträge zur Naturgeschichte* 14, 9–13.
- Canudo, J.I., Oms, O., Vila, B., Galobart, À., Fondevilla, V., Puértolas-Pascual, E., Sellés, A.G., Cruzado-Caballero, P., Dinarès-Turell, J., Vicens, E., Castanera, D., Company, J., Burrell, L., Estrada, R., Marmi, J., Blanco, A., 2016. The upper Maastrichtian dinosaur fossil record from the southern Pyrenees and its contribution to the topic of the Cretaceous–Palaeogene mass

- Carsey, D.O., 1926. Foraminifera of the Cretaceous of central Texas. University of Texas Bulletin 2612, 1–56.
- Casanovas, M.L., Santafé-Llopis, J.V., Isidro-Llorens, A., 1993. *Pararhabdodon isonensis* n. gen. n. sp. (Dinosauria). Estudio morfológico, radio-tomográfico y consideraciones biomecánicas 26-27:121-131. Paleontologia i Evolució 26–27, 121–132.
- Casanovas, M.L., Pereda Suberbiola, X., Santafé, J. V., Weishampel, D.B., 1999. A primitive euhadrosaurian dinosaur from the uppermost Cretaceous of the Ager syncline (southern Pyrenees, Catalonia). Geologie en Mijnbouw/Netherlands Journal of Geosciences 78, 345–356. <https://doi.org/10.1023/a:1003859501941>
- Cau, A., 2018. The assembly of the avian body plan: a 160 million year long process. Bollettino della Società Paleontologica Italiana 57, 1–25.
- Cavin, L., 1999. Osteichthyes from the Upper Cretaceous of Laño (Iberian Peninsula). Estudios del Museo de Ciencias Naturales de Álava 14, 105–110.
- Chadima, M., Hroudá, F., 2006. Remasoft 3.0 a user-friendly paleomagnetic data browser and analyzer. Travaux Geophysiques. 27, 20-21.
- Chanvry, E., Deschamps, R., Joseph, P., Puigdefàbregas, C., Poyatos-Moré, M., Serra-Kiel, J., García, D., Teinturier, S., 2018. The influence of intrabasinal tectonics in the stratigraphic evolution of piggyback basin fills: Towards a model from the Tremp-Graus-Ainsa Basin (South-Pyrenean Zone, Spain). Sedimentary Geology 377, 34–62. <https://doi.org/10.1016/j.sedgeo.2018.09.007>
- Chiappe, L. M., 2002. Osteology of the flightless *Patagopteryx deferrariisi* from the Late Cretaceous of Patagonia (Argentina); pp. 281–316 in L.M. Chiappe and L.M. Witmer (eds.), Mesozoic Birds. University of California Press, Berkeley.
- Chiappe, L. M., C.A. Walker., 2002. Skeletal morphology and systematics of the Cretaceous Euenantiornithes (Ornithothoraces: Enantiornithes); pp. 240–267 in L.M. Chiappe and L.M. Witmer (eds.), Mesozoic Birds. University of California Press, Berkeley.
- Chiarenza, A.A., Mannion, P.D., Lunt, D.J., Farnsworth, A., Jones, L.A., Kelland, S.-J., Allison, P.A., 2019. Ecological niche modelling does not support climatically-driven dinosaur diversity decline before the Cretaceous/Paleogene mass extinction. Nature Communications 10, 1091. <https://doi.org/10.1038/s41467-019-08997-2>
- Chiarenza, A.A., Farnsworth, A., Mannion, P.D., Lunt, D.J., Valdes, P.J., Morgan, J. V., Allison, P.A., 2020. Asteroid impact, not volcanism, caused the end-Cretaceous dinosaur extinction. Proceedings of the National Academy of Sciences 117, 17084–17093. <https://doi.org/10.1073/pnas.2006087117>
- Choi, S., Moreno-Azanza, M., Csiki-Sava, Z., Prondvai, E., Lee, Y.N., 2020. Comparative crystallography suggests maniraptoran theropod affinities for latest Cretaceous European ‘geckoid’ eggshell. Papers in Palaeontology 6, 265–292. <https://doi.org/10.1002/spp2.1294>
- Choukroune, P., 1989. The Ecos Pyrenean deep seismic profile reflection data and the overall structure of an orogenic belt. Tectonics 8, 23–39. <https://doi.org/10.1029/TC008i001p00023>
- Clarke, J.A., M.A. Norell., 2002. The morphology and phylogenetic position of *Apsaravis ukhaana* from the Late Cretaceous of Mongolia. American Museum Novitates 3387: 1–46.

- Clarke, J. A., Z. Zhou, F. Zhang., 2006. Insight into the evolution of avian flight from a new clade of Early Cretaceous ornithurines from China and the morphology of *Yixianornis grabaui*. *Journal of Anatomy* 208: 287–308.
- Codrea, V., Vremir, M., Jipa, C., Godefroit, P., Csiki, Z., Smith, T., Fărcaș, C., 2010. More than just Nopcsa's Transylvanian dinosaurs: A look outside the Hațeg Basin. *Palaeogeography, Palaeoclimatology, Palaeoecology* 293, 391–405. <https://doi.org/10.1016/j.palaeo.2009.10.027>
- Codrea, V.A., Venczel, M., Solomon, A., 2017. A new family of teioid lizards from the Upper Cretaceous of Romania with notes on the evolutionary history of early teioids. *Zoological Journal of the Linnean Society*. <https://doi.org/10.1093/zoolinnean/zlx008>
- Colin, J.-P., Néraudeau, D., Nel, A., Perrichot, V., 2011. Termite coprolites (Insecta: Isoptera) from the Cretaceous of western France: A palaeoecological insight. *Revue de Micropaléontologie* 54, 129–139. <https://doi.org/10.1016/j.revmic.2011.06.001>
- Company, J., 2004. Vertebrados continentales del Cretácico superior (Campaniense-Maastrichtiense) de Valencia. Universidad de Valencia. Doctoral Thesis, 410 pp.
- Company, J., Galobart, À., Gaete, R., 1998. First data on the hadrosaurid dinosaurs (Ornithischia, Dinosauria) from the Upper Cretaceous of Valencina, Spain. *Oryctos* 1, 121–126.
- Company, J., Ruiz-Omeñaca, J.I., Suberbiola, X.P., 1999. A long-necked pterosaur (Pterodactyloidea, Azhdarchidae) from the Upper Cretaceous of Valencia, Spain. *Geologie en Mijnbouw/Netherlands Journal of Geosciences* 78, 319–333. <https://doi.org/10.1023/a:1003851316054>
- Company, J., Pereda-Suberbiola, X., Ruiz-Omeñaca, J.I., 2009. Last Cretaceous dinosaur faunas from Eastern Iberia into its regional paleogeographic context. Faunal composition and palaeobiogeographical implications., in: *Actas de Las IV Jornadas Internacionales Sobre Paleontología de Dinosaurios y Su Entorno Salas de Los Infantes, Burgos*. Salas de los Infantes Burgos (Spain), pp. 17–44.
- Company, J., Cruzado-Caballero, P., Canudo, J.I., 2015. Presence of diminutive hadrosaurids (Dinosauria: Ornithomimidae) in the Maastrichtian of the south-central Pyrenees (Spain). *Journal of Iberian Geology* 41, 71–81. [https://doi.org/10.5209/rev\\_JIGE.2015.v41.n1.48656](https://doi.org/10.5209/rev_JIGE.2015.v41.n1.48656)
- Conti, S., Vila, B., Sellés, A.G., Galobart, À., Benton, M.J., Prieto-Márquez, A., 2020. The oldest lambeosaurine dinosaur from Europe: Insights into the arrival of Tsintaosaurini. *Cretaceous Research* 107, 104286. <https://doi.org/10.1016/j.cretres.2019.104286>
- Cook, T.D., Newbrey, M.G., Brinkman, D.B., Kirkland, J.I., 2014. Euselachians from the freshwater deposits of the Hell Creek Formation of Montana, in: *Through the End of the Cretaceous in the Type Locality of the Hell Creek Formation in Montana and Adjacent Areas*. Geological Society of America. [https://doi.org/10.1130/2014.2503\(08\)](https://doi.org/10.1130/2014.2503(08))
- Corral, J.-C., Pueyo, E.L., Berreteaga, A., Rodríguez-Pintó, A., Sánchez, E., Pereda-Suberbiola, X., 2016. Magnetostratigraphy and lithostratigraphy of the Laño vertebrate-site: Implications in the uppermost Cretaceous chronostratigraphy of the Basque-Cantabrian Region. *Cretaceous Research* 57, 473–489. <https://doi.org/10.1016/j.cretres.2015.07.015>
- Corral, J.C., Berreteaga, A., Poyato-Ariza, F., Bardet, N., Cappetta, H., Floquet, M., Astibia, H., Badiola, A., Pereda-Suberbiola, X., 2021. Stratigraphy, age, and vertebrate palaeontology of the latest Cretaceous Quintanilla la Ojada locality (Basque-Cantabrian Region, northern Spain): a synthesis. *Comptes Rendus Palevol* 20, 92–117.

- Costa, E., Garcés, M., López-Blanco, M., Beamud, E., Gómez-Paccard, M., Larrasoña, J.C., 2010. Closing and continentalization of the South Pyrenean foreland basin (NE Spain): magnetochronological constraints. *Basin Research* 22, 904–917. <https://doi.org/10.1111/j.1365-2117.2009.00452.x>
- Courtillot, V., Féraud, G., Maluski, H., Vandamme, D., Moreau, M.G., Besse, J., 1988. Deccan flood basalts and the Cretaceous/Tertiary boundary. *Nature* 333, 843–846. <https://doi.org/10.1038/333843a0>
- Courtillot, V., Renne, P.R., 2003. On the ages of flood basalt events. *Comptes Rendus Geoscience* 335, 113–140. [https://doi.org/10.1016/S1631-0713\(03\)00006-3](https://doi.org/10.1016/S1631-0713(03)00006-3)
- Courtillot, V., Fluteau, F., 2010. Cretaceous Extinctions: The Volcanic Hypothesis. *Science* 328, 973–974. <https://doi.org/10.1126/science.328.5981.973-b>
- Crawford, D.S., Evans, D.C., 2016. A large gavialoid (Crocodylia: Eusuchia) from the Upper Cretaceous Hell Creek Formation of South Dakota, U.S.A., in: IV Canadian Society of Vertebrate Palaeontology Meeting. Toronto, p. 20.
- Cruzado-Caballero, P., Canudo, J.I., Ruiz-Omeñaca, J.I., 2005. Nuevas evidencias de la presencia de hadrosaurios lambeosaurios (Dinosauria) en el Maastrichtense superior de la Península Ibérica (Arén, Huesca). *Geogaceta* 3, 47–50.
- Cruzado-Caballero, P., Canudo, J.I., Ruiz-Omeñaca, J.I., 2009. Los fémures de Blasi (Arén, Huesca, Spain): una contribución a los hadrosauroideos europeos del Maastrichtense superior, in: *Actas de Las IV Jornadas Internacionales Sobre Paleontología de Dinosaurios y Su Entorno. Colectivo Arqueológico y Paleontológico de Salas. Salas de los Infantes Burgos Spain*, pp. 197–205.
- Cruzado-Caballero, P., Pereda-Suberbiola, X., Ruiz-Omeñaca, J.I., 2010a. *Blasisaurus canudo* gen. et sp. nov., a new lambeosaurine dinosaur (hadrosauridae) from the latest cretaceous of Arén (Huesca, Spain). *Canadian Journal of Earth Sciences* 47, 1507–1517. <https://doi.org/10.1139/E10-081>
- Cruzado-Caballero, P., Ruiz-Omeñaca, J.I., Canudo, J.I., 2010b. Review of the fossil record of spanish hadrosaur remains, in: Moreno-Azanza, M., Díaz-Martínez, I., Gasca, J.M., Melero-Rubio, M., Rabal-Garcés, R. y Sauqué, V. (Eds.), *Cidaris. VIII Encuentro de Jóvenes Investigadores en Paleontología*, pp. 99–105.
- Cruzado-Caballero, P., Ruiz-Omeñaca, J.I., Canudo, J.I., 2010c. Evidencias de la coexistencia de dinosaurios hadrosaurinos y lambeosaurinos en el Maastrichtiano superior de la Península Ibérica (Arén, Huesca, España). *Ameghiniana* 47, 153–164. <https://doi.org/10.5710/AMGH.v47i2.6>
- Cruzado-Caballero, P., Puértolas-Pascual, E., Canudo, J.I., Castanera, D., Gasca, J.M., Moreno-Azanza, M., 2012. New hadrosaur remains from the Late Maastrichtian of Huesca (NE Spain), in: Royo-Torres, R., Gascó, F., Alcalá, L. (Eds.), *10th Annual Meeting of the European Association of Vertebrate Palaeontologists*, pp. 45–48.
- Cruzado-Caballero, P., Canudo, J.I., Moreno-Azanza, M., Ruiz-Omeñaca, J.I., 2013. New material and phylogenetic position of *Arenysaurus ardevoli*, a lambeosaurine dinosaur from the late Maastrichtian of Arén (Northern Spain). *Journal of Vertebrate Paleontology* 33, 1367–1384. <https://doi.org/10.1080/02724634.2013.772061>
- Cruzado-Caballero, P., Ruiz-Omeñaca, J.I., Gaete, R., Riera, V., Oms, O., Canudo, J.I., 2014. A new hadrosaurid dentary from the latest Maastrichtian of the Pyrenees (north Spain) and the high diversity of the duck-billed dinosaurs of the Ibero-Armorican Realm at the very end of

- Cruzado-Caballero, P., Fortuny, J., Llacer, S., Canudo, J.I., 2015. Paleoneuroanatomy of the European lambeosaurine dinosaur *Arenysaurus ardevoli*. *PeerJ* 2015, 1–16. <https://doi.org/10.7717/peerj.802>
- Cruzado-Caballero, P., Canudo, J.I., De Valais, S., Frigola, J., Barriuso, E., Fortuny, J., 2021. Bioerosion and palaeoecological association of osteophagous insects in the Maastrichtian dinosaur *Arenysaurus ardevoli*. *Lethaia*. <https://doi.org/10.1111/let.12456>
- Csiki, Z., Codrea, V., Jipa-Murzea, C., Godefroit, P., 2010a. A partial titanosaur (Sauropoda, Dinosauria) skeleton from the Maastrichtian of Nalat-Vad, Hateg Basin, Romania. *Neues Jahrbuch für Geologie und Paläontologie - Abhandlungen* 258, 297–324. <https://doi.org/10.1127/0077-7749/2010/0098>
- Csiki, Z., Grigorescu, D., Codrea, V., Therrien, F., 2010b. Taphonomic modes in the Maastrichtian continental deposits of the Hațeg Basin, Romania—Palaeoecological and palaeobiological inferences. *Palaeogeography, Palaeoclimatology, Palaeoecology* 293, 375–390. <https://doi.org/10.1016/j.palaeo.2009.10.013>
- Csiki, Z., Vremir, M., Brusatte, S.L., Norell, M.A., 2010c. An aberrant island-dwelling theropod dinosaur from the Late Cretaceous of Romania. *Proceedings of the National Academy of Sciences* 107, 15357–15361. <https://doi.org/10.1073/pnas.1006970107>
- Csiki-Sava, Z., Buffetaut, E., Ősi, A., Pereda-Suberbiola, X., Brusatte, S.L., 2015. Island life in the Cretaceous - faunal composition, biogeography, evolution, and extinction of land-living vertebrates on the Late Cretaceous European archipelago. *ZooKeys* 469, 1–161. <https://doi.org/10.3897/zookeys.469.8439>
- Csiki-Sava, Z., Vremir, M., Vasile, Ș., Brusatte, S.L., Dyke, G., Naish, D., Norell, M.A., Totoianu, R., 2016. The East Side Story – The Transylvanian latest Cretaceous continental vertebrate record and its implications for understanding Cretaceous–Paleogene boundary events. *Cretaceous Research* 57, 662–698. <https://doi.org/10.1016/j.cretres.2015.09.003>
- Csiki-Sava, Z., Vremir, M., Meng, J., Brusatte, S.L., Norell, M.A., 2018. Dome-headed, small-brained island mammal from the Late Cretaceous of Romania. *Proceedings of the National Academy of Sciences* 115, 4857–4862. <https://doi.org/10.1073/pnas.1801143115>
- Csiki-Sava, Z., Vremir, M., Meng, J., Vasile, Ș., Brusatte, S.L., Norell, M.A., 2022. Spatial and Temporal Distribution of the Island-Dwelling Kogaionidae (Mammalia, Multituberculata) in the Uppermost Cretaceous of Transylvania (Western Romania). *Bulletin of the American Museum of Natural History* 456. <https://doi.org/10.1206/0003-0090.456.1.1>
- Cuevas, J.L., 1992. Estratigrafía del «Garumniense» de la Conca de Tremp. Prepirineo de Lérida. *Acta Geológica Hispánica* 27, 95–108.
- Currie, P.J., Rigby, J.K., Sloan, R.E., 1990. Theropod teeth from the Judith River Formation of southern Alberta, Canada, in: Carpenter, K., Currie, P.J. (Eds.), *Dinosaur Systematics: Approaches and Perspectives*. Cambridge University Press, New York, pp. 107–125.
- Currie, P.J., Peng, J.-H., 1993. A juvenile specimen of *Sauornithoides mongoliensis* from the Upper Cretaceous of northern China. *Can J Earth Sci.* 30 (10):2224–2230. doi:10.1139/e93-193.
- Cushman, J.A., 1933. Some new foraminiferal genera. *Contributions from the Cushman Laboratory for Foraminiferal Research* 9, 32–38.

- Cushman, J. A., 1938. Cretaceous species of *Guembelina* and related genera. Contributions from the Cushman Laboratory for Foraminiferal Research. 14, 2-28.
- Dalla Vecchia, F.M., Riera, F.M., Oms, J.O., Dinarès-Turell, J., Gaete, R., Galobart, A., 2013. The last pterosaurs: First record from the uppermost Maastrichtian of the Tremp Syncline (Northern Spain). *Acta Geologica Sinica* 87, 1198–1227. <https://doi.org/10.1111/1755-6724.12146>
- Dameron, S.N., Leckie, R.M., Clark, K., MacLeod, K.G., Thomas, D.J., Lees, J.A., 2017. Extinction, dissolution, and possible ocean acidification prior to the Cretaceous/Paleogene (K/Pg) boundary in the tropical Pacific. *Palaeogeography, Palaeoclimatology, Palaeoecology* 485, 433–454. <https://doi.org/10.1016/j.palaeo.2017.06.032>
- Dartevelle, E., Casier, E., 1949. Les poissons fossiles du Bas-Congo et des régions voisines (Deuxieme partie). *Annales du Musée du Congo Belge* 2, 201–259.
- De Celis, A., Narváez, I., Ortega, F., 2020. Spatiotemporal palaeodiversity patterns of modern crocodiles (Crocodyliformes: Eusuchia). *Zoological Journal of the Linnean Society* 189, 635–656. <https://doi.org/10.1093/zoolinnean/zlz038>
- de França, M.A.G., Langer, 2005. A new freshwater turtle (Reptilia, Pleurodira, Podocnemidae) from the Upper Cretaceous (Maastrichtian) of Minas Gerais, Brazil. *Geodiversitas* 27, 391–411.
- de Lapparent de Broin, F. Murelaga, X., 1996. Turtles from Upper Cretaceous of Laño (Iberian Peninsula). *Comptes Rendus de l'Académie des Sciences. Série 2. Sciences de la Terre et des Planètes* 323, 729–735.
- Delfino, M., Codrea, V., Folie, A., Dica, P., Godefroit, P., Smith, T., 2008. A complete skull of *Allodaposuchus precedens* Nopcsa, 1928 (Eusuchia) and a reassessment of the morphology of the taxon based on the romanian remains. *Journal of Vertebrate Paleontology* 28, 111–122.
- DePalma, R.A., Smit, J., Burnham, D.A., Kuiper, K., Manning, P.L., Oleinik, A., Larson, P., Maurrasse, F.J., Vellekoop, J., Richards, M.A., Gurche, L., Alvarez, W., 2019. A seismically induced onshore surge deposit at the KPg boundary, North Dakota. *Proceedings of the National Academy of Sciences* 116, 8190–8199. <https://doi.org/10.1073/pnas.1817407116>
- De Porta, J., Kevdes, M., Solé de Porta, N., Civis, J., 1985. Palinología del Maastrichtiense del Barranco de la Posa, Lérida, España. Problemática regional. *Revista d'Investigacions Geològiques* 40, 5–28.
- Deramond, J., Souquet, P., Fondécave-Wallez, M.-J., Specht, M., 1993. Relationships between thrust tectonics and sequence stratigraphy surfaces in foredeeps: model and examples from the Pyrenees (Cretaceous-Eocene, France, Spain). *Geological Society, London, Special Publications* 71, 193–219. <https://doi.org/10.1144/GSL.SP.1993.071.01.09>
- Dercourt, J., Gaetani, M., Vrielynck, B., Barrier, E., Biju-Duval, B., Brunet, M.-F., Cadet, J.-P., Crasquin, S., Sandulescu, M., 2000. Atlas Peri-Tethys. *Palaeogeographical maps. CCGM/CGMW*, Paris.
- D'Hondt, S., 2005. Consequences of the Cretaceous/Paleogene Mass Extinction for Marine Ecosystems. *Annual Review of Ecology, Evolution, and Systematics* 36, 295–317. <https://doi.org/10.1146/annurev.ecolsys.35.021103.105715>
- Dias-Brito, D., Musacchio, E.A., Castro, J.D., Maranhão, M.S., Suárez, J.M., Rodrigues, R., 2001. Grupo Bauru: uma unidade continental do Cretaceo no Brasil - concepções baseadas em

- dados micropaleontologicos, isotopicos e estratigraficos. *Revue de Paléobiologie* 20, 245–304.
- Díaz-Molina, M., 1987. Sedimentacion sintectónica asociada a una subida relativa del nivel del mar durante el Cretácico Superior (Fm. Tremp, provincia de Lérida). *Estudios Geológicos*. Número extraordinario Galve-Tremp. 69–93.
- Díaz-Molina, M., Kálin, O., Benito, M.I., López-Martínez, N., Vicens, E., 2007. Depositional setting and early diagenesis of the dinosaur eggshell-bearing Aren Fm at Bastus, Late Campanian, south-central Pyrenees. *Sedimentary Geology* 199, 205–221. <https://doi.org/10.1016/j.sedgeo.2007.02.002>
- Díez-Canseco, D., Arz, J.A., Benito, M.I., Díaz-Molina, M., Arenillas, I., 2014. Tidal influence in redbeds: A palaeoenvironmental and biochronostratigraphic reconstruction of the Lower Tremp Formation (South-Central Pyrenees, Spain) around the Cretaceous/Paleogene boundary. *Sedimentary Geology* 312, 31–49. <https://doi.org/10.1016/j.sedgeo.2014.06.008>
- Díez-Canseco, D., Buatois, L.A., Mángano, M.G., Díaz-Molina, M., Benito, M.I., 2016. Ichnofauna from coastal meandering channel systems (Upper Cretaceous Tremp Formation, South-Central Pyrenees, Spain): delineating the fluvial-tidal transition. *Journal of Paleontology* 90, 250–268. <https://doi.org/10.1017/jpa.2016.12>
- Díez Díaz, V., Pereda Suberbiola, X., Sanz, J.L., 2013. The axial skeleton of the titanosaur *Lirainosaurus astibiae* (Dinosauria: Sauropoda) from the latest Cretaceous of Spain. *Cretaceous Research* 43, 145–160. <https://doi.org/10.1016/j.cretres.2013.03.002>
- d'Orbigny, A., 1839. Foraminifères. In: de la Sagra, R. (ed.) *Histoire physique et naturelle de l'île de Cuba*. A. Bertrand, Paris, France 1-224.
- Dunham, R.J., 1962. Classification of Carbonate Rocks According to Depositional Texture. In: Ham, W.E., Ed., *Classification of Carbonate Rocks*, AAPG, Tulsa, 108-121.
- Dzombak, R.M., Sheldon, N.D., Mohabey, D.M., Samant, B., 2020. Stable climate in India during Deccan volcanism suggests limited influence on K–Pg extinction. *Gondwana Research* 85, 19–31. <https://doi.org/10.1016/j.gr.2020.04.007>
- Eberth, D.A., Shannon, M., Noland, 2007. A Bonebeds database: classification, Biases and Patterns Occurrence, in: Rogers, R.R., Eberth, D.A., Fiorillo, A.R. (Eds.), *Bonebeds: Genesis, Analysis, and Paleobiological Significance*. University of Chicago Press, Chicago, pp. 103–220.
- Ehrenberg, C.G., 1840. Über die Bildung der Kreidefelsen und des Kreidemergels durch unsichtbare Organismen. *Abhandlungen der Königlichen Akademie der Wissenschaften zu Berlin* 59–147.
- Eichenseer, H., 1988. Facies Geology of Late Maastrichtian to Early Eocene Coastal and Shallow Marine Sediments (Tremp-Graus Basin, Northeastern Spain). Universität Tübingen. Doctoral Thesis, 129 pp.
- El Naggar, Z.R., 1966. Stratigraphy and Planktonic Foraminifera of the Upper Cretaceous-Lower Tertiary in the Esna Idfu Region, Nile Valley, Egypt, U.A.R. *Bulletin of the British Museum (Natural History)*. Geology, Supplement 2, 291 pp.
- Estes, R., 1969. Studies on Fossil Phyllodont Fishes: Interrelationships and Evolution in the Phyllodontidae (Albuloidei). *Copeia* 2, 317–331.
- Estes, R., 1981. *Handbuch der Paläoherpetologie/Encyclopedia of Paleoherpetology*. Part 2. Gymnophiona, Caudata. Gustav Fischer Verlag, Stuttgart xv-115

- Fassett, J.E., Zielinski, J.R., Budahn, R.A., 2002. Dinosaurs that did not die: Evidence for Paleocene dinosaurs in the Ojo Alamo Sandstone, San Juan Basin, New Mexico, in: Koerble, C., McLeod, K.G. (Eds.), *Catastrophic Events and Mass Extinctions: Impacts and beyond*: Geological Society of America Special Paper 356. pp. 307–336.
- Fastovsky, D.E., 1987. Paleoenvironments of Vertebrate-Bearing Strata during the Cretaceous–Paleogene Transition, Eastern Montana and Western North Dakota. *PALAIOS* 2, 282. <https://doi.org/10.2307/3514678>
- Fastovsky, D.E., Sheehan, P.M., 2005. The extinction of the dinosaurs in North America. *GSA Today* 15, 4–10.
- Fastovsky, D.E., Bercovici, A., 2016. The Hell Creek Formation and its contribution to the Cretaceous–Paleogene extinction: A short primer. *Cretaceous Research* 57, 368–390. <https://doi.org/10.1016/j.cretres.2015.07.007>
- Feist, M., Colombo, F., 1983. La limite Crétacé-Tertiaire dans le nord-est de l'Espagne, du point de vue des charophytes. *Géologie Méditerranéenne* 10, 303–325. <https://doi.org/10.3406/geolm.1983.1273>
- Fernandes, L.A., Magalhães Ribeiro, C.M., 2015. Evolution and palaeoenvironment of the Bauru Basin (Upper Cretaceous, Brazil). *Journal of South American Earth Sciences* 61, 71–90. <https://doi.org/10.1016/j.jsames.2014.11.007>
- Fiorillo, A.R., 1988. Taphonomy of Hazard Homestead Quarry (Ogallala Group), Hitchcock County, Nebraska. *Rocky Mountain Geology* 26, 57–97.
- Fisher, R. A., 1953. Dispersion on a sphere. *Proceedings of the Royal Society of London. Series A. Mathematical and Physical Sciences* 217 (1130), 295 - 305.
- Flügel, E., 2010. *Microfacies of Carbonate Rocks, Analysis, Interpretation and Application*. Springer-Verlag, Berlin, 976 pp.
- Folie, A., Codrea, V., 2005. New lissamphibians and squamates from the Maastrichtian of Hațeg Basin, Romania. *Acta Palaeontologica Polonica* 50, 57–71.
- Folk, R.L., 1980. *Petrology of Sedimentary Rocks*. Hemphill Pub. Co, 182 pp.
- Fondevilla, V., Dinarès-Turell, J., Oms, O., 2016. The chronostratigraphic framework of the South-Pyrenean Maastrichtian succession reappraised: Implications for basin development and end-Cretaceous dinosaur faunal turnover. *Sedimentary Geology* 337, 55–68. <https://doi.org/10.1016/j.sedgeo.2016.03.006>
- Fondevilla, V., Vicente, A., Battista, F., Sellés, A.G., Dinarès-Turell, J., Martín-Closas, C., Anadón, P., Vila, B., Razzolini, N.L., Galobart, À., Oms, O., 2017a. Geology and taphonomy of the L'Espinou dinosaur bonebed, a singular lagoonal site from the Maastrichtian of South-Central Pyrenees. *Sedimentary Geology* 355, 75–92. <https://doi.org/10.1016/j.sedgeo.2017.03.014>
- Fondevilla, V., Vila, B., Oms, O., Galobart, À., 2017b. Skin impressions of the last European dinosaurs. *Geological Magazine* 154, 393–398. <https://doi.org/10.1017/S0016756816000868>
- Fondevilla, V., Dalla Vecchia, F.M., Gaete, R., Galobart, À., Moncunill-Solé, B., Köhler, M., 2018. Ontogeny and taxonomy of the hadrosaur (Dinosauria, Ornithomimidae) remains from Basturs Poble bonebed (late early Maastrichtian, Tremp Syncline, Spain). *PLOS ONE* 13, e0206287. <https://doi.org/10.1371/journal.pone.0206287>

- Fondevilla, V., Riera, V., Vila, B., Sellés, A.G., Dinarès-Turell, J., Vicens, E., Gaete, R., Oms, O., Galobart, 2019. Chronostratigraphic synthesis of the latest Cretaceous dinosaur turnover in south-western Europe. *Earth-Science Reviews* 191, 168–189. <https://doi.org/10.1016/j.earscirev.2019.01.007>
- Forster, C. A., Sampson, S. D., Chiappe, L. M., Krause, D. W., 1998. The theropod ancestry of birds: new evidence from the Late Cretaceous of Madagascar. *Science*, 279(5358), 1915–1919.
- Fowler, D., 2020. The Hell Creek Formation, Montana: A Stratigraphic Review and Revision Based on a Sequence Stratigraphic Approach. *Geosciences* 10, 435. <https://doi.org/10.3390/geosciences10110435>
- Gaffney, E.S., Chatterjee, S., Rudra, D.K., 2001. *Kurmademys*, a New Side-Necked Turtle (Pelomedusoides: Bothremydidae) from the Late Cretaceous of India. *American Museum Novitates* 3321, 1–16. [https://doi.org/10.1206/0003-0082\(2001\)321<0001:KANSNT>2.0.CO;2](https://doi.org/10.1206/0003-0082(2001)321<0001:KANSNT>2.0.CO;2)
- Gale, A.S., Mutterlose, J., Batenburg, S., Gradstein, F.M., Agterberg, F.P., Ogg, J.G., Petrizzo, M.R., 2020. The Cretaceous Period, in: *Geologic Time Scale 2020*. Elsevier, pp. 1023–1086. <https://doi.org/10.1016/B978-0-12-824360-2.00027-9>
- Gardner, J.D., 2001. Monophyly and affinities of albanerpetontid amphibians (Temnospondyli; Lissamphibia). *Zoological Journal of the Linnean Society* 131, 309–352. <https://doi.org/10.1111/j.1096-3642.2001.tb02240.x>
- Gardner, J.D., 2002. Monophyly and intra-generic relationships of *Albanerpeton* (Lissamphibia; Albanerpetontidae). *Journal of Vertebrate Paleontology* 22, 12–22.
- Garrido Megías, A., Ríos Aragües, L.M., 1972. Síntesis geológica del Secundario y Terciario entre los ríos Cinca y Segre. *Boletín Instituto Geológico y Minero de España* 83, 1–47.
- Gasca, J.M., Moreno-Azanza, M., Bádenas, B., Díaz-Martínez, I., Castanera, D., Canudo, J.I., Aurell, M., 2017. Integrated overview of the vertebrate fossil record of the Ladruñán anticline (Spain): Evidence of a Barremian alluvial-lacustrine system in NE Iberia frequented by dinosaurs. *Palaeogeography, Palaeoclimatology, Palaeoecology* 472, 192–202. <https://doi.org/10.1016/j.palaeo.2017.01.050>
- Gayet, M., Meunier, F.J., Werner, C., 2002. Diversification in Polypteriformes and Special Comparison With the Lepisosteiformes. *Palaeontology* 45, 361–376. <https://doi.org/10.1111/1475-4983.00241>
- Gervais, P. 1871. Remarques sur les reptiles provenant des calcaires lithographiques de Cerin. *Comptes Rendus Académie Sciences, Paris*, 73, 603–607.
- Gheerbrant, E., Abrial, C., Cappetta, H., 1997. Nouveaux sites a microvertébrés continentaux du crétacé terminal des petites pyrénées (Haute-Garonne et Ariège, France). *Geobios* 30, 257–269. [https://doi.org/10.1016/S0016-6995\(97\)80031-9](https://doi.org/10.1016/S0016-6995(97)80031-9)
- Gheerbrant, E., Astibia, H., 2012. Addition to the Late Cretaceous Laño mammal faunule (Spain) and to the knowledge of European “Zhelestidae” (Lainodontinae nov.). *Bulletin de la Société Géologique de France* 183, 537–546. <https://doi.org/10.2113/gssgfbull.183.6.537>
- Ghinassi, M., Oms, O., Cosma, M., Finotello, A., Munari, G., 2020. Reading tidal processes where their signature is cryptic: The Maastrichtian meandering channel deposits of the Tremp Formation (Southern Pyrenees, Spain). *Sedimentology* sed.12840. <https://doi.org/10.1111/sed.12840>

- Gilabert, V., Batenburg, S.J., Arenillas, I., Arz, J.A., 2022. Contribution of orbital forcing and Deccan volcanism to global climatic and biotic changes across the Cretaceous-Paleogene boundary at Zumaia, Spain. *Geology* 50, 21–25. <https://doi.org/10.1130/G49214.1>
- Godefroit, P., Codrea, V., Weishampel, D.B., 2009. Osteology of *Zalmoxes shqiperorum* (Dinosauria, Ornithomimidae), based on new specimens from the Upper Cretaceous of Năălaț-Vad (Romania). *Geodiversitas* 31, 525–553. <https://doi.org/10.5252/g2009n3a3>
- Goldin, T.J., Melosh, H.J., 2009. Self-shielding of thermal radiation by Chicxulub impact ejecta: Firestorm or fizzle? *Geology* 37, 1135–1138. <https://doi.org/10.1130/G30433A.1>
- Goloboff, P.A., Catalano, S.A., 2016. TNT version 1.5, including a full implementation of phylogenetic morphometrics. *Cladistics* 32, 221–238. <https://doi.org/10.1111/cla.12160>
- Gómez-Gras, D., Roigé, M., Fondevilla, V., Oms, O., Boya, S., Remacha, E., 2016. Provenance constraints on the Tremp Formation paleogeography (southern Pyrenees): Ebro Massif VS Pyrenees sources. *Cretaceous Research* 57, 414–427. <https://doi.org/10.1016/j.cretres.2015.09.010>
- Grambast, L., 1962. Classification de l'embranchement des charophytes. *Naturalia Monspeliensia, Série Botanique* 14, 63–86.
- Grambast, L., 1971. Remarques phylogénétiques et biochronologiques sur les Septorella du Crétacé terminal de Provence et les charophytes associées. *Paléobiologie continentale* 2, 1–38.
- Grambast, L., 1975. Charophytes du Crétacé Supérieur de la region de Cuenca., in: 1er Symposium Sobre El Cretácico de La Cordillera Ibérica, Cuenca. Imprenta Magerit., Madrid, pp. 67–93.
- Grambast-Fessard, N., 1980. Les charophytes du Montien de Mons (Belgique). *Review of Palaeobotany and Palynology* 30, 67–88.
- Gradstein, F.M., Ogg, J.G., Schmitz, M., Ogg, G., 2012. *The Geologic Time Scale 2012*. Elsevier.
- Grande, L., 2010. An Empirical Synthetic Pattern Study of Gars (Lepisosteiformes) and Closely Related Species, Based Mostly on Skeletal Anatomy. *The Resurrection of Holostei*. *Copeia* 10 (2A), 1-871.
- Grande, L., Bemis, W.E., 1998. A comprehensive phylogenetic study of Amiidae fishes (Amiidae) based on comparative skeletal anatomy. An empirical search for interconnected patterns of natural history., *Society of Vertebrate Paleontology Memoir* 4.
- Gutzwiller, S. C., A. Su, P.M. O'Connor., 2013. Postcranial pneumaticity and bone structure in two clades of neognath birds. *The Anatomical Record* 296(6): 867–876.
- Han, F., Wang, Q., Wang, H., Zhu, X., Zhou, X., Wang, Z., Fang, K., Stidham, T.A., Wang, W., Wang, X., Li, X., Qin, H., Fan, L., Wen, C., Luo, J., Pan, Y., Deng, C., 2022. Low dinosaur biodiversity in central China 2 million years prior to the end-Cretaceous mass extinction. *Proceedings of the National Academy of Sciences* 119. <https://doi.org/10.1073/pnas.2211234119>
- Henderson, M.D., Peterson, J.E., 2006. An azhdarchid pterosaur cervical vertebra from the Hell Creek Formation (Maastrichtian) of southeastern Montana. *Journal of Vertebrate Paleontology* 26, 192–195.
- Hendrickx, C., Mateus, O., Araújo, R., 2015. A proposed terminology of theropod teeth (Dinosauria, Saurischia). *Journal of Vertebrate Paleontology* 35, e982797. <https://doi.org/10.1080/02724634.2015.982797>

- Henehan, M.J., Ridgwell, A., Thomas, E., Zhang, S., Alegret, L., Schmidt, D.N., Rae, J.W.B., Witts, J.D., Landman, N.H., Greene, S.E., Huber, B.T., Super, J.R., Planavsky, N.J., Hull, P.M., 2019. Rapid ocean acidification and protracted Earth system recovery followed the end-Cretaceous Chicxulub impact. *Proceedings of the National Academy of Sciences* 116, 22500–22504. <https://doi.org/10.1073/pnas.1905989116>
- Hildebrand, A.R., Penfield, G.T., Kring, D.A., Pilkington, M., Camargo Z., A., Jacobsen, S.B., Boynton, W. V., 1991. Chicxulub Crater: A possible Cretaceous/Tertiary boundary impact crater on the Yucatán Peninsula, Mexico. *Geology* 19, 867. [https://doi.org/10.1130/0091-7613\(1991\)019<0867:CCAPCT>2.3.CO;2](https://doi.org/10.1130/0091-7613(1991)019<0867:CCAPCT>2.3.CO;2)
- Hirsch, K.F., 1985. Fossil Crocodilian Eggs from the Eocene of Colorado. *Journal of Paleontology* 3, 531–542.
- Holroyd, P.A., Hutchison, J.H., 2002. Patterns of geographic variation in latest Cretaceous vertebrates: evidence from the turtle component, in: Hartman, J., Johnson, K.R., Nichols, D.J. (Eds.), *The Hell Creek Formation and the Cretaceous-Tertiary Boundary in the Northern Great Plains*. Geological Society of America Special Paper, 361. pp. 177–190.
- Holroyd, P.A., Wilson, G.P., Hutchison, J.H., 2014. Temporal changes within the latest Cretaceous and early Paleogene turtle faunas of northeastern Montana, in: *Through the End of the Cretaceous in the Type Locality of the Hell Creek Formation in Montana and Adjacent Areas*. Geological Society of America. [https://doi.org/10.1130/2014.2503\(11\)](https://doi.org/10.1130/2014.2503(11))
- Hope, S., 2002. The Mesozoic Radiation of Neornithes. In L.M. Chiappe and L.M. Witmer (eds.), *Mesozoic Birds*. University of California Press, Berkeley, pp. 281–316.
- Houde, P., H. Haubold., 1987. *Palaeotis weigelti* restudied: a small Middle Eocene ostrich (Aves: Struthioniformes). *Palaeovertebrata* 17: 27–42.
- Hull, P.M., Bornemann, A., Penman, D.E., Henehan, M.J., Norris, R.D., Wilson, P.A., Blum, P., Alegret, L., Batenburg, S.J., Bown, P.R., Bralower, T.J., Cournede, C., Deutsch, A., Donner, B., Friedrich, O., Jehle, S., Kim, H., Kroon, D., Lippert, P.C., Loroch, D., Moebius, I., Moriya, K., Peppe, D.J., Ravizza, G.E., Röhl, U., Schueth, J.D., Sepúlveda, J., Sexton, P.F., Sibert, E.C., Śliwińska, K.K., Summons, R.E., Thomas, E., Westerhold, T., Whiteside, J.H., Yamaguchi, T., Zachos, J.C., 2020. On impact and volcanism across the Cretaceous-Paleogene boundary. *Science* 367, 266–272. <https://doi.org/10.1126/science.aay5055>
- Hunter, J., Archibald, J.D., 2002. Mammals from the end of the age of dinosaurs in North Dakota and southeastern Montana, with a reappraisal of geographic differentiation among Lanciaan mammals, in: Hartman, J.H., Johnson, K.R., Nichols, D. (Eds.), *The Hell Creek Formation and the Cretaceous-Tertiary Boundary in the Northern Great Plains: An Integrated Continental Record of the End of the Cretaceous*. Boulder, Colorado, Geological Society of America Special Paper 361. pp. 191–216.
- Hutchison, J.H., Archibald, J.D., 1986. Diversity of turtles across the cretaceous/tertiary boundary in Northeastern Montana. *Palaeogeography, Palaeoclimatology, Palaeoecology* 55, 1–22. [https://doi.org/10.1016/0031-0182\(86\)90133-1](https://doi.org/10.1016/0031-0182(86)90133-1)
- Iori, F. V., Arrua-Campos, A.C., 2016. Os Crocodiliformes da Formação Marília (Bacia Bauru, Cretáceo Superior) na Região de Monte Alto, estado de São Paulo, Brasil. *Revista Brasileira de Paleontologia* 19, 537–546.
- Iori, F.V., Araújo-Júnior, H.I. de, Tavares, S.A.S., Marinho, T. da S., Martinelli, A.G., 2021. New theropod dinosaur from the Late Cretaceous of Brazil improves abelisaurid diversity. *Journal of South American Earth Sciences* 112, 103551. <https://doi.org/10.1016/j.jsames.2021.103551>

- Isasmendi, E., Torices, A., Canudo, J.I., Currie, P.J., Pereda-Suberbiola, X., 2022. Upper Cretaceous European theropod palaeobiodiversity, palaeobiogeography and the intra-Maastrichtian faunal turnover: new contributions from the Iberian fossil site of Laño. *Papers in Palaeontology*. <https://doi.org/10.1002/spp2.1419>
- Jablonski, D., 1994. Extinctions in the fossil record. *Philosophical Transactions of the Royal Society of London. Series B: Biological Sciences* 344, 11–17. <https://doi.org/10.1098/rstb.1994.0045>
- Jackson, F.D., Varricchio, D.J., 2010. Fossil eggs and eggshell from the lowermost Two Medicine Formation of western Montana, Sevenmile Hill locality. *Journal of Vertebrate Paleontology* 30, 1142–1156. <https://doi.org/10.1080/02724634.2010.483537>
- Jain, S.L., Bandyopadhyay, S., 1997. New titanosaurid (Dinosauria: Sauropoda) from the Late Cretaceous of central India. *Journal of Vertebrate Paleontology* 17, 114–136. <https://doi.org/10.1080/02724634.1997.10010958>
- Jeffrey, C., 1967. The Origin and Differentiation of the Archegoniate Land Plants: A Second Contribution. *Kew Bulletin* 21, 335. <https://doi.org/10.2307/4108533>
- Johnson, K.R., Nichols, D.J., Hartman, J.H., 2002. Hell Creek Formation: A 2001 synthesis. *Geological Society of America Special Papers* 361, 503–510. <https://doi.org/10.1130/0-8137-2361-2.503>
- Jolley, D.W., Daly, R., Gilmour, I., Kelley, S.P., 2013. Climatic oscillations stall vegetation recovery from K/Pg event devastation. *Journal of the Geological Society* 170, 477–482. <https://doi.org/10.1144/jgs2012-088>
- Jouve, S., Bardet, N., Jalil, N.-E., Pereda-Suberbiola, X., Bouya, B., Amaghaz, M., 2008. The oldest African crocodylian: phylogeny, paleobiogeography, and differential survivorship of marine reptiles through the Cretaceous-Tertiary boundary. *Journal of Vertebrate Paleontology* 28, 409–421.
- Joyce, W.G., Bandyopadhyay, S., 2020. A revision of the pelomedusoid turtle *Jainemys pisdurensis* from the Late Cretaceous (Maastrichtian) Lameta Formation of India. *PeerJ* 8, e9330. <https://doi.org/10.7717/peerj.9330>
- Kaiho, K., Oshima, N., Adachi, K., Adachi, Y., Mizukami, T., Fujibayashi, M., Saito, R., 2016. Global climate change driven by soot at the K-Pg boundary as the cause of the mass extinction. *Scientific Reports* 6, 28427. <https://doi.org/10.1038/srep28427>
- Kapur, V. V., Khosla, A., 2019. Faunal elements from the Deccan volcano-sedimentary sequences of India: A reappraisal of biostratigraphic, palaeoecologic, and palaeobiogeographic aspects. *Geological Journal* 54, 2797–2828. <https://doi.org/10.1002/gj.3379>
- Keller, G., Li, L., MacLeod, N., 1996. The Cretaceous/Tertiary boundary stratotype section at El Kef, Tunisia: how catastrophic was the mass extinction? *Palaeogeography, Palaeoclimatology, Palaeoecology* 119, 221–254. [https://doi.org/10.1016/0031-0182\(95\)00009-7](https://doi.org/10.1016/0031-0182(95)00009-7)
- Keller, G., Adatte, T., Pardo, A., Bajpai, S., Khosla, A., Samant, B., 2010. Cretaceous Extinctions: Evidence Overlooked. *Science* 328, 974–975. <https://doi.org/10.1126/science.328.5981.974-a>
- Khosla, A., Sertich, J.J.W., Prasad, G.V.R., Verma, O., 2009. Dyrosaurid remains from the Intertrappean Beds of India and the Late Cretaceous distribution of Dyrosauridae. *Journal of Vertebrate Paleontology* 29, 1321–1326. <https://doi.org/10.1671/039.029.0416>

- Kielan-Jaworowska, Z., Cifelli, R.L., Luo, Z.X., 2005. Mammals from the age of dinosaurs: origins, evolution, and structure. Columbia University Press, New York, 700 pp.
- Kiessling, W., Baron-Szabo, R.C., 2004. Extinction and recovery patterns of scleractinian corals at the Cretaceous-Tertiary boundary. *Palaeogeography, Palaeoclimatology, Palaeoecology* 214, 195–223. <https://doi.org/10.1016/j.palaeo.2004.05.025>
- Kirschvink, J.L., 1980. The least-squares line and plane and the analysis of the paleomagnetic data. *Geophysical Journal of the Royal Astronomical Society* 62, 699–718.
- Koenen, E.J.M., Ojeda, D.I., Bakker, F.T., Wieringa, J.J., Kidner, C., Hardy, O.J., Pennington, R.T., Herendeen, P.S., Bruneau, A., Hughes, C.E., 2021. The Origin of the Legumes is a Complex Paleopolyploid Phylogenomic Tangle Closely Associated with the Cretaceous–Paleogene (K–Pg) Mass Extinction Event. *Systematic Biology* 70, 508–526. <https://doi.org/10.1093/sysbio/syaa041>
- Kortabitarte, A., Elorza, J., Astibia Ayerra, H., 2008. Datos sedimentológicos y tafonómicos de enclaves finicretácicos con fósiles de vertebrados de la Formación Sobrepeña (Burgos, Región Vasco-Cantábrica). *Geo-Temas* 10, 1278–1280.
- Kraus, M.J., Hasiotis, S.T., 2006. Significance of Different Modes of Rhizolith Preservation to Interpreting Paleoenvironmental and Paleohydrologic Settings: Examples from Paleogene Paleosols, Bighorn Basin, Wyoming, U.S.A. *Journal of Sedimentary Research* 76, 633–646. <https://doi.org/10.2110/jsr.2006.052>
- Kring, D.A., 2007. The Chicxulub impact event and its environmental consequences at the Cretaceous–Tertiary boundary. *Palaeogeography, Palaeoclimatology, Palaeoecology* 255, 4–21. <https://doi.org/10.1016/j.palaeo.2007.02.037>
- Kriwet, J., Benton, M.J., 2004. Neoselachian (Chondrichthyes, Elasmobranchii) diversity across the Cretaceous–Tertiary boundary. *Palaeogeography, Palaeoclimatology, Palaeoecology* 214, 181–194. <https://doi.org/10.1016/j.palaeo.2004.02.049>
- Kumari, A., Singh, S., Khosla, A., 2021. Palaeosols and palaeoclimate reconstruction of the Maastrichtian Lameta Formation, Central India. *Cretaceous Research* 117, 104632. <https://doi.org/10.1016/j.cretres.2020.104632>
- Labandeira, C.C., Johnson, K.R., Wilf, P., 2002. Impact of the terminal Cretaceous event on plant–insect associations. *Proceedings of the National Academy of Sciences* 99, 2061–2066. <https://doi.org/10.1073/pnas.042492999>
- Labandeira, C.C., Rodríguez-Tovar, F.J., Uchman, A., 2016. The End-Cretaceous Extinction and Ecosystem Change, in: *The Trace-Fossil Record of Major Evolutionary Events*. pp. 265–300. [https://doi.org/10.1007/978-94-017-9597-5\\_5](https://doi.org/10.1007/978-94-017-9597-5_5)
- Landman, N.H., Goolaerts, S., Jagt, J.W.M., Jagt-Yazykova, E.A., Machalski, M., 2015. Ammonites on the Brink of Extinction: Diversity, Abundance, and Ecology of the Order Ammonoidea at the Cretaceous/Paleogene (K/Pg) Boundary. pp. 497–553. [https://doi.org/10.1007/978-94-017-9633-0\\_19](https://doi.org/10.1007/978-94-017-9633-0_19)
- Lankester, E.R., 1885. Protozoa, in: Baynes, T.S. (Ed.), *The Encyclopedia Britannica*. J. M. Stoddard Co, pp. 830–866.
- Larson, D.W., 2008. Diversity and variation of theropod dinosaur teeth from the uppermost Santonian Milk River Formation (Upper Cretaceous), Alberta: a quantitative method supporting identification of the oldest dinosaur tooth assemblage in Canada. *Canadian Journal of Earth Sciences* 45, 1455–1468. <https://doi.org/10.1139/E08-070>

- Laurent, Y., 2003. Les faunes de vertébrés continentaux du Maastrichtien supérieur d'Europe: systématique et biodiversité. *Strata* série 2 41, 1–81.
- Laurent, Y., Buffetaut, E., Le Loeuff, J., 2000. Un crane de thoracosaurine (Crocodylia, Crocodylidae) dans le Maastrichtien Supérieur du sud de la France. *Oryctos* 3, 19–27.
- Laurent, Y., Bilotte, M., Le Loeuff, J., 2002a. Late Maastrichtian continental vertebrates from southwestern France: correlation with marine fauna. *Palaeogeography, Palaeoclimatology, Palaeoecology* 187, 121–135. [https://doi.org/10.1016/S0031-0182\(02\)00512-6](https://doi.org/10.1016/S0031-0182(02)00512-6).
- Laurent, Y., Tong, H., Claude, J., 2002b. New side-necked turtle (Pleurodira: Bothremydidae) from the Upper Maastrichtian of the Petites-Pyrénées (Haute-Garonne, France). *Cretaceous Research* 23, 465–471. <https://doi.org/10.1006/cres.2002.1015>
- Le Loeuff, J., Buffetaut, E., Cavin, L., Laurent, Y., Martin, M., Martin, V., Tong, H., 1994a. Les hadrosaures des Corbières et des Petites Pyrénées. *Bulletin de la Société d'Etudes Scientifiques de l'Aude* 94, 19–21.
- Le Loeuff, J., Buffetaut, E., Martin, M., 1994b. The last stages of dinosaur faunal history in Europe: a succession of Maastrichtian dinosaur assemblages from the Corbières (southern France). *Geological Magazine* 131, 625–630. <https://doi.org/10.1017/S0016756800012413>
- Leonhardt, R., 2006. Analyzing rock magnetic measurements: The RockMagAnalyzer 1.0 software. *Comput. Geosci.* 32, 1420–1431. <https://doi.org/10.1016/j.cageo.2006.01.006>
- Leymerie, A., 1868. Présence de garumniens en Espagne. *Bulletin de la Société Géologique de France*. *Bulletin de la Société Géologique de France* 25, 906–911.
- Li, L., Keller, G., 1998. Maastrichtian climate, productivity and faunal turnovers in planktic foraminifera in South Atlantic DSDP sites 525A and 21. *Marine Micropaleontology* 33, 55–86. [https://doi.org/10.1016/S0377-8398\(97\)00027-3](https://doi.org/10.1016/S0377-8398(97)00027-3)
- Liebau, A., 1971. Die Ableitung der palökologischen Systematik einer oberkretazischen Lagune. *Paleoecology of Ostracodes*. *Bulletin des Centres de Recherche Pau-SNPA* 5.
- Liebau, A., 1973. El Maastrichtiense lagunar (Garumniense) de Isona., in: *Libro-Guia, XIII Coloquio Europeo Micropaleontologia*. pp. 87–112.
- Lofgren, D.L., Hotton, C.L., Runkel, A.C., 1990. Reworking of Cretaceous dinosaurs into Paleocene channel, deposits, upper Hell Creek Formation, Montana. *Geology* 18, 874. [https://doi.org/10.1130/0091-7613\(1990\)018<0874:ROCDIP>2.3.CO;2](https://doi.org/10.1130/0091-7613(1990)018<0874:ROCDIP>2.3.CO;2)
- Longrich NR, Currie PJ., 2009. A microraptorine (Dinosauria-Dromaeosauridae) from the Late Cretaceous of North America. *Proceedings of the National Academy of Sciences* 106 (13):5002–5007. doi:10.1073/pnas.0811664106.
- Longrich, N.R., Tokaryk, T., Field, D.J., 2011. Mass extinction of birds at the Cretaceous–Paleogene (K–Pg) boundary. *Proceedings of the National Academy of Sciences* 108, 15253–15257. <https://doi.org/10.1073/pnas.1110395108>
- Longrich, N.R., Bhullar, B.-A.S., Gauthier, J.A., 2012. Mass extinction of lizards and snakes at the Cretaceous–Paleogene boundary. *Proceedings of the National Academy of Sciences* 109, 21396–21401. <https://doi.org/10.1073/pnas.1211526110>
- Longrich, N.R., Martill, D.M., Andres, B., 2018. Late Maastrichtian pterosaurs from North Africa and mass extinction of Pterosauria at the Cretaceous–Paleogene boundary. *PLOS Biology* 16, e2001663. <https://doi.org/10.1371/journal.pbio.2001663>

- Longrich, N.R., Suberbiola, X.P., Pyron, R.A., Jalil, N.-E., 2020. The first duckbill dinosaur (Hadrosauridae: Lambeosaurinae) from Africa and the role of oceanic dispersal in dinosaur biogeography. *Cretaceous Research* 104678. <https://doi.org/10.1016/j.cretres.2020.104678>
- López-Martínez, N., Ardèvol, L., Arribas, M.E., Civis, J., Gonzalez-Delgado, A., 1998. The geological record in non-marine environments around the K/T boundary (Tremp Formation, Spain). *Bulletin de la Société géologique de France* 169, 11–20.
- López-Martínez, N., Canudo, J.I., Cuenca-Bescós, G., 1999. Latest Cretaceous Eggshells From Arén ( Southern Pyrenees , Spain ), in: First International Symposium on Dinosaur Eggs and Babies. Isona, pp. 35–36.
- López-Martínez, N., Peláez-Campomanes, P., 1999. New mammals from south-central Pyrenees (Trempe Formation, Spain) and their bearing on late Paleocene marine-continental correlations. *Bulletin de la Société Géologique de France* 170, 681–696.
- López-Martínez, N., Moratalla, J.J., Sanz, J.L., 2000. Dinosaurs nesting on tidal flats. *Palaeogeography, Palaeoclimatology, Palaeoecology* 160, 153–163. [https://doi.org/10.1016/S0031-0182\(00\)00063-8](https://doi.org/10.1016/S0031-0182(00)00063-8)
- López-Martínez, N., Canudo, J.I., Ardevol, L., Pereda-Suberbiola, X., Orue-Etxebarria, X., Cuenca-Bescós, G., Ruiz-Omeñaca, J.I., Murelaga, X., Feist, M., 2001. New dinosaur sites correlated with upper Maastrichtian pelagic deposits in the Spanish Pyrenees: Implications for the dinosaur extinction. *Cretaceous Research* 22, 41–61. <https://doi.org/10.1006/cres.2000.0236>
- López-Martínez, N., Arribas, M.E., Robador, A., Vicens, E., Ardèvol, L., 2006a. Los carbonatos danienses (Unidad 3) de la Fm Temp (Pirineos sur-centrales): paleogeografía y relación con el límite Cretácico-Terciario. *Revista de la Sociedad Geológica de España* 19, 233–255.
- López-Martínez, N., Dinarès-Turell, J., Elez Villar, J., 2006b. Chronostratigraphy of the Continental Paleocene Series From the South Central Pyrenees ( Spain ): New Magnetostratigraphic Constraints, in: Caballero, F., Apellaniz, E., Baceta, J.I., Bernaola, G., Orue-Etxebarria, X., Payros, A., Pujalte, V. (Eds.), *Climate & Biota of the Early Paleogene*. 83 pp.
- López-Martínez, N., Vicens, E., 2012. A new peculiar dinosaur egg, *Sankofa pyrenaica* oogen. nov. oosp. nov. from the Upper Cretaceous coastal deposits of the Aren Formation, south-central Pyrenees, Lleida, Catalonia, Spain. *Palaeontology* 55, 325–339. <https://doi.org/10.1111/j.1475-4983.2011.01114.x>
- Lucas, S.G., Sullivan, R.M., Cather, S.M., Jasinski, S.E., Fowler, D.W., Heckert, A.B., Spielmann, J.A., Hunt, A.P., 2009. No definitive evidence of Paleocene dinosaurs in the San Juan Basin. *Palaeontologia Electronica* 12 (2), 1–10.
- Lyons, S.L., Karp, A.T., Bralower, T.J., Grice, K., Schaefer, B., Gulick, S.P.S., Morgan, J. V., Freeman, K.H., 2020. Organic matter from the Chicxulub crater exacerbated the K–Pg impact winter. *Proceedings of the National Academy of Sciences* 117, 25327–25334. <https://doi.org/10.1073/pnas.2004596117>
- Lyson, T.R., Bercovici, A., Chester, S.G.B., Sargis, E.J., Pearson, D., Joyce, W.G., 2011a. Dinosaur extinction: closing the ‘3 m gap.’ *Biology Letters* 7, 925–928. <https://doi.org/10.1098/rsbl.2011.0470>
- Lyson, T.R., Joyce, W.G., Knauss, G.E., Pearson, D.A., 2011b. Boremys (Testudines, Baenidae) from the latest Cretaceous and early Paleocene of North Dakota: an 11-million-year range extension and an additional K/T survivor. *Journal of Vertebrate Paleontology* 31, 729–737. <https://doi.org/10.1080/02724634.2011.576731>

- Lyson, T.R., Longrich, N.R., 2011. Spatial niche partitioning in dinosaurs from the latest cretaceous (Maastrichtian) of North America. *Proceedings of the Royal Society B: Biological Sciences* 278, 1158–1164. <https://doi.org/10.1098/rspb.2010.1444>
- Lyson, T.R., Miller, I.M., Bercovici, A.D., Weissenburger, K., Fuentes, A.J., Clyde, W.C., Hagadorn, J.W., Butrim, M.J., Johnson, K.R., Fleming, R.F., Barclay, R.S., Maccracken, S.A., Lloyd, B., Wilson, G.P., Krause, D.W., Chester, S.G.B., 2019. Exceptional continental record of biotic recovery after the Cretaceous–Paleogene mass extinction. *Science* 366, 977–983. <https://doi.org/10.1126/science.aay2268>
- Makovicky, P.J., H.D. Sues., 1998. Anatomy and phylogenetic relationships of the theropod dinosaur *Microvenator celer* from the Lower Cretaceous of Montana. *American Museum Novitates* 3240:1–27.
- Makovicky, P. J., M.A. Norell., 2004. Troodontidae. In D.B. Weishampel, P. Dodson and H. Osmólska (eds.), *The Dinosauria: Second Edition*. University of California Press, pp. 184–195.
- Makovicky, P.J., S. Apesteguía, F.L. Agnolín., 2005. The earliest dromaeosaurid theropod from South America. *Nature* 437: 1007–1011.
- Maddison, W.P., Maddison, D.R., 2017. Mesquite: a modular system for evolutionary analysis. Version 3.31 [WWW Document]. URL <http://mesquiteproject.org>.
- Mannion, P.D., Calvo, J.O., 2011. Anatomy of the basal titanosaur (Dinosauria, Sauropoda) *Andesaurus delgadoi* from the mid-Cretaceous (Albian-early Cenomanian) Río Limay Formation, Neuquén Province, Argentina: implications for titanosaur systematics. *Zoological Journal of the Linnean Society* 155–181. <https://doi.org/10.1111/j.1096-3642.2011.00699.x>
- Mannion, P.D., Benson, R.B.J., Carrano, M.T., Tennant, J.P., Judd, J., Butler, R.J., 2015. Climate constrains the evolutionary history and biodiversity of crocodylians. *Nature Communications* 6, 8438. <https://doi.org/10.1038/ncomms9438>
- Marie, P., 1946. Sur *Laffitteina bibensis* et *Laffitteina monodi* nouveau genre et nouvelles espèces de foraminifères du Montien, *Bulletin de la Société Géologique de France* (1945) sér. 5, 15: 419–434.
- Marmi, J., Luján, Á.H., Riera, V., Gaete, R., Oms, O., Galobart, À., 2012. The youngest species of *Polysternon*: A new bothremydid turtle from the uppermost Maastrichtian of the southern Pyrenees. *Cretaceous Research* 35, 133–142. <https://doi.org/10.1016/j.cretres.2011.12.004>
- Marmi, J., Vila, B., Martín-Closas, C., Villalba-Breva, S., 2014. Reconstructing the foraging environment of the latest titanosaurs (Fumanya dinosaur tracksite, Catalonia). *Palaeogeography, Palaeoclimatology, Palaeoecology* 410, 380–389. <https://doi.org/10.1016/j.palaeo.2014.06.007>
- Marmi, J., Blanco, A., Fondevilla, V., Dalla Vecchia, F.M., Sellés, A.G., Vicente, A., Martín-Closas, C., Oms, O., Galobart, À., 2016. The Molí del Baró-1 site, a diverse fossil assemblage from the uppermost Maastrichtian of the southern Pyrenees (north-eastern Iberia). *Cretaceous Research* 57, 519–539. <https://doi.org/10.1016/j.cretres.2015.06.016>
- Marsh, O. C., 1879. The vertebrae of recent birds. *American Journal of Science* 17: 266–9.
- Marsh, O. C., 1880. *Odontornithes: A Monograph of the Extinct Toothed Birds of North America*. Washington: Government Printing Office, 201 pp.
- Martin, L.D., 1991. Mesozoic birds and the origin of birds. In H.P. Schultze and L. Trueb (eds.), *Origins of the higher groups of tetrapods: controversy and consensus*. Cornell University Press, pp. 485–540.

- Martin, L.D. 1992. The status of the Late Palaeocene birds *Gastornis* and *Remiornis*. Bulletin of the Natural History Museum of Los Angeles County Science Service 36, 97–108.
- Martin, J.E., Rabi, M., Csiki, Z., 2010. Survival of *Theriosuchus* (Mesoeucrocodylia: Atoposauridae) in a Late Cretaceous archipelago: a new species from the Maastrichtian of Romania. *Naturwissenschaften* 97, 845–854. <https://doi.org/10.1007/s00114-010-0702-y>
- Martinelli, A.G., Marinho, T. da S., Filippi, L.S., Ribeiro, L.C.B., Ferraz, M.L. da F., Cavellani, C.L., Teixeira, V. de P.A., 2015. Cranial bones and atlas of titanosaurs (Dinosauria, Sauropoda) from Late Cretaceous (Bauru Group) of Uberaba, Minas Gerais State, Brazil. *Journal of South American Earth Sciences* 61, 164–170. <https://doi.org/10.1016/j.jsames.2015.02.009>
- Masriera, A., Ullastre, J., 1990. Yacimientos inéditos de carófitas que contribuyen a fijar el límite Cretácico-Terciario en el Pirineo Catalán. *Revista de la Sociedad Geológica de España* 3, 33–42.
- Mateus, O., Puértolas-Pascual, E., Callapez, P.M., 2019. A new eusuchian crocodylomorph from the Cenomanian (Late Cretaceous) of Portugal reveals novel implications on the origin of Crocodylia. *Zoological Journal of the Linnean Society* 186, 501–528. <https://doi.org/10.1093/zoolinnean/zly064>
- Mayr, G., Codrea, V., Solomon, A., Bordeianu, M., Smith, T., 2020. A well-preserved pelvis from the Maastrichtian of Romania suggests that the enigmatic *Gargantuavis* is neither an ornithurine bird nor an insular endemic. *Cretaceous Research* 106, 104271. <https://doi.org/10.1016/j.cretres.2019.104271>
- Mayayo-Lainez, A., Alegre-Esteve, M., Bauluz, B., Canudo, J., 2021. First approach to the paleohistology of the hadrosaur dinosaurs from Blasi 2A (Trempe Formation, Maastrichtian, Huesca). *Ciências da Terra-Procedia* 1, 38–41.
- McCarthy, P.J., Guy Plint, A., 1998. Recognition of interfluve sequence boundaries: Integrating paleopedology and sequence stratigraphy. *Geology* 26, 387. [https://doi.org/10.1130/0091-7613\(1998\)026<0387:ROISBI>2.3.CO;2](https://doi.org/10.1130/0091-7613(1998)026<0387:ROISBI>2.3.CO;2)
- Méndez, A.H., Novas, F.E., Iori, F. V., 2012. First record of Megaraptora (Theropoda, Neovenatoridae) from Brazil. *Comptes Rendus Palevol* 11, 251–256. <https://doi.org/10.1016/j.crpv.2011.12.007>
- Méndez, A.H., Novas, F.E., Iori, F. V., 2014. New record of abelisauroid theropods from the Bauru Group (Upper Cretaceous), São Paulo State, Brazil. *REVISTA BRASILEIRA DE PALEONTOLOGIA* 17, 23–32. <https://doi.org/10.4072/rbp.2014.1.03>
- Mey, P.H.W., Nagtegaal, P.J.C., Roberti, K.J., Harteveldt, J.J.A., 1968. Lithostratigraphic subdivision of Post-Hercynian deposits in the South-Central Pyrenees, Spain. *Leidse Geologische Mededelingen* 41, 221–228.
- Mikhailov, K.E., 1991. Classification of fossil eggshells of amniotic vertebrates. *Acta Palaeontol. Pol.* 36, 193–2398.
- Mikhailov, K.E., 1997. Fossil and Recent Eggshell in Amniotic Vertebrates: Fine Structure, Comparative Morphology and Classification., *Special Papers in Palaeontology*. <https://doi.org/10.1017/S0016756898591509>
- Miller, K.G., Kominz, M.A., Browning, J. V., Wright, J.D., Mountain, G.S., Katz, M.E., Sugarman, P.J., Cramer, B.S., Christie-Blick, N., Peka, S.F., 2005. The Phanerozoic Record of Global Sea-Level Change. *Science* 310, 1293–1298. <https://doi.org/10.1126/science.1116412>

- Mocho, P., Pérez-García, A., Codrea, V.A., 2022. New titanosaurian caudal remains provide insights on the sauropod diversity of the Hațeg Island (Romania) during the Late Cretaceous. *Historical Biology* 1–36. <https://doi.org/10.1080/08912963.2022.2125807>
- Mohabey, D.M., Head, J.J., Wilson, J.A., 2011. A new species of the snake *Madtsoia* from the Upper Cretaceous of India and its paleobiogeographic implications. *Journal of Vertebrate Paleontology* 31, 588–595. <https://doi.org/10.1080/02724634.2011.560220>
- Mohabey, D.M., Samant, B., 2013. Deccan continental flood basalt eruption terminated Indian dinosaurs before the Cretaceous-Paleogene boundary. *Geological Society of India Special Publication* 1, 260–267.
- Molina, E., Canudo, J.I., Guernet, C., McDougall, K., Ortiz, N., Pascual, J.O., Pares, J.M., Samso, J.M., Serra-Kiel, J., Tosquella, J., 1992. The stratotypic revisited integrated stratigraphy across the Paleocene/Eocene boundary. *Revue de Micropaléontologie* 35, 143–156.
- Moreno-Azanza, M., Bauluz, B., Canudo, J.I., Puértolas-Pascual, E., Sellés, A.G., 2014. A re-evaluation of aff. *Megaloolithidae* eggshell fragments from the uppermost Cretaceous of the Pyrenees and implications for crocodylomorph eggshell structure. *Historical Biology* 26, 195–205. <https://doi.org/10.1080/08912963.2013.786067>
- Moreno-Azanza, M., Pérez-Pueyo, M., Puértolas-Pascual, E., Núñez-Lahuerta, C., Mateus, O., Bauluz, B., Bádenas, B., Canudo, J.I., 2022. A new crocodylomorph related ootaxon from the late Maastrichtian of the Southern Pyrenees (Huesca, Spain). *Hist. Biol.* 1–10. <https://doi.org/10.1080/08912963.2022.2098024>
- Morgan, J., Warner, M., Brittan, J., Buffler, R., Camargo, A., Christeson, G., Denton, P., Hildebrand, A., Hobbs, R., Macintyre, H., Mackenzie, G., Maguire, P., Marin, L., Nakamura, Y., Pilkington, M., Sharpton, V., Snyder, D., Suarez, G., Trejo, A., 1997. Size and morphology of the Chicxulub impact crater. *Nature* 390, 472–476. <https://doi.org/10.1038/37291>
- Morgan, J., Artemieva, N., Goldin, T., 2013. Revisiting wildfires at the K-Pg boundary. *Journal of Geophysical Research: Biogeosciences* 118, 1508–1520. <https://doi.org/10.1002/2013JG002428>
- Muñoz, J.A., 1992. Evolution of a continental collision belt: ECORS-Pyrenees crustal balanced cross-section, in: *Thrust Tectonics*. Springer Netherlands, Dordrecht, pp. 235–246. [https://doi.org/10.1007/978-94-011-3066-0\\_21](https://doi.org/10.1007/978-94-011-3066-0_21)
- Muñoz, J.A., Mencos, J., Roca, E., Carrera, N., Gratacós, O., Ferrer, O., Fernández, O., 2018. The structure of the South-Central-Pyrenean fold and thrust belt as constrained by subsurface data. *Geologica Acta*, 16, 439–460.
- Murelaga, X., Pereda Suberbiola, X., Astibia, H., Lapparent, F.D., 1998. Primeros datos sobre los quelonios del Cretácico superior de Lleida. *Geogaceta* 24, 239–242.
- Murelaga, X., Canudo, J.I., 2005. Descripción de los restos de quelonios del Maastrichtiense superior de Aren y Serraduy (Huesca). *Geogaceta* 28, 51–54.
- Murelaga, X., García Garmilla, F., Pereda Suberbiola, X., 2005. Primeros restos de vertebrados del Cretácico superior de Quecedo de Valdivieso (Burgos). *Geogaceta* 195–198.
- Musacchio, E.A., 1973. Charophytas y ostrácodos no marinos del Grupo Neuquén (Cretácico Superior) en algunos afloramientos de las provincias de Río Negro y Neuquén, República Argentina. *Revista del Museo de la Plata. Nueva Serie. Sección Paleontología* 8, 1–32.
- Mutti, E., Rosell, J., Ghibaudo, G., Obrador, A., 1975. The Upper Cretaceous Aren Sandstone in its type-area, in: *9th International Congress International Association of Sedimentologists, Excursion Guidebook*. pp. 7–15.

- Mutti, E., Sgavetti, M., 1987. Sequence stratigraphy of the Upper Cretaceous Aren strata in the Aren–Orcau region, south-central Pyrenees, Spain: distinction between eustatically and tectonically controlled depositional sequences. *Annali dell'Università di Ferrara* 1, 1–22.
- Nagtegaal, P.J.C., 1972. Depositional history and clay minerals of the Upper Cretaceous basin in the south-central Pyrenees, Spain. *Leidse Geologische Mededelingen* 47, 251–275.
- Nagtegaal, P.J.C., Van Vliet, A., Brouwer, J., 1983. Syntectonic coastal offlap and concurrent turbidite deposition: the upper cretaceous Aren sandstone in the south-central Pyrenees, Spain 34, 185–218.
- Narváez, I., Brochu, C.A., Escaso, F., Pérez-García, A., Ortega, F., 2015. New Crocodyliforms from Southwestern Europe and Definition of a Diverse Clade of European Late Cretaceous Basal Eusuchians. *PLOS ONE* 10, e0140679. <https://doi.org/10.1371/journal.pone.0140679>
- Narváez, I., Brochu, C.A., Escaso, F., Pérez-García, A., Ortega, F., 2016. New Spanish Late Cretaceous eusuchian reveals the synchronic and sympatric presence of two allodaposuchids. *Cretaceous Research* 65, 112–125. <https://doi.org/10.1016/j.cretres.2016.04.018>
- Nederbragt, A. J., 1991. Late Cretaceous biostratigraphy and development of Heterohelcidae (planktic foraminifera). *Micropaleontology*. 37: 329-372.
- Nichols, D.J., Johnson, K.R., 2008. *Plants and the K–T Boundary*. Cambridge University Press, Cambridge, England, 292 pp.
- Nopcsa, F., 1915. Die Dinosaurier der Siebenburgischen Landesteile Ungarns. *Mitteilungen aus dem Jahrbuch der königlich Ungarischen geologischen Reichsanstalt* 23, 3–24.
- Novas F.E., Pol D., 2005. New evidence on deinonychosaurian dinosaurs from the Late Cretaceous of Patagonia. *Nature* 433(7028),858–861. doi:10.1038/nature03285.
- Novas, F.E., Ribeiro, L.C., Carvalho, I.S., 2005. Maniraptoran theropod ungual from the Marília Formation (Upper Cretaceous), Brazil. *Revista del Museo Argentino de Ciencias Naturales* 7, 31–36.
- Novas, F.E., de Souza Carvalho, I., Ribeiro, L.C.B., Méndez, A.H., 2008. First abelisaurid bone remains from the Maastrichtian Marília Formation, Bauru Basin, Brazil. *Cretaceous Research* 29, 625–635. <https://doi.org/10.1016/j.cretres.2008.01.010>
- Novas, F.E., Chatterjee, S., Rudra, D.K., Datta, P.M., 2010. *Rahiolisaurus gujaratensis*, n. gen. n. sp., A New Abelisaurid Theropod from the Late Cretaceous of India. pp. 45–62. [https://doi.org/10.1007/978-3-642-10311-7\\_3](https://doi.org/10.1007/978-3-642-10311-7_3)
- Novas, F. E., F.B. Egli, F.L. Agnolin, F.A. Gianechini, I. Cerda., 2018. Postcranial osteology of a new specimen of *Buitreraptor gonzalezorum* (Theropoda, Unenlagiidae). *Cretaceous Research* 83, 127–167.
- Núñez-Lahuerta, C., Moreno-Azanza, M., Pérez-Pueyo, M., 2021. First approach for a taphonomic key for fossil eggs and eggshells accumulations using optic microscopy: The case of Blasi-2B (Upper Cretaceous, Spain). *Ciências Terra Procedia* 1, 42–45.
- O'Connor, J., L.M. Chiappe, A. Bell., 2011. Pre-modern birds: avian divergences in the Mesozoic. In G. Dyke, and G. Kaiser (eds.), *Living dinosaurs. The evolutionary history of modern birds*. John Wiley & Sons Ltd, Chichester, West Sussex, pp.39–114.
- O'Connor, J. K., K.Q. Gao, and L.M. Chiappe. 2010. A new ornithuromorph (Aves: Ornithothoraces) bird from the Jehol Group indicative of higher-level diversity. *Journal of Vertebrate Paleontology* 30(2), 311-321.

- O'Connor, P.M., 2004. Pulmonary pneumaticity in the postcranial skeleton of extant Aves: a case study examining Anseriformes. *Journal of Morphology* 261, 141–161.
- O'Connor, P.M., 2009. Evolution of archosaurian body plans: Skeletal adaptations of an air-sac-based breathing apparatus in birds and other archosaurs. *Journal of Experimental Zoology* 311A, 629–646.
- Ogg, J.G., Hinnov, L.A., Huang, C., 2012. Cretaceous, in: *The Geologic Time Scale*. Elsevier, pp. 793–853. <https://doi.org/10.1016/B978-0-444-59425-9.00027-5>
- Oliva-Urcia, B., Pueyo, E. L., 2019. Paleomagnetism in structural geology and tectonics. In *Teaching methodologies in structural geology and tectonics* (pp. 55-121). Springer, Singapore.
- Oms, O., Fondevilla, V., Riera, V., Marmi, J., Vicens, E., Estrada, R., Vila, B., 2016. Transitional environments of the lower Maastrichtian South-Pyrenean Basin (Catalonia, Spain): The Fumanya Member tidal flat. *Cretaceous Research* 57, 428–442. <https://doi.org/10.1016/j.cretres.2015.09.004>
- Osborn, H.F., 1905. *Tyrannosaurus* and other Cretaceous carnivorous dinosaurs. *Bulletin of the AMNH. Bulletin of the American Museum of Natural History* 21, 259–265.
- Ősi, A., Codrea, V., Prondvai, E., Csiki-Sava, Z., 2014. New ankylosaurian material from the Upper Cretaceous of Transylvania. *Annales de Paléontologie* 100, 257–271. <https://doi.org/10.1016/j.annpal.2014.02.001>
- Ostrom JH. 1969. Osteology of *Deinonychus antirrhopus*, and unusual theropod from the Lower Cretaceous of Montana. *Bulletin of the Peabody Museum of Natural History* 30:1-165
- Pearson, D.A., Schaefer, T., Johnson, K.R., Nichols, D.J., Hunter, J.P., 2002. Vertebrate biostratigraphy of the Hell Creek Formation in southwestern North Dakota and northwestern South Dakota. *Special Paper of the Geological Society of America* 361, 145–167. <https://doi.org/10.1130/0-8137-2361-2.145>
- Peláez-Campomanes, P., López-Martínez, N., Álvarez-Sierra, M.A., Daams, R., 2000. The earliest mammal of the European Paleocene: The multituberculate *Hainina*. *Journal of Paleontology* 74, 701–711. <https://doi.org/10.1017/S0022336000032819>
- Pereda-Suberbiola, X., Company, J., Ruiz-Omeñaca, J.I., 2007. Azhdarchid pterosaurs from the Late Cretaceous (Campanian-Maastrichtian) of the Iberian Peninsula: an update. , Munich (Germany), September 2007. Abstracts, 27., in: Munich Flugsaurier, The Wellnhofer Pterosaur Meeting. Munich (Germany), p. 27.
- Pereda-Suberbiola, X., Canudo, J.I., Company, J., Cruzado-Caballero, P., Ruiz-Omeñaca, J.I., 2009a. Hadrosauroid dinosaurs from the latest Cretaceous of the Iberian Peninsula. *Journal of Vertebrate Paleontology* 29, 946–951. <https://doi.org/10.1671/039.029.0317>
- Pereda-Suberbiola, X., Canudo, J.I., Cruzado-Caballero, P., Barco, J.L., López-Martínez, N., Oms, O., Ruiz-Omeñaca, J.I., 2009b. The last hadrosaurid dinosaurs of Europe: A new lambeosaurine from the Uppermost Cretaceous of Aren (Huesca, Spain). *Comptes Rendus - Palevol* 8, 559–572. <https://doi.org/10.1016/j.crpv.2009.05.002>
- Pereda-Suberbiola, X., Corral, J.C., Astibia, H., Badiola, A., Bardet, N., Berreteaga, A., Buffetaut, E., Buscalioni, A.D., Cappetta, H., Cavin, L., Díez Díaz, V., Gheerbrant, E., Murelaga, X., Ortega, F., Pérez-García, A., Poyato-Ariza, F., Rage, J.-C., Sanz, J.L., Torices, A., 2015a. Late cretaceous continental and marine vertebrate assemblages from the Laño quarry (Basque-Cantabrian Region, Iberian Peninsula): an update. *Journal of Iberian Geology* 41. [https://doi.org/10.5209/rev\\_JIGE.2015.v41.n1.48658](https://doi.org/10.5209/rev_JIGE.2015.v41.n1.48658)

- Pereda-Suberbiola, X., Pérez-García, A., Corral, J.C., Murelaga, X., Martin, G., Larrañaga, J., Bardet, N., Berreteaga, A., Company, J., 2015b. First dinosaur and turtle remains from the latest Cretaceous shallow marine deposits of Albaina (Laño quarry, Iberian Peninsula). *Comptes Rendus Palevol* 14, 471–482. <https://doi.org/10.1016/j.crpv.2014.11.003>
- Pérez-García, A., 2017. The Iberian fossil record of turtles: an update. *Journal of Iberian Geology* 43, 155–191. <https://doi.org/10.1007/s41513-017-0016-4>
- Pérez-García, A., Ortega, F., Murelaga, X., 2012. A new genus of Bothremydidae (Chelonii, Pleurodira) in the Cretaceous of Southwestern Europe. *Geobios* 45, 219–229. <https://doi.org/10.1016/j.geobios.2011.03.001>
- Pérez-García, A., Ortega, F., Bolet, A., Escaso, F., Houssaye, A., Martínez-Salanova, J., de Miguel Chaves, C., Mocho, P., Narváez, I., Segura, M., Torices, A., Vidal, D., Sanz, J.L., 2016. A review of the upper Campanian vertebrate site of Armuña (Segovia Province, Spain). *Cretaceous Research* 57, 591–623. <https://doi.org/10.1016/j.cretres.2015.08.008>
- Pérez-García, A., Codrea, V., 2018. New insights on the anatomy and systematics of *Kallokibotion* Nopcsa, 1923, the enigmatic uppermost Cretaceous basal turtle (stem Testudines) from Transylvania. *Zoological Journal of the Linnean Society* 182, 419–443. <https://doi.org/10.1093/zoolinnean/zlx037>
- Pérez-García, A., Ortega, F., Murelaga, X., 2021. *Iberoccitanemys atlanticum* (Lapparent de Broin & Murelaga, 1996) n. comb.: new data on the diversity and paleobiogeographic distributions of the Campanian-Maastrichtian bothremydid turtles of Europe. *Comptes Rendus Palevol*. <https://doi.org/10.5852/cr-palevol2021v20a32>
- Pérez-Pueyo, M., Castanera, D., Bádenas, B., Canudo, J.I., 2018. New evidences of Crocodylomorpha swim tracks in the Maastrichtian of Beranuy (Huesca, Spain, in: *Life Finds a Way. Libro de Resúmenes Del XVI Encuentro de Jóvenes Investigadores En Paleontología. Zarautz (Spain)*, pp. 137–140.
- Pérez-Pueyo, M., Puértolas-Pascual, E., Bádenas, B., 2019. Larra 4: desenterrando a los últimos vertebrados del Maastrichtiense terminal del pirineo aragonés. *Libro de Resúmenes del XVII Encuentro de Jóvenes Investigadores en Paleontología Nájera (Spain)*, pp. 159–163.
- Pérez-Pueyo, M., Cruzado-Caballero, P., Moreno-Azanza, M., Vila, B., Castanera, D., Gasca, J.M., Puértolas-Pascual, E., Bádenas, B., Canudo, J.I., 2021a. The Tetrapod Fossil Record from the Uppermost Maastrichtian of the Ibero-Armorican Island: An Integrative Review Based on the Outcrops of the Western Tremp Syncline (Aragón, Huesca Province, NE Spain). *Geosciences* 11, 162. <https://doi.org/10.3390/geosciences11040162>
- Pérez-Pueyo, M., Moreno-Azanza, M., Núñez-Lahuerta, C., Puértolas-Pascual, E., Bádenas, B., Canudo, J.I., 2021b. Eggshell association of the Late Maastrichtian (Late Cretaceous) at Blasi 2B fossil site: A scrambled of vertebrate diversity. *Ciências da Terra-Procedia* 1, 58–61.
- Pérez-Pueyo, M., Puértolas-Pascual, E., Moreno-Azanza, M., Cruzado-Caballero, P., Gasca, J.M., Núñez-Lahuerta, C., Canudo, J.I., 2021c. First record of a giant bird (Ornithuromorpha) from the uppermost Maastrichtian of the Southern Pyrenees, northeast Spain. *J. Vertebr. Paleontol.* 41. <https://doi.org/10.1080/02724634.2021.1900210>
- Peters, D.S., 1988. Ein vollständiges Exemplar von *Palaeotis weigelti* (Aves, Palaeognathae). *Courier Forschungsinstitut Senckenberg* 107, 223–233.
- Pires, M.M., Rankin, B.D., Silvestro, D., Quental, T.B., 2018. Diversification dynamics of mammalian clades during the K–Pg mass extinction. *Biology Letters* 14, 20180458. <https://doi.org/10.1098/rsbl.2018.0458>

- Plummer, H.J., 1931. Some Cretaceous foraminifera in Texas. University of Texas Bulletin 3101, 109–203.
- Pol, C., Buscalioni, A.D., Carballeira, J., Francés, V., López-Martínez, N., Marandat, B., Moratalla, J., Sanz, J.L., Sigé, B., Villatte, J., 1992. Reptiles and mammals from the Late Cretaceous new locality Quintanilla del Coco (Burgos Province, Spain). Neues Jahrbuch für Geologie und Paläontologie Abhandlungen 184, 279–314.
- Poyato-Ariza, F.J., Fielitz, C., Wenz, S., 1999. Marine actinopterygian fauna from the Upper Cretaceous of Albaina (Laño quarry, Northern Spain). Estudios del Museo Ciencias Naturales de Álava 14 (Número, 325–338).
- Prasad, G.V.R., Rage, J.C., 1995. Amphibians and squamates from the Maastrichtian of Naskal, India. Cretaceous Research 16, 95–107. <https://doi.org/10.1006/cres.1995.1006>
- Prasad, G.V., de Lapparent de Broin, F., 2002. Late Cretaceous crocodile remains from Naskal (India): comparisons and biogeographic affinities. Annales de Paléontologie 88, 19–71. [https://doi.org/10.1016/S0753-3969\(02\)01036-4](https://doi.org/10.1016/S0753-3969(02)01036-4)
- Prasad, G.V.R., Rage, J.C., 2004. Fossil frogs (Amphibia: Anura) from the Upper Cretaceous intertrappean beds of Naskal, Andhra Pradesh. Revue de Paléobiologie 23, 99–116.
- Prasad, G.V.R., Verma, O., Gheerbrant, E., Goswami, A., Khosla, A., Parmar, V., Sahni, A., 2010. First mammal evidence from the Late Cretaceous of India for biotic dispersal between India and Africa at the KT transition. Comptes Rendus Palevol 9, 63–71. <https://doi.org/10.1016/j.crpv.2009.12.003>
- Prieto-Márquez, A., Gaete, R., Rivas, G., Galobart, À., Boada, M., 2006. Hadrosauroid dinosaurs from the Late Cretaceous of Spain: *Pararhabdodon isonensis* revisited and *Koutalisaurus kohlerorum*, gen. et sp. nov. Journal of Vertebrate Paleontology 26, 929–943. [https://doi.org/10.1671/0272-4634\(2006\)26\[929:HDFTL\]2.0.CO;2](https://doi.org/10.1671/0272-4634(2006)26[929:HDFTL]2.0.CO;2)
- Prieto-Márquez, A., Wagner, J.R., 2009. *Pararhabdodon isonensis* and *Tsintaosaurus spinorhinus*: a new clade of lambeosaurine hadrosaurids from Eurasia. Cretaceous Research 30, 1238–1246. <https://doi.org/10.1016/j.cretres.2009.06.005>
- Prieto-Márquez, A., Dalla Vecchia, F.M., Gaete, R., Galobart, À., 2013. Diversity, Relationships, and Biogeography of the Lambeosaurine Dinosaurs from the European Archipelago, with Description of the New Aralosaurin *Canardia garonnensis*. PLoS ONE 8, e69835. <https://doi.org/10.1371/journal.pone.0069835>
- Prieto-Márquez, A., Fondevilla, V., Sellés, A.G., Wagner, J.R., Galobart, À., 2019. *Adynomosaurus arcanus*, a new lambeosaurine dinosaur from the Late Cretaceous Ibero-Armorican Island of the European archipelago. Cretaceous Research 96, 19–37. <https://doi.org/10.1016/j.cretres.2018.12.002>
- Prieto-Márquez, A., Carrera Farias, M., 2021. The late-surviving early diverging Ibero-Armorican ‘duck-billed’ dinosaur *Fylax* and the role of the Late Cretaceous European Archipelago in hadrosauroid biogeography. Acta Palaeontologica Polonica 66. <https://doi.org/10.4202/app.00821.2020>
- Puértolas, E., Canudo, J.I., Cruzado-Caballero, P., 2011. A new crocodylian from the Late Maastrichtian of Spain: Implications for the initial radiation of crocodyloids. PLoS ONE 6. <https://doi.org/10.1371/journal.pone.0020011>
- Puértolas-Pascual, E., Cruzado-Caballero, P., Canudo, J.I., Gasca, J.M., Moreno-Azanza, M., Castanera, D., Parrillas, J., Ezquerro, L., 2012. Nuevos yacimientos de vertebrados del

- Maastrichtiense superior ( Cretácico Superior ) de Huesca ( España ). VIII Congreso Geológico de España. Comunicaciones 269–272.
- Puértolas-Pascual, E., Canudo, J.I., Moreno-Azanza, M., 2014. The eusuchian crocodylomorph *Allodaposuchus subjuniperus* sp. nov., a new species from the latest Cretaceous (upper Maastrichtian) of Spain. *Historical Biology* 26, 91–109. <https://doi.org/10.1080/08912963.2012.763034>
- Puértolas-Pascual, E., Rabal-Garcés, R., Canudo, J.I., 2015. Exceptional crocodylomorph biodiversity of “La Cantalera” site (lower Barremian; Lower Cretaceous) in Teruel, Spain. *Palaeontologia Electronica* 18.2.28A, 1–16.
- Puértolas-Pascual, E., Blanco, A., Brochu, C.A., Canudo, J.I., 2016. Review of the Late Cretaceous–early Paleogene crocodylomorphs of Europe: Extinction patterns across the K-PG boundary. *Cretaceous Research* 57, 565–590. <https://doi.org/10.1016/j.cretres.2015.08.002>
- Puértolas-Pascual, E., Arenillas, I., Arz, J.A., Calvín, P., Ezquerro, L., García-Vicente, C., Pérez-Pueyo, M., Sánchez-Moreno, E.M., Villaláin, J.J., Canudo, J.I., 2018. Chronostratigraphy and new vertebrate sites from the upper Maastrichtian of Huesca (Spain), and their relation with the K/Pg boundary. *Cretaceous Research* 89, 36–59. <https://doi.org/10.1016/j.cretres.2018.02.016>
- Pueyo, E. L., 2000. Rotaciones paleomagnéticas en sistemas de pliegues y cabalgamientos. Tipos, causas, significado y aplicaciones (ejemplos del Pirineo Aragonés). Doctoral Thesis. Universidad de Zaragoza, 296 pp.
- Pueyo, E. L., Garcés, M., Mauritsch, H. J., Lewis, C., Scholger, R., Sancho, C., Molina, R., Schnepf, E., Larrasoña, J. C., Parés, J. M., Pocoví, A., Muñoz, A., Valero, B., Millán, H., Laplana, C., Oliva, B., González, P., 2006. Sampling, transportation and magnetic-free consolidation of extremely soft sediments for paleomagnetic purposes: a successful “recipe”. 121–128 pp. In: *MAGIBER I: Paleomagnetismo en la Península Ibérica*. Edited by: M. Calvo, M. Garcés, C. Gomes, J.C. Larrasoña, E. Pueyo y J.J. Villaláin. Universidad de Burgos, 129–135 pp
- Pueyo, E. L., Sánchez, E., Canudo, J. L., Pereda Suberbiola, X., Puértolas Pascual, E., Parrilla-Bel, J., Cruzado-Caballero, P., Pérez-Pueyo, M., Compairé, F., 2016. Magnetoestratigrafía del Cretácico Superior del sector Occidental de las Sierras Exteriores (Pirineo Occidental); implicaciones bioestratigráficas. *Geo-Temas*, 16 (1) 909–912.
- Puigdefàbregas, C., Muñoz, J.A., Marzo, M., 1986. Thrust belt development in the eastern Pyrenees and related depositional sequences in the southern foreland basin. In: Allen, P. A., Homewood, P. (Eds.), *Foreland basins*, Blackwell Publishing, pp. 229–246.
- Pujalte, V., Schmitz, B., 2005. The stratigraphy of the Tremp Group revisited (Garumnian, Tremp-Graus basin, South Pyrenees). *Geogaceta* 38, 79–82
- Pujalte, V., Baceta, J.I., Schmitz, B., Orue-Etxebarria, X., Payros, A., Bernaola, G., Apellaniz, E., Caballero, F., Robador, A., Serra-Kiel, J., Tosquella, J., 2009. Redefinition of the Ilerdian Stage (early Eocene). *Geologica Acta* 7, 177–194. <https://doi.org/10.1344/105.000000268>
- Pujalte, V., Schmitz, B., Baceta, J.I., 2014. Sea-level changes across the Paleocene–Eocene interval in the Spanish Pyrenees, and their possible relationship with North Atlantic magmatism. *Palaeogeography, Palaeoclimatology, Palaeoecology* 393, 45–60. <https://doi.org/10.1016/j.palaeo.2013.10.016>
- Purnell, M.A., Donoghue, P.C.J., 2005. Between death and data: biases in interpretation of the fossil record of conodonts. *The Palaeontological Association. Special Papers in Palaeontology* 25, 7–25.

- Rabi, M., Vremir, M., Tong, H., 2013. Preliminary Overview of Late Cretaceous Turtle Diversity in Eastern Central Europe (Austria, Hungary, and Romania) In: Brinkman, D., Holroyd, P., Gardner, J. (Eds.), *Morphology and Evolution of Turtles. Vertebrate Paleobiology and Paleoanthropology*. Springer Netherlands, pp. 307–336. [https://doi.org/10.1007/978-94-007-4309-0\\_19](https://doi.org/10.1007/978-94-007-4309-0_19)
- Ramón, M. J., Pueyo, E. L., 2012. Automatic calculation of demagnetization intervals; a new approach based on the virtual directions method and comparison with the linearity spectrum analysis. *Geotemas* 13, 1180-1183
- Ramón, M. J., 2013. Flexural unfolding of complex geometries in fold and thrust belts using paleomagnetic vectors. University of Zaragoza. Doctoral Thesis, 262 pp.
- Ramón, M.J., Pueyo E.L., Oliva-Urcia, B., Larrasoña, J.C., 2017. Virtual directions in paleomagnetism: A global and rapid approach to evaluate the NRM components and their stability. *Frontiers in Earth Science*, 5 (8), 14 pp. doi:10.3389/feart.2017.00008
- Ramos, A., Lopez-Mir, B., Wilson, E.P., Granado, P., Muñoz, J.A., 2020. 3D reconstruction of syn-tectonic strata deposited during the inversion of salt-related structures: insights from the Lliert syncline (South-central Pyrenees). *Geologica Acta*, 18.20, 1-19.
- Rana, R.S., Sati, K.K., 2000. Late Cretaceous-Palaeocene crocodilians from the Deccan Trap associated sedimentary sequences of peninsular India. *Journal of the Palaeontological Society of India* 45, 123–136.
- Rana, R.S., Mohabey, D.M., 2005. Lizard fauna from the Intertrappean (Late Cretaceous-Early Palaeocene) beds of Peninsular India. *Gondwana Geological Magazine* 8, 123–132.
- Range, M.M., Arbib, B.K., Johnson, B.C., Moore, T.C., Titov, V., Adcroft, A.J., Ansong, J.K., Hollis, C.J., Ritsema, J., Scotese, C.R., Wang, H., 2022. The Chicxulub Impact Produced a Powerful Global Tsunami. *AGU Advances* 3. <https://doi.org/10.1029/2021AV000627>
- Rauhut, O.W.M., 2003. The interrelationships and evolution of basal theropod dinosaurs. *Special papers in Palaeontology* 69, Palaeontological Association, London, 213 pp.
- Raup, D.M., Sepkoski, J.J., 1982. Mass Extinctions in the Marine Fossil Record. *Science* 215, 1501–1503. <https://doi.org/10.1126/science.215.4539.1501>
- Raup, D.M., Jablonski, D., 1993. Geography of End-Cretaceous Marine Bivalve Extinctions. *Science* 260, 971–973. <https://doi.org/10.1126/science.11537491>
- Renne, P.R., Goodwin, M.B., 2012. Direct U-Pb dating of Cretaceous and Paleocene dinosaur bones, San Juan Basin, New Mexico: COMMENT. *Geology* 40, e259–e259. <https://doi.org/10.1130/G32521C.1>
- Renne, P.R., Deino, A.L., Hilgen, F.J., Kuiper, K.F., Mark, D.F., Mitchell, W.S., Morgan, L.E., Mundil, R., Smit, J., 2013. Time Scales of Critical Events Around the Cretaceous-Paleogene Boundary. *Science* 339, 684–687. <https://doi.org/10.1126/science.1230492>
- Renne, P.R., Arenillas, I., Arz, J.A., Vajda, V., Gilabert, V., Bermúdez, H.D., 2018. Multi-proxy record of the Chicxulub impact at the Cretaceous-Paleogene boundary from Gorgonilla Island, Colombia. *Geology* 46, 547–550. <https://doi.org/10.1130/G40224.1>
- Riera, V., 2010. Estudio integrado (geología y paleontología) de la sucesión de dinosaurios (Maastrichtiense) de la vertiente surpirenaica. Universitat Autònoma de Barcelona. Doctoral Thesis 274 pp.

- Riera, V., Oms, O., Gaete, R., Galobart, À., 2009. The end-Cretaceous dinosaur succession in Europe: The Tremp Basin record (Spain). *Palaeogeography, Palaeoclimatology, Palaeoecology* 283, 160–171. <https://doi.org/10.1016/j.palaeo.2009.09.018>
- Robador, A., Samsó, J.M., Serra-Kiel, J., Tosquella, J., 1990. Field Guide, in: Barnolas, A., Robador, A., Serra-Kiel, J., Caus, E. (Eds.), *Introduction to the Early Paleogene Of the South Pyrenean Basin. Field Trip Guidebook*. pp. 131–159.
- Roberts, E.M., O'Connor, P.M., Clarke, J.A., Slotznick, S.P., Placzek, C.J., Tobin, T.S., Hannaford, C., Orr, T., Jinnah, Z.A., Claeson, K.M., Salisbury, S., Kirschvink, J.L., Pirrie, D., Lamanna, M.C., 2022. New age constraints support a K/Pg boundary interval on Vega Island, Antarctica: Implications for latest Cretaceous vertebrates and paleoenvironments. *GSA Bulletin*. <https://doi.org/10.1130/B36422.1>
- Robertson, D.S., Lewis, W.M., Sheehan, P.M., Toon, O.B., 2013. K-Pg extinction patterns in marine and freshwater environments: The impact winter model. *Journal of Geophysical Research: Biogeosciences* 118, 1006–1014. <https://doi.org/10.1002/jgrg.20086>
- Rogers, R.R., Kidwell, D.A., 2007. A conceptual framework for the genesis and analysis of vertebrate skeletal concentrations. In: Rogers, R.R., Eberth, D.A., Fiorillo, A.R. (Eds.), *Bonebeds: Genesis, Analysis, and Paleobiological Significance*. University of Chicago Press, Chicago, pp. 103–220.
- Robin, N., van Bakel, B.W.M., Hyžný, M., Cincotta, A., Garcia, G., Charbonnier, S., Godefroit, P., Valentin, X., 2019. The oldest freshwater crabs: claws on dinosaur bones. *Scientific Reports* 9, 20220. <https://doi.org/10.1038/s41598-019-56180-w>
- Rosell, J., Linares, R., Llompart, C., 2001. El “garumniense” prepirenaico. *Revista de la Sociedad Geológica de España* 14, 47–56.
- Russell, D.A., Manabe, M., 2002. Synopsis of the Hell Creek (uppermost Cretaceous) dinosaur assemblage, in: *The Hell Creek Formation and the Cretaceous-Tertiary Boundary in the Northern Great Plains: An Integrated Continental Record of the End of the Cretaceous*. Geological Society of America. <https://doi.org/10.1130/0-8137-2361-2.169>
- Sakamoto, M., Benton, M.J., Venditti, C., 2016. Dinosaurs in decline tens of millions of years before their final extinction. *Proceedings of the National Academy of Sciences* 113, 5036–5040. <https://doi.org/10.1073/pnas.1521478113>
- Salgado, L., Coria, R.A., Calvo, J.O., 1997. Evolution of titanosaurid sauropods: Phylogenetic analysis based on the postcranial evidence. *Ameghiniana* 34, 3–32.
- Santa Catharina, A., Kneller, B.C., Marques, J.C., McArthur, A.D., Cevallos-Ferriz, S.R.S., Theurer, T., Kane, I.A., Muirhead, D., 2022. Timing and causes of forest fire at the K–Pg boundary. *Scientific Reports* 12, 13006. <https://doi.org/10.1038/s41598-022-17292-y>
- Santafé, J.V., Casanovas, M.L., Llompart, C., 1997. *Els Dinosauris i el seu entorn geològic*. Diputació de Lleida 69 pp.
- Santos Brilhante, N., de França, T. C., Castro, F., Sanches da Costa, L., Currie, P. J., Kugland de Azevedo, S. A., Delcourt, R., 2022. A dromaeosaurid-like claw from the Upper Cretaceous of southern France. *Historical Biology*, 34(11), 1–10.
- Sanz, J.L., L.M. Chiappe, B.P. Pérez-Moreno, J.J. Moratalla, F. Hernández-Carrasquilla, A.D. Buscalioni, F. Ortega, F.J. Poyato-Ariza, D. Rasskin-Gutman, X. Martínez-Delclòs., 1997. A nestling bird from the Lower Cretaceous of Spain: implications for avian skull and neck evolution. *Science* 276, 1543–1546.

- Scannella, J.B., Fowler, D.W., 2014. A stratigraphic survey of *Triceratops* localities in the Hell Creek Formation, northeastern Montana (2006–2010). *Geological Society of America Special Papers* 503.
- Scasso, R.A., Concheyro, A., Kiessling, W., Aberhan, M., Hecht, L., Medina, F.A., Tagle, R., 2005. A tsunami deposit at the Cretaceous/Paleogene boundary in the Neuquén Basin of Argentina. *Cretaceous Research* 26, 283–297. <https://doi.org/10.1016/j.cretres.2004.12.003>
- Scheepers, P.J.J., Zijdeveld, J.D.A., 1992. Stacking in Paleomagnetism: Application to marine sediments with weak NRM. *Geophysical Research Letters*, 1914, 1519-1522.
- Schmidt, P. W., 1982. Linearity spectrum analysis of multi-component magnetizations and its application to some igneous rocks from south-eastern Australia. *Geophysical Journal International*, 70(3), 647-665.
- Schoene, B., Eddy, M.P., Samperton, K.M., Keller, C.B., Keller, G., Adatte, T., Khadri, S.F.R., 2019. U-Pb constraints on pulsed eruption of the Deccan Traps across the end-Cretaceous mass extinction. *Science* 363, 862–866. <https://doi.org/10.1126/science.aau2422>
- Schulte, P., Alegret, L., Arenillas, I., Arz, J.A., Barton, P.J., Bown, P.R., Bralower, T.J., Christeson, G.L., Claes, P., Cockell, C.S., Collins, G.S., Deutsch, A., Goldin, T.J., Goto, K., Grajales-Nishimura, J.M., Grieve, R.A.F., Gulick, S.P.S., Johnson, K.R., Kiessling, W., Koeberl, C., Kring, D.A., MacLeod, K.G., Matsui, T., Melosh, J., Montanari, A., Morgan, J. V., Neal, C.R., Nichols, D.J., Norris, R.D., Pierazzo, E., Ravizza, G., Rebolledo-Vieyra, M., Reimold, W.U., Robin, E., Salge, T., Speijer, R.P., Sweet, A.R., Urrutia-Fucugauchi, J., Vajda, V., Whalen, M.T., Willumsen, P.S., 2010a. The Chicxulub Asteroid Impact and Mass Extinction at the Cretaceous-Paleogene Boundary. *Science* 327, 1214–1218. <https://doi.org/10.1126/science.1177265>
- Schulte, P., Alegret, L., Arenillas, I., Arz, J.A., Barton, P.J., Bown, P.R., Bralower, T.J., Christeson, G.L., Claes, P., Cockell, C.S., Collins, G.S., Deutsch, A., Goldin, T.J., Goto, K., Grajales-Nishimura, J.M., Grieve, R.A.F., Gulick, S.P.S., Johnson, K.R., Kiessling, W., Koeberl, C., Kring, D.A., Macleod, K.G., Matsui, T., Melosh, J., Montanari, A., Morgan, J. V., Neal, C.R., Norris, R.D., Pierazzo, E., Ravizza, G., Rebolledo-Vieyra, M., Reimold, W.U., Robin, E., Salge, T., Speijer, R.P., Sweet, A.R., Urrutia-Fucugauchi, J., Vajda, V., Whalen, M.T., Willumsen, P.S., 2010b. Response—Cretaceous Extinctions. *Science* 328, 975–976. <https://doi.org/10.1126/science.328.5981.975>
- Scott, A.C., 2000. The Pre-Quaternary history of fire. *Palaeogeography, Palaeoclimatology, Palaeoecology* 164, 281–329. [https://doi.org/10.1016/S0031-0182\(00\)00192-9](https://doi.org/10.1016/S0031-0182(00)00192-9)
- Scott, A.C., 2010. Charcoal recognition, taphonomy and uses in palaeoenvironmental analysis. *Palaeogeography, Palaeoclimatology, Palaeoecology* 291, 11–39. <https://doi.org/10.1016/j.palaeo.2009.12.012>
- Séguret, M., 1972. Étude tectonique des nappes et séries decollées de la partie centrale du versant sud des Pyrénées. Caractère synsédimentaire, rôle de la compression et de la gravité. *Publications de l'Université des Sciences et Techniques du Languedoc (USTELA). Série Géologie Structurale* 2, 163.
- Sellés, A. G., Bravo, A. M., Delclòs, X., Colombo, F., Martí, X., Ortega-Blanco, J., Parellada, C., Galobart, À., 2013. Dinosaur eggs in the Upper Cretaceous of the Coll de Nargó area, Lleida Province, south-central Pyrenees, Spain: Oodiversity, biostratigraphy and their implications. *Cretaceous Research*, 40, 10-20.

- Sellés, A.G., Vila, B., Galobart, À., 2014a. *Spheroolithus europaeus*, oosp. nov. (late Maastrichtian, Catalonia), the youngest oological record of hadrosauroids in Eurasia. *Journal of Vertebrate Paleontology* 34, 725–729. <https://doi.org/10.1080/02724634.2013.819360>
- Sellés, A.G., Vila, B., Galobart, À., 2014b. Diversity of theropod ootaxa and its implications for the latest cretaceous dinosaur turnover in southwestern Europe. *Cretaceous Research* 49, 45–54. <https://doi.org/10.1016/j.cretres.2014.02.004>
- Sellés A. G., Galobart À., 2016. Reassessing the endemic European Upper Cretaceous dinosaur egg *Cairanoolithus*. *Historical Biology* 28(5), 583–596.
- Sellés, A.G., Marmi, J., Llácer, S., Blanco, A., 2016. The youngest sauropod evidence in Europe. *Historical Biology* 28, 930–940. <https://doi.org/10.1080/08912963.2015.1059834>
- Sellés, A. G., Blanco, A., Vila, B., Marmi, J., López-Soriano, F. J., Llácer, S., Frigola, J., Canals, M., Galobart, À., 2020. A small Cretaceous crocodyliform in a dinosaur nesting ground and the origin of sebecids. *Scientific reports*, 10(1), 1–11.
- Sellés, A.G., Vila, B., Brusatte, S.L., Currie, P.J., Galobart, À., 2021. A fast-growing basal troodontid (Dinosauria: Theropoda) from the latest Cretaceous of Europe. *Scientific Reports* 11, 4855. <https://doi.org/10.1038/s41598-021-83745-5>
- Senter P., 2007. A method for distinguishing dromaeosaurid manual unguals from pedal “sickle claws”. *Bulletin of the Gunma Museum of Natural History*. 11,1–6.
- Sepkoski, J.J., 1993. Ten years in the library: new data confirm paleontological patterns. *Paleobiology* 19, 43–51. <https://doi.org/10.1017/S0094837300012306>
- Serra-Kiel, P., Canudo, J., Dinares, J., Molina, E., Ortiz, N., Pascual, J., Samsó, J., Tosquella, J., 1994. Cronoestratigrafía de los sedimentos marinos del Terciario inferior de la Cuenca de Tremp-Graus (Zona Central Surpirenaica). *Revista de la Sociedad Española de Geología* 7, 273–299.
- Serra-Kiel, J., Vicedo, V., Baceta, J.I., Bernaola, G., Robador, A., 2020. Paleocene Larger Foraminifera from the Pyrenean Basin with a recalibration of the Paleocene Shallow Benthic Zones. *Geologica Acta* 18, 1–69. <https://doi.org/10.1344/GeologicaActa2020.18.8>
- Serrano, J.F., Sellés, A.G., Vila, B., Galobart, À., Prieto-Márquez, A., 2021. The osteohistology of new remains of *Pararhabdodon isonensis* sheds light into the life history and paleoecology of this enigmatic European lambeosaurine dinosaur. *Cretaceous Research* 118, 104677. <https://doi.org/10.1016/j.cretres.2020.104677>
- Sibuet, J.-C., Srivastava, S.P., Spakman, W., 2004. Pyrenean orogeny and plate kinematics. *Journal of Geophysical Research: Solid Earth* 109 (B08104). <https://doi.org/10.1029/2003JB002514>
- Smit, J., 1982. Extinction and evolution of planktonic foraminifera after a major impact at the Cretaceous/Tertiary boundary. pp. 329–352. <https://doi.org/10.1130/SPE190-p329>
- Smith, T., F. Quesnel, G. De Ploëg, D. De Franceschi, G. Métais, E. De Bast, F. Solé, A. Folie, A. Boura, J. Claude, C. Dupuis, C. Gagnaison, A. Iakovleva, J. Martin, F. Maubert, J. Prieur, E. Roche, J.-Y. Storme, R. Thomas, H. Tong, J. Yans, E. Buffetaut., 2014. First Clarkforkian equivalent Land Mammal Age in the latest Palaeocene basal Sparnacian facies of Europe: fauna, flora, paleoenvironment and (bio)stratigraphy. *PLoS ONE* 9 (1), e86229
- Smith, T., Codrea, V., 2015. Red Iron-Pigmented Tooth Enamel in a Multituberculate Mammal from the Late Cretaceous Transylvanian “Hațeg Island.” *PLOS ONE* 10, e0132550. <https://doi.org/10.1371/journal.pone.0132550>

- Solomon, A.A., Codrea, V.A., Venczel, M., Grellet-Tinner, G., 2020. A new species of large-sized pterosaur from the Maastrichtian of Transylvania (Romania). *Cretaceous Research* 110, 104316. <https://doi.org/10.1016/j.cretres.2019.104316>
- Soulié-Märsche, I., 1989. Étude comparée de gyrogonites de charophytes actuelles et fossiles et phylogénie des genres actuels. Imprimerie des Tilleuls, Millau, France. 237 pp.
- Soulié-Märsche, I., Joseph, C., 1991. Fiabilité des données morphométriques en micropaléontologie: Exemple des Charophytes. *Geobios* 24, 113–123. [https://doi.org/10.1016/S0016-6995\(66\)80016-5](https://doi.org/10.1016/S0016-6995(66)80016-5)
- Sprain, C.J., Renne, P.R., Wilson, G.P., Clemens, W.A., 2015. High-resolution chronostratigraphy of the terrestrial Cretaceous–Paleogene transition and recovery interval in the Hell Creek region, Montana. *Geological Society of America Bulletin* 127, 393–409. <https://doi.org/10.1130/B31076.1>
- Sprain, C.J., Renne, P.R., Clemens, W.A., Wilson, G.P., 2018. Calibration of chron C29r: New high-precision geochronologic and paleomagnetic constraints from the Hell Creek region, Montana. *GSA Bulletin* 130, 1615–1644. <https://doi.org/10.1130/B31890.1>
- Sprain, C.J., Renne, P.R., Vanderkluisen, L., Pande, K., Self, S., Mittal, T., 2019. The eruptive tempo of Deccan volcanism in relation to the Cretaceous–Paleogene boundary. *Science* 363, 866–870. <https://doi.org/10.1126/science.aav1446>
- Springer, M.S., Murphy, W.J., Eizirik, E., O'Brien, S.J., 2003. Placental mammal diversification and the Cretaceous–Tertiary boundary. *Proceedings of the National Academy of Sciences* 100, 1056–1061. <https://doi.org/10.1073/pnas.0334222100>
- Srivastava, A.K., Mankar, R.S., 2015. Lithofacies architecture and depositional environment of Late Cretaceous Lameta Formation, central India. *Arabian Journal of Geosciences* 8, 207–226. <https://doi.org/10.1007/s12517-013-1192-y>
- Stinnesbeck, W., Irlm, C., Salazar, C., 2012. The Last Cretaceous Ammonites in Latin America. *Acta Palaeontologica Polonica* 57, 717–728. <https://doi.org/10.4202/app.2011.0042>
- Sues, H.D., Averianov, A., 2014. Dromaeosauridae (Dinosauria: Theropoda) from the Bissekty Formation (Upper Cretaceous: Turonian) of Uzbekistan and the phylogenetic position of *Itemirus medullaris* Kurzanov, 1976. *Cretaceous Research* 51, 225–240.
- Swisher III, C.C., Dingus, L., Butler, R.F., 1993. <sup>40</sup>Ar/<sup>39</sup>Ar dating and magnetostratigraphic correlation of the terrestrial Cretaceous–Paleogene boundary and Puerco Mammal Age, Hell Creek – Tullock formations, eastern Montana. *Canadian Journal of Earth Sciences* 30, 1981–1996. <https://doi.org/10.1139/e93-174>
- Szabó, M., Gulyás, P., Ősi, A., 2016. Late Cretaceous (Santonian) *Atractosteus* (Actinopterygii, Lepisosteidae) remains from Hungary (Iharkút, Bakony Mountains). *Cretaceous Research* 60, 239–252. <https://doi.org/10.1016/j.cretres.2015.12.002>
- Szabó, M., Ősi, A., 2017. The continental fish fauna of the Late Cretaceous (Santonian) Iharkút locality (Bakony Mountains, Hungary). *Central European Geology* 60, 230–287. <https://doi.org/10.1556/24.60.2017.009>
- Szentesi, Z., Company, J., 2017. Late Maastrichtian small-sized herpetofauna from Valencia province, eastern Spain. *Historical Biology* 29, 43–52. <https://doi.org/10.1080/08912963.2015.1122004>
- Tabuce, R., Tortosa, T., Vianey-Liaud, M., Garcia, G., Lebrun, R., Godefroit, P., Dutour, Y., Berton, S., Valentin, X., Cheylan, G., 2013. New eutherian mammals from the Late Cretaceous of

- Aix-en-Provence Basin, south-eastern France. *Zoological Journal of the Linnean Society* 169, 653–672. <https://doi.org/10.1111/zoj.12074>
- Tambussi, C. P., R. De Mendoza, F.J. Degrange, M.B. Picasso., 2012. Flexibility along the neck of the Neogene terror bird *Andalgalornis steulleti* (Aves Phorusrhacidae). *PLoS One* 7(5), e37701.
- Tanaka, T., Y. Kobayashi, K.I. Kurihara, A.R. Fiorillo, M. Kano., 2018. The oldest Asian hesperornithiform from the Upper Cretaceous of Japan, and the phylogenetic reassessment of Hesperornithiformes. *Journal of Systematic Palaeontology* 16(8), 689–709.
- Tanner, L.H., Lucas, S.G., 2016. Stratigraphic distribution and significance of a 15 million-year record of fusain in the Upper Triassic Chinle Group, southwestern USA. *Palaeogeography, Palaeoclimatology, Palaeoecology* 461, 261–271. <https://doi.org/10.1016/j.palaeo.2016.08.034>
- Teixell, A., 1998. Crustal structure and orogenic material budget in the west central Pyrenees. *Tectonics* 17, 395–406. <https://doi.org/10.1029/98TC00561>
- Teixell, A., Muñoz, J.A., 2000. Evolución tectono-sedimentaria del Pirineo meridional durante el Terciario: una síntesis basada en la transversal del río Noguera Ribagorçana. *Revista de la Sociedad Geológica de España*, 13 (2), 251-264.
- Teixell, A., 2004. Estructura de los Pirineos: generalidades., in: SGE-IGME (Ed.), *Geología de España*. Madrid, pp. 321–323.
- Teixell, A., Labaume, P., Lagabrielle, Y., 2016. The crustal evolution of the west-central Pyrenees revisited: Inferences from a new kinematic scenario. *Comptes Rendus Geoscience* 348, 257–267. <https://doi.org/10.1016/j.crte.2015.10.010>
- Tennant, J.P., Mannion, P.D., Upchurch, P., 2016. Evolutionary relationships and systematics of Atoposauridae (Crocodylomorpha: Neosuchia): implications for the rise of Eusuchia. *Zoological Journal of the Linnean Society* 177, 854–936. <https://doi.org/10.1111/zoj.12400>
- Terray, L., O. Plateau, A. Abourachid, C. Böhmer, A. Delapré, X. de la Bernardie, R. Cornette., 2020. Modularity of the Neck in Birds (Aves). *Evolutionary Biology* 47: 97–110.
- Thiel, M., Gutow, L., 2005. The Ecology of Rafting in the Marine Environment. II. The Rafting Organisms and Community, in: *Oceanography and Marine Biology: An Annual Review*. pp. 279–418.
- Thomas, R. G., Smith, D. G., Wood, J. M., Visser, J., Calverley-Range, E. A., Koster, E. H., 1987. Inclined heterolithic stratification—terminology, description, interpretation and significance. *Sedimentary Geology*, 53(1-2), 123-179.
- Tobin, T.S., Ward, P.D., Steig, E.J., Olivero, E.B., Hilburn, I.A., Mitchell, R.N., Diamond, M.R., Raub, T.D., Kirschvink, J.L., 2012. Extinction patterns,  $\delta^{18}\text{O}$  trends, and magnetostratigraphy from a southern high-latitude Cretaceous–Paleogene section: Links with Deccan volcanism. *Palaeogeography, Palaeoclimatology, Palaeoecology* 350–352, 180–188. <https://doi.org/10.1016/j.palaeo.2012.06.029>
- Tolkien, J.R.R., 1954. *The Lord of the Rings*. Three Volumes. Harper Collins , London, England 1216 pp.
- Tong, Y., Wang, J., 1980. Subdivision of the upper Cretaceous and lower Tertiary of the Tantou Basin, the Lushi Basin and the Lingbao Basin of western Henan. *Vertebrata Palasiatica* 18, 21–27.

- Toon, O.B., Bardeen, C., Garcia, R., 2016. Designing global climate and atmospheric chemistry simulations for 1 and 10 km diameter asteroid impacts using the properties of ejecta from the K-Pg impact. *Atmospheric Chemistry and Physics* 16, 13185–13212. <https://doi.org/10.5194/acp-16-13185-2016>
- Torices, A., Currie, P.J., Canudo, J.I., Pereda-Suberbiola, X., 2015. Theropod dinosaurs from the upper cretaceous of the south pyrenees basin of Spain. *Acta Palaeontologica Polonica* 60, 611–626. <https://doi.org/10.4202/app.2012.0121>
- Turner, A.H., 2006. Osteology and phylogeny of a new species of *Araripesuchus* (Crocodyliformes: Mesoeucrocodylia) from the Late Cretaceous of Madagascar. *Historical Biology* 18, 255–369. <https://doi.org/10.1080/08912960500516112>
- Upchurch, P., Barrett, P.M., Dodson, P., 2019. 13. Sauropoda, in: *The Dinosauria*, Second Edition. University of California Press, pp. 259–322. <https://doi.org/10.1525/9780520941434-018>
- Văcărescu, M.R., Sava, Z.C., Bucur, M., Roman, A., Vasile, Ștefan, 2018. Theropod teeth from the Maastrichtian of the Hațeg Basin, Romania: dental morphotype diversity in an European context-preliminary results. In: *Proceedings of the 11th Romanian Symposium of Paleontology*, Bucharest, Romania, 27–28 September 2017; pp. 122–123
- Vajda, V., Raine, J.I., Hollis, C.J., 2001. Indication of Global Deforestation at the Cretaceous-Tertiary Boundary by New Zealand Fern Spike. *Science* 294, 1700–1702. <https://doi.org/10.1126/science.1064706>
- Vajda, V., Bercovici, A., 2014. The global vegetation pattern across the Cretaceous–Paleogene mass extinction interval: A template for other extinction events. *Global and Planetary Change* 122, 29–49. <https://doi.org/10.1016/j.gloplacha.2014.07.014>
- Valentin, X., Godefroit, P., Tabuce, R., Vianey-Liaud, M., Wenhao, W., Garcia, G., 2012. First late Maastrichtian (latest Cretaceous) vertebrate assemblage from provence (Vitrolles-la-Plaine, southern France). *Bernissart Dinosaurs and Early Cretaceous Terrestrial Ecosystems* 583–597.
- Vallati, P., De Sosa Tomas, A., Casal, G., 2020. A Maastrichtian terrestrial palaeoenvironment close to the K/Pg boundary in the Golfo San Jorge basin, Patagonia, Argentina. *Journal of South American Earth Sciences* 97, 102401. <https://doi.org/10.1016/j.jsames.2019.102401>
- Vangerow, E.F., 1954. Megasporen und andere pflanzlich Mikrofossilien aus den Aachen Kreide. *Palaeontographica (B)* 96, 24–38.
- Vasile, Ș., Csiki-Sava, Z., Venczel, M., 2013. A new madtsoiid snake from the Upper Cretaceous of the Hațeg Basin, western Romania. *Journal of Vertebrate Paleontology* 33, 1100–1119. <https://doi.org/10.1080/02724634.2013.764882>
- Vavrek, M.J., Larsson, H.C.E., 2010. Low beta diversity of Maastrichtian dinosaurs of North America. *Proceedings of the National Academy of Sciences of the United States of America* 107, 8265–8268.
- Venczel, M., Vasile, Ș., Csiki-Sava, Z., 2015. A Late Cretaceous madtsoiid snake from Romania associated with a megaloolithid egg nest – Paleocological inferences. *Cretaceous Research* 55, 152–163. <https://doi.org/10.1016/j.cretres.2015.02.009>
- Venczel, M., Gardner, J.D., Codrea, V.A., Csiki-Sava, Z., Vasile, Ș., Solomon, A.A., 2016. New insights into Europe's most diverse Late Cretaceous anuran assemblage from the Maastrichtian of western Romania. *Palaeobiodiversity and Palaeoenvironments* 96, 61–95. <https://doi.org/10.1007/s12549-015-0228-6>

- Verma, O., Khosla, A., Goin, F.J., Kaur, J., 2016. Historical biogeography of the Late Cretaceous vertebrates of India: Comparison of geophysical and paleontological data. *Cretaceous Period: Biotic Diversity and Biogeography: Bulletin* 71, 71, 317. *Cretaceous Period: Biotic Diversity and Biogeography: New Mexico Museum of Natural history and Science Bulletin* 71, 317–330.
- Vianey-Liaud, M., López-Martínez, N., 1997. Late Cretaceous Dinosaur Eggshells from the Tremp Basin, Southern Pyrenees, Lleida, Spain. *Journal of Paleontology* 71, 1157–1171.
- Vicens, E., Ardèvol, L., López-Martínez, N., Arribas, M.E., 2004. Rudists biostratigraphy in the Campanian–Maastrichtian of the south-central Pyrenees, Spain. *Courier Forschungsinstitut Senckenberg* 247, 113–127.
- Vicente, A., Martín-Closas, C., Arz, J.A., Oms, O., 2015. Maastrichtian–basal Paleocene charophyte biozonation and its calibration to the Global Polarity Time Scale in the southern Pyrenees (Catalonia, Spain). *Cretaceous Research* 52, 268–285. <https://doi.org/10.1016/j.cretres.2014.10.004>
- Vicente, A., Expósito, M., Sanjuan, J., Martín-Closas, C., 2016a. Small sized charophyte gyrogonites in the Maastrichtian of Coll de Nargó, Eastern Pyrenees: An adaptation to temporary floodplain ponds. *Cretaceous Research* 57, 443–456. <https://doi.org/10.1016/j.cretres.2015.07.017>
- Vicente, A., Villalba-Breva, S., Ferràndez-Cañadell, C., Martín-Closas, C., 2016b. Revision of the Maastrichtian–Palaeocene charophyte biostratigraphy of the Fontllonga reference section (Southern Pyrenees, Catalonia, Spain). *Geologica Acta* 14, 349–362. <https://doi.org/10.1344/GeologicaActa2016.14.4.2>
- Vicente, A., Csiki-Sava, Z., Martín-Closas, C., 2019. European charophyte evolution across the Cretaceous–Paleogene boundary. *Palaeogeography, Palaeoclimatology, Palaeoecology* 533, 109244. <https://doi.org/10.1016/j.palaeo.2019.109244>
- Vidal, L.M., 1874. Datos para el conocimiento del terreno Garumnense de Cataluña. *Boletín de la Comisión del Mapa Geológico de España, Facsímil Luis Mariano Vidal 1842-1922. Selección de obras sobre el Cretácico*.
- Vidal, L.M., 1921. Contribución a la paleontología del Cretáceo de Cataluña. *Real Academia de Ciencias y Artes Barcelona* 17, 89–109.
- Vila, B., Oms, O., Marmi, J., Galobart, A., 2008. Tracking Fumanya footprints (Maastrichtian, Pyrenees): historical and ichnological overview. *Oryctos* 8, 115–130.
- Vila, B., Jackson, F., Galobart, À., 2010. First data on dinosaur eggs and clutches from Pinyes locality (Upper Cretaceous, Southern Pyrenees). *Ameghiniana* 47 (1), 79–87.
- Vila, B., Oms, O., Marmi, J., Galobart, A., Riera, V., Estrada, R., Malchus, N., 2011. La transición Cretácico-Terciario en el Sur de los Pirineos. Parada 1. Geología y registro paleontológico del sinclinal de Vallcebre., in: *Guía de Campo. XXVII Jornadas de La Sociedad Española de Paleontología*. pp. 11–26.
- Vila, B., Galobart, À., Canudo, J.I., Le Loeuff, J., Dinarès-Turell, J., Riera, V., Oms, O., Tortosa, T., Gaete, R., 2012. The diversity of sauropod dinosaurs and their first taxonomic succession from the latest Cretaceous of southwestern Europe: Clues to demise and extinction. *Palaeogeography, Palaeoclimatology, Palaeoecology* 350–352, 19–38. <https://doi.org/10.1016/j.palaeo.2012.06.008>

- Vila, B., Oms, O., Fondevilla, V., Gaete, R., Galobart, À., Riera, V., Canudo, J.I., 2013. The Latest Succession of Dinosaur Tracksites in Europe: Hadrosaur Ichnology, Track Production and Palaeoenvironments. *PLoS ONE* 8. <https://doi.org/10.1371/journal.pone.0072579>
- Vila, B., Castanera, D., Marmi, J., Canudo, J.I., Galobart, À., 2015. Crocodile swim tracks from the latest Cretaceous of Europe. *Lethaia* 48, 256–266. <https://doi.org/10.1111/let.12103>
- Vila, B., Sellés, A.G., 2015. Re-evaluation of the age of some dinosaur localities from the southern Pyrenees by means of megaloolithid oospecies. *Journal of Iberian Geology* 41. [https://doi.org/10.5209/rev\\_JIGE.2015.v41.n1.48659](https://doi.org/10.5209/rev_JIGE.2015.v41.n1.48659)
- Vila, B., Sellés, A.G., Brusatte, S.L., 2016. Diversity and faunal changes in the latest Cretaceous dinosaur communities of southwestern Europe. *Cretaceous Research* 57, 552–564. <https://doi.org/10.1016/j.cretres.2015.07.003>
- Vila, B., Sellés, A., Moreno-Azanza, M., Razzolini, N.L., Gil-Delgado, A., Canudo, J.I., Galobart, À., 2022. A titanosaurian sauropod with Gondwanan affinities in the latest Cretaceous of Europe. *Nature Ecology & Evolution* 6, 288–296. <https://doi.org/10.1038/s41559-021-01651-5>
- Villalba-Breva, S., Martín-Closas, C., Marmi, J., Gomez, B., Fernández-Marrów, M.T., 2012. Peat-forming plants in the Maastrichtian coals of the Eastern Pyrenees. *Geologica Acta* 10, 189–207. <https://doi.org/10.1344/105.000001711>
- Villalba-Breva, S., Martín-Closas, C., 2013. Upper Cretaceous paleogeography of the Central Southern Pyrenean Basins (Catalonia, Spain) from microfacies analysis and charophyte biostratigraphy. *Facies* 59, 319–345. <https://doi.org/10.1007/s10347-012-0317-1>
- Vitek, N.S., Joyce, W.G., 2015. A Review of the Fossil Record of New World Turtles of the Clade Pan-Trionychidae. *Bulletin of the Peabody Museum of Natural History* 56, 185–244. <https://doi.org/10.3374/014.056.0204>
- Vlachos, E., Randolfe, E., Sterli, J., Leardi, J.M., 2018. Changes in the Diversity of Turtles (Testudinata) in South America from the Late Triassic to the Present. *Ameghiniana* 55, 619. <https://doi.org/10.5710/AMGH.18.09.2018.3226>
- Walker, C.A., G.J. Dyke., 2009. Euenantiornithine birds from the Late Cretaceous of El Brete (Argentina). *Irish Journal of Earth Sciences* 27, 15–62.
- Wang, M., O'Connor, J.K., Zhou, S., Zhou, Z., 2020. New toothed Early Cretaceous ornithuromorph bird reveals intraclade diversity in pattern of tooth loss. *Journal of Systematics Palaeontology*. 18, 631–645. <https://doi.org/10.1080/14772019.2019.1682696>
- Wang, X., Dyke, G.J., Codrea, V., Godefroit, P., Smith, T., 2011. A Euenantiornithine Bird from the Late Cretaceous Hateg Basin of Romania. *Acta Palaeontologica Polonica* 56, 853–857. <https://doi.org/10.4202/app.2010.0085>
- Watanabe, A., M. E. L. Gold, S.L. Brusatte, R.B. Benson, J. Choiniere, A. Davidson, M.A. Norell., 2015. Vertebral pneumaticity in the ornithomimosaur *Archaeornithomimus* (Dinosauria: Theropoda) revealed by computed tomography imaging and reappraisal of axial pneumaticity in Ornithomimosauria. *PloS One* 10(12), e0145168.
- Wedel, M.J., Cifelli, R.L., Sanders, R.K., 2000. Osteology, paleobiology, and relationships of the sauropod dinosaur *Sauroposeidon*. *Acta Palaeontologica Polonica* 45, 343–388.
- Weishampel, D.B., Norman, D.B., Grigorescu, D., 1993. *Telmatosaurus transsylvanicus* from the late Cretaceous of Romania: the most basal hadrosaurid dinosaur. *Palaeontology* 36, 361–385.

- Weishampel, D.B., Jianu, C., Csiki, Z., Norman, D.B., 2003. Osteology and phylogeny of *Zalmoxes* (n. g.), an unusual Euornithopod dinosaur from the latest Cretaceous of Romania. *Journal of Systematic Palaeontology* 1, 65–123. <https://doi.org/10.1017/S1477201903001032>
- Wiest, L.A., Lukens, W.E., Peppe, D.J., Driese, S.G., Tubbs, J., 2018. Terrestrial evidence for the Lilliput effect across the Cretaceous-Paleogene (K-Pg) boundary. *Palaeogeography, Palaeoclimatology, Palaeoecology* 491, 161–169. <https://doi.org/10.1016/j.palaeo.2017.12.005>
- Wiley, E.O., 1976. The phylogeny and biogeography of fossil and recent gars (Actinopterygii: Lepisosteidae). The University of Kansas. Museum of Natural History, Miscellaneous Publication 64, 1–111.
- Wilf, P., Johnson, K.R., 2004. Land plant extinction at the end of the Cretaceous: a quantitative analysis of the North Dakota megafloral record. *Paleobiology* 30, 347–368. [https://doi.org/10.1666/0094-8373\(2004\)030<0347:LPEATE>2.0.CO;2](https://doi.org/10.1666/0094-8373(2004)030<0347:LPEATE>2.0.CO;2)
- Wilson, G.P., 2013. Mammals across the K/Pg boundary in northeastern Montana, U.S.A.: dental morphology and body-size patterns reveal extinction selectivity and immigrant-fueled ecospace filling. *Paleobiology* 39, 429–469. <https://doi.org/10.1666/12041>
- Wilson, G.P., Demar Jr., D.G., Carter, G., 2014. Extinction and survival of salamander and salamander-like amphibians across the Cretaceous-Paleogene boundary in northeastern Montana, USA, in: Wilson, G.P., Clemens, W.A., Horner, J.R., Hartman, J. (Eds.), *Through the End of the Cretaceous in the Type Locality of the Hell Creek Formation in Montana and Adjacent Areas*, Geological Society of America Special Paper, 503. pp. 271–297.
- Wilson, J.A., 1999. Vertebral laminae in sauropods and other saurischian dinosaurs. *Journal of Vertebrate Paleontology* 19, 639–653.
- Wilson, J.A., Sereno, P.C., Srivastava, S., Bhatt, D.K., Khosla, A., Sahni, A., 2003. A new abelisaurid (Dinosauria, Theropoda) from the Lameta Formation (Cretaceous, Maastrichtian) of India. *Contributions from the Museum of Paleontology, University of Michigan* 31, 1–42.
- Wilson, J.A., Barrett, P.M., Carrano, M.T., 2011a. An associated partial skeleton of *Jainosaurus* cf. *septentrionalis* (Dinosauria: Sauropoda) from the Late Cretaceous of Chhota Simla, Central India. *Palaeontology* 54, 981–998. <https://doi.org/10.1111/j.1475-4983.2011.01087.x>
- Wilson, J.A., D’Emic, M.D., Ikejiri, T., Moacdieh, E.M., Whitlock, J.A., 2011b. A Nomenclature for Vertebral Fossae in Sauropods and Other Saurischian Dinosaurs. *PLoS One* 6, e17114. <https://doi.org/10.1371/journal.pone.0017114>
- Wilson, J.A., Mohabey, D.M., Lakra, P., Bhadrar, A., 2019. Titanosaur (Dinosauria: Sauropoda) vertebrae from the Upper Cretaceous Lameta Formation of western and central India. *Contributions from the Museum of Paleontology, University of Michigan* 33, 1–27.
- Witts, J.D., Whittle, R.J., Wignall, P.B., Crame, J.A., Francis, J.E., Newton, R.J., Bowman, V.C., 2016. Macrofossil evidence for a rapid and severe Cretaceous–Paleogene mass extinction in Antarctica. *Nature Communications* 7, 11738. <https://doi.org/10.1038/ncomms11738>
- Xu, X., M. A. Norell., 2004. A new troodontid dinosaur from China with avian-like sleeping posture. *Nature* 431, 838–841.
- Xue, X., Zhang, Y., Bi, Y., Yue, L., Chen, D.-K., 1996. *The Development and Environmental Changes of the Intermontane Basins in Eastern Part of the Qinling Mountains*. Geological Publishing House, Beijing.
- Zhang, F., G.P. Ericson, Z. Zhou., 2005. Description of a new enantiornithine bird from the Early Cretaceous of Hebei, northern China. *Canadian Journal of Earth Sciences* 41, 1097–1107.

- Zhao, Z.K., Wang, Q., Zhang, S.K., 2015. *Palaeovertebrata Sinica* Volume II: Amphibians, Reptilians and Avians Fascicle 7 (Serial no.11) Dinosaur Eggs. Science Press, Beijing.
- Zhou, Z., J. Clarke, F. Zhang, 2008. Insight into diversity, body size and morphological evolution from the largest Early Cretaceous enantiornithine bird. *Journal of Anatomy* 212 (5), 565–577.
- Zhou, S., Z. Zhou, J. O'Connor., 2014. A new piscivorous ornithuromorph from the Jehol Biota. *Historical Biology* 26(5), 608–618.
- Zuschin, M., Ebner, C., 2015. Actinopaleontological characterization and molluscan biodiversity of a protected tidal flat and shallow subtidal at the northern Red Sea. *Facies* 61, 5. <https://doi.org/10.1007/s10347-015-0428-6>



# **Annexes**



# **Annex I**





# Chronostratigraphy and new vertebrate sites from the upper Maastrichtian of Huesca (Spain), and their relation with the K/Pg boundary

E. Puértolas-Pascual <sup>a,d,\*</sup>, I. Arenillas <sup>e</sup>, J.A. Arz <sup>e</sup>, P. Calvín <sup>b</sup>, L. Ezquerro <sup>c</sup>,  
C. García-Vicente <sup>e</sup>, M. Pérez-Pueyo <sup>a</sup>, E.M. Sánchez-Moreno <sup>b</sup>, J.J. Villalaín <sup>b</sup>, J.I. Canudo <sup>a</sup>

<sup>a</sup> Grupo Aragosaurus-IUCA, Área de Paleontología, Dpto. Ciencias de la Tierra, Universidad de Zaragoza, 50009 Zaragoza, Spain

<sup>b</sup> Dpto. de Física, Facultad de Ciencias, Universidad de Burgos, 09001 Burgos, Spain

<sup>c</sup> Grupo GEOTRANSFER, Área de Estratigrafía, Dpto. Ciencias de la Tierra, Universidad de Zaragoza, 50009 Zaragoza, Spain

<sup>d</sup> Faculdade de Ciências e Tecnologia-GeoBioTec, Universidade Nova de Lisboa, 2829-526 Monte de Caparica, Portugal

<sup>e</sup> IUCA, Área de Paleontología, Dpto. Ciencias de la Tierra, Universidad de Zaragoza, 50009 Zaragoza, Spain

## ARTICLE INFO

### Article history:

Received 9 November 2017

Received in revised form

24 January 2018

Accepted in revised form 22 February 2018

Available online 24 February 2018

### Keywords:

K/Pg boundary

Maastrichtian

Magnetostratigraphy

Biostratigraphy

Vertebrates

Pyrenees

## ABSTRACT

The transitional-continental facies of the Tremp Formation within the South-Pyrenean Central Unit (Spain) contain one of the best continental vertebrate records of the Upper Cretaceous in Europe. This Pyrenean area is therefore an exceptional place to study the extinction of continental vertebrates across the Cretaceous/Paleogene (K/Pg) boundary, being one of the few places in Europe that has a relatively continuous record ranging from the upper Campanian to lower Eocene. The Serraduy area, located on the northwest flank of the Tremp syncline, has seen the discovery of abundant vertebrate remains in recent years, highlights being the presence of hadrosaurid dinosaurs and eusuchian crocodylomorphs. Nevertheless, although these deposits have been provisionally assigned a Maastrichtian age, they have not previously been dated with absolute or relative methods. This paper presents a detailed stratigraphic, magnetostratigraphic and biostratigraphic study for the first time in this area, making it possible to assign most vertebrate sites from the Serraduy area a late Maastrichtian age, specifically within polarity chron C29r. These results confirm that the vertebrate sites from Serraduy are among the most modern of the Upper Cretaceous in Europe, being very close to the K/Pg boundary.

© 2018 Elsevier Ltd. All rights reserved.

## 1. Introduction

Recognizing the K/Pg (Cretaceous/Paleogene) boundary in continental deposits is a complicated task due to several biases that affect the continental record (Smith et al., 2001; Barret et al., 2009; Butler et al., 2011; Mannion et al., 2011; Smith and McGowan, 2011; Upchurch et al., 2011). Even so, great efforts have been made in recent years to detect the continental K/Pg boundary and ascertain

its relation with faunal and floral extinctions, especially in North America (e.g., Fastovsky and Sheehan, 2005; Archibald et al., 2010; Brusatte et al., 2015; and references therein), but also in Europe (Canudo et al., 2016; and references therein) and Asia (Jiang et al., 2011; and references therein).

In the European scenario, the greatest difficulty in knowing how the vertebrate faunas were affected by the K/Pg extinction event is as a result of the fragmentary nature of the continental geological record during the Late Cretaceous and early Paleogene. Nonetheless, major advances have been made in the last few years, and new outcrops, mainly in Romania, France and Spain, are being discovered and datings carried out (Puértolas-Pascual et al., 2016; and references therein).

In Eastern Europe (Romania), the Maastrichtian continental vertebrate assemblages have been examined and dated by biostratigraphy, magnetostratigraphy and radioisotopic techniques (Antonescu et al., 1983; Van Itterbeeck et al., 2005; Codrea et al.,

\* Corresponding author: Faculdade de Ciências e Tecnologia-GeoBioTec, Universidade Nova de Lisboa, 2829-526 Monte de Caparica, Portugal.

E-mail addresses: [eduardo.puertolas@gmail.com](mailto:eduardo.puertolas@gmail.com), [puertolas@fct.unl.pt](mailto:puertolas@fct.unl.pt) (E. Puértolas-Pascual), [ias@unizar.es](mailto:ias@unizar.es) (I. Arenillas), [josearz@unizar.es](mailto:josearz@unizar.es) (J.A. Arz), [calvinballester@gmail.com](mailto:calvinballester@gmail.com) (P. Calvín), [lope@unizar.es](mailto:lope@unizar.es) (L. Ezquerro), [christiangarciavicente90@gmail.com](mailto:christiangarciavicente90@gmail.com) (C. García-Vicente), [manuppueyo@gmail.com](mailto:manuppueyo@gmail.com) (M. Pérez-Pueyo), [emsanchez@ubu.es](mailto:emsanchez@ubu.es) (E.M. Sánchez-Moreno), [villa@ubu.es](mailto:villa@ubu.es) (J.J. Villalaín), [jicanudo@unizar.es](mailto:jicanudo@unizar.es) (J.I. Canudo).

2010, 2012; Panaiotu and Panaiotu, 2010; Bojar et al., 2011; Panaiotu et al., 2011; Vremir et al., 2014; Csiki-Sava et al., 2015). However, the vertebrate sites are located in excessively broad age ranges, the correlation between the different sites remains problematic and more accurate datings are required (Buffetaut and Le Loeuff, 1991; Gheerbrant et al., 1999; Codrea et al., 2012; Vremir et al., 2014).

Similar concerns occur with respect to the Upper Cretaceous and lower Paleogene of France. Apart from the Provence area, where several biostratigraphic, magnetostratigraphic, chemostratigraphic and sedimentological studies with a good chronostratigraphic control have been carried out (Cojan et al., 2003; Cojan and Moreau, 2006), most of the northern Pyrenees still lack accurate datings or correlations (Buffetaut and Le Loeuff, 1991; Laurent et al., 2002). Therefore, despite the abundant Maastrichtian vertebrate fossil record recovered from southern France, only limited biostratigraphic data (Bessière et al., 1980, 1989; Bilotte, 1985; García and Vianey-Liaud, 2001; Marty, 2001) and one new magnetostratigraphic study (Fondevilla et al., 2016b) are available, and further studies and correlations are still necessary (Dinarès-Turell et al., 2014).

The continental vertebrate record of the uppermost Cretaceous of Spain is one of the most complete and most studied in Europe (e.g., Company and Szentesi, 2012; Ortega et al., 2015; Pereda-Suberbiola et al., 2015; Canudo et al., 2016). Most of these vertebrate sites are located within the Tremp Basin, in the Pyrenees of Aragon and Catalonia (Spain), specifically in the Maastrichtian transitional and continental facies of the Tremp Formation. The Tremp Formation has been exhaustively prospected and studied, providing abundant new vertebrate fossil remains including dinosaurs, crocodylomorphs, testudines, mammals, fishes, amphibians and squamates (e.g., López-Martínez et al., 1999, 2001; Peláez-Campomanes et al., 2000; Pereda-Suberbiola et al., 2009; Riera et al., 2009; Blain et al., 2010; Cruzado-Caballero et al., 2010, 2013, 2015; Puértolas et al., 2011; Marmi et al., 2012, 2016; Vila et al., 2012, 2013, 2015; Blanco et al., 2014, 2015a, 2015b, 2016, 2017; Moreno-Azanza et al., 2014; Puértolas-Pascual et al., 2014, 2016; Sellés et al., 2014a, 2014b, 2016; Company et al., 2015; Torices et al., 2015; Canudo et al., 2016).

In addition to the record of the vertebrates themselves, there is a relatively continuous geological record ranging from the Maastrichtian to the end of the Thanetian (López-Martínez et al., 2006), which is probably the best dated and correlated in Europe for this time interval and which may contain the Cretaceous/Paleogene boundary. This makes the southern Pyrenees and the Tremp Basin one of the best areas in the world for studying vertebrate associations across the K/Pg boundary, allowing comparisons with the extinction patterns reported from other parts of the world (Brusatte et al., 2015; Csiki-Sava et al., 2015; Canudo et al., 2016; Puértolas-Pascual et al., 2016).

Ever since the 1980s, therefore, a great effort has been put into dating the fossil vertebrate sites and searching for the K/Pg boundary within the transitional and continental deposits of this sector of the Pyrenees. Outstanding in this context are works on the biostratigraphy of rudists (Vicens et al., 2004), charophytes and palynomorphs (Feist and Colombo, 1983; Médus et al., 1988; Galbrun et al., 1993; López-Martínez et al., 2001; Villalba-Breva and Martín-Closas, 2011, 2013; Villalba-Breva et al., 2012; Vicente et al., 2015), foraminifers (López-Martínez et al., 2001; Díez-Canseco et al., 2014), on eggshells (Vila et al., 2011; Sellés et al., 2013; Sellés and Vila, 2015), magnetostratigraphy (Galbrun et al., 1993; Oms et al., 2007; Pereda-Suberbiola et al., 2009; Vila et al., 2011, 2012; Canudo et al., 2016; Fondevilla et al., 2016a) and dinosaur occurrences (Riera et al., 2009; Vila et al., 2016).

The Serraduy area, located in the Aragonese northwestern branch of the Tremp Basin, has been prospected by the

Aragosaurus-IUCA research group of the University of Zaragoza for over 10 years. This has resulted in the discovery of around 40 new paleontological sites with hundreds of vertebrate remains. These findings include important specimens such as the holotype of the eusuchian crocodylomorph *Agaresuchus subjuniiperus* (Puértolas-Pascual, Canudo and Moreno-Azanza, 2014) and the smallest hadrosaurid known in Europe to date (Company et al., 2015), probably a new dwarf taxon.

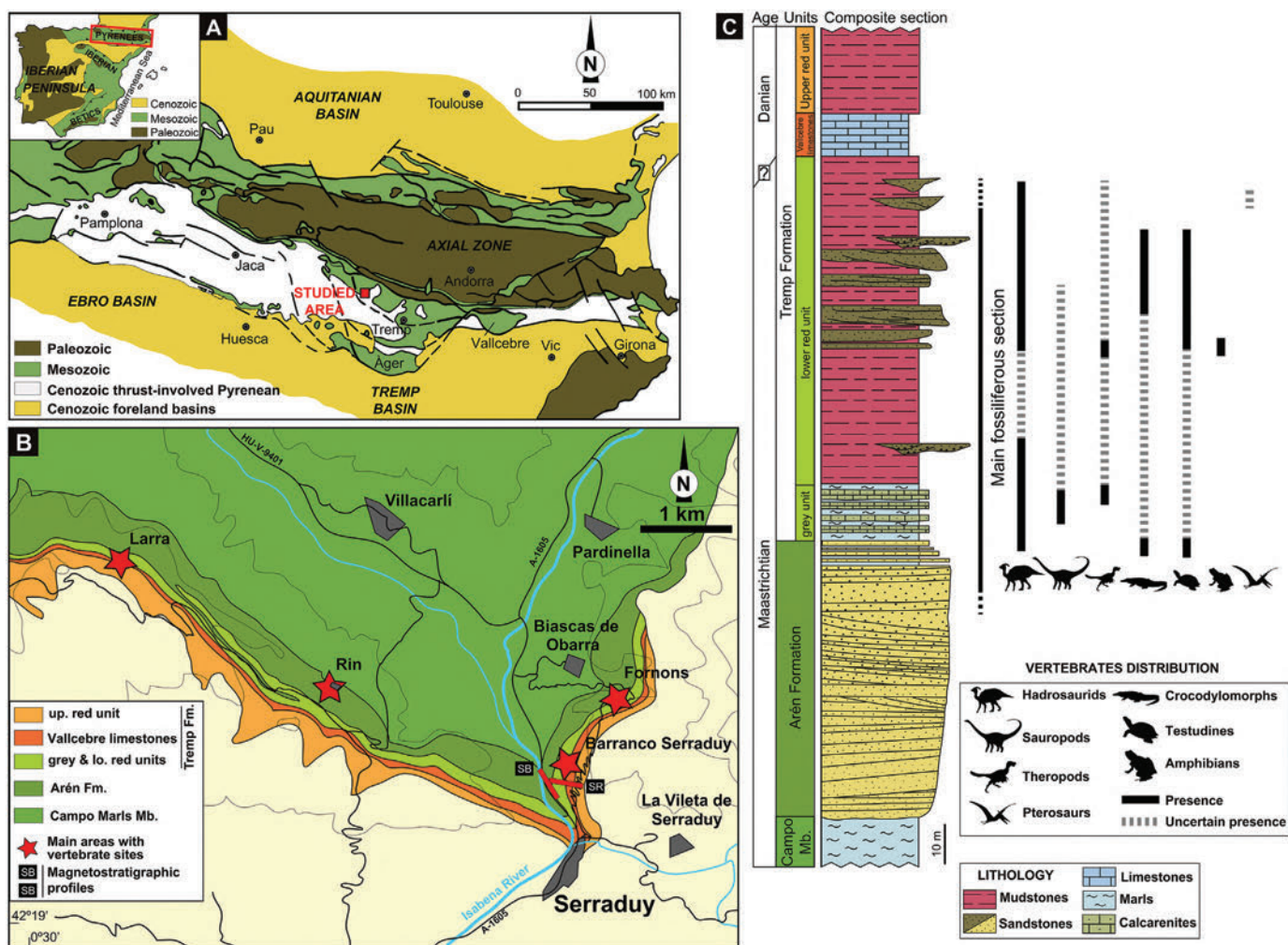
Despite the importance and potential of these vertebrate sites, a chronostratigraphic framework for the Serraduy sector has not yet been provided. Serraduy is located between other areas with vertebrate sites such as Campo to the west and Arén to the east, corresponding to the northwestern-most branch of the Tremp Formation within the Tremp Basin. In these nearby sectors (Campo and Arén, Huesca), previous magnetostratigraphic studies have stated that the vertebrate sites of the Tremp Formation in these areas lie within magnetic polarity chrons C30n and C29r, being late Maastrichtian in age (Pereda-Suberbiola et al., 2009; Canudo et al., 2016).

On the basis of works of magnetostratigraphy (Fondevilla et al., 2016a) and biostratigraphy (Díez-Canseco et al., 2014) on the more eastward-lying Isona sector of the Tremp syncline, however, some authors have detected the possible presence of important hiatuses in some areas of the Tremp Basin. These gaps reveal that most of the succession and vertebrate content in that area correlates to the early Maastrichtian (mostly chron C31r), suggesting an older age (Fondevilla et al., 2016a) for many vertebrate sites than previously thought (Vila et al., 2012). In accordance with these new datings (Pereda-Suberbiola et al., 2009; Díez-Canseco et al., 2014; Canudo et al., 2016; Fondevilla et al., 2016a), the chronostratigraphic study of the areas of Campo-Serraduy-Arén may thus acquire greater relevance, given that the lower part of the Tremp Formation exposed in Campo and Arén contains the only continental record of chron C30n in the whole Tremp syncline (Fondevilla et al., 2016a).

To test all these hypotheses, we here describe for the first time the magnetostratigraphy, biostratigraphy and a preliminary study of the fossil vertebrate assemblage of the Serraduy area. According to our biostratigraphic and magnetostratigraphic results, most of the “lower red unit” of the Tremp Formation up to the top would be included within magnetic polarity chron C29r, and most of the vertebrate sites would therefore have a late Maastrichtian age, being located very close to the K/Pg boundary. Unfortunately, the paleomagnetic and biostratigraphic data from the lower half of the studied sections are not conclusive enough to give a specific age or reveal the presence of hiatuses in this area.

## 2. Geographical and geological context

The studied area is located in the Aragonese part of the Tremp Basin within the Pyrenean range (Serraduy area, Huesca, Spain) (Fig. 1A, B). The Pyrenees are a 430-km-long east-west-oriented continental collisional fold-and-thrust belt, located in the north-eastern Iberian Peninsula between France and Spain (Fig. 1A); they formed as the result of the oblique collision and compressive episodes between the Iberian microplate and the European plate. This process took place during the Alpine orogeny, from Late Cretaceous until early Miocene times (Garrido-Megías and Ríos, 1972; Puigdefabregas and Souquet, 1986; Muñoz, 1992; Ardèvol et al., 2000; Sibuet et al., 2004; Teixell, 2004). The Tremp Basin is located within the South-Pyrenean Central Unit or SPCU (Séguret, 1972), which corresponds with the central sector of the Southern Pyrenees (between the Noguera thrust fault in the north and the Sierras Marginales frontal thrust in the south) (Fig. 1A). Several syn-sedimentary synclines (Ager, Tremp, Coll de Nargo and Vallcebre)



**Fig. 1.** Geographical and geological situation of the Serraduy sector (Huesca, Spain). A. location of the Pyrenees within the Iberian Peninsula; B. geological map of the Serraduy sector; the red stars indicate the areas with the highest concentration of vertebrate sites; the red rectangles indicate the magnetostratigraphic sections (SB, SR) studied in this work; C. composite stratigraphic section of the studied profiles and stratigraphic vertebrate distribution. (For interpretation of the references to color/colour in this figure legend, the reader is referred to the Web version of this article.)

associated with the emplacement of south-verging thrust-sheets developed during the Late Cretaceous, acting as different sub-basins (Oms et al., 2016; Fonddevilla et al., 2016a). The fossil remains studied here are from the Arén and Tremp Formations (Mey et al., 1968) within the Tremp Basin and the northern flank of the east-west-oriented Tremp syncline.

The Tremp Formation, which forms part of what is informally known as the “Garumnian” facies (Leymerie, 1862), was deposited during the Upper Cretaceous–Paleocene, when the Pyrenees Basin was completely filled by coastal and continental deposits due to the end-Cretaceous marine regression (Rosell et al., 2001), representing the last infilling episode of the South-Pyrenean Basin (Mey et al., 1968; López-Martínez et al., 1999; Oms et al., 2016). The SPCU has an extension of 5000 km<sup>2</sup>, of which the Tremp Formation is estimated to encompass about 1000 km<sup>2</sup> (López-Martínez et al., 2006). This formation crops out in the central and western part of the SPCU, reaching a thickness of about 900 m in the depocenter near the locality of Tremp (López-Martínez et al., 1999). In the northern areas, such as the Tremp syncline, the bottom of the Tremp Formation is underlain by and laterally interdigitated with upper Campanian–Maastrichtian mixed-platform marine deposits that correspond to the beach, barrier-island and deltaic sandstones

of the Arén Formation (Fig. 1C) (Ardèvol et al., 2000). In the southern outcrops, such as the Àger syncline, the Arén Formation is replaced by more calcareous deposits corresponding with the limestones Les Serres Formation (Souquet, 1967; López-Martínez et al., 2006). Above, the Tremp Formation is overlain by Ilerdian (lower Eocene) marine sediments of the alveoline limestones Cadí Formation, or marly deposits laterally equivalent to the Figols Group (Fonnesu, 1984; Eichenseer and Luterbacher, 1992; López-Martínez et al., 1999, 2006).

The sedimentary succession of the Tremp Formation can be linked with two main stages of compressive tectonics (Puigdefàbregas and Souquet, 1986). The first stage occurred during the late Santonian–late Maastrichtian and was characterized by active tectonics, particularly intense during the late Santonian and Campanian, which caused the inversion of the previous Mesozoic rift structures and the development of a foreland basin. During this period, the basin was filled by mainly siliciclastic deposits which progressively passed to marine facies towards the west, where the open sea was located. The second stage occurred during the late Maastrichtian–early Eocene, this being a period of smooth tectonics and almost uniform subsidence represented predominantly by carbonate-marl deposits.

The Tremp Formation has been divided into different local units by several authors. Cuevas (1992), and later Pujalte and Schmitz (2005), divided the series into five formations and four members, elevating the Tremp Formation to the category of group. However, the classification of the Tremp Formation as a group is not widespread within the literature and some authors indicate that the boundaries between the formations of this group can be confusing (Riera et al., 2009). For this reason, Galbrun et al. (1993) and Rosell et al. (2001) divided the Tremp Formation into informal units with a wider regional rank. The correspondence between the different units of each author is as follows (Fig. 2): “grey unit” or “Grey Garumnian” of Rosell et al. (2001) (Posa Formation according to Cuevas, 1992; Unit 1 according to Galbrun et al., 1993); “lower red unit” or “Lower Red Garumnian” of Rosell et al. (2001) (Conques Formation and Talarn Formation according to Cuevas, 1992; Unit 2 according to Galbrun et al., 1993); “Vallcebre limestones” and lateral equivalents of Rosell et al. (2001) (Suterranya Formation and St. Salvador de Toló Formation according to Cuevas, 1992; Unit 3 according to Galbrun et al., 1993); “upper red unit” or “Upper Red Garumnian” of Rosell et al. (2001) (Esplugafreda Formation and Claret Formation according to Cuevas, 1992; Unit 4 according to Galbrun et al., 1993). In this study we have used the division proposed by Rosell et al. (2001) since this is the most widespread in the literature. Thus, the four units into which the Tremp Formation is divided are the following (Galbrun et al., 1993; López-Martínez et al., 1999, 2006; Rosell et al., 2001):

“Grey unit” (Posa Formation, Cuevas, 1992): Peritidal deposits composed of grey marls, calcarenites and limestones. The fossil assemblage is formed by marine to freshwater taxa, such as charophytes, foraminifers, molluscs, ostracods, rudists, corals, plants and vertebrates (Liebau, 1973; Álvarez-Sierra et al., 1994; Arribas et al., 1996; López-Martínez et al., 2001, 2006; Díez-Canseco et al., 2014; Vicente et al., 2015; Canudo et al., 2016). In some sectors of the Tremp Basin, swampy deposits with an abundant accumulation of vegetal remains and lignite are observed (Oms et al., 2014). This unit was deposited in wide and shallow protected areas of variable salinity that are interpreted as tidal-plain, lagoonal and estuarine environments, located laterally and proximally to the barrier-island or deltaic deposits of the Arén Formation (Nagtegaal et al., 1983; Díaz-Molina, 1987; Ardèvol et al., 2000; López-Martínez et al., 2006; Riera et al., 2009; Díez-Canseco et al., 2014).

“Lower red unit” (Conques Formation–Tarn Formation, Cuevas, 1992): Detrital deposits composed of violet, brown, ochre, greenish or reddish lutites with a high degree of bioturbation and alternated with brown and ochre hybrid sandstones organized in channeled or tabular strata. This unit may also contain grey marls and microconglomerates and, more rarely, limestones and gypsum. In several areas, such as the Ager and Vallcebre synclines, the top of the “lower red unit” is characterized by the presence of the so-called “Reptile Sandstone”, where the last vertebrate remains before the K/Pg boundary can be found just a few meters below the overlying “Vallcebre limestones” (Llompert, 1979; Masriera and Ullastre, 1983; Lopez-Martínez et al., 1998; Vicente et al., 2015; Canudo et al., 2016; Gómez-Gras et al., 2016). Between the last levels with evidence of dinosaurs and the Danian “Vallcebre limestones” and lateral equivalents, there is a transitional section composed of lutitic–marly deposits and local intercalations of gypsum, where the presence of fossils is practically non-existent. This transitional section, which may contain the K/Pg boundary, is associated with a change in the sedimentary conditions from detrital to chemical deposits (López-Martínez et al., 2006). Among the fossil content of this unit, red algae, foraminifers, charophytes, ostracods, crustaceans, molluscs, plants and vertebrate remains have been recovered (Liebau, 1973; López-Martínez et al., 1998, 2001, 2006; Díez-Canseco et al., 2014; Vicente et al., 2015; Canudo et al., 2016). This unit has been interpreted as overbank facies deposited on tidal floodplains laterally associated with point bars of tide-influenced meandering fluvial channels (Díaz-Molina, 1987; Eichenseer, 1987; Cuevas, 1992; Rosell et al., 2001; López-Martínez et al., 2006; Oms et al., 2007; Riera et al., 2009; Díez-Canseco et al., 2014).

“Vallcebre limestones” and lateral equivalents (Esplugafreda Formation, Cuevas, 1992): Carbonatic unit composed of highly recrystallized, nodular and brecciated whitish massive limestones. It is highly variable in thickness, ranging from being absent (Islclés, Tremp and Barcedana–Toló sections) or just 4 m thick (Serraduy section) up to 100 m thick (Sta. M<sup>a</sup> de Meyá and Campo sections) (López-Martínez et al., 2006). The fossil content is very scarce, but *Microcodium*, charophytes, benthic and planktonic foraminifers, ostracods, molluscs, dasyclad algal and calcispheres may appear (López-Martínez et al., 2006; Díez-Canseco et al., 2014). This unit has been associated with lacustrine environments of variable

Rosell (1965)	Liebau (1965)	Eichenseer & Krauss (1985)	Cuevas (1992)	Galbrun et al. (1993)	Rosell et al. (2001)	Pujalte & Schmitz (2005)					
upper Garum	Conca Garumniense	Transitional marine-continental	<del>La Guixera Mb.</del> Claret Fm.	Unit 4	upper red Garumnian	<del>La Guixera Mb.</del> Claret Fm. <del>Egl. de Claret Mb.</del>					
middle Garum			Red beds			Esplugafreda Fm. <del>St. Salvador de Toló Fm.</del>	Esplugafreda Fm.				
lower Garum		Canalis	Perilagoonal brown marls	Talarn Fm. <del>Tossal d'Obà Mb.</del> Conques Fm. <del>Basturs Mb.</del> La Gubera Mb.	Unit 2	lower red Garumnian	<del>Tossal d'Obà Mb.</del> Conques Fm. <del>Basturs Mb.</del>				
				Xullí			Lagoonal lignitic marls	Posa Fm.	Unit 1	Gray Garumnian	Posa Fm.
				Posa							
			Orcau	Arén Formation							

Fig. 2. Lithostratigraphic subdivision of the Tremp Formation according to different authors. Modified from Cuevas (1992) and Riera (2010).

salinity near the coast (Rosell et al., 2001; López-Martínez et al., 2006). The  $^{87}\text{Sr}/^{86}\text{Sr}$  isotopic ratio and the presence of euhaline seawater dasycladal algae and planktonic foraminifera may indicate sporadic connections of these lakes with the open sea (López-Martínez et al., 2006; Díez-Canseco et al., 2014). Unlike the Arén Formation and the lower units of the Tremp Formation, the K/Pg transitional strata and the Danian “Vallcebre limestones” and lateral equivalents are isochronous throughout the Tremp Basin (López-Martínez et al., 2006; Vila et al., 2013).

“Upper red unit” (Esplugafreda Formation–Claret Formation, Cuevas, 1992): This Paleocene unit is the most heterolithic, and is formed by a succession of lutites, sandstones, carbonates and gypsums. The bottom is characterized by the presence of lutites with an intense red color. Towards the top, the succession may contain conglomerates, paleosols and occasionally evaporite deposits, indicating a paleoclimatic shift towards more arid conditions. The presence of oncolites, stromatolites and *Microcodium* is also common (Rossi, 1993; Arribas et al., 1996; López-Martínez et al., 2006). This unit shows a new phase of detrital sedimentation in the basin with thick textured deposits including conglomerates, especially in the eastern sector of the Tremp syncline. In contrast, in the Ager syncline and the northwest sector of the Tremp syncline, the presence of carbonated deposits representing internal platform environments is more common (López-Martínez et al., 2006).

### 3. Stratigraphy

#### 3.1. Stratigraphic succession of the Serraduy area

The characterization of the sedimentary succession of the Tremp Basin in the Serraduy area is mainly derived from two detailed stratigraphic sections studied in the field, the Larra (La) and Barranco Serraduy (BS) profiles (Fig. 3A), an exhaustive analysis of several outcrops in the whole area, as well as a new detailed mapping (Fig. 3B). The Larra profile is located in the western sector and comprises a 67-m-thick outcropping succession, whereas the Barranco Serraduy profile, which is 175 m thick, is situated in the eastern area (Fig. 3). On the basis of these profiles, the studied infill consists of sandstones that progressively pass into heterolithic deposits comprising marls, calcarenites, mudstones, sandstones and limestones. According to regional data, these deposits correspond to the Arén Formation and the lower part of the Tremp Formation, with an age range from Maastriatian to Danian.

The lower part of the succession corresponds to the Arén Formation and presents a well-exposure of outcrops, about 67 m thick, in the Barranco Serraduy area (Fig. 3A). This unit consists of brownish fine to coarse-grained sandstones with a massive texture, with medium to large-scale trough cross-bedding or parallel and cross-lamination contained in m-thick tabular beds. The presence of fragmentary dinosaur, turtle and crocodylomorph bones at the top of this formation is common. The unit exhibits a coarsening-upwards trend, except for the last seven meters, which change to a fining-upwards trend, and the sandstones grade up into an alternation of greyish massive marls and brownish calcarenites that represents the transition to the Tremp Formation (Fig. 3A). This transition is easily recognized in the area as a whole and is characterized by intensive bioturbation, oxide haloes, abundant bioclasts of bivalves and isolated bone remains.

The Tremp Formation is a very heterogeneous lithological unit that has been divided into four subunits (the “grey unit”, “lower red unit”, “Vallcebre limestones” and “upper red unit”). In this work, we focus only on the three lower subunits, which represent mixed carbonate–terrigenous deposits at the base, a middle section

composed mainly of terrigenous deposits and an upper carbonated part.

The basal deposits, the “grey unit” (~15 m thick), correspond to a succession of greyish massive marls and calcarenites in dm- to m-thick tabular strata (Fig. 3A), with bioturbation, carbonate nodules, soft intraclasts and oxide haloes. Invertebrates such as bivalves, ostracods and gastropods, and vertebrate remains such as dinosaur and turtle bones, are common in the calcarenite levels.

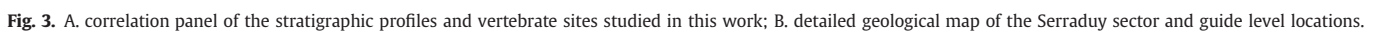
The “lower red unit” consists of m-thick tabular mudstone bodies with tabular or channeled dm- to m-thick intercalations of fine- to coarse-grained sandstones, and rare cm- to dm-thick calcaretes and marls; isolated channels comprising very coarse-grained sandstones are also present. The thickness of the unit changes from 56 to 77 m between the Larra and Barranco Serraduy profiles respectively (Fig. 3A). The mudstones (of varied colors) are massive, with common bioturbation and carbonate nodule mottling. The presence of coal, amber and microvertebrate remains is also common in the darkish beds. The root traces are filled with sand, carbonates or oxidations. Occasionally, they intercalate with cm- to dm-thick lenticular strata of brownish fine-grained sandstones with irregular bases and vertically bioturbated towards the top. The brownish sandstones appear in tabular or erosive levels: the former are massive beds although they sometimes present parallel lamination, scattered floating pebbles and vertical burrows; the latter exhibit a pervasive development of sedimentary structures dominated by trough cross-bedding, parallel and cross lamination, and asymmetric ripples. Rare calccrete levels with spherical carbonate nodules or crusts and frequent oxidizations have also been recognized. These deposits, especially the coarse- and very coarse-grained, include most of the vertebrate paleontological sites in the Serraduy area, with a great variety of fossil remains including hadrosaurid, testudine and crocodylomorph bones, as well as hadrosaurid and crocodylomorph ichnites.

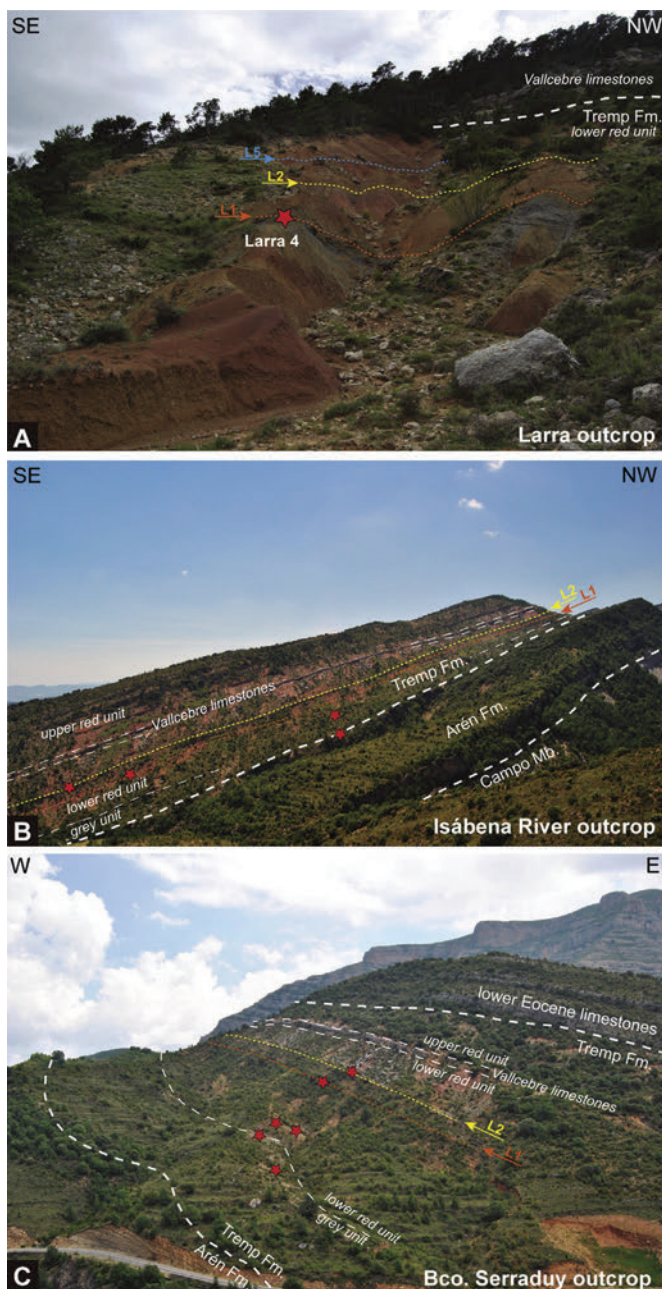
The upper part of the profiles comprises a 5-m-thick tabular body of whitish limestones (mudstone to wackestone), with scarce fossil content mainly restricted to foraminifers and charophytes. This has been ascribed to the “Vallcebre limestones” subunit (Fig. 3). Above it is the upper part of the Tremp Formation called the “upper red unit”. This unit is more terrigenous and has similar lithological characteristics to the “lower red unit”. Nevertheless, its fossil content is scarce, and no vertebrate remains have been recovered.

#### 3.2. Stratigraphic correlation

The stratigraphic correlation of the area has been based mainly on photogeology, the accurate physical correlation of beds in the field, and the lithological features of sedimentary bodies. The “grey unit” and the “Vallcebre limestones” represent two distinctive rock bodies, and this has also allowed the physical correlation between profiles (Figs. 3B and 4). Since most of the studied sediments of the “lower red unit” do not clearly crop out (Fig. 4), the detailed physical correlation of deposits has only been possible for thick sandstone beds located along the subunit (Figs. 3 and 4). These sandstones form m-thick tabular packages that have been physically correlated from visual inspection during fieldwork, as well as from analysis of aerial photographs (1:18000-scale) and 1:5000-scale satellite orthoimages.

In the area as a whole, the lower and upper boundaries of the “grey unit” and the lower boundary of the “Vallcebre limestones” are considered good correlation levels since: i) the thickness of these subunits is relatively homogeneous (Fig. 3A); ii) the contacts between subunits are not related with erosive surfaces; iii) the boundaries present the same lithofacies and sedimentary characteristics in different zones; and iv) lateral facies changes to other





**Fig. 4.** Landscape views of the main areas with outcrops and paleontological vertebrate sites in the Serraduy sector. A. outcrop of the Larra stratigraphic section located on the west side of the Isábena River; B. succession of the Arén and Tremp Formation in the sector located west of the Isábena River; C. succession of the Arén and Tremp Formation in the Barranco Serraduy sector located east of the Isábena River. Red stars point to the main areas with vertebrate sites; the white dotted lines mark the contact between different units; and the colored dotted lines point to the location of the different guide levels. (For interpretation of the references to color/colour in this figure legend, the reader is referred to the Web version of this article.)

units are not recognized. Thus, these boundaries can be considered continuous and isochronous limits, at least in the study area, allowing their use as a regional datum.

On the other hand, the correlation of the “lower red unit” is based on five characteristic packages of sandstones, two of which can be recognized in the whole area and permit the correlation between the Larra and Barranco Serraduy profiles (Fig. 3A, B). Throughout the whole area, the first correlation level (L1 in Figs. 3 and 4) presents numerous dinosaur ichnites at the base and is

always associated with a purple-greyish mudstone (Fig. 3A). In the western area, L1 comprises a tabular body of brownish fine- to medium-grained sandstones with parallel lamination that grade upwards to massive sandstones with bioturbation on the top. The underlying tabular body of grey-purple mudstones exhibits root bioturbation, vegetal remains and fossil vertebrates. Towards the southeast, L1 passes laterally into a thick body of greyish medium- to coarse-grained sandstones, which is composed of tabular and channelled strata. These beds are interfingered with purple bioturbated mudstones and show hadrosaurid dinosaur tracks at the base (Fig. 3A).

The second level (L2 in Figs. 3 and 4) comprises fine- to medium-grained massive sandstones with intense pedogenization and bioturbation in the western zone; L2 shows a negative-upwards trend. L2 corresponds to greyish sandstones that are fine- to very coarse-grained with trough cross-bedding, cross-lamination and ripples. This level displays sharp variations in thickness between the Larra and Isábena River outcrops. Towards the east, in the Barranco Serraduy outcrop, the variation in thickness continues to increase, and L2 forms a group of strata (~7 m thick) with a coarsening-upwards trend located 5 m above L1. The presence of hadrosaurid ichnites is also common at the base.

Level 3 is a cm-thick bed of brown fine-grained massive sandstones with scarce lateral continuity. L3 is located near to the Isábena River outcrop (Fig. 3B) and is not observed in other areas.

The fourth correlation level, which is up to one meter thick, is constituted by brown medium-grained sandstones with parallel lamination that passes vertically into cross-lamination. L4 presents a characteristic small slump (~20 cm thick) at the base and massive bioturbated sandstones (~15 cm thick) in the upper part. This level is easily recognizable in both western and eastern areas, from the Isábena River outcrop to near Barranco Serraduy (Fig. 3B).

The fifth level (L5 in Figs. 3 and 4A) is a fining-upward bed composed of 20 cm of greyish microconglomerates with slight channel geometry at the base and 60 cm of fine-grained massive sandstones with bioturbation. In the western area, from the Larra to Isábena River outcrops (Figs. 4A, B), this level presents good lateral continuity (Fig. 3B) and shows spectacular hadrosaurid dinosaur ichnites at its base.

On the basis of the vertical arrangement of the guide levels, chronostratigraphic refinement is possible for the studied sediments. Comparison of the thickness of the “lower red unit” between the Larra and Barranco Serraduy profiles shows clear variations, the succession being thicker in the latter (Fig. 3A). Accordingly, the average sedimentation rate for the Barranco Serraduy succession was slightly higher than for the Larra section. Consequently, the correlation results also allow us to constrain the vertical position of paleontological sites. This new correlation reveals that the most recent Cretaceous vertebrate remains correspond to dinosaur tracks and bones in L5 (the Camino de Rin 2 site) near the Larra section, which is located ca. 15 m lower than the Danian “Vallcebre limestones” (Fig. 3A).

### 3.3. Sedimentological interpretation

Characterization of the sedimentary environments requires exhaustive sedimentological analysis in order to establish and interpret correctly the different facies associations not studied in this work. Even so, the Serraduy area deposits may correspond with the evolution from coastal to continental environments, an interpretation previously proposed by several authors for the Tremp Basin (e.g., Díaz-Molina, 1987; Eichenseer, 1987; Cuevas, 1992; Rosell et al., 2001; López Martínez et al., 2006; Díaz-Molina et al., 2007; Oms et al., 2007, 2016; Riera et al., 2009; Villalba-Breva

et al., 2012; Díez-Canseco et al., 2014; Canudo et al., 2016; Fondevilla et al., 2016a).

The sedimentary features, especially the sedimentary structures and grain-size distribution, indicate that the Arén Formation in this area corresponds with a barrier-island or deltaic environment. The presence of m-scale coarsening-upwards sequences, facies associations and stacking patterns in the studied interval are similar to those described by Navarrete et al. (2013) for barrier-island and washover fan deposits interbedded within mudflat lagoonal deposits. The Tremp Formation mainly represents terrestrial environments, but the presence of planktonic foraminifers (see below) indicates continuous entrances of marine water into the more protected areas. Thus, the lowermost subunit (“grey unit”) has been interpreted as a transitional marine-to-continental environment connecting tidal systems with the barrier island. The “lower red unit” is predominantly composed of reddish-brownish and greyish-darkish mudstones representative of back-barrier mudflats, whereas the brownish tabular and erosive sandstones represent fluvial channels and their overbank deposits in the floodplains. Thus, frequent water-level oscillations and cyclic flooding of the mudflat area can be inferred from the sedimentary features. Several characteristics, such as mottling, oxide haloes and crusts, resulted from the migration and differential accumulation of iron, also indicating common water-table oscillations. In this context, the reddish colors of the mudstones suggest frequent subaerial exposure, probably in low water-level events. The vertical bioturbation and carbonate precipitation in the traces indicate the existence of vegetation with root penetration in search of the water level during dry periods. Darkish and greyish mudstones were deposited under anoxic conditions that favored the preservation of organic matter. This facies indicates the occurrence of high water-level periods, in which the mudflat areas were flooded. Isolated and anastomosed channeled sandstone bodies with freshwater charophytes (see below) indicate the existence of low-energy, meandering fluvial channels. Tabular, poorly sorted sandstone bodies and bioturbation traces filled with sands in mudstones reveal sharp flooding events related to high-energy water discharges. These floods occurred as a consequence of the overflow in the fluvial channels and the floodplain. The “Vallcebre limestones” represent the establishment of an extensive freshwater lake.

#### 4. Material and methods

In order to ensure the replicability of this research, all the paleontological material figured in this study, including the vertebrate remains and foraminifers, is properly labeled with MPZ abbreviations (Museo Paleontológico de la Universidad de Zaragoza) and housed in the Museo de Ciencias Naturales de la Universidad de Zaragoza (Zaragoza, Spain).

The methodology applied in this study (magnetostratigraphy and biostratigraphy) is detailed and explained in the corresponding section.

#### 5. Magnetostratigraphy

##### 5.1. Paleomagnetic sampling and laboratory procedures

115 levels were sampled as part of the Serraduy magnetostratigraphic study, 21 from the Arén Formation (SB) and 94 from the Tremp Formation (SR). Both magnetostratigraphic profiles were generated in the vicinity of the Barranco Serraduy (BS) stratigraphic section. SB consists of 6 levels of blue-grey marls from the Campo Member, and 14 levels of sandstones with one level of grey marls from the Arén Formation. In the SR profile, 17 levels correspond to the “grey unit” of marls and calcarenites of the Tremp Formation.

Another 73 levels are defined as an alternation of red, grey and versicolor mudstones, with some levels of sandstones in the so-called “lower red unit”. Finally, 4 levels of the Paleocene “Vallcebre limestones” were sampled at the top of the SR section (Fig. 5).

The complete SB profile was sampled with a portable gas-powered and water-cooled drill and directly oriented in the field with a magnetic compass and an inclinometer, providing from 1 to 3 samples per level, each divisible into 1–3 standard-sized specimens. In the SR profile, 62 levels were drilled with a portable electrical water-cooled drill, hand samples (blocks) were taken from 29 levels and in 3 levels both drilled and hand samples were collected. These were oriented *in situ* with a magnetic compass. Hand samples were collected because of how easily broken up (being disaggregated) the finest materials corresponding to the “lower red unit” were. They were consolidated with sodium silicate dissolved in distilled water to try to make the consolidator percolate to the interior of each piece. Once hardened, about 3 cubes per block were sectioned with a disc cutter, maintaining the face perpendicular to the strike line and parallel to the dip line, both oriented in the field, as the marker for the paleomagnetic analysis.

The sampled levels in the SB profile were established each 1 m from the SB01 to SB06 marls, every 2–4 m at the beginning of the sandstones, and every 6 m afterward, due to the homogeneity of the materials. The sampled SR profile levels were separated by 1 m whenever possible. In total a sequence of 173 m was sampled.

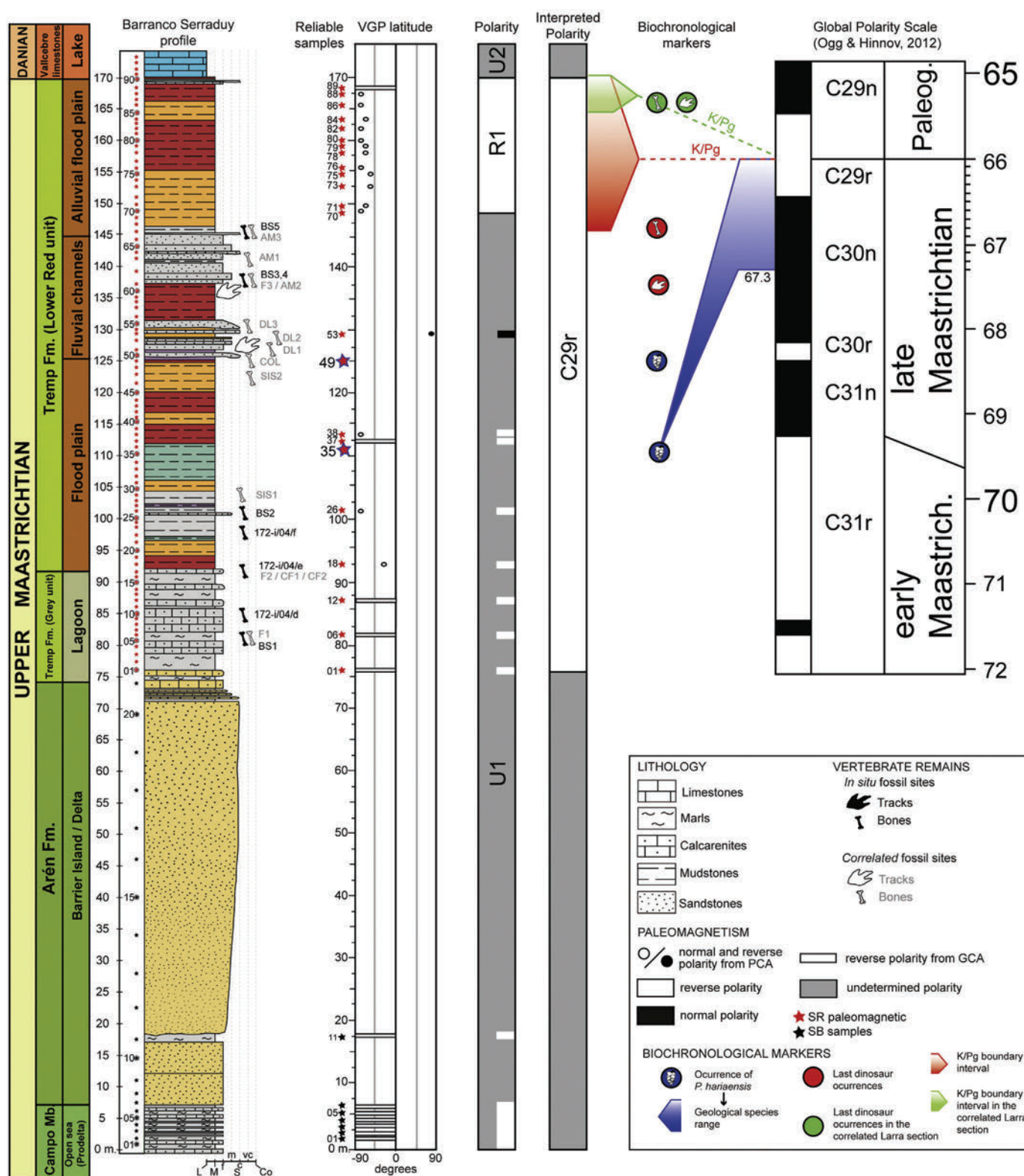
Thermal (Th) and alternating field (Af) demagnetizations were carried out in the paleomagnetic laboratory of the University of Burgos, using a 755 superconducting magnetometer (2G) with an alternating field inductor demagnetizer system (for automatic Af), a TD48-DC (ASC) oven and a LDA3 (Agico) alternating field demagnetizer (for manual Af). A total of 198 samples (1–3 samples per level) were demagnetized with different stepwise temperatures and applied alternating fields according to the sample lithology. 145 of these were Th-demagnetized, heating up to 400–575 °C for marls, sandstones, calcarenites and limestones, and up to 475–675 °C for mudstones (several samples of all lithologies were heated up to 675 °C in order to check their magnetic behaviors), 39 with automatic Af, 14 with manual Af trying to improve the accuracy of the method, and an Af protocol with an initial thermal step of 130 °C to delete the part of the signal carried by goethite (all Af up to 100 mT).

Principal component analysis (PCA) and great circle (GC) analysis were performed with Remasoft 3.0 software (Chadima and Hrouda, 2006). Virtual Geomagnetic Poles (VGPs) were calculated, through the isolated paleomagnetic directions considered primary. In cases where overlapping prevents the isolation of stable paleomagnetic components, GCs were calculated. Together with the stratigraphic column, the VGP latitudes obtained from PCA paleomagnetic directions are symbolized with a point, whereas for the primary components verified by GC a bar occupies the status corresponding to normal or inverse latitude (−90°–0° or 0°–90°) (Fig. 5).

In addition, rock-magnetic measurements were carried out at the University of Burgos with a variable field translation balance (VFTB). Powdered whole-rock specimens from 14 representative samples from all lithologies were submitted to experiments on IRM acquisition and backfield curves, hysteresis loops and strong field magnetization versus temperature (Ms-T) curves. Analysis of these measurements was performed with RockMagAnalyzer 1.0 software (Leonhardt, 2006).

##### 5.2. Paleomagnetic behavior

The natural remanent magnetization (NRM) behavior was analyzed separately in accordance with the lithology because of



**Fig. 5.** Lithology, paleontological site positions, and the proposed magnetostratigraphy from the Barranco Serraduy section. VGP latitude logs along the Arén Formation (SB) and Trempe Formation (SR) profiles are shown by circles (black or white) when the polarity has been calculated from paleomagnetic directions obtained by principal component analysis (PCA) or by bars (white) when it has been obtained by great circle analysis (GCA) (Ogg et al., 2012).

the big variations among lithologies. Sandstones and green/violet mudstones in general show low NRM intensities (0.1–0.5 mA/m) and a heterogeneous paleomagnetic behavior, being paleomagnetically unstable (it is not possible to isolate a reliable

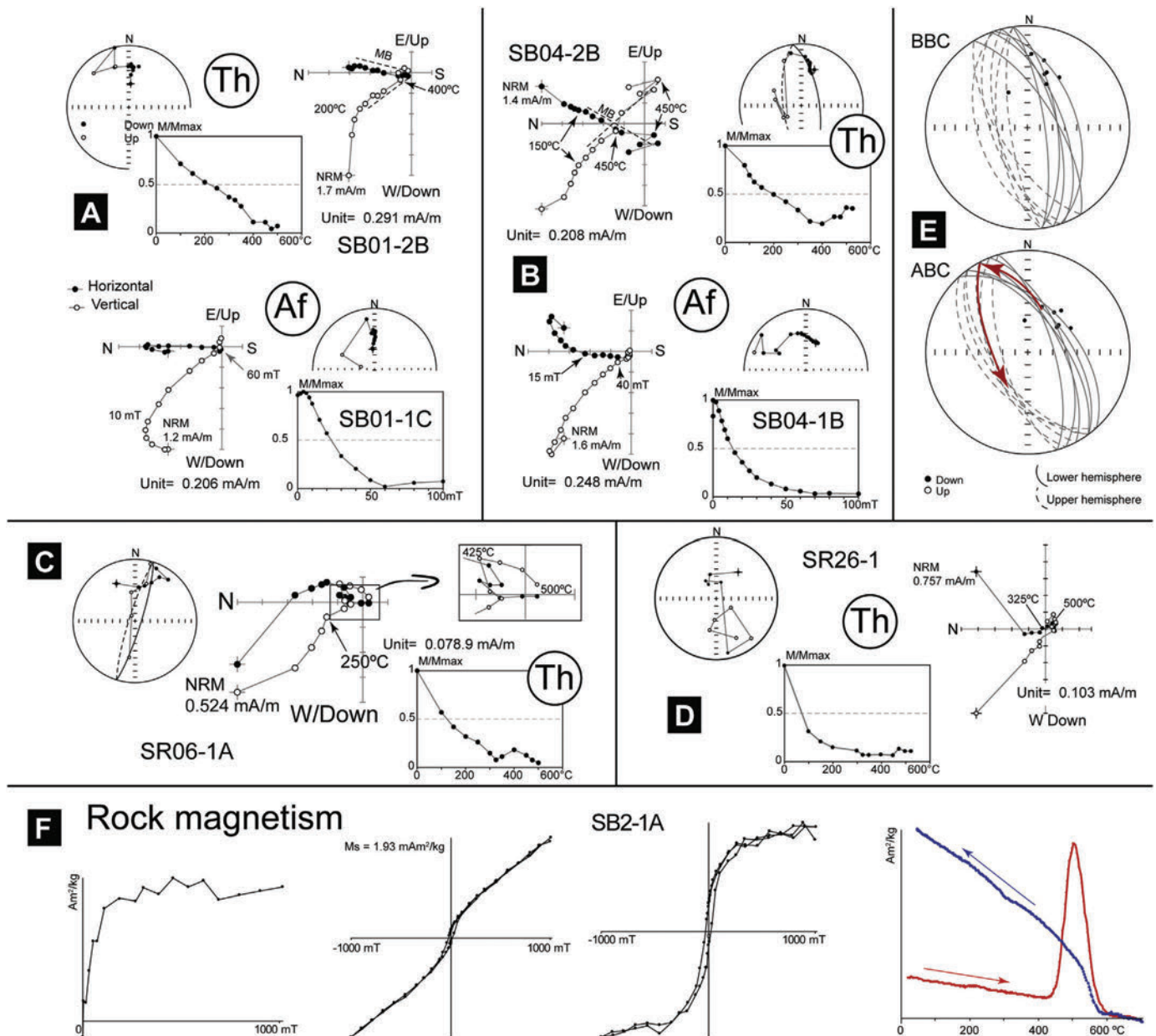
paleomagnetic component). In marls and red beds two paleomagnetic components can be identified on the basis of the unblocking temperature ranges and the coherence of the directional data.

### 5.3. Blue-grey marls

These rocks appear below the Arén Formation (Campo Member), at the bottom of the Tresp Formation (“grey unit”) and intercalated with continental sediments of the Tresp Formation (“lower red unit”) (Fig. 5).

Marls of the Campo Member (samples SB01-SB06 and SB11) show homogeneous paleomagnetic behavior, with NRM intensities between 1.1 and 1.78 mA/m, and display two different components in thermal (Th) demagnetization. A low-temperature component MB (unblocking temperatures between 250/300–450 °C) with a northwards direction and positive inclinations

(Fig. 6A) is isolated in all samples. This component does not go to the origin in some samples (Fig. 6B, C), going systematically to the southern quadrant with negative inclination (Fig. 6B). Great circle analysis (Fig. 6E) allows us to infer this high-temperature component (up to 500 °C) with negative inclination (component MA), but this cannot be isolated because of spurious component formation during heating. Alternating field (Af) demagnetization diagrams show only one recognizable component (6/15–40/60 mT), which corresponds with component MB (Fig. 6A) with a slight overlapping with MA when this appears, as can be observed in the equal-area demagnetization diagram (Fig. 6B), but it is noteworthy that the overlapped component is almost trending to



**Fig. 6.** A–D, demagnetization diagrams, in geographic coordinates, showing the paleomagnetic behaviors in representative samples of carbonatic rocks; A–B, samples from the SB and SR sections showing an overlap between two components with opposite direction; D, sample of the SR section with a normal polarity component at low temperatures and a dispersed high temperature cluster; E, equal area projection of the MB component and the demagnetization great circles calculated in these rocks, before and after bedding correction (BBC and ABC respectively). Note the path from normal polarity to reverse polarity followed by all samples; F, representative rock magnetic experiments of this lithology. From left to right, acquisition of the isothermal remanent magnetization (IRM), non-corrected and corrected hysteresis loop, and thermomagnetic curve. The low coercivity may indicate the presence of magnetite as the main magnetic mineral, as can be observed in the IRM and hysteresis loops; the thermomagnetic curve shows an important growth of magnetite up to 400 °C.

the origin, preventing recognition of the presence of two components.

The NRM intensity is lower in the marls of the Tremp Formation (SR samples), around 0.4–0.5 mA/m. A low-temperature component (250–400 °C) is recognizable, and with some exceptions it goes to the origin, mainly in the basal marls (SR01–SR17); this component shows the same behavior as the already described MB component for the SB samples. However, a few samples (SR-01A, SR26-1) show an overlapping of components either (i) in the definition of great circles (Fig. 6E), indicating the presence of a high component (Fig. 6C), or (ii) by a cluster-end showing a south declination and negative inclination (Fig. 6D).

Therefore, most samples of SB and SR marls show the low-temperature MB component (between 250/300 °C and 350/400 °C) with normal polarity (positive inclination towards the north). This component does not go to the origin because of the presence of a high-temperature component (up to 350/400 °C) with reversed polarity, which cannot be isolated because of the formation of spurious components but is clearly evidenced by analyzing the great circles.

According to the NRM behavior (low coercivity and unblocking temperatures between 150 and 500 °C), and the magnetic rock properties (Fig. 6F), both components are carried by magnetite. Thermomagnetic curves show a major growth of magnetic minerals (magnetite according to the Curie temperature in the cooling curve) in agreement with that observed in the NRM.

### 5.3.1. Red mudstones

Red and orange mudstones appear throughout the Tremp Formation, mainly in the upper section. Most samples show low–medium NRM intensities ranging from 0.1 to 1.8 mA/m, but some of them have higher intensities around 3 mA/m. Low-intensity samples (~0.2–0.8 mA/m) usually show a single component (Fig. 7A) with unblocking temperatures from 350/550 °C up to 620 °C; however, the end of the component is obliterated because of a spurious component generated during heating. In some samples, generally those of a higher intensity (>1 mA/m), component A overlaps with an intermediate temperature component between 350 °C and 550 °C (Fig. 7B, C); this overlapping component has low inclination and does not go to the origin. In these samples, component RA can be observed at temperatures up to 500 °C (Fig. 7B). Finally, SR53 (Fig. 7D) shows high intensity and a single component with positive inclination toward the north, which can be interpreted as component RA according to its unblocking temperatures (550–625 °C).

The unblocking temperatures and high coercivity (Fig. 7) point to hematite as the carrier of component RA. This is in agreement with the rock magnetism experiments (Fig. 7E), which are characterized by a high-coercivity magnetic phase with Curie temperatures over 600 °C. Differences between the cooling and the heating in the thermomagnetic curve indicate the growth of magnetic minerals (probably magnetite or maghemite) during heating, at temperatures above 600 °C.

### 5.4. Interpretation of the paleomagnetic components

Carbonatic rocks show the presence of two components with different unblocking temperatures. Component B, carried by magnetite, is characterized by low to intermediate unblocking temperatures (300–450 °C) and does not go to the origin. Several works (e.g. Juárez et al., 1994; Villalain et al., 1994; Osete et al., 2007) evidence the presence of low to intermediate unblocking temperatures (below 450–500 °C) for diagenetic secondary magnetite, and a high-temperature component (above 450 °C) corresponding with primary magnetite. The unblocking

temperatures of secondary minerals are usually lower than those of primary ones. This is because of the small size of secondary minerals, which range from the superparamagnetic to the stable single domain (see Jackson and Swanson-Hysell, 2012). This suggests a secondary origin for component B found in the marls, but does not ensure a primary origin for the high-temperature component since the presence of two secondary magnetizations is also possible.

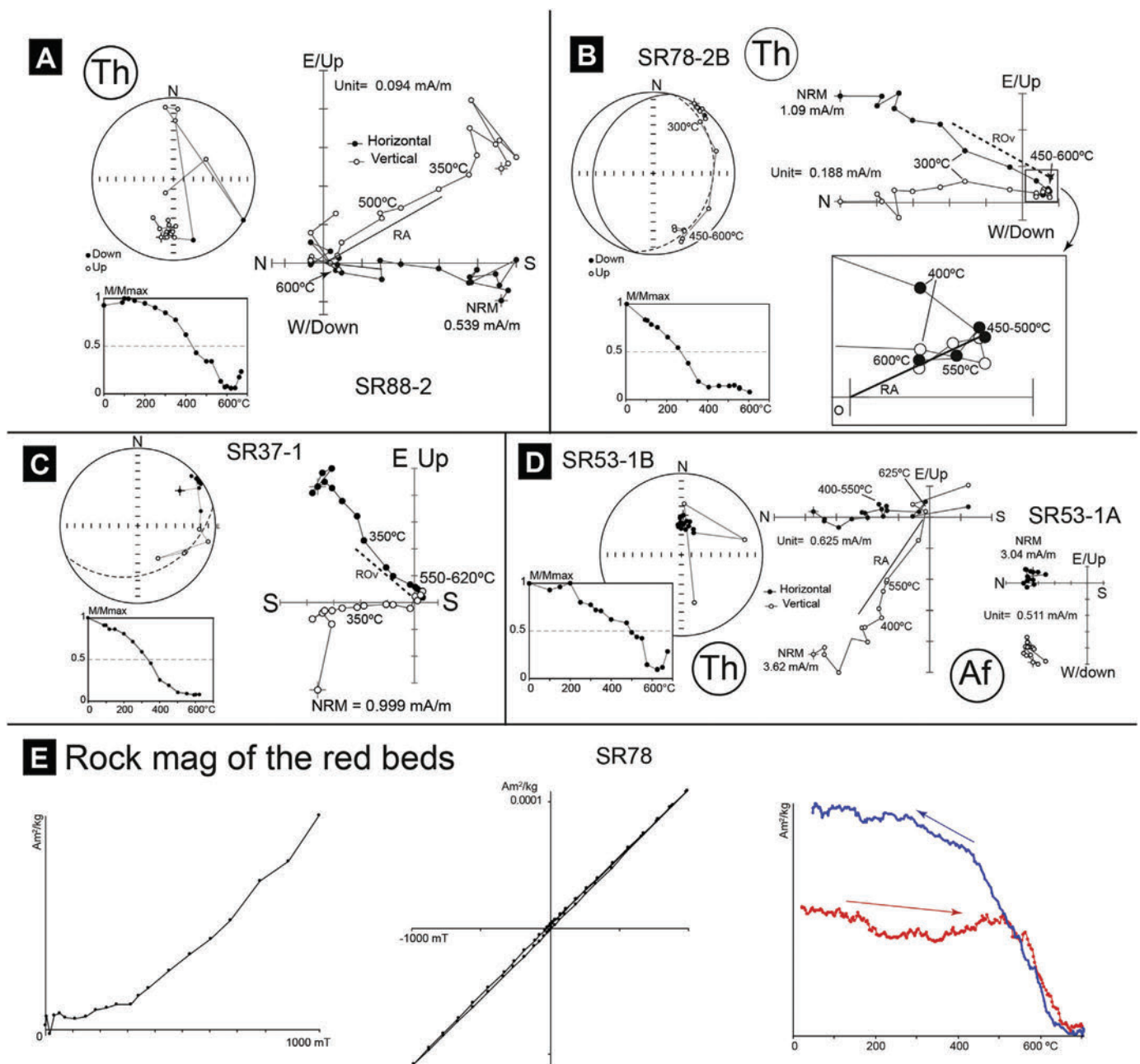
The paleopole reference for the Late Cretaceous of Iberia from the Lisbon Volcanics (Van der Voo and Zijdeveld, 1971) corresponds to an expected direction for the section location of  $D = 1.08^\circ$  and  $I = 47.39^\circ$ . In spite of the low dip of the studied materials, the mean direction of component B is in better agreement before than after the bedding correction (BBC and ABC respectively, Fig. 8B). This fact agrees with a secondary origin for this component. We can thus consider component B to be a chemical remanent magnetization (CRM). This was acquired probably during the early diagenesis, but after the tilting of the series (note that the tilting is Maastrichtian–early Paleocene [Simó et al., 1985], slightly post-dating the age of the rocks). Component B partially obliterates the high-temperature component (A), which cannot be calculated because of the growth of magnetic minerals during heating. However, this is clearly evidenced by the demagnetization great circles.

Comparisons between the demagnetization great circles (Fig. 8C) calculated in carbonates (the NW–SE GC) and in red beds (the NE–SW GC) are coherent with the calculated direction of component A (Fig. 8A). This agrees with the correspondence between component A as calculated in red beds and the high-temperature component observed in carbonates.

As regards the assessment of the primary nature of component A in red beds, several hitches appear in this work regarding the interpretation of both components: (i) the thickness of the Upper Cretaceous in this locality is limited; (ii) the series shows significant changes in lithology and coloration which can produce different behavior in recording the paleomagnetic components; (iii) the absence of conglomerates and a near uniform and low dip (around  $20^\circ$  towards the east) along the section preclude the use of the field test to establish the primary nature of one of the components; and finally (iv) the presence of only one polarity prevents the use of the reversal test. However, several magnetostratigraphic works performed on longer sections of the same rocks (both in lithology and age) of the Tremp Basin (Galbrun et al., 1993; Oms et al., 2007; Pereda-Suberbiola et al., 2009; Vila et al., 2011, 2012; Canudo et al., 2016; Fondevilla et al., 2016a) show the presence of a component in red beds with similar paleomagnetic behavior. Reversal and tilt tests reveal a better concordance between the paleomagnetic direction and the reference in these works, showing a primary origin for this component. In accordance with these works, therefore, we consider that the component A observed in red beds is probably primary and can be considered a detrital remanence (DRM) carried by hematite.

### 6. Biostratigraphy

Planktonic foraminifera have been the basis for the micropaleontological dating of Pyrenean sections, from the deep sea to the continental shelf, mainly for Cretaceous materials. In the South-Central Pyrenees, the dinosaur-rich sites of the Arén Formation located west of the Tremp syncline have been correlated with deep marine sediments containing planktonic foraminifera from the uppermost Maastrichtian *Abathomphalus mayaroensis* (Bolli, 1951) Zone near Campo (López-Martínez et al., 2001). Non-reworked planktonic foraminifera from the Maastrichtian were found in the “lower red unit” (Tremp Formation), suggesting transport after death landwards from the outer/inner shelf by tidal currents (Díez-



**Fig. 7.** A–D. demagnetization diagrams showing, in geographic coordinates, the paleomagnetic behaviors in representative samples of red beds; A. components RA and RB with the same polarity; B and C. component RB does not go to the origin and a non-zero end cluster reveals component RA with reversed polarity; in SR78-2B, RA is partially demagnetized before the growth of the magnetic mineral during heating (up to 620 °C); D. RA and RB with normal polarity; E. representative rock magnetic experiments of this lithology. From left to right, IRM, hysteresis loop and thermomagnetic curve. The high coercivity observed in the IRM and in the hysteresis loop and the presence of a magnetic phase with Curie temperatures above 620 °C indicate the presence of hematite as the main magnetic phase. The higher magnetization of the cooling curve indicates the growth of magnetite during heating. (For interpretation of the references to color/colour in this figure legend, the reader is referred to the Web version of this article.)

Canseco et al., 2014). This and other biostratigraphic studies with planktonic foraminifera (Vicente et al., 2015) have indicated an early to late Maastrichtian age for the “grey unit” and “lower red unit” of the Tremp Formation and Danian for the “Vallcebre limestones”.

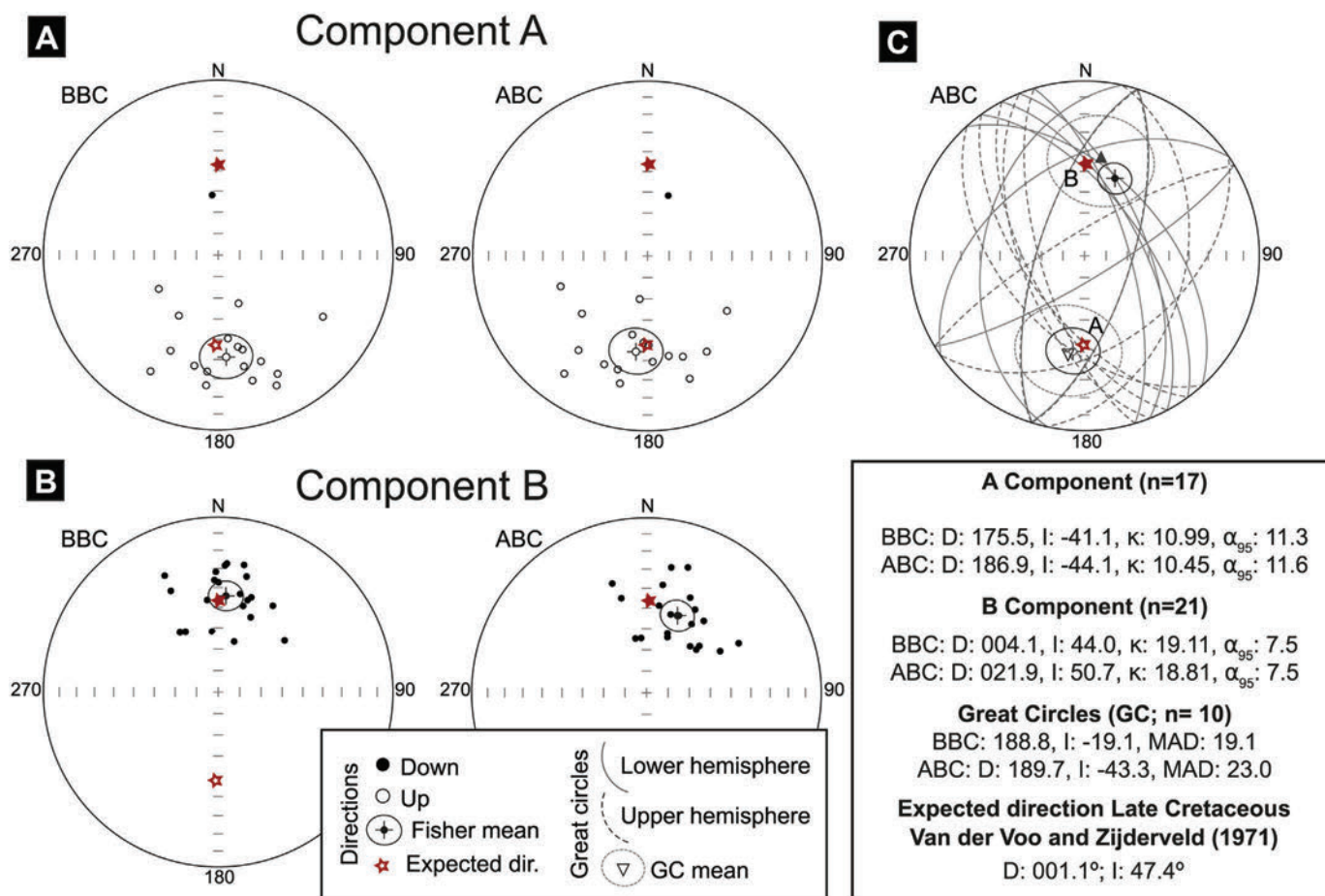
#### 6.1. Micropaleontological sampling and methodology

For micropaleontological studies, 94 samples were analyzed from the “grey” and “lower red units” of the Tremp Formation and the lower part of the “Vallcebre limestones”. Rock samples were disaggregated in water with diluted  $H_2O_2$ , washed through a 63- $\mu$ m

sieve, and then oven-dried at 50 °C. In each sample, between 100 and 200 specimens of foraminifera were picked from the residues and mounted on micropaleontological slides. Some were selected for scanning electron microscopy using a JEOL JSM 6400 SEM at the Microscopy Service of the Universidad de Zaragoza (Spain), and SEM photographs are provided in Fig. 9.

#### 6.2. Foraminiferal assemblages

Foraminifera are absent from the “grey unit” of the Tremp Formation. In the lower part of the “lower red unit”, all samples contain planktonic foraminifera, and benthic foraminifera are very



**Fig. 8.** Equal-area projection of component A (A) and component B (B) with their respective Fisher means (Fisher, 1953), before and after bedding correction (BBC and ABC respectively); C. calculated demagnetization great circles (GC) and mean direction of both components; note that both components overlap with the GC mean intersection, component A being almost coincident with its mean. n: number of samples. NW-SW GCs correspond with carbonates and NE-SW GCs with red beds. (For interpretation of the references to color/colour in this figure legend, the reader is referred to the Web version of this article.)

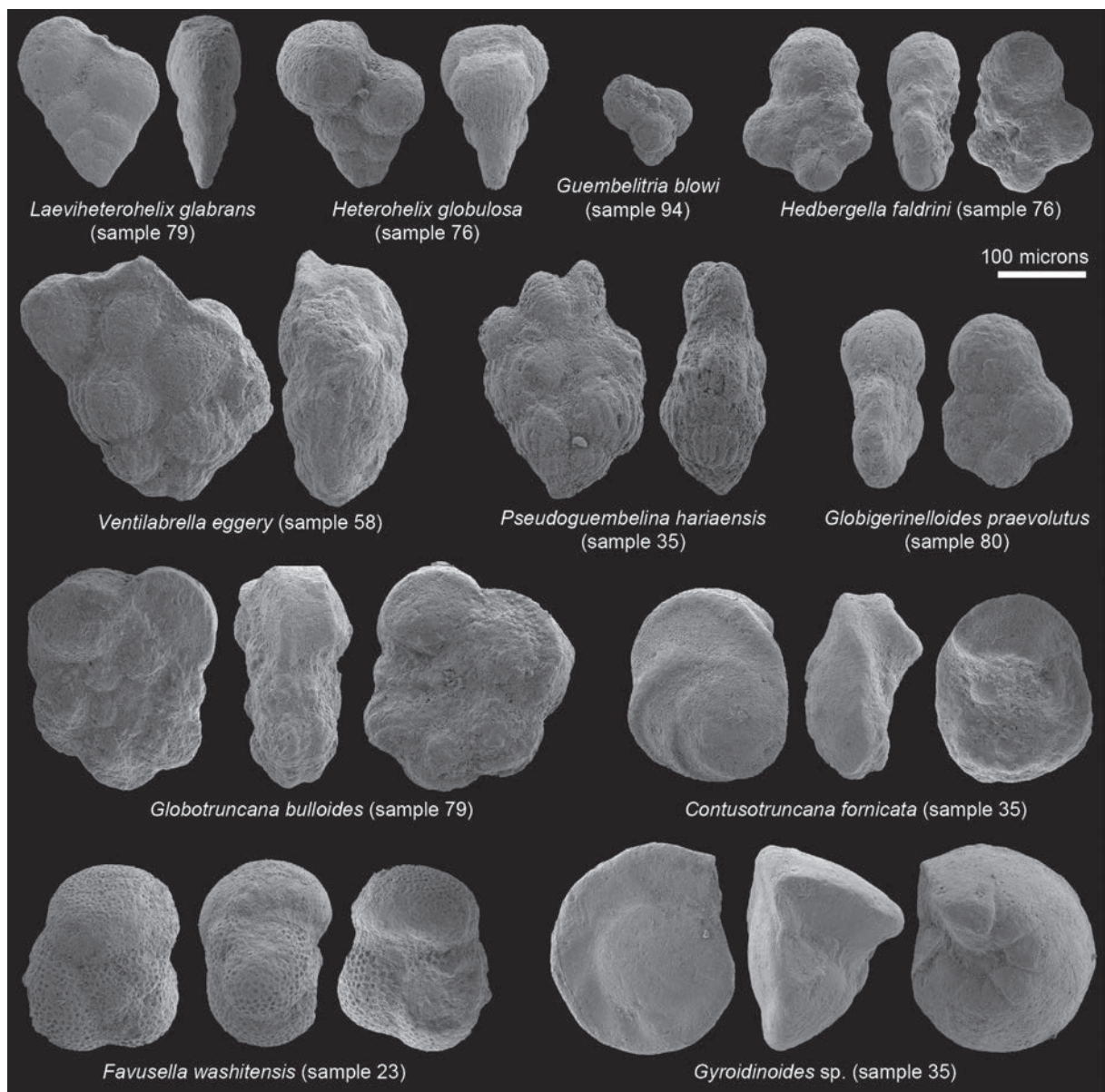
scarce. There are also relatively abundant fragments of echinoderms, marine bivalves and continental microfossils such as calcified charophyte fructifications. The preservation of the microfossils varies from poor to moderate (Fig. 9).

In the “lower red unit” of Barranco Serraduy, planktonic foraminifers indicate mixed assemblages with species of different ages. Some species are exclusively Maastrichtian, such as *Pseudoguembelina hariaensis* Nederbragt, 1991 and *Globotruncanita fareedi* (El Naggar, 1966). Other species have their first record before the Maastrichtian, but their ranges span this stage (*Heterohelix globulosa* (Ehrenberg, 1840), *Htx. planata* (Cushman, 1938), *Htx. labelliosa* Nederbragt, 1991, *Htx. glabrans* (Cushman, 1938), *Pseudotextularia nuttalli* (Voorwijk, 1937), *Globigerinelloides yaucoensis* (Pessagno, 1967), *Gdes. bollii* Pessagno, 1967, *Gdes. praevolutus* Petters, 1977, *Globotruncana arca* (Cushman, 1926), *Gna. aegyptiaca* Nakkady, 1950, *Gna. bulloides* Vogler, 1941, *Gna. linneiana* (d’Orbigny, 1839), *Gna. mariei* Banner and Blow, 1960, and *Contusotruncana fornicata* (Plummer, 1931)). Finally, other species predate the Maastrichtian (*Ventilabrella eggeri* Cushman, 1928, *Sigalia deflaensis* (Sigal, 1952), *Hedbergella flandrini* Porthault, 1970 (in Donze et al., 1970), *Dicarinella primitiva* (Dalbiez, 1955), *Ticinella raynaudi* Sigal, 1966, *Favusella washitensis* (Carsey, 1926), and *Whiteinella* spp.). The small benthic foraminifera mainly consist of calcareous trochospiral plano-convex species (such as *Anomalinoides* spp. and *Gyroidinoides* spp.) and planispiral *Lenticulina* spp.

### 6.3. Interpretation of foraminiferal faunas

Since planktonic foraminifers are almost absent from the “grey unit”, no unequivocal age attributions have been obtained for this interval. Although the distinction of *in situ* and *ex situ* specimens is difficult, the foraminiferal assemblages identified in the “lower red unit” suggest that they are reworked and mixed: some of the planktonic foraminifer species identified are of different ages, and most of the benthic foraminifers indicate a contradictory bathyal depth. The studied stratigraphical interval cannot be assigned to any biozone with reworked specimens, but at least a minimum age can be assigned based on the most modern species identified in these horizons. The presence of *P. hariaensis* specimens in samples 35 and 49 suggests that the last 60 m of the “lower red unit” are late Maastrichtian in age, since the first appearance of *P. hariaensis* was calibrated at 67.3 Ma (upper part of chron C30n) according to the time-scale GTS 2012 (Gradstein et al., 2012).

In the “Vallcebre limestones”, a few specimens of *Guembelitra cretacea* Cushman, 1933 and *Guembelitra blowi* Arz, Arenillas and Nández, 2010 have been identified in samples 80 and 94. *Guembelitra* is the only genus whose survival beyond the Cretaceous/Paleogene mass extinction event has been clearly proven (Smit, 1982). However, these specimens are probably reworked, as the uppermost occurrence of *Guembelitra* is in the lower Danian, and these *Guembelitra* specimens were found in horizons equivalent to



**Fig. 9.** Some representative planktonic and benthic foraminifer species identified in the Barranco Serraduy section. From left to right and from top to bottom: *Laeviheterohelix glabrans* (MPZ 2018/25), *Heterohelix globulosa* (MPZ 2018/23), *Guembelitra blowi* (MPZ 2018/28), *Hedbergella faldini* (MPZ 2018/24), *Ventilabrella eggeri* (MPZ 2018/22), *Pseudoguembelina hariaensis* (MPZ 2018/21), *Globigerinelloides praevolutus* (MPZ 2018/27), *Globotruncana bulloides* (MPZ 2018/26), *Contusotruncana fornicata* (MPZ 2018/20), *Favusella washitensis* (MPZ 2018/18), *Gyroidinoides* sp. (MPZ 2018/19).

the Suterranya Limestone Formation belonging to the upper Danian (Diez-Canseco et al., 2014).

## 7. Vertebrate assemblage

Considering the limited extent of the outcroppings of the Tremp Formation in the Serraduy area compared to the rest of the outcrops within the Tremp syncline, this sector represents one of the areas with the richest and most diverse vertebrate assemblages in the Tremp Basin. In a studied area of approximately 1.5 km<sup>2</sup> of outcrops of the Tremp Formation, nearly 40 paleontological sites with more than 600 vertebrate remains distributed in about 17 stratigraphic levels have been found (Table 1). Although most of this material is currently under study, a preliminary review of the fossils recovered in recent years (mainly between 2009 and 2016) has allowed the identification of dinosaurs (sauropods, hadrosauroids and

theropods), crocodylomorphs, testudines and amphibians. Within the paleontological site Camino de Rin 2, located in the upper part of the “lower red unit”, a bone fragment has been recovered that could correspond to a pterosaur mandible. However, this fossil remnant is still under laboratory preparation. The presence of pterosaurs in the Serraduy area thus remains uncertain. The most representative material recovered in the area will be described below.

### 7.1. Dinosaurs

#### 7.1.1. Hadrosauroids

The most abundant taxa recovered in Serraduy correspond to hadrosauroids, representing between 60% and 75% of the identified dinosaur remains. This percentage variation is a consequence of the doubtful assignment of some remains to Hadrosauridae? due to

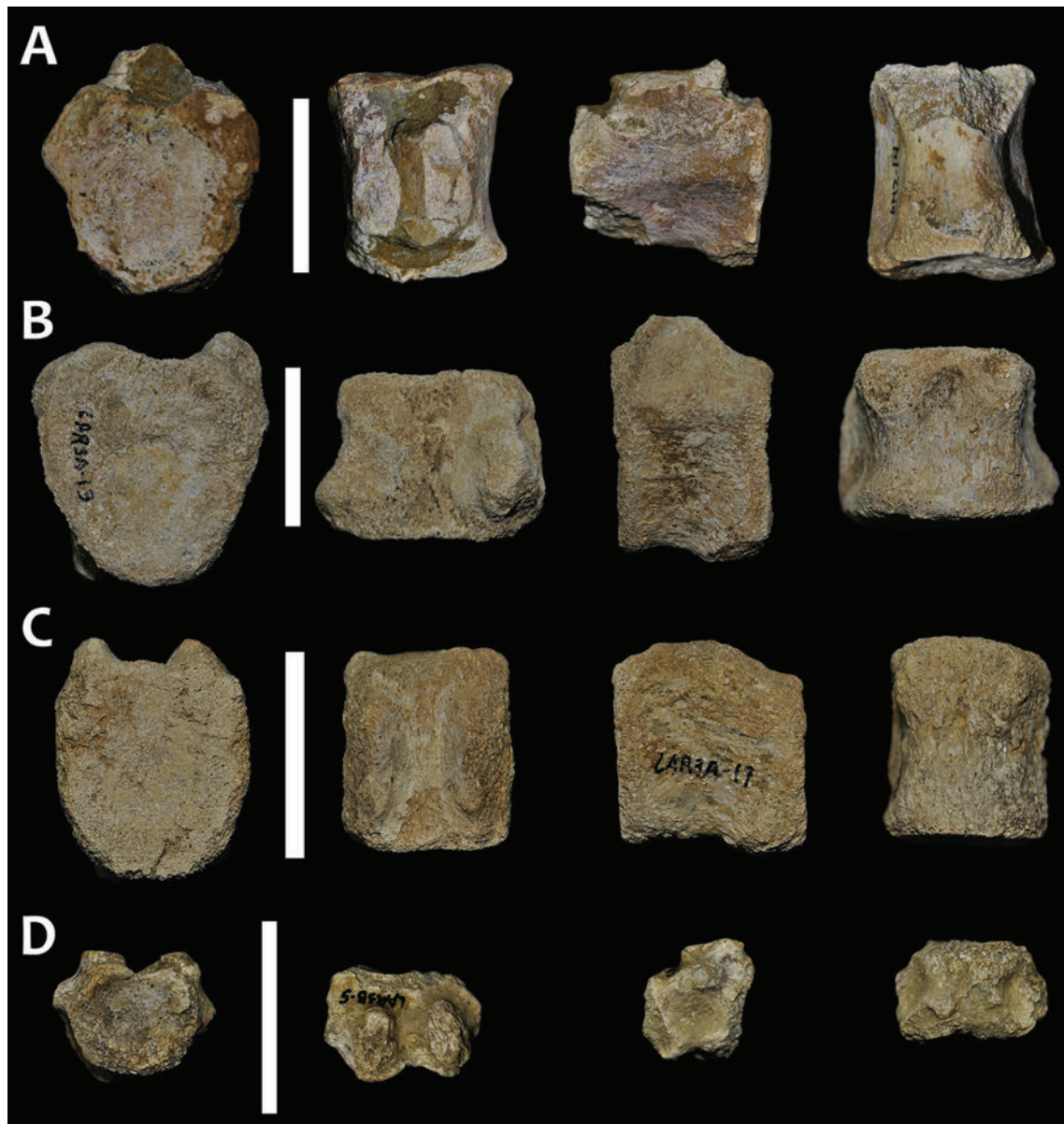
**Table 1**

Vertebrate faunal list for Serraduy (Huesca, Spain), upper Maastrichtian.

Site	Abbreviation	Taxa	Site	Abbreviation	Taxa
172-i/04/a	172-i/04/a	Hadrosauridae indet.	Camino Rin 2	CRIN2	Hadrosauridae? indet. Theropoda? indet. Pterosauria? indet. Hadrosauridae? indet. Dinosauria indet. Avialae? indet. Bothremydidae indet. Hadrosauridae indet. Avialae? indet. Bothremydidae indet. cf. Allodaposuchidae
172-i/04/b	172-i/04/b	Dinosauria indet.	Dolor 1	DL1	Dinosauria indet.
172-i/04/c	172-i/04/c	Dinosauria indet.	Dolor 2	DL2	Hadrosauridae indet. Dinosauria indet.
172-i/04/d	172-i/04/d	Dinosauria indet.	Dolor 3	DL3	Hadrosauridae indet. Dinosauria indet.
172-i/04/e	172-i/04/e	Hadrosauridae indet. Theropoda indet.	Barranco Extremadura	EXT	Hadrosauridae indet. Bothremydidae indet. cf. <i>Thoracosaurus</i> Dinosauria indet. Hadrosauridae indet. Bothremydidae indet.
172-i/04/f	172-i/04/f	Hadrosauridae indet.	Fornons 1	F1	Dinosauria indet.
Amor 1	AM1	Dinosauria indet. Hadrosauridae indet. Bothremydidae indet.	Fornons 2	F2	Hadrosauridae indet. Dinosauria indet.
Amor 2	AM2	Hadrosauridae indet. Bothremydidae indet.	Fornons 3	F3	Hadrosauridae? indet.
Amor 3	AM3	Dinosauria indet. Hadrosauridae? indet. Bothremydidae indet.	Larra 1	LAR1	Dinosauria indet. Theropoda? indet. Vertebrata indet. Eusuchia indet.
Barranco Serraduy 1	BS1	<i>Agaresuchus subjuniperus</i> Dinosauria indet. Hadrosauridae indet.	Larra 2	LAR2	Dinosauria indet. Ornithopoda indet. Hadrosauridae indet. Bothremydidae indet. cf. Allodaposuchidae
Barranco Serraduy 2	BS2	Dinosauria indet. Hadrosauridae indet.	Larra 3	LAR3	Dinosauria indet. Hadrosauridae indet. Eusuchia indet.
Barranco Serraduy 3	BS3	Vertebrata indet.	Larra 4	LAR4	Hadrosauridae indet. Coelurosauria indet. Bothremydidae indet. cf. Allodaposuchidae
Barranco Serraduy 4	BS4	Dinosauria indet. Hadrosauridae indet. Sauropoda indet. Bothremydidae indet. Eusuchia indet.	Larra 5	LAR5	Discoglossidae indet. Hadrosauridae indet.
Barranco Serraduy 5	BS5	Hadrosauridae indet. Bothremydidae indet.	Larra 6	LAR6	Dinosauria indet. Bothremydidae indet. cf. Allodaposuchidae
Camino Fornons 1	CF1	Dinosauria indet. Hadrosauridae indet. Theropoda? indet. Sauropoda? indet. Osteichthyes indet. Bothremydidae indet.	Pedregal	PED	
Camino Fornons 2	CF2	Hadrosauridae indet. cf. Allodaposuchidae	Rin 1 y 2	RIN1-2	Dinosauria indet.
Color	COL	Dinosauria indet. Hadrosauridae indet. Bothremydidae indet.	San Cristobal	SCRI	Dinosauria indet. Hadrosauridae indet.
Camino Rin 1	CRIN1	Theropoda? indet.	Sierra de Sis 1	SIS1	Dinosauria indet. Hadrosauridae indet. Bothremydidae indet.
			Sierra de Sis 2	SIS2	Dinosauria indet. Hadrosauridae indet.

their fragmentary nature. Around 20% of the bones were classified as Dinosauria indet., being unable to perform a more precise taxonomic assignment until now. The distribution of hadrosauroids through the studied stratigraphic sections and paleontological sites is also very extensive (Fig. 1), it being possible to find remains from the top of the Arén Formation through to the last levels with vertebrates before the K/Pg boundary, within the “lower red unit” of the Tremp Formation.

Most of the hadrosauroid remains are disarticulated and correspond to vertebral elements, which represent more than half of the identified bones (Fig. 10). Most vertebrae are caudal, although there are representative elements from most of the vertebral column. In addition, fragments from ribs, chevrons, femora (Fig. 11D), pubis, isolated teeth, dentaries, maxilla, autopodial bones (Fig. 11B), humerus, scapula, isolated teeth, tibiae (Fig. 11C), ulna and coracoid (Fig. 11A) have also been identified.



**Fig. 10.** Vertebrae of Hadrosauridae indet. from Serraduy. A. caudal (juvenile MPZ 2017/796 from AM2 site); B. caudal (adult MPZ 2017/797 from LAR3 site); C. caudal (juvenile MPZ 2017/798 from LAR3 site); D. cervical (adult? MPZ 2017/799 from LAR3 site). In posterior/anterior, dorsal, lateral and ventral views respectively. Scale bar = 3 cm.

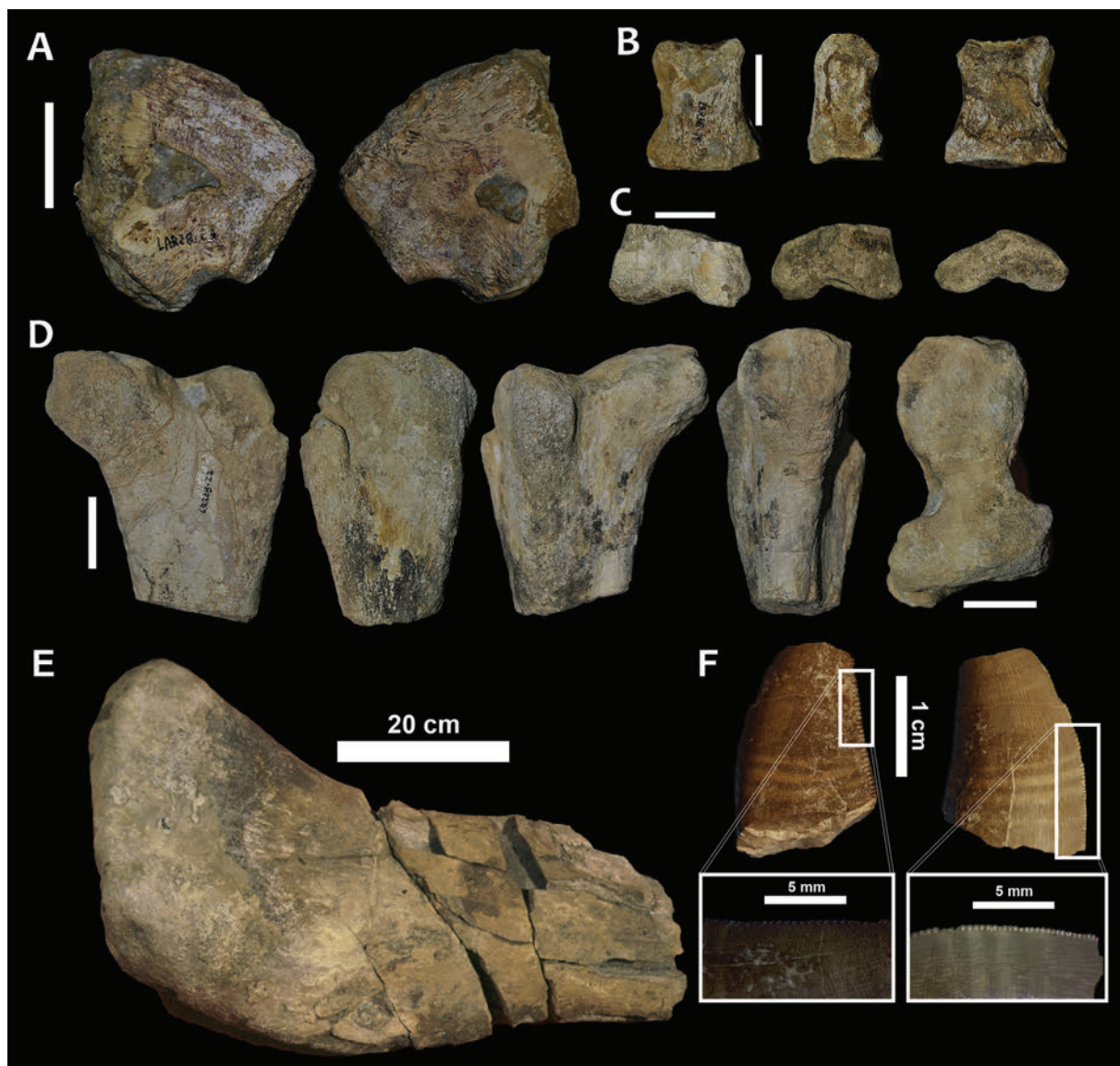
Because most of the material is fragmentary and/or poorly diagnostic, most of the remains have been assigned to Hadrosauroidea indet. and Hadrosauridae indet.

One of the most interesting aspects observed in Serraduy is the joint presence of mature medium to large-sized hadrosaurids and mature small-sized hadrosaurids that may represent new insular dwarf species (Cruzado-Caballero et al., 2014; Company et al., 2015; Blanco et al., 2015b). The hypothesis of the presence of dwarf hadrosaurids in Serraduy is based on the recovery of several small vertebrae with mostly fused neural arches, several diminutive limb bones and a histological study of several rib fragments and representative elements such as a humerus and a femur (Company et al., 2015). These remains represented the first case of dwarfism in hadrosaurids registered in the Iberian Peninsula, this being the smallest hadrosaurid known in Europe to date (Company et al., 2015). In addition, the large amount of recovered vertebrae with unfused neural arches also

indicates the presence of a great number of immature individuals in the area.

The presence of hadrosauroid ichnites is very widespread throughout the sector, their preservation as natural casts (convex hyporeliefs) being common at the base of most sandstone channel beds (Fig. 12). All these ichnites have been attributed to the ichnogenus *Hadrosauropodus* (Vila et al., 2013).

In addition, some eggshell fragments have also been recovered. Due to their external sagenotuberculate ornamental pattern, these eggshells have been tentatively assigned to *Spheroolithus europaeus* Sellés, Vila and Galobart, 2014a. However, to confirm this assignment further exhaustive microscopic study will be necessary. *Spheroolithus europaeus* was first defined near the village of Pont d'Orrit (Lleida, Spain) within the “grey unit” of the Tremp Formation (chron C30n, late Maastrichtian), representing the youngest oological record of hadrosauroids in Eurasia (Sellés et al., 2014a). The recovered eggshells from Serraduy have been identified up



**Fig. 11.** Dinosaur remains from Serraduy. A. coracoid of Hadrosauridae indet. (MPZ 2017/800 from LAR2 site) in medial and lateral views; B. phalanx of Hadrosauridae indet. (MPZ 2017/801 from LAR3 site) in dorsal, lateral and ventral views; C. tibia (distal fragment) of Hadrosauridae indet. (MPZ 2017/802 from LAR3 site) in anterior, posterior and distal views; D. femur (proximal fragment) of Hadrosauridae indet. (MPZ 2017/803 from LAR3 site) in anterior, lateral, posterior, medial and proximal views; E. femur (proximal fragment) of Titanosauria indet. (MPZ 99/143 from femur site) in posterior view; F. teeth of Theropoda indet. (MPZ 2017/804 from 172-i/04/e site) in lingual and labial view (white boxes show the detailed denticles). Scale bar without number = 3 cm.

until the lower-mid part of the “lower red unit” of the Tremp Formation (172-i/04/f paleontological site). If their assignment to *Spheroolithus europaeus* is confirmed, these eggshells would therefore be even more modern than those recovered at the Pont d’Orrit locality.

#### 7.1.2. Theropods

The presence of theropods within the Serraduy area is not very abundant, representing between 1% and 4% of the identified dinosaur remains. These theropod bones have been found from the “grey unit” to the middle part of the “lower red unit” of the Tremp Formation, thus constituting the youngest reliable record of non-avian theropods in the Iberian Peninsula and one of the youngest records in Europe.

The most important record corresponds to two isolated teeth that belong to two different taxa, a medium–large form and a

small-sized theropod. The first specimen (MPZ 2017/804; Fig. 11F) corresponds to a medium–large tooth with serrated carinae, which was recovered at the top of the “grey unit” of the Tremp Formation, very close to the 172-i/04/e paleontological site. This tooth is very similar to Morphotype 1 described by Torices et al. (2015) in the Spanish sites of Blasi (Huesca, upper Maastrichtian), Montrebei (Lleida, upper Campanian–lower Maastrichtian) and Laño (Burgos, upper Campanian–lower Maastrichtian). Due to its limited diagnostic value, this morphotype has been assigned to Theropoda indet. (López-Martínez et al., 2001; Torices et al., 2004, 2015; Pereda-Suberbiola et al., 2015). The second specimen corresponds to a small tooth with smooth carinae, which was recovered at the Larra 4 paleontological site within the “lower red unit” of the Tremp Formation. This tooth is very similar to the teeth assigned to Coelurosauria indet. from Blasi (Huesca, upper Maastrichtian), Montrebei (Lleida, upper Campanian–lower Maastrichtian), Laño



Fig. 12. Dinosaur ichnites of *Hadrosauropodus* indet. from Serraduy (Pedregal site).

(Burgos, upper Campanian–lower Maastrichtian) and Vicari 4 (Lleida, upper Campanian) (López-Martínez et al., 2001; Torices et al., 2004, 2015; Pereda-Suberbiola et al., 2015).

The other remains, also recovered in the “grey unit” and the “lower red unit” of the Tremp Formation, correspond to a possible cervical vertebra of an avian theropod (Cruzado-Caballero et al., 2012) and fragmentary long bones and a vertebral fragment that may correspond to undetermined theropods. Nevertheless, for the proper taxonomic assignation of these remains, further detailed studies will be necessary.

#### 7.1.3. Sauropods

Among the dinosaur remains, the presence of sauropods is the scarcest, amounting to around 1% of the identified remains. The most important item is a proximal left femur fragment (MPZ 99/143; Fig. 11E) assigned to Titanosauria indet. (Canudo, 2001; Vila et al., 2012). This femur was recovered in the “grey unit” of the Tremp Formation, representing one of the youngest sauropods yet documented in Eurasia (Canudo, 2001; Vila et al., 2012; Sellés et al., 2016).

Other possible sauropod remains consist of a caudal vertebra from the Barranco de Serraduy 4 site (Cruzado-Caballero et al., 2012) and a proximal fragment from a big autopodial bone from the Camino de Fornons 1 site. However, due to the fragmentary nature of these bones, their assignment to Sauropoda still remains doubtful. For the proper assignation of these specimens, further studies as well as the recovery of new remains will be necessary. Both these remains appeared in the middle part of the “lower red unit”, so if their assignment to Sauropoda is confirmed, they would be more modern than the femur, extending the presence of sauropods to chron C29r, as already seen in other sectors of the Tremp Basin (Sellés et al., 2016).

#### 7.2. Testudines

Another common clade, comprising about 5% of the remains found in Serraduy, is Testudines. The presence of testudines has been recognized from the top of the Arén Formation to the last deposits with vertebrates of the “lower red unit” of the Tremp Formation. This clade is represented entirely by isolated and disarticulated plates, in most cases preventing a more accurate identification or classification in the preliminary study, and rendering further systematic studies necessary. Nevertheless, when the plates are well preserved, it is possible to observe their smooth and

brilliant ornamentation crossed by very fine dichotomic sulci, suggesting highly vascularized shell bones. This characteristic ornamentation pattern is widely used to recognize bothremydids (e.g., de Lapparent de Broin and Murelaga, 1996; Murelaga and Canudo, 2005; Marmi et al., 2012), so most of these plates are assigned to Bothremydidae indet.

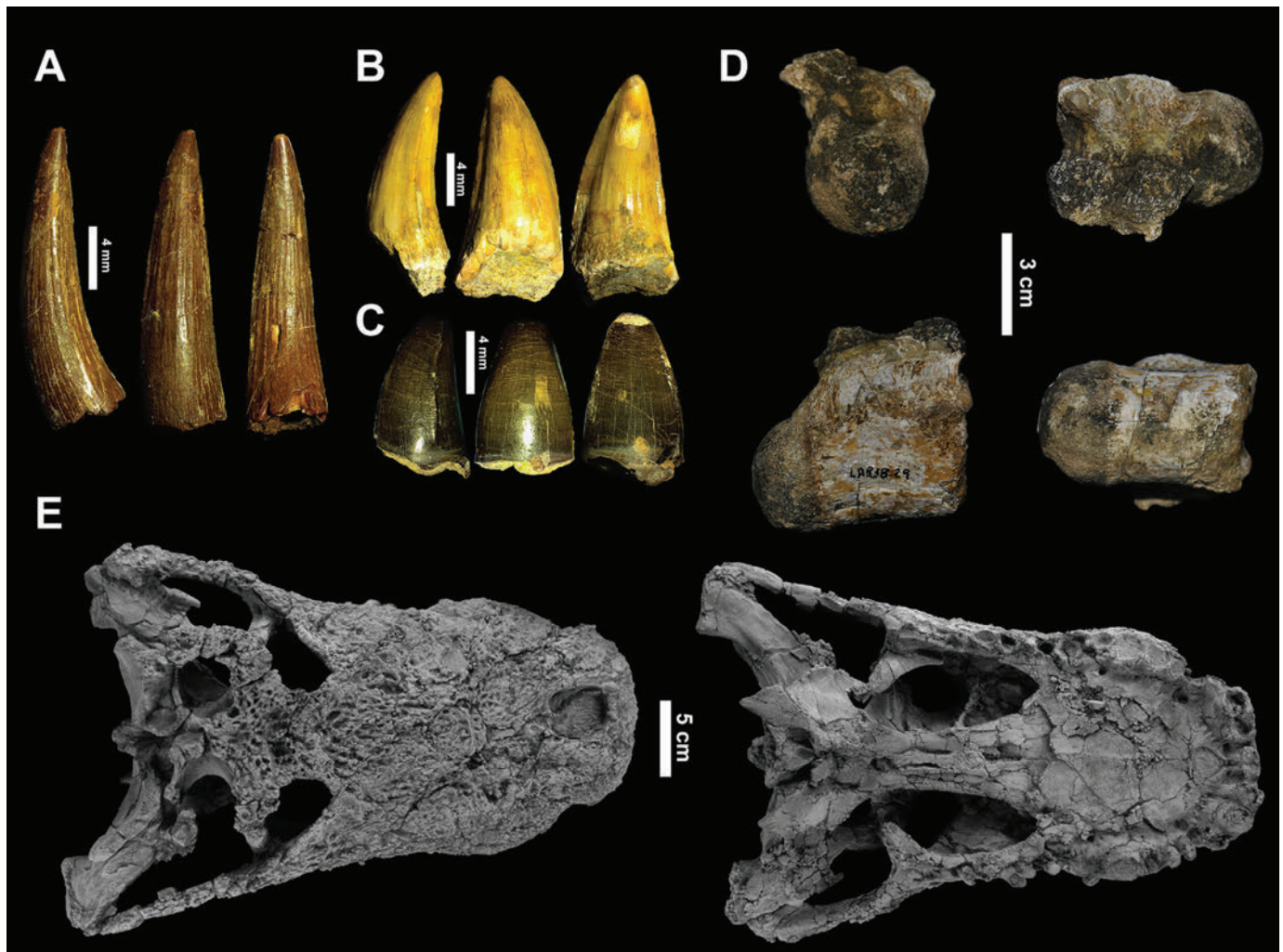
In addition, better-preserved plates allowed more accurate anatomical identification, and a left xiphiplastron and a right mesoplastron belonging to Bothremydidae from the Rim 2 site at the top of the Arén Formation have been recognized (Murelaga and Canudo, 2005).

#### 7.3. Crocodylomorphs

Representing about 4% of the recovered bone remains, crocodylomorphs are one of the most representative taxa in Serraduy. This group of archosaurs is mainly represented by isolated teeth, although some ichnites, a eusuchian vertebra, osteoderm fragments and a complete skull have also been found (Fig. 13E). All the recovered remains have been assigned to Eusuchia. These have a highly extended stratigraphic distribution, remains being found from the top of the Arén Formation up until the last levels with vertebrates before the K/Pg boundary.

The most important taxon corresponds to the complete skull of the eusuchian crocodylomorph originally erected in Serraduy with the name of *Allodaposuchus subjuniiperus* (Puértolas-Pascual et al., 2014) (MPZ 2012/288; Fig. 13E). This taxon was later assigned to the new genus *Agaresuchus* and included within Allodaposuchidae (Narváez et al., 2016), a clade of endemic European eusuchian crocodylomorphs with a record until the K/Pg boundary. *Agaresuchus subjuniiperus* was recovered in one of the last Maastrichtian sandstone strata (Amor 3 site), so this taxon may represent the last and youngest record of Allodaposuchidae before the K/Pg extinction event (Puértolas-Pascual et al., 2014).

As regards isolated teeth, at least two different morphotypes have been distinguished. The first morphotype (Fig. 13A) corresponds to a slender conical tooth ornamented with well-marked longitudinal ridges, which was found at the top of the Arén Formation (Barranco de Extremadura site). These teeth have been assigned to cf. *Thoracosaurus* (Puértolas-Pascual et al., 2016). This marine genus belonging to Gavialoidea is typical of the Upper Cretaceous–lower Paleocene of Europe and North America, which is consistent with its presence within the shallow marine facies of the Arén Formation. Teeth of the second morphotype (Fig. 13B, C)



**Fig. 13.** Crocodylomorph (Eusuchia) remains from Serraduy. A. teeth of cf. *Thoracosaurus* (MPZ 2017/806 from EXT site); B. teeth of cf. *Allodaposuchidae* (MPZ 2017/807 from DL3 site); C. teeth of cf. *Allodaposuchidae* (MPZ 2017/808 from PED site); D. dorsal vertebra of Eusuchia indet. (MPZ 2017/805 from LAR3B site); E. skull holotype of *Agaresuchus subjuniperus* (MPZ 2012/288) (from AM3 site).

have been recovered from the “grey unit” up until the last levels with vertebrates within the “lower red unit” of the Tremp Formation. This morphotype corresponds to generalist conical teeth with an ornamentation that varies from smooth to gently longitudinally-ridged enamel. This generalist morphology is widely distributed within Crocodylomorpha and has little taxonomic value (e.g., Prasad and Broin, 2002; Turner, 2006; Andrade and Bertini, 2008; Buscalioni et al., 2008). However, as this dental morphology is also typical of Allodaposuchidae, the most common clade in Europe during the Campanian–Maastrichtian, this morphotype has been tentatively assigned to cf. *Allodaposuchidae*. Additionally, several isolated teeth similar to those present in *A. subjuniperus* were recovered in the same site where the holotype was recovered, so these teeth have been assigned to cf. *Agaresuchus subjuniperus*.

Other bone remains correspond to osteoderm fragments and a procoelous dorsal vertebra (Fig. 13D) that have been assigned to Eusuchia indet. Further evidence of Crocodylomorpha is the presence of about five tracks (MPZ 2012/832) composed of scratch marks and one pedal impression located on a fluvial channel deposit in the uppermost part of the “lower red unit” of the Tremp Formation (Serraduy Norte site, chron C29r). The scratch marks resemble *Characichnos* whereas the pes track has been assigned to cf. *Crocodylopodus* (Vila et al., 2015).

#### 7.4. Amphibians

Due to their small size, amphibian remains have only been recovered by washing and sieving techniques. In the area of Serraduy, one of the paleontological sites with the greatest potential for the study of macrovertebrates and microvertebrates is Larra 4, located within the “lower red unit” of the Tremp Formation. This site is located in a dark grey lutite layer with a high organic content, where vegetal remains (wood and amber fragments), macrovertebrates (dinosaurs, crocodylomorphs and testudines) and microvertebrates are highly abundant. Most of the microvertebrate remains are very fragmentary and need a more thorough systematic study for their proper identification.

Nevertheless, a very preliminary study of the micropaleontological content allowed us to identify several remains that may correspond with amphibians. The most outstanding remains are several distal parts of humeri. In spite of the low taxonomic value of the humerus (Evans and Milner, 1993), the large and spherical humeral ball shifted laterally and a rather long ulnar epicondyle allow us tentatively to assign these specimens to Discoglossidae indet., being very similar to other humeri assigned to this clade in other sites within the Tremp Basin (Blain et al., 2010; Blanco et al., 2016).

## 8. Discussion

Considering component A as primary (see “Magnetostratigraphy” section), the local magnetic stratigraphy of the Serraduy section can be correlated with the geomagnetic polarity time scale (GPTS) (Gradstein et al., 2012). According to our results, the “grey unit” and the “lower red unit” of the Tremp Formation can be assigned to a reverse polarity chron (Fig. 5).

The presence of the planktonic foraminifer *P. hariaensis* in sample SR35 indicates that this level has a maximum age of 67.3 Ma (maximum age range of the species), or younger if it is reworked. The age range for this species is between 67.3 and 66.0 Ma, its lowermost and uppermost occurrences being coincident respectively with the upper part of C30n and the K/Pg boundary in the middle part of C29r. According to López-Martínez et al. (2006) and Díez-Canseco et al. (2014), the “Vallcebre limestones unit” and lateral equivalents are late Danian in age. Because this biostratigraphic information indicates that the K/Pg boundary is located between the “lower red unit” and the “Vallcebre limestones unit”, all the reverse polarity section between levels SR35 and SR90 can thus only correspond with chron C29r (Fig. 5). As a result, the K/Pg boundary can be located within the last 25 m of the “lower red unit”, between the last horizon with dinosaur remains and the “Vallcebre limestone unit” (Fig. 5). Correlating the profile of Barranco Serraduy with Larra, located further west, the K/Pg boundary can be located with more precision within the last 5 m of the “lower red unit” (Figs. 3, 5).

Therefore, the upper section of the “lower red unit” is well defined as reverse polarity, pointing to the C29r (Fig. 5). However, some inconsistencies can be observed in the middle part of this formation. SR37, above the level marked by *P. hariaensis*, has

reversed polarity (indicating C29r), whereas level SR53 shows normal polarity. Therefore, one part of this paleomagnetic information must be wrong. As regards its paleomagnetic properties, level SR35 has similar behavior to samples from the uppermost levels, with a non-zero ending cluster up to 500 °C with reversed polarity. Otherwise, component RA of level SR53 (Fig. 7D) has been defined by its unblocking temperature range; however, it is possible that this component corresponds with the CRM defined as RB. The lithology of both samples can also be analyzed: the paleomagnetic component defined in SR35 is more reliable than that defined in SR53 because the former is sampled in red mudstones, similar to the upper section where coherent paleomagnetic components appear, whereas SR53 is in a level of shale located between sandstones. The greater porosity of sandstones could have favored chemical processes in level SR53. In the light of these considerations, we consider that the section between levels SR37 and SR90 belongs to subchron C29r.

The lower section of the Tremp Formation also shows reversed polarities (see “Magnetostratigraphy” section), so at the beginning it is possible to ascribe this to subchron C29r (Fig. 14). However, Fondevilla et al. (2016a) provide evidence of the presence of a major hiatus affecting chrons C31n, C30r and C30n in the Isona section located in the eastern sector of the Tremp syncline (Fig. 14), probably related to an abrupt migration of the basin depocenter. This would imply the presence of consecutive deposits associated with chrons C31r and C29r, with a hiatus lacking most of the upper Maastrichtian. Nevertheless, according to the magnetostratigraphic works of Pereda-Suberbiola et al. (2009) on Arén, and Canudo et al. (2016) on Campo, this major hiatus seems not to have affected the most western sectors of the Tremp Basin (Fig. 14). Therefore, the sections of Campo and Arén acquire greater relevance because the

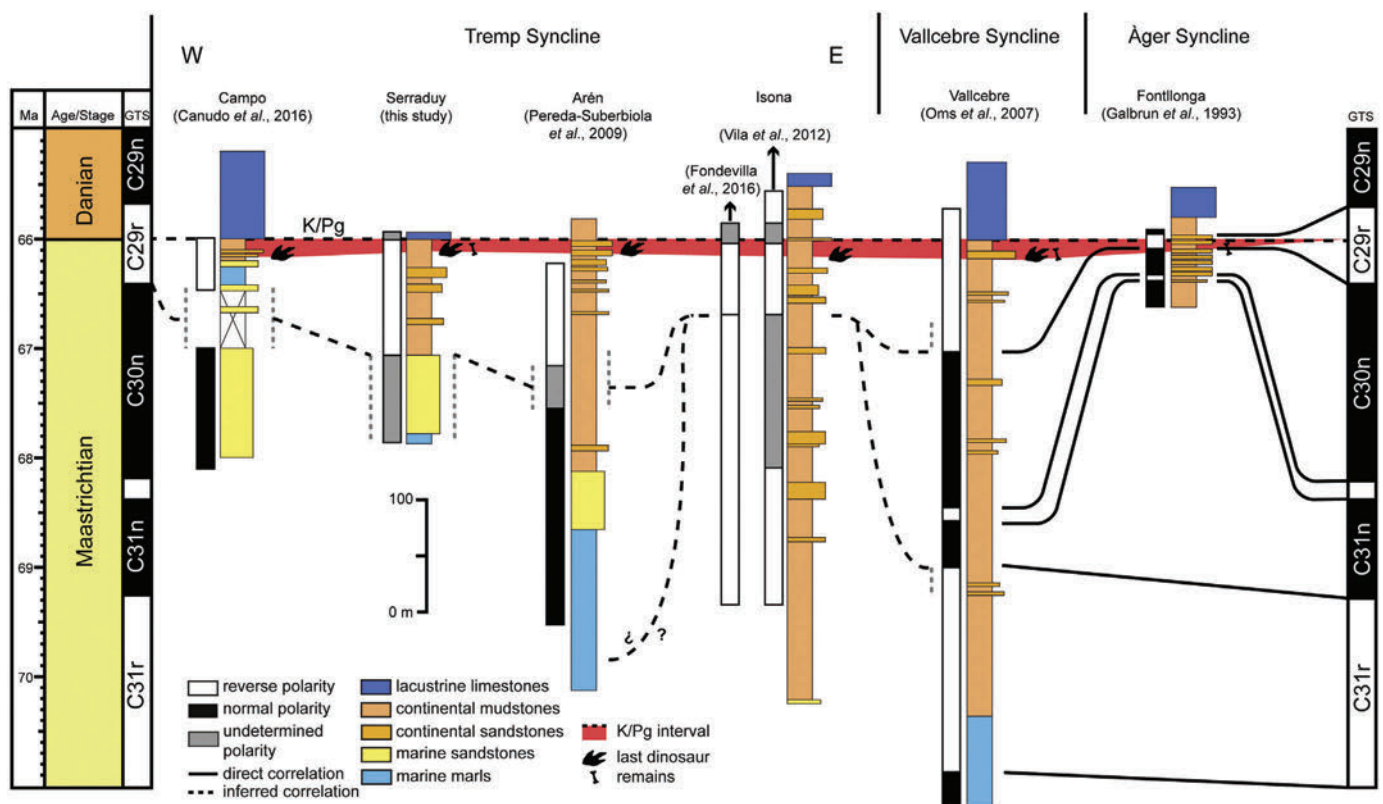


Fig. 14. Chronostratigraphic framework with indication of lithostratigraphy, paleomagnetic data, correlation and the K/Pg transition in the main Maastrichtian South Pyrenean continental sections with magnetostratigraphic data.

“lower red unit” exposed there is the only continental record of chron C30n in the whole Tremp syncline (Fondevilla et al., 2016a).

In summary, the magnetostratigraphic data presented in this work show that both the marls and red beds of the Tremp Formation in the Serraduy area are of reverse polarity. Biostratigraphic data ensure that the upper part of this formation (the last 60 m of the “lower red unit”) belong to chron C29r. However, although this cannot be fully confirmed for the lower part of the Tremp Formation (the “grey unit” and beginning of the “lower red unit”), these units probably also belong to the same chron C29r, unless there exists a hiatus such as that observed by Fondevilla et al. (2016a) in the Isona section. It should be pointed out that this hiatus has not been observed in Campo and Arén (Pereda-Suberbiola et al., 2009; Canudo et al., 2016), the sections closest to the Serraduy area.

## 9. Conclusions

In this work, a chronostratigraphic framework for the vertebrate sites of the Arén and Tremp Formations within the Serraduy sector of the Tremp Basin is proposed for the first time. The joint study of stratigraphy, field correlations, magnetostratigraphy and biostratigraphy has allowed most of the vertebrate sites in this area to be dated to within chron C29r, making this one of the areas with dinosaur sites closest to the K/Pg boundary anywhere in Europe. In addition, a complete faunal list of the taxa recovered in the Serraduy area is presented. This shows a great diversity of theropods, sauropods and hadrosaur dinosaurs, eusuchian crocodylomorphs, testudines, amphibians and probably pterosaurs.

The presence of dinosaurs (ichnites and bones) in the highest levels of the series has pinpointed the range of the K/Pg boundary to the last 5 m of the “lower red unit” within the Tremp Formation, below the “Vallcebre limestones”. This suggests a high abundance of hadrosaurid dinosaurs, eusuchian crocodylomorphs, amphibians and testudines just before the great extinction event of the Late Cretaceous.

Although everything points to a late Maastrichtian age for the studied deposits, the lower half of the section unfortunately shows unclear paleomagnetic signals and inconclusive biostratigraphic content, so it has been assigned an undetermined polarity. The magnetostratigraphic results also seem to indicate the presence of a reverse polarity chron in the lower half of the section, yet we do not have the biostratigraphic data to be able to assign it to a specific chron (C31r, C30r or C29r). For this reason, the continuity of the lower part of the series or the presence of possible hiatuses cannot be determined. Further studies in the adjacent outcrops located between Serraduy and Campo (e.g. Rin or Larra sections) and between Serraduy and Arén (e.g. Isclès section) could be crucial to achieve more accurate knowledge of the chronostratigraphic framework of the northwestern-most branch of the Tremp Basin.

In conclusion, these results show the great paleontological potential of the Serraduy area, which is one of the few and most important places in the world for studying, within continental deposits, the great extinction event which affected planet Earth at the end of the Cretaceous.

## Acknowledgements

This work was supported by the Spanish Ministry of Economy and Competitiveness (grant numbers CGL2014-53548-P, CGL2015-64422-P and CGL2017-85038-P), cofinanced by the European Regional Development Fund; and by the Department of Education and Science of the Aragonese Government (grant numbers DGA groups H54 and E05), cofinanced by the European Social Fund (ESF). The paleomagnetic study was possible thanks to the complementary grants (beneficiaries of FPU, grant number CGL2010-

16447/BTE: Brief Stays and Temporary Transfers, year 2015) supported by the Spanish Ministry of Culture, Education and Sports; and the Laboratory of paleomagnetism of the University of Burgos (Spain). Eduardo Puértolas Pascual is the recipient of a postdoctoral grant (SFRH/BPD/116759/2016) funded by the Fundação para a Ciência e Tecnologia (FCT-MCTES). Special thanks to R. Silva, V. Burriel, M. Gallego, A. Alonso, C. Nuñez, J. Galán, J. Parrilla, J.C. García and X. Pereda for their help in the field work; and J. Larrañaga and G. Martín for the discovery of the Larra paleontological sites. Many thanks to P. Cruzado for her helpful comments. Rupert Glasgow edited the text in English.

## References

- Álvarez-Sierra, M.A., Arribas, M.E., Ardévol, L., Civis, J., Daams, R., Krauss, S., López-Martínez, N., De La Peña, A., Soler, R., Vianey-Liaud, M., 1994. El límite Cretácico-Terciario en la sección de Fontllonga (cuenca de Ager, provincia de Lérida). In: *Jaca (Spain), II Congreso Del Grupo Español Del Terciario, Comunicaciones*, pp. 23–26.
- Andrade, M.B., Bertini, R.J., 2008. Morphology of the dental carinae in *Mariliasuchus amarali* (Crocodylomorpha, Notosuchia) and the pattern of tooth serration among basal Mesoeucrocodylia. *Arquivos do Museu Nacional (rio de Janeiro)* 63–82.
- Antonescu, E., Lupu, D., Lupu, M., 1983. Correlation palinologique du Crétacé terminal du sud-est des Monts Metaliferi et des Depressions de Hațeg et de Rusca Montană. *Anuarul Institutului de Geologie și Geofizică* 59, 71–77.
- Archibald, J.D., Clemens, W.A., Padian, K., Rowe, T., Macleod, N., Barrett, P.M., Gale, A., Holroyd, P., Sues, H.-D., Arens, N.C., Horner, J.R., Wilson, G.P., Goodwin, M.B., Brochu, C.A., Lofgren, D.L., Hurlbert, S.H., Hartman, J.H., Eberth, D.A., Wignall, P.B., Currie, P.J., Weil, A., Prasad, G.V.R., Dingus, L., Courtillot, V., Milner, A., Milner, A., Bajpai, S., Ward, D.J., Sahni, A., 2010. Cretaceous Extinctions: Multiple Causes. *Science* 328, 973. <https://doi.org/10.1126/science.328.5981.973-a>.
- Ardévol, L., Klimowitz, J., Malagón, J., Nagtegaal, P.J.C., 2000. Depositional Sequence Response to Foreland Deformation in the Upper Cretaceous of the Southern Pyrenees, Spain. *AAPG Bulletin* 84, 566. <https://doi.org/10.1306/C9EBCE55-1735-11D7-8645000102C1865D>.
- Arribas, M.E., Ardévol, L., López-Martínez, N., 1996. Lacustrine peritidal carbonates in the Upper Cretaceous Tremp Formation (Ager Syncline, South Pyrenean Foreland Basin, Spain), 17th Regional African European Meeting of Sedimentology. Abstracts 15.
- Arz, J.A., Arenillas, I., Nájera, C., 2010. Morphostatistical analysis of Maastrichtian populations of *Guebelitria* from El Kef, Tunisia. *Journal of Foraminiferal Research* 40, 148–164.
- Banner, F.T., Blow, W.H., 1960. Some primary types of species belonging to the superfamily Globigerinaceae. Contributions from the Cushman Foundation for Foraminiferal Research 11, 1–41.
- Barrett, P.M., McGowan, A.J., Page, V., 2009. Dinosaur diversity and the rock record. *Proceedings Biological Sciences* 276, 2667. <https://doi.org/10.1098/rspb.2009.0352>.
- Bessière, G., Tambareau, Y., Villatte, J., 1980. Le passage Crétacé-Tertiaire dans les Hautes-Corbieres. *Bulletin de la Société d'Histoire naturelle de Toulouse* 116, 283–303.
- Bessière, G., Bilotte, M., Crochet, B., Peybernès, B., Tambareau, Y., Villatte, J., 1989. Livret explicatif de la carte géologique de la France (Feuille 1077: Quillan). Editions du Bureau des Recherches Géologiques et Minières, Orléans, p. 98.
- Bilotte, M., 1985. Le Crétacé supérieur des plate-formes est-pyrénéennes. *Strata* 5, 1–438.
- Blain, H.A., Canudo, J.I., Cuenca-Bescós, G., López-Martínez, N., 2010. Amphibians and squamate reptiles from the latest Maastrichtian (Upper Cretaceous) of Blasi 2 (Huesca, Spain). *Cretaceous Research* 31, 433–446. <https://doi.org/10.1016/j.cretres.2010.06.001>.
- Blanco, A., Szabó, M., Blanco-Lapaz, À., Marmi, J., 2017. Late Cretaceous (Maastrichtian) Chondrichthyes and Osteichthyes from northeastern Iberia. *Palaeogeography, Palaeoclimatology, Palaeoecology* 465, 278–294. <https://doi.org/10.1016/j.palaeo.2016.10.039>.
- Blanco, A., Puértolas-Pascual, E., Marmi, J., Vila, B., Sellés, A.G., 2014. *Allodaposuchus palustris* sp. nov. from the Upper Cretaceous of Fumanya (South-Eastern Pyrenees, Iberian Peninsula): Systematics, Palaeoecology and Palaeobiogeography of the Enigmatic Allodaposuchian Crocodylians. *PLoS One* 9, 1–34. <https://doi.org/10.1371/journal.pone.0115837>.
- Blanco, A., Fortuny, J., Vicente, A., Luján, A.H., García-Marçà, J.A., Sellés, A.G., 2015a. A new species of *Allodaposuchus* (Eusuchia, Crocodylia) from the Maastrichtian (Late Cretaceous) of Spain: phylogenetic and paleobiological implications. *PeerJ* 3, e1171. <https://doi.org/10.7717/peerj.1171>.
- Blanco, A., Prieto-Márquez, A., Esteban-Trivigno, S.D., 2015b. Diversity of hadrosauroid dinosaurs from the Late Cretaceous Ibero-Armorican Island (European Archipelago) assessed from dentary morphology. *Cretaceous Research* 56, 447–457. <https://doi.org/10.1016/j.cretres.2015.04.001>.

- Blanco, A., Bolet, A., Blain, H.A., Fondevilla, V., Marmi, J., 2016. Late Cretaceous (Maastrichtian) amphibians and squamates from northeastern Iberia. *Cretaceous Research* 57, 624–638. <https://doi.org/10.1016/j.cretres.2015.07.005>.
- Bojar, A.-V., Halas, S., Bojar, H.-P., Grigorescu, D., Vasile, S., 2011. Upper Cretaceous volcanoclastic deposits from the Hațeg basin, south Carpathians (Romania): K-Ar ages and intrabasinal correlation. *Geochronometria* 38, 182. <https://doi.org/10.2478/s13386-011-0023-8>.
- Bolli, H.M., 1951. The genus *Globotruncana* in Trinidad. *Journal of Paleontology* 25 (2), 187–199.
- Brusatte, S.L., Butler, R.J., Barrett, P.M., Carrano, M.T., Evans, D.C., Lloyd, G.T., Mannion, P.D., Norell, M.A., Peppe, D.J., Upchurch, P., Williamson, T.E., 2015. The extinction of the dinosaurs. *Biological Reviews* 90, 628–642. <https://doi.org/10.1111/brv.12128>.
- Buffetaut, E., Loeuff, J.L., 1991. Late Cretaceous dinosaur faunas of Europe: Some correlation problems. *Cretaceous Research* 12, 159–176. [https://doi.org/10.1016/S0195-6671\(05\)80022-9](https://doi.org/10.1016/S0195-6671(05)80022-9).
- Buscalioni, A.D., Fregenal, M.A., Bravo, A., Poyato-Ariza, F.J., Sanchíz, B., Báez, A.M., Cambra Moo, O., Martín Closas, C., Evans, S.E., Marugán Lobón, J., 2008. The vertebrate assemblage of Buenache de la Sierra (Upper Barremian of Serranía de Cuenca, Spain) with insights into its taphonomy and palaeoecology. *Cretaceous Research* 29, 687–710. <https://doi.org/10.1016/j.cretres.2008.02.004>.
- Butler, R.J., Benson, R.B.J., Carrano, M.T., Mannion, P.D., Upchurch, P., 2011. Sea level, dinosaur diversity and sampling biases: investigating the 'common cause' hypothesis in the terrestrial realm. *Proceedings of the Royal Society of London B: Biological Sciences* 278, 1165–1170. <https://doi.org/10.1098/rspb.2010.1754>.
- Canudo, J.I., 2001. Descripción de un fragmento proximal de fémur de Titanosauridae (Dinosauria, Sauropoda) del Maastrichtense superior de Serraduy (Huesca). *Actas de las XVII Jornadas de la Sociedad Española de Paleontología. Los fósiles y la paleogeografía* (Albarracín, 2001). *Albarracín* 1, 255–262.
- Canudo, J.I., Oms, O., Vila, B., Galobart, A., Fondevilla, V., Puértolas-Pascual, E., Sellés, A.G., Cruzado-Caballero, P., Dinarès-Turell, J., Vicens, E., Castanera, D., Company, J., Burrell, L., Estrada, R., Marmi, J., Blanco, A., 2016. The upper Maastrichtian dinosaur fossil record from the southern Pyrenees and its contribution to the topic of the Cretaceous–Palaeogene mass extinction event. *Cretaceous Research* 57, 540–551. <https://doi.org/10.1016/j.cretres.2015.06.013>.
- Carsey, D.O., 1926. Foraminifera of the Cretaceous of central Texas. *University of Texas Bulletin* 2612, 1–56.
- Chadima, M., Hrouda, F., 2006. Remasoft 3.0 a user-friendly paleomagnetic data browser and analyzer. *Travaux Géophysiques* 27, 20–21.
- Codrea, V., Vremir, M., Jipa, C., Godefroit, P., Csiki, Z., Smith, T., Fărcaș, C., 2010. More than just Nopcsa's Transylvanian dinosaurs: A look outside the Hațeg Basin. *Palaeogeography, Palaeoclimatology, Palaeoecology* 293, 391–405. <https://doi.org/10.1016/j.palaeo.2009.10.027>.
- Codrea, V., Godefroit, P., Smith, T., 2012. First discovery of Maastrichtian (latest Cretaceous) terrestrial vertebrates in Rusca Montană Basin (Romania). *Bernisart Dinosaur and Early Cretaceous Terrestrial Ecosystems*. Indiana University Press, Bloomington, pp. 570–581.
- Cojan, I., Moreau, M.-G., 2006. Correlation of Terrestrial Climatic Fluctuations with Global Signals During the Upper Cretaceous–Danian in a Compressive Setting (Provence, France). *Journal of Sedimentary Research* 76, 589. <https://doi.org/10.2110/jsr.2006.045>.
- Cojan, I., Renard, M., Emmanuel, L., 2003. Palaeoenvironmental reconstruction of dinosaur nesting sites based on a geochemical approach to eggshells and associated palaeosols (Maastrichtian, Provence Basin, France). *Palaeogeography, Palaeoclimatology, Palaeoecology* 191, 111–138. [https://doi.org/10.1016/S0031-0182\(02\)00655-7](https://doi.org/10.1016/S0031-0182(02)00655-7).
- Company, J., Szentesi, Z., 2012. Amphibians from the Late Cretaceous Sierra Perenchiza Formation of the Chera Basin, Valencia Province, Spain. *Cretaceous Research* 37, 240–245. <https://doi.org/10.1016/j.cretres.2012.04.003>.
- Company, J., Cruzado-Caballero, P., Canudo, J.I., 2015. Presence of diminutive hadrosaurids (Dinosauria: Ornithomimidae) from the Maastrichtian of the south-central Pyrenees (Spain). *Journal of Iberian Geology* 41.
- Cruzado-Caballero, P., Pereda-Suberbiola, X., Ruiz-Omeñaca, J.I., 2010. *Blasisaurus canudo* gen. et sp. nov., a new lambeosaurine dinosaur (Hadrosauridae) from the Latest Cretaceous of Arén (Huesca, Spain). *Canadian Journal of Earth Sciences* 47, 1507–1517. <https://doi.org/10.1139/E10-081>.
- Cruzado-Caballero, P., Puértolas-Pascual, E., Canudo, J.I., Castanera, D., Gasca, J.M., Moreno-Azanza, M., 2012. New hadrosaur remains from the Late Maastrichtian of Huesca (NE Spain). In: *Abstracts 10th Annual Meeting of the European Association of Vertebrate Palaeontologists*, pp. 45–48.
- Cruzado-Caballero, P., Canudo, J.I., Moreno-Azanza, M., Ruiz-Omeñaca, J.I., 2013. New material and phylogenetic position of *Arenysaurus ardevoli*, a lambeosaurine dinosaur from the late Maastrichtian of Arén (northern Spain). *Journal of Vertebrate Paleontology* 33, 1367–1384. <https://doi.org/10.1080/02724634.2013.772061>.
- Cruzado-Caballero, P., Ruiz-Omeñaca, J.I., Gaete, R., Riera, V., Oms, O., Canudo, J.I., 2014. A new hadrosaurid dentary from the latest Maastrichtian of the Pyrenees (north Spain) and the high diversity of the duck-billed dinosaurs of the Ibero-Armorican Realm at the very end of the Cretaceous. *Historical Biology* 26, 619–630. <https://doi.org/10.1080/08912963.2013.822867>.
- Cruzado-Caballero, P., Fortuny, J., Llacer, S., Canudo, J., 2015. Paleoneuroanatomy of the European lambeosaurine dinosaur *Arenysaurus ardevoli*. *PeerJ* 3, e802. <https://doi.org/10.7717/peerj.802>.
- Csiki-Sava, Z., Buffetaut, E., Ősi, A., Pereda-Suberbiola, X., Brusatte, S.L., 2015. Island life in the Cretaceous-faunal composition, biogeography, evolution, and extinction of land-living vertebrates on the Late Cretaceous European archipelago. *ZooKeys* 1. <https://doi.org/10.3897/zookeys.469.8439>.
- Cuevas, J.L., 1992. Estratigrafía del "garumniense" de la Conca de Tremp: Prepirineo de Lérida. *Acta Geológica Hispánica* 27, 95–108.
- Cushman, J.A., 1926. The foraminifera of the Velasco shale of the Tampico embayment. *Bulletin of the American Association of Petroleum Geologists* 10 (6), 581–612.
- Cushman, J.A., 1928. Foraminifères du Stampien du Bassin de Paris. *Bulletin de la Société des Sciences de Seine-et-Oise* 9, 47–63.
- Cushman, J.A., 1933. Some new foraminiferal genera. *Contributions from the Cushman Laboratory for Foraminiferal Research* 9 (2), 32–38.
- Cushman, J.A., 1938. Cretaceous species of *Gümbelina* and related genera. *Contributions from the Cushman Laboratory for Foraminiferal Research* 14 (1), 2–28.
- Dalbiez, F., 1955. The genus *Globotruncana* in Tunisia. *Micropaleontology* 1 (2), 161–171.
- de Lapparent de Broin, F., Murelaga, X., 1996. Une nouvelle faune de chéloniens dans le Crétacé supérieur européen. *Comptes Rendus de l'Académie des Sciences. Série 2. Sciences de la Terre et des Planètes* 323, 729–735.
- Díaz-Molina, M., 1987. Sedimentación sintectónica asociada a una subida relativa del nivel del mar durante el Cretácico superior (Fm. Tremp, provincia de Lérida). *Estudios Geológicos* 43, 69–93.
- Díaz-Molina, M., Kálin, O., Benito-Moreno, M.I., López-Martínez, N., Vicens, E., 2007. Depositional setting and early diagenesis of the dinosaur eggshell-bearing Aren Fm at Bastus, Late Campanian, south-central Pyrenees. *Sedimentary Geology* 199, 205–221.
- Díez-Canseco, D., Arz, J.A., Benito, M.I., Díaz-Molina, M., Arenillas, I., 2014. Tidal influence in redbeds: A palaeoenvironmental and biostratigraphic reconstruction of the Lower Tremp Formation (South-Central Pyrenees, Spain) around the Cretaceous/Paleogene boundary. *Sedimentary Geology* 312, 31–49. <https://doi.org/10.1016/j.sedgeo.2014.06.008>.
- Dinarès-Turell, J., Fondevilla, V., Oms, O., Le Loeuff, J., Vila, B., Estrada, R., Riera, V., 2014. Magnetostratigraphic dating of the Maastrichtian terrestrial successions from the Pyrenees: State of the art and new data from Aude (France). In: Marmi, J., Oms, O., Vila, B., Galobart, A., Estrada, R., Dinarès-Turell, J. (Eds.), *Paleontología i Evolució, mem. especial* 7, p. 68.
- Donze, P., Porthault, B., Thomel, G., Villoutreys, O. de, 1970. Le Sénonien inférieur de Puget-Théniers (Alpes-Maritimes) et sa microfaune. *Geobios* 3, 81–82.
- d'Orbigny, A., 1839. Foraminifères. In: *de la Sagra, R. (Ed.), Histoire physique et naturelle de l'île de Cuba*. A. Bertrand, Paris, France, p. 224.
- Ehrenberg, C.G., 1840. Über die Bildung der Kreidefelsen und des Kreidemergels durch unsichtbare Organismen. *Abhandlungen der Königlichen Akademie der Wissenschaften zu Berlin* 1838, 59–147.
- Eichenseer, H., 1987. Facies geology of late Maastrichtian to Early Eocene coastal and shallow marine sediments, tremp-graus basin, northeastern Spain. *Arb. Mus. Geol. Pal. Univ. Tübingen*, p. 237.
- Eichenseer, H., Luterbacher, H., 1992. The marine paleogene of the tremp region (NE Spain): depositional sequences, facies history, biostratigraphy and controlling factors. *Facies* 27, 119–151. <https://doi.org/10.1007/BF02536808>.
- El Naggar, Z.R., 1966. Stratigraphy and Planktonic Foraminifera of the Upper Cretaceous-Lower Tertiary: *Bulletin of the British Museum (Natural History). Geology, Supplement* 2, 291.
- Evans, S.E., Milner, A.R., 1993. Frogs and Salamanders from the Upper Jurassic Morrison Formation (Quarry Nine, Como Bluff) of North America. *Journal of Vertebrate Paleontology* 13, 24–30.
- Fastovsky, D.E., Sheehan, P.M., 2005. The extinction of the dinosaurs in North America. *Gsa Today* 15, 4–10.
- Feist, M., Colombo, F., 1983. La limite Cretace-Tertiaire dans le nord-est de l'Espagne, du point de vue des charophytes. *Géologie Méditerranéenne* 10, 303–326.
- Fisher, R., 1953. Dispersion on a sphere. *Proceedings of the Royal Society of London. Series A. Mathematical and Physical Sciences* 217 (1130), 295–305.
- Fondevilla, V., Dinarès-Turell, J., Oms, O., 2016a. The chronostratigraphic framework of the South-Pyrenean Maastrichtian succession reappraised: Implications for basin development and end-Cretaceous dinosaur faunal turnover. *Sedimentary Geology* 337, 55–68. <https://doi.org/10.1016/j.sedgeo.2016.03.006>.
- Fondevilla, V., Dinarès-Turell, J., Vila, B., Le Loeuff, J., Estrada, R., Oms, O., Galobart, A., 2016b. Magnetostratigraphy of the Maastrichtian continental record in the Upper Aude Valley (northern Pyrenees, France): Placing age constraints on the succession of dinosaur-bearing sites. *Cretaceous Research* 57, 457–472. <https://doi.org/10.1016/j.cretres.2015.08.009>.
- Fonnesu, F., 1984. Estratigrafia física y análisis de facies de la secuencia de Figols entre el río Noguera Pallaresa e Isclès (provs. de Lérida y Huesca). *Universitat Autònoma, Departament de Estratigrafia i Geologia Històrica*.
- Galbrun, B., Feist, M., Colombo, F., Rocchia, R., Tambareau, Y., 1993. Magnetostratigraphy and biostratigraphy of Cretaceous-Tertiary continental deposits, Ager Basin, Province of Lerida, Spain. *Palaeogeography, Palaeoclimatology, Palaeoecology* 102, 41–52. [https://doi.org/10.1016/S0031-0182\(93\)90004-3](https://doi.org/10.1016/S0031-0182(93)90004-3).
- García, G., Vianey-Liaud, M., 2001. Dinosaur eggshells as biochronological markers in Upper Cretaceous continental deposits. *Palaeogeography, Palaeoclimatology, Palaeoecology* 169, 153–164. [https://doi.org/10.1016/S0031-0182\(01\)00215-2](https://doi.org/10.1016/S0031-0182(01)00215-2).
- Garrido-Megías, A., Ríos, L., 1972. Síntesis geológica del Secundario y Terciario entre los ríos Cinca y Segre (Pirineo central de la vertiente surpirenaica, provincias de Huesca y Lérida). *Boletín Geológico y Minero de España* 83, 1–47.

- Gheerbrant, E., Codrea, V., Hosu, A., 1999. Découverte de vertébrés dans les Calcaires de Rona (Thanétien ou Sparnacien), Transylvanie, Roumanie: les plus anciens mammifères cénozoïques d'Europe Orientale. *Birkhäuser*.
- Gómez-Gras, D., Roigé, M., Fondevilla, V., Oms, O., Boya, S., Remacha, E., 2016. Provenance constraints on the Tresp Formation paleogeography (southern Pyrenees): Ebro Massif VS Pyrenees sources. *Cretaceous Research* 57, 414–427. <https://doi.org/10.1016/j.cretres.2015.09.010>.
- Gradstein, F.M., Ogg, J.G., Schmitz, M., Ogg, G., 2012. The geologic time scale 2012. Elsevier.
- Jackson, M., Swanson-Hysell, N.L., 2012. Rock magnetism of remagnetized carbonate rocks: another look. Geological Society, London, Special Publications 371, 229. <https://doi.org/10.1144/SP371.3>.
- Jiang, X., Liu, Y., Ji, S., Zhang, X., Xu, L., Jia, S., Lü, J., Yuan, C., Li, M., 2011. Dinosaur-bearing strata and K/T boundary in the Luanchuan-Tantou Basin of western Henan Province, China. *Science China Earth Sciences* 54, 1149. <https://doi.org/10.1007/s11430-011-4186-1>.
- Juárez, M.T., Osete, M.L., Meléndez, G., Langereis, C.G., Zijdeveld, J.D.A., 1994. Oxfordian magnetostratigraphy of the Aguilón and Tosos sections (Iberian Range, Spain) and evidence of a pre-Oligocene overprint. *Physics of the Earth and Planetary Interiors* 85, 195–211. [https://doi.org/10.1016/0031-9201\(94\)90017-5](https://doi.org/10.1016/0031-9201(94)90017-5).
- Laurent, Y., Bilote, M., Le Loeuff, J., 2002. Late Maastrichtian continental vertebrates from southwestern France: correlation with marine fauna. *Palaeogeography, Palaeoclimatology, Palaeoecology* 187, 121–135. [https://doi.org/10.1016/S0031-0182\(02\)00512-6](https://doi.org/10.1016/S0031-0182(02)00512-6).
- Leonhardt, R., 2006. Analyzing rock magnetic measurements: The Rock-MagAnalyzer 1.0 software. *Computers & Geosciences* 32, 1420–1431. <https://doi.org/10.1016/j.cageo.2006.01.006>.
- Leymerie, A., 1862. Aperçu géognostique des Petites Pyrénées et particulièrement de la montagne d'Ausseg. *Bulletin de la Société Géologique de France* 19, 1091–1096.
- Liebau, A., 1973. El Maastrichtense lagunar (Garumnense) de Isona. Libro-Guia. XIII Coloquio Europeo Micropaleontología, pp. 87–112.
- Llompart, C., 1979. Yacimiento de huellas de pisadas de reptil en el Cretácico prepirenaico. *Acta geológica hispánica* 14, 333–336.
- López-Martínez, N., Ardevol, L., Arribas, M.E., Civis, J., Gonzalez-Delgado, A., 1998. The geological record in non-marine environments around the K/T boundary (Tresp Formation, Spain). *Bulletin de la Société Géologique de France* 169, 11.
- López-Martínez, N., Fernández-Marrón, M.T., Valle, M.F., 1999. The succession of vertebrates and plants across the Cretaceous-Tertiary boundary in the Tresp Formation, Ager valley (south-central Pyrenees, Spain). *Geobios* 32, 617–627.
- López-Martínez, N., Canudo, J.I., Ardevol, L., Suberbiola, X.P., Orue-Etxebarria, X., Cuenca-Bescós, G., Ruiz-Omeñaca, J.I., Murelaga, X., Feist, M., 2001. New dinosaur sites correlated with Upper Maastrichtian pelagic deposits in the Spanish Pyrenees: implications for the dinosaur extinction pattern in Europe. *Cretaceous Research* 22, 41–61. <https://doi.org/10.1006/cres.2000.0236>.
- López-Martínez, N., Arribas, M.E., Robador, A., Vicens, E., Ardevol, L., 2006. Los carbonatos danianos (Unidad 3) de la FM Tresp (Pirineos Sur-Centrales): paleogeografía y relación con el límite Cretácico-Terciario. *Revista de la Sociedad Geológica de España* 19, 233–255.
- Mannion, P.D., Upchurch, P., Carrano, M.T., Barrett, P.M., 2011. Testing the effect of the rock record on diversity: a multidisciplinary approach to elucidating the generic richness of sauropodomorph dinosaurs through time. *Biological Reviews* 86, 157–181. <https://doi.org/10.1111/j.1469-185X.2010.00139.x>.
- Marmi, J., Luján, Á.H., Riera, V., Gaete, R., Oms, O., Galobart, À., 2012. The youngest species of *Polysternon*: A new bothremiid turtle from the uppermost Maastrichtian of the southern Pyrenees. *Cretaceous Research* 35, 133–142. <https://doi.org/10.1016/j.cretres.2011.12.004>.
- Marmi, J., Blanco, A., Fondevilla, V., Dalla Vecchia, F.M., Sellés, A.G., Vicente, A., Martín-Closas, C., Oms, O., Galobart, À., 2016. The Molí del Baró-1 site, a diverse fossil assemblage from the uppermost Maastrichtian of the southern Pyrenees (north-eastern Iberia). *Cretaceous Research* 57, 519–539. <https://doi.org/10.1016/j.cretres.2015.06.016>.
- Marty, D., 2001. Sedimentology, Paleogeology and Stratigraphy of the Palustrine Facies Rognacien at the K/T-boundary in Southern France. *Geologisch-Paläontologisches Institut*.
- Masriera, A., Ullastre, J., 1983. Essai de synthèse stratigraphique des couches continentales de la fin du Crétacé des Pyrénées catalanes (NE de l'Espagne). *Géologie Méditerranéenne* 20, 283–290.
- Médus, J., Feist, M., Rocchia, R., Batten, D.J., Boclet, D., Colombo, F., Tambareau, Y., Villatte, J., 1988. Prospects for recognition of the palynological Cretaceous Tertiary boundary and an iridium anomaly in nonmarine facies of the eastern Spanish Pyrenees: a preliminary report. *Newsletters on Stratigraphy* 18, 123–138. <https://doi.org/10.1127/nos/18/1988/123>.
- Mey, P.H.W., Nagtegaal, P.J.C., Roberti, K.J., Hartvelt, J.J.A., 1968. Lithostratigraphic subdivision of post-Hercynian deposits in the south-central Pyrenees, Spain. *Leidse Geologische Mededelingen* 41, 221–228.
- Moreno-Azanza, M., Bauluz, B., Canudo, J.I., Puértolas-Pascual, E., Sellés, A.G., 2014. A re-evaluation of aff. *Megaloolithidae* eggshell fragments from the uppermost Cretaceous of the Pyrenees and implications for crocodylomorph eggshell structure. *Historical Biology* 26, 195–205. <https://doi.org/10.1080/08912963.2013.786067>.
- Muñoz, J.A., 1992. Evolution of a continental collision belt: ECORS-Pyrenees crustal balanced cross-section. *Thrust tectonics*, pp. 235–246.
- Murelaga, X., Canudo, J.I., 2005. Descripción de los restos de quelonios del Maastrichtense superior de Aren y Serraduy (Huesca). *Geogaceta* 38, 51–54.
- Nagtegaal, P.J.C., Van Vliet, A., Brouwer, J., 1983. Syntectonic coastal offlap and concurrent turbidite deposition: The Upper Cretaceous Aren sandstone in the South-Central Pyrenees, Spain. *Sedimentary Geology* 34, 185–218. [https://doi.org/10.1016/0037-0738\(83\)90086-6](https://doi.org/10.1016/0037-0738(83)90086-6).
- Nakkady, S.E., 1950. A new foraminiferal fauna from the Esna Shales and Upper Cretaceous Chalk of Egypt. *Journal of Paleontology* 675–692.
- Narváez, I., Brochu, C.A., Escaso, F., Pérez-García, A., Ortega, F., 2016. New Spanish Late Cretaceous eusuchian reveals the synchronic and sympatric presence of two allodaposuchids. *Cretaceous Research* 65, 112–125. <https://doi.org/10.1016/j.cretres.2016.04.018>.
- Navarrete, R., Rodríguez-López, J.P., Liesa, C.L., Soria, A.R., Veloso, F., de, M.L., 2013. Changing physiography of rift basins as a control on the evolution of mixed siliciclastic-carbonate back-barrier systems (Barremian Iberian Basin, Spain). *Sedimentary Geology* 289, 40–61. <https://doi.org/10.1016/j.sedgeo.2013.02.003>.
- Nederbragt, A.J., 1991. Late Cretaceous Biostratigraphy and Development of Heterohelicidae (Planktic Foraminifera). *Micropaleontology* 37, 329–372. <https://doi.org/10.2307/1485910>.
- Ogg, J.G., Hinnov, L.A., Huang, C., 2012. Chapter 27-Cretaceous. In: *The Geologic Time Scale*. Elsevier, Boston, pp. 793–853. <https://doi.org/10.1016/B978-0-444-59425-9.00027-5>.
- Oms, O., Dinarès-Turell, J., Vicens, E., Estrada, R., Vila, B., Galobart, À., Bravo, A.M., 2007. Integrated stratigraphy from the Vallcebre Basin (southeastern Pyrenees, Spain): New insights on the continental Cretaceous-Tertiary transition in southwest Europe. *Palaeogeography, Palaeoclimatology, Palaeoecology* 255, 35–47. <https://doi.org/10.1016/j.palaeo.2007.02.039>.
- Oms, O., Pérez-Cano, J., Fondevilla, V., Anadón, P., Ibáñez-Insa, J., Rejas, M., Fernandez-Turiel, J.L., Dinarès-Turell, J., Pardo, P., Estrada, R., 2014. On the search of the K-PG boundary in the terrestrial record in Europe: preliminary geochemical data from the Puig Pedrós section (Tresp basin, Catalonia, Spain). Abstract book Reconstructing the terrestrial end-Cretaceous paleoenvironments in Europe (Tresp, 2014). *Paleontología i Evolució Special Memoir* 7, 74.
- Oms, O., Fondevilla, V., Riera, V., Marmi, J., Vicens, E., Estrada, R., Anadón, P., Vila, B., Galobart, À., 2016. Transitional environments of the lower Maastrichtian South-Pyrenean Basin (Catalonia, Spain): The Fumanya Member tidal flat. *Cretaceous Research* 57, 428–442. <https://doi.org/10.1016/j.cretres.2015.09.004>.
- Ortega, F., Bardet, N., Barroso-Barcenilla, F., Callapez, P.M., Cambra-Moo, O., Gómez, V.D., Díaz, V.D., Domingo, L., Elvira, A., Escaso, F., García-Oliva, M., Gómez, B., Houssaye, A., Knoll, F., Marcos-Fernández, F., Martín, M., Mocho, P., Narváez, I., García, A.P., Peyrot, D., Segura, M., Serrano, H., Torices, A., Vidal, D., Sanz, J.L., 2015. The biota of the Upper Cretaceous site of "Lo Hueco" (Cuenca, Spain). *Journal of Iberian Geology* 41.
- Osete, M.-L., Gialanella, P.-R., Gómez, J.J., Villalán, J.J., Goy, A., Heller, F., 2007. Magnetostratigraphy of Early-Middle Toarcian expanded sections from the Iberian Range (central Spain). *Earth and Planetary Science Letters* 259, 319–332. <https://doi.org/10.1016/j.epsl.2007.04.048>.
- Panaiotu, C.G., Panaiotu, C.E., 2010. Palaeomagnetism of the Upper Cretaceous Sănpetru Formation (Hațeg Basin, South Carpathians). *Palaeogeography, Palaeoclimatology, Palaeoecology* 293, 343–352. <https://doi.org/10.1016/j.palaeo.2009.11.017>.
- Panaiotu, A.G., Ciobănet, D., Panaiotu, C.G., Panaiotu, C.E., Csiki, Z., 2011. New palaeomagnetic data from the Hațeg Basin, Romania. In: Abstract Book, 8th Romanian Symposium of Paleontology, Bucharest (Romania). Ed. Ars Docendi, Bucharest, pp. 84–85.
- Peláez-Campomanes, P., López-Martínez, N., Álvarez-Sierra, M.A., Daams, R., 2000. The Earliest Mammal of the European Paleocene: The Multituberculata *Hainina*. *Journal of Paleontology* 74, 701–711.
- Pereda-Suberbiola, X., Canudo, J.I., Cruzado-Caballero, P., Barco, J.L., López-Martínez, N., Oms, O., Ruiz-Omeñaca, J.I., 2009. The last hadrosaurid dinosaurs of Europe: A new lambeosaurine from the Uppermost Cretaceous of Aren (Huesca, Spain). *Comptes Rendus Palevol* 8, 559–572. <https://doi.org/10.1016/j.crpv.2009.05.002>.
- Pereda-Suberbiola, X., Corral, J.C., Astibia, H., Badiola, A., Bardet, N., Berreteaga, A., Buffetaut, E., Buscalioni, A.D., Cappetta, H., Cavin, L., Díez Díaz, V., Gheerbrant, E., Murelaga, X., Ortega, F., Pérez-García, A., Poyato-Ariza, F., Rage, J.-C., Sanz, J.L., Torices, A., 2015. Late cretaceous continental and marine vertebrate assemblages from the Laño quarry (Basque-Cantabrian Region, Iberian Peninsula): an update. *Journal of Iberian Geology* 41 (1), 101–124.
- Pessagno, E.A., 1967. Upper Cretaceous planktonic foraminifera from the western Gulf Coastal Plain. *Paleontolog. Research Institution*.
- Petters, S.W., 1977. Upper Cretaceous planktonic foraminifera from the subsurface of the Atlantic Coastal Plain of New Jersey. *Journal of Foraminiferal Research* 7 (3), 165–187.
- Plummer, H.J., 1931. Some Cretaceous foraminifera in Texas. *University of Texas Bulletin* 3101, 109–203.
- Prasad, G.V.R., de Lapparent de Broin, F., 2002. Late Cretaceous crocodile remains from Naskal (India): comparisons and biogeographic affinities. *Annales de Paléontologie* 88, 19–71. [https://doi.org/10.1016/S0573-3969\(02\)01036-4](https://doi.org/10.1016/S0573-3969(02)01036-4).
- Puértolas, E., Canudo, J.I., Cruzado-Caballero, P., 2011. A New Crocodylian from the Late Maastrichtian of Spain: Implications for the Initial Radiation of Crocodyliids. *PLoS One* 6, e20011. <https://doi.org/10.1371/journal.pone.0020011>.
- Puértolas-Pascual, E., Canudo, J.I., Moreno-Azanza, M., 2014. The eusuchian crocodylomorph *Allodaposuchus subjuniperus* sp. nov., a new species from the latest

- Cretaceous (upper Maastrichtian) of Spain. *Historical Biology* 26, 91–109. <https://doi.org/10.1080/08912963.2012.763034>.
- Puértolas-Pascual, E., Blanco, A., Brochu, C.A., Canudo, J.I., 2016. Review of the Late Cretaceous-early Paleogene crocodylomorphs of Europe: Extinction patterns across the K-PG boundary. *Cretaceous Research* 57, 565–590. <https://doi.org/10.1016/j.cretres.2015.08.002>.
- Puigdefábregas, C., Souquet, P., 1986. Tecto-sedimentary cycles and depositional sequences of the Mesozoic and Tertiary from the Pyrenees. *Tectonophysics* 129, 173–203.
- Pujalte, V., Schmitz, B., 2005. Revisión de la estratigrafía del Grupo Tremp («Garumniense», Cuenca de Tremp-Graus, Pirineos meridionales). *Geogaceta* 38, 79–82.
- Riera, V., 2010. Estudio integrado (geología y paleontología) de la sucesión de dinosaurios (Maastrichtiense) de la vertiente surpirenaica. *Universitat Autònoma de Barcelona*.
- Riera, V., Oms, O., Gaete, R., Galobart, À., 2009. The end-Cretaceous dinosaur succession in Europe: The Tremp Basin record (Spain). *Palaeogeography, Palaeoclimatology, Palaeoecology* 283, 160–171. <https://doi.org/10.1016/j.palaeo.2009.09.018>.
- Rosell, J., Linares, R., Llompart, C., 2001. El «Garumniense» prepirenaico. *Revista de la Sociedad Geológica de España* 14, 47–56.
- Rossi, C., 1993. Sedimentología y diagénesis del Paleoceno superior-Eoceno inferior en la Cuenca de Ager (Sierras Marginales, Prepireneo de Lérida). Unpublished PhD. Thesis Universidad Complutense Madrid.
- Séguret, M., 1972. Étude tectonique des nappes et séries décollées de la partie centrale du versant sud des Pyrénées. *Publications de l'Université des Sciences et Techniques du Languedoc (USTELA). Série Géologie Structurale* 2, 163.
- Sellés, A.G., Vila, B., 2015. Re-evaluation of the age of some dinosaur localities from the southern Pyrenees by means of megaloolithid oospecies. *Journal of Iberian Geology* 41 (1), 125–139.
- Sellés, A.G., Bravo, A.M., Delclòs, X., Colombo, F., Martí, X., Ortega-Blanco, J., Parellada, C., Galobart, À., 2013. Dinosaur eggs in the Upper Cretaceous of the Coll de Nargó area, Lleida Province, south-central Pyrenees, Spain: Oodiversity, biostratigraphy and their implications. *Cretaceous Research* 40, 10–20. <https://doi.org/10.1016/j.cretres.2012.05.004>.
- Sellés, A.G., Vila, B., Galobart, À., 2014a. Spheroolithus europaeus, oosp. nov. (late Maastrichtian, Catalonia), the youngest oological record of hadrosauroids in Eurasia. *Journal of Vertebrate Paleontology* 34, 725–729. <https://doi.org/10.1080/02724634.2013.819360>.
- Sellés, A.G., Vila, B., Galobart, À., 2014b. Diversity of theropod ootaxa and its implications for the latest Cretaceous dinosaur turnover in southwestern Europe. *Cretaceous Research* 49, 45–54. <https://doi.org/10.1016/j.cretres.2014.02.004>.
- Sellés, A.G., Marmi, J., Llácer, S., Blanco, A., 2016. The youngest sauropod evidence in Europe. *Historical Biology* 28, 930–940. <https://doi.org/10.1080/08912963.2015.1059834>.
- Sibuet, J.-C., Srivastava, S.P., Spakman, W., 2004. Pyrenean orogeny and plate kinematics. *Journal of Geophysical Research: Solid Earth* 109. <https://doi.org/10.1029/2003JB002514> n/a–n/a.
- Sigal, J., 1952. Aperçu stratigraphique sur la micropaleontologie du Cretace. *Monographies Regionales* 1 (26), 3–43.
- Sigal, J., 1966. Contribution à une monographie des Rosalines. I. Le genre *Ticinella* Reichel, souche des Rotalipores. *Eclogae Geologicae Helvetiae* 59, 185–217.
- Simó, A., Puigdefábregas, C., Gili, E., 1985. Transition from shelf to basin on an active slope, upper Cretaceous, Tremp area, southern Pyrenees. In: *International Association of Sedimentologists 6th European Regional Meeting Excursion Guidebook*. International Association of Sedimentologists, Lleida, Spain, pp. 63–108.
- Smit, J., 1982. Extinction and evolution of planktonic foraminifera after a major impact at the Cretaceous/Tertiary boundary. *Geological Society of America Special Papers* 190, 329–352.
- Smith, A.B., McGowan, A.J., 2011. The ties linking rock and fossil records and why they are important for palaeobiodiversity studies. *Geological Society, London, Special Publications* 358, 1. <https://doi.org/10.1144/SP358.1>.
- Smith, A.B., Gale, A.S., Monks, Neale E.A., 2001. Sea-Level Change and Rock-Record Bias in the Cretaceous: A Problem for Extinction and Biodiversity Studies. *Paleobiology* 27, 241–253.
- Souquet, P., 1967. Le Crétacé supérieur sudpyrénéen en Catalogne. Aragon et Navarre: These Doctorale Science Naturelles, Université de Toulouse, France.
- Teixell, A., 2004. Estructura cortical de la Cordillera Pirenaica. *Geologia de Espana* 320–321.
- Torices, A., Ruiz-Omeñaca, J.I., Canudo, J.I., López-Martínez, N., 2004. Nuevos datos sobre los dinosaurios terópodos (Saurischia: Theropoda) del Cretácico superior de los Pirineos Sur-Centrales (Huesca y Lleida). *Geotemas* 6, 71–74.
- Torices, A., Currie, P.J., Canudo, J.I., Pereda-Suberbiola, X., 2015. Theropod Dinosaur from the Upper Cretaceous of the South Pyrenees Basin of Spain. *Acta Palaeontologica Polonica* 60, 611–626. <https://doi.org/10.4202/app.2012.0121>.
- Turner, A.H., 2006. Osteology and phylogeny of a new species of *Araripesuchus* (Crocodyliformes: Mesoeucrocodylia) from the Late Cretaceous of Madagascar. *Historical Biology* 18, 255–369. <https://doi.org/10.1080/08912960500516112>.
- Upchurch, P., Mannion, P.D., Benson, R.B.J., Butler, R.J., Carrano, M.T., 2011. Geological and anthropogenic controls on the sampling of the terrestrial fossil record: a case study from the Dinosauria. *Geological Society, London, Special Publications* 358, 209. <https://doi.org/10.1144/SP358.14>.
- Van Der Voo, R., Zijdeveld, J.D.A., 1971. Renewed paleomagnetic study of the Lisbon volcanics and implications for the rotation of the Iberian Peninsula. *Journal of Geophysical Research* 76, 3913–3921. <https://doi.org/10.1029/JB076i017p03913>.
- Van Itterbeek, J., Markevich, V.S., Codrea, V., 2005. Palynostratigraphy of the Maastrichtian dinosaur-and mammal sites of the Râul Mare and Barbat Valleys (Hațeg Basin, Romania). *Geologica Carpathica* 56, 137–147.
- Vicens, E., Ardèvol, L., López-Martínez, N., Arribas, M.E., 2004. Rudist biostratigraphy in the Campanian-Maastrichtian of the south-central Pyrenees, Spain. *Courier-Forschungsinstitut Senckenberg* 113–128.
- Vicente, A., Martín-Closas, C., Arz, J.A., Oms, O., 2015. Maastrichtian–basal Paleocene charophyte biozonation and its calibration to the Global Polarity Time Scale in the southern Pyrenees (Catalonia, Spain). *Cretaceous Research* 52, 268–285. <https://doi.org/10.1016/j.cretres.2014.10.004>.
- Vila, B., Riera, V., Bravo, A.M., Oms, O., Vicens, E., Estrada, R., Galobart, À., 2011. The chronology of dinosaur oospecies in south-western Europe: Refinements from the Maastrichtian succession of the eastern Pyrenees. *Cretaceous Research* 32, 378–386. <https://doi.org/10.1016/j.cretres.2011.01.009>.
- Vila, B., Galobart, À., Canudo, J.I., Le Loëuff, J., Dinarès-Turell, J., Riera, V., Oms, O., Tortosa, T., Gaete, R., 2012. The diversity of sauropod dinosaurs and their first taxonomic succession from the latest Cretaceous of southwestern Europe: Clues to demise and extinction. *Palaeogeography, Palaeoclimatology, Palaeoecology* 350–352, 19–38. <https://doi.org/10.1016/j.palaeo.2012.06.008>.
- Vila, B., Oms, O., Fondevilla, V., Gaete, R., Galobart, À., Riera, V., Canudo, J.I., 2013. The Latest Succession of Dinosaur Tracksites in Europe: Hadrosaur Ichnology, Track Production and Palaeoenvironments. *PLoS One* 8, e72579. <https://doi.org/10.1371/journal.pone.0072579>.
- Vila, B., Castanera, D., Marmi, J., Canudo, J.I., Galobart, À., 2015. Crocodile swim tracks from the latest Cretaceous of Europe. *Lethaia* 48, 256–266. <https://doi.org/10.1111/let.12103>.
- Vila, B., Sellés, A.G., Brusatte, S.L., 2016. Diversity and faunal changes in the latest Cretaceous dinosaur communities of southwestern Europe. *Cretaceous Research* 57, 552–564. <https://doi.org/10.1016/j.cretres.2015.07.003>.
- Villalain, J.J., Osete, M.L., Vegas, R., García-Dueñas, V., Heller, F., 1994. Widespread Neogene remagnetization in Jurassic limestones of the South-Iberian palaeomargin (Western Betics, Gibraltar Arc). *Physics of the Earth and Planetary Interiors* 85, 15–33. [https://doi.org/10.1016/0031-9201\(94\)90005-1](https://doi.org/10.1016/0031-9201(94)90005-1).
- Villalba-Breva, S., Martín-Closas, C., 2011. A characean thallus with attached gyrogonites and associated fossil charophytes from the Maastrichtian of the Eastern Pyrenees (Catalonia, Spain). *Journal of Phycology* 47, 131–143. <https://doi.org/10.1111/j.1529-8817.2010.00947.x>.
- Villalba-Breva, S., Martín-Closas, C., 2013. Upper Cretaceous paleogeography of the Central Southern Pyrenean Basins (Catalonia, Spain) from microfacies analysis and charophyte biostratigraphy. *Facies* 59, 319–345. <https://doi.org/10.1007/s10347-012-0317-1>.
- Villalba-Breva, S., Martín-Closas, C., Marmi, J., Gomez, B., Fernández-Marrón, M.T., 2012. Peat-forming plants in the Maastrichtian coals of the Eastern Pyrenees. *Geologica Acta: An International Earth Science Journal* 10. <https://doi.org/10.1344/105.000001711>.
- Vogler, J., 1941. Ober-Jura und Kreide von Misol. *Beitrage zur Geologie von Niederländisch-Indian* 4, pp. 243–293.
- Voorwijk, G.H., 1937. Foraminifera from the upper Cretaceous of Habana, Cuba. *Proceedings of the Koninklijke Nederlandse Akademie van Wetenschappen* 40, 190–198.
- Vremir, M., Bălc, R., Csiki-Sava, Z., Brusatte, S.L., Dyke, G., Naish, D., Norell, M.A., 2014. Petrești-Arini – An important but ephemeral Upper Cretaceous continental vertebrate site in the southwestern Transylvanian Basin, Romania. *Cretaceous Research* 49, 13–38. <https://doi.org/10.1016/j.cretres.2014.02.002>.

# ZUBÍA

REVISTA DE CIENCIAS

MONOGRÁFICO

31

*ier*

Instituto de Estudios Riojanos

ZUBÍA. MONOGRÁFICO  
REVISTA DE CIENCIAS.  
Nº 31 (2019). Logroño (España).  
P. 1-366, ISSN: 1131-5423



INSTITUTO DE ESTUDIOS RIOJANOS

# ZUBÍA

---

REVISTA DE CIENCIAS

Monográfico Núm. 31

**PALEONTOLOGÍA IBÉRICA:  
NUEVAS TENDENCIAS Y PERSPECTIVAS**

Coordinadores:

ANGÉLICA TORICES HERNÁNDEZ, MIREIA FERRER VENTURA,  
PABLO NAVARRO LORBÉS Y RAÚL SAN JUAN PALACIOS



Gobierno de La Rioja  
Instituto de Estudios Riojanos  
LOGROÑO  
2019

## LARRA 4: DESENTERRANDO A LOS ÚLTIMOS VERTEBRADOS DEL MAASTRICHTIENSE TERMINAL DEL PIRINEO ARAGONÉS

MANUEL PÉREZ-PUEYO<sup>1</sup>  
EDUARDO PUÉRTOLAS-PASCUAL<sup>1,2</sup>  
JOSÉ IGNACIO CANUDO<sup>1</sup>  
BEATRIZ BÁDENAS<sup>1</sup>

### RESUMEN

Larra 4 es un yacimiento del Pirineo aragonés que presenta una rica asociación fósil de restos de vertebrados, incluyendo dinosaurios hadrosáuridos y terópodos, crocodiloformas, anfibios y peces. Por su edad (Maastrichtiense terminal). Este yacimiento aporta información relevante sobre la diversidad de los ecosistemas en este sector de Iberia al final del Cretácico. Además, el nivel en que se encuentra el yacimiento, una caliza intraclástica con mezcla de fósiles marinos y continentales intercalada entre facies lutíticas de llanura aluvial, indican una un proceso generador y una historia tafonómica complejos.

**PALABRAS CLAVE:** Maastrichtiense superior, Huesca, Fm. Trepmp, Dinosauria, Crocodylomorpha

### 1. INTRODUCCIÓN

Las sucesiones sedimentarias continentales con registro fósil de vertebrados del Maastrichtiense (Cretácico Superior) son escasas en Europa, siendo las situadas en el noroeste de Rumanía, el sur de Francia y el noroeste de España las que presentan un registro más continuo (Csiki-Sava *et al.*, 2015). En la Península Ibérica, los afloramientos mejor estudiados del Maastrichtiense se localizan en la cuenca de Trepmp (Huesca y Lérida). Durante los últimos 30 años se han caracterizado los depósitos de esta cuenca

1. Grupo Aragosaurus-IUCA, Facultad de Ciencias, Universidad de Zaragoza, C/ Pedro Cerbuna, 12, 50009 Zaragoza. manuppueyo@unizar.es, jicanudo@unizar.es, bbadenas@unizar.es.

2. Departamento de Ciências da Terra. Faculdade de Ciências e Tecnologia. Universidade Nova de Lisboa, Monte da Caparica, Campus FCT, 2829-516, Caparica, Portugal; puertolas@fct.unl.pt.

a nivel estratigráfico, sedimentológico y paleontológico, y en particular, en su sector aragonés se han encontrado en los últimos años una inusitada paleobiodiversidad de vertebrados (Canudo *et al.*, 2016; Puértolas-Pascual *et al.*, 2018 y referencias contenidas). Además, se han realizado estudios geocronológicos para datar la sucesión sedimentaria del Cretácico final en esta parte de la cuenca (Canudo *et al.*, 2016; Puértolas-Pascual *et al.*, 2018). Los afloramientos cercanos a Serraduy (Huesca) son los que han mostrado un mayor potencial paleontológico, con más de cincuenta yacimientos localizados. Uno de los yacimientos más significativos por su posición estratigráfica y riqueza fosilífera es Larra 4, descubierto recientemente por los aficionados J. Larrañaga and G. Martín, y que está siendo estudiado por el grupo Aragosaurus-IUCA. El objetivo de este trabajo es hacer una evaluación preliminar de la paleobiodiversidad y génesis de Larra 4.

## 2.CONTEXTO GEOGRÁFICO Y GEOLÓGICO

Larra 4 está localizado al sur del municipio de Valle de Lierp (NE de la provincia de Huesca). Geológicamente, el yacimiento está situado en la Fm. Tremp, la cual es parte del relleno sedimentario de la Cuenca de Tremp, que actualmente forma parte de la Unidad Surpirenaica Central de la Cordillera Pirenaica.

La Fm. Tremp es una unidad sedimentaria de carácter transicional y continental que se depositó desde el final del Cretácico Superior hasta el Paleoceno Inferior, y a nivel regional está dividida en cuatro unidades informales (Rosell *et al.*, 2001). En la zona de estudio, las dos unidades inferiores denominadas “Garum Gris” y “Garum Rojo Inferior” corresponden al Maastrichtiense, estando el límite Cretácico-Paleógeno en los últimos metros del “Garum Rojo Inferior”, por debajo de las “calizas lacustres de Vallcebre”, de edad Paleoceno (Canudo *et al.*, 2016). Por otra parte, Puértolas-Pascual *et al.* (2018) sitúan el “Garum Gris” y el “Garum Rojo Inferior” dentro del cron C29r, lo que implica que el depósito de estas dos unidades se produjo en esta zona durante de los últimos cientos de miles de años del Maastrichtiense. El “Garum Gris” es una unidad de margas y calizas limosas/arenosas de ambientes de lagoon, mientras que el “Garum Rojo Inferior” está dominado por lutitas de llanura aluvial y areniscas correspondientes a canales, con cierta influencia mareal.

## 3.DESCRIPCIÓN DEL YACIMIENTO

Larra 4 se ubica en la parte media del Garum Rojo Inferior. El nivel fosilífero es una capa de caliza intraclástica gris de unos 40 cm de espesor de media, si bien se acuña lateralmente dada su geometría lenticular. La capa

está intercalada entre dos niveles de lutitas margosas grises bioturbadas, de unos 50 cm de espesor cada uno. A escala de afloramiento, tanto las lutitas grises como el nivel de caliza intraclástica de Larra-4 se acuñan lateralmente. Este conjunto de facies está englobado en un tramo lutítico ocre-rojizo potente de la serie.

La caliza intraclástica es granosostenida con matriz micrítica. De entre los granos destacan mayoritariamente (85%) intraclastos carbonatados micríticos redondeados ( $\varphi \sim 0,2$  cm), ocasionalmente con envueltas oncolíticas irregulares. También hay granos cuarzo (10 %), mal clasificados ( $\varphi^{<1 \text{ mm}}$ ) y de redondeamiento variable (subredondeados a subangulosos). El 5% restante de granos son fósiles de macro- y microvertebrados, pinzas de decápodos, microforaminíferos, restos vegetales y ámbar. Los fósiles de macrovertebrados están desarticulados y su tamaño oscila entre 15 cm a 2 cm. Presentan evidencias de fragmentación bioestratinómica. De base a techo de la capa se observa granodecrecimiento y bioturbación. En concreto, se reconocen dos familias de trazas rellenas de sedimento lutítico: galerías de en torno a 1 cm de grosor que parten del techo de la capa, y otras de pocos mm, afectando a las primeras. Tentativamente se han identificado como afines morfológicamente a *Planolites*.

En el yacimiento se ha recogido material en superficie, y se ha desarrollado una excavación para valorarlo, en la misma se han recuperado 73 fósiles de vertebrados referenciados. También se ha lavado-tamizado una muestra 7 kg de sedimento, a fin de valorar el potencial micropaleontológico del yacimiento.

#### 4. REGISTRO FÓSIL DE GRUPOS DE VERTEBRADOS

La asociación fósil de vertebrados descrita en este trabajo está depositada en el Museo de Ciencias Naturales de la Universidad de Zaragoza (MPZ) (Canudo, 2018). La asociación incluye:

4.1. Osteichthyes y chondrichthyes. Los osteíctios y condricios son escasos, habiéndose identificado preliminarmente un diente medial de Rajiformes y dientes de Pycnodontiformes indeterminados.

4.2. Anura. Se han recuperado algunos fragmentos distales de húmeros y un fragmento de ilion de anfibios, identificados preliminarmente como anuros por su similitud con los descritos en niveles similares (Blain *et al.*, 2010).

4.3. Testudines. Los quelonios tan solo están representados por placas desarticuladas y aisladas, y por lo general fragmentadas, lo que dificulta reconocer su posición en el caparazón o en el plastrón. Las placas son lisas, y algunas de ellas presentan finos surcos dicotómicos (Fig. 1A) señalando un caparazón altamente vascularizado. Este carácter permite asignarlas a Bothremydidae indet. (Murelaga y Canudo, 2005).

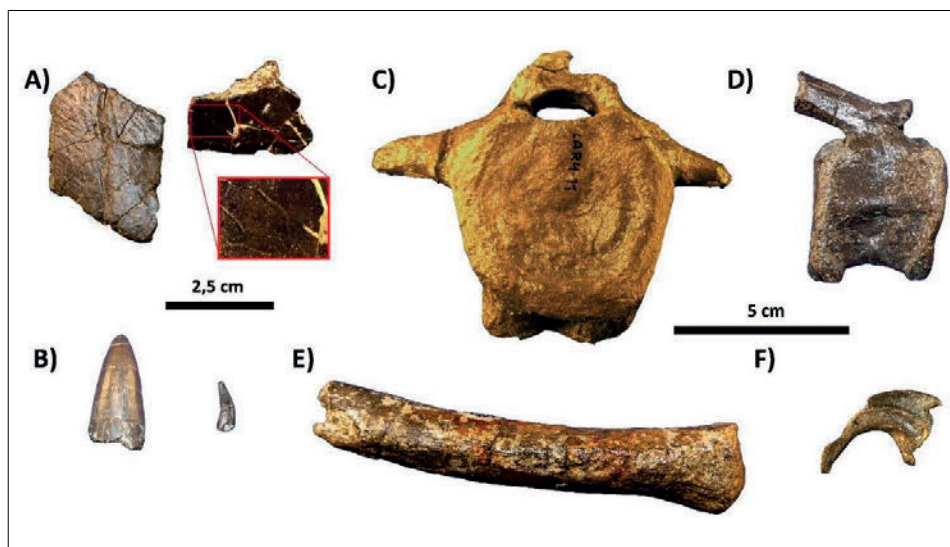


Figura 1. Restos de vertebrados de Larra 4. A. Fragmentos de placas de tortugas Bothremydidae indet. (MPZ 2019/193 y 197), con detalle de los surcos. B. Dientes de crocodilomorfos Allodaposuchidae indet. (MPZ 2019/ 184 y 200). C. Vértebra caudal anterior de Hadrosauridae (MPZ 2019/206). D. Vértebra caudal posterior de Hadrosauridae (MPZ 2019/209). E. Ulna derecha de Theropoda indet. (MPZ2019/194). F) II falange ungual pedal de Dromaeosauridae indet. (MPZ/2019/196).

4.4. Crocodylomorpha. Se han hallado dientes aislados de crocodilomorfos y un fragmento de osteodermo. Los dientes representan un mismo morfotipo (Fig. 1B), de forma cónica, con ornamentación lisa o ligeramente estriada. Este morfotipo es bastante común dentro de Crocodylomorpha, no obstante, en niveles estratigráficos cercanos (Puértolas-Pascual *et al.*, 2018) se han hallado dientes similares asignados a Allodaposuchidae indet. y un taxón de esta familia (*Agaresuchus subjuniiperus*), que presenta también este tipo de dentición. Por este motivo, los dientes se han asignado a Allodaposuchidae indet.

4.5 Dinosauria. Incluye restos de Hadrosauria y Theropoda. Los hadrosáuridos están representado por restos aislados, que incluyen un fragmento de maxilar, un atlas, vértebras caudales anteriores (Fig. 1C) y posteriores (Fig. 1D), un fragmento distal de fémur y fragmentos de arcos neurales, costillas y arcos hemales. El relativo pequeño tamaño de estos huesos y la presencia de arcos neurales bien soldados a los centros vertebrales indican que corresponderían a hadrosaurios adultos de pequeña talla, que probablemente pertenezcan al taxón enano citado por Company *et al.* (2015). Los terópodos están representados por un diente asignado a Coelurosauria indet. (Puértolas-Pascual *et al.*, 2018), un fragmento distal de ulna asignado a Theropoda indet. (Fig. 1E) y como pieza más relevante, la II falange ungual pedal de un dromeosáurido (Fig. 1F).

Esta falange está aplastada lateromedialmente y presenta una sección con forma de lágrima y morfología falciforme, con una marcada curvatura.

## 5. DISCUSIÓN Y CONCLUSIONES

Las lutitas grises bioturbadas en las que se encuentra intercalado el nivel de caliza intraclástica de Larra 4 corresponderían a depósitos de una charca de escasa extensión y lámina de agua. Esta zona encharcada estaría situada dentro de una amplia llanura aluvial, que corresponde a los depósitos lutíticos ocreos y rojizos. El nivel de caliza intraclástica de Larra 4 se interpreta como el depósito de al menos un evento en el que se produjo erosión, transporte y mezcla de granos de origen continental y marino (*e.g.* foraminíferos, decápodos), que quedó preservado dentro del área encharcada. No obstante, estudios sedimentológicos y tafonómicos más exhaustivos son necesarios para poder determinar la causa última de este evento, si bien la presencia de organismos marinos hace que la hipótesis más plausible es que se trate de un evento de alta energía desde áreas costeras cercanas (tormenta o tsunami). Durante el Maastrichtiense superior los ecosistemas de Iberia estaban dominados por hadrosáuridos, y en menor medida, saurópodos y terópodos de pequeño y gran tamaño (Vila *et al.*, 2016). La asociación de Larra 4 presenta fósiles de dos de estos grupos (hadrosáuridos y terópodos), lo que apoya la hipótesis (Csiki-Sava *et al.*, 2015) de que al final del Maastrichtiense (C29r) estos ecosistemas no habían experimentado un declive marcado previo al K/Pg. La diversidad del ecosistema se ve apoyada también por la presencia de fósiles de crocodilomorfos, testudinos, anfibios y osteíctios. La recuperación de más restos y un estudio pormenorizado de cada grupo permitirá reconstruir con mayor precisión la biodiversidad que existía en esta área de Iberia al final del Maastrichtiense.

## AGRADECIMIENTOS

Este artículo forma parte del Proyecto GL2017-85038-P (Ministerio de Ciencia e Innovación) y del Gobierno de Aragón (Grupo Aragosaurus: Recursos geológicos y Paleoambientes). M.P-P está apoyado por una beca del Ministerio de Educación, Cultura y Deporte (FPU 16/03064).

## REFERENCIAS BIBLIOGRÁFICAS

- Blain, H.A., Canudo, J.I., Cuenca-Bescós, G., López-Martínez, N. (2010). "Amphibians and squamate reptiles from the latest Maastrichtian (Upper Cretaceous) of Blasi 2 (Huesca, Spain)". *Cretaceous Research* 31, pp. 433-446.
- Canudo, J.I. (2018). "The collection of type fossils of the Natural Science Museum of the University of Zaragoza (Spain)". *Geoheritage* 10, pp. 385-392.

- Canudo, J.I., Oms, O., Vila, B., Galobart, À., Fondevilla, V., Puértolas-Pascual, E., Sellés, ... Blanco, A. (2016.) "The upper Maastrichtian dinosaur fossil record from the southern Pyrenees and its contribution to the topic of the Cretaceous-Palaeogene mass extinction event." *Cretaceous Research* 57, pp. 540-551.
- Company, J., Cruzado-Caballero, P., Canudo, J.I. (2015). "Presence of diminutive hadrosaurids (Dinosauria: Ornithopoda) from the Maastrichtian of the southcentral Pyrenees (Spain)." *Journal of Iberian Geology* 41, pp. 71-81.
- Csiki-Sava, Z., Buffetaut, E., Ösi, A., Pereda-Suberbiola, X., Brusatte, S.L. (2015). "Island life in the Cretaceous-faunal composition, biogeography, evolution, and extinction of land-living vertebrates on the Late Cretaceous European archipelago". *ZooKeys* 1, pp. 1-161.
- Murelaga, X., Canudo, J.I. (2005). "Descripción de los restos de quelonios del Maastrichtiense superior de Aren y Serraduy (Huesca)." *Geogaceta* 38, pp. 51-54.
- Puértolas-Pascual, E., Arenillas, I., Arz, J.A., Calvín, P., Ezquerro, L., García-Vicente, C., Pérez-Pueyo, M., Sánchez-Moreno, E.M., Villalaín, J.J., Canudo, J.I. (2018). Chronostratigraphy and new vertebrate sites from the upper Maastrichtian of Huesca (Spain), and their relation with the K/Pg boundary." *Cretaceous Research*, 89, pp. 36-59.2
- Rosell, J., Linares, R., Llompart, C. (2001). "El "Garumniense" prepirenaico." *Revista de la Sociedad Geológica de España* 14, 47-56.
- Vila, B., Sellés, A.G., Brusatte, S.L., 2016. "Diversity and faunal changes in the latest Cretaceous dinosaur communities of South-Western Europe." *Cretaceous Research*, 57, 552-564.



## First record of a giant bird (Ornithuromorpha) from the uppermost Maastrichtian of the Southern Pyrenees, northeast Spain

Manuel Pérez-Pueyo, Eduardo Puértolas-Pascual, Miguel Moreno-Azanza, Penélope Cruzado-Caballero, José Manuel Gasca, Carmen Núñez-Lahuerta & José Ignacio Canudo

To cite this article: Manuel Pérez-Pueyo, Eduardo Puértolas-Pascual, Miguel Moreno-Azanza, Penélope Cruzado-Caballero, José Manuel Gasca, Carmen Núñez-Lahuerta & José Ignacio Canudo (2021): First record of a giant bird (Ornithuromorpha) from the uppermost Maastrichtian of the Southern Pyrenees, northeast Spain, Journal of Vertebrate Paleontology, DOI: [10.1080/02724634.2021.1900210](https://doi.org/10.1080/02724634.2021.1900210)

To link to this article: <https://doi.org/10.1080/02724634.2021.1900210>



View supplementary material [↗](#)



Published online: 26 Apr 2021.



Submit your article to this journal [↗](#)



View related articles [↗](#)



View Crossmark data [↗](#)



ARTICLE

## FIRST RECORD OF A GIANT BIRD (ORNITHUROMORPHA) FROM THE UPPERMOST MAASTRICHTIAN OF THE SOUTHERN PYRENEES, NORTHEAST SPAIN

MANUEL PÉREZ-PUEYO, <sup>1\*</sup> EDUARDO PUÉRTOLAS-PASCUAL, <sup>1,2,3</sup> MIGUEL MORENO-AZANZA, <sup>1,2,3</sup>  
PENÉLOPE CRUZADO-CABALLERO, <sup>1,4,5,6</sup> JOSÉ MANUEL GASCA, <sup>1</sup> CARMEN NÚÑEZ-LAHUERTA, <sup>1,2,3</sup>  
and JOSÉ IGNACIO CANUDO <sup>1</sup>

<sup>1</sup>Grupo Aragosaurus-IUCA, Facultad de Ciencias, Universidad de Zaragoza, C/Pedro Cerbuna, 12, 50009 Zaragoza, Spain, manuppueyo@unizar.es, jicanudo@unizar.es;

<sup>2</sup>GeoBioTec. Departamento de Ciências da Terra. Faculdade de Ciências e Tecnologia. Universidade Nova de Lisboa, Monte da Caparica, Campus FCT, 2829-516, Caparica, Portugal;

<sup>3</sup>Espaço NovaPaleo, Museu de Lourinhã, Lourinhã, Portugal;

<sup>4</sup>Instituto de Investigación en Paleobiología y Geología (IIPG), CONICET, General Roca, 8332, Río Negro, Argentina;

<sup>5</sup>Universidad Nacional de Río Negro-IIPG, General Roca, Río Negro, Argentina;

<sup>6</sup>Departamento de Biología Animal, Edafología y Geología, Universidad de La Laguna, San Cristóbal de La Laguna, Santa Cruz de Tenerife, Spain

**ABSTRACT**—Throughout the evolutionary history of Avialae, several members of this clade have evolved into giant forms, in different time periods and ecological contexts. In Europe, the first birds that show this condition, the Gargantuaviidae, occur during the Late Cretaceous (late Campanian–early Maastrichtian), but it is during the Paleogene when more groups evolve large forms. However, until now, there was no record of any giant bird during the late Maastrichtian of Europe, close to the K/Pg boundary. Here we describe a cervical vertebra (MPZ 2019/264) from Beranuy (Huesca, NE Spain), which is the first fossil evidence of a giant bird from the late Maastrichtian of Europe, within Chron C29r. The vertebra displays some features, such as a well-marked heterocoelous articulation, lateral pneumatic foramina, ventral carotid processes, and a low neural spine, that support its inclusion within the clade Ornithuromorpha. This phylogenetic assignment is supported by two cladistic analyses. The vertebra is clearly different from the one assigned to *Gargantuavis*, meaning that it belonged to a distinct taxon. Although the kinship between these two taxa of giant birds is still unclear, this finding demonstrates that large-sized birds were part of the ecological communities of the Ibero-Armorican island from the late Campanian to the Late Maastrichtian, being present during the last hundreds of thousands of years prior to the K/Pg extinction event.

**SUPPLEMENTAL DATA**—Supplemental materials are available for this article for free at [www.tandfonline.com/UJVP](http://www.tandfonline.com/UJVP)

Citation for this article: Pérez-Pueyo, M., E. Puértolas-Pascual, M. Moreno-Azanza, P. Cruzado-Caballero, J. M. Gasca, C. Núñez-Lahuerta, and J. I. Canudo. 2021. First record of a giant bird (Ornithuromorpha) from the uppermost Maastrichtian of the Southern Pyrenees, northeast Spain. *Journal of Vertebrate Paleontology*. DOI: 10.1080/02724634.2021.1900210

### INTRODUCTION

The term ‘giant bird’ is used to refer to all avialans (extant and extinct) that have evolved into large-sized forms, standing out from other members of their respective clades. The most common use of this term in the literature refers to terrestrial and flightless birds (e.g., Baskin, 1995; Buffetaut and Le Loeuff, 1998; Worthy et al., 2016; Angst and Buffetaut, 2017; Pavia et al., 2017) that move in a cursorial or graviportal way and are large in size, according to a human scale. Ecologically, these kinds of giant birds are diverse in habitats and diets (Fig. 1A). For example, the extant *Struthio* (ostrich) lives in open habitats and is predominantly herbivorous (Winkler et al., 2020a), whereas the extant *Casuaris* (cassowary) inhabits different types of forest with a mainly frugivorous diet (Winkler et al., 2020b), and the extinct phorusrhacids preferred open habitats and were carnivorous (Degrange et al., 2010; Angst and Buffetaut, 2017). However, there are other different cases of gigantism

within Avialae, including flying forms such as the teratorn *Argentavis* (Campbell and Tonni, 1980) or the pelagornithid *Pelagornis* (Ksepka, 2014), and aquatic flightless birds such as the penguin *Anthropornis* (Wiman, 1905). It is important to note that the term ‘giant bird’ does not have a phylogenetic nor geographic connotation, since throughout the evolutionary history of Avialae, different clades of birds (Fig. 1A) have evolved into large flightless forms in different chronological periods, distinct continents, and assuming diverse ecological roles.

Avialae is the only clade of dinosaurs that crossed the K/Pg boundary, and even though most of the giant forms occurred after this biotic crisis there are some cases of gigantism before this event. Nowadays, all the extant giant bird species belong to the clade Palaeognathae (Angst and Buffetaut, 2017), which includes African, South American, and Australasian representatives. However, the fossil record shows that Europe also harbored several different groups of giant flightless birds.

### Late Cretaceous–Paleogene Giant Flightless Bird Record of Europe

The first evidence of large birds from the Late Cretaceous European archipelago is the taxon *Gargantuavis philoinos*

\*Corresponding author

Color versions of one or more of the figures in the article can be found online at [www.tandfonline.com/ujvp](http://www.tandfonline.com/ujvp).

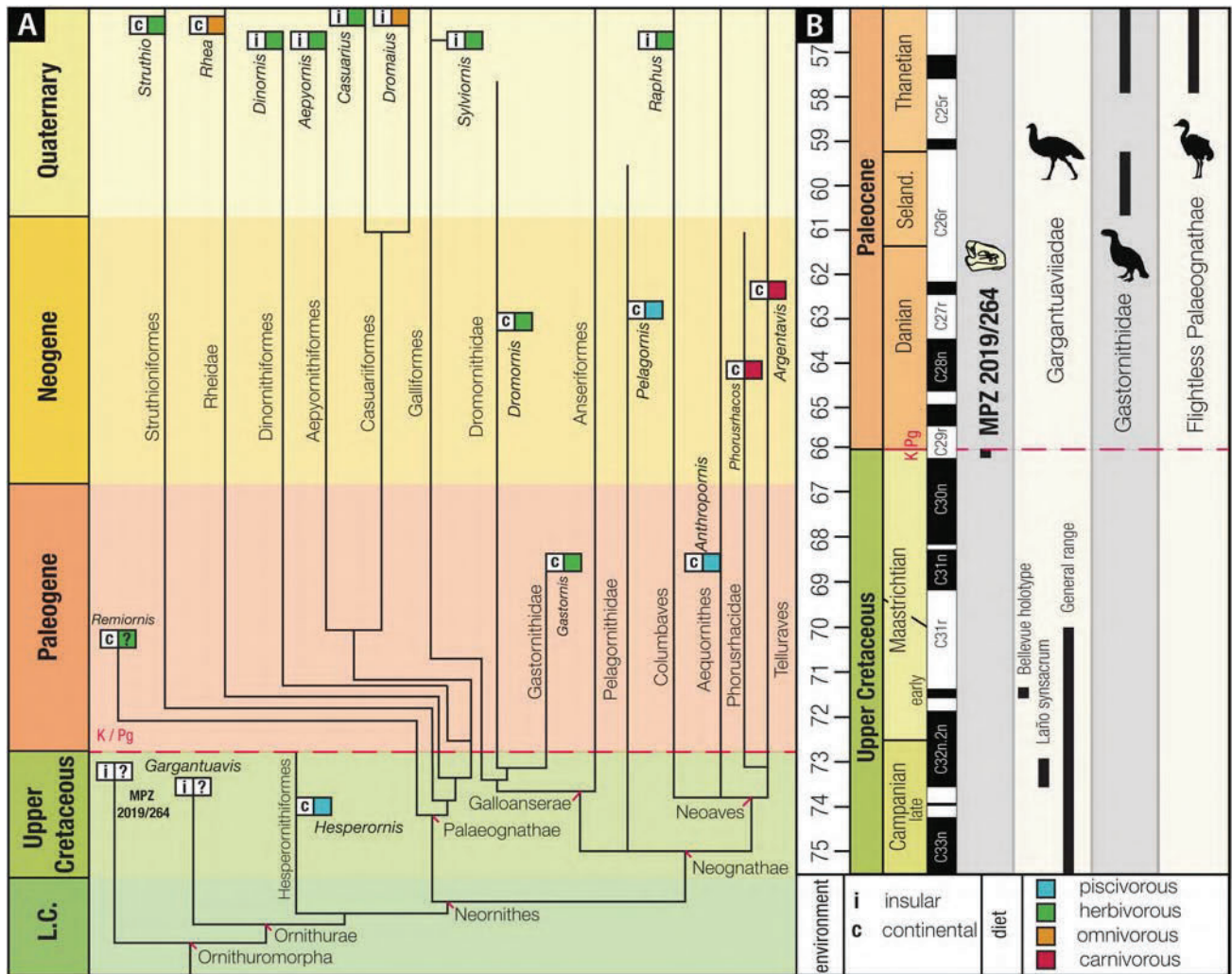


FIGURE 1. **A**, simplified phylogeny of Avialae, focusing on the main clades with giant taxa. Several examples are given, with ecological information. Note that the geological time is not to scale. Phylogeny modified after Mayr (2017) and completed with information from Mitchell et al. (2014) for Palaeognathae and Worthy et al. (2017) for Galloanserae; **B**, chronostratigraphic distribution of the main groups of large-sized birds of Europe between the Late Cretaceous and the Paleocene. The chronostratigraphic time scale was obtained by a combination of Ogg et al. (2012) and Vandenberghe et al. (2012). **Abbreviations:** L. C., Lower Cretaceous; **Seland.**, Selandian.

Buffetaut and Le Loeuff, 1998. This is a taxon with uncertain affinities, known from fragmentary material, whose holotype is a synsacrum found at the Bellevue site in the south of France (Campagne-sur-Aude, Aude) (Fig. 2). Several sites in southern France have yielded *Gargantuavis* remains. These include pelvic elements and a femur from Fox-Amphoux (Var) (Buffetaut et al., 1995, 2015, 2019), a cervical vertebra, pelvic elements, and a femur from Cruzy (Hérault) (Buffetaut and Angst, 2013, 2016, 2019), and a femur from Villeshassans (Hérault) (Buffetaut and Le Loeuff, 1998). *Gargantuavis* has also been reported in Spain, represented by a synsacrum from the Laño quarry in the province of Burgos (Fig. 2) (Angst et al., 2017). All these remains suggest that this taxon, included in the clade Gargantuaviidae (Buffetaut and Angst, 2019), was endemic to the Ibero-Armorican Island. However, the synsacrum and the ilia recently described and assigned to Gargantuaviidae indet. from the early Maastrichtian of Romania (Fig. 2) would extend the presence of this clade to the paleobiogeographic region of Hateg Island (Mayr et al., 2020). The stratigraphic range of *Gargantuavis* would thus be limited to between the upper Campanian and

the lower Maastrichtian (Fig. 1B) based on the fossil faunal assemblages and magnetostratigraphic studies of the sites (Corral et al., 2016; Fondevilla et al., 2016b; Angst and Buffetaut, 2017).

During the Paleogene, several clades of giant birds are represented in Europe. The first after the K/Pg boundary is Gastornithidae, found in the Selandian deposits of Walbeck (Germany) (Mayr, 2007; Buffetaut and Angst, 2014) and the Thanetian deposits of northern France and Belgium (Angst and Buffetaut, 2017) (Fig. 2). This clade is even more abundant during the Eocene (Fig. 2), with gastornithid remains in northern France, Germany, and England spanning the whole of the Ypresian and up to the middle Lutetian (Angst and Buffetaut, 2017). Although scarcer, the fossil record also shows large-sized ratites (e.g., Palaeognathae) living alongside gastornithids during the late Paleocene (Thanetian) of Europe, represented by *Remiornis heberti* Lemoine, 1881 from northern France (Fig. 2) (Martin, 1992; Smith et al., 2014). In the Eocene, the presence of flightless Palaeognathae is documented by *Palaeotis weigelti* Lambrecht, 1928 during the early and middle Lutetian of

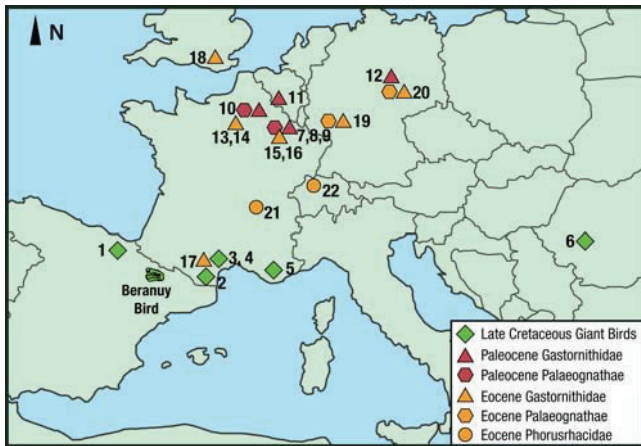


FIGURE 2. Late Cretaceous-Paleogene European paleontological sites with fossils of giant birds: 1. Laño (Spain), 2. Campagne-sur-Aude (France), 3. Villespassans (France), 4. Cruzy (France), 5. Fox-Amphoux (France), 6. Nălaț-Vad (Romania). Gastornithidae: 7. Cernay-lès-Reims (France), 8. Mont-de-Berru (France), 9. Louvois (France), 10. Petit Pâtis (Rivecourt) (France), 11. Mesvin (Belgium), 12. Walbeck (Germany), 13. Meudon (France), 14. Passy (France), 15. Monthelon (France), 16. Mutigny (France), 17. Saint-Papoul (France), 18. Croydon (England), 19. Messel (Germany), 20. Geiseltal (Germany), 21. Lissieu (France), 22. Egerkingen (Switzerland).

Germany (Figs. 1B, 2), although this taxon is not a large-sized bird (Houde and Habould, 1987; Peters, 1988). As well as the skeletal remains, there are several sites from the Paleocene of southern France and northern Spain with eggshells of *Ornitholithus*, an avian oogenus whose producer has been postulated to be a gastornithid (Dughi and Sirugue, 1962; Angst et al., 2014a) or a ratite (Kerourio and Aujard, 1987).

Finally, the last giant birds of the Paleogene in Europe were members of the clade Phorusrhacidae during the late Lutetian of France and Switzerland (Figs. 1B, 2). This fragmentary material has been identified as *Eleutherornis* Schaub, 1940 (Angst et al., 2013), a phorusrhacid, rendering this group the only one present in Europe during the late Lutetian, since gastornithids seem to become extinct in Europe during the middle Lutetian.

All the European large-sized birds belong to Neornithes, except *Gargantuavis*, which has been classified, on the basis of the characters of its referred cervical vertebra and the femur, as closely related or within Ornithurae (Buffetaut and Angst, 2013, 2019, 2020). Recently, Mayr et al. (2020) questioned this phylogenetic proposal, pointing out the resemblances between the pelvis of *Gargantuavis* and that of *Balaur bondoc* Csiki, Vremir, Brusatte, and Norell, 2010 and placing it outside Ornithothoraces. They put forward the hypothesis that *Gargantuavis*, *Balaur*, and *Elopteryx* are part of a distinctive European clade of derived theropods during the Late Cretaceous (Mayr et al., 2020), though Buffetaut and Angst (2020) reject this hypothesis, considering gargantuaviids as basal ornithurines, and the result of insular evolution in the European archipelago during the Late Cretaceous. Nevertheless, the incompleteness of the known fossil material precludes a more accurate classification of *Gargantuavis*.

Thus, giant birds were present in most European ecosystems from the early Maastrichtian to the Eocene (Buffetaut and Angst, 2014; Angst and Buffetaut, 2017), and include the enigmatic *Gargantuavis*, gastornithids, and phorusrhacids (Fig. 1B). This record goes even further in Eastern Europe, where the presence of large-sized palaeognaths has been documented from the Neogene to the early Pleistocene (Boev and Spassov, 2009;

Zelenkov et al., 2019). However, no record of Mesozoic giant birds close to the K/Pg boundary has yet been documented, creating a hiatus between the early Maastrichtian and the middle Paleocene (Fig. 1B) and raising the question of whether any lineage of giant bird was present around the K/Pg boundary. In this paper, we describe an isolated vertebra from Beranuy (Huesca, NE Spain), which is the first fossil evidence of a giant bird from the Late Cretaceous of the Tremp Basin. It also represents the first record of ornithuromorphs in Chron C29r in Europe (66.3–66.052 Ma) (Fig. 1B). This fossil is therefore the youngest record of a Mesozoic giant bird on the continent, filling a gap between the late Campanian–early Maastrichtian giant birds and those of the Paleogene.

## MATERIAL AND METHODS

The fossil vertebra MPZ 2019/264 studied in this paper is housed in the Museo de Ciencias Naturales de la Universidad de Zaragoza (Canudo, 2018). The specimen was embedded in a carbonate sandy matrix when it was collected in the field. Prior to being studied, the fossil was cleaned using both physical and chemical methods (10% diluted formic acid immersions) to remove the surrounding rocky matrix. The anatomical descriptions follow the terminology of several authors: Baumel and Witmer (1993) to describe the main anatomical features, Britt (1993, 1997) to describe the internal pneumatic cavities, taking into account the recommendations of Wedel et al. (2000) and Wilson (1999) for vertebral laminae and Wilson et al. (2011) for pneumatic fossae.

A micro-CT scan was performed using a GE V|Tome|X scanner at the CENIEH (Centro Nacional de Investigación sobre la Evolución Humana, Burgos, Spain). In order to examine the internal features of the vertebra, the images obtained from the scanner were processed using Dragonfly software (Version 4.1, Object Research Systems (ORS) Inc., Montreal, Canada, 2018; software available at <http://www.theobjects.com/dragonfly>).

To analyse the phylogenetic affinities of MPZ 2019/264 we included it in two datasets (Analysis A1 and A2). Both datasets were edited using Mesquite V.3.31 (Maddison and Maddison, 2017) and analysed using TNT v.1.5 (Goloboff and Catalano, 2016). The codifications for MPZ 2019/264 can be found in Supplemental Data 1.

For Analysis A1 we used the dataset of Cau (2018), which includes 1781 characters coded for 132 taxa, with representatives of the main pan-avian clades, in order to explore the avialan affinities of the studied specimen. MPZ 2019/264 was scored for 32 characters (1.8% of the total). All characters were equally weighted and four of them were treated as ordered (13, 296, 398, and 469).

Analysis A2 was carried out by including MPZ 2019/264 in the dataset of Wang et al. (2020), which is more focused on Mesozoic birds, including a total of 280 characters coded for 72 taxa. MPZ 2019/264 was scored for five characters (1.8% of the total). All characters were equally weighted, and 36 multistate characters were treated as ordered (1, 3, 8, 28, 31, 43, 51, 56, 64, 67, 69, 70, 72, 74, 92, 107, 117, 159, 168, 176, 183, 193, 205, 213, 214, 216, 219, 222, 229, 233, 234, 249, 261, 265, 268, and 270). For both analyses, a heuristic tree search was performed, starting from 1000 replicates of Wagner trees followed by TBR branch swapping and holding 10 trees per replication. This was followed with an additional round of tree bisection and reconnection (TBR), using trees in memory. Branch support was assessed with the Bremer decay index and 1000 replicates of standard bootstrap analysis.

**Institutional Abbreviations**—LP, Institut d'Estudis Illerendencs, Lleida, Spain; MACN-N, Museo Argentino de Ciencias Naturales, "Bernardino Rivadavia" Buenos Aires, Argentina; MC-MN, Musée de l'Association Culturelle, Archéologique et Paléontologique de l'Ouest Biterrois, Cruzy, Hérault, France;

**MHNT.PAL**, Muséum d'Histoire Naturelle, Toulouse, Haute-Garonne, France; **MPZ**, Museo de Ciencias Naturales de la Universidad de Zaragoza, Zaragoza, Spain; **ZIN PH**, Paleoherpétological Collection, Zoological Institute, Russian Academy of Sciences, Saint Petersburg, Russia.

## GEOGRAPHIC AND GEOLOGICAL CONTEXT

MPZ 2019/264, described in this paper, was found by members of the *Aragosaurus*-IUCA research group of the University of Zaragoza at the ‘Dolor’ fossil site. This paleontological site is situated to the north of the village of Serraduy, but within the limits of the municipality of Beranuy, situated furthest north. Both towns are in the Aragonese Pyrenees, in the region of Ribagorza (Huesca), north-eastern Spain (Figs. 2, 3A,B).

The Pyrenees is an alpine mountain chain, formed between the Late Cretaceous and the Miocene by the collision of the European plate and the Iberian microplate (Teixell, 1998). The chain is structured as an asymmetric belt of thrusts and folds, verging towards both sides of the orogen (Muñoz, 1992). In the southern Pyrenees, the migration of the main thrust sheets generated a NW–SE foreland basin known as the South-Pyrenean Basin, which was connected to the Atlantic by its western margin, and was filled with Cretaceous and Paleogene deposits (Teixell, 2004). The basin was compartmentalized into several sub-basins due to the propagation of several thrust sheets (Puigdefàbregas et al., 1992), which are preserved as synclines (Trempe, Áger, Coll de Nargó and Vallcebre), the Trempe Syncline being the largest of these. Beranuy is situated in the western part of the north flank of the Trempe syncline (Fig. 3A).

From the beginning of the Maastrichtian, the basin was affected by a fall in sea level (Oms et al., 2016), leading to the sedimentary infill of transitional and continental deposits of the Arén and Trempe formations. The Trempe Formation, informally known as the ‘Garumnian’ (Mey et al., 1968), was deposited

between the Maastrichtian and the Paleocene. It is a diachronous and sedimentologically heterogeneous unit, and its lithostratigraphy is complex, with several proposals existing for its division (see Fondevilla et al., 2019). In this paper, we use the division into four informal units proposed by Rosell et al. (2001) (Fig. 3B, C):

(1) ‘Gray Garumnian’: this is characterized by a mixed lithology of gray marls, limestones, sandstones, and coal layers, with abundant freshwater and brackish invertebrate fossils. It is interpreted as transitional deposits in lagoonal, tidal flat, estuarine, and marsh environments (Rosell et al., 2001; Díez-Canseco et al., 2014; Oms et al., 2016).

(2) ‘Lower Red Garumnian’: a mainly detrital succession of variegated mudstones (ochre, reddish, purple, brown, gray) with intercalations of sandstone levels, interpreted as a fluvial environment with coastal influence (tidal/perilagoonal flats with associated meandering channels) (Rosell et al., 2001; Vila et al., 2013; Díez-Canseco et al., 2014).

These two units have been dated as Maastrichtian by magnetostratigraphic and biostratigraphic methods (Canudo et al., 2016; Puértolas-Pascual et al., 2018; Fondevilla et al., 2019); it has been proposed that the K/Pg boundary is situated near the top of the ‘Lower Red Unit’, although it may not be preserved (Fondevilla et al., 2016a).

(3) ‘Vallcebre limestones and equivalent units’: a carbonate interval represented by lacustrine limestones interpreted as deposits of coastal lakes. This unit is discontinuous laterally and varies greatly in width. In the Trempe Basin, it is an isochronous unit, dated as late Danian (López-Martínez et al., 2006; Díez-Canseco et al., 2014).

(4) ‘Upper Red Garumnian’: this is formed by a succession of red mudstones, sandstones, conglomerates, with an occasional presence of paleosoils, gypsum, and limestones. It is interpreted as deposits of fluvial settings in a more arid environment, dated as Selandian to Thanetian (Rosell et al., 2001; López-Martínez et al., 2006).

The fossil site of ‘Dolor’ is located in the middle part of the ‘Lower Red Garumnian’ (Fig. 3B, C) and was first reported by Cruzado-Caballero et al. (2012). The vertebra was found in a sandstone block that had fallen from an outcrop of a detrital interval comprising several sandstone levels, two of them containing vertebrate fossils. Although the precise fossiliferous layer could not be determined, the aforementioned sandstone package is continuous regionally, allowing the site to be correlated with the nearby stratigraphic section of Serraduy (BS, Barranco Serraduy), previously dated by means of magnetostratigraphy and biostratigraphy (Puértolas-Pascual et al., 2018), identifying the Cretaceous part of the Trempe Formation as belonging to the lower half of Chron C29r. This indicates that the ‘Dolor’ site corresponds to the last 300 ka of the Cretaceous (Fig. 1B). Besides MPZ 2019/264, the ‘Dolor’ outcrop has yielded vertebrate fossil remains of hadrosaurid dinosaurs (Cruzado-Caballero et al., 2012), eusuchian crocodylomorphs (Puértolas-Pascual et al., 2016; Blanco et al., 2020), and testudines (Puértolas-Pascual et al., 2018). All the fossil sites in this area contain a vertebrate assemblage with a high degree of elements in common with the ‘Dolor’ site. In these localities in the Trempe Formation, the crocodylomorph *Agaresuchus subjuniiperus* Puértolas-Pascual, Canudo and Moreno-Azanza, 2014 and abundant hadrosaurid dinosaur remains, including small-sized individuals identified as dwarf hadrosaurids (Company et al., 2015), have previously been reported. This faunal assemblage is concordant with other late Maastrichtian communities of dinosaurs, characterized by the predominance of hadrosaurid dinosaurs and the lack of rhabdodontids and nodosaurids (Le Loeuff et al., 1994; Vila et al., 2016; Fondevilla et al., 2019), reinforcing the idea of a late Maastrichtian age for MPZ 2019/264.

TABLE 1. Main measurements of MPZ 2019/264. The measurements with an asterisk are estimated or represent just the preserved bone.

Measurement	Description of the measure	Length
M1	Maximum length	4.64 cm*
M2	Maximum height	3.23 cm*
M3	Cranial width	2.92 cm*
M4	Caudal width	3.17 cm*
M5	Distance between articular surfaces	4.35 cm
M6	Length of the centrum (ventral view)	4.57 cm*
M7	Length of the neural arch (Distance between the borders of the neural canal) (dorsal view)	4.34 cm
M8	Height of cranial articular surface	0.23 cm
M9	Width of cranial articular surface	1.33 cm
M10	Height of caudal articular surface	1.61 cm*
M11	Width of caudal articular surface (dorsal margin)	1.42 cm
M12	Width of caudal articular surface (narrowest part)	0.9 cm
M13	Length of the ventral keel	1.19* cm
M14	Cranial height of the neural canal	1.02 cm
M15	Cranial width of the neural canal	1.07 cm
M16	Caudal height of the neural canal	1.4 cm
M17	Caudal width of the neural canal	1.76 cm
M18	Width of the dorsal spine	0.52 cm
M19	Length of dorsal spine	1.66 cm*
M20	Distance between postzygapophyses (between their middle point)	2.64 cm
M6/M8	Relation between centrum length and dorsoventral height of the cranial surface (Cau, 2018: character 222)	19.8

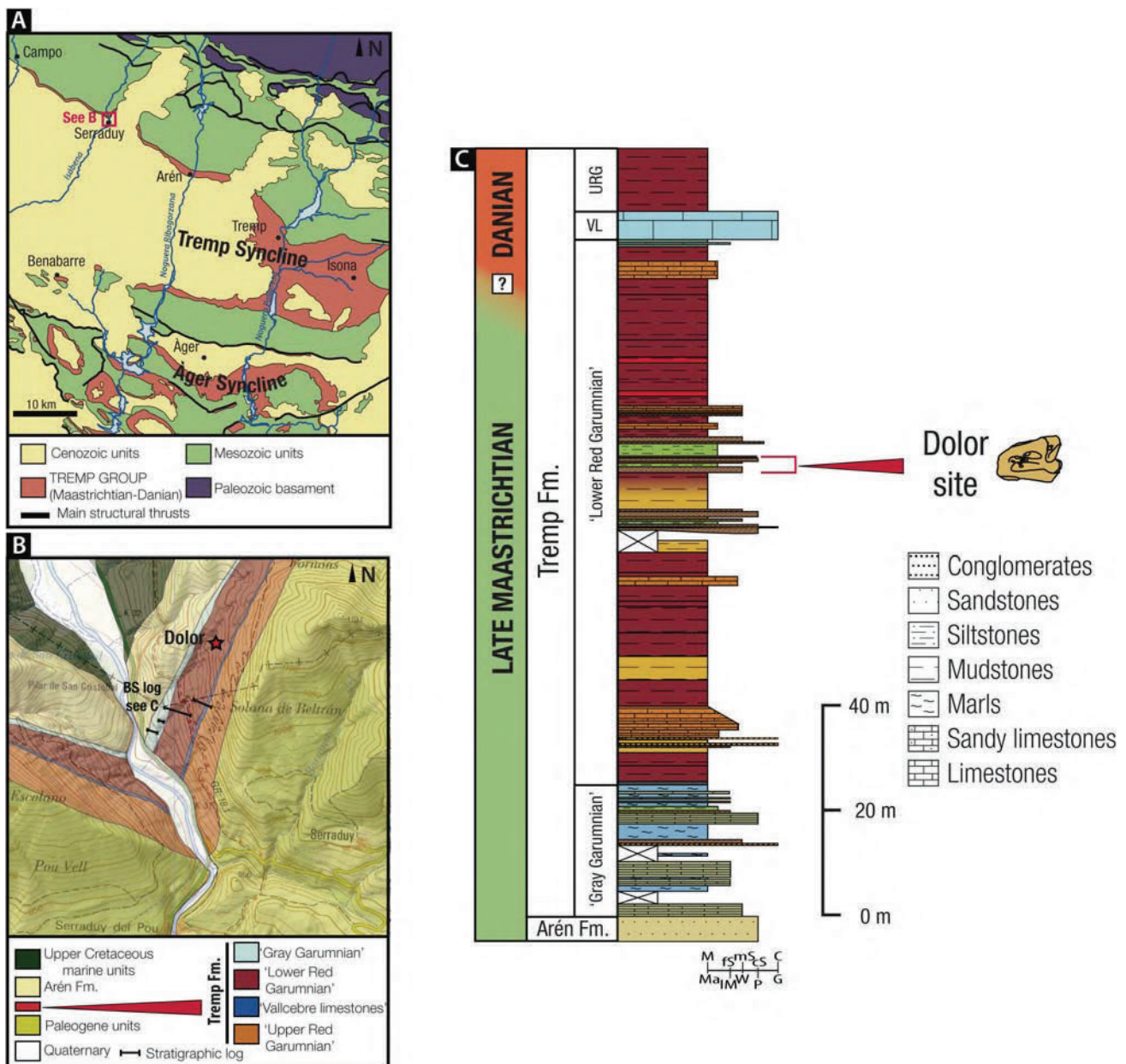


FIGURE 3. Geographic and geological context of the Dolor site. **A**, regional view of the Tremp and Àger synclines in the South-Central Pyrenees (modified from López-Martínez and Vicens, 2012); **B**, local geological map of the surroundings of the town of Serraduy, showing the location of the Amor site (base map modified from Instituto Geográfico Nacional (IGN)); **C**, Stratigraphic log of the Tremp Fm. in the Serraduy outcrops (Barranco Serraduy log), with the stratigraphic position of the Dolor site. **Abbreviations:** VL, Vallcebre limestones; URG, Upper Red Garumnian. **Lithology and grain size chart, upper line (siliciclastic):** C, conglomerate; cS, coarse sandstone; fS, fine sandstone; M, mudstone; mS, medium sandstone. **Lower line (carboantes):** G, grainstone; IM, mudstone; Ma, marl; P, packstone; W, wackstone.

## SYSTEMATIC PALEONTOLOGY

Avialae Gauthier, 1986  
 Ornithothoraces Chiappe, 1995  
 Ornithuromorpha Chiappe, 2002

## DESCRIPTION

MPZ 2019/264 is an isolated cervical vertebra, which is not deformed and moderately well preserved (Fig. 4). It shows

some bone modifications due to taphonomic effects, such as a low stage of weathering (stage 1, Behrensmeyer, 1978) and a low-to-medium stage of abrasion (stage 1–2; Fiorillo, 1988). It lacks the caudal articular surface, the prezygapophysis, and part of the transverse processes. Some small specific areas show a heavily pneumatized inner bone tissue exposed by the effect of abrasion.

The centrum is craniocaudally elongated (Cau, 2018, character 222:1), with the cranial articular surface dorsoventrally shorter. The mediolateral width of the cranial and caudal articular

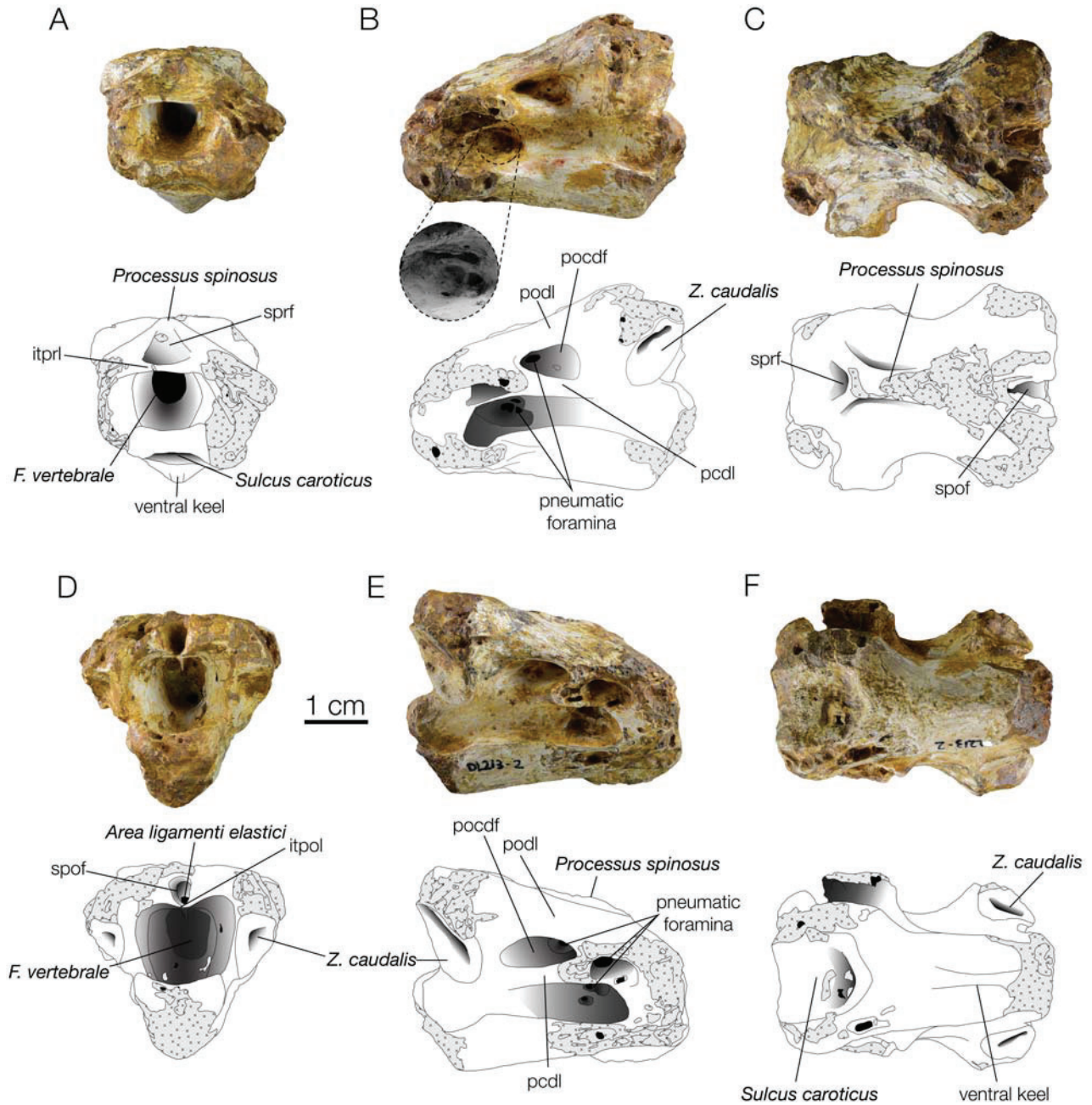


FIGURE 4. MPZ 2019/264. Cervical vertebra from the Dolor site (Serraduy, NE Spain). **A**, cranial view; **B**, right lateral view, with a detailed view of the pneumatic foramen; **C**, dorsal view; **D**, caudal view; **E**, left lateral view; **F**, ventral view. Each photograph has a schematic drawing with the main osteological elements pointed out. Gray texture identifies eroded or broken areas. **Abbreviations:** **itpol**, interpostzygapophyseal lamina; **itprl**, interprezygapophyseal lamina; **pcdl**, posterior centrodiapophyseal lamina; **pocdf**, postzygapophyseal centrodiapophyseal fossa; **podl**, postzygodiapophyseal lamina; **sprf**, spinoprezygapophyseal fossa; **spof**, spinopostzygapophyseal fossa. Scale bar equals 1 cm.

surfaces are similar (Table 1). In ventral view, the centrum shows a smooth ventral medial keel (Cau, 2018, character 207:1; Wang et al., 2020, character 54:1) in its caudal section, which gradually disappears cranially towards the sulcus caroticus (Fig. 4A, F). The caudal part of the ventral surface of the centrum is connected with the cranial part through a craniodorsally inclined triangular facet (Fig. 4F). In ventral view, the cranial area of the centrum possesses a smooth wide medial depression or sulcus caroticus, which is laterally limited by two ridges or prominences (Cau, 2018, character 210:1) (Fig. 4A, F). These ridges indicate

the presence of carotid processes (processi carotici) (Cau, 2018, character 520:1; Wang et al., 2020, character 52:1) that would be located at the lateroventral margins of the cranial region of the centrum; however, they are not preserved. In lateral view, the centrum shows on both lateral sides an elongated groove that is craniodorsally oriented (Fig. 4B, E), which, together with the ventral keel, gives the centrum an inverted-arrow-shaped section in caudal view (Fig. 4D). On both lateral sides of the cranial half of the centrum, there is a pneumatic foramen (pleurocoel), divided into two subforamina by a bone

septum (Wang et al., 2020, character 50:0) (Fig. 4B). The subforamina would be partially covered by the ansae costotransversariae, but they are also not preserved. Thus, it is impossible to determine the size and the position of the transverse foramina (foramina transversarium). However, we can infer that they would be situated far from the centrum, as the part of the transverse processes that is preserved exceeds the width of the centrum (Fig. 4A). Each transverse foramen would also be connected with the inner part of the neural arch through a pneumatic foramen, which is situated in a slightly anterior position just above the foramina of the centrum (Fig. 4E). The caudal articular surface (facies articularis caudalis) is almost completely eroded, except for its dorsal margin (Fig. 4D). This dorsal margin extends more posteriorly than the caudal margin of the postzygapophyses (Cau, 2018, character 782:1, character 1083:0) (Fig. 4B, E, F) (Table 1). This latter feature, along with the shape of the cranial articular surface (facies articularis cranialis), which is narrow, concave transversely, convex dorsoventrally, and with concave dorsal and ventral margins (Figs. 4A and 5F), points to a well-developed, heterocoelous (i.e. saddle-shaped) articulation. Although most of the morphology of the caudal articular face is unknown, the lateromedially convex shape (Fig. 4B, D, E) of the preserved dorsal margin would also suggest a heterocoelous articulation, with a transversely convex and dorsoventrally concave articular surface (Cau, 2018, character 684:1; Wang et al., 2020, character 51:1&2).

The caudal aperture of the neural canal (foramen vertebrae) is bigger than the cranial one (Fig. 4A, D) (Table 1). There is also a thin inner medial keel in the dorsal roof of the caudal region of the neural canal (Fig. 4D). The neural arch is lateromedially wider than it is dorsoventrally high. In lateral view, its dorsal surface is tilted and faces dorsocranially, as well as the neural canal (foramen vertebrae) (Figs. 4B, E, 5F). It has a pneumatic, dorsoventrally compressed, oval foramen in the middle part of each lateral side (Fig. 4B, E), that is enclosed within the postzygapophyseal centrodiapophyseal fossa (podcf, sensu Wilson et al., 2011). This fossa is bounded dorsally by a well-marked, craniolaterally oriented postzygodiapophyseal lamina (podl) (Cau, 2018; character 848:1) and ventrally by a posterior centrodiapophyseal lamina (pcdl) (Fig. 4B, E). This latter lamina is craniolaterally directed and does not face ventrally (Cau, 2018, character 1424:1). The prezygapophyses (zygapophysis cranialis) are not preserved (Fig. 4A); however, they would be situated laterally to the lateral sides of the centrum, since they are not in the well-preserved craniomedial portion of the arch (Cau, 2018, character 216:1). The postzygapophyses (zygapophysis caudalis) are elliptical and craniocaudally elongated, and are situated near the base of the neural arch (Fig. 4B, D, E). Their articular facets are slightly concave, lateroventrally oriented and subvertical, oriented at an angle of about 70°, with respect to the horizontal plane. Although the dorsal margins of the postzygapophyses are not well preserved, they seem relatively flat, without any kind of bump-like protuberance, suggesting that they lack well-developed epipophyses (torus dorsalis) (Fig. 4C, D, E) (Cau, 2018, character 208:0; Wang et al., 2020, character 53:1). A horizontal, interpostzygapophyseal lamina (itpol) (Fig. 4D) (Cau, 2018, character 1162:1) joins both postzygapophyses medially. The neural spine (processus spinosus) is craniocaudally elongated, being slightly less than half the length of the neural arch (Cau, 2018, character 211:1) (Table 1), and situated in its middle part (Cau, 2018, character 213:0) (Fig. 4C). Although the distalmost part of its dorsal margin is not preserved, the neural spine shows a slight vertical development (Cau, 2018, character 212:0) (Fig. 4A, B, E). Just ahead of the cranial margin of the spine, there is a shallow depression, which corresponds to the spinoprezygapophyseal fossa (sprf) (Fig. 4A, C). In caudal view, just below the base of the spine and above the

neural canal, there is a lateromedially narrow but dorsoventrally deep fossa, which would correspond to the spinopostzygapophyseal fossa (spof). Within this fossa, there is a tiny foramen (Fig. 4D), corresponding to the insertion of the elastic interlaminar ligament (area ligamenti elastici).

The CT-scan images of MPZ 2019/264 reveal its inner pneumatic system (Fig. 5). They show that both centrum and neural arch are strongly pneumatized, with an asymmetric pattern of distribution of the camerae. Its pneumatic system could be described as ‘camellate’ (sensu Wedel et al., 2000), as it is constituted by numerous small and irregular chambers or camellae separated by thin bone walls. This system is only connected with the exterior through the six pneumatic foramina or pleurocoels (three per side) (Figs. 4B, E, 5). An extended description of the inner pneumatic structure of the vertebra can be found in Supplemental Data 2.

Determining the position of MPZ 2019/264 in the neck is difficult, given the lack of any associated material. The absence of hypapophyses in its ventral surface rules it out as one of the cranial-most or one of the cervicothoracic vertebrae. The presence of two elongated ridges on the ventral surface of the centrum, which would support the carotid processes, may indicate an intermediate position in the neck. Rauhut (2003) notes the presence of a ventral keel in the cranial cervical vertebrae of several dinosaurs, including theropods. For all these reasons, we situate MPZ 2019/264 in the cranial middle part of the neck. In addition, the spacing between the two ventral ridges and the shape of the cranial articulation of the centrum (thin dorsoventrally and elongated transversely) may indicate that the vertebra was capable of dorsal bending and limited ventral bending. This supports the notion that this vertebra was situated at a transitional point between section I and II of the neck (see Boas, 1929; Tambussi et al., 2012), again suggesting a middle-cranial position. Recently, Terray et al. (2020) have proposed a modular structure for the neck of birds, differentiating nine different morphofunctional modules. MPZ/2019/264 shares features with module 2 and module 7 and fits better (despite some differences) within module 7. This module is characterized by vertebrae with an elongated centrum, small neural spine, well-marked sulcus caroticus and ventrolaterally oriented postzygapophyses, which do not project further than the caudal margin of the centrum. Module 7 vertebrae are specific to long-necked birds, and usually occupy posterior positions, but they can also occupy anterior to medium positions, as is the case in *Struthio* (see Terray et al., 2020).

## CLADISTIC ANALYSIS

To test the affinity of MPZ 2019/264 within Avialae, it was included in an extensive matrix comprising a sample of all major pan-avian clades (Cau, 2018). Our Analysis A1 resulted in 21,624 MPTs of 6,795 steps (consistency index of 0.244; retention index of 0.563). The general topology of the consensus tree (Fig. 6A) is the same as that originally recovered by Cau (2018; see Supplemental Figure 1 for the full consensus tree), although the addition of MPZ 2019/264 has resulted in the collapse of the clade Ornithothoraces. MPZ 2019/264 is recovered as a sister taxon of *Piscivoravis*, an Early Cretaceous ornithuromorph, closely related to the Carinatae (Zhou et al., 2014; Cau, 2018), based on the relatively long centrum (A1 character 222:1), a condition shared with some Neornithes such as *Meleagris* (turkey), but also with some dromaeosaurs such as *Fukuivenator* and *Halszkaraptor*. Nevertheless, its position within Ornithothoraces is supported by the presence of a saddle-shaped articular surface, a character exclusive to this clade and shared with most of its members (A1 character 648:1). The presence of a ventral keel on the centrum (A1 character 207:1) also supports its inclusion within Ornithothoraces.

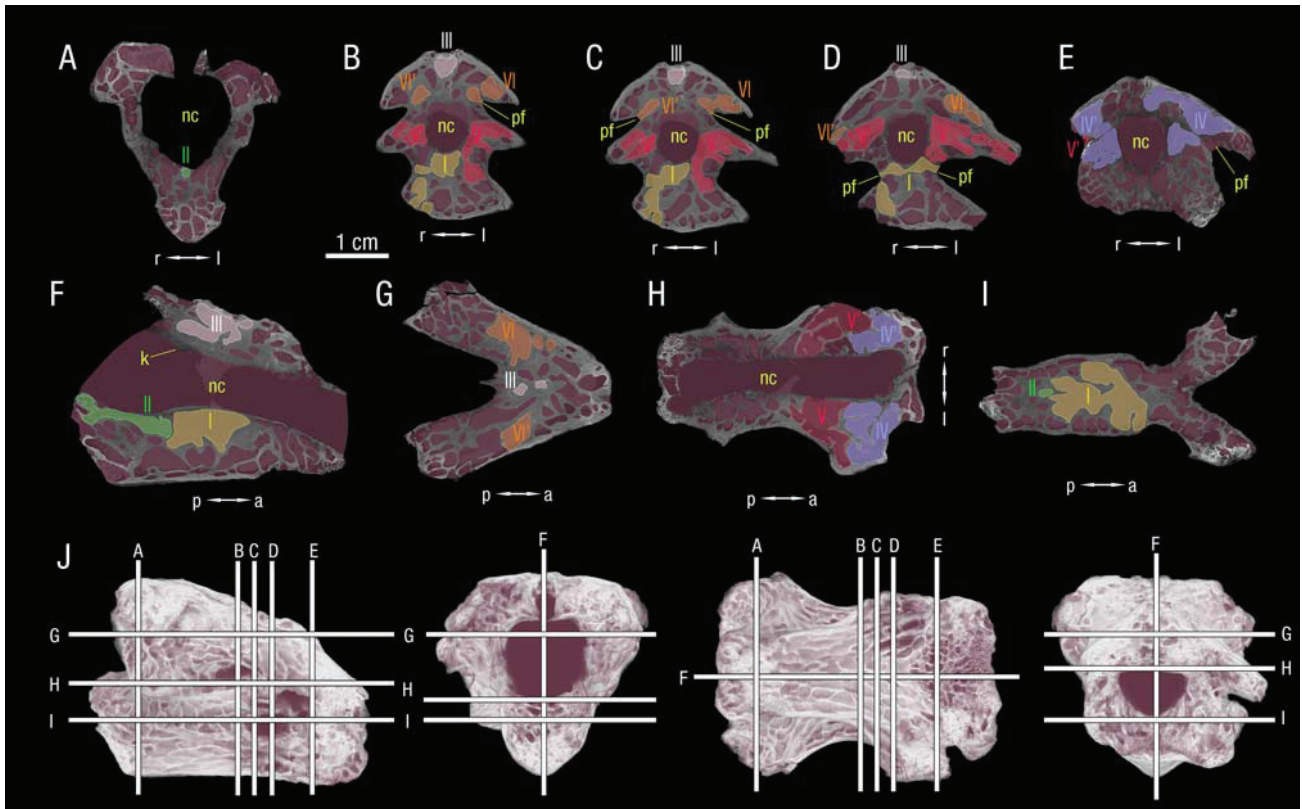


FIGURE 5. CT-scan cross-sections of MPZ 2019/264. **Abbreviations:** a, anterior; k, keel; l, left; nc, neural canal; p, posterior; pf, pneumatic foramen; r, right.

To further specify the position of MPZ 2019/264 within Ornithothoraces, a second analysis (A2) was carried out, using the dataset of Wang et al. (2020), which focuses on Mesozoic birds. This resulted in 4,872 trees of 1,271 steps (consistency index of 0.306; retention index of 0.665). The consensus tree (Fig. 6) is identical to that recovered by Wang et al. (2020). MPZ 2019/264 is recovered as an ornithuromorph ornithothoraces, forming a clade with *Patagopteryx*, *Apsaravis* and *Vorona*, based on certain derived conditions shared with *Apsaravis*, such as the presence of pneumatic foramina at the level of the parapophysis-diapophysis (A2, character 50:0), and heterocoelous articular surfaces (A2, character 51:1–2). The placement within Ornithuromorpha is nonetheless well supported on the basis of the presence of a prominent carotid process, a synapomorphy of this clade (A2, character 52:1).

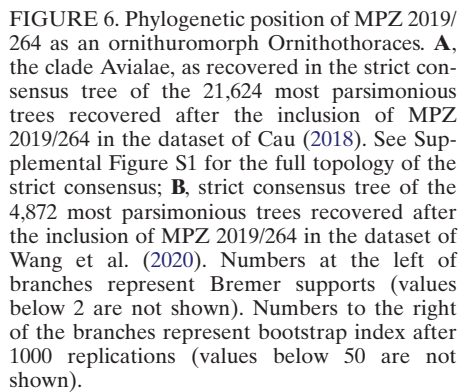
## DISCUSSION

### Comparisons and Taxonomic Attribution

The key feature of MPZ 2019/264 with relevant phylogenetic implications is its heterocoelous vertebral articulation (A1, character 684:1; A2, character 51:1&2). This characteristic has been recognized as an avialan character (Marsh, 1879; Martin, 1991), mainly in the clade Ornithuromorpha (Clarke and Norell, 2002; Clarke et al., 2006; O'Connor et al., 2011), but also in a few enantiornitheans such as *Vescornis* (Zhang et al., 2005), *Pengornis* (Zhou et al., 2008) and the enantiornithean LP-4450-IEI from El Montsec (Sanz et al., 1997). A few paravian theropods, such as dromaeosaurids (e.g., *Buitreraptor*) and troodontids (e.g., *Mei*), also show a slight, incipient saddle-shaped

articulation (Xu and Norell, 2004; Novas et al., 2018), but not as developed as in MPZ 2019/264. On the other hand, the cervical vertebra from Beranuy shares some characters with these paravian theropods, such as the presence of lateral pneumatic excavations (e.g., Makovicky and Sues, 1998; Makovicky and Norell, 2004; Sues and Averianov, 2014) (Fig. 7B2), and the presence of a camellate inner pneumatic system. This system is present in most coelurosaurs (Benson et al., 2012), but in MPZ 2019/264 it is clearly more complex than those in most non-avian theropods, and more similar to that of modern birds (compare for example *Archaeornithomimus* and *Catharacta*) (Gutzwiler et al., 2013; Watanabe et al., 2015). Another feature shared with troodontids and dromaeosaurids is the presence of carotid processes on the ventral surface (Makovicky and Norell, 2004; Makovicky et al., 2005) (A1, character 520:1; A2, character 52:1). Unlike these two clades, MPZ 2019/264 lacks well-developed epiphyses above the postzygapophysis, it is more elongated craniocaudally (Fig. 7A1, B1), and its caudal articular face would project far beyond the postzygapophyses (Fig. 7A2, B2).

The systematic attribution of MPZ 2019/264 within Avialae is well supported even though it is an isolated element, as some of its characters are decisive. First is the above-mentioned well-developed heterocoelous articulation, which would situate it within Ornithothoraces (Ornithuromorpha + Enantiornithes), and most probably within Ornithuromorpha (O'Connor et al., 2011). On the other hand, the presence of well-marked lateral pneumatic foramina (pleurocoels) in the centrum (A2, character 50:0) is a character that is present within Ornithuromorpha and Ornithurae, but not in Enantiornithes (Chiappe and Walker, 2002; O'Connor et al., 2011). In most neornitheans the



Comparisons with the sister clade of Enantiornithes, Ornithuromorpha, should begin with the cervical vertebra MC-MN 478 (Fig. 7C), referred to *Gargantuavis* (Buffetaut and Angst, 2013). This vertebra was identified as belonging to a giant bird that would be included within Ornithuromorpha and closely

For comparison, other Late Cretaceous birds of relatively 'large' size, with preserved cervical vertebrae include *Patagopteryx* (Alvarenga and Bonaparte, 1992; Chiappe, 2002), a non-flying hen-sized ornithuromorph bird from Argentina. The anterior cervical vertebrae of *Patagopteryx* (MACN-N-03)

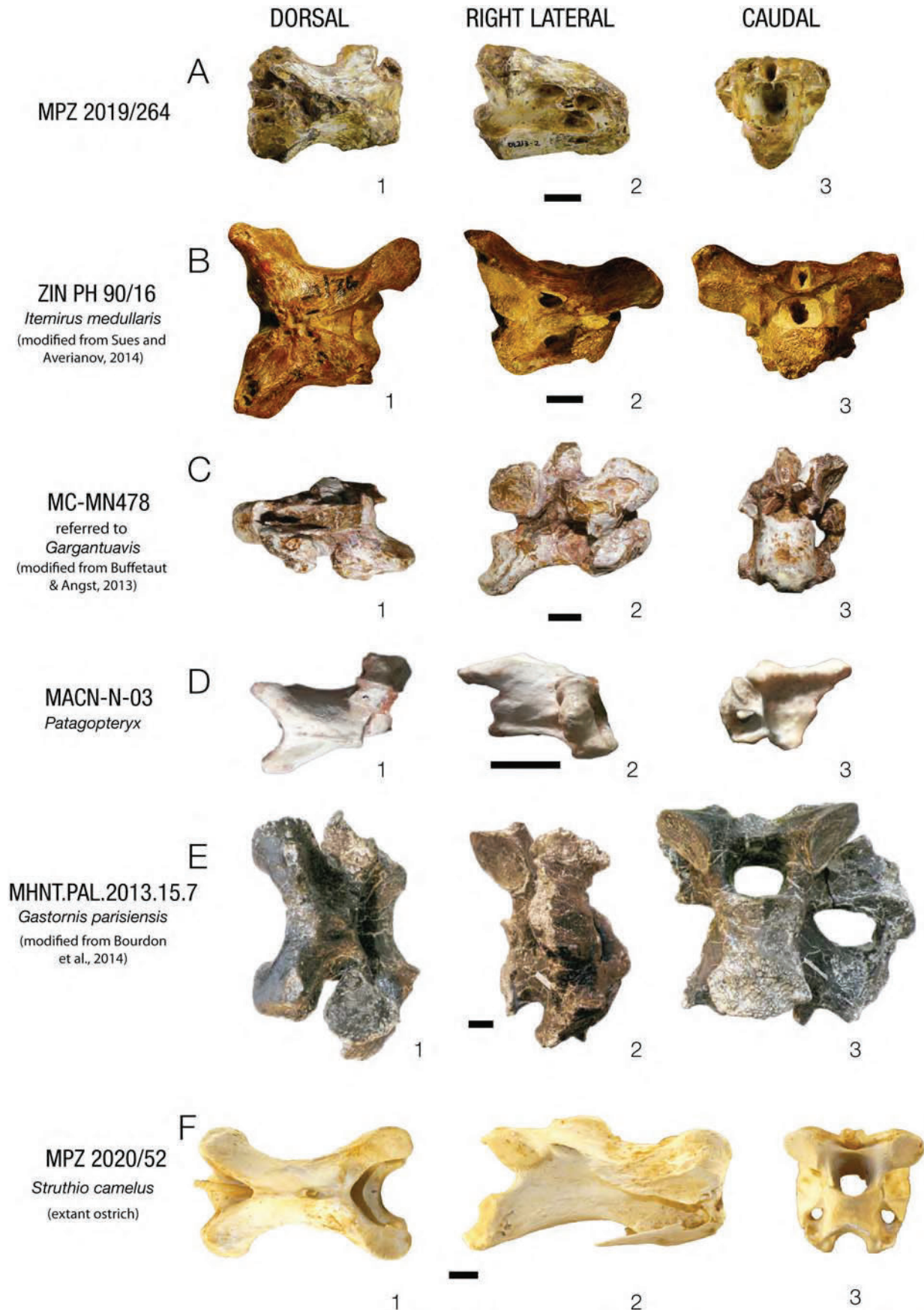


FIGURE 7. Comparative plate of **A**, MPZ 2019/264 with several cervical vertebrae of maniraptoran theropods in dorsal (1), right lateral (2) and caudal (3) views; **B**, ZIN PH 90/16, *Itemirus medullaris*. Dromaeosauridae (modified from Sues and Averianov, 2014) (mirrored); **C**, MC-MN478, referred to *Gargantuavis*. Ornithurae? (modified from Buffetaut and Angst, 2013); **D**, MACN-N-03, *Patagopteryx deferrariisi*. Ornithuromorpha (mirrored); **E**, MHNT.PAL.2013.15.7, *Gastornis parisiensis*. Gastornithidae (modified from Bourdon et al., 2014); **F**, MPZ 2020/52 *Struthio camelus*. Palaeognathae. Scale bar equals 1 cm.

(Fig. 7D) are smaller in size, lack pneumatic foramina in their centrum or neural arch, have tiny epipophyses above the postzygapophyses (Fig. 7D2, D3), and the centrum does not project beyond the postzygapophyses (Fig. 7D2). On the other hand, MACN-N-03 and MPZ 2019/264 share the elongated shape, the low and long neural spine, and their well-developed heterocoelous articulation. Other ornithuromorphs, such as *Longicrusavis* (O'Connor et al., 2010) and *Piscivoravis* (Zhou et al., 2014), have elongated anterior-middle centra (A1, character 222:1), heterocoelous articulation, a keeled ventral surface, long and low neural spines (A1, character 212:0), and they lack pneumatic foramina. The ornithurine *Apsaravis* (Clarke and Norell, 2002) shares some characteristics with MPZ 2019/264, such as the heterocoelous articulation and the presence of pleurocoels in the centra, in a caudal position relative to the diapophyses, as well as the ventral keel and the absence of epipophyses.

MPZ 2019/264 also differs from the cervical vertebrae of Hesperornithiformes, the large Late Cretaceous diving ornithurines. Hesperornithiforms such as *Hesperornis* and *Chupkaornis* (e.g., Marsh, 1880; Tanaka et al., 2018) possess more craniocaudally elongated heterocoelous cervical vertebrae, without pneumaticity, but with the postzygapophyses projecting further than the centrum, and epipophyses above the postzygapophyses.

MPZ 2019/264 is not similar to the giant flightless birds present in Europe during the Paleogene either. The cervical vertebrae of neornithine giant birds, gastornithids (Bourdon et al., 2014), and phorusrhacids (Alvarenga et al., 2011; Tambussi et al., 2012) are clearly more robust and bigger than MPZ 2019/264 (Fig. 7E). The cervical vertebrae of gastornithids, such as *Gastornis*, are craniocaudally compressed (Fig. 7E1, E2), they lack pneumatic foramina, the caudal articular surface does not project further than the postzygapophyses, and they have marked epipophyses. The cervical vertebrae of phorusrhacids, such as *Andalgalornis* or *Paraphysornis*, do not show pneumatic openings; their postzygapophyses extend further than the caudal articular surface and they generally have a bony bridge between the transverse processes and the middle part of the neural arch. Finally, comparison with Paleogene palaeognaths is difficult since their remains are scarce. Sometimes there are no cervical vertebrae preserved, as is the case with *Remiornis* (Martin, 1992; Smith et al., 2014), and sometimes they are preserved in two-dimensional slabs, as is the case with *Palaeotis* (Houde and Haubold, 1987; Peters, 1988). Comparison of MPZ 2019/264 with modern palaeognaths (e.g., *Struthio*) (Fig. 7F) shows that they share the absence of epipophyses above the postzygapophyses, and have a low, long neural spine (Fig. 7F1, F2), and a caudal articular surface that projects further than the postzygapophyses. On the other hand, palaeognaths have more elongated vertebrae, generally without pneumatic foramina, but when present, they are very reduced (Apostolaki et al., 2015).

Even though the affinities of *Gargantuavis* within Ornithuromorpha have been questioned on the basis of the pelvic material (Mayr et al., 2020), MC-MN 478, the vertebra assigned to *Gargantuavis* from Montpelo-Nord (Cruzy, France), clearly has avialan features (Buffetaut et al., 2013; 2020). Whether or not the Montpelo-Nord vertebra belongs to *Gargantuavis*, there is no doubt of its avialan affinities, it being more derived than the avialan vertebra MPZ 2019/264. This suggests that at least two different taxa of large-sized birds inhabited the Ibero-Armorican Island during the Late Cretaceous, although it seems they did not coexist at the same time (Fig. 1B). Due to the scarceness and fragmentary nature of most of these remains, establishing their phylogenetic position is complicated and, until new fossils are discovered, the degree of kinship between them will remain unknown. Further research should exercise caution in the assignment of new giant bird material from the Late Cretaceous of the Ibero-Armorican Island.

It is also important to note that in both cladistics analyses carried out, bootstrap values are low (Fig. 6). The inclusion of MPZ 2019/264 in both datasets does have an impact on the general topology of the tree and does not significantly lower the already low bootstrap values and Bremer indexes recovered for both consensus topologies (Cau, 2018; Wang et al., 2020). This is due to the scarce number of characters of MPZ 2019/264 scored in both matrixes (1.8% of the overall number in both analyses). In any case, we consider our consensus topologies informative, but more complete material from this putative ornithuromorph and related taxa would help to refine its phylogenetic position and the robustness of the phylogenetic hypothesis.

### Paleoecological Implications

The Beranuy vertebra (MPZ 2019/264) points to the presence of a medium-sized (cassowary-sized) to big bird, with a slender and probably long neck, as indicated by the elongated shape of the vertebra. This character is unlike the craniocaudally compressed vertebra and more robust necks present in Cenozoic giant birds such as *Gastornis* and *Andalgalornis* (e.g., Tambussi et al., 2012; Bourdon et al., 2014). The high degree of pneumatization of MPZ 2019/264 and the presence of pneumatic foramina connected with inner camellae is unambiguous proof of the presence of an avian pulmonary system with air sacs (O'Connor, 2006). It also suggests that at least all the cervical vertebrae and the anterior dorsal vertebrae were pneumatic too (Benson et al., 2012). If we extrapolate from the patterns of pneumaticity in extant birds, this animal would have at least an 'extended' pattern (O'Connor, 2009), with pneumaticity extending through the axial skeleton, the girdles and the proximal appendicular elements.

The ecological role of this giant bird is difficult to ascertain given the limitations of the anatomical information and the absence of direct evidence of its feeding or locomotion habits, and any correlation with extant birds must be very cautious. Extant analogs of giant flightless terrestrial birds are mainly palaeognaths and show a wide range of feeding habits, such the herbivorous *Struthio* (Winkler et al., 2020b), the omnivorous *Rhea* (Winkler et al., 2020c), and the frugivorous *Casuaris* (Winkler et al., 2020b) (Fig. 1A). However, there are also neognaths that could be considered giant flightless birds, such as the megapode *Alectura* or the rail *Porphyrio hochstetteri*, both being omnivorous (Elliot and Kirwan, 2020; del Hoyo et al., 2020). Extinct giant flightless birds, such as Aepyornithiformes (Tovondrafale et al., 2014), Dinornithiformes (Wood et al., 2013), Dromornithidae (Murray and Vickers-Rich, 2004) and Gastornithidae (Angst et al., 2014b) have been identified as herbivores. The only exception to this tendency is Phorusrhacidae, which were carnivorous (Degrange et al., 2010) (Fig. 1A). We cannot rule out neither that this bird was able to fly or was adapted to aquatic life, since there are examples of giant flying birds such as the pelagornithids (Ksepka, 2014) and giant aquatic birds such as *Hesperornis* (Marsh, 1880) or penguins such as *Anthropornis* (Wiman, 1905) (Fig. 1A). Nevertheless, most extant aquatic and diving birds lack pneumaticity in their postcranial skeleton (O'Connor, 2009), as does *Hesperornis* (Marsh, 1880). It thus also seems implausible that the Beranuy bird was adapted to an aquatic lifestyle.

In addition to inferences from extant and extinct analogs, the context of the Beranuy bird within the late Maastrichtian biota must be considered. Vertebrate communities in the southern Pyrenees area in the late Maastrichtian would include several bigger predators such as abelisaurid theropods (e.g., cf. *Arcovenator*), maniraptoran theropods (e.g., dromaeosaurids and troodontids) (Torices et al., 2015; Fondevilla et al., 2019

and references therein), and several crocodylomorphs (Puértolas-Pascual et al., 2016; Blanco et al., 2020; and references therein). The Beranuy bird also coexisted with large-sized herbivores, including at least two types of titanosaur sauropods and diverse hadrosaurid ornithopods (Fondevilla et al., 2019 and references therein). Among the herbivorous dinosaurs, there were some small-sized forms (Blanco et al., 2015; Company et al., 2015). And there were also large-sized flying animals, since azhdarchid pterosaurs inhabited the Ibero-Armorican Island during the late Maastrichtian (Buffetaut et al., 1997; Dalla Vecchia et al., 2013). Thus, it can be inferred that putative competitors would not have been lacking, whatever ecological role the Beranuy bird may have had (e.g., terrestrial/flying, carnivorous/herbivorous/omnivorous). In any case, the fossil from Beranuy provides direct evidence that giant birds were part of the paleocommunities of the late Maastrichtian, which is a new and interesting finding given its proximity to the biotic crisis of K/Pg. In fact, this new report reinforces the idea that rich and diverse vertebrate assemblages were present through until the latest Mesozoic in the Ibero-Armorican Island (e.g., Vila et al., 2016). Its large size is difficult to explain given the coexistence of several predators in the same ecosystem, since birds tend to become flightless and bigger in islands that are predator-free (Mayr, 2017). One solution to this question is that the bird perhaps occupied a niche or had habitat preferences out of the reach of most predators, as has been proposed for *Patagopteryx* (Chiappe, 2002), and was not competing directly with other herbivores.

It is important to underscore that *Gargantuavis* and the Beranuy bird did not coexist at the same time, since *Gargantuavis* only inhabited the Ibero-Armorican Island from the upper Campanian to lower Maastrichtian. *Gargantuavis* seems to have disappeared during the faunal turnover that took place at the end of the early Maastrichtian (Le Loeuff et al., 1994; Vila et al., 2016; Fondevilla et al., 2019), and it may have been replaced ecologically by the Beranuy taxon during the late Maastrichtian. Only further fossil material from this new taxon will help resolve such unknowns regarding the paleoecology of this extinct giant bird.

## CONCLUSIONS

The vertebra MPZ 2019/264 was found at the ‘Dolor’ site in the southern Pyrenees (municipality of Beranuy, Huesca province, Spain) in uppermost Maastrichtian deposits within Chron C29r (66.3–66.052 Ma). It represents the first evidence of a giant bird from the late Maastrichtian of the Ibero-Armorican Island. This vertebra belongs to a cassowary-sized bird, and its most notable character is the presence of a well-developed heterocoelous articulation, which differentiates it from paravian theropods already recognized in the island. Other characters such as the lateral pneumatic foramina and the low neural spine distinguish MPZ 2019/264 from MC-MN 478 (the vertebra from Cruzy, France), which has been assigned to the other giant bird that inhabited the European archipelago, *Gargantuavis philoinos*. Moreover, these taxa were not contemporary, *Gargantuavis* being limited to the late Campanian–early Maastrichtian, and the Beranuy bird to the latest Maastrichtian. Given all these comparisons and the chronological record, we can conclude that MPZ 2019/264 belongs to a new taxon of giant bird, whose phylogenetic affinities are still uncertain due to the scarcity of the fossil material, but which can clearly be included within the clade Ornithuromorpha and probably positioned outside Ornithurae. Both cladistic analyses that were performed situate MPZ 2019/264 within the clade Ornithuromorpha and are concordant with the comparisons. Nevertheless, these results should be taken with caution

given the fragmentary condition of these taxa. This finding represents the youngest evidence of a Mesozoic bird in Europe to date, and suggests that a giant bird taxon formed part of the biological communities that inhabited the Ibero-Armorican Island during the last hundreds of thousands of years before the K/Pg extinction event. New findings would allow more to be known about the phylogeny, systematics and paleobiology of this enigmatic extinct bird.

## ACKNOWLEDGMENTS

This research forms part of the project CGL2017-85038-P, subsidized by the Spanish Ministry of Science and Innovation, the European Regional Development Fund, the Government of Aragón (Grupo Aragosaurus: Recursos geológicos y Paleomambientes), the project PTDC/CTA-PAL/31656/2017, subsidized by the Fundação para a Ciência e a Tecnologia, and the project UIDB/04035/2020, subsidized by GeoBioTec. M.P-P is supported by a PhD grant from the Spanish Ministry of Education, Culture and Sport (Grant Number FPU 16/03064). M.M-A and E.P-P are supported by postdoctoral grants funded by the Fundação para a Ciência e a Tecnologia, Portugal (Grant numbers SFRH/BPD/113130/2015, SFRH/BPD/116759/2016, PTDC/CTA-PAL/31656/2017).

The Government of Aragón (Dirección General de Patrimonio Cultural) funded the fieldwork campaign during which MPZ 2019/264 was found (DGA Exp231\_08-2009). We thank E. Buffetaut and M. Ezcurra for granting access, respectively, to the Cruzy vertebra (MC-MN 478) at the Musée de l'Association Culturelle, Archéologique et Paléontologique de l'Ouest Biterrois, (Cruzy, Hérault, France) and to the holotype of *Patagopteryx* (MACN-N-03) at the Museo Argentino de Ciencias Naturales (Buenos Aires, Argentina). We want to acknowledge Paleoymás for the preparation of the fossil, the technician B. Notario (CENIEH) for her help with the CT-scanning, and I. Pérez for her help with the photography of MPZ 2019/264. R. Glasgow reviewed the text in English. We thank E. Buffetaut and an anonymous reviewer for their valuable comments on the original manuscript, that have helped to improve the text. We also thank L. Zanno for her editorial work.

## ORCID

Manuel Pérez-Pueyo  <http://orcid.org/0000-0002-6792-1563>  
 Eduardo Puértolas-Pascual  <http://orcid.org/0000-0003-0759-7105>  
 Miguel Moreno-Azanza  <http://orcid.org/0000-0002-7210-1033>  
 Penélope Cruzado-Caballero  <http://orcid.org/0000-0002-5819-8254>  
 José Manuel Gasca  <http://orcid.org/0000-0002-8427-6199>  
 Carmen Núñez-Lahuerta  <http://orcid.org/0000-0002-2882-6061>  
 José Ignacio Canudo  <http://orcid.org/0000-0003-1732-9155>

## LITERATURE CITED

- Alvarenga, H. M. F., and J. F. Bonaparte. 1992. A new flightless land bird from the Cretaceous of Patagonia; pp. 51–64 in K. E. Campbell (ed.), *Papers in Avian Paleontology, Honoring Pierce Brodkorb*. Science Series 36. Natural History Museum of Los Angeles County, Los Angeles.
- Alvarenga, H. M. F., L. Chiappe, and S. Bertelli. 2011. Phorusrhacids: the terror birds; pp. 187–208 in G. Dyke, and G. Kaiser (eds.), *Living dinosaurs. The evolutionary history of modern birds*. John Wiley & Sons Ltd, Chichester, West Sussex.
- Angst, D., and E. Buffetaut. 2017. *Paleobiology of Giant Flightless Birds*. ISTE Press – Elsevier, London, 281 pp.
- Angst, D., E. Buffetaut, J. C. Corral, and X. Pereda-Suberbiola. 2017. First record of the Late Cretaceous giant bird *Gargantuavis philoinos* from the Iberian Peninsula. *Annales de Paléontologie* 103:135–139.

- Angst, D., E. Buffetaut, C. Lécuyer, and R. Amiot. 2013. "Terror Birds" (Phorusrhacidae) from the Eocene of Europe imply trans-Tethys dispersal. *PLoS ONE* 8:e80357.
- Angst, D., C. Lécuyer, R. Amiot, E. Buffetaut, F. Fourel, F. Martineau, S. Legendre, A. Abourachid, and A. Herrel. 2014b. Isotopic and anatomical evidence of an herbivorous diet in the Early Tertiary giant bird *Gastornis*. Implications for the structure of Paleocene terrestrial ecosystems. *Naturwissenschaften* 101:313–322.
- Angst, D., E. Buffetaut, C. Lécuyer, R. Amiot, F. Smektala, S. Giner, A. Mechin, P. Mechin, A. Amoros, L. Leroy, M. Guiomar, H. Tong, and A. Martinez. 2014a. Fossil avian eggs from the Palaeogene of southern France: new size estimates and a possible taxonomic identification of the egg-layer. *Geological Magazine* 152:70–79.
- Apostolaki, N. E., E. J. Rayfield, and P. M. Barrett. 2015. Osteological and soft-tissue evidence for pneumatization in the cervical column of the ostrich (*Struthio camelus*) and observations on the vertebral columns of non-volant, semi-volant and semi-aquatic birds. *PLoS One* 10:e0143834.
- Baskin, J. A. 1995. The giant flightless bird *Titanis walleri* (Aves: Phorusrhacidae) from the Pleistocene coastal plain of south Texas. *Journal of Vertebrate Paleontology* 15:842–844.
- Baumel, J. J., and L. M. Witmer. 1993. Osteologia; pp. 45–132 in J. J. Baumel, A. S. King, J. E. Breazile, H. E. Evans and J. C. Vanden Berge (eds.), *Handbook of Avian Anatomy: Nomina Anatomica Avium*. Publications of the Nuttall Ornithological Club, Cambridge, Massachusetts.
- Behrensmeyer, A. K. 1978. Taphonomic and ecologic information from bone weathering. *Paleobiology* 4:150–162.
- Benson, R. B., R. J. Butler, M. T. Carrano, and P. M. O'Connor. 2012. Air-filled postcranial bones in theropod dinosaurs: physiological implications and the 'reptile'-bird transition. *Biological Reviews* 87:168–193.
- Blanco, A., A. Prieto-Márquez, and S. De Esteban-Trivigno. 2015. Diversity of hadrosauroid dinosaurs from the late Cretaceous Ibero-Armorian Island (European Archipelago) assessed from dentary morphology. *Cretaceous Research* 56:447–457.
- Blanco, A., E. Puértolas-Pascual, J. Marmi, B. Moncunill-Solé, S. Llácer, and G.E. Rössner. 2020. Late Cretaceous (Maastrichtian) crocodyliforms from north-eastern Iberia: a first attempt to explain the crocodyliform diversity based on tooth qualitative traits. *Zoological Journal of the Linnean Society* 189:584–617.
- Boas, J. E. V. 1929. Biologisch-anatomische Studien über den Hals der Vögel. Det Kongelige Danske Videnskabernes Selskabs Skrifter, Naturvidenskabelig og Matematisk Afdeling 9:105–222.
- Boev, Z. N., and N. Spassov. 2009. First record of ostriches (Aves, Struthioniformes, Struthionidae) from the late Miocene of Bulgaria with taxonomic and zoogeographic discussion. *Geodiversitas* 31:493–507.
- Bourdon, E., C. Mourer-Chauvire, and Y. Laurent. 2014. The birds (Aves) from the Early Eocene of La Borie, southern France. *Acta Palaeontologica Polonica* 61:175–190.
- Britt, B. B. 1993. Pneumatic postcranial bones in dinosaurs and other archosaurs. Ph.D. Dissertation. University of Calgary, 383 pp.
- Britt, B. B. 1997. Postcranial pneumaticity; pp. 590–593 in P.J. Currie, and K. Padian (eds.), *Encyclopedia of dinosaurs*. Academic Press, San Diego.
- Buffetaut, E., and D. Angst. 2013. New evidence of a giant bird from the Late Cretaceous of France. *Geological Magazine* 150:173–176.
- Buffetaut, E., and D. Angst. 2014. Stratigraphic distribution of large flightless birds in the Palaeogene of Europe and its palaeobiological and palaeogeographical implications. *Earth-Science Reviews* 138:394–408.
- Buffetaut, E., and D. Angst. 2016. Pelvic elements of the giant bird *Gargantuavis* from the Upper Cretaceous of Cruzy (southern France), with remarks on pneumatization. *Cretaceous Research* 66:1–6.
- Buffetaut, E., and D. Angst. 2019. A femur of the Late Cretaceous giant bird *Gargantuavis* from Cruzy (southern France) and its systematic implications. *Palaeovertebrata* 42:e3.
- Buffetaut, E., and D. Angst. 2020. *Gargantuavis* is an insular basal ornithurine: a comment on Mayr et al., 2020, 'A well preserved pelvis from the Maastrichtian of Romania suggests that the enigmatic *Gargantuavis* is neither an ornithurine bird nor an insular endemic'. *Cretaceous Research* 112:104438.
- Buffetaut, E., and J. Le Loeuff. 1998. A new giant ground bird from the Upper Cretaceous of southern France. *Journal of the Geological Society* 155:1–4.
- Buffetaut, E., J. Le Loeuff, P. Mechin, and A. Mechin-Salessy. 1995. A large French Cretaceous bird. *Nature* 377:110.
- Buffetaut, E., D. Angst, P. Mechin, and A. Mechin-Salessy. 2015. New remains of the giant bird *Gargantuavis philoinos* from the Late Cretaceous of Provence (south-eastern France). *Palaeovertebrata* 39:1–6.
- Buffetaut, E., D. Angst, P. Mechin, and A. Mechin-Salessy. 2019. A femur of the giant bird *Gargantuavis* from the Late Cretaceous of Var (south-eastern France). *Carnets natures* 6:47–52.
- Buffetaut, E., Y. Laurent, J. Le Loeuff, and M. Bilotte. 1997. A terminal Cretaceous giant pterosaur from the French Pyrenees. *Geological Magazine* 134:553–556.
- Campbell, K. E., and E. P. Tonni. 1980. A new genus of Teratorn from the Huayquerian of Argentina [Aves: Teratornithidae]. *Contributions in Science-Natural History Museum Los Angeles County* 330:59–68.
- Canudo, J. I. 2018. The collection of type fossils of the Natural Science Museum of the University of Zaragoza (Spain). *Geoheritage* 10:385–392.
- Canudo, J. I., O. Oms, B. Vila, À. Galobart, V. Fondevilla, E. Puértolas-Pascual, A.G. Sellés, P. Cruzado-Caballero, J. Dinarès-Turell, E. Vicens, D. Castanera, J. Company, L. Burrell, R. Estrada, J. Marmi, and A. Blanco. 2016. The upper Maastrichtian dinosaur fossil record from the southern Pyrenees and its contribution to the topic of the Cretaceous–Palaeogene mass extinction event. *Cretaceous Research* 57:540–551.
- Cau, A. 2018. The assembly of the avian body plan: a 160 million year long process. *Bollettino della Società Paleontologica Italiana* 57:1–25.
- Chiappe, L. M. 1995. The phylogenetic position of the Cretaceous birds of Argentina: Enantiornithes and *Patagopteryx deferrariisi*. *Courier Forschungsinstitut Senckenberg* 181:55–63.
- Chiappe, L. M. 2002. Osteology of the flightless *Patagopteryx deferrariisi* from the Late Cretaceous of Patagonia (Argentina); pp. 281–316 in L. M. Chiappe and L. M. Witmer (eds.), *Mesozoic Birds*. University of California Press, Berkeley.
- Chiappe, L. M., and C. A. Walker. 2002. Skeletal morphology and systematics of the Cretaceous Euenantiornithes (Ornithothoraces: Enantiornithes); pp. 240–267 in L. M. Chiappe and L. M. Witmer (eds.), *Mesozoic Birds*. University of California Press, Berkeley.
- Clarke, J. A., and M. A. Norell. 2002. The morphology and phylogenetic position of *Apsaravis ukhaana* from the Late Cretaceous of Mongolia. *American Museum Novitates* 3387:1–46.
- Clarke, J. A., Z. Zhou, and F. Zhang. 2006. Insight into the evolution of avian flight from a new clade of Early Cretaceous ornithurines from China and the morphology of *Yixianornis grabaui*. *Journal of Anatomy* 208:287–308.
- Company, J., P. Cruzado-Caballero, and J. I. Canudo. 2015. Presence of diminutive hadrosaurids (Dinosauria: Ornithomimidae) from the Maastrichtian of the southcentral Pyrenees (Spain). *Journal of Iberian Geology* 41:71–81.
- Corral, J. C., E. L. Pueyo, A. Berreteaga, A. Rodríguez-Pintó, E. Sánchez, and X. Pereda-Suberbiola. 2016. Magnetostratigraphy and lithostratigraphy of the Laño vertebrate-site: implications in the uppermost Cretaceous chronostratigraphy of the Basque-Cantabrian Region. *Cretaceous Research* 57:473–489.
- Cruzado-Caballero, P., E. Puértolas-Pascual, J. I. Canudo, D. Castanera, J. M. Gasca, and M. Moreno-Azanza. 2012. New hadrosaur remains from the Late Maastrichtian of Huesca (NE Spain). *Fundamental. 10th EAVP meeting*. Teruel 20:45–48. (Fundación Conjunto Paleontológico de Teruel-Dinópolis, ed.).
- Csiki, Z., M. Vremir, S. L. Brusatte, and M. A. Norell. 2010. An aberrant island-dwelling theropod dinosaur from the Late Cretaceous of Romania. *Proceedings of the National Academy of Sciences* 107:15357–15361.
- Dalla Vecchia, F. M., V. Riera, O. Oms, J. Dinarès-Turell, R. Gaete, and À. Galobart. 2013. The last pterosaurs: First record from the uppermost Maastrichtian of the Tremp Syncline (Northern Spain). *Acta Geologica Sinica-English Edition* 87:1198–1227.
- Degrange, F. J., C. P. Tambussi, K. Moreno, L. M. Witmer, and S. Wroe. 2010. Mechanical analysis of feeding behavior in the extinct "terror bird" *Andalgalornis steulleti* (Gruiformes: Phorusrhacidae). *PLoS ONE*, 5:e11856.
- Díez-Canseco, D., J. A., Arz, M. I. Benito, M. Díaz-Molina, and I. Arenillas. 2014. Tidal influence in redbeds: A palaeoenvironmental and biochronostratigraphic reconstruction of the Lower Tremp

- Formation (South-Central Pyrenees, Spain) around the Cretaceous/Paleogene boundary. *Sedimentary Geology* 312:31–49.
- Dughi, R., and F. Sirugue. 1962. Distribution verticale des oeufs d'oiseaux fossiles de l'Eocène de Basse-Provence. *Bulletin de la Société Géologique de France* 4:69–78.
- Elliott, A., and G. M. Kirwan. 2020. Australian Brushturkey (*Alectura lathami*), version 1.0. In J. del Hoyo, A. Elliott, J. Sargatal, D. A. Christie, and E. de Juana, (eds.), *Birds of the World* Cornell Lab of Ornithology, Ithaca. <https://doi.org/10.2173/bow.ausbrt1.01>
- Fiorillo, A. R. 1988. Taphonomy of Hazard Homestead Quarry (Ogallala Group), Hitchcock County, Nebraska. *Rocky Mountain Geology* 26:57–97.
- Fondevilla, V., J. Dinarès-Turell, and O. Oms. 2016a. The chronostratigraphic framework of the South-Pyrenean Maastrichtian succession reappraised: Implications for basin development and end-Cretaceous dinosaur faunal turnover. *Sedimentary Geology* 337:55–68.
- Fondevilla, V., J. Dinarès-Turell, B. Vila, J. Le Loeuff, R. Estrada, O. Oms, and À. Galobart. 2016b. Magnetostratigraphy of the Maastrichtian continental record in the Upper Aude Valley (northern Pyrenees, France): placing age constraints on the succession of dinosaur-bearing sites. *Cretaceous Research* 57:457–472.
- Fondevilla, V., V. Riera, B. Vila, J. Dinarès-Turell, E. Vicens, R. Gaete, O. Oms, and À. Galobart. 2019. Chronostratigraphic synthesis of the latest Cretaceous dinosaur turnover in south-western Europe. *Earth-Science Reviews* 191:168–189.
- Gauthier, J. 1986. Saurischian monophyly and the origin of birds. *Memoirs of the California Academy of Sciences* 8:1–55.
- Goloboff, P. A., and S. A. Catalano. 2016. TNT version 1.5, including a full implementation of phylogenetic morphometrics. *Cladistics* 32:221–238.
- Gutzwiller, S. C., A. Su, and P. M. O'Connor. 2013. Postcranial pneumaticity and bone structure in two clades of neognath birds. *The Anatomical Record* 296:867–876.
- Houde, P., and H. Haubold. 1987. *Palaeotis weigelti* restudied: a small Middle Eocene ostrich (Aves: Struthioniformes). *Palaeovertebrata* 17:27–42.
- Hope, S. 2002. The Mesozoic Radiation of Neornithes; pp. 281–316 in L. M. Chiappe and L. M. Witmer (eds.), *Mesozoic Birds*. University of California Press, Berkeley.
- del Hoyo, J., N. Collar, and C. J. Sharpe. 2020. South Island Takahe (*Porphyrio hochstetteri*), version 1.0. In J. del Hoyo, A. Elliott, J. Sargatal, D. A. Christie, and E. de Juana (eds.), *Birds of the World* Cornell Lab of Ornithology, Ithaca. <https://doi.org/10.2173/bow.takahe3.01>
- Kerourio, P., and C. Aujard. 1987. Les oeufs d'oiseaux géants du Midi de la France. *Monde et Minéraux* 78:12–16.
- Ksepka, D. T. 2014. Flight performance of the largest volant bird. *Proceedings of the National Academy of Sciences* 111:10624–10629.
- Lambrecht, K. 1928. *Palaeotis weigelti* n. g. sp., eine fossil trappe aus der mitteozänen Braunkohle des Geiseltales. *Jahrbuch hallesch. Verband* 7:1–11.
- Le Loeuff, J., E. Buffetaut, and M. Martin. 1994. The last stages of dinosaur faunal history in Europe: a succession of Maastrichtian dinosaur assemblages from the Corbières (southern France). *Geological Magazine* 131:625–630.
- Lemoine, V. 1881. Recherches sur les oiseaux fossiles des terrains tertiaires inférieurs des environs de Reims. F. Kuller, Pt II, Reims, pp 75 – 170.
- López-Martínez, N., M. E. Arribas, A. Robador, E. Vicens, and L. Ardèvol. 2006. Los carbonatos danienses (Unidad 3) de la Formación Tremp (Pirineos sur-centrales): paleogeografía y relación con el límite Cretácico-Terciario. *Revista de la Sociedad Geológica de España* 19:213–255.
- López-Martínez, N., and E. Vicens. 2012. A new peculiar dinosaur egg, *Sankofa pyrenaica* oogen. nov. oosp. nov. from the Upper Cretaceous coastal deposits of the Aren Formation, south-central Pyrenees, Lleida, Catalonia, Spain. *Palaeontology* 55:325–339.
- Maddison, W. P., and D. R. Maddison. 2017. Mesquite: a modular system for evolutionary analysis. Version 3.31 <http://mesquiteproject.org>.
- Makovicky, P. J., S. Apesteguía, and F. L. Agnolín. 2005. The earliest dromaeosaurid theropod from South America. *Nature* 437:1007–1011.
- Makovicky, P. J., and M. A. Norell. 2004. Troodontidae; pp. 184–195 in D. B. Weishampel, P. Dodson and H. Osmólska (eds.), *The Dinosauria*: Second Edition. University of California Press, Berkeley.
- Makovicky, P. J., and H. D. Sues. 1998. Anatomy and phylogenetic relationships of the theropod dinosaur *Microvenator celer* from the Lower Cretaceous of Montana. *American Museum Novitates* 3240:1–27.
- Marsh, O. C. 1879. The vertebrae of recent birds. *American Journal of Science* 17: 266–9.
- Marsh, O. C. 1880. *Odontornithes: A Monograph of the Extinct Toothed Birds of North America*. Government Printing, Washington, 201 pp.
- Martin, L. D. 1991. Mesozoic birds and the origin of birds; pp. 485–540 in H. P. Schultze and L. Trueb (eds.), *Origins of the higher groups of tetrapods: controversy and consensus*. Cornell University Press, Ithaca.
- Martin, L. D. 1992. The status of the Late Palaeocene birds *Gastornis* and *Remiornis*. *Bulletin of the Natural History Museum of Los Angeles County Science Service* 36:97–108.
- Mayr, G. 2007. The birds from the Palaeocene fissure filling of Walbeck (Germany). *Journal of Vertebrate Paleontology* 27:394–408.
- Mayr, G. 2017. *Avian Evolution: The Fossil Record of Birds and its Paleobiological Significance*. Wiley-Blackwell, Chichester, 312 pp.
- Mayr, G., V. Codrea, A. Solomon, M. Bordeianu, and T. Smith. 2020. A well-preserved pelvis from the Maastrichtian of Romania suggests that the enigmatic *Gargantuavis* is neither an ornithurine bird nor an insular endemic. *Cretaceous Research* 106:104271.
- Mey, P. H. W., P. J. C. Nagtegaal, K. J. Roberti, and J. J. A. Hartevelt. 1968. Lithostratigraphic subdivision of post-Hercinian deposits in the south-central Pyrenees, Spain. *Leidsche Geologische Mededelingen* 41:221–228.
- Mitchell, K., J. B. Llamas, J. Soubrier, N. J. Rawlence, T. H. Worthy, J. Wood, S. Y. Lee, and A. Cooper. 2014. Ancient DNA reveals elephant birds and kiwi are sister taxa and clarifies ratite bird evolution. *Science* 344:898–900.
- Muñoz, J. A. 1992. Evolution of a continental collision belt: ECORS-Pyrenees crustal balanced section; pp. 235–246 in K. R. McClay (ed.), *Thrust tectonics*. Chapman and Hall, London.
- Murray, P. F., and P. Vickers-Rich. 2004. Magnificent mihrungs: the colossal flightless birds of the Australian dreamtime. *Indiana University Press, Bloomington*, 41 pp.
- Novas, F. E., F. B. Egli, F. L. Agnolín, F. A. Gianechini, and I. Cerda. 2018. Postcranial osteology of a new specimen of *Buitreraptor gonzalezorum* (Theropoda, Unenlagiidae). *Cretaceous Research* 83:127–167.
- O'Connor, J., L. M. Chiappe, and A. Bell. 2011. Pre-modern birds: avian divergences in the Mesozoic; pp. 39–114 in G. Dyke, and G. Kaiser (eds.), *Living dinosaurs. The evolutionary history of modern birds*. John Wiley & Sons Ltd, Chichester.
- O'Connor, J. K., K. Q. Gao, and L. M. Chiappe. 2010. A new ornithomorph (Aves: Ornithothoraces) bird from the Jehol Group indicative of higher-level diversity. *Journal of Vertebrate Paleontology* 30:311–321.
- O'Connor, P. M. 2004. Pulmonary pneumaticity in the postcranial skeleton of extant Aves: a case study examining Anseriformes. *Journal of Morphology* 261:141–161.
- O'Connor, P. M. 2006. Postcranial pneumaticity: an evaluation of soft-tissue influences on the postcranial skeleton and the reconstruction of pulmonary anatomy in archosaurs. *Journal of Morphology* 267:1199–1226.
- O'Connor, P. M. 2009. Evolution of archosaurian body plans: Skeletal adaptations of an air-sac-based breathing apparatus in birds and other archosaurs. *Journal of Experimental Zoology* 311A:629–646.
- Ogg, J. G., and L. A. Hinnov. 2012. Cretaceous; pp. 793–853 in F.M. Gradstein, J.G. Ogg, M.D. Schmitz and G.M. Ogg (eds.), *The Geological Time Scale*. Elsevier, Amsterdam.
- Oms, O., V. Fondevilla, V. Riera, J. Marmi, E. Vicens, R. Estrada, P. Anadón, B. Vila, B., and À. Galobart. 2016. Transitional environments of the lower Maastrichtian South-Pyrenean Basin (Catalonia, Spain): the Fumanya Member tidal flat. *Cretaceous Research* 57:428–442.
- Pavia, M., H. J. Meijer, M. A. Rossi, and U. B. Göhlich. 2017. The extreme insular adaptation of *Garganornis ballmanni* Meijer, 2014: a giant Anseriformes of the Neogene of the Mediterranean Basin. *Royal Society Open Science* 4:160722.
- Peters, D. S. 1988. Ein vollständiges Exemplar von *Palaeotis weigelti* (Aves, Palaeognathae). *Courier Forschungsinstitut Senckenberg* 107:223–233.







- Puértolas-Pascual, E., I. Arenillas, J. A. Arz, P. Calvín, L. Ezquerro, C. García-Vicente, M. Pérez-Pueyo, E. M. Sánchez-Moreno, J. J. Villalán, and J. I. Canudo. 2018. Chronostratigraphy and new vertebrate sites from the upper Maastrichtian of Huesca (Spain), and their relation with the K/Pg boundary. *Cretaceous Research* 89:36–59.
- Puértolas-Pascual, E., A. Blanco, C.A. Brochu, and J. I. Canudo. 2016. Review of the Late Cretaceous-early Paleogene crocodylomorphs of Europe: Extinction patterns across the K-PG boundary. *Cretaceous Research* 57:565–590.
- Puértolas-Pascual, E., J. I. Canudo, and M. Moreno-Azanza. 2014. The eusuchian crocodylomorph *Allodaposuchus subjuniperus* sp. nov., a new species from the latest Cretaceous (upper Maastrichtian) of Spain. *Historical Biology* 26:91–109.
- Puigdefàbregas, C., J. A. Muñoz, and J. Vergés. 1992. Thrusting and foreland evolution in the Southern Pyrenees; pp. 247–254 in K. McClay (ed.), *Thrust Tectonics*. Chapman & Hall, London.
- Rauhut, O. W. M. 2003. The interrelationships and evolution of basal theropod dinosaurs. *Special papers in Palaeontology* 69, Palaeontological Association, London, 213 pp.
- Rosell, J., R. Linares, and C. Llombart. 2001. El “Garumniense” prepirineico. *Revista de la Sociedad Geológica de España* 14:47–56.
- Sanz, J. L., L. M. Chiappe, B. P. Pérez-Moreno, J. J. Moratalla, F. Hernández-Carrasquilla, A. D. Buscalioni, F. Ortega, F. J. Poyato-Ariza, D. Rasskin-Gutman, and X. Martínez-Delclòs. 1997. A nestling bird from the Lower Cretaceous of Spain: implications for avian skull and neck evolution. *Science* 276:1543–1546.
- Schaub, S. 1940. Ein Ratitenbecken aus dem Böhnerz von Egerkingen. *Eclogae Geol. Helvetiae* 32, 274–284.
- Smith, T. F., F. Quesnel, G. De Ploëg, D. De Franceschi, G. Métais, E. De Bast, F. Solé, A. Folie, A. Boura, J. Claude, C. Dupuis, C. Gagnaison, A. Iakovleva, J. Martin, F. Maubert, J. Prieur, E. Roche, J.-Y. Storme, R. Thomas, H. Tong, J. Yans, and E. Buffetaut. 2014. First Clarkforkian equivalent Land Mammal Age in the latest Palaeocene basal Sparnacian facies of Europe: fauna, flora, paleoenvironment and (bio)stratigraphy. *PLoS ONE* 9:e86229.
- Sues, H. D., and A. Averianov. 2014. Dromaeosauridae (Dinosauria: Theropoda) from the Bissekty Formation (Upper Cretaceous: Turonian) of Uzbekistan and the phylogenetic position of *Itemirus medullaris* Kurzanov, 1976. *Cretaceous Research* 51:225–240.
- Tanaka, T., Y. Kobayashi, K. I. Kurihara, A. R. Fiorillo, and M. Kano. 2018. The oldest Asian hesperornithiform from the Upper Cretaceous of Japan, and the phylogenetic reassessment of Hesperornithiformes. *Journal of Systematic Palaeontology* 16:689–709.
- Tambussi, C. P., R. De Mendoza, F. J. Degrangé, and M. B. Picasso. 2012. Flexibility along the neck of the Neogene terror bird *Andalgalornis steulleti* (Aves Phorusrhacidae). *PLoS ONE* 7:e37701.
- Teixell, A. 1998. Crustal structure and orogenic material budget in the West Central Pyrenees. *Tectonics* 17:395–406.
- Teixell, A., 2004. Estructura de los Pirineos: generalidades; pp. 321–323 in Vera J.A. (ed.), *Geología de España*. SGE-IGME, Madrid.
- Terray, L., O. Plateau, A. Abourachid, C. Böhmer, A. Delapré, X. de la Bernardie, and R. Cornette. 2020. Modularity of the neck in birds (Aves). *Evolutionary Biology* 47:97–110.
- Torices, A., P. J. Currie, J. I. Canudo, and X. Pereda-Suberbiola. 2015. Theropod dinosaurs from the Upper Cretaceous of the South Pyrenees Basin of Spain. *Acta Palaeontologica Polonica* 60:611–626.
- Tovondrafale, T., T. Razakamanana, K. Hiroko, and A. Rasoamiamanan. 2014. Paleoeological analysis of elephant bird (Aepyornithidae) remains from the Late Pleistocene and Holocene formations of southern Madagascar. *Malagasy Nature* 8:1–13.
- Vandenbergh, N., F. J. Hilgen, R. P. Speijer, J. G., Ogg, F. M., Gradstein, O. Hammer, C. J. Hollis, and J. J. Hooker. 2012. The Palaeogene period; pp. 855–921 in F.M. Gradstein, J. G. Ogg, M. D. Schmitz and G. M. Ogg (eds.), *The Geological Time Scale*. Elsevier, Amsterdam.
- Vila, B., O. Oms, V. Fondevilla, R. Gaete, À. Galobart, V. Riera, and J. I. Canudo. 2013. The latest succession of dinosaur tracksites in Europe: hadrosaur ichnology, track production and palaeoenvironments. *PLoS ONE* 8:e72579.
- Vila, B., A. G. Sellés, and Brusatte, S. L. 2016. Diversity and faunal changes in the latest Cretaceous dinosaur communities of South-Western Europe. *Cretaceous Research* 57:552–564.
- Walker, C. A., and G. J. Dyke. 2009. Euenantiornithine birds from the Late Cretaceous of El Brete (Argentina). *Irish Journal of Earth Sciences* 27:15–62.
- Wang, M., J. O’Connor, S. Zhou, and Z. Zhou. 2020. New toothed Early Cretaceous ornithomorph bird reveals intraclade diversity in pattern of tooth loss. *Journal of Systematic Palaeontology* 18:631–645.
- Watanabe, A., M. E. L. Gold, S. L. Brusatte, R. B. Benson, J. Choiniere, A. Davidson, and M. A. Norell. 2015. Vertebral pneumaticity in the ornithomimosaur *Archaeornithomimus* (Dinosauria: Theropoda) revealed by computed tomography imaging and reappraisal of axial pneumaticity in Ornithomimosauria. *PLoS ONE* 10:e0145168.
- Wedel, M. J., R. L. Cifelli, and R. K. Sanders. 2000. Osteology, paleobiology, and relationships of the sauropod dinosaur *Sauroposeidon*. *Acta Palaeontologica Polonica* 45:343–388.
- Wilson, J. A. 1999. Vertebral laminae in sauropods and other saurischian dinosaurs. *Journal of Vertebrate Paleontology* 19:639–653.
- Wilson, J. A., M. D. D’Emic, T. Ikejiri, E. M. Moacdieh, and J. A. Whitlock. 2011. A nomenclature for vertebral fossae in sauropods and other saurischian dinosaurs. *PLoS ONE* 6:e17114.
- Wiman, C. 1905. Über die alttertiären Vertebraten der Seymourinsel, 3, *Wiss. Ergeb. Schwedischen Südpolar-Exped. 1901–1903*, pp. 37.
- Winkler, D. W., S. M. Billerman, and I. J. Lovette. 2020a. Ostriches (Struthionidae), version 1.0. in S. M. Billerman, B. K. Keeney, P. G. Rodewald, and T. S. Schulenberg (eds.), *Birds of the World*. Cornell Lab of Ornithology, Ithaca. <https://doi.org/10.2173/bow.struth1.01>
- Winkler, D. W., S. M. Billerman, and I. J. Lovette. 2020b. Cassowaries and Emu (Casuariidae), version 1.0. in S. M. Billerman, B. K. Keeney, P. G. Rodewald, and T. S. Schulenberg (eds.), *Birds of the World*. Cornell Lab of Ornithology, Ithaca. <https://doi.org/10.2173/bow.casuar1.01>
- Winkler, D. W., S. M. Billerman, and I. J. Lovette. 2020c. Rheas (Rheidae), version 1.0. in S. M. Billerman, B. K. Keeney, P. G. Rodewald, and T. S. Schulenberg (eds.), *Birds of the World*. Cornell Lab of Ornithology, Ithaca. <https://doi.org/10.2173/bow.rheida1.01>
- Wood, J. R., J. M. Wilmshurst, S. J. Richardson, N. J. Rawlence, S. J., Wagstaff, T. H. Worthy, and A. Cooper. 2013. Resolving lost herbivore community structure using coprolites of four sympatric moa species (Aves: Dinornithiformes). *Proceedings of the National Academy of Sciences* 110:16910–16915.
- Worthy, T. H., F. J. Degrangé, W. D. Handley, and M. S. Lee. 2017. The evolution of giant flightless birds and novel phylogenetic relationships for extinct fowl (Aves, Galloanseres). *Royal Society Open Science* 4:170975.
- Worthy, T. H., M. Mitri, W. D. Handley, M. S. Lee, A. Anderson, and C. Sand. 2016. Osteology supports a stem-galliform affinity for the giant extinct flightless bird *Sylviornis neocaledoniae* (Sylviornithidae, Galloanseres). *PLoS ONE* 11:e0150871.
- Xu, X., and M. A. Norell. 2004. A new troodontid dinosaur from China with avian-like sleeping posture. *Nature* 431:838–841.
- Xu, X., Zheng, X., Sullivan, C. et al. 2015. A bizarre Jurassic maniraptoran theropod with preserved evidence of membranous wings. *Nature* 521, 70–73. <https://doi.org/10.1038/nature14423>.
- Zelenkov, N. V., A. V. Lavrov, D. B. Startsev, I. A. Vislobokova, and A. V. Lopatin. 2019. A giant early Pleistocene bird from eastern Europe: unexpected component of terrestrial faunas at the time of early Homo arrival. *Journal of Vertebrate Paleontology* 39:e1605521.
- Zhang, F., G. P. Ericson, and Z. Zhou. 2005. Description of a new enantiornithine bird from the Early Cretaceous of Hebei, northern China. *Canadian Journal of Earth Sciences* 41:1097–1107.
- Zhou, Z., J. Clarke, and F. Zhang. 2008. Insight into diversity, body size and morphological evolution from the largest Early Cretaceous enantiornithine bird. *Journal of Anatomy* 212:565–577.
- Zhou, S., Z. Zhou, and J. O’Connor. 2014. A new piscivorous ornithomorph from the Jehol Biota. *Historical Biology* 26:608–618.

Submitted May 22, 2020; revisions received September 17, 2020; accepted November 29, 2020.

Handling Editor: Lindsay Zanno.

## Review

# The Tetrapod Fossil Record from the Uppermost Maastrichtian of the Ibero-Armorican Island: An Integrative Review Based on the Outcrops of the Western Tresp Syncline (Aragón, Huesca Province, NE Spain)

Manuel Pérez-Pueyo <sup>1,\*</sup> , Penélope Cruzado-Caballero <sup>1,2,3,4</sup> , Miguel Moreno-Azanza <sup>1,5,6</sup> , Bernat Vila <sup>7</sup>, Diego Castanera <sup>1,7</sup> , José Manuel Gasca <sup>1</sup> , Eduardo Puértolas-Pascual <sup>1,5,6</sup>, Beatriz Bádenas <sup>1</sup> and José Ignacio Canudo <sup>1</sup> 



**Citation:** Pérez-Pueyo, M.; Cruzado-Caballero, P.; Moreno-Azanza, M.; Vila, B.; Castanera, D.; Gasca, J.M.; Puértolas-Pascual, E.; Bádenas, B.; Canudo, J.I. The Tetrapod Fossil Record from the Uppermost Maastrichtian of the Ibero-Armorican Island: An Integrative Review Based on the Outcrops of the Western Tresp Syncline (Aragón, Huesca Province, NE Spain). *Geosciences* **2021**, *11*, 162. <https://doi.org/10.3390/geosciences11040162>

Academic Editors:  
Angelos G. Maravelis and  
Jesus Martinez-Frias

Received: 25 February 2021  
Accepted: 26 March 2021  
Published: 2 April 2021

**Publisher's Note:** MDPI stays neutral with regard to jurisdictional claims in published maps and institutional affiliations.



**Copyright:** © 2021 by the authors. Licensee MDPI, Basel, Switzerland. This article is an open access article distributed under the terms and conditions of the Creative Commons Attribution (CC BY) license (<https://creativecommons.org/licenses/by/4.0/>).

- <sup>1</sup> Grupo Aragosaurus-IUCA, Facultad de Ciencias, Universidad de Zaragoza, C/Pedro Cerbuna, 12, 50009 Zaragoza, Aragón, Spain; pcruzado@ull.edu.es (P.C.-C.); mmazanza@fct.unl.pt (M.M.-A.); diego.castanera@icp.cat (D.C.); jmgaska@hotmail.com (J.M.G.); puertolas@fct.unl.pt (E.P.-P.); bbadenas@unizar.es (B.B.); jicanudo@unizar.es (J.I.C.)
- <sup>2</sup> Área de Paleontología, Departamento de Biología Animal, Edafología y Geología, Universidad de La Laguna, 38200 San Cristóbal de La Laguna, Santa Cruz de Tenerife, Spain
- <sup>3</sup> Instituto de Investigación en Paleobiología y Geología (IIPG), Universidad Nacional de Río Negro, 8500 Río Negro, Argentina
- <sup>4</sup> IIPG, UNRN, Consejo Nacional de Investigaciones Científicas y Técnicas (CONICET), 2300 Buenos Aires, Argentina
- <sup>5</sup> GEOBIOTEC, Department of Earth Sciences, NOVA School of Science and Technology, Campus de Caparica, 2829-516 Caparica, Portugal
- <sup>6</sup> Espaço Nova Paleo, Museu de Lourinhã, Rua João Luis de Moura 95, 2530-158 Lourinhã, Portugal
- <sup>7</sup> Institut Català de Paleontologia Miquel Crusafont, Universitat Autònoma de Barcelona, c/ Escola Industrial 23, 08201 Sabadell, Barcelona, Spain; bernat.vila@icp.cat
- \* Correspondence: manuppueyo@unizar.es

**Abstract:** The South-Pyrenean Basin (northeastern Spain) has yielded a rich and diverse record of Upper Cretaceous (uppermost Campanian–uppermost Maastrichtian) vertebrate fossils, including the remains of some of the last European dinosaurs prior to the Cretaceous–Paleogene (K–Pg) extinction event. In this work, we update and characterize the vertebrate fossil record of the Arén Sandstone and Tresp formations in the Western Tresp Syncline, which is located in the Aragonese area of the Southern Pyrenees. The transitional and continental successions of these sedimentary units are dated to the late Maastrichtian, and exploration of their outcrops has led to the discovery of numerous fossil remains (bones, eggshells, and tracks) of dinosaurs, including hadrosauroids, sauropods, and theropods, along with other tetrapods such as crocodylomorphs, testudines, pterosaurs, squamates, and amphibians. In particular, this fossil record contains some of the youngest lambeosaurine hadrosaurids (*Arenysaurus* and *Blasisaurus*) and Mesozoic crocodylomorphs (*Arenysuchus* and *Agaresuchus subjuniperus*) in Europe, complementing the lower Maastrichtian fossil sites of the Eastern Tresp Syncline. In addition, faunal comparison with the fossil record of Hațeg island reveals the great change in the dinosaur assemblages resulting from the arrival of lambeosaurine hadrosaurids on the Ibero-Armorican island, whereas those on Hațeg remained stable. In the light of its paleontological richness, its stratigraphic continuity, and its calibration within the last few hundred thousand years of the Cretaceous, the Western Tresp Syncline is one of the best places in Europe to study the latest vertebrate assemblages of the European Archipelago before the end-Cretaceous mass extinction.

**Keywords:** late Maastrichtian; Western Tresp Syncline; Southern Pyrenees; tetrapods; Ibero-Armorican island

## 1. Introduction

The Cretaceous–Paleogene (K–Pg) extinction event is undoubtedly one of the most debated topics in the evolutionary history of life on the planet. Ever since a catastrophic meteorite impact at the end of the Maastrichtian was proposed as the major cause of the extinction [1], scientific debate on this event has been of ongoing significance. At the end of the Cretaceous, a set of destabilizing events occurred on Earth, including a marine regression [2], climate changes [3,4], the volcanic activity of the Deccan Volcanic Province (India) with the emission of a huge amount of gases and volcanic material into the atmosphere [5–8], and the impact of an asteroid in Chicxulub (Mexico) 66 Ma ago [1,9–12]. Although all these causes seem to have contributed to the extinction to a certain degree, the meteorite impact hypothesis shows the most solid arguments for having been the major disturbing mechanism [12–16].

Whatever the cause, the K–Pg extinction eradicated nearly 70% of the living species on Earth [17,18]. Among vertebrates, this event led to the disappearance of several groups, including non-avian dinosaurs, enantiornithine birds, pterosaurs, mosasaurs, plesiosaurs, and several lineages of crocodylomorphs, among others [19–23]. However, the mechanism by which they became extinct and how fast they did so remain difficult questions for researchers, as is the issue of how determinant the Chicxulub impact was on the stability of the ecosystems. Except for the Hell Creek Formation in North America, whose vertebrate faunas are well known [22,24,25] and their chronostratigraphic framework is well constrained [26–29], the main difficulty in assessing the end-Cretaceous extinction is the lack of well-studied sedimentary formations with vertebrate remains encompassing the K–Pg boundary. In Europe, a great effort has been made in recent decades to characterize the terrestrial uppermost Cretaceous–Paleocene formations, especially in Spain, France, and Romania (e.g., [30–33]). The best-known deposits are those from the so-called Ibero-Armorican island, which encompassed the current south of France and the north-east of Spain (Languedoc, Provence, and the Pyrenees), and other outcrops in the east, northwest, and center of Spain and part of Portugal. Of these regions, the South-Pyrenean Basin is the best-known area. Since the end of the 20th century, several research teams have worked on the uppermost Campanian–Danian outcrops in this area, improving our knowledge of the biodiversity of fossil vertebrates, the environments they inhabited, and the chronostratigraphic framework [31,33,34].

The main objectives of this paper are to review the paleontological and stratigraphical data of the western sector of the Tremp Syncline (Figure 1a), which are characterized by the thickest and most continuous upper Maastrichtian succession in the South-Pyrenean Basin, and to integrate these data within the Ibero-Armorican Maastrichtian record as a whole. Work in this area has led to the discovery of more than 50 vertebrate fossil sites and the erection of four taxa. Such a record enables us to characterize the extinction patterns of the tetrapods of the Ibero-Armorican island, especially in the last few hundred thousand years of the Maastrichtian, and to ascertain how the ecological communities were affected by the asteroid impact and its consequences.

## 2. The Geological and Stratigraphic Framework of the Western Tremp Syncline (Aragonese Outcrops of the Tremp Fm)

The Western Tremp Syncline is the westernmost edge of the Tremp Syncline or Tremp–Graus Basin, the largest of the sub-basins into which the Southern Pyrenees was compartmentalized by several structural highs [35]. The Pyrenees is a mountain range located in the northeast of the Iberian Peninsula between Spain and France (Figure 1a). It is structured as an asymmetric range, a NW–SE oriented belt of folds and thrusts, which was formed as a product of the collision between the European plate and the Iberian microplate. This collision took place during the Alpine orogeny between the Late Cretaceous and the Miocene [36–39]. The thrust sheets of the orogen controlled the development of a series of compartmentalized foreland basins, parallel to the axis of the orogen, which were active in different tectonic stages. The South-Pyrenean Basin was active between the Late

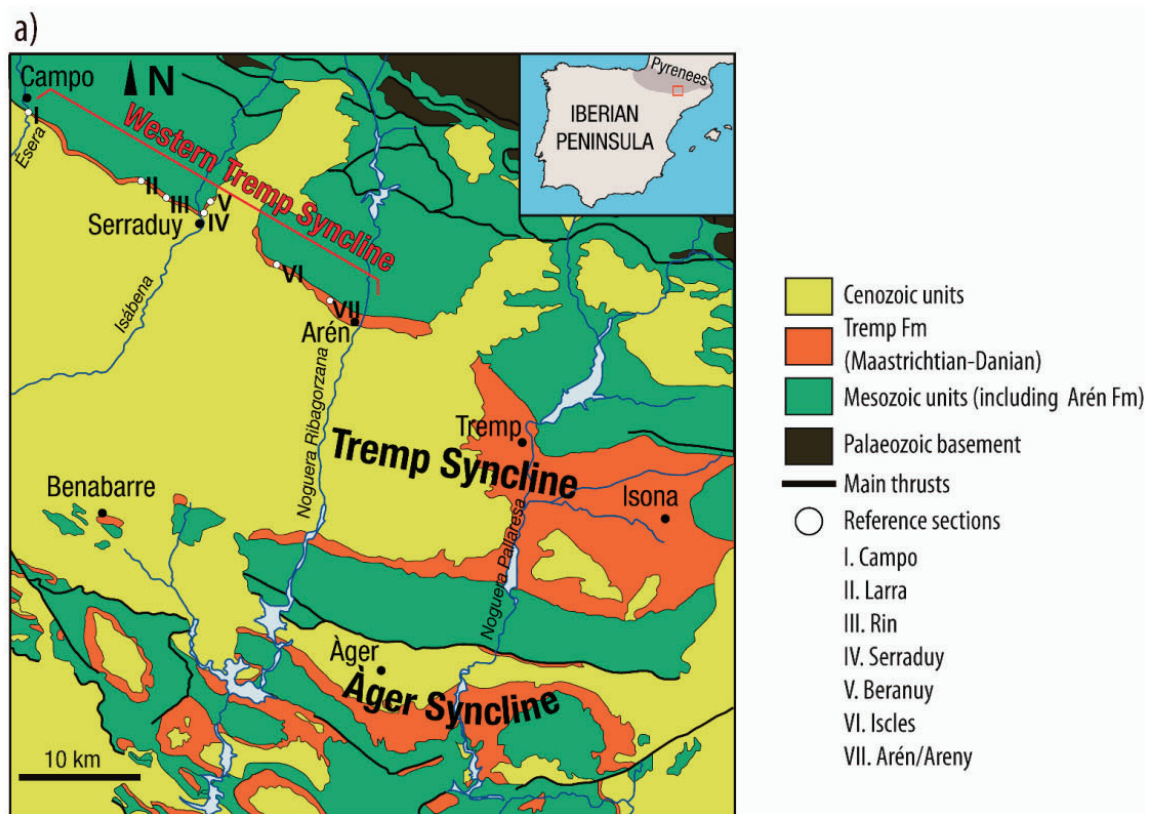
Cretaceous and the Oligocene and was connected with the Atlantic Ocean until the Late Eocene [40]. For this reason, its sedimentary record consists mainly of marine sediments, although at the end of the Late Cretaceous, as a consequence of the global sea level fall [2], the basin was progressively filled with westward-prograding turbiditic and deltaic sediments (Santonian-Maastrichtian) [41] and transitional and continental deposits (lower to upper Maastrichtian) [35,42]. Continental sedimentation lasted up to the Paleocene.

The Tremp Syncline or Tremp-Graus Basin is limited in the north by the Bóixols thrust sheet and in the south by the Montsec thrust sheet (Figure 1a). In the Tremp Syncline, the uppermost Cretaceous-lowermost Paleocene transitional and continental deposits consist of two closely related stratigraphic units, the Arén and Tremp formations (see lithostratigraphy by [43]; Figure 1b). The uppermost Cretaceous outcrops of the Western Tremp Syncline (*sensu* [33]) studied here comprise those located between the rivers Noguera Ribagorçana and Ésera. Thus, they constitute the part of the Tremp Syncline situated within the region of Aragón (Huesca province) (Figure 1a).

The Arén Sandstone Fm [44] is a middle Campanian–Maastrichtian transitional unit constituted by a thick succession of calcarenites with large-scale cross-bedding, which is composed mainly of quartz grains and bioclasts [45]. It represents deposition in different transitional sedimentary environments including delta [46], barrier-island [45,47], and beach deposits [48,49]. These deposits pass laterally and vertically to the Tremp Fm, since their boundary is not isochronous.

The Tremp Fm [44], traditionally known as the ‘Garumnian Facies’ [50], is a coastal to continental heterogeneous and diachronous lithostratigraphic unit that ranges between the Maastrichtian and the Paleocene. It can be subdivided into four minor lithostratigraphic units, which have received different names in the successive stratigraphic subdivisions proposed (Figure 1b) [42–44,51,52]. The scheme used here is that of Rosell et al. (2001) [43], who divided the Tremp Fm into four informal units recognizable throughout the South-Pyrenean Basin.

The lowermost unit is the so-called “Grey Garumnian”, which is characterized by a succession of grey marls and mudstones, with intercalations of sandstones, limestones, and coal beds and a rich fossil content of brackish and continental invertebrate faunas. It is interpreted as transitional deposits, including lagoon, tidal mud flats, swamp and marsh sub-environments [42,43,47,51,53–56]. The overlying unit is the ‘Lower Red Garumnian’, which is composed of reddish, brown ochre, and multi-colored mudstones, with local paleosoils and intercalated lenticular sandstone packages, sometimes with channelized bases and point-bar deposits. There are also carbonate intercalations of lacustrine origin. The ‘Lower Red Garumnian’ has been interpreted either as fluvial and alluvial deposits [43,51,55] or as deltaic-plain and perilagoonal deposits in the Western Tremp Syncline [54]. The fluvial deposits show features indicative of a marked tidal influence in the basin [54,56–58]. The ‘Grey Garumnian’ and ‘Lower Red Garumnian’ successions studied here are of Maastrichtian age, having been dated by means of the biostratigraphy of planktonic foraminifera and charophytes [56,59–61] and by magnetostratigraphy [31,62–64]. Nevertheless, due to sedimentary evolution and syntectonic activity during the Maastrichtian, the age of these units varies throughout the basin, being younger westwards [41,63]. Thus, the lower Maastrichtian is only represented in the eastern part of the basin, whereas the upper Maastrichtian is much better recorded in its western part. This distribution implies the presence in the eastern part of a sedimentary hiatus within the ‘Lower Red Garumnian’, between chron C31r and chron C29r [63].



b)

Mey et al. (1968)	Rosell et al. (2001)	Cuevas (1992)	Pujalte & Schmitz (2005)
Tresp Fm	'Upper Red Garumnian'	La Guixera Mb Claret Fm	La Guixera Mb Claret Fm Cg. Claret Mb
	'Vallcebre limestones & equivalents'	Esplugafreda Fm St. Salvador de Toló Fm	Esplugafreda Fm St. Salvador de Toló Fm
	'Lower Red Garumnian'	Talarn Fm Tossal d'Oba Mb Conques Fm Basturs Mb	Talarn Fm Tossal d'Oba Mb Conques Fm Basturs Mb
	'Grey Garumnian'	La Posa Fm	La Posa Fm Fumanya Mb*
Arén Fm & lateral equivalents	Arén Fm & lateral equivalents	Arén Fm & lateral equivalents	Arén Fm & lateral equivalents

\* defined by Oms et al., 2016

**Figure 1.** Geological and stratigraphic setting of the Tresp Syncline. (a) Geological map of the area of the South-Pyrenean Basin where the Tresp and Àger synclines are located. Reference sections of the Western Tresp Syncline are marked with Roman numerals: I Campo, II Larra, III Rin, IV Serraduy, V Beranuy, VI Isclès, VII Arén/Areny (map modified after [65]); (b) Stratigraphic proposals for the late Campanian-Paleocene deposits of the Tresp Syncline (modified after [66]).

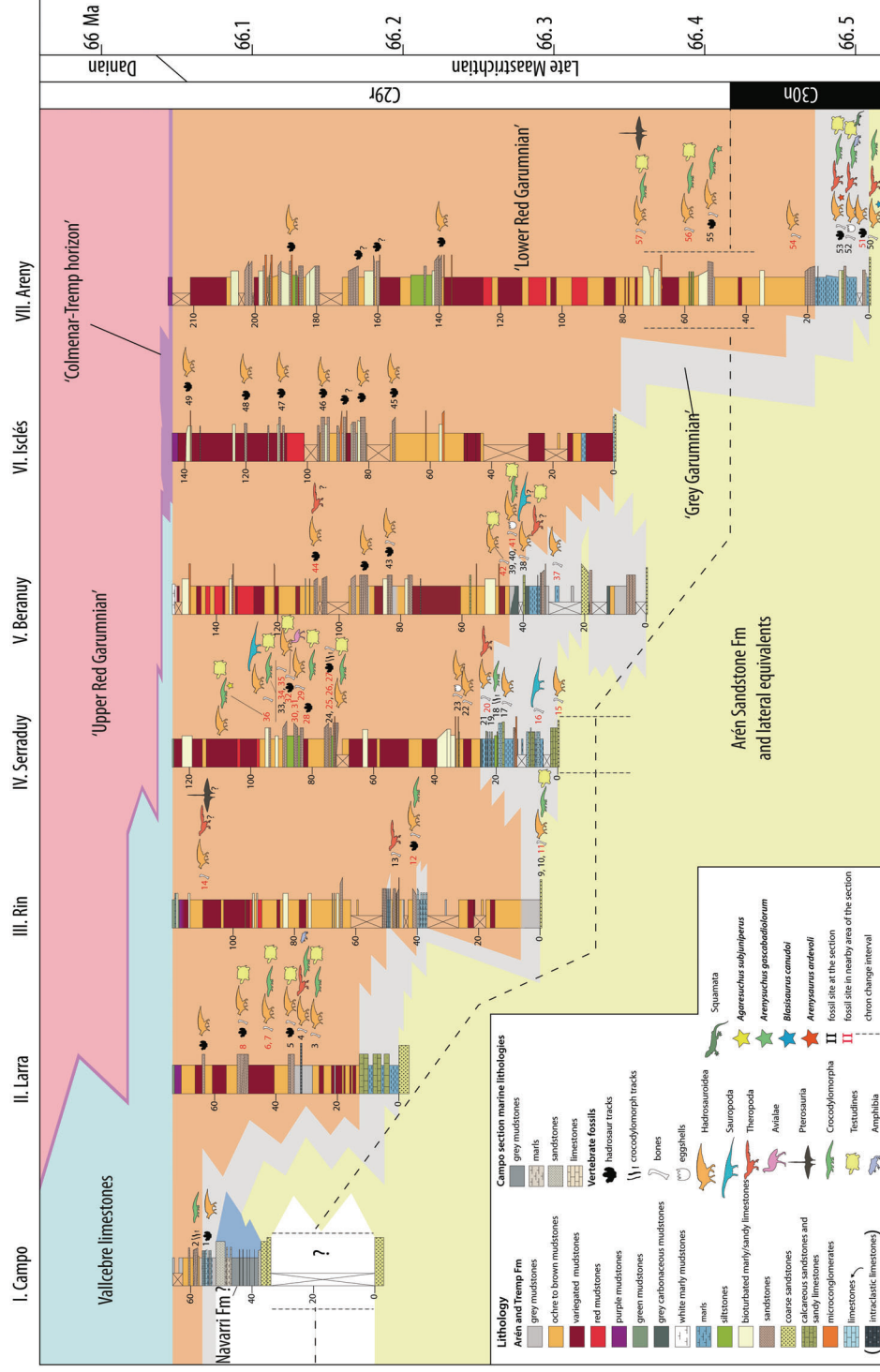
The third unit of the Tresp Fm is the ‘Vallcebre limestones and equivalents’, which is a laterally discontinuous sedimentary unit of limestones with charophytes and *Microcodium* and which represents coastal lacustrine deposits [43,67]. In the Eastern Tresp Syncline, this unit has been dated as late Danian [56], which would indicate the existence of a disconformity. The K-Pg boundary would accordingly be situated somewhere between the topmost part of the ‘Lower Red Garumnian’ and the boundary with the ‘Vallcebre limestones’, with dinosaur-bearing sites lying just a few meters below the Vallcebre limestones ([31,64]; Figure 2). However, up to now, the boundary has never been recognized in the Tresp Syncline within this stratigraphic interval [43]. Finally, the last unit is the ‘Upper Red Garumnian’, which is a succession of red mudstones, sandstones, and conglomerates, with the occasional presence of paleosoils, gypsum, and limestones, representing fluvial and alluvial environments [43,51]. Its age is constrained in the Tresp Syncline between the Selandian and the late Thanetian [68,69], and at the top of the unit, the Paleocene-Eocene Thermal Maximum has been recognized [70]. It is also worth mentioning the Colmenar-Tresp Horizon [54], which is a stratigraphic level of caliche paleosoils and gypsum that can be traced across the basin. This horizon overlies the more modern sedimentary units westwards, marking a progressive unconformity within the Garumnian deposits.

The lithostratigraphic schemes used by other authors are indicated in Figure 1b. The ‘Grey Garumnian’ of Rosell et al. (2001) [43] (Figure 1b) is equivalent to the Posa Fm, whereas the ‘Lower Red Garumnian’ is equivalent to the Conques and Tarn formations of Cuevas (1992) [51]. Paleogene units also change their names. Thus, the ‘Vallcebre limestones and equivalents’ are equal to the Sant. Salvador de Toló and Suterranya formations, and the ‘Upper Red Garumnian’ is equivalent to the Esplugafreda and Claret formations. Furthermore, Cuevas (1992) [51] named as members the limestones intercalated with the mudstones of the Lower and Upper Red Garumnian, including (from older to younger) the Basturs, Tossal d’Oba, and la Guixera members (Figure 1b). Later, Pujalte and Schmitz (2005) [52] and Oms et al. (2016) [42] followed the proposal by Cuevas (1992) [51], with some modifications. Pujalte and Schmitz (2005) define the Claret Conglomerates member within the Claret Fm, and Oms et al. (2016) differentiate the Fumanya Member (lower Maastrichtian tidal flat deposits within La Posa Fm), which is preserved only in the eastern part of the South-Pyrenean Basin.

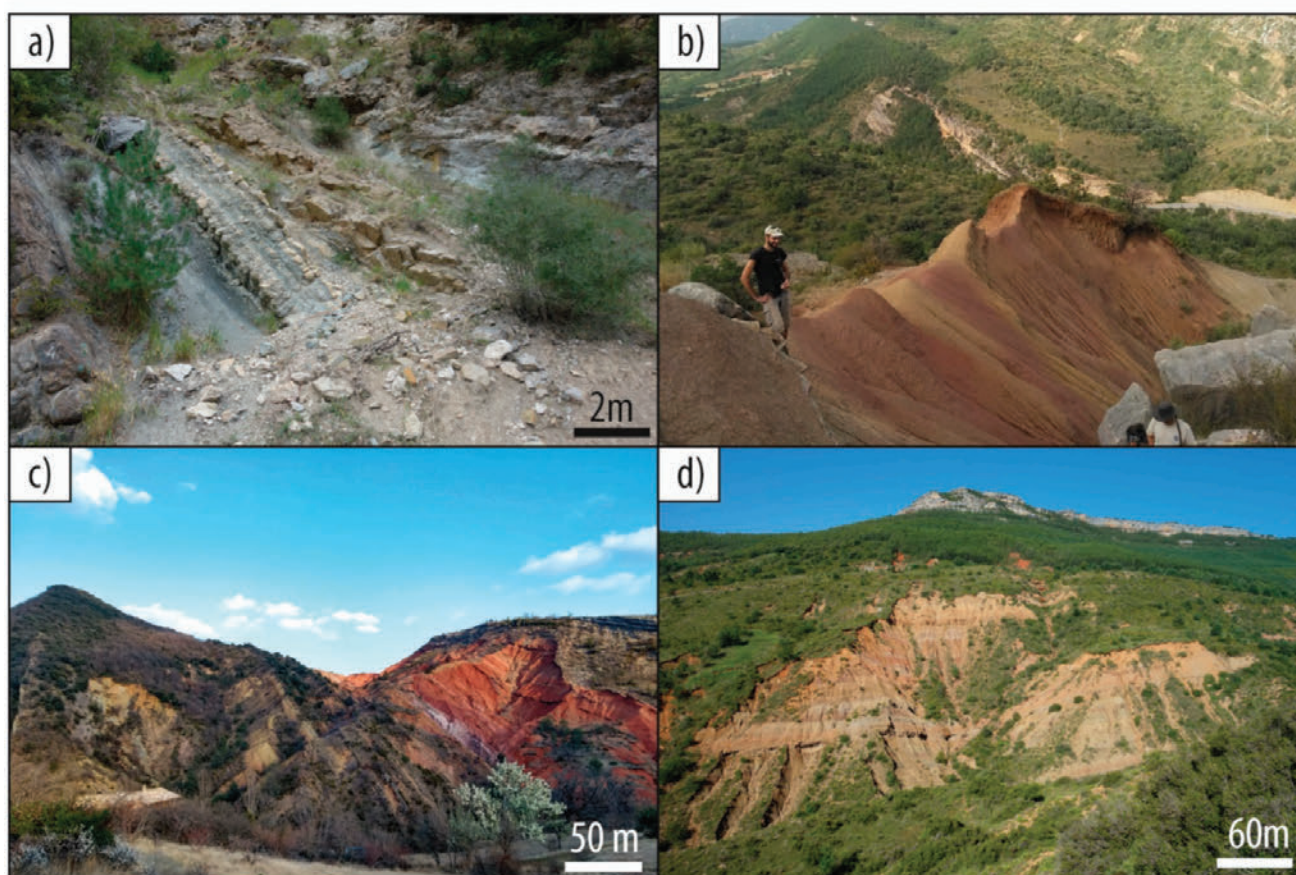
In the Western Tresp Syncline studied here, there are some sedimentological particularities that sometimes make it difficult to locate the formations and boundaries proposed in the Eastern Tresp Syncline. The boundary between the Conques and Tarn formations (equivalent units to the ‘Lower Red Garumnian’) is defined by the sharp contact between mudstones and conglomerates, or a swift change of light-colored mudstones to red mudstones and sandstones [51]; however, neither of these contacts can be observed in the Western Tresp Syncline. Moreover, chronostratigraphic data in the eastern part of the Tresp Syncline [63,71] restrict the Conques Fm to the early Maastrichtian (within chron C31r) and the Tarn Fm to the late Maastrichtian (chron C29r), a great part of the late Maastrichtian not being recorded (hiatus between C31r and C29r). By contrast, in the Western Tresp Syncline, the lateral equivalents to these units (‘Lower Red Garumnian’) are dated to within the late Maastrichtian chron C30n–C29r [31,62,64,72], thus being the only part of the basin where chron C30n is recorded. According to the lithostratigraphic and depositional model proposed by Ardèvol et al. (2000) [41] and updated by Fondevilla et al. (2016) [63], the Tarn Fm is limited to the eastern part of the basin (see [63], Figure 8c). As a direct correlation is not possible, since part of the succession is overlaid by discordant Neogene conglomerates (Figure 1a), it is quite difficult to determine whether the ‘Lower Red Garumnian’ in the Western Tresp Syncline corresponds to an upper Maastrichtian Conques Fm or the Tarn Fm. A similar pattern is observed with the ‘Vallcebre limestone’ of the Western Tresp Syncline, which cannot be directly correlated with the St. Salvador de Toló and Suterranya formations to the east due to their lateral discontinuity. Finally, westwards, the continental deposits of the Tresp Fm pass laterally to the marine Laspún and Navarri formations [69,73].

### 3. The Upper Maastrichtian Tetrapod Fossil Record of the Western Tremp Syncline and Its Integration within the Ibero-Armorican Island Record

The sedimentary succession of the Tremp Fm in the Western Tremp Syncline here under study encompasses sedimentary rocks belonging to the ‘Grey Garumnian’ and ‘Lower Red Garumnian’, and therefore, the late Maastrichtian between the upper part of chron C30n and chron C29r (Figure 2). The studied area is the part of the Tremp Syncline where the thickest succession of the upper Maastrichtian is preserved (more than 210 m). In these upper Maastrichtian sediments, there is a diverse and significant record of vertebrate fossils, including avian and non-avian dinosaurs, crocodylomorphs, testudines, squamates, amphibians, and fishes. More than 1200 fossil remains have been recovered from the hilly outcrops, with 57 different fossil localities identified. In order to facilitate our explanation of the Western Tremp Syncline fossil record, we have clustered the paleontological sites by their closeness to certain reference stratigraphic logs, which are called the Campo (I), Larra (II), Rin (III), Serraduy (IV), Beranuy (V), Isclés (VI), and Areny (VII) sections (Figures 1a, 2 and 3). A table summing up the assemblage from all the sites can be found in the Supplementary Materials Table S1. All the fossils are housed at the Natural Science Museum of the University of Zaragoza (Spain) (MPZ) [74].



**Figure 2.** Correlation panel of the Western Tremp Syncline (W-E oriented) with the stratigraphic position of the vertebrate fossil sites: (1) Campo 1, (2) Campo 2, (3) Larra 3, (4) Larra 4, (5) Larra 5, (6) Larra 1, (7) Larra 2, (8) Larra 6, (9) Rin1, (10) Rin2, (11) Barranco Extremadura, (12) Pedregal, (13) Camino Rin 1, (14) Camino Rin 2, (15) Fuente San Cristobal, (16) Femur, (17) Barranco Serraduy 1, (18) Beranuy, (19) 172-i/04/d, (20) 172-i/04/c, (21) 172-i/04/b, (22) Barranco Serraduy 2, (23) 172-i/04/f, (24) Barranco Serraduy 3, (25) 172-i/04/a, (26) Color, (27) Serraduy Norte, (28) Dolor 1, (29) Dolor 2, (30) Dolor 3, (31) 172-i/04/b, (32) Amor 1, (33) Barranco Serraduy 4, (34) Barranco Serraduy 5, (35) Amor 2, (36) Amor 3, (37) Fornons 1, (38) Camino Fornons 1, (39) Camino Fornons 2, (40) Veracruz 1, (41) Fornons 2, (42) Sierra del Sis 1, (43) Sierra del Sis 2, (44) Fornons 3, (45) Isclés 1, (46) Isclés 2, (47) Isclés 3, (48) Isclés 4, (49) Isclés 5, (50) Blasi 1, (51) Areny 1, (52) Blasi 2a and 2b, (53) Blasi 3, (54) Blasi 3, 4, (55) Elias, (56) Blasi 4, (57) Blasi 5 (Larra log is modified from Puértolas Pascual et al. (2018), magnetostratigraphic data from [31,64,75]).



**Figure 3.** Upper Maastrichtian outcrops of the Western Tremp Syncline (Aragón, NE Spain). (a) Campo section (I); (b) Serraduy section (IV); (c) Isclés section (VI); (d) Arén/Areny section (VII).

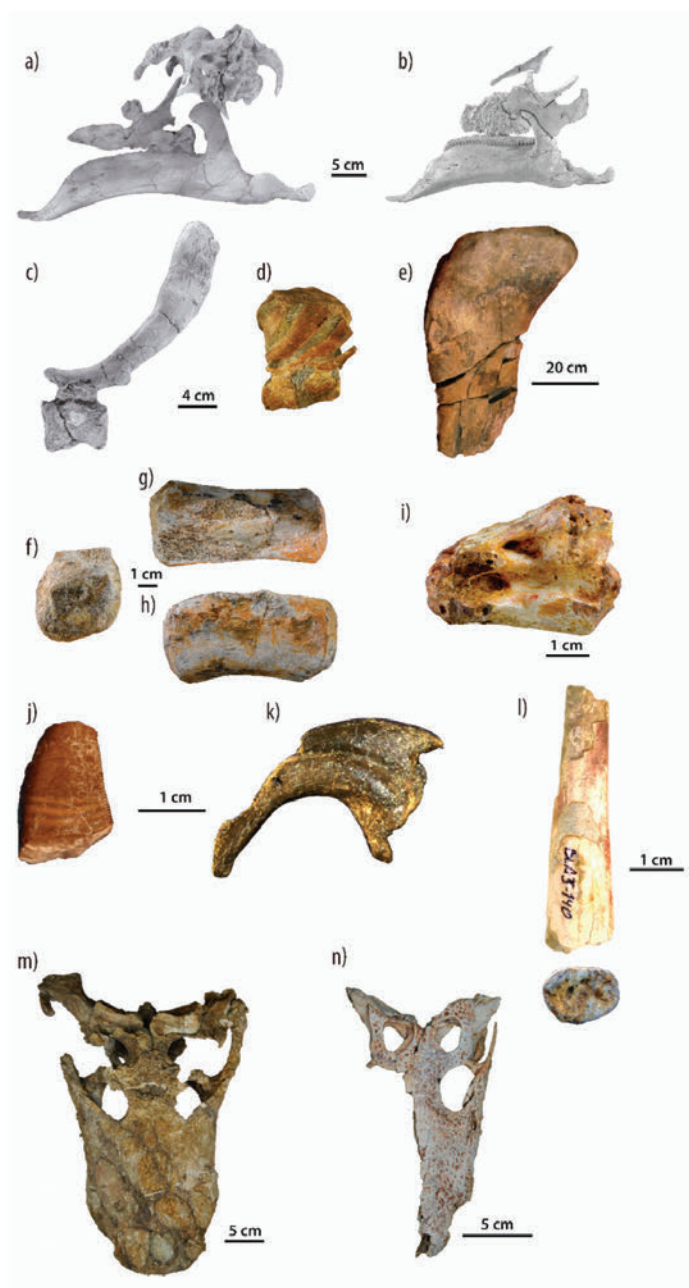
### 3.1. Dinosauria

#### 3.1.1. Hadrosauroidea

Hadrosauroid dinosaurs are the clade of Cretaceous ornithomorphs with the most abundant fossil record, especially in the Northern Hemisphere. In Europe, the best record of hadrosauroids has been recovered from France and Spain. In Spain, it is concentrated principally in the South-Pyrenean Basin (the provinces of Huesca and Lleida, NE Spain) [23,62,75–81].

In the Western Tremp Syncline, hadrosauroids are recorded in the upper Maastrichtian sediments of the Arén Sandstone Fm and the ‘Grey and Lower Red Garumnian’ of the Tremp Fm; these are among the youngest non-avian dinosaurs in the world [64]. The first hadrosauroid bones were found in the 1990s near the locality of Arén (Areny in Catalan) (Huesca, Aragón) by the geologists Lluís Ardèvol and Fabián López Olmedo during geological mapping work. Early work on several sites (Blasi 1 to 5 and Blasi 3,4) by a multidisciplinary team yielded fossil remains of indeterminate euhadrosaurids together with bones and eggshells of several dinosaurs and other terrestrial and aquatic vertebrates [72] (Figure 2). Later studies on specimens from the Blasi 1 and Blasi 3 sites resulted in the erection of two lambeosaurine hadrosaur species: *Blasisaurus canudo* Cruzado-Caballero, Pereda-Suberbiola, and Ruiz-Omeñaca 2010a [82] (Figures 3 and 4b)

and *Arenysaurus ardevoli* Pereda-Suberbiola, Canudo, Cruzado-Caballero, Barco, López-Martínez, Oms and Ruiz-Omeñaca [62,83] (Figures 3 and 4a,c). Both sites fall within the upper part of chron C30n [62]. These two species are recovered within Arenysaurini, which is a recently erected clade of lambeosaurines from Europe [84].



**Figure 4.** Main tetrapod remains from the Western Tremp Syncline. (a) Cranial elements of *Arenysaurus ardevoli* (MPZ2008/17, MPZ2008/256, MPZ2008/258, MPZ2008/259, MPZ2011/01), in left lateral view (modified from Cruzado-Caballero et al., 2013); (b) cranial elements of *Blasisaurus canudoii* (MPZ 99/664, MPZ 99/665, MPZ99/666a, MPZ99/666b, MPZ99/667, MPZ 2009/348), in left lateral view; (c) mid-caudal vertebra of *Arenysaurus* (MPZ204/480), in left lateral view (modified from Cruzado-Caballero et al., 2013); (d) articulated mid-caudal vertebrae of the small hadrosaurid from Serraduy (MPZ 2013-371), in left lateral view; (e) femur (proximal end) of *Titanosauria* indet. from Serraduy (MPZ 99/143), in posterior view (modified from Puértolas-Pascual et al., 2018); (f–h) posterior caudal vertebra of *Titanosauria* indet. (MPZ2021/1), in anterior view (f); dorsal view (g); left lateral view (h); (i) cervical vertebra of *Ornithuromorpha* indet. (MPZ 2019/264), in left lateral view; (j) cf. *Arcovenator* tooth (MPZ 2017/804), in lingual view; (k) pedal ungual II of *Dromaeosauridae* indet. (MPZ 2019/196), in lateral view; (l) fragmentary bone of *Pterosauria* indet. (MPZ 2021/54) (note the thin cortex in the transverse section); (m) skull of *Agaresuchus subjuniperus* (MPZ 2012/288), in dorsal view; (n) skull of *Arenysuchus gascabadiolorum* (MP Z2011/184), in dorsal view.

In addition to this, other remains of indeterminate hadrosaurids and euhadrosaurids have been described from the Blasi sites [76,78,85–87]. The findings from these sites have also led to the first description of a pathological bone from a hadrosaurid in Spain [88] and the first paleo-neuroanatomical description of a European lambeosaurine, *Arenysaurus ardevoli* [89]. Recent studies on the paleohistology of the hadrosauroids from the Blasi sites reveal the presence of hadrosaurid individuals at different ontogenetic stages, including early and late juveniles, subadults, and mature adults [90,91]. New areas with hadrosaurid remains have been found in the vicinities of Serraduy (Isábena, Huesca, Aragón) and Beranuy (Huesca, Aragón) (Figure 2) [23,64,77,79,92–94]. The new sites are characterized by the presence of fossil remains of the smallest adult hadrosaurids (maybe affected by insular dwarfism) from Europe, which coexisted alongside larger hadrosaurids [79] (Figure 4d).

This rich osteological record of hadrosauroids in the Western Tremp Syncline is complemented by several track sites. These tracks appear in several levels from Arén to Campo (Huesca, Aragón), with large ornithopod footprints, many of which have been referred to the ichnogenus *Hadrosauropodus* [31,64,95,96] (Figures 3 and 5a,b), spanning from the top of chron C30n into chron C29r. Recently, in the Blasi 2B site, eggshells attributable to hadrosaurid dinosaurs have been tentatively referred to *Spheroolithus* aff. *europaeus* Sellés, Vila, Galobart 2014 [97,98].

### 3.1.2. Sauropoda

The sauropod remains in the Western Tremp Syncline are very scarce compared to those in the eastern part, where titanosaur bones, eggshells, and tracks are moderately abundant [33,71,99]. A remarkable specimen is the proximal half of a femur (MPZ 99/143) that probably corresponds to a large and indeterminate titanosaur [71,100] (Figure 4e). MPZ 99/143 was recovered northwest of the town of Serraduy, in the ‘Grey Garumnian’ unit (‘Femur’ site in Figure 2). Interestingly, the femur was originally correlated to the top of chron C30n, but the chronostratigraphical data indicate that this fossil lies within chron C29r [31,64]. Thus, this femur is one of the youngest records of titanosaurian sauropods in the Ibero-Armorican island, along with those recorded in fossil sites in the Catalonia region, including the ‘Molí del Baró-2’ femur [71], the vertebra from ‘El Portet’ site [101], and the skin impressions and footprints from the ‘Mirador de Vallcebre’ [102]. In addition, Cruzado-Caballero et al. (2012) [77] reported a caudal vertebral centrum that was found in the ‘Lower Red Garumnian’ unit near Serraduy and Beranuy. The caudal vertebra (MPZ 2021/1) is from the ‘Barranco Serraduy 4’ site (Serraduy) (Figures 2 and 4f–h), which is situated stratigraphically above the ‘Femur’ site, making it the youngest evidence of sauropods in the Western Tremp Syncline. MPZ 2021/1 is a slightly deformed centrum from a posterior caudal vertebra, which is elongated craniocaudally and compressed dorsoventrally. It is amphiplatyan, with both articular surfaces flat to slightly concave and with a rounded contour (Figure 4f,h). In anteroposterior view, the centrum has a subcircular outline (Figure 4f). Its ventral surface is slightly concave and lacks chevron facets (Figure 4h). Together with its length and the absence of transverse processes, this indicates that it was situated distally in the caudal series [103]. The neural arch is not preserved, but its attachment facets can be observed in the anterior area of the centrum (Figure 4g), which is a synapomorphy of Titanosauriformes [104]. The amphiplatyan condition in the middle and posterior caudal vertebrae is plesiomorphic within Titanosauria [104,105]. Some basal titanosaurs show this condition, as is the case of *Andesaurus* [106,107] or the distalmost vertebrae of *Lirainosaurus* [103]. Therefore, we tentatively refer it to Titanosauriformes indet., but for the reasons mentioned above, its ascription to Titanosauria cannot be ruled out.



**Figure 5.** Tetrapod tracks from the Western Tresp Syncline. (a) *Hadrosauropodus* trackway from the Areny 1 site; (b) foot cast of a hadrosaurid dinosaur from the 172-i/04/a site; (c) crocodylomorph tracks from the Serraduy Norte site.

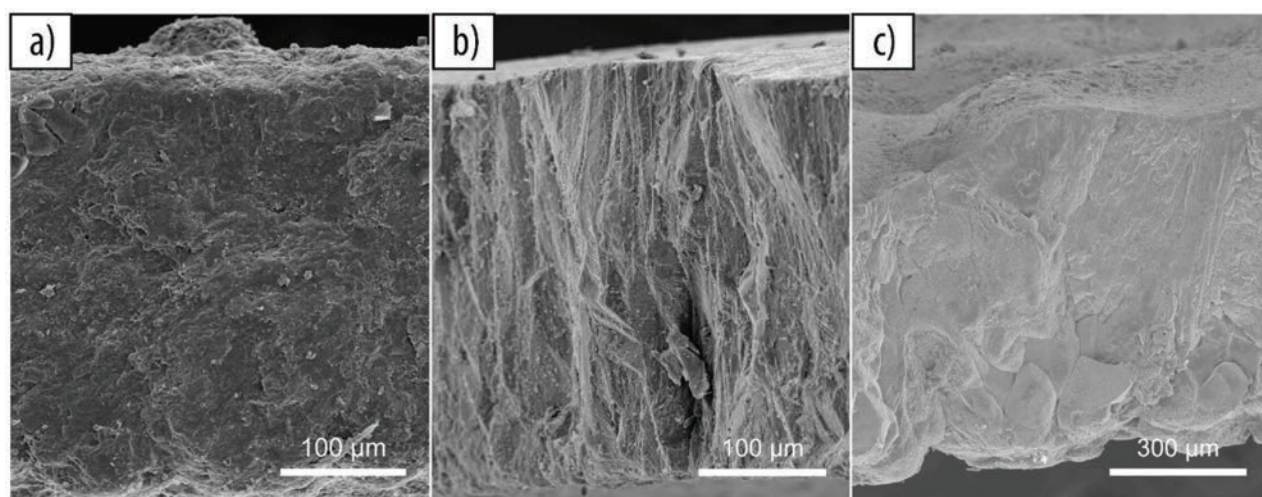
### 3.1.3. Theropoda

Theropod fossils are scarce in the Western Tresp Syncline, and these are mainly represented by teeth, eggshells, and some isolated bones. Torices et al. (2015) [108] describe several teeth from the Blasi sites of Arén/Areny (Figure 2). They identify one

morphotype as Coelurosauria indet. (MPZ 98/79 to 82) and three morphotypes belonging to maniraptoran theropods, including *Richardoestesia* sp. (MPZ 98/72 to 74, MPZ 2004/7), cf. *Paronychodon* (MPZ 98/76 to 78), and Dromaeosauridae indet. (MPZ 2004/6). Finally, they describe two different morphotypes of large teeth whose assignation is problematic and that are referred to Theropoda indet. 1 (MPZ 98/67, MPZ 2004/3 to 5, 8) and Theropoda indet. 2 (MPZ 98/68), although a possible relation with neoceratosaurs is suggested. In fact, these two morphotypes were identified by Pérez-García et al. (2016) as cf. *Arcovenator* [109], which is an abelisaurid species from the Campanian of southern France. The Blasi sites 1, 2, and 3 are dated to within chron C30n [62] (Figure 2). Two more theropod teeth have been described from the fossil sites of 172-i/04/e (Serraduy) and Larra 4 (Valle de Lierp) [64]. The first tooth (MPZ 2017/804) (Figure 4j) is large and resembles the Theropoda indet. morphotype 1 (cf. *Arcovenator*) from Torices et al. (2015) [108], and the second one has been identified as Coelurosauria indet. Both sites are situated in outcrops of the ‘Lower Red Garumnian’ dated to within chron C29r [64].

Postcranial fossils of theropods are not very common and are usually fragmentary. A pedal ungual II (MPZ 2019/196) (Figure 4k) and the proximal part of an ulna (MPZ 2019/194) from a dromaeosaurid theropod were found at the Larra 4 site (Valle de Lierp, Huesca, Aragón, Spain) (Figure 2) [93]. Other sites in the Serraduy area have yielded fragmentary remains of indeterminate theropods (Figure 2). As regards avian theropods, a cervical vertebra from a large ornithuromorph bird has recently been described from the Tresp Fm outcrops between Serraduy and Bascas de Obarra (Beranuy, Huesca) (MPZ 2019/264) [110] (Figures 2 and 4i). It has been dated as uppermost Maastrichtian (C29r) [64] and represents the youngest record of a Mesozoic bird in Europe.

Up to now, theropod eggshells have only been found in the site Blasi 2B (‘Grey Garumnian’ at Arén/Areny, C30n; Figure 2). This site has a diverse theropod eggshell assemblage, which was briefly described by López-Martínez et al. (1999) [111]. The authors recognized up to six different types of prismatic eggshells, whereas more recent research [98,112] recognized at least four different types (Figure 6a,b), including two different morphotypes attributable to the oogenus *Pseudogeckoolithus*, which has recently been referred to maniraptoran theropods [113]. Further research is necessary to ascertain the exact number of theropod ootaxa present at Blasi 2B.



**Figure 6.** Tetrapod eggshells from the Western Tresp Syncline. (a) *Pseudogeckoolithus* sp. from the Blasi 2B site; (b) Prismaticoolithidae indet. from Blasi 2B; (c) *Krokolithes* sp. from the Veracruz 1 site.

### 3.2. Pterosauria

The presence of pterosaurs in the upper Maastrichtian of the Tresp Syncline has only been reported from the site of Torrebillas-2 in the Eastern Tresp Syncline, within chron

C29r [114]. In the Western Tremp Syncline, Puértolas-Pascual et al. (2018) [64] reported a possible mandible of a pterosaur from the upper part of the ‘Lower Red Garumnian’ near Serraduy (Isábena). This specimen has been reexamined, and although its identification as a dentary has been refuted, its affinity to a pterosaurian bone cannot be ruled out. However, until a future study identifies this bone more precisely, it cannot be assigned to Pterosauria. Nevertheless, we have identified a fragment of a long bone from the Blasi 5 site (Figures 2 and 4l) that shows a very thin cortex (thinner than the pterosaur bones from Barranc de Torrebilles-2 [114]) and is hollow inside. This bone could be the first pterosaur fossil identified in the Western Tremp Syncline. Blasi 5 is situated in the upper part of the ‘Lower Red Garumnian’ and is dated to within chron C29r (Figure 2) [62].

### 3.3. *Crocodylomorpha*

The crocodylomorph record in the Western Tremp Syncline is dominated by eusuchians. Two skulls belonging to two different genera have been identified. The first one is *Arenysuchus gascabadiolorum* Puértolas, Canudo, Cruzado-Caballero 2011 [115] (MPZ 2011/184) (Figure 4n), from the Elias site near Arén/Areny (‘Lower Red Garumnian’, C29r, Figure 2). Phylogenetically, MPZ 2011/184 was initially placed within Crocodyloidea (crown-group Crocodylia) [115], but later cladistic studies have situated it as a more basal eusuchian within Allodaposuchidae [116–120]. The second species is the allodaposuchid *Agaresuchus subjuniperus* Puértolas-Pascual, Canudo, Moreno-Azanza 2014 [121] (MPZ 2012/288) (Figure 4m). MPZ 2012/288 was initially identified as a member of the genus *Allodaposuchus* [121], but it was later reassigned to *Agaresuchus* [119]. This crocodylomorph comes from the Amor 3 site near the town of Serraduy, from one of the uppermost levels of the ‘Lower Red Garumnian’ (C29r, Figure 2). As such, it could be one of the youngest crocodylomorphs on the Ibero-Armorican island before the K-Pg extinction. In addition, allodaposuchids are also represented by isolated teeth in several sites throughout the C30n–C29r interval (Figure 2) [23,64,93,94,122]. All these teeth are conical with pointed crowns, showing the typical morphology of crocodylomorphs with a generalist diet. These dental morphologies have been observed in several allodaposuchid species from the Late Cretaceous of Europe (e.g., [122]). As the presence of other crocodylomorph clades with generalist dentition cannot be ruled out, these teeth were assigned to cf. Allodaposuchidae, since this is the most abundant clade in this region and time interval.

Gavialoidea is another clade of crocodylomorphs that may be present in the upper Maastrichtian of the Western Tremp Syncline. A few elongated conical teeth with basiapical ridges have been assigned to cf. *Thoracosaurus*. These are restricted to the transitional environments of the Arén Fm and the ‘Grey Garumnian’ unit of the Tremp Fm close to Arén/Areny, Beranuy and Serraduy (Figure 2) [23,64,122].

Hylaeochampsidae are represented by tribodont teeth from the Blasi 2B site, which were identified as cf. *Acynodon* (MPZ-2017/1137) [23,64,72,122]. The eusuchian record is augmented by teeth, osteoderms, and vertebrae from the Blasi and Serraduy sites, whose taxonomical position within Eusuchia is difficult to assign with precision. They are accordingly identified as Eusuchia indet. [23,64,72,122] (Figure 2).

López-Martínez et al. (2001) [72] pointed out the presence of “trematochampsid”-like and alligatoroid teeth from the sites of Blasi 1, 2, and 3 (Figure 2). However, although the authors did not provide pictures or specimen numbers, the morphotypes in question probably correspond to more recently erected taxa that had not been described at the time of publication of that paper. The “trematochampsid”-like teeth may correspond to non-eusuchian crocodylomorphs more typical of the Late Cretaceous of Europe, such as *Sabresuchus* or *Doratodon*, and the alligatoroid teeth probably correspond to allodaposuchids. In addition, Blanco et al. (2020) [122] mentioned the presence of a conical tooth (MPZ 2010/948) with enamel striations and crenulated carinae assigned to Mesoeucrocodylia indet.

There are also crocodylomorph eggshells from the Blasi 2 site (upper part of C30n, Figure 2). These were first reported as megaloolithid eggshells [111], but they were

later [123] described as having a crocodyloid morphotype and were identified as *Krokolithes* sp. Hirsch, 1985 [124], implying that these eggs were laid by crocodylomorphs. Something similar has occurred with the eggshells found at the Veracruz 1 site close to Biascas de Obarra, (Beranuy section, C29r, Figure 2), which were first identified as hadrosaurid eggshells [94] (Figure 6c), but after a more thorough study, their crocodylomorph affinities have been ascertained, and a description is in preparation.

Finally, the crocodylomorph record also includes several swimming and plantigrade tracks from the Serraduy, Beranuy, and Campo outcrops, all within chron C29r [23,125,126] (Figures 2 and 5c). This is the youngest record of crocodylomorph tracks in Europe. These tracks represent digit scratch marks produced by the manus and pes of buoyant crocodylomorphs, and they have been assigned to the ichnogenus *Characichnos*. One pedal impression has been assigned to cf. *Crocodylopodus*, and although its assignation cannot be confirmed with certainty due to the scarce material, this is the youngest occurrence of this ichnotaxon [125].

### 3.4. Testudines

Testudines are represented mainly by disarticulated plates of the carapace or the plastron, which appear at most of the paleontological sites from the topmost part of the Arén Fm to the upper levels of the 'Lower Red Garumnian' (Figure 2). Most of these remains show fine ornamentation comprising thin dichotomic grooves, which is a distinctive character of the bothremydids [127]. Among these remains, Murelaga and Canudo (2005) [128] describe several plates from the Blasi sites near Arén/Areny (Figure 2), including nuchal, pleural, and peripheral plates, a hyoplastron, a hypoplastron, and a xiphiplastron from bothremydid turtles. At the site of Rin 2, near the town of Serraduy (Isabena municipality), situated in the topmost part of the Arén Fm, Murelaga and Canudo (2005) [128] describe a xiphiplastron and a mesoplastron from a bothremydid. Pérez-Pueyo et al. (2019a, 2019b) [93,94] also describe indeterminate plates from this kind of turtle from the Larra 4 (Valle de Lierp) and Veracruz 1 (Biascas de Obarra, Beranuy) sites (Figure 2). Thus, the record of this group of pleurodiran turtles extends from the upper part of chron C30r to near the K-Pg boundary interval. It is also important to note that Murelaga and Canudo (2005) [128] identify a peripheral plate from a solemydid turtle from the Blasi 2 site (Figure 2). This shows its characteristic vermiculate ornamentation, although it is not well preserved.

### 3.5. Amphibia and Squamata

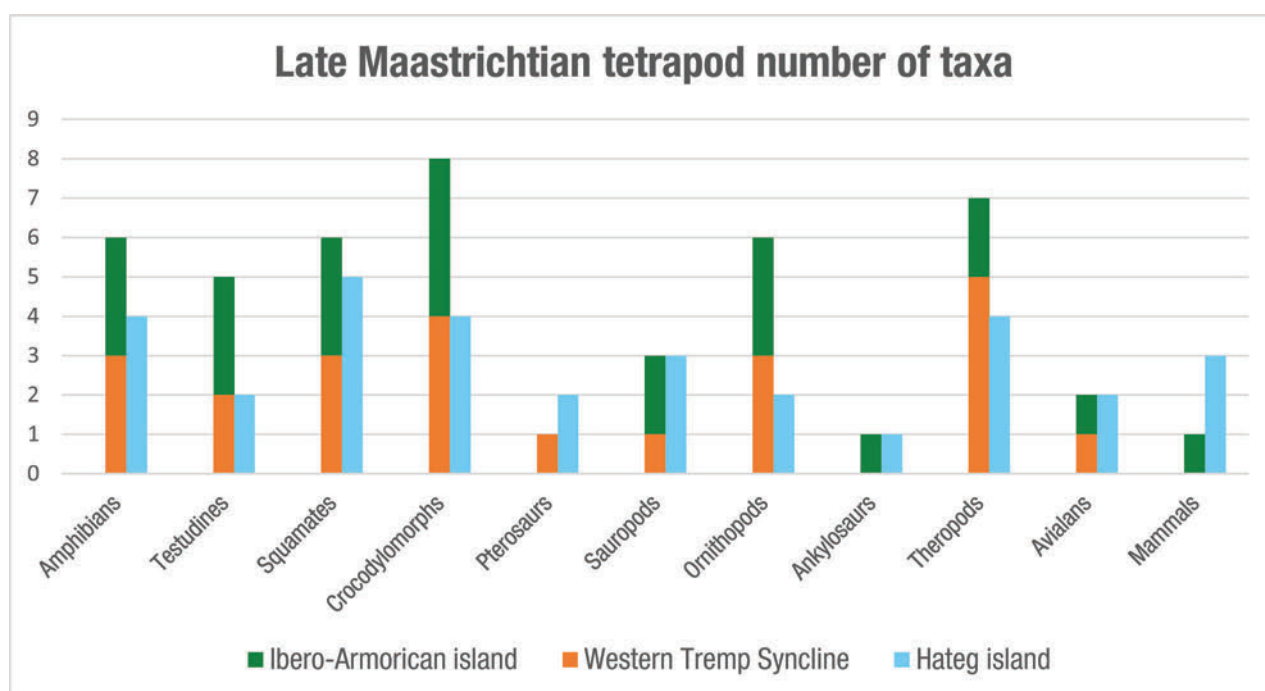
The Blasi 2 site has yielded a rich microvertebrate fossil assemblage, which includes the bones of small tetrapods, mainly amphibians and squamates [129] (Figure 2). Amphibian remains dominate, with at least one albanerpetontid (resembling the North American taxon *Albanerpeton nexuosum*) and two anurans, a discoglossid and a palaeobatrachid. The squamate remains comprise at least two undetermined lizards, one anguid lizard, and a snake. Blasi 2B is dated to the top of chron C30n in the 'Grey Garumnian' and is the only well-studied microvertebrate site in the Western Tremp Syncline. However, it is noteworthy that the Larra 4 site (Valle de Lierp) (C29r) has yielded remains from discoglossid amphibians [64], making it the youngest microvertebrate site in the Western Tremp Syncline.

### 3.6. The Tetrapod Fossil Record from the Upper Maastrichtian of the Ibero-Armorican Island

The tetrapod fossil record of the Western Tremp Syncline adds several unique taxa to the late Maastrichtian assemblages of the Ibero-Armorican island, yielding the youngest record of some groups prior to the Paleocene. To date, the upper Maastrichtian record of the Ibero-Armorican island is limited to the South Pyrenean Basin in northeast Spain; the Sobrepueña Fm, Torme Fm, and equivalent outcrops in northwest Spain [130,131]; east Spain near Tous (Valencia) [132,133]; and the Haute-Garonne and Aude departments in southern France [33,134]. During the Maastrichtian, the dinosaur faunas underwent a change in dominant herbivores during the so-called "Maastrichtian Dinosaur Turnover" [33,34,135].

During the early Maastrichtian, ecosystems were inhabited by rhabdodontid ornithopods, titanosaurian sauropods and ankylosaurs, whereas in the late Maastrichtian, these communities were replaced by hadrosaurid ornithopods and new titanosaurian forms. However, nodosaurid ankylosaurs still persisted up to chron C30r, coexisting with these new assemblages for nearly 2 Myr [33].

Lambeosaurine hadrosaurids were present in the Ibero-Armorican island from the late early Maastrichtian, mostly recorded from the Pyrenees (Spanish and French). The lambeosaurine from Els Nerets (Vilamitjana, Catalonia, NE Spain) is the oldest evidence of hadrosaurids in Europe, which was dated to within chron C31r [81]. Lambeosaurines are also present within chron C29r, with some fossils falling very close to the K-Pg boundary. At present, there are five species of lambeosaurine hadrosaurids described from the region, comprising *Adynomosaurus* from the Costa de Les Solanes site (Basturs, Catalonia) [136], *Arenysaurus* [62], *Blasisaurus* [82] from Areny and Blasi sites (Ribagorça, Aragón, NE Spain), *Pararhabdodon* from the Sant Romà d'Abella site (Lleida, Catalonia, NE Spain) [80,137–139], and *Canardia* from the Lacarn and Tricouté sites (Haute-Garonne, southern France) [80]. Additional hadrosauroid remains include the aforementioned lambeosaurinae from Els Nerets [81] and other indeterminate lambeosaurines from Basturs Poble and Les Llaus (Lleida, Catalonia) [80,140–142]; a non-hadrosaurid hadrosauroid from Fontllonga-R (Fontllonga, Catalonia, NE Spain) [75]; an indeterminate euhadrosaurid from Blasi 3,4 [78]; and a small hadrosaurid from Serraduy [79]. Outside the Pyrenees, there is a dentary from La Solana (Tous, Valencia, E Spain) that has been identified as belonging to an indeterminate hadrosaurid [75,143]. Finally, there is a hadrosauroid femur from the Albaina site (Laño, Condado de Treviño, Burgos, NW Spain) [144]. With six to twelve taxa, hadrosauroids are the most speciose clade of dinosaurs in the Tremp Basin, five to eight of them being lambeosaurine hadrosaurids (Table 1, Figures 7 and 8).



**Figure 7.** Bar chart with the minimum number of tetrapod taxa (genera) present in the Ibero-Armorican island and Hateg island during the late Maastrichtian.

**Table 1.** Number of tetrapod taxa present on the Ibero-Armorican and Hațeg islands during the late Maastrichtian. Red numbers mark possible additional taxa.

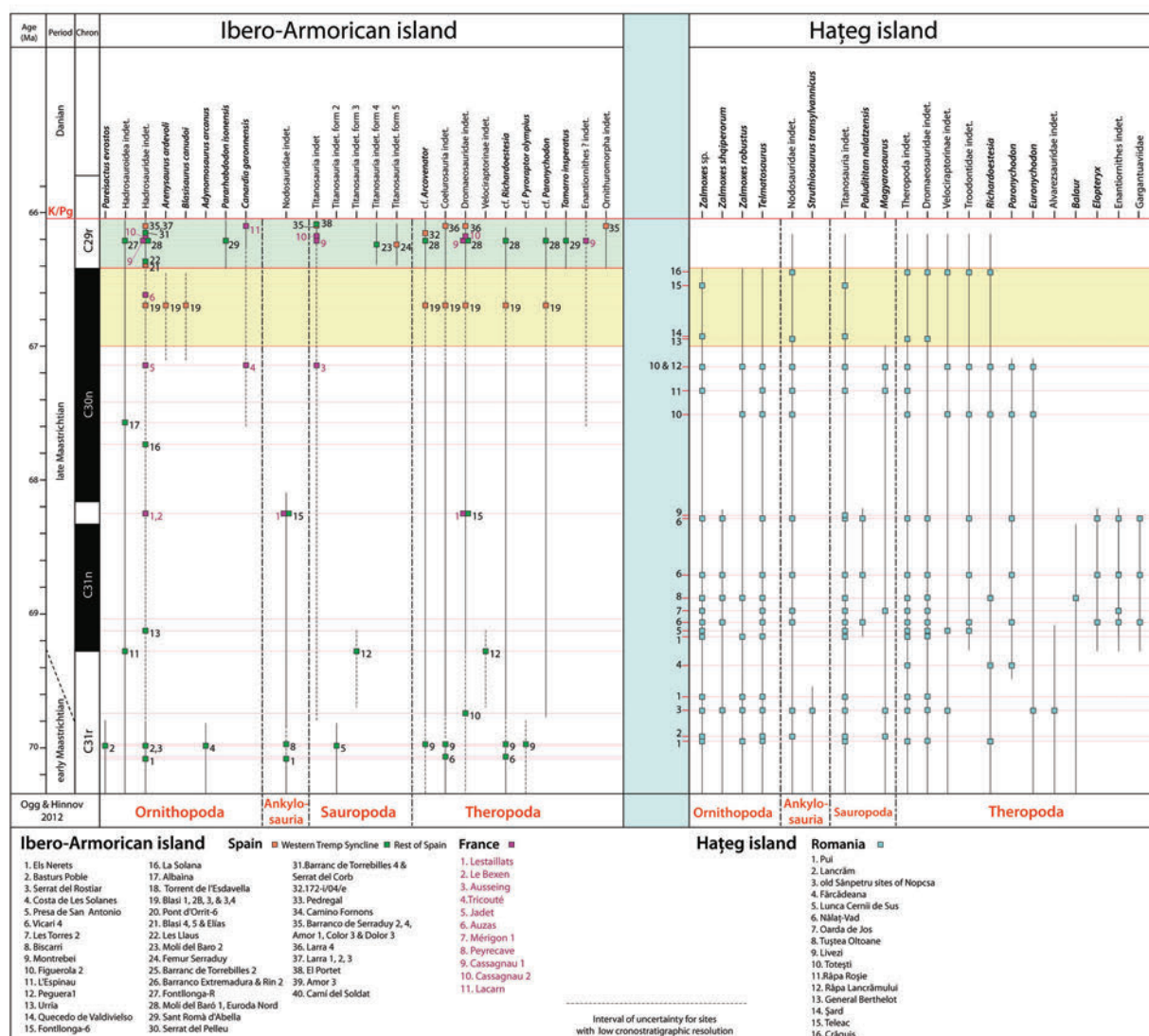
Taxon	Ibero-Armorican Island	Western Trepmp Syncline	Hațeg Island
<b>Amphibia</b>	<b>6</b>	<b>3</b>	<b>4</b>
Anura	4	2	3
Albanerpetontidae	1	1	1
Salamandridae	1	—	—
<b>Squamata</b>	<b>6 + 2?</b>	<b>3 + 2?</b>	<b>5</b>
‘Scincomorpha’	1	1?	1
Anguimorpha	1	1	1
Teiioidea	1	—	1
Borioteiioidea	—	—	1
Scleroglossa	1	1	—
Iguanidae	1	1?	—
Amphisbaenia	1?	—	—
Varanoidea	1?	—	—
Alethinophidia	1	1	1
<b>Testudines</b>	<b>5</b>	<b>2</b>	<b>2</b>
Meiolaniformes	—	—	1
Pan-Pleurodira	3	1	1
Pan-Cryptodira	2	1	—
<b>Crocodylomorpha</b>	<b>8</b>	<b>4</b>	<b>4</b>
Notosuchia ( <i>Doratodon</i> )	1	—	1
Neosuchia (‘Atoposauridae’)	1	—	1
Basal Eusuchia	4	2	1
(Allodaposuchidae)			
Basal Eusuchia			
(Hylaeochampsidae, cf. <i>Acynodon</i> )	1	1	1
Eusuchia (Gavialoidea)	1	1	—
<b>Pterosauria</b>	<b>1</b>	<b>1</b>	<b>2</b>
Azhdarchidae	1	1	2
<b>Dinosauria</b>	<b>18 + 1? (6)</b>	<b>10 (1)</b>	<b>12 + 1? (3)</b>
<b>Sauropoda</b>	<b>3</b>	<b>1</b>	<b>3</b>
Titanosauria	3	1	3
<b>Theropoda</b>	<b>8 + 1?</b>	<b>6</b>	<b>6 + 1? (3)</b>
Alvarezsauridae	—	—	1?
Abelisauroidae	1	1	—
Coelurosauria indet.	1	1	—
Maniraptora	5	3	3 (2)
Paraves with uncertain affinities ( <i>Balaur</i> , <i>Elopteryx</i> )	—	—	1 (1)
Enantiornithes	1?	—	1
Ornithuromorpha	1	1	1
<b>Ornithopoda</b>	<b>6 (6)</b>	<b>3 (1)</b>	<b>2</b>
Rhabdodontidae	—	—	1
Hadrosauroidae	6 (6)	3 (1)	1
<b>Ankylosauria</b>	<b>1</b>	<b>—</b>	<b>1</b>
Nodosauridae	1	—	1
<b>Mammalia</b>	<b>1?</b>	<b>—</b>	<b>3</b>
Multituberculata	—	—	3
Theria	1?	—	—

Ankylosaurs are represented during the late Maastrichtian by isolated and fragmentary material referred to nodosaurids from several sites in the Southern Pyrenees within the Lleida province (Catalonia, NE Spain), including Els Nerets [145], Fontllonga-6 [111], and Biscarri [146]. They are also present at the Lestaillats site, in the Petite Pyrénées (Haute-

Garonne, southern France) [134]. Their last occurrence is documented at the Fontllonga-6 and Lestaillats sites, dated to within chrons C30r and C30n (Figure 8).

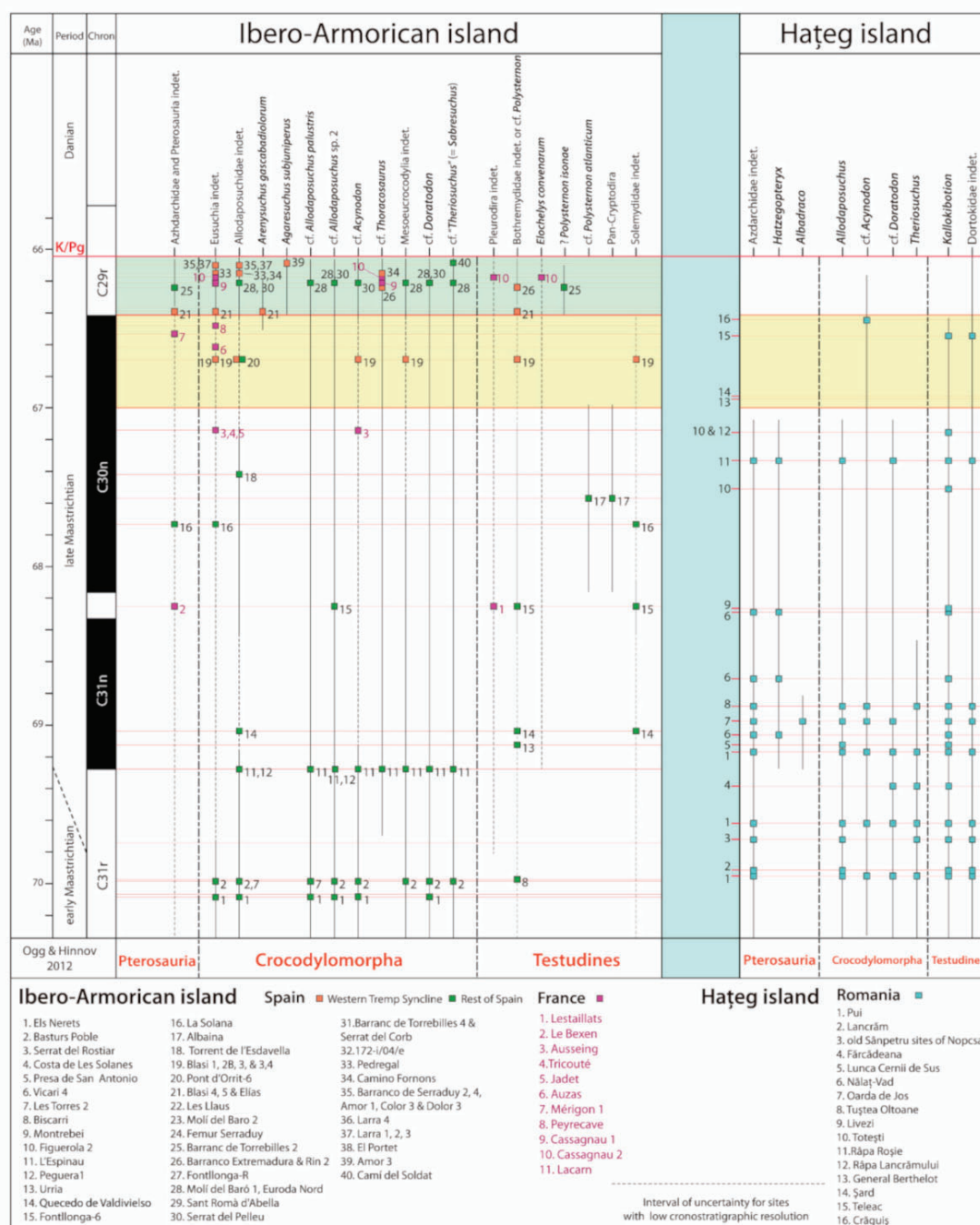
Titanosaurs from the upper Maastrichtian of the Ibero-Armorican island consist mainly of three undetermined but distinct taxa represented by three femur morphotypes [71] (Figures 7 and 8). The femur from Serraduy corresponds to a large titanosaur, whereas the other two femora represent small-medium titosaurs. Although not formally described, these titosaurs represent different taxa from those of the early Maastrichtian assemblage [71]. This distinction is additionally supported by the distinct ootaxa association reported from the pre- and post-turnover assemblages, respectively [33,99].

Theropods from the late Maastrichtian of the Ibero-Armorican island are mainly abelisaurids and maniraptorans [64,93,108,147,148], and they have been found only in the South-Pyrenean Basin. Due to their fragmentary and incomplete nature, the number of taxa is difficult to determine. Based on tooth morphotypes from the Southern Pyrenees, at least one abelisaurid taxon inhabited the island during the late Maastrichtian (Theropoda indet. 1 and 2 or cf. *Arcovenator*; [108]) (Figures 7 and 8). Maniraptorans are also represented mainly by teeth from the Southern Pyrenees, with at least three taxa identified in this way (*Richardoestesia*, *Paronychodon*, and Dromaeosauridae indet. from [108]), and by the troodontid *Tamarro insperatus* Sellés, Vila, Brusatte, Currie and Galobart 2021 [149], which were recently described on the basis of skeletal remains (Table 1, Figures 7 and 8). However, the real abundance of theropods is hard to establish, since there are several fragmentary skeletal remains attributable to undetermined dromaeosaurids, and an oological record comprising several ootaxa of maniraptoran-like eggshells, including *Prismatoolithus trempii* Sellés, Vila, Galobart 2014 [150], and *Pseudogeckoolithus* Vianey-Liaud and López-Martínez 1997 [151] ([98,113,150]). Avialan dinosaurs are represented by the giant ornithuromorph bird from Beranuy [110] and a putative enantiornithine from southern France [152] (Table 1, Figures 7 and 8).



**Figure 8.** Dinosaur groups and species occurrences in the Ibero-Armorican island and Hațeg island during the late Maastrichtian. Hațeg island data are based on [32] with updated information. The yellow band marks the temporal interval used for comparison, whereas the green band marks the last  $\approx 350$  ka of the Maastrichtian, with a record only in the Ibero-Armorican island. Magnetostratigraphic scale based on [153] and calibration for the K-Pg boundary based on [28].

The pterosaur record in the late Maastrichtian is scarce, with some isolated and fragmentary bones from the Pyrenees of France [154–156] and Spain [114] and from the upper Maastrichtian outcrops near Valencia (Spain) [157,158] (Figure 9). All of them have been identified as belonging to undetermined giant azhdarchids.



**Figure 9.** Pterosaur, crocodylomorph, and testudines groups and species occurrences in the Ibero-Armorican island and Hațeg island during the late Maastrichtian. Hațeg island data based on [32] with updated information. The yellow band marks the temporal interval used for comparison, whereas the green band marks the last  $\approx 350$  ka of the Maastrichtian, with a record only in the Ibero-Armorican island. Magnetostratigraphic scale based on [153] and calibration for the K-Pg boundary based on [28].

During the late Maastrichtian, the crocodylomorphs of the Ibero-Armorican island show great abundance, with a similar number of taxa to that during the early Maastrichtian [23]. The best-represented clade is the eusuchian Allodaposuchidae, with two taxa described from the Western Tresp Syncline (*Agaresuchus subjuniperus* and *Arenysuchus*),

and probably *Allodaposuchus palustris*, whose characteristic teeth have been found up to chron C29r [122,148]. In addition, Blanco et al. (2020) [122] described *Allodaposuchus* sp. 2 on the basis of a dentary from the Fontllonga-6 site (C30r), which seems to be different from the allodaposuchids previously described and could represent a new taxon. Finally, there are plenty of isolated teeth of allodaposuchids [64,121,148,159] that due to their conical generalist shape are difficult to ascribe to specific taxa.

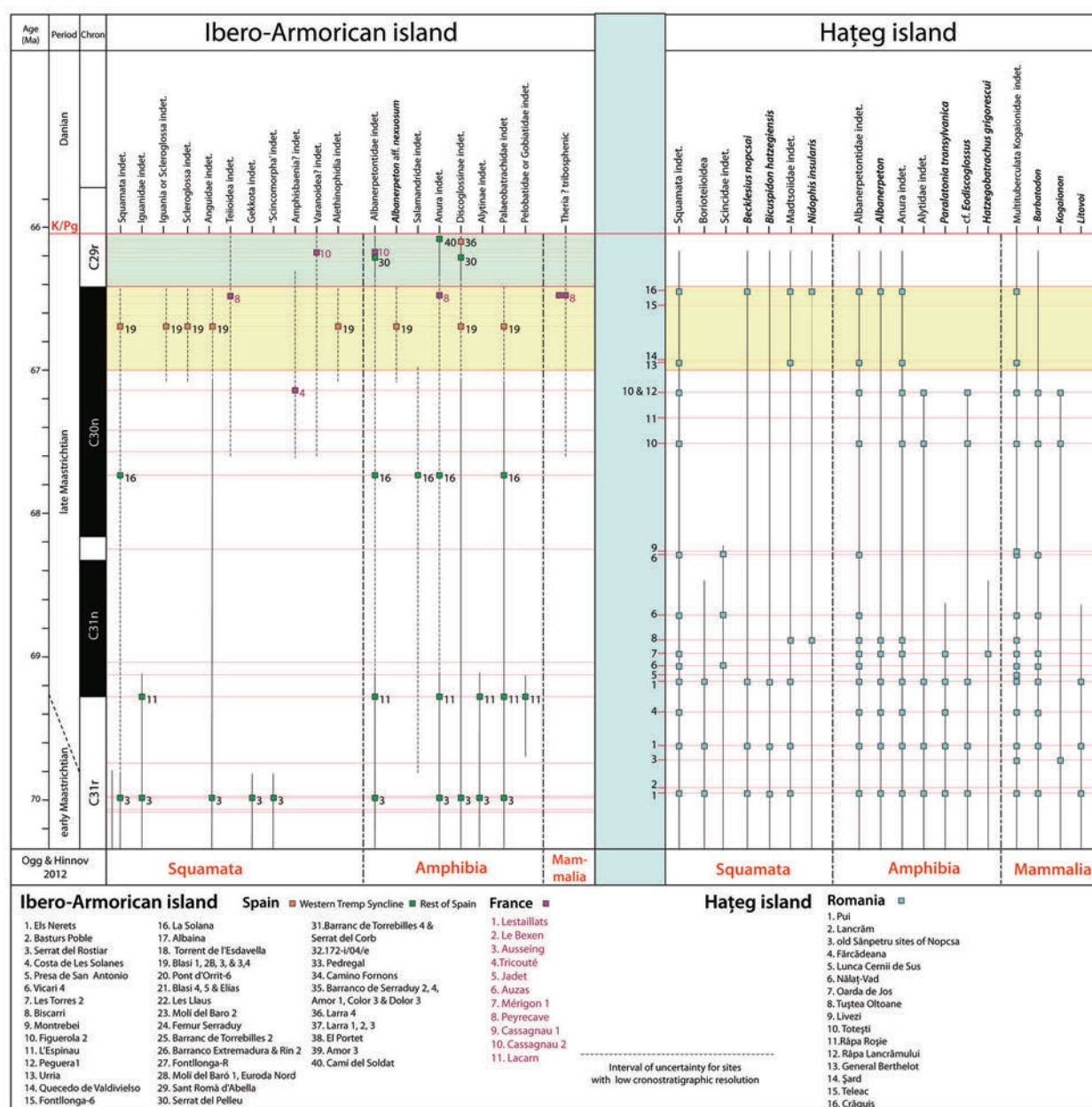
Gavialoidea is represented by a skull and other associated remains from the site of Cassagnau (Haute-Garonne, southern France). These have been ascribed to *Thoracosaurus neocesariensis* [160]. This assignment has been debated, as the remains could belong to a new taxon [161]. In addition, more teeth referred to cf. *Thoracosaurus* have been found in the Spanish Pyrenees, including the record of the Western Tresp Syncline [64,122].

The diversity of hylaeochampsids, “atoposaurids”, and notosuchians during the late Maastrichtian is difficult to determine, since most of their fossils are isolated teeth. There are several teeth referred to cf. *Acynodon* from France [162,163] and the Spanish Pyrenees, including the Western Tresp Syncline [122]. “Atoposaurids” are represented by teeth identified as cf. *Theriosuchus*; these are from the Spanish Pyrenees [122,148] but not the Western Tresp Syncline. “Atoposauridae” is here written in quotes, since Tennant et al. (2016) [164] have argued that some taxa assigned to this clade, such as “*Theriosuchus*” *ibericus* and “*Theriosuchus*” *sympiestodon*, belong to Paralligatoridae and have accordingly grouped these taxa under the new genus *Sabresuchus*. There are also some teeth from the Spanish Pyrenees identified as the notosuchian cf. *Doratodon* [122,148]. It should further be noted that plenty of undetermined eusuchian and crocodylomorph remains have been discovered in the French and Spanish Pyrenees (see [23] and references therein), as well as fossil tracks of crocodylomorphs [125], but due to their limited diagnostic value, it is difficult to ascertain their taxonomic status more precisely. There are also indeterminate eusuchian remains from La Solana (Valencia) [132] and Quecedo de Valdivielso (Burgos, NW Spain) [165,166]. Thus, Ibero-Armorican crocodylomorphs are represented during the late Maastrichtian by a minimum of eight taxa (Table 1, Figures 7 and 9).

The record of testudines during the late Maastrichtian of the Ibero-Armorican island is poorer than during the early Maastrichtian. In the Pyrenees, pleurodiran turtles are represented by the bothremydid *Elochelys convenarum* Laurent, Tong, Claude [167] from southern France and another bothremydid turtle from Isona. This represents the species *Polysternon isonae* Marmi, Luján, Riera, Gaete, Oms, Galobart [168], although Pérez-García [169] considers this a *nomen dubium*, lacking enough diagnostic characters for a new species, and classifies the remains as *Foxemydina* indet. Isolated remains of indeterminate bothremydidids are also present in other sites in the Pyrenees [128,170] and in the northwestern Spanish sites of Urria and Quecedo de Valdivielso (Burgos) [165,166]. In the fossil site of Albaina, there is a plate identified as cf. *Polysternon atlanticum* [144]. Pan-cryptodirans are represented by the remains of solemydid turtles from the Pyrenees, from the sites of Blasi and Fontllonga-6 [128,170], and from La Solana (Valencia) [132,133]. Pereda-Suberbiola et al. (2015) [144] describe a plate from a putative pan-cryptodiran that differs from solemydidids. This makes a minimum of three pan-pleurodirans and two pan-cryptodirans in the Ibero-Armorican island during the late Maastrichtian (Table 1, Figures 7 and 9).

Small-sized upper Maastrichtian tetrapods from the Ibero-Armorican island are represented only by amphibians and squamates from the Spanish and French Pyrenees [129,134,152,171] and from Valencia [172] (Figure 10). The first group consists of albanerpetontids, with at least one taxon present, identified in Blasi 2 as *Albanerpeton* aff. *nexuosum* [129], plus several albanerpetontid remains from the L’Espinau and Serrat del Rostiar 1 sites (Lleida, Catalonia, NE Spain) [171], Cassagnau 1 (Haute-Garonne, southern France) [134,152], and La Solana [172]. In La Solana, the presence of a salamandrid is also documented [172]. Anurans may be represented by at least four different groups with one discoglossid and one palaeobatrachid recognized at Blasi 2, L’Espinau, and Serrat del Rostiar [129,171], and an alytid and a putative pelobatid or gobiatid at L’Espinau [171].

It is noteworthy that there are remains of a palaeobatrachid from Valencia [172] that shows differences from the Blasi 2 taxon and could represent another taxon.



**Figure 10.** Squamate, amphibian and mammal groups and species occurrences in the Ibero-Armorican island and Hațeg island during the late Maastrichtian. Hațeg island data based on [32] with updated information. The yellow band marks the temporal interval used for comparison, whereas the green band marks the last ~350 ka of the Maastrichtian, with a record only in the Ibero-Armorican island. Magnetochronostratigraphic scale based on [153] and calibration for the K-Pg boundary based on [28].

Upper Maastrichtian squamates are represented by the previously described fossils from Blasi 2 [129], with two undetermined lizards, one anguid lizard, and an alethinophid snake. Additionally, in the Pyrenees, the site of Serrat del Rostiar 1 (Lleida, Catalonia) has yielded several squamate remains [171] including geckos, anguid, and “scincomorph” lizards, and an indeterminate iguanid. An indeterminate iguanid can also be found at L'Espinau. The Serrat del Rostiar 1 site is dated to within chron C31r in the early Maastrichtian, but due to its stratigraphic position, it lies very close to the boundary with

the late Maastrichtian, so we have extended its faunal assemblage to the lower part of the late Maastrichtian (Figure 10). In the French Pyrenees, there is also evidence of a large varanoid, “scincomorph” lizards, and other indeterminate squamates [134,152]. Outside the Pyrenees, there are also undetermined squamate remains at the La Solana site [132].

It is interesting to note that during the late Maastrichtian, there is almost no evidence of mammals in the Spanish record of the Ibero-Armorican island, despite the fact that their presence is documented during the early Maastrichtian [173–175] and the earliest Paleocene [176,177]. The only evidence of mammals during the late Maastrichtian is some tribosphenic teeth from the Peyrecave site, in the Petites Pyrénées (Haute-Garonne, southern France). These would have belonged to a therian mammal [152,178].

## 4. Discussion

### 4.1. Comparison with the Upper Maastrichtian Vertebrate Assemblage from the Hațeg Island

To assess the composition of the dinosaur communities of the European Archipelago at the end of the Cretaceous and thus how they faced the K-Pg extinction event, we performed a faunal comparison between the inferred communities of Ibero-Armorican tetrapods and those of Hațeg island, which is another European landmass with a well-known Maastrichtian tetrapod assemblage (Table 1, Figures 7 and 8). The Hațeg island encompasses part of present-day Transylvania (western Romania) [179]. During the Late Cretaceous, it was inhabited by an unusual community of vertebrates, with several groups showing dwarfism and other peculiar adaptations to insularity [30,180]. The upper Maastrichtian vertebrate fossils of Hațeg island are recovered mainly from the Sînpetru, Densuș-Ciula and Sebeș formations, which range from the Santonian-Campanian to the upper Maastrichtian (see [32] for a detailed chronostratigraphic framework). In the late Maastrichtian, the dinosaur assemblage consisted of rhabdodontids, hadrosauroids, titanosaurian sauropods and nodosaurid ankylosaurs, similar to the early Maastrichtian assemblages of the region; this presumably indicates that a major dinosaur turnover did not occur during the early–late Maastrichtian transition. This represents a remarkable difference with respect to the replacement pattern observed in the Ibero-Armorican island [33]. Here, we summarize the tetrapod assemblages of Hațeg island present in tiers 3 and 4 of Csiki-Sava et al. (2016) [32], which is equivalent to the uppermost part of the lower Maastrichtian (C31r) and to the upper Maastrichtian (C31n, C30n, C30r, but not chron C29r) (Figures 8–10). In order to focus on the youngest time interval in the latest Maastrichtian in which contemporary tetrapod communities are preserved in both islands, we thus select the last 800–850 ky of the Maastrichtian, which comprises the upper part of chron C30n (yellow fringe in Figures 8–10) and the Maastrichtian part of chron C29r (green fringe in Figures 8–10). As can be observed, there are C29r vertebrate sites only in the Ibero-Armorican island (Figures 8–10).

#### 4.1.1. Dinosauria

Despite both islands having very similar assemblages of dinosaurs during the early Maastrichtian, this dramatically changed in the late Maastrichtian due to the aforementioned faunal turnover on the Ibero-Armorican island. Regarding herbivorous dinosaurs, in the last 800 ky prior to the K-Pg event (during the upper part of chron C30n and lower part of C29r), the communities of the Ibero-Armorican island were dominated by lambeosaurine hadrosaurids and titanosaurian sauropods (Table 1, Figures 7 and 8). The lambeosaurines were represented by at least four medium-sized taxa (*Arenysaurus*, *Blasisaurus*, *Canardia*, and *Pararhabdodon*), which was probably a small-sized hadrosaurid that had undergone insular dwarfism [79], and a non-hadrosaurid hadrosauroid [75]. Titanosaurs have not yet been documented in chron C30n, but they are present in C29r (Figure 8), and it is reasonable to assume that those forms present in C29r would be present in the upper part of C30n. These correspond to a large and a small–medium form [71]. In Hațeg island, by contrast, the herbivorous communities show a higher clade diversity, with rhabdodontids, hadrosauroids, nodosaurian ankylosaurs, and titanosaurs.

The small-sized rhabdodontids were represented by two species of the genus *Zalmoxes*, *Z. robustus* and *Z. shqiperorum* [32,181,182], although the latter seems not to have reached the upper part of chron C30n (Figure 8). Hadrosauroids are represented only by the small-sized non-hadrosaurid hadrosauroid *Telmatosaurus* [32,183]. However, the latter could be a wastebasket taxon, and hadrosauroid diversity in the latest Maastrichtian could be higher [184]. Ankylosaurs also reached the latest Maastrichtian, although only isolated teeth and fragmentary fossils have been found [32,185–187]. However, the holotype of *Struthiosaurus transylvanicus* [188] might be situated in the basal part of the upper Maastrichtian (tier 3, [32]). Titanosaurs are represented by dwarf and medium-sized forms, which cohabited the island during the late Maastrichtian [189–192], although their record is absent in the lower part of C29r. At least three taxa are recognized, including *Paludititan* and *Magyarosaurus* (Table 1, Figure 8), but most of the recovered material is indeterminate and is in review [193], so the diversity of sauropods remains uncertain [32].

These differences between the two islands are clearly caused by the reorganization of the ecosystems after the arrival of lambeosaurines and new titanosaur faunas on the Ibero-Armorican island [33,34]. This group of hadrosaurids arrived on the island around the mid-part of chron C31r, in the late early Maastrichtian [33]. This arrival apparently occurred in several waves, but it was all of Asian origin [80,83,84], and it represented a complete shift in the herbivorous dinosaur assemblages of the island. Hadrosaurids have been recognized as very efficient plant-eaters mainly on account of the advantages of their dental battery and feeding strategies [194–196]. Although they coexisted for some time with rhabdodontids and ankylosaurs, rhabdodontids seem to have been unable to compete and did not reach the upper part of the late Maastrichtian, disappearing from the island around the C31r–C31n boundary, followed by the nodosaurid ankylosaurians in chron C30n [33] (Figure 8). By contrast, it seems that lambeosaurine hadrosaurids did not reach Hațeg island, and the Hațeg herbivorous assemblage remained stable until the K–Pg boundary. Consequently, in Hațeg island, there is no evidence of herbivore turnover due to ecosystem reorganization after the arrival of newcomers.

As regards non-avian theropods, the fossil record in both islands is composed mainly of isolated teeth, making it difficult to assess their diversity. Both islands were inhabited by several taxa of small to medium-sized maniraptoran theropods: at least three in the Ibero-Armorican island (*Richardoestesia*, *Paronychodon*, and a dromaeosaurid morphotype) and (historically) at least five morphotypes in Hațeg, including *Richardoestesia*, *Paronychodon*, *Euronychodon*, a “troodontid”, and a “velociraptorine dromaeosaurid” [32,185,197] (Table 1; Figure 8). However, new research simplifies the teeth from Hațeg to within three morphospaces: Dromaeosauridae, *Richardoestesia* and *Euronychodon* [198]. The recent discovery of the troodontid *Tamarro* in the Ibero-Armorican island [149] represents the fourth maniraptoran theropod of the island and the first not described based on isolated teeth. It implies that troodontids were then present in both islands. However, significant differences between the islands exist regarding the medium to big-sized theropods. In the Ibero-Armorican island, there was at least one abelisaurid (cf. *Arcovenator*) during chron C30n, which would be the main predator. In the Hațeg island, there is no record of this kind of theropod, nor of any kind of medium to big-sized theropod (Figure 8). Nor is there any evidence of the enigmatic theropods *Balaur* [199,200] and *Elopteryx* [32] in the latest Maastrichtian of Hațeg island, although they are present in the lower part of the upper Maastrichtian (Figure 8). Finally, some small teeth have been found in the Ibero-Armorican island in the upper part of chron C30n; these have been referred to indeterminate small coelurosaurians (Figure 8).

Avialae are not recorded during C30n in either of the two islands (Figure 8), but in the Ibero-Armorican island, a putative enantiornithine [152] and a large ornithuromorph [110] are present during chron C29r, so their presence could be inferred in the upper part of chron C30n. In Hațeg island, enantiornithine birds [201] and gargantuaviids [202] have been recognized, but just in the lower part of the upper Maastrichtian (C31n–C30r; Figure 8).

These faunal differences between the islands indicate that the Ibero-Armorican land-mass, despite its insular condition, allowed the dispersal of faunas at some points in time. This is supported by the presence of ‘Ibero-Armorican’ groups outside the island (arenysaurins and titanosaurs in Africa; [84,203]) and by the arrival of Gondwanan theropods (abelisaurids; [204]) or Laurasian hadrosaurids (lambeosaurines; [139]). By contrast, the immigrants arriving at Hațeg island at the Campanian–Maastrichtian boundary did not include Asian lambeosaurines but distinct velociraptorines and possibly alvarezsaurids [30] that probably followed different migratory routes. The arrival of such newcomers seems not to have significantly altered the evolution of its “primitive” dinosaur faunas or their ecological roles, and some of them became smaller in size as a consequence of “insular dwarfism” ([180]) whereas others showed peculiar ecological adaptations (e.g., aberrant theropods [200]).

#### 4.1.2. Pterosauria

Pterosaurs are represented by large azhdarchids during the late Maastrichtian of both islands, although the record in Ibero-Armorica is scarcer and more fragmentary [114,154,157]. In Hațeg, during the late Maastrichtian, at least two different taxa of giant azhdarchids (*Hatzegopteryx* [191,205,206] and *Albadraco* [207]) (Table 1) coexisted, despite there being no record of them in the upper part of C30n and C29r. However, it seems plausible that they were present since there are remains of indeterminate azhdarchids in that interval (Figure 9). It has been suggested that in Hațeg island, these giant azhdarchids would have occupied the role of large predators due to the absence of large theropods in the island [206]. Their ecological role in the Ibero-Armorican island is more difficult to determine, since there were medium–large theropods (abelisaurids) dwelling on the island.

#### 4.1.3. Crocodylomorpha

The main clades of Crocodylomorpha present in the latest Cretaceous of Europe already inhabited the continent millions of years before the extinction at the K-Pg boundary. The most common clade is Allodaposuchidae, whose earliest record is from the Santonian of Hungary [208]. Subsequently, these basal eusuchians became the dominant crocodylomorphs during the Campanian and Maastrichtian of Europe. During the late Maastrichtian of the Ibero-Armorican island, indeterminate allodaposuchids (mostly isolated teeth) are present in most stratigraphic levels up to the uppermost part of the Maastrichtian part of chron C29r (Figure 9). Many of these teeth may fall within C29r and belong to *Arenysuchus gascabadiolorum*, *Agaresuchus subjuniperus*, or other unknown species, but their generalist morphology does not allow a more specific assignment. Other remains with a more peculiar morphology may belong to the lower Maastrichtian species *Al. palustris*, and thus, its record would cover almost the entire Maastrichtian [122]. In addition, remains very similar to a specimen that Blanco et al. (2020) [122] assigned to *Allodaposuchus* sp. 2 are present throughout the upper Maastrichtian. Therefore, during the late Maastrichtian and up to the K-Pg boundary, there was a great abundance of defined species of allodaposuchids in the Ibero-Armorican island, with at least three species and a fourth possible new species. This contrasts with the allodaposuchid situation observed in Hațeg island during this time interval, where only remains assigned to *Allodaposuchus* sp. have been described (e.g., [32]). Whether these remains belong to the Romanian species *Al. precedens* or to other taxa is difficult to establish, since most occurrences are based on undiagnostic postcranial material or isolated teeth with generalist morphologies typical of several contemporary European taxa such as *Arenysuchus* and *Agaresuchus*. Another difference between the allodaposuchids of the two islands is that the last record in Hațeg occurs in the middle part of chron C30n. Whether their absence during the last million years before the K-Pg boundary is real or due to some kind of bias cannot be determined in the present work. However, it should be noted that in most Maastrichtian microvertebrate sites in Europe, the conical teeth of Allodaposuchidae are among the most common remains, appearing in a wide variety

of sedimentary environments [122]. Consequently, the hypothesis that the clade truly disappeared at the end of the Maastrichtian, and that this disappearance is not merely an artifact of biases, must be considered.

Another common clade of basal eusuchians during the late Maastrichtian of Europe is Hylaeochampsidae, specifically the genus *Acynodon*. This genus is known from the Campanian to the late Maastrichtian of Europe (e.g., [23]). Most of the late Maastrichtian remains assigned to this taxon are isolated teeth with a peculiar button-like (molariform, tribodont) morphology associated with durophagy. Although this dental morphology is present in several lineages among Crocodylomorpha (e.g., *Bernissartia*), so far, the only European Late Cretaceous taxon with this morphology is *Acynodon*. For this reason, these teeth are usually assigned to cf. *Acynodon*. In contrast to the allodaposuchids, there is a similar record of the clade on both islands, covering most of the late Maastrichtian. The last record of cf. *Acynodon* (and the last record of Crocodylomorpha in Hațeg) occurs at the end of chron C30n. This last appearance is based on an isolated blunt tooth recovered in Crăguș, which is a very rich area for microvertebrates ([32]). However, the presence of *Acynodon* and other vertebrates in Hațeg island during chron C29r cannot be ascertained, as there is no sedimentary record for this period [32] (Figure 9).

During the late Maastrichtian, the only clade whose presence is recorded in the Ibero-Armorican island but not in Hațeg is Crocodylia, with a single representative, the genus *Thoracosaurus*. The presence of this genus is based on an almost complete skull, teeth, osteoderms, and vertebrae recovered within chron C29r of Cassagnau 1 and 2 (Haute-Garonne, France) [134,160]. In addition, isolated slender conical teeth tentatively assigned to cf. *Thoracosaurus* have been recovered from deposits of the lower and upper part of the upper Maastrichtian of the Tremp Basin in Spain [122]. The scarce representatives of the crown group Crocodylia during the Late Cretaceous of Europe, and the fact that most of the *Thoracosaurus* remains have been recovered in marine and coastal paleoenvironments (e.g., [23,122,160,161]), could explain the scarcity of remains in the continental deposits of the Ibero-Armorican island and their absence in Hațeg. Interestingly, *Thoracosaurus* is the only European crocodylomorph that has been recovered below and above the K-Pg boundary.

Only two clades of non-eusuchian crocodylomorphs have been found in the Maastrichtian of Europe, “Atoposauridae” and Notosuchia. Most of the “atoposaurid” record in the Upper Cretaceous of Europe is based on isolated teeth similar to those present in *Sabresuchus* (= *Theriosuchus*) *sympiestodon* [209], whose type material was found in the lower Maastrichtian of the Densuș-Ciula Fm but also reported from upper Maastrichtian sites on Hațeg island, although it does not reach the upper part of the upper Maastrichtian [32,210] (Figure 9). Remains assigned to this taxon are also present throughout the upper Maastrichtian of the Ibero-Armorican island [23,148]. As regards Notosuchia, many ziphodont teeth similar to *Doratodon carcharidens* from the Campanian of Austria and the Santonian of Hungary [211] have been found in the Maastrichtian of the Ibero-Armorican island and Hațeg (e.g., [32,122]). As happens with other crocodylomorphs, there is a record of both clades throughout the upper Maastrichtian of the Ibero-Armorican island, but they disappear at the top of chron C30n in Hațeg.

As we have already pointed out, the most striking difference between the Crocodylomorpha record of the Ibero-Armorican island and Hațeg is the almost complete absence of crocodylomorphs from the top of chron C30n in Hațeg island. Several factors could explain this, such as geological and sampling biases. However, the abundance of microfossil sites from the top of chron C30n in Hațeg, together with the fact that crocodylomorphs are usually among the most abundant remains found in this kind of site [32], make it difficult to justify their absence by biases alone. Further studies are needed to clarify this question.

Therefore, the crocodylomorph fossil assemblage of Europe during the Maastrichtian is mostly composed of endemic European taxa such as Allodaposuchidae, Hylaeochampsidae, and *Sabresuchus*. This would imply sporadic connections and faunal exchanges between the two islands, probably via the Adriatic–Australpine domain [116], and subse-

quent isolation processes that allowed endemism and differentiation at species and even the genus level. Isolated cases of intercontinental faunal exchange are explained by the presence of taxa with Gondwanan affinities such as *Notosuchia* (*Doratodon*) in the Maastrichtian of both islands, and the presence of taxa with North American affinities such as *Crocodylia* (*Thoracosaurus*) in the late Maastrichtian of the Ibero-Armorican island. The presence of *Doratodon* is explained by several episodic Cretaceous faunal and geographical links between Africa and Europe [211], such as a Turonian–Coniacian immigration wave that connected eastern Europe and northern Africa [30,212]. The presence of *Thoracosaurus*, a common taxon in North America, could be explained by the more aquatic and cosmopolitan nature of this taxon, which was able to move great distances across the ocean or, for example, via the Thulean Land Bridge [115].

#### 4.1.4. Testudines

The record of turtles in the two islands shows a certain contrast. The diversity of testudines in the Ibero-Armorican island appears to be greater than in Hațeg, with three freshwater taxa of bothremydid pleurodirans (*Elochelys*, *Polysternon isonae?* and *Polysternon atlanticum*) reaching the C29r (Figure 9), and at least one taxon of a solemydid cryptodiran and an indeterminate pan-cryptodiran. By contrast, in Hațeg, there are no cryptodiran turtles.

Hațeg turtles are represented only by two main groups that span the whole Maastrichtian: the basal turtle (stem Testudines) *Kallokibotion*, and the dortokids, which are stem pleurodirans and are present during the upper part of chron C30r [32,213,214] (Table 1, Figure 9).

#### 4.1.5. Amphibia and Squamata

The upper Maastrichtian assemblages of amphibians in the Ibero-Armorican island (upper part of chron C30n) consist of albanerpetontids, discoglossid anurans, palaeobatrachids, and probably salamandrids (Figure 10). In Hațeg island, the assemblages are dominated by albanerpetontids and alytid anurans [32,215], the latter represented by two taxa (*Paralatonina transylvanica* and cf. *Eodiscoglossus*). However, there is no direct evidence of these two taxa in the upper part of C30n (Figure 10). Moreover, the presence of the bombinatorid *Hatzegobatrachus* is documented in the lower part of the upper Maastrichtian [215]. The absence of palaeobatrachids in Hațeg island is also noteworthy.

The squamate assemblages of both islands are diverse and have some groups in common (anguimorph and “scincomorph” lizards, teioids) but also show some differences (Table 1, Figure 10). In Hațeg island, there are borioteioid lizards (*Bicuspidon hatzegiensis*) and paramacellodids, which are represented by *Becklesius nopcsai* [32,216–218]. Snakes are represented by the madtsoiid *Nidophis insularis* [219,220], which shows Gondwanan affinities. This clade of snakes has no record in the upper Maastrichtian deposits of the Ibero-Armorican island but is present in the lower Maastrichtian [30,221]. In the Ibero-Armorican island, there are certain groups that do not appear in Hațeg, such as varanoids and iguanids (Table 1, Figure 10).

#### 4.1.6. Mammalia

During the late Maastrichtian, mammals were part of the communities of both islands, but there is almost no information about those of the Ibero-Armorican island, except the alleged therian teeth from Peyrecave [152,178], which is situated in the upper part of the upper Maastrichtian. By contrast, mammals from Hațeg island are well known, with at least three taxa of kogaionid multituberculate mammals: *Barbatodon*, *Kogaionon*, and *Litovoi* [32,222–224] (Table 1) (Figures 7 and 10). Kogaionids were a group of multituberculates endemic to Hațeg island that survived up to the top of the Maastrichtian and made it to the Paleocene, diversifying and dispersing through Europe [225].

#### 4.2. Evaluation of the Tetrapod Diversity of the Ibero-Armorican Island and Its Biases

Despite the high number of fossiliferous localities that are known in the last million years of the Cretaceous in the Tremp Basin (over 50, see Figure 2), the fossil record of tetrapods is certainly limited by a series of factors including geological history, rock outcrop area, taphonomy, and study and sampling biases [226–229], as well as uncertainties in the taxonomic identification of specimens and the dating of the fossil-bearing deposits. Such biases (resulting, for example, from variations in the fossilization potential of vertebrate remains, interruptions in deposition in continental environments, anagenetic evolutionary lineages, syn-sedimentary and post-sedimentary erosion, etc.) strongly influence the measurement of diversity (i.e., taxonomic richness over a given time period). Some of them are shared with the coeval fossil records of continental to transitional fossiliferous deposits [230,231], but others are specific to the Ibero-Armorican island.

As far as geological and rock outcrop area biases are concerned, the available outcrops of the uppermost Maastrichtian beds are limited by the following factors: the geological history of the basin, the outcrop area, and the number of exposures. The relatively extensive Ibero-Armorican island has reduced potential for fossiliferous outcrops, due to its geological history. In the Pyrenean region, the Alpine orogeny has had an important impact on the availability of outcrops and localities. Thus, a significant reduction in outcrops occurred due to a series of thrusts that caused a shortening of circa 120 km [232]. Second, highly erosive fluvial and glacial valleys generated during and after the last glaciation have eroded Mesozoic formations for thousands of years, further limiting potential outcrops. The number of exposures (i.e., sedimentary bedrock that is visibly exposed at the surface) is constrained by the Pyrenean climate, which favors a high level of vegetation cover. However, in general terms, the southern Pyrenean regions are less forested than the northern foothills, and this enhances the number of available exposures.

As regards taphonomic biases, it is worth mentioning that because of the fragmentary character of the fossil remains commonly found in the Lower Red Garumnian of the Tremp Basin (channel-lag bone accumulations from fluvial-deltaic channelized sandstones, modes 1 and 2 of [233]), major uncertainties exist in the taxonomy of most of the collected specimens. Consequently, their taxonomic assignment is usually to what is commonly held to be a family rank (e.g., Azhdarchidae, Bothremydidae, Titanosauridae, Rhabdodontidae, Solemydidae) or a superfamily rank (Hadrosauroidea, Varanoidea) (Figures 8–10). A similar scenario has been observed in the Hațeg Basin [32]. This reveals that our understanding of the real taxonomic diversity in both regions is preliminary, and diversity comparisons between the regions at lower taxonomic levels (genus or species level) are still not possible. Furthermore, we concur with previous authors [234,235] that the diversity of dinosaurs varies in different paleobioprovinces because of climatic, environmental, or biotic conditions that caused differences in dinosaur evolution. Therefore, endemism or variations in speciation due to the particularities of insular ecosystems are assumed.

With respect to study and sampling biases, the accessibility of sedimentary rock exposures and variations in the efforts of paleontologists in the region are the two main factors affecting the fossil record. First, the complex relief of the Western Tremp Basin reduces accessibility to some of the outcrops (Figure 3), hindering the collection of large macroremains or representative amounts of bulk rock for sieving. Sampling efforts made by paleontologists are unequal as well. Indeed, there are microvertebrate fossil assemblages present in the Maastrichtian outcrops of the Tremp Basin that have not been sampled. One exception is the great effort made by some teams in the 1990s in their pursuit of mammal microfossils [177]. This otherwise unsuccessful survey resulted in the discovery of important localities such as Blasi 2 and Fontllonga 6 [129,151]. Prospecting efforts are currently being carried out in selected localities—L’Espinau, Veracruz 1 [43,57,171]—but an extensive microfossil sampling campaign is lacking. Regarding macrovertebrates, the greater amount of hadrosaur and crocodylomorph fossils—probably because their osteological remains are both more resilient and more easily identifiable compared with other vertebrate clades—produced a clear study bias in the faunal diversity of the Tremp

Formation. These two clades of vertebrates have been the subject of further studies probably because their fossils are more informative or better preserved and thus allow greater taxonomic resolution. By contrast, other groups such as pterosaurs, turtles, sauropods, and theropods have a more fragmentary and less diagnostic fossil record that makes assessment of their abundance more difficult.

Finally, however, one of the key strengths of the fossil record in the Tresp Basin is the dating of the fossil-bearing deposits. In this context, detailed correlations of stratigraphic successions and magnetochrons coupled with accurate age constraints provided by planktic foraminifera [56,60,64] provide a solid chronostratigraphic framework.

By all these reasons, interpreting if there was or not a decline in the diversity of some groups of tetrapods before the K-Pg boundary in the islands of the European archipelago is difficult. However, the discovery during the last years of new taxa whose presence was not known in the islands (e.g., the troodontid *Tamarro* [149], the ornithomorph from Beranuy [110], or the azhdarchid *Albadraco* [207]) points that the late Maastrichtian tetrapod ecosystems were in fact more diverse than what the studied fossil record had pointed up to the day. By this reason, it seems plausible to think that diversity was far from declining prior to the extinction, but this would perhaps be a daredevil judgment, since a higher resolution of the Maastrichtian fossil record (in number of specimens and age constraints) is needed in the Maastrichtian to observe differences and clear trends in the evolution of diversity.

## 5. Conclusions

The vertebrate record of the Western Tresp Syncline comprises some of the youngest sedimentary deposits with vertebrate fossils in the late Maastrichtian of Europe, with a continuous succession from the upper part of chron C30r to chron C29r ( $\approx 67$ –66.052 Ma). Among the upper Maastrichtian outcrops of the Tresp and Arén Sandstone formations in this area, more than 50 fossil sites have been recognized. Fossils have been recovered belonging to hadrosauroid ornithomorphs, including the holotypes of *Arenysaurus* and *Blasisaurus*, titanosaurian sauropods, abelisaurid and maniraptoran theropods, a large avialan ornithomorph, pterosaurs, non-eusuchian and eusuchian crocodylomorphs, including the holotypes *Arenysuchus* and *Agaresuchus subjuniperus*, pleurodiran and cryptodiran turtles, squamates, and amphibians. This record is augmented by a relatively diverse oological record, albeit one in need of further study, and ichnites of both dinosaurs (*Hadrosauropodus*) and crocodylomorphs (*Characichnos* and cf. *Crocodylopodus*).

A first attempt at comparing Late Cretaceous European regions indicates that the Ibero-Armorican island and Hačeg island show diverse and thriving communities of vertebrates during the late Maastrichtian, with certain differences in the faunas probably caused by their different paleobiogeographic evolution. Despite these differences, it seems that both European islands flourished during the late Maastrichtian. The rich record of the Ibero-Armorican island and its chronostratigraphic framework indicate that its tetrapod assemblages were thriving just a few hundred thousand years before the K-Pg extinction, and some groups even just tens of thousands of years before.

Despite its small size and relatively inaccessible outcrops, the Western Tresp Syncline is a privileged area when it comes to studying the last Mesozoic ecological communities of tetrapods in Europe, and it is key to understanding how they were affected by the K-Pg extinction event. Further research in this area would help to unveil missing taxa and shed light on these communities and the environment in which they lived.

**Supplementary Materials:** The following are available online at <https://www.mdpi.com/article/10.3390/geosciences11040162/s1>, Table S1: Arén and Tresp Fm Aragonese sites.

**Author Contributions:** Conceptualization, M.P.-P.; writing—original draft preparation, M.P.-P.; writing—review and editing, P.C.-C., M.M.-A., E.P.-P., D.C., B.V., J.M.G., B.B., J.I.C. supervision, E.P.-P., B.B., J.I.C. All authors have read and agreed to the published version of the manuscript.

**Funding:** This research was funded by the Spanish Ministry of Science and Innovation, the European Regional Development Fund, the Government of Aragón (Grupo Aragosaurus: Recursos geológicos y Paleoambientes), project CGL2017-85038-P; by the Fundação para a Ciência e a Tecnologia, project PTDC/CTA-PAL/31656/2017 and GeoBioTec, project (UIDB/04035/2020). M.P.-P. is supported by a Ph.D grant from the Spanish Ministry of Education, Culture and Sport (Grant Number FPU 16/03064). M.M.-A. and E.P.-P. are supported by postdoctoral grants funded by the Fundação para a Ciência e a Tecnologia, Portugal (Grant numbers SFRH/BPD/113130/2015, SFRH/BPD/116759/2016, PTDC/CTA-PAL/31656/2017). D.C. is supported by the Beatriu de Pinós postdoctoral programme (BP2017-00195) of the Government of Catalonia's Secretariat for Universities and Research of the Ministry of Economy and Knowledge. B.V. is part of the consolidated research group 2017 SGR 01666 of the Agència de Gestió i Ajuts Universitaris i de Recerca (AGAUR). Additional support was also provided by the CERCA Programme of the Generalitat de Catalunya.

**Acknowledgments:** We would like to acknowledge Isabel Pérez for the photographs of MPZ 2021/1, and Diego Torromé for the photograph of the Serraduy outcrops. We would also like to thank the Servicio General de Apoyo a la Investigación-SAI, Universidad de Zaragoza for the SEM photographs. We would like to thank the valuable comments of two anonymous reviewers, which have contributed substantially to the improvement of this work. Rupert Glasgow reviewed the text in English.

**Conflicts of Interest:** The authors declare no conflict of interest. The funders had no role in the design of the study; in the collection, analyses, or interpretation of data; in the writing of the manuscript, or in the decision to publish the results.

## References

- Alvarez, L.W.; Alvarez, W.; Asaro, F.; Michel, H.V. Extraterrestrial cause for the Cretaceous-Tertiary extinction. *Science* **1980**, *208*, 1095–1108. [[CrossRef](#)] [[PubMed](#)]
- Miller, K.G.; Kominz, M.A.; Browning, J.V.; Wright, J.D.; Mountain, G.S.; Katz, M.E.; Sugarman, P.J.; Cramer, B.S.; Christie-Blick, N.; Peka, S.F. The Phanerozoic Record of Global Sea-Level Change. *Science* **2005**, *310*, 1293–1298. [[CrossRef](#)] [[PubMed](#)]
- Li, L.; Keller, G. Maastrichtian climate, productivity and faunal turnovers in planktic foraminifera in South Atlantic DSDP sites 525A and 21. *Mar. Micropaleontol.* **1998**, *33*, 55–86. [[CrossRef](#)]
- Barnet, J.S.K.; Littler, K.; Kroon, D.; Leng, M.J.; Westerhold, T.; Röhl, U.; Zachos, J.C. A new high-resolution chronology for the late Maastrichtian warming event: Establishing robust temporal links with the onset of Deccan volcanism. *Geology* **2018**, *46*, 147–150. [[CrossRef](#)]
- Courtillot, V.; Féraud, G.; Maluski, H.; Vandamme, D.; Moreau, M.G.; Besse, J. Deccan flood basalts and the Cretaceous/Tertiary boundary. *Nature* **1988**, *333*, 843–846. [[CrossRef](#)]
- Courtillot, V.E.; Renne, P.R. On the ages of flood basalt events. *Comptes Rendus Geosci.* **2003**, *335*, 113–140. [[CrossRef](#)]
- Tobin, T.S.; Ward, P.D.; Steig, E.J.; Olivero, E.B.; Hilburn, I.A.; Mitchell, R.N.; Diamond, M.R.; Raub, T.D.; Kirschvink, J.L. Extinction patterns,  $\delta^{18}\text{O}$  trends, and magnetostratigraphy from a southern high-latitude Cretaceous–Paleogene section: Links with Deccan volcanism. *Palaeogeogr. Palaeoclimatol. Palaeoecol.* **2012**, *350–352*, 180–188. [[CrossRef](#)]
- Schoene, B.; Eddy, M.P.; Samperton, K.M.; Keller, C.B.; Keller, G.; Adatte, T.; Khadri, S.F.R. U–Pb constraints on pulsed eruption of the Deccan Traps across the end-Cretaceous mass extinction. *Science* **2019**, *363*, 862–866. [[CrossRef](#)]
- Hildebrand, A.R.; Penfield, G.T.; Kring, D.A.; Pilkington, M.; Camargo, Z.A.; Jacobsen, S.B.; Boynton, W.V. Chicxulub Crater: A possible Cretaceous/Tertiary boundary impact crater on the Yucatán Peninsula, Mexico. *Geology* **1991**, *19*, 867. [[CrossRef](#)]
- Renne, P.R.; Arenillas, I.; Arz, J.A.; Vajda, V.; Gilabert, V.; Bermúdez, H.D. Multi-proxy record of the Chicxulub impact at the Cretaceous–Paleogene boundary from Gorgonilla Island, Colombia. *Geology* **2018**, *46*, 547–550. [[CrossRef](#)]
- Maruoka, T. Mass Extinction at the Cretaceous–Paleogene (K–Pg) boundary. In *Astrobiology*; Springer: Singapore, 2019; pp. 303–320.
- Lyons, S.L.; Karp, A.T.; Bralower, T.J.; Grice, K.; Schaefer, B.; Gulick, S.P.S.; Morgan, J.V.; Freeman, K.H. Organic matter from the Chicxulub crater exacerbated the K–Pg impact winter. *Proc. Natl. Acad. Sci. USA* **2020**, *117*, 25327–25334. [[CrossRef](#)]
- Schulte, P.; Alegret, L.; Arenillas, I.; Arz, J.A.; Barton, P.J.; Bown, P.R.; Bralower, T.J.; Christeson, G.L.; Claeys, P.; Cockell, C.S.; et al. The Chicxulub asteroid impact and mass extinction at the Cretaceous–Paleogene boundary. *Science* **2010**, *327*, 1214–1218. [[CrossRef](#)]
- Witts, J.D.; Whittle, R.J.; Wignall, P.B.; Crame, J.A.; Francis, J.E.; Newton, R.J.; Bowman, V.C. Macrofossil evidence for a rapid and severe Cretaceous–Paleogene mass extinction in Antarctica. *Nat. Commun.* **2016**, *7*, 11738. [[CrossRef](#)]
- Chiarenza, A.A.; Farnsworth, A.; Mannion, P.D.; Lunt, D.J.; Valdes, P.J.; Morgan, J.V.; Allison, P.A. Asteroid impact, not volcanism, caused the end-Cretaceous dinosaur extinction. *Proc. Natl. Acad. Sci. USA* **2020**, *117*, 17084–17093. [[CrossRef](#)]
- Dzombak, R.M.; Sheldon, N.D.; Mohabey, D.M.; Samant, B. Stable climate in India during Deccan volcanism suggests limited influence on K–Pg extinction. *Gondwana Res.* **2020**, *85*, 19–31. [[CrossRef](#)]
- Raup, D.M.; Sepkoski, J.J. Mass extinctions in the marine fossil record. *Science* **1982**, *215*, 1501–1503. [[CrossRef](#)]
- Jablonski, D. Extinctions in the fossil record. *Philos. Trans. R. Soc. London Ser. B Biol. Sci.* **1994**, *344*, 11–17. [[CrossRef](#)]
- Bardet, N. Extinction events among Mesozoic marine reptiles. *Hist. Biol.* **1994**, *7*, 313–324. [[CrossRef](#)]

20. Longrich, N.R.; Tokaryk, T.; Field, D.J. Mass extinction of birds at the Cretaceous–Paleogene (K–Pg) boundary. *Proc. Natl. Acad. Sci. USA* **2011**, *108*, 15253–15257. [\[CrossRef\]](#)
21. Longrich, N.R.; Martill, D.M.; Andres, B. Late Maastrichtian pterosaurs from North Africa and mass extinction of Pterosauria at the Cretaceous–Paleogene boundary. *PLOS Biol.* **2018**, *16*, e2001663. [\[CrossRef\]](#)
22. Brusatte, S.L.; Butler, R.J.; Barrett, P.M.; Carrano, M.T.; Evans, D.C.; Lloyd, G.T.; Mannion, P.D.; Norell, M.A.; Peppe, D.J.; Upchurch, P.; et al. The extinction of the dinosaurs. *Biol. Rev.* **2015**, *90*, 628–642. [\[CrossRef\]](#)
23. Puértolas-Pascual, E.; Blanco, A.; Brochu, C.A.; Canudo, J.I. Review of the late cretaceous–early paleogene crocodylomorphs of Europe: Extinction patterns across the K–PG boundary. *Cretac. Res.* **2016**, *57*, 565–590. [\[CrossRef\]](#)
24. Pearson, D.A.; Schaefer, T.; Johnson, K.R.; Nichols, D.J.; Hunter, J.P. Vertebrate biostratigraphy of the Hell Creek Formation in southwestern North Dakota and northwestern South Dakota. *Spec. Pap. Geol. Soc. Am.* **2002**, *361*, 145–167. [\[CrossRef\]](#)
25. Lyson, T.R.; Longrich, N.R. Spatial niche partitioning in dinosaurs from the latest Cretaceous (Maastrichtian) of North America. *Proc. R. Soc. B Biol. Sci.* **2011**, *278*, 1158–1164. [\[CrossRef\]](#)
26. Johnson, K.R.; Nichols, D.J.; Hartman, J.H. Hell Creek Formation: A 2001 synthesis. *Geol. Soc. Am. Spec. Pap.* **2002**, *361*, 503–510.
27. LeCain, R.; Clyde, W.C.; Wilson, G.P.; Riedel, J. Magnetostratigraphy of the Hell Creek and lower Fort Union Formations in northeastern Montana. In *Through the End of the Cretaceous in the Type Locality of the Hell Creek Formation in Montana and Adjacent Areas*; Geological Society of America: Boulder, CO, USA, 2014.
28. Sprain, C.J.; Renne, P.R.; Clemens, W.A.; Wilson, G.P. Calibration of chron C29r: New high-precision geochronologic and paleomagnetic constraints from the Hell Creek region, Montana. *GSA Bull.* **2018**, *130*, 1615–1644. [\[CrossRef\]](#)
29. Fowler, D. The Hell Creek Formation, Montana: A stratigraphic review and revision based on a sequence stratigraphic approach. *Geosciences* **2020**, *10*, 435. [\[CrossRef\]](#)
30. Csiki-Sava, Z.; Buffetaut, E.; Ősi, A.; Pereda-Suberbiola, X.; Brusatte, S.L. Island life in the Cretaceous—Faunal composition, biogeography, evolution, and extinction of land-living vertebrates on the Late Cretaceous European archipelago. *Zookeys* **2015**, *469*, 1–161. [\[CrossRef\]](#) [\[PubMed\]](#)
31. Canudo, J.I.; Oms, O.; Vila, B.; Galobart, À.; Fondevilla, V.; Puértolas-Pascual, E.; Sellés, A.G.; Cruzado-Caballero, P.; Dinarès-Turell, J.; Vicens, E.; et al. The upper Maastrichtian dinosaur fossil record from the southern Pyrenees and its contribution to the topic of the Cretaceous–Palaeogene mass extinction event. *Cretac. Res.* **2016**, *57*, 540–551. [\[CrossRef\]](#)
32. Csiki-Sava, Z.; Vremir, M.; Vasile, Ş.; Brusatte, S.L.; Dyke, G.; Naish, D.; Norell, M.A.; Totoianu, R. The east side story—The Transylvanian latest Cretaceous continental vertebrate record and its implications for understanding Cretaceous–Paleogene boundary events. *Cretac. Res.* **2016**, *57*, 662–698. [\[CrossRef\]](#)
33. Fondevilla, V.; Riera, V.; Vila, B.; Sellés, A.G.; Dinarès-Turell, J.; Vicens, E.; Gaete, R.; Oms, O. Galobart Chronostratigraphic synthesis of the latest Cretaceous dinosaur turnover in south-western Europe. *Earth Sci. Rev.* **2019**, *191*, 168–189. [\[CrossRef\]](#)
34. Vila, B.; Sellés, A.G.; Brusatte, S.L. Diversity and faunal changes in the latest Cretaceous dinosaur communities of southwestern Europe. *Cretac. Res.* **2016**, *57*, 552–564. [\[CrossRef\]](#)
35. Gómez-Gras, D.; Roigé, M.; Fondevilla, V.; Oms, O.; Boya, S.; Remacha, E. Provenance constraints on the Tremp Formation paleogeography (southern Pyrenees): Ebro Massif VS Pyrenees sources. *Cretac. Res.* **2016**, *57*, 414–427. [\[CrossRef\]](#)
36. Puigdefàbregas, C.; Muñoz, J.A.; Marzo, M. *Thrust Belt Development in the Eastern Pyrenees and Related Depositional Sequences in the Southern Foreland Basin*; Wiley: Hoboken, NJ, USA, 1986.
37. Muñoz, J.A. Evolution of a continental collision belt: ECORS-Pyrenees crustal balanced cross-section. In *Thrust Tectonics*; Springer: Dordrecht, The Netherlands, 1992; pp. 235–246.
38. Teixell, A. Crustal structure and orogenic material budget in the west central Pyrenees. *Tectonics* **1998**, *17*, 395–406. [\[CrossRef\]](#)
39. Teixell, A. Estructura de los Pirineos: Generalidades. In *Geología de España*; SGE-IGME: Madrid, Spain, 2004; pp. 321–323.
40. Costa, E.; Garcés, M.; López-Blanco, M.; Beamud, E.; Gómez-Paccard, M.; Larrasoña, J.C. Closing and continentalization of the South Pyrenean foreland basin (NE Spain): Magnetochronological constraints. *Basin Res.* **2009**, *36*, 349–364. [\[CrossRef\]](#)
41. Ardévol, L.; Klimowitz, J.; Malagón, J.; Nagtegaal, P.J.C. Depositional sequence response to foreland deformation in the upper Cretaceous of the Southern Pyrenees, Spain. *Am. Assoc. Pet. Geol. Bull.* **2000**, *84*, 566–588. [\[CrossRef\]](#)
42. Oms, O.; Fondevilla, V.; Riera, V.; Marmi, J.; Vicens, E.; Estrada, R.; Vila, B. Transitional environments of the lower Maastrichtian South-Pyrenean Basin (Catalonia, Spain): The Fumanya Member tidal flat. *Cretac. Res.* **2016**, *57*, 428–442. [\[CrossRef\]](#)
43. Rosell, J.; Linares, R.; Llompart, C. El “garumniense” prepirenaico. *Rev. Soc. Geol. España* **2001**, *14*, 47–56.
44. Mey, P.H.W.; Nagtegaal, P.J.C.; Roberti, K.J.; Hartvelt, J.J.A. Lithostratigraphic subdivision of Post-Hercynian deposits in the South-Central Pyrenees, Spain. *Leidse Geol. Meded.* **1968**, *41*, 221–228.
45. Nagtegaal, P.J.C.; Van Vliet, A.; Brouwer, J. Syntectonic coastal offlap and concurrent turbidite deposition: The Upper Cretaceous Aren sandstone in the South-Central Pyrenees, Spain. *Sediment. Geol.* **1983**, *34*, 185–218. [\[CrossRef\]](#)
46. Mutti, E.; Sgavetti, M. Sequence stratigraphy of the Upper Cretaceous Aren strata in the Aren–Orcau region, south-central Pyrenees, Spain: Distinction between eustatically and tectonically controlled depositional sequences. *Ann. Univ. Ferrara* **1987**, *1*, 1–22.
47. Nagtegaal, P.J.C. Depositional history and clay minerals of the Upper Cretaceous basin in the south-central Pyrenees, Spain. *Leidse Geol. Meded.* **1972**, *47*, 251–275.
48. Mutti, E.; Rosell, J.; Ghibaudo, G.; Obrador, A. The Upper Cretaceous Aren Sandstone in its type-area. In *Proceedings of the 9th International Congress International Association of Sedimentologists*, Nice, France, 1 January–30 November 1975; pp. 7–15.

49. Díaz-Molina, M.; Kälin, O.; Benito, M.I.; Lopez-Martinez, N.; Vicens, E. Depositional setting and early diagenesis of the dinosaur eggshell-bearing Aren Fm at Bastus, Late Campanian, south-central Pyrenees. *Sediment. Geol.* **2007**, *199*, 205–221. [\[CrossRef\]](#)
50. Leymerie, A. Présence de garumnien en Espagne. Bulletin de la Société Géologique de France. *Bull. Soc. Géol. Fr.* **1868**, *25*, 906–911.
51. Cuevas, J.L. Estratigrafía del «Garumniense» de la Conca de Tremp. Prepirineo de Lérida. *Acta Geológica Hispánica* **1992**, *27*, 95–108.
52. Pujalte, V.; Schmitz, B. The stratigraphy of the Tremp Group revisited (Garumnian, Tremp-Graus basin, South Pyrenees). *Geogaceta* **2005**, *38*, 79–82.
53. Díaz-Molina, M. Sedimentación sintectónica asociada a una subida relativa del nivel del mar durante el Cretácico Superior (Fm. Tremp, provincia de Lérida). *Estud. Geol. Núm. Extraordin. Galve Tremp*. **1987**, *43*, 69–93.
54. Eichenseer, H. *Facies Geology of Late Maastrichtian to Early Eocene Coastal and Shallow Marine Sediments (Tremp-Graus Basin, Northeastern Spain)*; Universität Tübingen: Tübingen, Germany, 1988.
55. Riera, V.; Oms, O.; Gaete, R.; Galobart, À. The end-Cretaceous dinosaur succession in Europe: The Tremp Basin record (Spain). *Palaeogeogr. Palaeoclimatol. Palaeoecol.* **2009**, *283*, 160–171. [\[CrossRef\]](#)
56. Díez-Canseco, D.; Arz, J.A.; Benito, M.I.; Díaz-Molina, M.; Arenillas, I. Tidal influence in redbeds: A palaeoenvironmental and biostratigraphic reconstruction of the Lower Tremp Formation (South-Central Pyrenees, Spain) around the Cretaceous/Paleogene boundary. *Sediment. Geol.* **2014**, *312*, 31–49. [\[CrossRef\]](#)
57. Blanco, A.; Szabó, M.; Blanco-Lapaz, À.; Marmi, J. Late Cretaceous (Maastrichtian) Chondrichthyes and Osteichthyes from northeastern Iberia. *Palaeogeogr. Palaeoclimatol. Palaeoecol.* **2017**, *465*, 278–294. [\[CrossRef\]](#)
58. Ghinassi, M.; Oms, O.; Cosma, M.; Finotello, A.; Munari, G. Reading tidal processes where their signature is cryptic: The Maastrichtian meandering channel deposits of the Tremp Formation (Southern Pyrenees, Spain). *Sedimentology* **2020**. [\[CrossRef\]](#)
59. Villalba-Breva, S.; Martín-Closas, C. Upper Cretaceous paleogeography of the Central Southern Pyrenean Basins (Catalonia, Spain) from microfacies analysis and charophyte biostratigraphy. *Facies* **2013**, *59*, 319–345. [\[CrossRef\]](#)
60. Vicente, A.; Martín-Closas, C.; Arz, J.A.; Oms, O. Maastrichtian-basal Paleocene charophyte biozonation and its calibration to the Global Polarity Time Scale in the southern Pyrenees (Catalonia, Spain). *Cretac. Res.* **2015**, *52*, 268–285. [\[CrossRef\]](#)
61. Vicente, A.; Villalba-Breva, S.; Ferrández-Cañadell, C.; Martín-Closas, C. Revision of the Maastrichtian-Palaeocene charophyte biostratigraphy of the Fontllonga reference section (Southern Pyrenees, Catalonia, Spain). *Geol. Acta* **2016**, *14*, 349–362. [\[CrossRef\]](#)
62. Pereda-Suberbiola, X.; Canudo, J.I.; Cruzado-Caballero, P.; Barco, J.L.; López-Martínez, N.; Oms, O.; Ruiz-Omeñaca, J.I. The last hadrosaurid dinosaurs of Europe: A new lambeosaurine from the Uppermost Cretaceous of Aren (Huesca, Spain). *Comptes Rendus Palevol* **2009**, *8*, 559–572. [\[CrossRef\]](#)
63. Fondevilla, V.; Dinarès-Turell, J.; Oms, O. The chronostratigraphic framework of the South-Pyrenean Maastrichtian succession reappraised: Implications for basin development and end-Cretaceous dinosaur faunal turnover. *Sediment. Geol.* **2016**, *337*, 55–68. [\[CrossRef\]](#)
64. Puértolas-Pascual, E.; Arenillas, I.; Arz, J.A.; Calvín, P.; Ezquerro, L.; García-Vicente, C.; Pérez-Pueyo, M.; Sánchez-Moreno, E.M.; Villalán, J.J.; Canudo, J.I. Chronostratigraphy and new vertebrate sites from the upper Maastrichtian of Huesca (Spain), and their relation with the K/Pg boundary. *Cretac. Res.* **2018**, *89*, 36–59. [\[CrossRef\]](#)
65. López-Martínez, N.; Vicens, E. A new peculiar dinosaur egg, *Sankofa pyrenaica* oogen. nov. oosp. nov. from the Upper Cretaceous coastal deposits of the Aren Formation, south-central Pyrenees, Lleida, Catalonia, Spain. *Palaeontology* **2012**, *55*, 325–339. [\[CrossRef\]](#)
66. Riera, V. *Estudio Integrado (Geología y Paleontología) de la Sucesión de Dinosaurios (Maastrichtiense) de la Vertiente Surpirenaica*; Universitat Autònoma de Barcelona: Barcelona, Spain, 2010.
67. López-Martínez, N.; Arribas, M.E.; Robador, A.; Vicens, E.; Ardévol, L. Los carbonatos danienses (Unidad 3) de la Fm Temp (Pirineos sur-centrales): Paleogeografía y relación con el límite Cretácico-Terciario. *Rev. Soc. Geol. Esp.* **2006**, *19*, 233–255.
68. Robador, A.; Samsó, J.M.; Serra-Kiel, J.; Tosquella, J. Field guide. In *Introduction to the early Paleogene of the south Pyrenean basin. Field trip Guidebook*; Barnolas, A., Robador, A., Serra-Kiel, J., Caus, E., Eds.; IGME: Barcelona, Spain, 1990; pp. 131–159.
69. Serra-Kiel, P.; Canudo, J.I.; Dinares, J.; Molina, E.; Ortiz, N.; Pascual, J.O.; Samsó, J.M.; Tosquella, J. Cronoestratigrafía de los sedimentos marinos del Terciario inferior de la Cuenca de Tremp-Graus (Zona Central Surpirenaica). *Rev. Soc. Esp. Geol.* **1994**, *7*, 273–299.
70. Pujalte, V.; Schmitz, B.; Baceta, J.I. Sea-level changes across the Paleocene–Eocene interval in the Spanish Pyrenees, and their possible relationship with North Atlantic magmatism. *Palaeogeogr. Palaeoclimatol. Palaeoecol.* **2014**, *393*, 45–60. [\[CrossRef\]](#)
71. Vila, B.; Galobart, À.; Canudo, J.I.; Le Loeuff, J.; Dinarès-Turell, J.; Riera, V.; Oms, O.; Tortosa, T.; Gaete, R. The diversity of sauropod dinosaurs and their first taxonomic succession from the latest Cretaceous of southwestern Europe: Clues to demise and extinction. *Palaeogeogr. Palaeoclimatol. Palaeoecol.* **2012**, *350–352*, 19–38. [\[CrossRef\]](#)
72. López-Martínez, N.; Canudo, J.I.; Ardevol, L.; Pereda-Suberbiola, X.; Orue-Etxebarria, X.; Cuenca-Bescós, G.; Ruiz-Omeñaca, J.I.; Murelaga, X.; Feist, M. New dinosaur sites correlated with upper Maastrichtian pelagic deposits in the Spanish Pyrenees: Implications for the dinosaur extinction. *Cretac. Res.* **2001**, *22*, 41–61. [\[CrossRef\]](#)
73. Garrido Mejías, A.; Ríos Aragües, L.M. Síntesis geológica del Secundario y Terciario entre los ríos Cinca y Segre. *Bol. Inst. Geol. Min. Esp.* **1972**, *83*, 1–47.

74. Canudo, J.I. The Collection of Type Fossils of the Natural Science Museum of the University of Zaragoza (Spain). *Geoheritage* **2018**, *10*, 385–392. [[CrossRef](#)]
75. Pereda-Suberbiola, X.; Canudo, J.I.; Company, J.; Cruzado-Caballero, P.; Ruiz-Omeñaca, J.I. Hadrosauroid dinosaurs from the latest Cretaceous of the Iberian Peninsula. *J. Vertebr. Paleontol.* **2009**, *29*, 946–951. [[CrossRef](#)]
76. Cruzado-Caballero, P.; Ruiz-Omeñaca, J.I.; Canudo, J.I. Review of the fossil record of Spanish hadrosaur remains. In Proceedings of the VIII Encuentro de Jóvenes Investigadores en Paleontología, Enciso, Spain, 21–22 April 2010; Volume 30, pp. 99–105.
77. Cruzado-Caballero, P.; Puértolas-Pascual, E.; Canudo, J.I.; Castanera, D.; Gasca, J.M.; Moreno-Azanza, M. New hadrosaur remains from the Late Maastrichtian of Huesca (NE Spain). In Proceedings of the 10th Annual Meeting of the European Association of Vertebrate Palaeontologists, Teruel, Spain, 19–24 June 2012; pp. 45–48.
78. Cruzado-Caballero, P.; Ruiz-Omeñaca, J.I.; Gaete, R.; Riera, V.; Oms, O.; Canudo, J.I. A new hadrosaurid dentary from the latest Maastrichtian of the Pyrenees (north Spain) and the high diversity of the duck-billed dinosaurs of the Ibero-Armorican Realm at the very end of the Cretaceous. *Hist. Biol.* **2014**, *26*, 619–630. [[CrossRef](#)]
79. Company, J.; Cruzado-Caballero, P.; Canudo, J.I. Presence of diminutive hadrosaurids (Dinosauria: Ornithopoda) in the Maastrichtian of the south-central Pyrenees (Spain). *J. Iber. Geol.* **2015**, *41*, 71–81. [[CrossRef](#)]
80. Prieto-Márquez, A.; Dalla Vecchia, F.M.; Gaete, R.; Galobart, À. Diversity, relationships, and biogeography of the lambeosaurine dinosaurs from the European archipelago, with description of the new aralosaurin *Canardia garonnensis*. *PLoS ONE* **2013**, *8*, e69835. [[CrossRef](#)]
81. Conti, S.; Vila, B.; Sellés, A.G.; Galobart, À.; Benton, M.J.; Prieto-Márquez, A. The oldest lambeosaurine dinosaur from Europe: Insights into the arrival of Tsintaosaurini. *Cretac. Res.* **2020**, *107*, 104286. [[CrossRef](#)]
82. Cruzado-Caballero, P.; Pereda-Suberbiola, X.; Ruiz-Omeñaca, J.I. *Blasisaurus canudo* gen. et sp. nov., a new lambeosaurine dinosaur (hadrosauridae) from the latest cretaceous of Arén (Huesca, Spain). *Can. J. Earth Sci.* **2010**, *47*, 1507–1517. [[CrossRef](#)]
83. Cruzado-Caballero, P.; Canudo, J.I.; Moreno-Azanza, M.; Ruiz-Omeñaca, J.I. New material and phylogenetic position of *Arenysaurus ardevoli*, a lambeosaurine dinosaur from the late Maastrichtian of Arén (Northern Spain). *J. Vertebr. Paleontol.* **2013**, *33*, 1367–1384. [[CrossRef](#)]
84. Longrich, N.R.; Suberbiola, X.P.; Pyron, R.A.; Jalil, N.-E. The first duckbill dinosaur (Hadrosauridae: Lambeosaurinae) from Africa and the role of oceanic dispersal in dinosaur biogeography. *Cretac. Res.* **2020**, 104678. [[CrossRef](#)]
85. Cruzado-Caballero, P.; Canudo Sanagustín, J.; Ruiz-Omeñaca, J.I. Nuevas evidencias de la presencia de hadrosaurios lambeosaurios (Dinosauria) en el Maastrichtiense superior de la Península Ibérica (Arén, Huesca). *Geogaceta* **2005**, *3*, 47–50.
86. Cruzado-Caballero, P.; Canudo, J.I.; Ruiz-Omeñaca, J.I. Los fémures de Blasi (Arén, Huesca, Spain): Una contribución a los hadrosauroides Europeos del Maastrichtiense superior. In Proceedings of the Actas de las IV Jornadas Internacionales sobre Paleontología de Dinosaurios y su Entorno, Burgos, Spain, 5–9 September 2009; pp. 197–205.
87. Cruzado-Caballero, P.; Ruiz-Omeñaca, J.I.; Canudo, J.I. Evidencias de la coexistencia de dinosaurios hadrosaurinos y lambeosaurinos en el Maastrichtiano superior de la Península Ibérica (Arén, Huesca, España). *Ameghiniana* **2010**, *47*, 153–164. [[CrossRef](#)]
88. Canudo, I.; Cruzado-Caballero, P.; Moreno-Azanza, M. Possible theropod predation evidence in hadrosaurid dinosaurs from the Upper Maastrichtian (Upper Cretaceous) of Arén (Huesca, Spain). *Kaupia Darmstädter Beiträge zur Naturgeschichte* **2005**, *14*, 9–13.
89. Cruzado-Caballero, P.; Fortuny, J.; Llacer, S.; Canudo, J.I. Paleoneuroanatomy of the European lambeosaurine dinosaur *Arenysaurus ardevoli*. *Peer J.* **2015**, *2015*, 1–16. [[CrossRef](#)]
90. Mayayo-Lainez, A. Paleohistología y Mineralogía de los Dinosaurios Hadrosaurios del Maastrichtiense de Arén (Huesca). Master's Thesis, University of Zaragoza, Zaragoza, Spain, 2020.
91. Mayayo-Lainez, A.; Alegre-Esteve, M.; Bauluz, B.; Canudo, J. First approach to the paleohistology of the hadrosaur dinosaurs from Blasi 2A (Trespín Formation, Maastrichtian, Huesca). *Ciências Terra-Procedia* **2021**, *1*, 38–41.
92. Puértolas-Pascual, E.; Cruzado-Caballero, P.; Canudo, J.I.; Gasca, J.M.; Moreno-Azanza, M.; Castanera, D.; Parrillas, J.; Ezquerro, L. Nuevos yacimientos de vertebrados del Maastrichtiense superior (Cretácico Superior) de Huesca (España). In Proceedings of the VIII Geological Congress of Spain, Oviedo, Spain, 17–19 July 2012; pp. 269–272.
93. Pérez Pueyo, M.; Puértolas-Pascual, E.; Bádenas, B. Larra 4: Desenterrando a los últimos vertebrados del maastrichtiense terminal del pirineo aragonés. *Zubia* **2019**, *31*, 159–163.
94. Pérez-Pueyo, M.; Gilabert, V.; Moreno-Azanza, M.; Puertolas-Pascual, E.; Bádenas, B.; Canudo, J.I. Late Maastrichtian fossil assemblage of Veracruz 1 site (Beranuy, NE Spain): Wildfires and bones in a transitional environment. In Proceedings of the VIII Jornadas Internacionales sobre Paleontología de Dinosaurios y su Entorno, Burgos, Spain, 5–9 September 2019; pp. 111–113.
95. Barco, J.L.; Ardevol, L.; Canudo, J.I. Descripción de los primeros rastros asignados a Hadrosauridae (Ornithopoda, Dinosauria) del Maastrichtiense de la Península Ibérica (Areny, Huesca). *Geogaceta* **2001**, *30*, 235–238.
96. Vila, B.; Oms, O.; Fondevilla, V.; Gaete, R.; Galobart, À.; Riera, V.; Canudo, J.I. The Latest Succession of Dinosaur Tracksites in Europe: Hadrosaur Ichthyology, Track Production and Palaeoenvironments. *PLoS ONE* **2013**, *8*, e72579. [[CrossRef](#)] [[PubMed](#)]
97. Sellés, A.G.; Via, B.; Galobart, À. *Spheroolithus europaeus*, oosp. nov. (late Maastrichtian, Catalonia), the youngest oological record of hadrosauroids in Eurasia. *J. Vertebr. Paleontol.* **2014**, *34*, 725–729. [[CrossRef](#)]

98. Pérez-Pueyo, M.; Moreno-Azanza, M.; Núñez-Lahuerza, C.; Puértolas-Pascual, E.; Bádenas, B.; Canudo, J.L. Eggshell association of the Late Maastrichtian (Late Cretaceous) at Blasi 2B fossil site: A scrambled of vertebrate diversity. *Ciências da Terra-Procedia* 2021, 1, 58–61. [\[CrossRef\]](#)
99. Vila, B.; Sellés, A.G. Re-evaluation of the age of some dinosaur localities from the southern Pyrenees by means of megaloolithid oospecies. *J. Iber. Geol.* 2015, 41. [\[CrossRef\]](#)
100. Canudo, J.L. Descripción de un fragmento proximal de fémur de Titanosauridae (Dinosauria, Sauropoda) del Maastrichtense superior de Serraduy (Huesca). In Proceedings of the XVII Jornadas de la Sociedad Española de Paleontología, Albarraçin, Spain, 18–20 October 2001; pp. 255–262.
101. Sellés, A.G.; Marmi, J.; Llácer, S.; Blanco, A. The youngest sauropod evidence in Europe. *Hist. Biol.* 2016, 28, 930–940. [\[CrossRef\]](#)
102. Fondevilla, V.; Vila, B.; Oms, J.; Galobart, A. Skin impressions of the last European dinosaurs. *Geol. Mag.* 2017, 154, 393–398. [\[CrossRef\]](#)
103. Díez Díaz, V.; Perea Suberbiola, X.; Sanz, J.L. The axial skeleton of the titanosaur *Lirainosaurus astibiae* (Dinosauria: Sauropoda) from the latest Cretaceous of Spain. *Cretac. Res.* 2013, 43, 145–160. [\[CrossRef\]](#)
104. Salgado, L.; Coria, R.A.; Calvo, J.O. Evolution of titanosaurid sauropods: Phylogenetic analysis based on the postcranial evidence. *Ameghiniana* 1997, 34, 3–32.
105. Upchurch, P.; Barrett, P.M.; Dodson, R. 13. Sauropoda. In *The Dinosauria*, 2nd ed.; University of California Press: Berkeley, CA, USA, 2019; pp. 259–322.
106. Calvo, J.O.; Bonaparte, J.F. *Andesaurus delgadoi* gen. et. sp. nov. (Saurischia-Sauropoda), dinosaurio Titanosauridae de la Formación Río Limay (Albiano-Cenomaniano), Neuquén, Argentina. *Ameghiniana* 1991, 28, 303–310.
107. Mannion, P.D.; Calvo, J.O. Anatomy of the basal titanosaur (Dinosauria, Sauropoda) *Andesaurus delgadoi* from the mid-Cretaceous (Albian-early Cenomanian) Río Limay Formation, Neuquén Province, Argentina: Implications for titanosaur systematics. *Zool. J. Linn. Soc.* 2011, 155–181. [\[CrossRef\]](#)
108. Torices, A.; Currie, P.J.; Canudo, J.L.; Perea Suberbiola, X. Theropod dinosaurs from the upper cretaceous of the south pyrenees basin of Spain. *Acta Palaeontol. Pol.* 2015, 60, 611–626. [\[CrossRef\]](#)
109. Pérez-García, A.; Ortega, F.; Bolet, A.; Escaso, F.; Housaye, A.; Martínez-Salanova, J.; de Miguel Chaves, C.; Mocho, P.; Narváez, I.; Segura, M.; et al. A review of the upper Campanian vertebrate site of Armuña (Segovia Province, Spain). *Cretac. Res.* 2016, 57, 591–623. [\[CrossRef\]](#)
110. Pérez-Pueyo, M.; Puértolas-Pascual, E.; Moreno-Azanza, M.; Cruzado-Caballero, P.; Gasca, J.M.; Núñez-Lahuerza, C.; Canudo, J.L. First record of a giant bird (Ornithomorphia) from the uppermost Maastrichtian of the Southern Pyrenees, NE Spain. *J. Vertebr. Paleontol.* 2021, 41, e1900210.
111. López-Martínez, N.; Canudo, J.L.; Cuenca-Bescós, G. Latest cretaceous eggshells from Arén (Southern Pyrenees, Spain). In Proceedings of the First International Symposium on Dinosaur Eggs and Babies, Isona, Spain, 23–26 September 1999; pp. 35–36.
112. Núñez-Lahuerza, C.; Moreno-Azanza, M.; Pérez-Pueyo, M. First approach for a taphonomic key for fossil eggs and eggshells accumulations using optic microscopy: The case of Blasi-2B (Upper Cretaceous, Spain). *Ciências Terra Procedia* 2021, 1, 42–45.
113. Choi, S.; Moreno-Azanza, M.; Csiki-Sava, Z.; Prondvai, E.; Lee, Y.N. Comparative crystallography suggests maniraptoran theropod affinities for latest Cretaceous European 'geckoid' eggshells. *Pap. Palaeontol.* 2020, 6, 265–292. [\[CrossRef\]](#)
114. Dalla Vecchia, F.M.; Riera, F.M.; Oms, J.O.; Dináres-Turell, J.; Gaete, R.; Galobart, A. The last pterosaurs: First record from the uppermost Maastrichtian of the Tremp Syncline (Northern Spain). *Acta Geol. Sin.* 2013, 87, 1198–1227. [\[CrossRef\]](#)
115. Puértolas, E.; Canudo, J.L.; Cruzado-Caballero, P. A new crocodylian from the late Maastrichtian of Spain: Implications for the initial radiation of crocodylioids. *PLoS ONE* 2011, 6. [\[CrossRef\]](#)
116. Blanco, A.; Puértolas-Pascual, E.; Marmi, J.; Vila, B.; Sellés, A.G. *Allodaposuchus palustris* sp. nov. from the Upper Cretaceous of Fumanya (South-Eastern Pyrenees, Iberian Peninsula): Systematics, Palaeoecology and Palaeobiogeography of the Enigmatic *Allodaposuchus* Crocodylians. *PLoS ONE* 2014, 9, e115837. [\[CrossRef\]](#)
117. Blanco, A.; Fortuny, J.; Vicente, A.; Luján, A.H.; García-Marzá, J.A.; Sellés, A.G. A new species of *Allodaposuchus* (Eusuchia, Crocodylia) from the Maastrichtian (Late Cretaceous) of Spain: Phylogenetic and paleobiological implications. *Peer J.* 2015, 3, e1171. [\[CrossRef\]](#)
118. Narváez, I.; Brochu, C.A.; Escaso, F.; Pérez-García, A.; Ortega, F. New Crocodylians from Southwestern Europe and Definition of a Diverse Clade of European Late Cretaceous Basal Eusuchians. *PLoS ONE* 2015, 10, e0140679. [\[CrossRef\]](#)
119. Narváez, I.; Brochu, C.A.; Escaso, F.; Pérez-García, A.; Ortega, F. New Spanish Late Cretaceous eusuchian reveals the synchronous and sympatric presence of two allodaposuchids. *Cretac. Res.* 2016, 65, 112–125. [\[CrossRef\]](#)
120. Mateus, O.; Puértolas-Pascual, E.; Callapez, P.M. A new eusuchian crocodylomorph from the Cenomanian (Late Cretaceous) of Portugal reveals novel implications on the origin of Crocodylia. *Zool. J. Linn. Soc.* 2019, 186, 501–528. [\[CrossRef\]](#)
121. Puértolas-Pascual, E.; Canudo, J.L.; Moreno-Azanza, M. The eusuchian crocodylomorph *Allodaposuchus subjuniperus* sp. nov., a new species from the latest Cretaceous (upper Maastrichtian) of Spain. *Hist. Biol.* 2014, 26, 91–109. [\[CrossRef\]](#)
122. Blanco, A.; Puértolas-Pascual, E.; Marmi, J.; Moncunill-Solé, B.; Llácer, S.; Rössner, G.E. Late Cretaceous (Maastrichtian) crocodylians from north-eastern Iberia: A first attempt to explain the crocodyliiform diversity based on tooth qualitative traits. *Zool. J. Linn. Soc.* 2020, 189, 584–617. [\[CrossRef\]](#)

123. Moreno-Azanza, M.; Bauluz, B.; Canudo, J.I.; Puértolas-Pascual, E.; Sellés, A.G. A re-evaluation of aff. Megaloolithidae eggshell fragments from the uppermost Cretaceous of the Pyrenees and implications for crocodylomorph eggshell structure. *Hist. Biol.* **2014**, *26*, 195–205. [\[CrossRef\]](#)
124. Hirsch, K.F. Fossil crocodilian eggs from the eocene of Colorado. *J. Paleontol.* **1985**, *3*, 531–542.
125. Vila, B.; Castanera, D.; Marmi, J.; Canudo, J.I.; Galobart, À. Crocodile swim tracks from the latest Cretaceous of Europe. *Lethaia* **2015**, *48*, 256–266. [\[CrossRef\]](#)
126. Pérez-Pueyo, M.; Castanera, D.; Bádenas, B.; Canudo, J.I. New evidences of Crocodylomorpha swim tracks in the Maastrichtian of Beranuy (Huesca, Spain). In Proceedings of the XVI Encuentro de Jóvenes Investigadores en Paleontología, Zarautz, Spain, 11–14 April 2018; pp. 137–140.
127. De Lapparent de Broin, F.; Murelaga, X. Turtles from Upper Cretaceous of Lano (Iberian Peninsula). *Comptes Rendus l'Académie Sci.* **1996**, *323*, 729–735.
128. Murelaga, X.; Canudo, J.I. Descripción de los restos de quelonios del Maastrichtiense superior de Aren y Serraduy (Huesca). *Geogaceta* **2005**, *28*, 51–54.
129. Blain, H.A.; Canudo, J.I.; Cuenca-Bescós, G.; López-Martínez, N. Amphibians and squamate reptiles from the latest Maastrichtian (Upper Cretaceous) of Blasi 2 (Huesca, Spain). *Cretac. Res.* **2010**, *31*, 433–446. [\[CrossRef\]](#)
130. Berreteaga, A.; Pereda Suberbiola, X.; Floquet, M.; Olivares, M.; Etxebarria, N.; Iriarte, E.; Badiola Kortabitarte, A.; Elorza, J.; Astibia Ayerra, H. Datos sedimentológicos y tafonómicos de enclaves finicretácicos con fósiles de vertebrados de la Formación Sobrepeña (Burgos, Región Vasco-Cantábrica). *Geo-Temas* **2008**, *10*, 1278–1280.
131. Corral, J.-C.; Pueyo, E.L.; Berreteaga, A.; Rodríguez-Pintó, A.; Sánchez, E.; Pereda-Suberbiola, X. Magnetostratigraphy and lithostratigraphy of the Laño vertebrate-site: Implications in the uppermost Cretaceous chronostratigraphy of the Basque-Cantabrian Region. *Cretac. Res.* **2016**, *57*, 473–489. [\[CrossRef\]](#)
132. Company, J. Vertebrados continentales del Cretácico superior (Campaniense- Maastrichtiense) de Valencia. Ph.D. Thesis, Universidad de Valencia, Valencia, Spain, 2004.
133. Company, J.; Pereda-Suberbiola, X.; Ruiz-Omeñaca, J.I. Last Cretaceous dinosaur faunas from Eastern Iberia into its regional paleogeographic context. Faunal composition and palaeobiogeographical implications. In Proceedings of the IV Jornadas Internacionales sobre Paleontología de Dinosaurios y su Entorno Salas de los Infantes, Burgos, Spain, 5–9 September 2009; pp. 17–44.
134. Laurent, Y.; Bilotte, M.; Le Loeuff, J. Late Maastrichtian continental vertebrates from southwestern France: Correlation with marine fauna. *Palaeogeogr. Palaeoclimatol. Palaeoecol.* **2002**, *187*, 121–135. [\[CrossRef\]](#)
135. Le Loeuff, J.; Buffetaut, E.; Martin, M. The last stages of dinosaur faunal history in Europe: A succession of Maastrichtian dinosaur assemblages from the Corbières (southern France). *Geol. Mag.* **1994**, *131*, 625–630. [\[CrossRef\]](#)
136. Prieto-Márquez, A.; Fondevilla, V.; Sellés, A.G.; Wagner, J.R.; Galobart, À. *Adynomosaurus arcanus*, a new lambeosaurine dinosaur from the Late Cretaceous Ibero-Armorican Island of the European archipelago. *Cretac. Res.* **2019**, *96*, 19–37. [\[CrossRef\]](#)
137. Casanovas-Cladellas, M.L.; Santafé-Llopis, J.V.; Isidro-Llorens, A. *Pararhabdodon isonensis* n. gen. n. sp. (Dinosauria). Estudio morfológico, radio-tomográfico y consideraciones biomecánicas 26–27:121–131. *Paleontol. Evol.* **1993**, *26–27*, 121–132.
138. Serrano, J.F.; Sellés, A.G.; Vila, B.; Galobart, À.; Prieto-Márquez, A. The osteohistology of new remains of *Pararhabdodon isonensis* sheds light into the life history and paleoecology of this enigmatic European lambeosaurine dinosaur. *Cretac. Res.* **2021**, *118*, 104677. [\[CrossRef\]](#)
139. Prieto-Márquez, A.; Wagner, J.R. *Pararhabdodon isonensis* and *Tsintaosaurus spinorhinus*: A new clade of lambeosaurine hadrosaurids from Eurasia. *Cretac. Res.* **2009**, *30*, 1238–1246. [\[CrossRef\]](#)
140. Prieto-Márquez, A.; Gaete, R.; Rivas, G.; Galobart, À.; Boada, M. Hadrosauroid dinosaurs from the Late Cretaceous of Spain: *Pararhabdodon isonensis* revisited and *Koutalisaurus kohlerorum*, gen. et sp. nov. *J. Vertebr. Paleontol.* **2006**, *26*, 929–943. [\[CrossRef\]](#)
141. Blanco, A.; Prieto-Márquez, A.; De Esteban-Trivigno, S. Diversity of hadrosauroid dinosaurs from the Late Cretaceous Ibero-Armorican Island (European Archipelago) assessed from dentary morphology. *Cretac. Res.* **2015**, *56*, 447–457. [\[CrossRef\]](#)
142. Fondevilla, V.; Dalla Vecchia, F.M.; Gaete, R.; Galobart, À.; Moncunill-Solé, B.; Köhler, M. Ontogeny and taxonomy of the hadrosaur (Dinosauria, Ornithopoda) remains from Basturs Poble bonebed (late early Maastrichtian, Tremp Syncline, Spain). *PLoS ONE* **2018**, *13*, e0206287. [\[CrossRef\]](#)
143. Company, J.; Galobart Lorente, À.; Gaete, R. First data on the hadrosaurid dinosaurs (Ornithischia, Dinosauria) from the Upper Cretaceous of Valencia, Spain. *Oryctos* **1998**, *1*, 121–126.
144. Pereda-Suberbiola, X.; Pérez-García, A.; Corral, J.C.; Murelaga, X.; Martín, G.; Larrañaga, J.; Bardet, N.; Berreteaga, A.; Company, J. First dinosaur and turtle remains from the latest Cretaceous shallow marine deposits of Albaina (Laño quarry, Iberian Peninsula). *Comptes Rendus Palevol.* **2015**, *14*, 471–482. [\[CrossRef\]](#)
145. Santafé, J.V.; Casanovas, M.L.; Llopart, C. *Els Dinosaurios i el Seu Entorn Geològic*; Diputació de Lleida: Lleida, Spain, 1997.
146. López-Martínez, N.; Moratalla, J.J.; Sanz, J.L. Dinosaurs nesting on tidal flats. *Palaeogeogr. Palaeoclimatol. Palaeoecol.* **2000**, *160*, 153–163. [\[CrossRef\]](#)
147. Baiano, M.; Galobart, À.; Dalla, F.M.; Vila, B. Aplicación de la microtomografía en el estudio de dientes aislados de dinosaurios terópodos. In Proceedings of the XII Encuentro de Jóvenes investigadores en Paleontología, Boltaña, Spain, 9–12 April 2014; pp. 57–59.

148. Marmi, J.; Blanco, A.; Fondevilla, V.; Dalla Vecchia, F.M.; Sellés, A.G.; Vicente, A.; Martín-Closas, C.; Oms, O.; Galobart, À. The Molí del Baró-1 site, a diverse fossil assemblage from the uppermost Maastrichtian of the southern Pyrenees (north-eastern Iberia). *Cretac. Res.* **2016**, *57*, 519–539. [\[CrossRef\]](#)
149. Sellés, A.G.; Vila, B.; Brusatte, S.L.; Currie, P.J.; Galobart, À. A fast-growing basal troodontid (Dinosauria: Theropoda) from the latest Cretaceous of Europe. *Sci. Rep.* **2021**, *11*, 4855. [\[CrossRef\]](#)
150. Sellés, A.G.; Vila, B.; Galobart, À. Diversity of theropod ootaxa and its implications for the latest cretaceous dinosaur turnover in southwestern Europe. *Cretac. Res.* **2014**, *49*, 45–54. [\[CrossRef\]](#)
151. Vianey-Liaud, M.; Lopez-Martinez, N. Late Cretaceous Dinosaur Eggshells from the Tremp Basin, Southern Pyrenees, Lleida, Spain. *J. Paleontol.* **1997**, *71*, 1157–1171. [\[CrossRef\]](#)
152. Laurent, Y. Les faunes de vertébrés continentaux du Maastrichtien supérieur d'Europe: Systématique et biodiversité. *Strat. Série* **2003**, *41*, 1–81.
153. Ogg, J.G.; Hinnov, L.A.; Huang, C. Cretaceous. In *The Geologic Time Scale*; Elsevier: Amsterdam, The Netherlands, 2012; pp. 793–853.
154. Buffetaut, E.; Clarke, J.B.; Le Loeuff, J. A terminal Cretaceous pterosaur from the Corbières (southern France) and the problem of pterosaur extinction. *Bull. Soc. Geol. Fr.* **1996**, *167*, 753–759.
155. Buffetaut, E.; Laurent, Y.; Le Loeuff, J.; Bilotte, M. A terminal Cretaceous giant pterosaur from the French Pyrenees. *Geol. Mag.* **1997**, *134*, 553–556. [\[CrossRef\]](#)
156. Buffetaut, E. Late Cretaceous pterosaurs from France: A review. *Zitteliana* **2008**, *28*, 249–255.
157. Company, J.; Ruiz-Omeñaca, J.I.; Suberbiola, X.P. A long-necked pterosaur (Pterodactyloidea, Azhdarchidae) from the Upper Cretaceous of Valencia, Spain. *Geol. Mijnbouw/Netherlands J. Geosci.* **1999**, *78*, 319–333. [\[CrossRef\]](#)
158. Pereda-Suberbiola, X.; Company, J.; Ruiz-Omeñaca, J.I. Azhdarchid pterosaurs from the Late Cretaceous (Campanian-Maastrichtian) of the Iberian Peninsula. In Proceedings of the Munich Flugsaurier, The Wellnhofer Pterosaur Meeting, Munich, Germany, 10–14 September 2007; p. 27.
159. Blanco, A.; Méndez, J.M.; Marmi, J. The fossil record of the uppermost Maastrichtian Reptile Sandstone (Tremp Formation, northeastern Iberian Peninsula). *Span. J. Paleontol.* **2015**, *30*, 147–160. [\[CrossRef\]](#)
160. Laurent, Y.; Buffetaut, E.; Le Loeuff, J. Un crane de thoracosaurine (Crocodylia, Crocodylidae) dans le Maastrichtien Supérieur du sud de la France. *Oryctos* **2000**, *3*, 19–27.
161. Brochu, C.A. A new Late Cretaceous gavialoid crocodylian from eastern North America and the phylogenetic relationships of thoracosaurines. *J. Vertebr. Paleontol.* **2004**, *24*, 610–633. [\[CrossRef\]](#)
162. Le Loeuff, J.; Buffetaut, E.; Cavin, L.; Laurent, Y.; Martin, M.; Martin, V.; Tong, H. Les hadrosaures des Corbières et des Petites Pyrénées. *Bull. Soc. Etudes Sci. Aude* **1994**, *94*, 19–21.
163. Buffetaut, E.; Le Loeuff, J. Late Cretaceous dinosaurs from the foothills of the Pyrenees. *Geol. Today* **1997**, *13*, 60–68. [\[CrossRef\]](#)
164. Tennant, J.P.; Mannion, P.D.; Upchurch, P. Evolutionary relationships and systematics of Atoposauridae (Crocodylomorpha: Neosuchia): Implications for the rise of Eusuchia. *Zool. J. Linn. Soc.* **2016**, *177*, 854–936. [\[CrossRef\]](#)
165. Murelaga, X.; García Garmilla, F.; Pereda Suberbiola, X. Primeros restos de vertebrados del Cretácico Superior de Quecedo de Valdivieso (Burgos). *Geogaceta* **2005**, 195–198.
166. Berreteaga, A. Estudio Estratigráfico, Sedimentológico y Paleontológico de los Yacimientos con Fósiles de Vertebrados del Cretácico Final de la Región Vasco-Cantábrica. Ph.D. Thesis, University of the Basque Country, Bilbao, Spain, 2008.
167. Laurent, Y.; Tong, H.; Claude, J. New side-necked turtle (Pleurodira: Bothremydidae) from the Upper Maastrichtian of the Petites-Pyrénées (Haute-Garonne, France). *Cretac. Res.* **2002**, *23*, 465–471. [\[CrossRef\]](#)
168. Marmi, J.; Luján, Á.H.; Riera, V.; Gaete, R.; Oms, O.; Galobart, À. The youngest species of *Polysternon*: A new bothremydid turtle from the uppermost Maastrichtian of the southern Pyrenees. *Cretac. Res.* **2012**, *35*, 133–142. [\[CrossRef\]](#)
169. Pérez-García, A. Las tortugas mesozoicas de la Península Ibérica. Ph.D. Thesis, Universidad Complutense de Madrid, Madrid, Spain, 2012.
170. Murelaga, X.; Pereda Suberbiola, X.; Astibia, H.; Lapparent, F.D. Primeros datos sobre los quelonios del Cretácico superior de Lleida. *Geogaceta* **1998**, *24*, 239–242.
171. Blanco, A.; Bolet, A.; Blain, H.-A.; Fondevilla, V.; Marmi, J. Late Cretaceous (Maastrichtian) amphibians and squamates from northeastern Iberia. *Cretac. Res.* **2016**, *57*, 624–638. [\[CrossRef\]](#)
172. Szentesi, Z.; Company, J. Late Maastrichtian small-sized herpetofauna from Valencia province, eastern Spain. *Hist. Biol.* **2017**, *29*, 43–52. [\[CrossRef\]](#)
173. Pol, C.; Buscalioni, A.D.; Carballeira, J.; Francés, V.; López-Martínez, N.; Marandat, B.; Moratalla, J.; Sanz, J.L.; Sigé, B.; Villatte, J. Reptiles and mammals from the Late Cretaceous new locality Quintanilla del Coco (Burgos Province, Spain). *Neues Jahrb. Geol. Paläontol. Abh.* **1992**, *184*, 279–314.
174. Gheerbrant, E.; Astibia, H. Addition to the Late Cretaceous Laño mammal faunule (Spain) and to the knowledge of European “Zhelestidae” (Lainodontinae nov.). *Bull. Soc. Géol. Fr.* **2012**, *183*, 537–546. [\[CrossRef\]](#)
175. Tabuce, R.; Tortosa, T.; Vianey-Liaud, M.; Garcia, G.; Lebrun, R.; Godefroit, P.; Dutour, Y.; Berton, S.; Valentin, X.; Cheylan, G. New eutherian mammals from the Late Cretaceous of Aix-en-Provence Basin, south-eastern France. *Zool. J. Linn. Soc.* **2013**, *169*, 653–672. [\[CrossRef\]](#)

176. Peláez-Campomanes, P.; López-Martínez, N.; Álvarez-Sierra, M.A.; Daams, R. The earliest mammal of the European Paleocene: The multituberculate Hainina. *J. Paleontol.* **2000**, *74*, 701–711. [\[CrossRef\]](#)
177. López-Martínez, N.; Peláez-Campomanes, P. New mammals from south-central Pyrenees (Trespín Formation, Spain) and their bearing on late Paleocene marine-continental correlations. *Bull. Soc. Géol. Fr.* **1999**, *170*, 681–696.
178. Gheerbrant, E.; Abrial, C.; Cappetta, H. Nouveaux sites à microvertébrés continentaux du Crétacé terminal des Petites Pyrénées (Haute-Garonne et Ariège, France). *Geobios* **1997**, *30*, 257–269. [\[CrossRef\]](#)
179. Nopcsa, F. Über das Vorkommen der Dinosaurier in Siebenbürgen. *Verhandlungen der Zool. Gesellschaft* **1914**, *54*, 12–14.
180. Benton, M.J.; Csiki, Z.; Grigorescu, D.; Redelstorff, R.; Sander, P.M.; Stein, K.; Weishampel, D.B. Dinosaurs and the island rule: The dwarfed dinosaurs from Hațeg Island. *Palaeogeogr. Palaeoclimatol. Palaeoecol.* **2010**, *293*, 438–454. [\[CrossRef\]](#)
181. Godefroit, P.; Codrea, V.; Weishampel, D.B. Osteology of *Zalmoxes shqiperorum* (Dinosauria, Ornithomimidae), based on new specimens from the Upper Cretaceous of Nălaț-Vad (Romania). *Geodiversitas* **2009**, *31*, 525–553. [\[CrossRef\]](#)
182. Weishampel, D.B.; Jianu, C.; Csiki, Z.; Norman, D.B. Osteology and phylogeny of *Zalmoxes* (n. g.), an unusual Ornithomimid dinosaur from the latest Cretaceous of Romania. *J. Syst. Palaeontol.* **2003**, *1*, 65–123. [\[CrossRef\]](#)
183. Weishampel, D.B.; Norman, D.B.; Grigorescu, D. *Telmatosaurus transsylvanicus* from the late Cretaceous of Romania: The most basal hadrosaurid dinosaur. *Palaeontology* **1993**, *36*, 361–385.
184. Dalla Vecchia, F.M. An overview of the latest Cretaceous hadrosaurid record in Europe. In *Hadrosaurs*; Eberth, D.A., Evans, D.C., Eds.; Indiana University Press: Bloomington, IN, USA, 2014; pp. 268–297.
185. Codrea, V.; Smith, T.; Dica, P.; Folie, A.; Garcia, G.; Godefroit, P.; Van Itterbeeck, J. Dinosaur egg nests, mammals and other vertebrates from a new Maastrichtian site of the Hațeg Basin (Romania). *Comptes Rendus Palevol* **2002**, *1*, 173–180. [\[CrossRef\]](#)
186. Vasile, S.; Csiki, Z.; Grigorescu, D. The first report of continental fossil remains from Crăguș (Hațeg Basin, Romania), and their stratigraphical significance. In Proceedings of the Eighth Romanian Symposium on Paleontology, Bucharest, Romania, 29–30 September 2011; pp. 127–128.
187. Ősi, A.; Codrea, V.; Prondvai, E.; Csiki-Sava, Z. New ankylosaurian material from the Upper Cretaceous of Transylvania. *Ann. Paléontol.* **2014**, *100*, 257–271. [\[CrossRef\]](#)
188. Nopcsa, F. Die dinosaurier der siebenbürgischen landesteile ungarns. *Mitteilungen aus dem Jahrb. der königlich Ung. Geol. Reichsanstalt* **1915**, *23*, 3–24.
189. Csiki, Z.; Codrea, V.; Jipa-Murzea, C.; Godefroit, P. A partial titanosaur (Sauropoda, Dinosauria) skeleton from the Maastrichtian of Nălaț-Vad, Hațeg Basin, Romania. *Neues Jahrb. Geol. Paläontol. Abhandlungen* **2010**, *258*, 297–324. [\[CrossRef\]](#)
190. Codrea, V.; Vremir, M.; Jipa, C.; Godefroit, P.; Csiki, Z.; Smith, T.; Fărcaș, C. More than just Nopcsa's Transylvanian dinosaurs: A look outside the Hațeg Basin. *Palaeogeogr. Palaeoclimatol. Palaeoecol.* **2010**, *293*, 391–405. [\[CrossRef\]](#)
191. Vremir, M.M. New faunal elements from the late Cretaceous (Maastrichtian) continental deposits of Sebeș area (Transylvania). *Terra Sebus* **2010**, *2*, 635–684.
192. Csiki, Z.; Vremir, M. A large-sized (?) Late Maastrichtian titanosaur from Rapa Rosie, Sebeș. In Proceedings of the 8th Romanian Symposium of Paleontology, Bucharest, Romania, 29–30 September 2011; pp. 28–29.
193. Mannion, P.D.; Díez Díaz, V.; Csiki-Sava, Z.; Upchurch, P.; Cuff, A.R. Dwarfs among giants: Resolving the systematics of the titanosaurian sauropod dinosaurs from the Late Cretaceous of Romania. In Proceedings of the XVII Conference of the EAVP, Brussels, Belgium, 1–6 July 2019; p. 65.
194. Erickson, G.M.; Krick, B.A.; Hamilton, M.; Bourne, G.R.; Norell, M.A.; Lilleodden, E.; Sawyer, W.G. Complex dental structure and wear biomechanics in hadrosaurid dinosaurs. *Science* **2012**, *338*, 98–101. [\[CrossRef\]](#)
195. LeBlanc, A.R.H.; Reisz, R.R.; Evans, D.C.; Baillet, A.M. Ontogeny reveals function and evolution of the hadrosaurid dinosaur dental battery. *BMC Evol. Biol.* **2016**, *16*, 152. [\[CrossRef\]](#)
196. Chin, K.; Feldmann, R.M.; Tashman, J.N. Consumption of crustaceans by megaherbivorous dinosaurs: Dietary flexibility and dinosaur life history strategies. *Sci. Rep.* **2017**, *7*, 11163. [\[CrossRef\]](#)
197. Vremir, M.; Dyke, G.; Totoianu, R. Repertoire of the late cretaceous vertebrate localities from Sebescedil; area, Alba county (Romania). *Terra Sebus* **2015**, *7*, 695–724.
198. Văcărescu, M.R.; Sava, Z.C.; Bucur, M.; Roman, A.; Vasile, Ș. Theropod dental diversity in the Maastrichtian of the Hațeg Basin, Romania Hațeg Basin have yielded a diverse and unique assemblage of vertebrate. In Proceedings of the 11th Romanian Symposium of Paleontology, Bucharest, Romania, 27–28 September 2017; pp. 122–123.
199. Brusatte, S.L.; Vremir, M.; Csiki-Sava, Z.; Turner, A.H.; Watanabe, A.; Erickson, G.M.; Norell, M.A. The Osteology of *Balaur bondoc*, an Island-Dwelling Dromaeosaurid (Dinosauria: Theropoda) from the Late Cretaceous of Romania. *Bull. Am. Museum Nat. Hist.* **2013**, *374*, 1–100. [\[CrossRef\]](#)
200. Csiki, Z.; Vremir, M.; Brusatte, S.L.; Norell, M.A. An aberrant island-dwelling theropod dinosaur from the Late Cretaceous of Romania. *Proc. Natl. Acad. Sci. USA* **2010**, *107*, 15357–15361. [\[CrossRef\]](#) [\[PubMed\]](#)
201. Wang, X.; Dyke, G.J.; Codrea, V.; Godefroit, P.; Smith, T. A Euenantiornithine Bird from the Late Cretaceous Hațeg Basin of Romania. *Acta Palaeontol. Pol.* **2011**, *56*, 853–857. [\[CrossRef\]](#)
202. Mayr, G.; Codrea, V.; Solomon, A.; Bordeianu, M.; Smith, T. A well-preserved pelvis from the Maastrichtian of Romania suggests that the enigmatic *Gargantuavis* is neither an ornithurine bird nor an insular endemic. *Cretac. Res.* **2020**, *106*, 104271. [\[CrossRef\]](#)

203. Sallam, H.M.; Gorscak, E.; O'Connor, P.M.; El-Dawoudi, I.A.; El-Sayed, S.; Saber, S.; Kora, M.A.; Sertich, J.J.W.; Seiffert, E.R.; Lamanna, M.C. New Egyptian sauropod reveals Late Cretaceous dinosaur dispersal between Europe and Africa. *Nat. Ecol. Evol.* **2018**, *2*, 445–451. [\[CrossRef\]](#) [\[PubMed\]](#)
204. Tortosa, T.; Buffetaut, E.; Vialle, N.; Dutour, Y.; Turini, E.; Cheylan, G. A new abelisaurid dinosaur from the Late Cretaceous of southern France: Palaeobiogeographical implications. *Ann. Paléontol.* **2014**, *100*, 63–86. [\[CrossRef\]](#)
205. Buffetaut, E.; Grigorescu, D.; Csiki, Z. A new giant pterosaur with a robust skull from the latest Cretaceous of Romania. *Naturwissenschaften* **2002**, *89*, 180–184. [\[CrossRef\]](#) [\[PubMed\]](#)
206. Naish, D.; Witton, M.P. Neck biomechanics indicate that giant Transylvanian azhdarchid pterosaurs were short-necked arch predators. *Peer J.* **2017**, *5*, e2908. [\[CrossRef\]](#)
207. Solomon, A.A.; Codrea, V.A.; Venczel, M.; Grellet-Tinner, G. A new species of large-sized pterosaur from the Maastrichtian of Transylvania (Romania). *Cretac. Res.* **2020**, *110*, 104316. [\[CrossRef\]](#)
208. Rabi, M.; Delfino, M. A reassessment of the “alligatoroid” eusuchian from the Late Cretaceous of Hungary and its taxonomic implications. In Proceedings of the 10th Annual Meeting of the European Association of Vertebrate Palaeontologists, Teruel, Spain, 19–24 June 2012; pp. 203–206.
209. Martin, J.E.; Rabi, M.; Csiki, Z. Survival of *Theriosuchus* (Mesoeucrocodylia: Atoposauridae) in a Late Cretaceous archipelago: A new species from the Maastrichtian of Romania. *Naturwissenschaften* **2010**, *97*, 845–854. [\[CrossRef\]](#)
210. Martin, J.E.; Rabi, M.; Csiki-Sava, Z.; Vasile, Ş. Cranial morphology of *Theriosuchus sympietodon* (Mesoeucrocodylia, Atoposauridae) and the widespread occurrence of *Theriosuchus* in the Late Cretaceous of Europe. *J. Paleontol.* **2014**, *88*, 444–456. [\[CrossRef\]](#)
211. Rabi, M.; Sebők, N. A revised Eurogondwana model: Late Cretaceous notosuchian crocodyliforms and other vertebrate taxa suggest the retention of episodic faunal links between Europe and Gondwana during most of the Cretaceous. *Gondwana Res.* **2015**, *28*, 1197–1211. [\[CrossRef\]](#)
212. Sellés, A.G.; Blanco, A.; Vila, B.; Marmi, J.; López-Soriano, F.J.; Llácer, S.; Frigola, J.; Canals, M.; Galobart, À. A small Cretaceous crocodyliform in a dinosaur nesting ground and the origin of sebecids. *Sci. Rep.* **2020**, *10*, 15293. [\[CrossRef\]](#)
213. Rabi, M.; Vremir, M.; Tong, H. Preliminary Overview of Late Cretaceous Turtle Diversity in Eastern Central Europe (Austria, Hungary, and Romania). In *Morphology and Evolution of Turtles. Vertebrate Paleobiology and Paleoanthropology*; Brinkman, D., Holroyd, P., Gardner, J., Eds.; Springer: Dordrecht, The Netherlands, 2013; pp. 307–336.
214. Pérez-García, A.; Codrea, V. New insights on the anatomy and systematics of *Kallokibotion* Nopcsa, 1923, the enigmatic uppermost Cretaceous basal turtle (stem Testudines) from Transylvania. *Zool. J. Linn. Soc.* **2018**, *182*, 419–443. [\[CrossRef\]](#)
215. Venczel, M.; Gardner, J.D.; Codrea, V.A.; Csiki-Sava, Z.; Vasile, Ş.; Solomon, A.A. New insights into Europe’s most diverse Late Cretaceous anuran assemblage from the Maastrichtian of western Romania. *Palaeobiodivers. Palaeoenviron.* **2016**, *96*, 61–95. [\[CrossRef\]](#)
216. Grigorescu, D.; Venczel, M.; Csiki, Z.; Limborea, R. New microvertebrate fossil assemblages from the Uppermost Cretaceous of the Haţeg Basin (Romania). *Geol. Mijnb.* **1999**, *78*, 301–314. [\[CrossRef\]](#)
217. Folie, A.; Codrea, V. New lissamphibians and squamates from the Maastrichtian of Haţeg Basin, Romania. *Acta Palaeontol. Pol.* **2005**, *50*, 57–71.
218. Codrea, V.A.; Venczel, M.; Solomon, A. A new family of teioid lizards from the Upper Cretaceous of Romania with notes on the evolutionary history of early teioids. *Zool. J. Linn. Soc.* **2017**. [\[CrossRef\]](#)
219. Vasile, Ş.; Csiki-Sava, Z.; Venczel, M. A new madtsoiid snake from the Upper Cretaceous of the Haţeg Basin, western Romania. *J. Vertebr. Paleontol.* **2013**, *33*, 1100–1119. [\[CrossRef\]](#)
220. Venczel, M.; Vasile, Ş.; Csiki-Sava, Z. A Late Cretaceous madtsoiid snake from Romania associated with a megaloolithid egg nest—Paleoecological inferences. *Cretac. Res.* **2015**, *55*, 152–163. [\[CrossRef\]](#)
221. Pereda-Suberbiola, X.; Corral, J.C.; Astibia, H.; Badiola, A.; Bardet, N.; Berreteaga, A.; Buffetaut, E.; Buscalioni, A.D.; Cappetta, H.; Cavin, L.; et al. Late Cretaceous continental and marine vertebrate assemblages from the Laño quarry (Basque-Cantabrian Region, Iberian Peninsula): An update. *J. Iber. Geol.* **2015**, *41*. [\[CrossRef\]](#)
222. Csiki, Z.; Grigorescu, D.; Rücklin, M. A new multituberculate specimen from the Maastrichtian of Pui, Romania and a reassessment of affinities of *Barbatodon*. *Acta Palaeontol. Rom.* **2005**, *5*, 73–86.
223. Smith, T.; Codrea, V. Red iron-pigmented tooth enamel in a multituberculate mammal from the Late Cretaceous Transylvanian “Haţeg Island”. *PLoS ONE* **2015**, *10*, e0132550. [\[CrossRef\]](#)
224. Csiki-Sava, Z.; Vremir, M.; Meng, J.; Brusatte, S.L.; Norell, M.A. Dome-headed, small-brained island mammal from the Late Cretaceous of Romania. *Proc. Natl. Acad. Sci. USA* **2018**, *115*, 4857–4862. [\[CrossRef\]](#)
225. De Bast, E.; Smith, T. The oldest Cenozoic mammal fauna of Europe: Implication of the Hainin reference fauna for mammalian evolution and dispersals during the Paleocene. *J. Syst. Palaeontol.* **2017**, *15*, 741–785. [\[CrossRef\]](#)
226. Brocklehurst, N.; Kammerer, C.F.; Fröbisch, J. The early evolution of synapsids, and the influence of sampling on their fossil record. *Paleobiology* **2013**, *39*, 470–490. [\[CrossRef\]](#)
227. Purnell, M.A.; Donoghue, P.C.J. Between death and data: Biases in interpretation of the fossil record of conodonts—The Palaeontological Association. *Spec. Pap. Palaeontol.* **2005**, *25*, 7–25.
228. Benton, M.J.; Dunhill, A.M.; Lloyd, G.T.; Marx, F.G. Assessing the quality of the fossil record: Insights from vertebrates. *Geol. Soc. Lond. Spec. Publ.* **2011**, *358*, 63–94. [\[CrossRef\]](#)

- 
229. Benton, M.J.; Pearson, P.N. Speciation in the fossil record. *Trends Ecol. Evol.* **2001**, *16*, 405–411. [[CrossRef](#)]
230. Grigorescu, D.; Csiki-Sava, Z.; Vasile, Ș.; Butiseacă, G.-A. Taphonomic biases in macro- and microvertebrate assemblages from the Maastrichtian of the Hațeg Basin (Romania) and their relevance in the reconstruction of a fossil ecosystem. In Proceedings of the 9th Annual Meeting of the European Association of Vertebrate Palaeontologists, Heraklion, Greece, 14–19 June 2011; pp. 28–29.
231. Chiarenza, A.A.; Mannion, P.D.; Lunt, D.J.; Farnsworth, A.; Jones, L.A.; Kelland, S.-J.; Allison, P.A. Ecological niche modelling does not support climatically-driven dinosaur diversity decline before the Cretaceous/Paleogene mass extinction. *Nat. Commun.* **2019**, *10*, 1091. [[CrossRef](#)]
232. Teixell, A.; Labaume, P.; Lagabrielle, Y. The crustal evolution of the west-central Pyrenees revisited: Inferences from a new kinematic scenario. *Comptes Rendus Geosci.* **2016**, *348*, 257–267. [[CrossRef](#)]
233. Fondevilla, V.; Vila, B.; Galobart, À.; Oms, O. Taphonomic modes in the dinosaur-bearing Tremp Formation (Maastrichtian, Southern Pyrenees). In Proceedings of the XIV Annual Meeting of the European Association of Vertebrate Palaeontologists, Haarlem, The Netherlands, 6–10 July 2016; p. 223.
234. Upchurch, P.; Mannion, P.D.; Benson, R.B.J.; Butler, R.J.; Carrano, M.T. Geological and anthropogenic controls on the sampling of the terrestrial fossil record: A case study from the Dinosauria. *Geol. Soc. Lond. Spec. Publ.* **2011**, *358*, 209–240. [[CrossRef](#)]
235. Le Loeuff, J. Paleobiogeography and biodiversity of Late Maastrichtian dinosaurs: How many dinosaur species went extinct at the Cretaceous-Tertiary boundary? *Bull. Soc. Géol. Fr.* **2012**, *183*, 547–559. [[CrossRef](#)]

# **Annex II**



# Legend

## Sedimentary facies

 Coarse bioclastic sandstones with large scale cross-stratification (Arén Sandstone Fm)




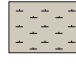

### 'Grey' and 'Lower Red Garumnian'

 Marls	 Fine sandstones with plant bioturbations	 Bioturbated marly/sandy limestones
 Grey mudstones and siltstones	 Wavy sandstones	 Carbonated sandstones and sandy limestones
 Dark grey marly mudstones rich in organic matter	 Foreset sandstones	 Intraclastic limestones
 Ochre to brown mudstones	 Cross-bedded sandstones	 Bioclastic carophyte packstone
 Variegated hydromorph mudstones	 Microconglomerates	 Micritic limestones
 Red mudstones	 Bioclastic sandstones	

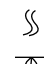
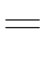
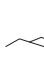




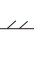








### 'Vallcebre limestones' and Colmenar-Tremp Horizon

 White marly mudstones	 Green mudstones	 Lacustrine limestones
 Purple mudstones	 Gypsum	









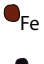
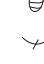















### Marine facies of Campo section

 Mudstones	 Fine sandstones	 Lumaquelic sandstones
 Marls	 Bioclastic packstones	





### Sedimentary structures

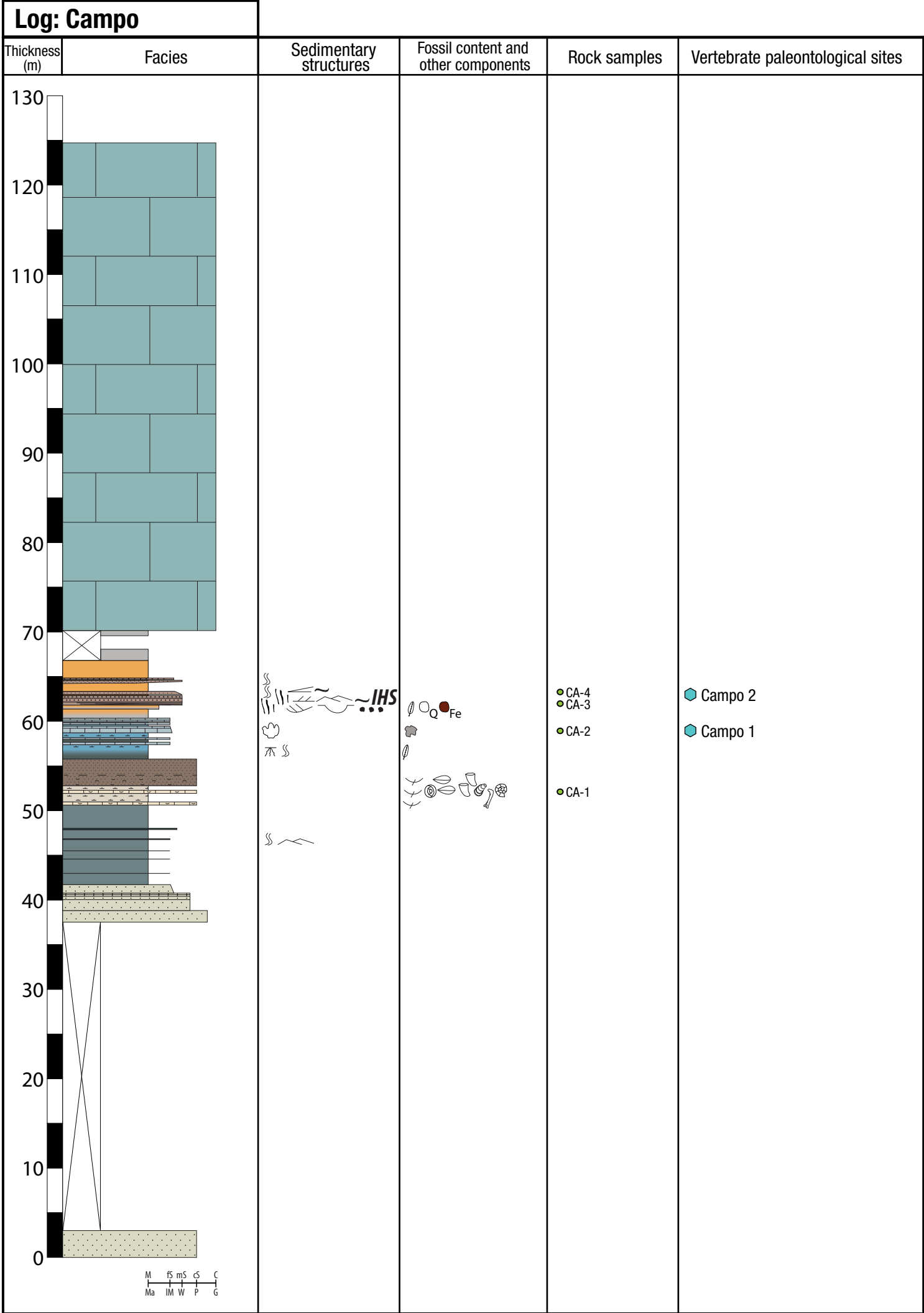
 Bioturbation	 Parallel lamination	 Ripples
 Root marks-mottling	 Low-angle cross-bedding	 Inclined heterolithic stratification
 Crocodylomorph tracks	 Planar cross-bedding	 Imbricated shells
 Hadrosaur tracks	 Trough cross-bedding	 Scour/erosive base
 Sauropods tracks	 Hummocky cross-bedding	
 Lag deposits/ Pebbles lineation	 Mud drapes/ flaser cross-bedding	

### Fossil content and other components

 Vegetal remains	 Veneroid bivalves	 Quartz/detritic pebbles
 Charcoal	 Oysters	 Carbonated pebbles
 Algae fragments	 Rudists	 Ferrous nodules
 Carophytes	 Gastropods	 Mud pebbles
 Bioclasts	 Ammonoids	 Carbonate nodules
 Foraminifera	 Vertebrate bones	 Gypsum nodules
 Decapods	 Eggshell fragments	 Glauconite
 Ostracods	 Calcspheres	 Oncoids
 Termite coprolites		

### Samples and sites

 Hard rock sample (thin-section)
 Soft rock sample
 Site in the section
 Site in the nearby area of the section



## Log: El Castellaz

Thickness (m)	Facies	Sedimentary structures	Fossil content and other components	Rock samples	Vertebrate paleontological sites
80					
70					
60				● EC-4	
50					
40				● EC-3 ● EC-2	<div>El Castellaz 2</div>
30					<div>El Castellaz 5</div> <div>El Castellaz 4</div> <div>El Castellaz 3</div> <div>El Castellaz 6</div>
20					
10				● EC-1	<div>El Castellaz 1</div> <div>El Castellaz 7</div>
0					

### Log: Valle de Lierp

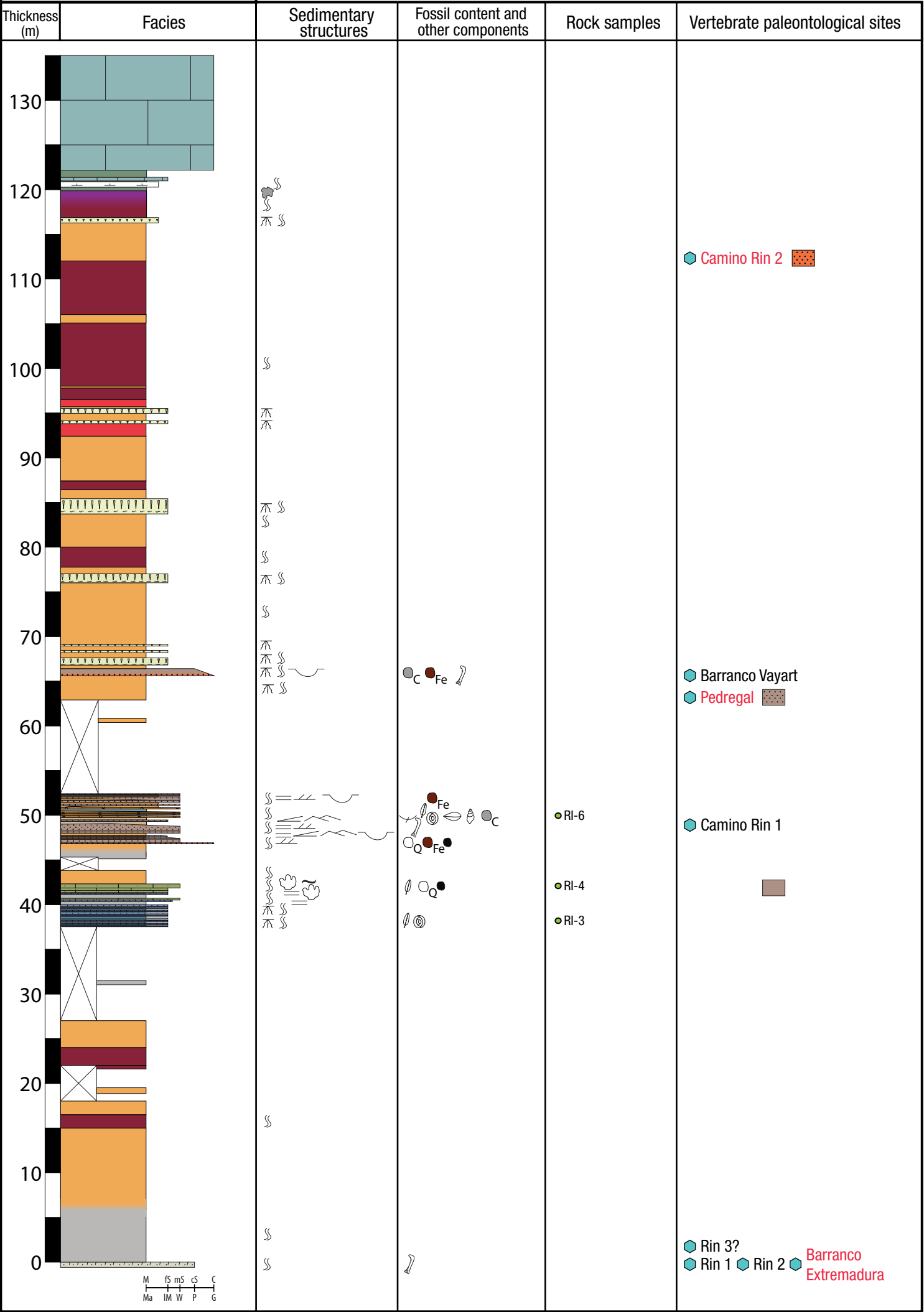
Thickness (m)	Facies
80	Black shale
75	Black shale
70	Black shale
65	Black shale
60	Black shale
55	Black shale
50	Black shale
45	Black shale
40	Black shale
35	Black shale
30	Black shale
25	Black shale
20	Black shale
15	Black shale
10	Black shale
5	Black shale
0	Black shale

Geological Log: Valle de Lierp

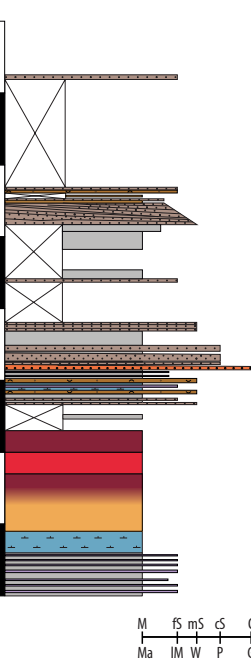

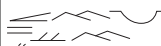








The log shows a sequence of facies from 0 to 80 meters. The facies are: Black shale (0-80m), Black shale (80-85m), Black shale (85-90m), Black shale (90-95m), Black shale (95-100m), Black shale (100-105m), Black shale (105-110m), Black shale (110-115m), Black shale (115-120m), Black shale (120-125m), Black shale (125-130m), Black shale (130-135m), Black shale (135-140m), Black shale (140-145m), Black shale (145-150m), Black shale (150-155m), Black shale (155-160m), Black shale (160-165m), Black shale (165-170m), Black shale (170-175m), Black shale (175-180m), Black shale (180-185m), Black shale (185-190m), Black shale (190-195m), Black shale (195-200m), Black shale (200-205m), Black shale (205-210m), Black shale (210-215m), Black shale (215-220m), Black shale (220-225m), Black shale (225-230m), Black shale (230-235m), Black shale (235-240m), Black shale (240-245m), Black shale (245-250m), Black shale (250-255m), Black shale (255-260m), Black shale (260-265m), Black shale (265-270m), Black shale (270-275m), Black shale (275-280m), Black shale (280-285m), Black shale (285-290m), Black shale (290-295m), Black shale (295-300m), Black shale (300-305m), Black shale (305-310m), Black shale (310-315m), Black shale (315-320m), Black shale (320-325m), Black shale (325-330m), Black shale (330-335m), Black shale (335-340m), Black shale (340-345m), Black shale (345-350m), Black shale (350-355m), Black shale (355-360m), Black shale (360-365m), Black shale (365-370m), Black shale (370-375m), Black shale (375-380m), Black shale (380-385m), Black shale (385-390m), Black shale (390-395m), Black shale (395-400m), Black shale (400-405m), Black shale (405-410m), Black shale (410-415m), Black shale (415-420m), Black shale (420-425m), Black shale (425-430m), Black shale (430-435m), Black shale (435-440m), Black shale (440-445m), Black shale (445-450m), Black shale (450-455m), Black shale (455-460m), Black shale (460-465m), Black shale (465-470m), Black shale (470-475m), Black shale (475-480m), Black shale (480-485m), Black shale (485-490m), Black shale (490-495m), Black shale (495-500m), Black shale (500-505m), Black shale (505-510m), Black shale (510-515m), Black shale (515-520m), Black shale (520-525m), Black shale (525-530m), Black shale (530-535m), Black shale (535-540m), Black shale (540-545m), Black shale (545-550m), Black shale (550-555m), Black shale (555-560m), Black shale (560-565m), Black shale (565-570m), Black shale (570-575m), Black shale (575-580m), Black shale (580-585m), Black shale (585-590m), Black shale (590-595m), Black shale (595-600m), Black shale (600-605m), Black shale (605-610m), Black shale (610-615m), Black shale (615-620m), Black shale (620-625m), Black shale (625-630m), Black shale (630-635m), Black shale (635-640m), Black shale (640-645m), Black shale (645-650m), Black shale (650-655m), Black shale (655-660m), Black shale (660-665m), Black shale (665-670m), Black shale (670-675m), Black shale (675-680m), Black shale (680-685m), Black shale (685-690m), Black shale (690-695m), Black shale (695-700m), Black shale (700-705m), Black shale (705-710m), Black shale (710-715m), Black shale (715-720m), Black shale (720-725m), Black shale (725-730m), Black shale (730-735m), Black shale (735-740m), Black shale (740-745m), Black shale (745-750m), Black shale (750-755m), Black shale (755-760m), Black shale (760-765m), Black shale (765-770m), Black shale (770-775m), Black shale (775-780m), Black shale (780-785m), Black shale (785-790m), Black shale (790-795m), Black shale (795-800m), Black shale (800-805m), Black shale (805-810m), Black shale (810-815m), Black shale (815-820m), Black shale (820-825m), Black shale (825-830m), Black shale (830-835m), Black shale (835-840m), Black shale (840-845m), Black shale (845-850m), Black shale (850-855m), Black shale (855-860m), Black shale (860-865m), Black shale (865-870m), Black shale (870-875m), Black shale (875-880m), Black shale (880-885m), Black shale (885-890m), Black shale (890-895m), Black shale (895-900m), Black shale (900-905m), Black shale (905-910m), Black shale (910-915m), Black shale (915-920m), Black shale (920-925m), Black shale (925-930m), Black shale (930-935m), Black shale (935-940m), Black shale (940-945m), Black shale (945-950m), Black shale (950-955m), Black shale (955-960m), Black shale (960-965m), Black shale (965-970m), Black shale (970-975m), Black shale (975-980m), Black shale (980-985m), Black shale (985-990m), Black shale (990-995m), Black shale (995-1000m), Black shale (1000-1005m), Black shale (1005-1010m), Black shale (1010-1015m), Black shale (1015-1020m), Black shale (1020-1025m), Black shale (1025-1030m), Black shale (1030-1035m), Black shale (1035-1040m), Black shale (1040-1045m), Black shale (1045-1050m), Black shale (1050-1055m), Black shale (1055-1060m), Black shale (1060-1065m), Black shale (1065-1070m), Black shale (1070-1075m), Black shale (1075-1080m), Black shale (1080-1085m), Black shale (1085-1090m), Black shale (1090-1095m), Black shale (1095-1100m), Black shale (1100-1105m), Black shale (1105-1110m), Black shale (1110-1115m), Black shale (1115-1120m), Black shale (1120-1125m), Black shale (1125-1130m), Black shale (1130-1135m), Black shale (1135-1140m), Black shale (1140-1145m), Black shale (1145-1150m), Black shale (1150-1155m), Black shale (1155-1160m), Black shale (1160-1165m), Black shale (1165-1170m), Black shale (1170-1175m), Black shale (1175-1180m), Black shale (1180-1185m), Black shale (1185-1190m), Black shale (1190-1195m), Black shale (1195-1200m), Black shale (1200-1205m), Black shale (1205-1210m), Black shale (1210-1215m), Black shale (1215-1220m), Black shale (1220-1225m), Black shale (1225-1230m), Black shale (1230-1235m), Black shale (1235-1240m), Black shale (1240-1245m), Black shale (1245-1250m), Black shale (1250-1255m), Black shale (1255-1260m), Black shale (1260-1265m), Black shale (1265-1270m), Black shale (1270-1275m), Black shale (1275-1280m), Black shale (1280-1285m), Black shale (1285-1290m), Black shale (1290-1295m), Black shale (1295-1300m), Black shale (1300-1305m), Black shale (1305-1310m), Black shale (1310-1315m), Black shale (1315-1320m), Black shale (1320-1325m), Black shale (1325-1330m), Black shale (1330-1335m), Black shale (1335-1340m), Black shale (1340-1345m), Black shale (1345-1350m), Black shale (1350-1355m), Black shale (1355-1360m), Black shale (1360-1365m), Black shale (1365-1370m), Black shale (1370-1375m), Black shale (1375-1380m), Black shale (1380-1385m), Black shale (1385-1390m), Black shale (1390-1395m), Black shale (1395-1400m), Black shale (1400-1405m), Black shale (1405-1410m), Black shale (1410-1415m), Black shale (1415-1420m), Black shale (1420-1425m), Black shale (1425-1430m), Black shale (1430-1435m), Black shale (1435-1440m), Black shale (1440-1445m), Black shale (1445-1450m), Black shale (1450-1455m), Black shale (1455-1460m), Black shale (1460-1465m), Black shale (1465-1470m), Black shale (1470-1475m), Black shale (1475-1480m), Black shale (1480-1485m), Black shale (1485-1490m), Black shale (1490-1495m), Black shale (1495-1500m), Black shale (1500-1505m), Black shale (1505-1510m), Black shale (1510-1515m), Black shale (1515-1520m), Black shale (1520-1525m), Black shale (1525-1530m), Black shale (1530-1535m

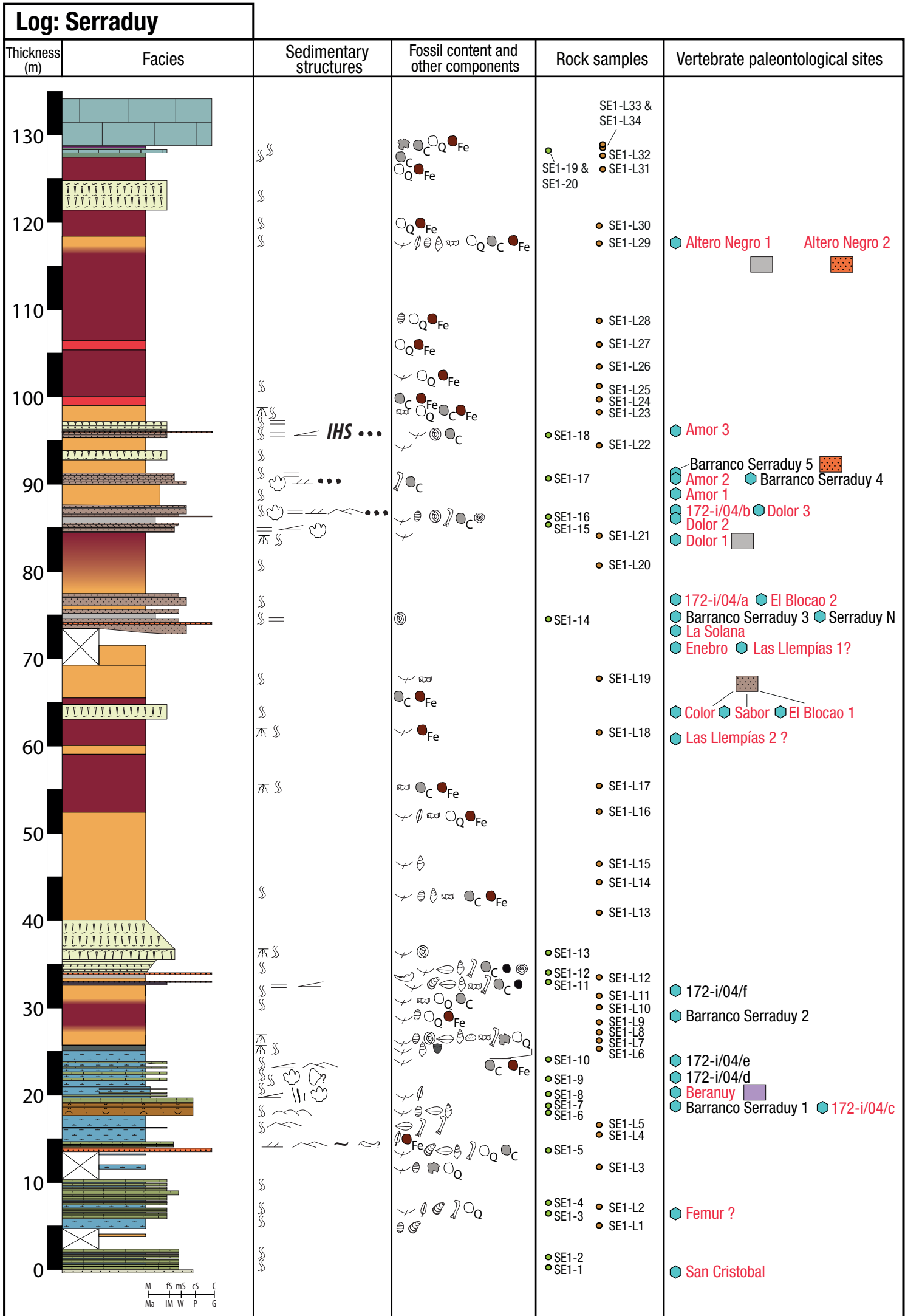
Thickness (m)	Facies	Sedimentary structures	Fossil content and other components	Rock samples	Vertebrate paleontological sites
80					
70					
60					Larra 2C
50					Larra 2B Larra 1? Larra 2A
40					
30				LAR4	Larra 6 Larra 10 Larra 7 Larra 4
20					Larra 3B Larra 5 Larra 8 Barranco Generator Larra 3A Larra 3C ? Larra 9?
10					
0					

Log: Rin 1

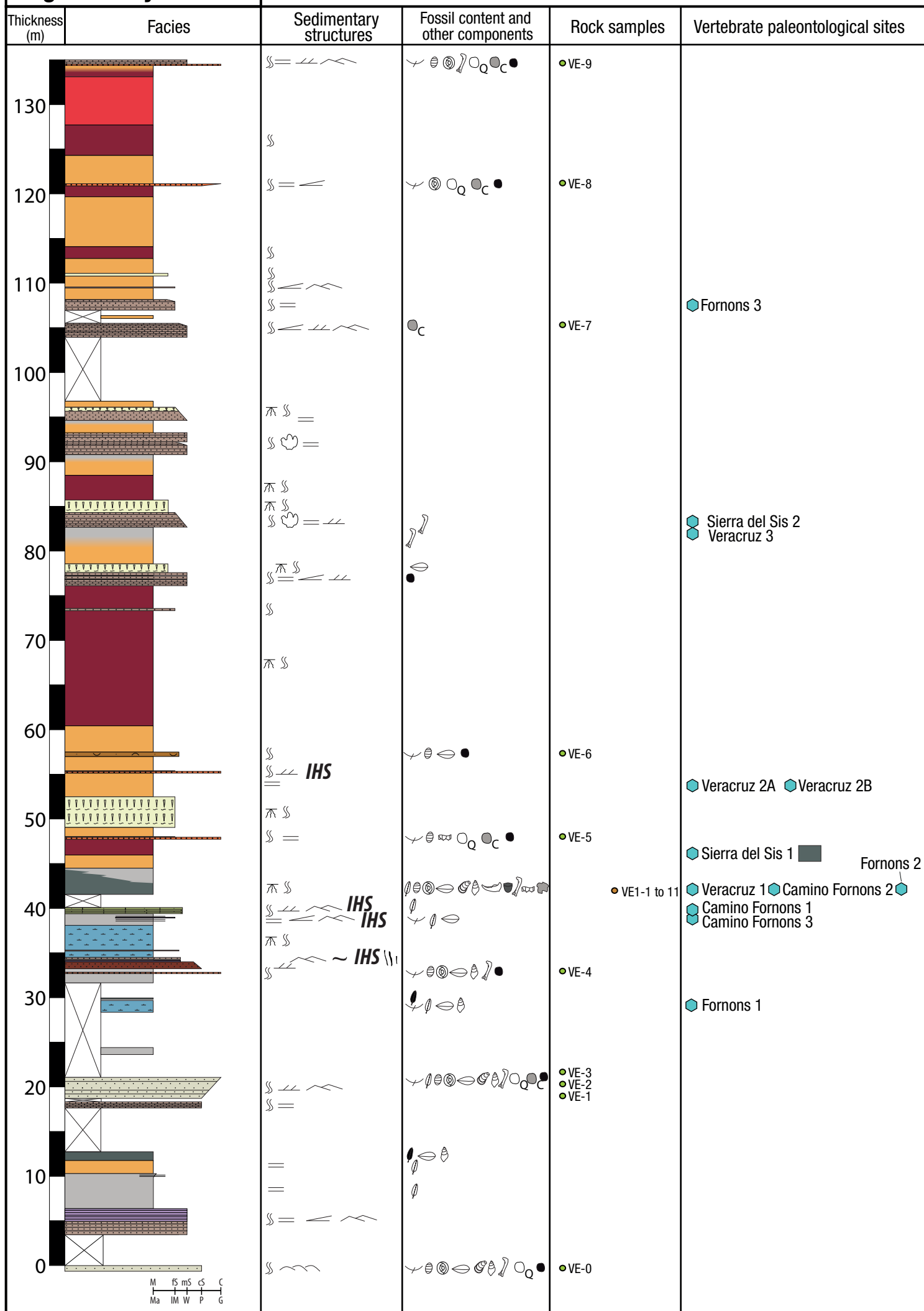


Log: Rin 2

Thickness (m)	Facies	Sedimentary structures	Fossil content and other components	Rock samples	Vertebrate paleontological sites
<div><div>40</div><div>30</div><div>20</div><div>10</div><div>0</div></div> <div><div>M Ma fS IM mS W cS P C G</div></div>		<div><i>IHS</i></div> <div><i>IHS</i></div> <div></div> <div></div>	<div></div> <div></div> <div></div>	<div> RI-5</div> <div> RI-2 RI-1</div>	<div> Camino Rin 3</div>

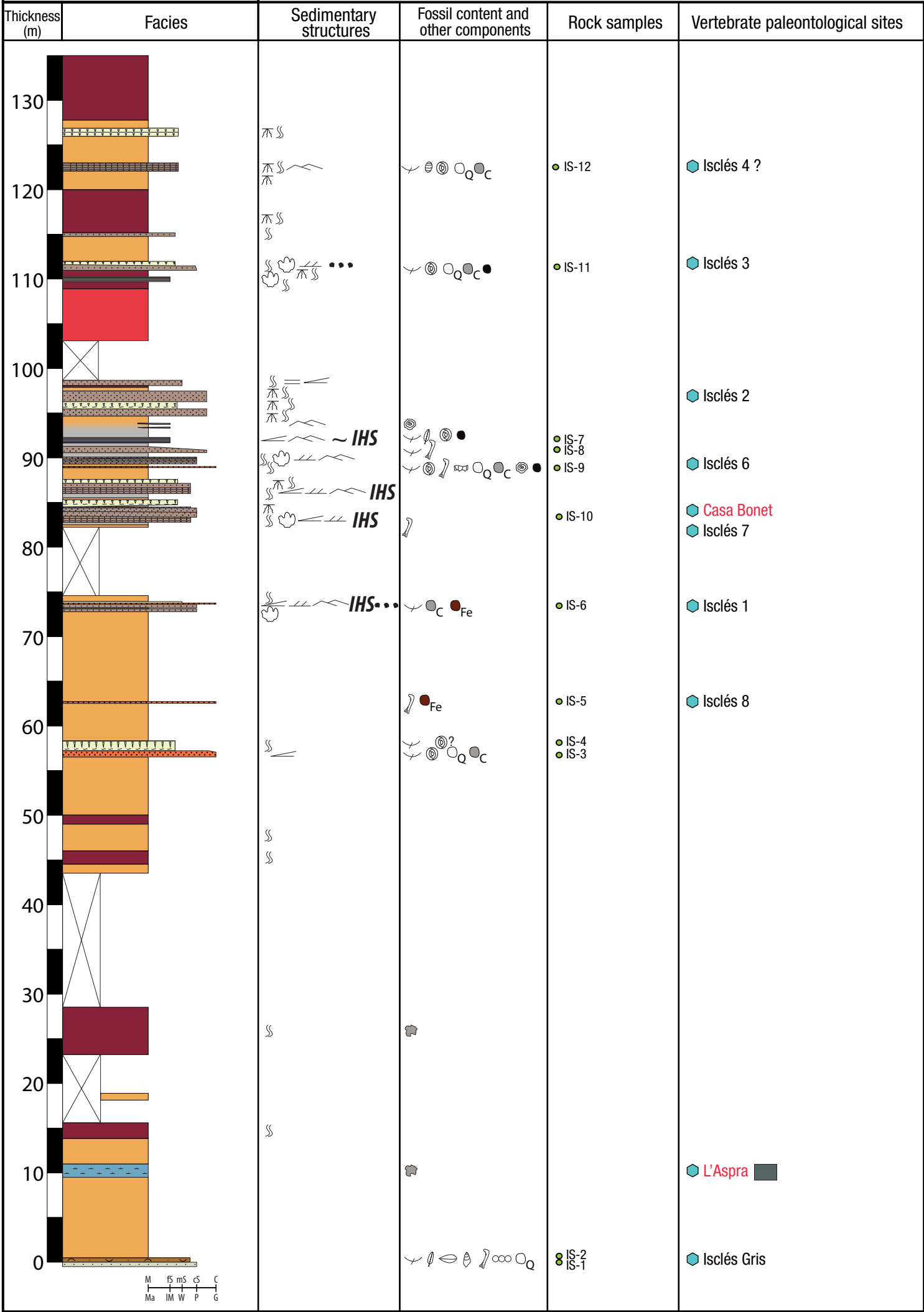


# Log: Beranuy



Log: Beranuy					
Thickness (m)	Facies	Sedimentary structures	Fossil content and other components	Rock samples	Vertebrate paleontological sites
<div> <div>160</div> <div>150</div> <div>140</div> </div> <div> <div>M</div> <div>fs</div> <div>mS</div> <div>cS</div> <div>C</div> <div>Ma</div> <div>IM</div> <div>W</div> <div>P</div> <div>G</div> </div>				<div>●VE-10</div>	

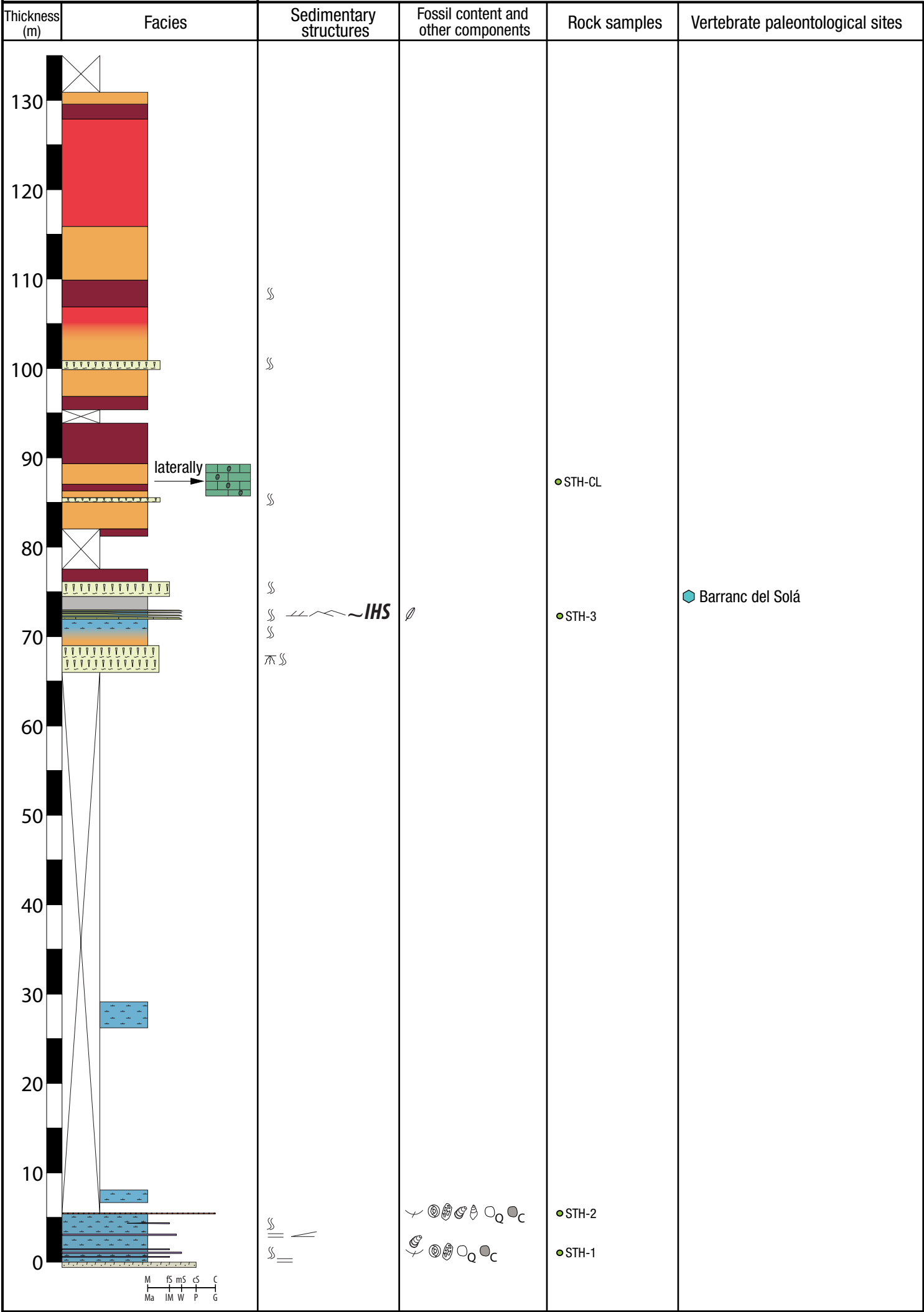
Log: Isclés



**Log: Isclés**

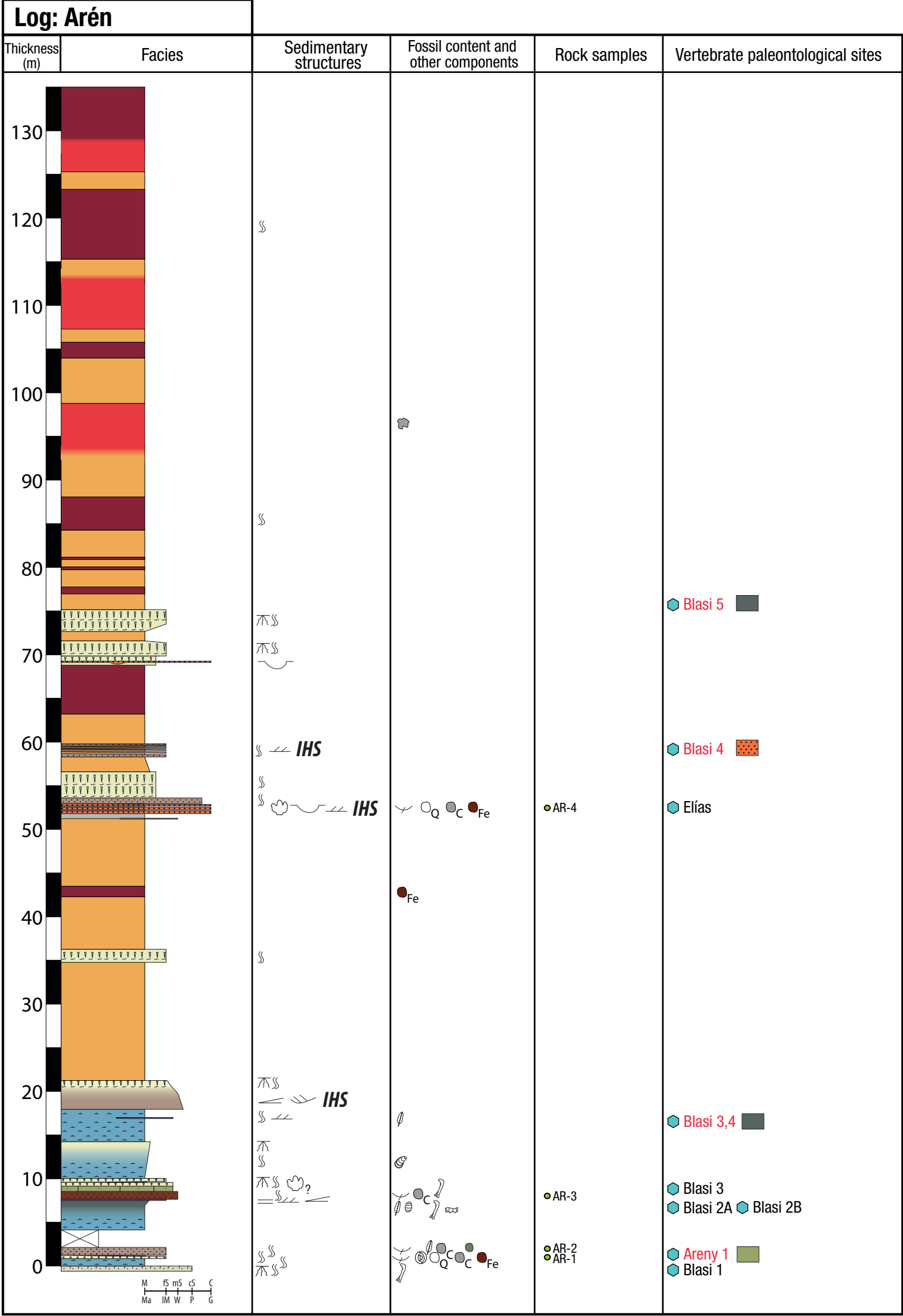
Log: Isclés					
Thickness (m)	Facies	Sedimentary structures	Fossil content and other components	Rock samples	Vertebrate paleontological sites
150				IS-14	
140				IS-13	
					Isclés 5 ?

Log: San Pere de Cornudella



## Log: San Pere de Cornudella

Thickness (m)	Facies	Sedimentary structures	Fossil content and other components	Rock samples	Vertebrate paleontological sites
230					
220					
210					
200					
190					
180					
170					
160				● STH-6	
150				● STH-5	
140					



## Log: Arén

Thickness (m)	Facies	Sedimentary structures	Fossil content and other components	Rock samples	Vertebrate paleontological sites
240					
230					
220					
210					
200					
190					
180					
170					
160					
150					
140					

# **Annex III**



New discovery	Fossil site	N° in Fig. 6. 1.	Age	Stratigraphic unit	Sedimentary facies	Taxa	Taphonomic mode	Tracks	References
	172-i/04/a	52	C29r	LRG	Cross-bedded sandstones	Hadrosauroidea indet. <i>Hadrosauropodus</i> sp.	Isolated bones	Positive hyporeliefs	Vila et al., 2013 Puértolas-Pascual et al., 2018
	172-i/04/b	56	C29r	LRG	Cross-bedded sandstones	Dinosauria indet.	Isolated bones		Puértolas-Pascual et al., 2018
	172-i/04/c	37	C29r	GG	Bioclastic sandstones	Dinosauria indet.	Isolated bones		Puértolas-Pascual et al., 2018 Cruzado-Caballero et al., 2012
	172-i/04/d	39	C29r	GG	Carbonated sandstones and sandy limestones	Dinosauria indet. Bothremydidae indet.	Isolated bones	Negative epireliefs	Puértolas-Pascual et al., 2012 Puértolas-Pascual et al., 2018 Cruzado-Caballero et al., 2012
	172-i/04/e	40	C29r	GG	Carbonated sandstones and sandy limestones	Hadrosauroidea indet. Theropoda indet. cf. <i>Arcovenator</i>	Undifferentiated bonebed		Puértolas-Pascual et al., 2012 Puértolas-Pascual et al., 2018 Cruzado-Caballero et al., 2012
	172-i/04/f	42	C29r	LRG	Ochre mudstones	Hadrosauroidea indet.	Undifferentiated bonebed		Puértolas-Pascual et al., 2012 Puértolas-Pascual et al., 2018
X	Altero Negro 1	63	C29r	LRG	Grey mudstones	Dinosauria indet. Hadrosauroidea indet. Bothremydidae indet.	Macrofossil bonebed		
X	Altero Negro 2	64	C29r	LRG	Microconglomerates	Dinosauria indet. Hadrosauroidea indet. Eusuchia indet. Bothremydidae indet.	Macrofossil bonebed		

	Amor 1	58	C29r	LRG	Ochre mudstones	Dinosauria indet. Hadrosauroidea indet. Bothremydidae indet.	Articulated/associated elements		Cruzado-Caballero et al., 2012 Puértolas-Pascual et al., 2012 Company et al., 2015 Puértolas-Pascual et al., 2018
	Amor 2	59	C29r	LRG	Cross-bedded sandstones	Hadrosauroidea indet. Bothremydidae indet.	Articulated/associated elements		Cruzado-Caballero et al., 2012 Puértolas-Pascual et al., 2012 Puértolas-Pascual et al., 2018
	Amor 3	62	C29r	LRG	Microconglomerates	Dinosauria indet. Hadrosauroidea indet. Dromaeosauridae indet. Bothremydidae indet. <i>Agaresuchus subjuniperus</i>	Macrofossil bonebed		Cruzado-Caballero et al., 2012 Puértolas-Pascual et al., 2012 Puértolas-Pascual et al., 2014 Puértolas-Pascual et al., 2018
	Areny 1	90	C30n	GG	Carbonated sandstones and sandy limestones	<i>Hadrosauropodus</i> sp.	-	Negative epireliefs	Barco et al., 2001 Vila et al., 2013
X	Barranc del Solá	88	C29r/C30n	GG	Grey mudstones	Hadrosauroidea indet.	Isolated bones		
	Barranco Extremadura	28	C30n	Aren Fm	Coarse bioclastic sandstones with large scale cross-stratification	Dinosauria indet. Hadrosauroidea indet. Bothremydidae indet. cf. <i>Thoracosaurus</i>	Macrofossil bonebed		Puértolas-Pascual et al. 2018 Blanco et al., 2020
X	Barranco Generator	10	C29r	LRG	Ochre mudstones	Hadrosauroidea indet.	Isolated bones		
	Barranco Serraduy 1	36	C29r	GG	Carbonated sandstones and sandy limestones	Dinosauria indet. Hadrosauroidea indet.	Macrofossil bonebed		Cruzado-Caballero et al., 2012 Puértolas-Pascual et al., 2012 Puértolas-Pascual et al., 2018
	Barranco Serraduy 2	41	C29r	LRG	Variegated hydromorphic mudstones	Dinosauria indet. Hadrosauroidea indet.	Undifferentiated bonebed		Cruzado-Caballero et al., 2012 Puértolas-Pascual et al., 2012

									Company et al., 2015 Puértolas-Pascual et al., 2018
	Barranco Serraduy 3	50	C29r	LRG	Cross-bedded sandstones	Vertebrata indet.	Isolated bones		Puértolas-Pascual et al., 2018 Cruzado-Caballero et al., 2012 Puértolas-Pascual et al., 2012 Company et al., 2015 Puértolas-Pascual et al., 2016 Puértolas-Pascual et al., 2018 Cruzado-Caballero et al., 2012 Puértolas-Pascual et al., 2012 Puértolas-Pascual et al., 2018
	Barranco Serraduy 4	60	C29r	LRG	Cross-bedded sandstones	Dinosauria indet. Hadrosauroidae indet. Sauropoda indet. Bothremydidae indet. Eusuchia indet.	Macrofossil bonebed	Positive hyporeliefs	
	Barranco Serraduy 5	61	C29r	LRG	Microconglomerates	Hadrosauroidae indet. Bothremydidae indet.	Macrofossil bonebed		
X	Barranco Vayart	32	C29r	LRG	Cross-bedded sandstones	Pterosauria indet. Eusuchia indet.	Isolated bones		
X	Beranuy	38	C29r	GG	Wavy sandstones	Crocodylomorpha swim tracks	-	Positive hyporeliefs	Pérez-Pueyo et al. 2018 López-Martínez et al., 2001 Cruzado-Caballero et al., 2009 Cruzado-Caballero et al., 2010a Cruzado-Caballero et al., 2010c Torices et al., 2015 Puértolas-Pascual et al., 2016
	Blasi 1	89	C30n	Aren Fm	Coarse bioclastic sandstones with large scale cross-stratification	Hadrosauroidae indet. Euhadrosauria indet. <i>Blasisaurus canudoii</i> Theropoda indet. cf. <i>Arcovenator</i> cf. <i>Allodaposuchus</i> cf. <i>Thoracosaurus</i>	Articulated/ass ociated elements		

Blasi 2a  
&2b

91  
and  
92

C30n

GG

Dark grey marly mudstones rich in organic matter

Hadrosauroidea indet.  
Euhadrosauria indet.  
Theropoda indet.  
cf. *Arcovenator*  
Coelurosauria indet.  
Dromaeosauridae  
indet.  
cf. *Richardoestesia*  
cf. *Paronychodon*  
Mesoeucrocodylia  
indet.  
Eusuchia indet.  
Allodaposuchidae  
indet.  
cf. *Allodaposuchus*  
aff. *Acynodon*  
Trematochampsid-like  
teeth  
Bothremydidae indet.  
Solemydidae sp.  
Indeterminate lizard 1  
(Iguania or  
Scleroglossa)  
Indeterminate lizard 2  
(Scleroglossa)  
Anguidae indet.  
Alethinophidia indet  
*Albanerpeton* aff.  
*nexuosum*  
Discoglossidae  
aff. *Paradiscoglossus*  
Palaeobatrachidae  
indet.

Microfossil  
bonebed

López-Martínez et  
al., 1999  
López-Martínez et  
al., 2001  
Murelaga & Canudo,  
2005  
Blain et al., 2010  
Moreno-Azanza et  
al., 2013  
Torices et al., 2015  
Puértolas-Pascual et  
al., 2016  
Blanco et al., 2020  
Pérez-Pueyo et al.,  
2019a

Blasi 3	93	C30n	GG	Foreset sandstones	Hadrosauroidea indet. Lambeosaurinae indet. Arenysaurus ardevoli Theropoda indet. cf. <i>Arcovenator</i> Eusuchia indet. cf. <i>Allodaposuchus</i> Trematochampsid-like teeth Bothremydidae indet.	Articulated/associated elements	López-Martínez et al., 2001 Canudo et al., 2005 Cruzado-Caballero et al., 2005 Murelaga & Canudo, 2005 Cruzado-Caballero et al., 2009 Pereda-Suberbiola et al., 2009 Cruzado-Caballero et al., 2013 Cruzado-Caballero et al., 2015 Torices et al., 2015 Puértolas-Pascual et al., 2016
Blasi 3,4	94	C29r/C30n	GG	Dark grey marly mudstones rich in organic matter	Euhadrosauroidea indet.	Isolated bones	Cruzado-Caballero et al., 2013 Cruzado Caballero et al., 2014 López-Martínez et al., 2001 Murelaga & Canudo, 2005
Blasi 4	96	C29r/C30n	LRG	Cross-bedded sandstones	Hadrosauroidea indet. Lambeosaurinae indet. Eusuchia indet. Bothremydidae indet.	Macrofossil bonebed	Cruzado-Caballero et al., 2010c Puértolas-Pascual et al., 2016 López-Martínez et al., 2001 Murelaga & Canudo, 2005
Blasi 5	97	C29r/C30n	LRG	Grey mudstones	Hadrosauroidea indet. Hadrosaurinae indet. Pterosauria indet. Eusuchia indet. Bothremydidae indet.	Macrofossil bonebed	Cruzado-Caballero et al., 2010c Puértolas-Pascual et al., 2016

	Camino Fornons 1	67	C29r	GG	Carbonated sandstones and sandy limestones	Dinosauria indet. Hadrosauroidea indet. Theropoda? indet. Sauropoda? indet. Bothremydidae indet. Osteichthyes indet.	Macrofossil bonebed		Puértolas-Pascual et al., 2018
	Camino Fornons 2	68	C29r	GG	Dark grey marly mudstones rich in organic matter	Hadrosauroidea indet. cf. Allodaposuchidae indet. cf. <i>Thoracosaurus</i>	Undifferentiated bonebed		Puértolas-Pascual et al., 2018 Blanco et al., 2020
X	Camino Fornons 3	66	C29r	GG	Grey mudstones	Plantae indet.	-		
	Camino Rin 1	30	C29r	LRG	Cross-bedded sandstones	Dinosauria indet. Theropoda? indet.	Isolated bones		Puértolas-Pascual et al., 2018
	Camino Rin 2	33	C29r	LRG	Microconglomerates	Hadrosauroidea indet. Theropoda? indet. Pterosauria? indet. <i>Hadrosauropodus</i> sp.	Macrofossil bonebed	Positive hyporeliefs	Puértolas-Pascual et al., 2018
X	Camino Rin 3	25	C29r	LRG	Cross-bedded sandstones	Hadrosauroidea indet.	Articulated/associated elements		
	Campo 1	1	C29r	GG	Micritic limestones	<i>Hadrosauropodus</i> sp.	-	Positive hyporeliefs	Canudo et al. 2016
	Campo 2	2	C29r	LRG	Cross-bedded sandstones	Crocodylomorpha swim tracks	-	Positive hyporeliefs	Canudo et al. 2016
X	Casa Bonet	82	C30n	LRG	Cross-bedded sandstones	<i>Hadrosauropodus</i> sp.	-	Positive hyporeliefs	
	Color	44	C29r	LRG	Cross-bedded sandstones	Dinosauria indet. Hadrosauroidea indet. Bothremydidae indet.	Macrofossil bonebed		Cruzado-Caballero et al., 2012 Puértolas-Pascual et al., 2012 Company et al., 2015 Puértolas-Pascual et al., 2018 Cruzado-Caballero et al., 2012
	Dolor 1	54	C29r	LRG	Grey mudstones	Hadrosauroidea? indet.	Isolated bones		Puértolas-Pascual et al., 2012 Puértolas-Pascual et al., 2018

	Dolor 2	55	C29r	LRG	Cross-bedded sandstones	Dinosauria indet. Bothremydidae indet.	Macrofossil bonebed		Cruzado-Caballero et al., 2012 Puértolas-Pascual et al., 2012 Puértolas-Pascual et al., 2018 Cruzado-Caballero et al., 2012 Puértolas-Pascual et al., 2012 Company et al., 2015 Puértolas-Pascual et al., 2018 Blanco et al., 2020 Pérez-Pueyo et al., 2021
	Dolor 3	57	C29r	LRG	Cross-bedded sandstones	Hadrosauroidea indet. Ornithuromorpha indet. Allodaposuchidae indet. Bothremydidae indet.	Macrofossil bonebed		
X	El Blocao 1	46	C29r	LRG	Cross-bedded sandstones	<i>Hadrosauropodus</i> sp.	-	Positive hyporeliefs	
X	El Blocao 2	53	C29r	LRG	Cross-bedded sandstones	Dinosauria indet.	Undifferentiate d bonebed		
X	El Castellaz 1	3	C29r	LRG	Bioturbated marly/sandy limestones	Hadrosauroidea indet. Bothremydidae indet.	Isolated bones		
X	El Castellaz 2	9	C29r	LRG	Cross-bedded sandstones	Hadrosauroidea indet. Eusuchia indet.	Macrofossil bonebed		
X	El Castellaz 3	6	C29r	LRG	Ochre mudstones	Dinosauria indet.	Undifferentiate d bonebed		
X	El Castellaz 4	7	C29r	LRG	Ochre mudstones	Dinosauria indet. Hadrosauroidea indet.?	Isolated bones		
X	El Castellaz 5	8	C29r	LRG	Ochre mudstones	Vertebrata indet.	Undifferentiate d bonebed		
X	El Castellaz 6	5	C29r	LRG	Level not located	Hadrosauroidea indet.	Undifferentiate d bonebed		
X	El Castellaz 7	4	C29r	LRG	Bioturbated marly/sandy limestones	<i>Hadrosauropodus</i> sp.?	-	Positive hyporeliefs	
	Elías	95	C29r/C 30n	LRG	Microconglomerates	<i>Arenysuchus</i> <i>gascabadiolorum</i>	Articulated/ass ociated elements		Puértolas et al., 2011
X	Enebro	47	C29r	LRG	Ochre mudstones	Vertebrata indet. Dinosauria indet. Hadrosauroidea indet	Undifferentiate d bonebed		

	Femur	35	C29r	GG	Level not located	Titanosauria indet.	Isolated bones		Canudo, 2001 Vila et al., 2012 Puértolas-Pascual et al., 2018
	Fornons 1	65	C29r	GG	Dark grey marly mudstones rich in organic matter	Dinosauria indet. Hadrosauroida indet.	Undifferentiated bonebed		Puértolas-Pascual et al., 2018
	Fornons 2	69	C29r	GG	Dark grey marly mudstones rich in organic matter	Dinosauria indet. Hadrosauroida? indet.	Undifferentiated bonebed		Puértolas-Pascual et al., 2018
	Fornons 3	76	C29r	LRG	Cross-bedded sandstones	Dinosauria indet. <i>Hadrosauropodus</i> sp. Theropoda? indet.	Macrofossil bonebed	Positive hyporeliefs	Cruzado-Caballero et al., 2012 Puértolas-Pascual et al., 2012 Puértolas-Pascual et al., 2018
	Islés 1	80	C30n	LRG	Cross-bedded sandstones	<i>Hadrosauropodus</i> sp.	-	Positive hyporeliefs	Vila et al., 2015
	Islés 2	84	C29r	LRG	Cross-bedded sandstones	<i>Hadrosauropodus</i> sp.	-	Positive hyporeliefs	Vila et al., 2015
	Islés 3	85	C29r	LRG	Cross-bedded sandstones	<i>Hadrosauropodus</i> sp.	-	Positive hyporeliefs	Vila et al., 2015
	Islés 4	86	C29r	LRG	Cross-bedded sandstones	<i>Hadrosauropodus</i> sp.	-	Positive hyporeliefs	Vila et al., 2015
	Islés 5	87	C29r	LRG	Cross-bedded sandstones	<i>Hadrosauropodus</i> sp.	-	Positive hyporeliefs	Vila et al., 2015
X	Islés 6	83	C30n	LRG	Level not located	Dinosauria indet. Hadrosauroida indet. Bothremydidae indet.	Undifferentiated bonebed		
X	Islés 7	81	C30n	LRG	Grey mudstones	Dinosauria indet.	Undifferentiated bonebed		
X	Islés 8	79	C30n	LRG	Ochre mudstones	Hadrosauroida indet.	Isolated bones		
X	Islés Gris	77	C30n	GG	Bioclastic sandstones	Vertebrata indet.	Isolated bones		
X	La Solana	49	C29r	LRG	Cross-bedded sandstones	Hadrosauroida indet.	Isolated bones		
	Larra 1	21	C29r	LRG	Level not located	Eusuchia indet.	Isolated bones		Puértolas-Pascual et al., 2016 Puértolas-Pascual et al., 2018
X	Larra 10	20	C29r	LRG	Cross-bedded sandstones	Bothremydidae indet. cf. <i>Polysternon</i> ?	Articulated/associated elements		

	Larra 2A	22	C29r	LRG	Ochre mudstones	Dinosauria indet. Ornithopoda indet. Hadrosauroidae indet. Bothremydidae indet. cf. Allodaposuchidae indet.	Macrofossil bonebed	Puértolas-Pascual et al., 2018
	Larra 2B	23	C29r	LRG	Cross-bedded sandstones	Dinosauria indet. Hadrosauroidae indet.	Macrofossil bonebed	Puértolas-Pascual et al., 2018
X	Larra 2C	24	C29r	LRG	Microconglomerates	Bothremydidae indet.	Isolated bones	
	Larra 3A	11	C29r	LRG	Microconglomerates	Dinosauria indet. Hadrosauroidae indet. Bothremydidae indet.	Macrofossil bonebed	Puértolas-Pascual et al., 2016 Puértolas-Pascual et al., 2018
	Larra 3B	14	C29r	LRG	Cross-bedded sandstones	Dinosauria indet. Hadrosauroidae indet. cf. Allodaposuchidae indet. Bothremydidae indet.	Macrofossil bonebed	Puértolas-Pascual et al., 2018
X	Larra 3C	12	C29r	LRG	Level not located	Dinosauria indet. Hadrosauroidae indet.	Undifferentiated bonebed	
	Larra 4	17	C29r	LRG	Intraclastic limestone	Hadrosauroidae indet. Coelurosauria indet. Dromaeosauridae indet. cf. Allodaposuchidae indet. Bothremydidae indet. Discoglossidae indet. Actinistia indet.	Macrofossil bonebed	Puértolas-Pascual et al., 2018 Pérez-Pueyo et al., 2019a
	Larra 5	15	C29r	LRG	Bioturbated marly/sandy limestones	Hadrosauroidae indet. Bothremydidae indet.	Macrofossil bonebed	Puértolas-Pascual et al., 2018
	Larra 6	19	C29r	LRG	Bioturbated marly/sandy limestones	Hadrosauroidae indet. Bothremydidae indet.	Macrofossil bonebed	Puértolas-Pascual et al., 2018
X	Larra 7	18	C29r	LRG	Ochre mudstones	Dinosauria indet.	Isolated bones	
X	Larra 8	16	C29r	LRG	Microconglomerates	Hadrosauroidae indet. Eusuchia indet.	Macrofossil bonebed	
X	Larra 9	13	C29r	LRG	Ochre mudstones	Bothremydidae indet.	Undifferentiated bonebed	
X	Las Llampías 1	48	C29r	LRG	Level not located	Theropoda indet.	Isolated bones	
X	Las Llampías 2	43	C29r	LRG	Level not located	Hadrosauroidae indet.	Isolated bones	

X	L'Aspra	78	C30n	GG	Dark grey marly mudstones rich in organic matter	Dinosauria indet.	Isolated bones		
	Pedregal	31	C29r	LRG	Cross-bedded sandstones	Hadrosauroidae indet. <i>Hadrosauropodus</i> sp. cf. <i>Allodaposuchidae</i> indet.	Macrofossil bonebed	Positive hyporeliefs	Puértolas-Pascual et al., 2018 Blanco et al., 2020
	Rin 1	26	C30n	Aren Fm	Coarse bioclastic sandstones with large scale cross-stratification	Dinosauria indet. Sauropoda indet.? <i>Eusuchia</i> indet.	Macrofossil bonebed		Puértolas-Pascual et al., 2018
	Rin 2	27	C30n	Aren Fm	Coarse bioclastic sandstones with large scale cross-stratification	Dinosauria indet. <i>Bothremydidae</i> indet.	Isolated bones		Murelaga & Canudo, 2005 Puértolas-Pascual et al., 2018
X	Rin 3	29	C30n	GG	Level not located	Dinosauria indet. Hadrosauroidae indet.	Macrofossil bonebed		
X	Sabor	45	C29r	LRG	Cross-bedded sandstones	Hadrosauroidae indet.	Isolated bones		
	San Cristobal	34	C29r	Aren Fm	Coarse bioclastic sandstones with large scale cross-stratification	Dinosauria indet. Hadrosauroidae indet.	Macrofossil bonebed		Puértolas-Pascual et al., 2018
	Serraduy Norte	51	C29r	LRG	Cross-bedded sandstones	<i>Characichnos</i> cf. <i>Crocodylopus</i> <i>Hadrosauropodus</i> sp.	-	Positive hyporeliefs	Vila et al. 2013 Vila et al., 2015
	Sierra del Sis 1	71	C29r	GG	Dark grey marly mudstones rich in organic matter	Dinosauria indet. Hadrosauroidae indet. <i>Bothremydidae</i> indet.	Macrofossil bonebed		Puértolas-Pascual et al., 2018
	Sierra del Sis 2	75	C29r	LRG	Cross-bedded sandstones	Dinosauria indet. Hadrosauroidae indet.	Undifferentiated bonebed		Puértolas-Pascual et al., 2018
X	Veracruz 1	70	C29r	GG	Dark grey marly mudstones rich in organic matter	Hadrosauroidae indet. cf. <i>Richardoestes</i> sp. <i>Allodaposuchidae</i> indet. morph. 1 <i>Allodaposuchidae</i> indet. morph. 2 cf. <i>Allodaposuchus palustris</i> <i>Bothremydidae</i> indet. <i>Albanerpetontidae</i> indet. <i>Osteichthyes</i> indet.	Microfossil bonebed		Pérez-Pueyo et al. 2019b
X	Veracruz 2A	72	C29r	LRG	Ochre mudstones	Dinosauria indet. Hadrosauroidae indet.	Macrofossil bonebed		

X	Veracruz 2B	73	C29r	LRG	Ochre mudstones	Dinosauria indet. Hadrosauroidea indet. Theropoda indet.	Undifferentiated bonebed
X	Veracruz 3	74	C29r	LRG	Grey mudstones	Hadrosauroidea indet. cf. Allodaposuchidae indet.	Isolated bones



# **Annex IV**



**Microchara cristata Grambast 1971**

Nº	Altura	Anchura	nº de vueltas	ISI
1	449.4538	338.5043	7	133
2	517.3834	381.333	7	136
3	442.0081	396.7114	7	111
4	518.3952	397.591	8	130
5	496.802	392.2837	7	127
6	415.1077	386.3388	7	107
7	462.7618	364.949	7	127
8	493.4506	392.951	8	126
9	355.2476	314.0105	7	113
10	519.4051	410.5593	7	127
11	529.0678	465.5841	7	114
12	483.5278	496.7141	8	97
13	412.1517	362.9092	8	114
14	460.2069	427.9534	7	108
15	505.7745	439.3325	8	115
16	527.6627	401.4167	7	131
17	523.0913	399.2351	7	131
18	504.9969	454.1896	7	111
19	461.628	386.3388	8	119
20	508.8732	370.0584	8	138
21	495.3936	415.0025	7	119
22	549.7916	397.591	7	138
23	522.8407	452.0695	7	116
24	333.5662	358.1856	8	93
25	509.9876	408.7471	7	125
26	443.2906	338.6333	8	131
27	464.8332	401.3079	8	116
28	471.456	399.2351	8	118
29	512.2942	421.683	7	121
30	458.7814	388.7052	7	118
31	485.6904	404.5592	8	120
32	461.0601	411.3032	8	112
33	481.0832	386.3388	7	125
34	515.3538	403.5866	8	128
35	515.0147	433.5292	7	119
36	576.7701	416.7875	7	138
37	535.2223	355.2476	8	151
38	489.2736	386.3388	7	127
39	526.171	467.2693	7	113
40	514.7603	439.6307	8	117
41	547.1642	450.1334	8	122
42	426.2152	374.049	7	114
43	532.687	439.3325	7	121
44	484.7004	376.7245	7	129

45	445.1583	383.5026	8	116
46	505.7745	390.2748	8	130
47	452.1661	419.8149	7	108
48	508.444	378.4593	8	134
49	439.2332	364.4701	9	121
50	514.7603	429.8878	10	120
51	475.8812	351.7889	10	135
52	378.4593	352.6568	10	107
53	454.1896	372.1764	9	122
54	477.4386	364.949	9	131
55	486.3194	383.6164	9	127
56	472.2888	351.1677	8	134
57	415.0025	329.2177	9	126
58	458.7814	357.0867	10	128
59	475.8812	369.7042	9	129
60	473.2126	421.683	10	112
61	484.8806	443.0935	9	109
62	486.3194	383.2748	9	127
63	495.3936	429.8878	9	115
64	489.1843	376.7245	10	130
65	508.444	413.7379	10	123
66	440.821	375.6799	9	117
67	437.7393	390.2748	9	112
68	491.8551	414.792	9	119
69	435.2382	408.2127	9	107
70	546.3656	383.1609	9	143
71	511.9532	453.3235	10	113
72	461.0601	393.0621	9	117
73	518.3952	401.3079	9	129
74	428.8708	378.69	9	113
75	542.113	448.6759	9	121
76	433.63	378.113	10	115
77	422.614	389.939	10	108
78	510.5011	439.3325	9	116
79	485.2407	431.51	9	112
80	493.5391	439.3325	9	112
81	485.2407	417.2063	9	116
82	508.8732	395.2778	9	129
83	500.9162	405.7448	9	123
84	497.5047	372.0591	9	134
85	597.0817	455.7253	9	131
86	440.821	347.7941	10	127
87	452.1661	373.4649	9	121
88	515.3538	383.2748	10	134
89	391.3921	339.7919	9	115
90	448.9678	355.1247	9	126

91	506.0335	412.1517	10	123
92	537.9891	416.7875	9	129
93	526.6687	444.2746	9	119
94	461.0601	393.0621	10	117
95	514.7603	437.5398	9	118
96	459.4472	405.7448	9	113
97	508.1863	386.3388	9	132
98	484.9706	401.3079	10	121
99	438.0385	384.1852	9	114
100	496.6262	427.0341	9	116
101	782.5611	662.9299	9	118
102	773.4683	630.5193	10	123
103	734.074	661.6771	9	111
104	757.207	616.8663	9	123
105	669.0279	631.1424	9	106
106	762.0358	705.3136	9	108
107	823.5083	679.5837	9	121
108	775.7234	664.1145	9	117
109	800.9274	647.737	9	124
110	696.6545	494.8645	9	141
111	833.6273	652.4392	10	128
112	753.7389	559.8659	9	135
113	738.8176	570.987	10	129
114	654.2438	486.0499	8	135
115	681.4446	572.5908	8	119
116	886.3841	628.0907	9	141
MEAN	116	521	429	8 122

<i>Microchara punctata</i> Feist in Feist and Colombo 1983					
Nº	Altura	Anchura	nº de vueltas	ISI	
1	392.6002	317.0176	8	124	
2	350.6412	252.0488	8	139	
3	395.6098	319.472	9	124	
4	377.6521	279.6867	9	135	
5	348.3234	289.6459	8	120	
6	306.6268	268.9295	9	114	
7	383.0523	326.7245	8	117	
8	394.4381	307.0039	8	128	
9	352.8617	261.4017	9	135	
10	373.0276	313.623	8	119	
11	351.22	284.00	8	124	
12	313.57	296	8	106	
MEAN	12	362	293	8	124

**Peckichara sertulata Grambast 1971**

Nº	Altura	Anchura	nº de vueltas	ISI
1	790.4451	677.0731	8	116.744425
2	826.8951	684.4499	8	120.811633
3	689.9149	618.7747	8	111.496947
4	825.0446	678.1042	9	121.669295
5	835.511	684.4499	8	122.070439
6	668.7667	659.8266	8	101.354917
7	747.4557	656.9082	8	113.783889
8	713.2556	606.3709	8	117.626951
9	748.6815	677.0731	8	110.57617
10	684.4499	560.7232	8	122.065557
11	770.6403	686.87	7	112.195947
12	683.7477	611.1054	7	111.887033
13	817.3875	803.5402	7	101.723287
14	734.9064	597.6665	8	122.962622
15	854.3237	769.1089	8	111.079679
16	815.6762	738.3447	9	110.473631
17	747.6309	719.8375	8	103.861066
18	793.4228	689.2816	7	115.108658
19	783.732	692.9464	8	113.101389
20	760.6593	599.2718	8	126.930601
21	744.1182	637.8183	7	116.666173
22	798.4702	716.4322	7	111.450909
23	786.1242	706.6126	8	111.252502
24	652.8406	594.0021	8	109.905436
25	785.902	681.7009	9	115.285457
26	814.9799	727.3208	9	112.05233
27	798.3608	661.6771	8	120.65716
28	766.8344	712.4593	8	107.632029
29	823.7204	702.149	8	117.314188
30	832.2117	755.1859	8	110.199581
31	819.0419	746.2278	8	109.757624
32	805.0604	745.4081	9	108.002636
33	897.1571	710.4953	8	126.272067
34	826.6838	741.1781	7	111.536458
35	810.0892	661.9411	7	122.380858
36	834.308	727.3809	8	114.70029
37	780.997	694.6458	8	112.430968
38	769.7332	661.9411	9	116.284243
39	739.7628	635.7611	8	116.358613
40	756.5146	611.7482	8	123.664377
41	685.8521	526.171	8	130.347758
42	852.6865	657.2405	8	129.737364
43	885.5956	831.3193	8	106.528935
44	850.4302	762.0358	8	111.59977

45	822.8718	691.6218	8	118.977135
46	723.9508	689.2816	7	105.029759
47	781.556	612.2476	8	127.653583
48	828.1616	709.5727	8	116.71272
49	766.6635	740.1168	8	103.586826
50	722.1995	623.8352	8	115.767674
51	874.3308	806.6319	7	108.392787
52	666.1497	554.7729	8	120.076107
53	738.8176	589.056	8	125.424
54	887.0736	759.9701	9	116.724803
55	784.4003	736.1531	8	106.553963
56	861.602	842.3817	7	102.281662
57	644.8994	562.6668	9	114.614795
58	751.3598	668.832	8	112.339093
59	873.5312	767.0621	8	113.880115
60	780.2138	658.2363	7	118.530959
61	732.5853	686.2339	9	106.754461
62	815.6762	750.4874	8	108.686195
63	715.3953	661.6771	7	108.118492
64	846.8797	773.4683	8	109.491197
65	790.6108	647.8045	7	122.04466
66	864.8397	728.2809	9	118.750842
67	828.0033	783.2861	8	105.708923
68	834.308	807.1731	7	103.36172
69	768.4273	727.3809	8	105.643041
70	720.3226	597.0817	7	120.640542
71	857.7415	775.4418	8	110.613266
72	891.9337	699.8441	8	127.447484
73	710.4953	616.7955	8	115.191388
74	785.5129	672.9327	9	116.729786
75	806.9566	533.3424	8	151.30179
76	859.0642	739.4085	8	116.182624
77	775.4418	665.3626	9	116.544242
78	781.7236	693.828	8	112.668212
79	756.5724	702.3355	8	107.722363
80	790.5557	769.96	8	102.674905
81	707.1068	641.0962	8	110.29652
82	870.3761	748.1564	8	116.336116
83	894.0853	727.3809	9	122.918446
84	792.9823	764.3247	8	103.749401
85	720.3226	616.0871	8	116.918955
86	741.1781	710.8025	7	104.273423
87	758.4171	673.4516	8	112.616423
88	852.4816	779.878	8	109.30961
89	751.011	619.48	8	121.232485
90	734.5498	617.1494	8	119.023011

91	798.7983	714.1734	7	111.849349
92	697.4689	586.9021	8	118.839053
93	666.1497	586.6045	7	113.560278
94	674.7473	562.7444	7	119.902979
95	884.4607	803.5946	8	110.063047
96	826.8951	727.0806	7	113.72812
97	814.9799	668.2441	7	121.958413
98	825.4151	824.5682	7	100.102708
99	832.7363	704.942	8	118.128342
100	806.9566	763.9246	8	105.633017
101	860.8415	801.1455	8	107.451331
102	780.6055	631.7647	8	123.559531
103	788.5646	629.549	8	125.258653
104	748.6815	706.3653	8	105.990696
105	594.7368	588.4626	7	101.066202
106	788.2322	673.1923	8	117.088713
107	609.2446	555.1663	7	109.740919
108	768.3703	674.035	8	113.995609
109	788.7861	740.2349	8	106.558891
110	718.8662	656.1766	8	

MEAN	110	781	687	8	113
------	-----	-----	-----	---	-----

**Peckichara llobregatensis Feist in Feist and Colombo 1983**

Nº	Altura	Anchura	nº de vueltas	ISI
1	565.7626	624.7445	6	91
2	520.6647	418.4605	7	124
3	536.9329	562.6668	7	95
4	504.7374	486.3194	7	104
5	425.6	414.792	6	103
6	519.4051	413.8434	6	126
7	446.7251	442.0081	8	101
8	550.1885	440.4246	7	125
9	524.0921	514.336	6	102
10	542.5156	568.4577	5	95
11	440.821	381.7908	5	115
12	461.3442	434.8367	7	106
13	462.573	528.6549	7	87
14	363.9905	347.6685	6	105
15	428.7689	413.7379	6	104
16	432.1168	581.6706	6	74
17	484.8806	543.3199	7	89
18	543.3199	504.9969	7	108
19	564.8357	564.8357	5	100
20	449.551	450.1334	7	100
21	474.5027	508.444	7	93
22	403.5866	436.3405	7	92
23	405.7448	326.0188	6	124
24	434.8367	322.2465	7	135
25	506.551	529.0678	8	96
26	422.3039	443.1921	7	95
27	447.8966	423.4399	6	106
28	449.551	449.551	6	100
29	487.8435	400	7	122
30	448.9678	448.6759	6	100
31	588.1657	585.263	7	100
32	412.1517	440.821	6	93
33	562.6668	517.0457	6	109
34	519.6573	566.3798	7	92
35	463.9869	474.7787	7	98
36	516.9613	467.2693	7	111
37	512.2942	405.7448	7	126
38	451.0057	479.9017	8	94
39	415.0025	453.3235	6	92
40	522.8407	493.4506	6	106
41	414.792	423.4399	6	98
42	439.3325	402.2861	7	109
43	580.9945	481.0832	7	121
44	521.0839	516.1158	6	101

45	475.973	429.5829	6	111
46	472.8433	494.5996	6	96
47	663.5882	635.555	6	104
48	495.658	448.6759	7	110
49	461.0601	478.8997	6	96
50	456.2999	378.4593	7	121
51	534.7325	525.4235	5	102
52	429.8878	392.5062	7	110
53	483.5278	462.7618	6	104
54	507.8424	474.7787	6	107
55	542.0324	497.6802	6	109
56	556.4234	527.6627	6	105
57	538.1514	552.6435	6	97
58	510.9286	510.6722	7	100
59	565.6855	577.678	7	98
60	542.757	487.3957	6	111
61	524.0921	552.0901	6	95
62	438.8353	330.2771	6	133
63	402.8284	364.949	7	110
64	339.7919	357.6976	7	95
65	491.1443	506.8095	7	97

MEAN	65	486	471	6	104
------	----	-----	-----	---	-----

**Platychara**

Nº	Altura	Anchura	nº de vueltas	ISI	Comentarios
1	378.49	443.40	6	85	
2	358.75	433.46	6	83	
3	323.32	362.02	5	89	
4	364.12	386.27	6	94	
5	280.31	411.47	6	68	
6	250.63	434.46	6	58	
7	328.65	412.15	6	80	
8	343.20	396.65	6	87	
9	390.39	416.23	6	94	
10	349.87	409.35	6	85	
11	393.08	423.62	5	93	
12	338.78	420.09	6	81	
13	344.28	386.88	6	89	
14	273.14	367.17	6	74	
15	320.19	394.50	6	81	
16	360.00	366.83	6	98	
17	367.59	407.95	6	90	
18	336.49	366.49	6	92	
19	361.17	459.72	5	79	
20	389.91	417.87	6	93	
21	307.59	397.94	5	77	
22	354.23	431.60	6	82	
23	368.94	435.75	6	85	
24	356.50	418.05	5	85	
25	368.27	413.09	6	89	
26	280.31	349.60	5	80	
27	371.83	406.88	6	91	
28	298.90	361.38	6	83	
29	293.13	396.38	5	74	
30	384.66	445.60	6	86	
31	270.17	347.33	6	78	
32	373.83	393.67	6	95	
33	312.69	395.60	6	79	
34	393.83	405.66	5	97	
35	347.51	391.30	6	89	
36	390.03	395.44	6	99	
37	355.84	424.50	6	84	
38	345.22	407.49	6	85	
39	379.39	418.65	5	91	
40	255.59	357.54	6	71	
41	332.31	448.48	6	74	
42	361.17	468.71	5	77	
43	306.38	389.87	5	79	
44	342.65	410.38	6	83	

45	273.82	312.34	6	88
46	323.80	384.10	6	84
47	357.89	466.58	6	77
48	287.52	336.26	5	86
49	334.36	362.07	6	92
50	363.09	446.30	6	81
51	348.8	397.1625	6	88
52	334.6388	444.7305	6	75
53	364.5845	429.7612	6	85
54	321.9296	383.1695	5	84
55	321.3992	412.0363	6	78
56	333.6641	398.5659	6	84
57	377.5011	436.6	5	86
58	356.4969	429.1833	6	83
59	328.7942	386.3942	6	85
60	442.2474	441.7912	5	100
61	314.3239	369.1924	6	85
62	312.3936	359.5726	5	87
63	318.9772	387.8766	6	82
64	300.8091	384.3013	6	78
65	252.8493	371.788	6	68
66	279.7018	325.9515	6	86
67	290.0999	336.4416	6	86
68	336.6259	388.8351	6	87
69	312.1452	372.8294	6	84
70	357.1923	429.9776	5	83
71	245.3147	345.3591	5	71
72	339.7903	384.3416	6	88
73	334.3606	390.0299	6	86
74	340.884	466.3175	5	73
75	387.5566	434.9271	5	89
76	341.5658	386.073	6	88
77	361.165	449.8969	5	80
78	299.4137	378.7726	6	79
79	359.9175	448.5158	5	80
80	331.2849	391.6966	6	85
81	388.6356	460.9651	5	84
82	292.2838	419.3493	6	70
83	352.4715	404.1308	5	87
84	356.4969	382.075	5	93
85	373.536	398.7215	6	94
86	401.5125	465.4519	5	86
87	306.3777	362.0229	5	85
88	315.9481	407.1895	5	78
89	308.9488	366.2822	5	84
90	266.5266	386.8756	5	69

91	338.8303	397.3577	5	85
92	359.0978	430.9145	5	83
93	339.9272	413.5017	5	82
94	284.0488	368.6459	6	77
95	354.0521	451.2738	5	78
96	384.4627	423.325	5	91
97	397.9428	413.5393	5	96
98	364.5845	438.7262	5	83
99	317.5151	401.0487	5	79
100	401.0487	418.646	5	96
101	312.3439	421.5626	5	74
102	324.7598	351.9871	5	92
103	297.7514	374.6554	5	79
104	312.0955	410.9432	5	76
105	321.7851	358.7521	5	90

MEAN	105	337	402	6	84
------	-----	-----	-----	---	----

#### *Feistiella malladae*

Nº	Altura	Anchura	nº de vueltas	ISI	Comentarios
1	561.9763	455.0728	8	123	
2	768.219	701.0157	8	110	

MEAN	2	665	578	8	117
------	---	-----	-----	---	-----

#### *Lamprothamnium sp.*

Nº	Altura	Anchura	nº de vueltas	ISI	Comentarios
1	618.6251	416.8639	8	148	
2	659.4726	502.653	8	131	
3	538.2938	406.2743	8	132	
4	637.9787	468.9709	9	136	

MEAN	4	614	449	8	137
------	---	-----	-----	---	-----

**Microchara nana Vicente et Martín-Closas 2015**

Nº	Altura	Anchura	nº de vueltas	ISI	Comentarios
1	266.23	257.39		6	103
2	329.11	274.26		7	120
3	310.38	259.96		6	119
4	290.64	264.04		7	110
5	293.91	249.16		7	118
6	317.66	247.77		8	128
7	278.96	248.70		7	112
8	298.31	245.77		7	121
9	252.85	215.14		7	118
10	275.73	279.69		6	99
11	246.83	229.96		6	107
12	379.79	272.67		7	139
13	320.92	275.52		7	116
14	296.65	210.93		8	141
15	272.35	242.57		6	112
16	323.16	309.72		6	104
17	317.24	257.24		7	123
18	363.60	328.99		7	111
19	272.22	226.84		6	120
20	371.26	301.200		6	123
21	268.36	241.00		7	111
22	267.17	252.81		6	106
MEAN	22	301	259	7	117

<i>Microchara laevigata???</i>					
Nº	Altura	Anchura	nº de vueltas	ISI	Comentarios
1	678.5129	511.6733		6	133
2	771.2981	647.2659		7	119
3	744.4248	659.3546		7	113
4	649.8975	438.8745		7	148
MEAN	4	711	564	7	128

<i>Lycnothamnus begudianus Gambrast 1962</i>					
Nº	Altura	Anchura	nº de vueltas	ISI	Comentarios
1	1021.38	831.32		9	123
2	982.38	871.13		10	113
3	1120.20	989.20		10	113
4	1130.95	1000.00		10	113
5	1050.06	819.26		10	128
6	1065.42	953.28		10	112
7	1065.58	932.90		9	114
8	962.98	973.04		10	99
9	1216.84	1033.63		10	118
10	1036.50	923.73		9	112
11	938.73	834.26		10	113
12	1070.45	877.92		10	122
13	1075.74	907.27		10	119
14	961.67	835.51		9	115
15	1046.56	905.35		10	116
16	1024.29	860.69		10	119
17	939.94	836.35		9	112
18	1006.53	751.48		10	134
19	886.24	716.37		10	124
MEAN	19	1032	887	10	117



# **APPENDIX I**



## **APPENDIX I: List of scientific papers included in this Doctoral Thesis**

- 1) Puértolas-Pascual, E., Arenillas, I., Arz, J.A., Calvín, P., Ezquerro, L., García-Vicente, C., **Pérez-Pueyo, M.**, Sánchez-Moreno, E.M., Villalaín, J.J, Canudo, J.I. (2018). Chronostratigraphy and new vertebrate sites from the upper Maastrichtian of Huesca (Spain), and their relation with the K/Pg boundary. *Cretaceous Research*, 89, 36-59. <https://doi.org/10.1016/j.cretres.2018.02.016>

**Impact factor:** 2.120 - 8/57 **Q1 Paleontology** Science Citation Index Expanded (SCIE)

**PhD candidate contribution:** M.P.P participated in some field workdays, helping in the stratigraphic location of several vertebrate sites. He also participated in the preparation and revision of the final text of the manuscript.

- 2) **Pérez-Pueyo, M.**, Cruzado-Caballero, P., Moreno-Azanza, M., Vila, B., Castanera, D., Gasca, J.M., Puértolas-Pascual, E., Bádenas, B., Canudo, J.I. (2021). The Tetrapod Fossil Record from the Uppermost Maastrichtian of the Ibero-Armorican Island: An Integrative Review Based on the Outcrops of the Western Tresp Syncline (Aragón, Huesca Province, NE Spain). *Geosciences*, 11 (4), 162. <https://doi.org/10.3390/geosciences11040162>

**Impact factor:** No impact factor - 124/245 **Q3 Geosciences, Multidisciplinary** Emerging Sources Citation Index (ESCI)

**PhD candidate contribution:** M.P.P. reviewed and summarized all the upper Maastrichtian vertebrate record of Spain, Portugal and southern France, and summarized it in a data base. Another task performed was the comparison of the reviewed record with the record from Romania (Hateg island). He also carried out the field work to situate all the vertebrate sites of the Western Tresp Syncline in different stratigraphic logs. He took care of the conceptualization, the writing and elaboration of figures of the manuscript.

- 3) **Pérez-Pueyo, M.**, Puértolas-Pascual, E., Moreno-Azanza, M., Cruzado-Caballero, P., Gasca, J.M., Núñez-Lahuerta, C., Canudo, J.I. (2021). First record of a giant bird

(Ornithuromorpha) from the uppermost Maastrichtian of the Southern Pyrenees, NE Spain. *Journal of Vertebrate Paleontology*, 41, e1900210. <https://doi.org/10.1080/02724634.2021.1900210>

**Impact factor:** 2.558 - 9/54 **Q1 Paleontology** Science Citation Index Expanded (SCIE)

**PhD candidate contribution:** M.P.P commissioned the CT-scan of the fossil, studied and compare it. He also codified the cladistic dataset and run the analysis He lead the the conceptualization, the writing and elaboration of figures of the manuscript.

- 4) Moreno-Azanza, M., **Pérez-Pueyo, M.**, Puértolas-Pascual, E., Núñez-Lahuerta, C., Mateus, O., Bauluz, B., Bádenas, B., Canudo, J.I. (2022). A new crocodylomorph related ootaxon from the late Maastrichtian of the Southern Pyrenees (Huesca, Spain). *Historical Biology*. Publicado online el 21 de julio de 2022 (pendiente de asignación de volumen).

<https://doi.org/10.1080/08912963.2022.2098024>

**Impact factor:** 1.942 - 24/54 **Q2 Paleontology** Science Citation Index Expanded (SCIE) (data SCIE from 2021)

**PhD candidate contribution:** M.P.P collected the eggshells and took part in the microscopy sessions (SEM and optic) to characterize the new ootaxa. It also collaborated with the conception, the writing and the preparation of the manuscript. M.P.P also created part of the graphic support of the paper

- 5) **Pérez-Pueyo, M.**, Puértolas-Pascual, E., Canudo, J.I., Bádenas, B. (2019). Larra 4: Desenterrando a los últimos vertebrados del Maastrichtiense terminal del Pirineo aragonés. *Zubia*, 31, 175-180.

**Impact factor:** None

**PhD candidate contribution:** MPP studied and described the fossils and the stratigraphic features of the site. He carried out the conceptualization, the writing and elaboration of figures of the manuscript

- 6) **Pérez-Pueyo, M.**, Moreno-Azanza, M., Núñez-Lahuerta, C., Puértolas-Pascual, E., Bádenas, B., Canudo, J.I. (2021). Eggshell association of the Late Maastrichtian (Late Cretaceous) at Blasi 2B fossil site: A scrambled of vertebrate diversity. *Ciências da Terra-Procedia*, 1, 58-61.

<https://doi.org/10.21695/cterraproc.v1i0.410>

**Impact factor:** None

**PhD candidate contribution:** M.P.P collected the eggshells and led the microscopy sessions (SEM and optic) to characterize the eggshells. He took care of the conceptualization, the writing and elaboration of figures of the manuscript